

March 2021

A Comparison of Intertidal Metazoan Biodiversity Between Previously Oiled Sheared and Intact Marsh Margins and Between Multiple Salinity Zones in the Coastal Marshes of Louisiana

Patrick M. Rayle

Louisiana State University and Agricultural and Mechanical College

Follow this and additional works at: https://digitalcommons.lsu.edu/gradschool_theses



Part of the [Biodiversity Commons](#), [Bioinformatics Commons](#), [Biology Commons](#), [Environmental Microbiology and Microbial Ecology Commons](#), and the [Molecular Biology Commons](#)

Recommended Citation

Rayle, Patrick M., "A Comparison of Intertidal Metazoan Biodiversity Between Previously Oiled Sheared and Intact Marsh Margins and Between Multiple Salinity Zones in the Coastal Marshes of Louisiana" (2021). *LSU Master's Theses*. 5287.

https://digitalcommons.lsu.edu/gradschool_theses/5287

This Thesis is brought to you for free and open access by the Graduate School at LSU Digital Commons. It has been accepted for inclusion in LSU Master's Theses by an authorized graduate school editor of LSU Digital Commons. For more information, please contact gradetd@lsu.edu.

**A COMPARISON OF INTERTIDAL METAZOAN BIODIVERSITY BETWEEN
PREVIOUSLY OILED SHEARED AND INTACT MARSH MARGINS AND
BETWEEN MULTIPLE SALINITY ZONES IN THE COASTAL MARSHES OF
LOUISIANA**

A Thesis

Submitted to the Graduate Faculty of the
Louisiana State University and
Agricultural and Mechanical College
in partial fulfilment of the
requirements for the degree of
Master of Science

in

The Department of Entomology

by

Patrick Michael Rayle
B.S., Louisiana State University, 2015
May 2021

Acknowledgements

This research was made possible through grants from the Gulf of Mexico Research Initiative. I would like to extend my thanks to Dr. Lane Foil, my major professor, for his help in the experimental design and writing of this thesis. I would also like to extend my thanks to my committee members Dr. Claudia Husseneder for her assistance in the bioinformatics methods of this thesis, and Dr. Brant Faircloth for many helpful insights. I would also like to acknowledge many members of the Foil Lab, both past and present: Dr. Mike Becker, Erin Stevens, Darius Davis, Julian Lucero, and Igor Sokolov for their field and logistical support, Ben Aker, for his statistical expertise, and Colleen Walsh, Amy Mitchell, Fallon Ross, and Dakota Mengel for their assistance with lab work. I acknowledge the ecological expertise of Dr. Michael Kaller, who gave important insights on how to handle the intersection of bioinformatics and ecology. Many thanks go to the team behind the World Register of Marine Species (WoRMS Editorial Board 2020, marinespecies.org) for keeping detailed, consistent, and expert-reviewed records of taxonomic strings and other data for marine species online and freely available. I also acknowledge Dr. W. Kelley Thomas, Jeffrey Hall, Joseph Sevigny, Devin Thomas, Krystalynne Morris, and the other team members at the Hubbard Center for Genome Studies at the University of New Hampshire for handling our sequencing and computing needs and for their continued support. Lastly, I would like to thank Michael, Joanne, Christopher and Stephen Rayle for their constant love and support, and Brandi Wozniak for her unending love and patience during my time in graduate school.

Table of Contents

Acknowledgements.....	ii
List of Tables	v
List of Figures	viii
Abstract.....	xii
Introduction	1
Chapter 1. Literature Review	3
1.1. Tidal Marshes.....	3
1.2. Marsh Ecosystem Services.....	3
1.3. Natural and Anthropogenic Threats to Salt Marshes.....	4
1.4. Proposed solutions to combat global salt marsh losses	8
1.5. Louisiana specific issues	9
1.6. Proposed solutions to Louisiana issues	9
1.7. Meiofauna as a measure of marsh health and recovery.....	11
1.8. DNA metabarcoding and associated analyses.....	11
Chapter 2. A Comparison of Intertidal Metazoan Infauna Biodiversity between Previously Oiled Sheared and Intact Marsh Margins in Bay Jimmy, Louisiana, Using DNA Extraction of Whole Sediments	14
2.1. Introduction.....	14
2.2. Materials and Methods	16
2.3. Results.....	25
2.4. Discussion	81
Chapter 3. A Comparison of Intertidal Metazoan Meiofauna Biodiversity between Previously Oiled Sheared and Intact Marsh Margins in Bay Jimmy, Louisiana, Using DNA Extraction of the Organic Portion of Sediments	94
3.1. Introduction.....	94
3.2. Materials and methods	97

3.3. Results.....	103
3.4. Discussion	152
Chapter 4. A Comparison of Intertidal Metazoan Biodiversity among Three Different Salinity Zones and Two Different Bays in the Marshes of Louisiana	
4.1. Introduction	164
4.2. Materials and Methods	166
4.3. Results.....	173
4.4. Discussion	237
Summary and Conclusions.....	250
Glossary.....	252
Literature Cited	254
Vita	280

List of Tables

Table 2.1. Mean and standard deviation values for soil chemistry analyses, 1	27
Table 2.2. Mean and standard deviation values for soil chemistry analyses, 2.	27
Table 2.3. Mean and standard deviation values for soil chemistry analyses, 3	28
Table 2.4. ANOVA results for Carbon (%)	29
Table 2.5. ANOVA results for Nitrogen (%)	29
Table 2.6. ANOVA results for Percent Organic Matter	30
Table 2.7. ANOVA results for C/N ratios	30
Table 2.8. Sub-Domain level taxonomy assignments for the full 18S sequence dataset	32
Table 2.9. OTU diversity profile	40
Table 2.10. Shared and total number of OTUs for samples from sheared and intact margins	42
Table 2.11. Shared and total numbers of OTUs for samples collected from different marsh islands.....	42
Table 2.12. Shared and total numbers of OTUs for samples from elevation positions.....	43
Table 2.13. Assignment of OTUs to phyla, orders and the lowest feasible level and OTU incidence	48
Table 2.14. Unique OTUs in the samples from sheared and intact margins.	62
Table 2.15. Unique OTUs in the samples from different islands.	64
Table 2.16. Empirical and estimated similarity indices between communities from different margins, islands, and elevation positions	68
Table 2.17. Estimated pairwise similarity matrix for island communities, Sørensen index	70
Table 2.18. Estimated pairwise similarity matrix for elevation transect communities, Sørensen index....	70
Table 2.19. Adonis test results.....	75
Table 2.20. Adonis test results for Dragon Island samples only	76
Table 2.21. Adonis test results for Horseshoe Island samples only.....	77

Table 2.22. Adonis test results for Stingray Island samples only	77
Table 2.23. Songbird differentials	80
Table 3.1. Sub-Domain level taxonomy assignments for the full floated 18S sequence dataset.....	104
Table 3.2. OTU diversity profile	113
Table 3.3. Shared and total number of OTUs for samples from sheared and intact margins	115
Table 3.4. Shared and total numbers of OTUs for samples from different islands	115
Table 3.5. Shared and total numbers of OTUs for samples from different elevation positions	116
Table 3.6. Assignment of OTUs to phyla, orders, and lowest feasible level and OTU incidence.....	121
Table 3.7. Unique taxa in the samples from sheared and intact margins.	132
Table 3.8. Unique taxa in the samples from different islands.	134
Table 3.9. Empirical and estimated similarity indices between communities from different margins, islands, and elevation positions	139
Table 3.10. Estimated pairwise similarity matrix for island communities, Sørensen index	141
Table 3.11. Estimated pairwise similarity matrix for elevation transect communities, Sørensen index..	142
Table 3.12. Adonis test results.....	146
Table 3.13. Adonis test output for Dragon Island samples.....	147
Table 3.14. Adonis test output for Horseshoe Island samples	147
Table 3.15. Adonis test output for Stingray Island samples	148
Table 3.16. Songbird differentials	151
Table 4.1. Mean and standard deviation values for soil chemistry analyses	174
Table 4.2. Historic data ranges for soil chemical analyses in Gulf Coast marshes.....	175
Table 4.3. Sub-Domain level taxonomy assignments for the full 18S sequence dataset	181

Table 4.4. OTU diversity profile	192
Table 4.5. Shared and total number of OTUs for samples from Barataria and Caillou Bays.....	194
Table 4.6. Shared and total number of OTUs for samples from different salinity zones	194
Table 4.7. Shared and total number of OTUs for samples from the different distances from the marsh edge	195
Table 4.8. Assignment of OTUs to phyla, orders and the lowest feasible level and OTU incidence	201
Table 4.9. Unique OTUs from Barataria and Caillou Bays.....	216
Table 4.10. Unique OTUs from the different salinity zones.....	219
Table 4.11. Empirical and estimated similarity indices between communities collected from different bays, salinity zones, and distances from the marsh edge	226
Table 4.12. Estimated pairwise similarity matrix for salinity zone communities, Sørensen index.....	228
Table 4.13. Estimated pairwise similarity matrix for the distance from marsh edge communities, Sørensen index.....	228
Table 4.14. Adonis test results.....	232
Table 4.15. Songbird differentials	234

List of Figures

Fig. 2.1. Sheared and intact margins photo comparison	17
Fig. 2.2. Taxa bar plots for the full 18S sequence dataset	33
Fig. 2.3. Alpha rarefaction curves	34
Fig. 2.4. Sample-based rarefaction curves for the full metazoa dataset.....	35
Fig. 2.5. Sample-based rarefaction curves for samples from sheared and intact marsh margins	36
Fig. 2.6. Sample-based rarefaction curves for samples from the different islands.....	36
Fig. 2.7. Sample-based rarefaction curves for samples from the different elevation positions ..	37
Fig. 2.8. Coverage-based rarefaction curves for the full metazoa dataset	38
Fig. 2.9. Coverage-based rarefaction curves for samples from sheared and intact marsh margins	38
Fig. 2.10. Coverage-based rarefaction curves for samples from the different islands	39
Fig. 2.11. Coverage-based rarefaction curves for samples from the different elevation positions	39
Fig. 2.12. Observed OTU richness and richness estimations from four estimator models.....	41
Fig. 2.13. Taxa bar plots for the metazoa dataset	44
Fig. 2.14. Percentage of total OTU incidences by phylum	46
Fig. 2.15. Percentage of the total OTUs per phylum assignment	47
Fig. 2.16. The OTU richness for sheared and intact sites, split by island of origin.	66
Fig. 2.17. Faith's PD for sheared and intact sites, split by island of origin	67
Fig. 2.18. Plot of the first two dimensions of the NMDS ordination of the Sørensen distance matrix, grouped by margin type	72

Fig. 2.19. Plot of the first two dimensions of the NMDS ordination of the Sørensen distance matrix, grouped by island of origin.....	73
Fig. 2.20. Plot of the first two dimensions of the NMDS ordination of the Sørensen distance matrix, grouped by margin type and island of origin	74
Fig. 2.21. Plot of the first two dimensions of the NMDS ordination of the Sørensen distance matrix for samples from Stingray Island.....	78
Fig. 3.1. Taxa bar plots for the full floated 18S sequence dataset	106
Fig. 3.2. Alpha rarefaction curves	107
Fig. 3.3. Sample-based rarefaction curves for the full floated metazoa dataset	108
Fig. 3.4. Sample-based rarefaction curves for samples from sheared and intact margins	109
Fig. 3.5. Sample-based rarefaction curves for samples from the different islands.....	109
Fig. 3.6. Sample-based rarefaction curves for samples from the different elevation positions	110
Fig. 3.7. Coverage-based rarefaction curves for the full floated metazoa dataset	111
Fig. 3.8. Coverage-based rarefaction curves for samples from sheared and intact marsh margins	111
Fig. 3.9. Coverage-based rarefaction curves for samples from the different islands	112
Fig. 3.10. Coverage-based rarefaction curves for samples from the different elevation positions	112
Fig. 3.11. Observed OTU richness and richness estimations	114
Fig. 3.12. Taxa bar plots for the floated metazoa dataset.....	117
Fig. 3.13. Percentage of total OTU incidences by phylum.....	119
Fig. 3.14. Percentage of the total OTUs per phylum assignment.....	120
Fig. 3.15. The OTU richness values for sheared and intact sites, with individual box plots for	

each island and elevation position	137
Fig. 3.16. Faith's PD values for sheared and intact sites, with individual box plots for each island and elevation position.	138
Fig. 3.17. Plot of the first two dimensions of the NMDS ordination of the Sørensen distance matrix, grouped by margin type	143
Fig. 3.18. Plot of the first two dimensions of the NMDS ordination of the Sørensen distance matrix, grouped by island of origin	144
Fig. 3.19. Plot of the first two dimensions of the NMDS ordination of the Sørensen distance matrix, grouped by margin type and island of origin	145
Fig. 4.1. Average monthly salinity recorded at CRMS sites in Barataria and Caillou Bays	167
Fig. 4.2. Soil phosphorus boxplots	179
Fig. 4.3. Taxa bar plots for the full 18S sequence dataset	182
Fig. 4.4. Alpha rarefaction curves	183
Fig. 4.5. Sample-based rarefaction curves for the full metazoa dataset	184
Fig. 4.6. Sample-based rarefaction curves for samples from the different bays	185
Fig. 4.7. Sample-based rarefaction curves for samples from the different salinity zones	186
Fig. 4.8. Sample-based rarefaction curves for samples from different distances from the marsh edge	187
Fig. 4.9. Coverage-based rarefaction for the full metazoa dataset	188
Fig. 4.10. Coverage-based rarefaction for samples from different bays	189
Fig. 4.11. Coverage-based rarefaction for samples from different salinity zones	190
Fig. 4.12. Coverage-based rarefaction for samples from different distances from the marsh edge	191
Fig. 4.13. Observed OTU richness and richness estimations	193

Fig. 4.14. Taxa bar plots for the full salinity zone metazoa dataset	196
Fig. 4.15. Percentage of total OTU incidences by phylum	199
Fig. 4.16. Percentage of OTUs per phylum assignment.....	200
Fig. 4.17. The OTU richness values, divided by bay, salinity zone, and distance from marsh edge.	224
Fig. 4.18. Faith's PD values, divided by bay, salinity zone, and distance from marsh edge.	225
Fig. 4.19. Plot of the first two dimensions of the NMDS ordination of the Sørensen distance matrix, grouped by salinity zone	229
Fig. 4.20. Plot of the first two dimensions of the NMDS ordination of the Sørensen distance matrix, grouped by salinity zone and bay	230
Fig. 4.21. Plot of the first two dimensions of the NMDS ordination of the Sørensen distance matrix, grouped by salinity zone, bay, and distance from marsh edge.....	231

Abstract

Marshes in Louisiana are under threat from numerous natural and anthropogenic sources. A consequence of these threats are sheared marsh margins, which result from the impact of storm surge on previously oiled, weakened marsh. These conditions occurred in Louisiana marshes after Hurricane Isaac in 2012 followed the Deepwater Horizon oil spill in 2010, particularly in the shorelines surrounding Bay Jimmy. The second and third chapters of this thesis focus on the differences in biodiversity between the sheared and intact marsh margins in impacted sites in Bay Jimmy. Metabarcoding methods were used to determine community composition of the sediment within marsh margins to test the hypothesis that the sheared and intact margins contained different communities. In the second chapter, DNA was extracted directly from sediments, while in the third chapter, the organic portion of the sediment was extracted before DNA extraction to focus on meiofauna. Meiofauna are near-microscopic animals which are a key component of marsh health. There was a significant difference in community composition between the sheared and intact margin samples in both chapters, but the commonly detected taxa were shared between both types of margin, leaving rare unique taxa in each margin type. An advanced rate of marsh loss has been reported for Louisiana estuaries primarily due to the construction of flood control structures. Freshwater diversions of the Mississippi have been proposed to combat marsh loss by delivering sediment into marshes. However, the potential significance of changes in the salinity regime on commercially important salt marshes are unknown. The final chapter of this thesis describes a survey of meiofauna present in fresh, brackish, and salt marsh zones within Caillou and Barataria Bays in Louisiana to create an inventory of taxa which could be used as baseline for changes in salinity. Metabarcoding methods were used to determine community composition within samples from these sites. The communities from the freshwater and salt marshes separated distinctly while the brackish marsh community overlapped both of the other zones. The results suggest that the communities detected in the freshwater and salt marsh samples are potentially useful as indicators for detecting salinity regime changes.

Introduction

Tidal marshes occur throughout the world in the intertidal zones of coastlines and estuaries at temperate latitudes (Odum 1971, Chapman 1977). In North America, tidal marshes are present on both the Pacific and Atlantic coastlines: the majority of these marshes are concentrated in the Gulf of Mexico region (up to 58%). Marshes provide a number of ecological services, including acting as nursery habitat for commercially important species (Boesch and Turner 1984, Beck et al. 2001) and acting as a buffer zone against storm surge for vulnerable coastal communities (Barbier et al. 2011, Gedan et al. 2011).

Unfortunately, tidal marshes are being lost at an alarming rate, with roughly half of the coastal wetlands in the United States alone lost since 1970 due to anthropogenic activities. Marshes in Louisiana were initially built by deltaic processes of the Mississippi River (Roberts and Coleman 1996), but flood control structures have isolated the marsh from the sediment source (Blum and Roberts 2009). These marshes have lost more than 4800 km² worth of land area since the 1930's (Couvillion et al. 2017). This marsh loss is due to numerous factors, including erosion, subsidence, pollution, and hurricanes. Subsidence is a natural process which occurs as the deposited sediment compacts if the marsh is not resupplied with sediment (Kirwan and Megonigal 2013, Kirwan et al. 2016). Erosion is also a natural process, but one which has been exacerbated by canals dug throughout the marshes of Louisiana, many of them for industrial purposes (Scaife et al. 1983, Turner and McClenachan 2018). Decades of industrial exploitation in the region has also put these marshes at risk for pollution events, such as the 2010 Deepwater Horizon oil spill (DHOS), which impacted coastlines across the northern Gulf of Mexico (Michel et al. 2013). In marshes that were oiled but did not suffer immediate die-off, the belowground biomass of marsh plants was reduced resulting in weakened marsh (Lin et al. 2016, Rabalais and Turner 2016). Hurricanes and other tropical weather patterns cause storm surge and wind damage, which can cause hundreds of square meters of immediate marsh loss (Morton and Barras 2011).

The combination of weakened marsh from the DHOS and the impact of Hurricane Isaac in 2012 resulted in sheared marsh shorelines surrounding Bay Jimmy, Louisiana (Ragoonwala et al. 2016). In order to examine the impacts of the shearing of margins, the sediment invertebrate community must be studied. Broadly, the infauna (all sediment-dwelling invertebrates), and more specifically, the meiofauna (sediment-dwelling invertebrates ranging from 45 µm to 500 µm) are of interest for this study. Infauna and meiofauna are used as environmental indicators and were extensively sampled in the region to track the recovery from the DHOS (Fleeger et al. 2015, 2018, 2019). The goal of chapters 2 and 3 of this thesis was to compare the biodiversity within the sheared and intact margins of sites in Bay Jimmy to determine if shearing impacts community structure. The focus of chapter 2 was on infauna and the focus of chapter 3 was on meiofauna.

Meiofauna are difficult and time-consuming to identify to species level, even for experts. Using metabarcoding methods can circumvent the process of meiofauna identification and allow for rapid, responsive studies of meiofauna (Creer et al. 2016). Metabarcoding functions by extracting short regions of DNA from environmental samples and matching these regions against DNA databases, such as GenBank (Benson et al. 2011) or SILVA (Quast et al.

2013). Many regions of DNA, often referred to as barcodes, have been proposed for the purpose of identifying environmental samples, including 16S, 18S, COI, trnL, and ITS (Drummond et al. 2015, Ruppert et al. 2019); methods for the chapters in this thesis used regions from the 18S gene to select for eukaryotes (Creer et al. 2016, Jacquiod et al. 2016). Other regions which also select for eukaryotes, including the COI gene, may not be specific enough for a broad range of taxa to be identified (Creer et al. 2010, Deagle et al. 2014).

Louisiana has pledged \$50 billion to 79 marsh restoration and protection projects under the Coastal Protection and Restoration Authority (CPRA 2012, 2017, Peyronnin et al. 2013). Several of these projects are focused on reconnecting the Mississippi River to the marshes through diversion structures. In addition to returning the sediment supply to the marshes, these projects will also change the salinity regime of the marshes (Elsey-Quirk et al. 2019). Salinity regime changes will likely impact the marsh plant community and potentially the viability of commercial fisheries in the area (Elsey-Quirk et al. 2019). Surveillance tools for determining long term impacts of salinity on impacted areas are needed. Composition changes in invertebrate communities due to salinity regime change may occur more quickly than changes in plant communities (Bertness 1991a); meiofauna are of particular interest. The goal of chapter 4 of this thesis was to inventory meiofaunal biodiversity at marsh sites which have consistent long-term salinity values of fresh, brackish, and saltwater. These studies potentially will allow for the delineation of likely taxa that may act as bioindicators of long-term salinity regime change.

The overall goal of this study was to use metabarcoding methods to examine the soil invertebrate communities present in Louisiana marshes. The aims of the study were to elucidate the effects of marsh margin shearing and changing salinity on the infauna, and potentially allow future studies to select bioindicators associated with these impacts.

Chapter 1. Literature Review

1.1. Tidal Marshes

Tidal marshes are periodically flooded coastal grasslands primarily populated by halophyte species typically occurring in protected coastal environments (Chapman 1977). These marshes are connected to marine systems, and many are found within the lower estuarine portion of river systems. Tidal marshes are built and maintained either by tidal action redistributing marine sediments onto the marsh platform or by riverine sediment deposition during yearly flood pulses (Barbier et al. 2011). These coastal estuaries are affected by many variable abiotic factors including inundation period, salinity, and temperature, which influence the distribution of organisms which are adapted to and can survive long term in this environment. Tidal marshes are a transitional ecosystem between terrestrial or freshwater and marine environments, and as such salinity can vary from 0 ppt to 35 ppt due to saltwater inundation (Odum et al. 1984, Greenberg and Maldonado 2006). Tidal marshes can be divided into brackish and salt marsh based on the typical salinity levels (Chapman 1977). Salt marshes tend to have lower elevations and exist in the areas where tidal influence is strongest, while brackish marshes tend to have higher elevations and exist near the furthest extent of tidal influence. Plant diversity in these marshes is negatively correlated with salinity, and areas with heavy inundation tend to support near monocultures of halophyte plants such as the *Spartina* grasses or *Salicornia* succulents (Chapman 1977, Greenberg and Maldonado 2006). The salt marshes in the Gulf of Mexico and Atlantic tend to be dominated by the grass *Spartina alterniflora* Loisel, while the brackish marshes support a wider community including *Spartina patens* Aiton, the rush *Juncus roemerianus* Scheele, the graminoid *Distichlis spicata* L., the elder *Iva frutescens* L., and bulrushes in the genus *Schoenoplectus* (Greenberg and Maldonado 2006).

Unfortunately, coastal environments are in decline both globally (Barbier et al. 2011) and in North America (Kennish 2001). Louisiana marshes are among the most important coastal wetlands in the United States that contribute massively to the economy and provide a number of ecosystem services (Engle 2011), but these marshes are experiencing extreme rates of land loss. These marshes have lost an area the size of the state of Delaware since 1932 (Couvillion et al. 2017) and may lose an additional area twice this size by the year 2100 (Blum and Roberts 2009).

1.2. Marsh Ecosystem Services

Coastal marshes offer many ecosystem services to human communities (Barbier et al. 2011). Tidal marshes can serve as absorption and friction zones for storm surge and high waves during tropical weather patterns (Costanza et al. 2008, Wamsley et al. 2010), providing protection for vulnerable coastal communities (McGranahan et al. 2007). Globally, tropical weather patterns also may become more extreme and frequent in the future due to climate change, increasing the need for coastal protection (Nicholls et al. 1999). Marsh plants help to retain sediments in coastal areas both by resisting shearing with root mass (Howes et al. 2010) and by increasing soil cohesion via the addition of organic matter (Feagin et al. 2009). Preservation and creation of marshes may be key to expanding coastal defenses as the cost of creation and maintenance of coastal engineering projects increases (Temmerman et al. 2013).

Tidal marshes impact the biogeochemical cycles of carbon and nitrogen. These marshes can act as a carbon sink, through vertical accretion via burial of organic material and through the expansion of marshes (Sapkota and White 2019, Suir et al. 2019, Cragg et al. 2020). Wetlands are the largest biological component of the global carbon pool in terrestrial ecosystems, and marshes have among the fastest rates of carbon sequestration of all wetlands (Chmura et al. 2003, Bridgham et al. 2006). In addition, marshes produce a negligible amount of the greenhouse gas methane during decomposition when compared to freshwater wetlands, such as peatlands (Chmura et al. 2003). Marsh plants impact the global nitrogen cycle by facilitating denitrification microbes which promote removal of anthropogenic nitrogen from coastal waters (Hopkinson and Giblin 2008, Schutte et al. 2020). Microbial denitrification typically occurs around the rooting zone of wetland plants (Reddy et al. 1989).

Many of the organisms which are native to salt marshes are members of the food webs which support commercially important species, which makes these marshes valuable nurseries (Chesney et al. 2000). Juvenile nekton which include commercially important crabs, shrimp and finfish inhabit salt marshes at early points in the lifecycle (Beck et al. 2001). Penaeid shrimp use carbon from marsh plant sources when entering estuarine systems as larvae (Riera et al. 2000). *Spartina* plants offer shelter from predation to juvenile nekton (Boesch and Turner 1984), and marsh meiofauna act as a food source to the nekton (Coull 1990). Oyster reefs, which are frequently found in the same estuaries as marshes, are both commercially important as a food source and provide ecosystem services by filtering nutrients and creating new habitat (Coen et al. 2007, Lemasson et al. 2017). The organisms in marshes also generate value through tourism and recreation largely based on sport fishing and hunting activities (Bell 1997).

1.3. Natural and Anthropogenic Threats to Salt Marshes

Salt marshes are in decline due to a wide variety of factors. Extreme weather events such as hurricanes (Barras 2009, Palaseanu-Lovejoy et al. 2013) or droughts (McKee et al. 2004) can cause the demise of marsh plants and destruction of the structure of the marsh itself. Hurricanes are among the most damaging disturbances for any environment. Storm surge, wind shear, and wave action can be massively destructive as salt marshes absorb their impacts (Morton and Barras 2011). Hurricane damage can also leave behind shorelines which have increased erosion rates for years after the storm has passed (Deis et al. 2019). Additionally, storm surge can force saltwater inland, damaging freshwater habitats (Sasser et al. 1986). Generally speaking, shearing of marsh edges during hurricanes is more severe in freshwater marshes, but does occur in salt marshes as well (Howes et al. 2010). Climate change also threatens to increase the severity and frequency of hurricanes, potentially impacting salt marshes and other coastal environments in the future (Knutson et al. 2010).

In many places, salt marsh habitats have been reclaimed or repurposed to allow for agriculture or human development (Kennish 2001, Syvitski et al. 2009). Compaction of marsh sediments can reduce the elevation of marshes, leading to plant drowning and eventual marsh death (Yuill et al. 2009, Couvillion et al. 2017). Erosion due to channelization of marshes can cause losses in plants by undercutting banks and increasing stress on plants (Nyman et al. 1994, Turner and McClenachan 2018). Relative sea level rise (due to mean sea level rise as a part of global climate change) threatens to drown marshes by outpacing vertical accretion of the

marsh (Mendelssohn and McKee 1988, Jankowski et al. 2017), but most marshes are able to maintain high rates of vertical accretion (Kirwan et al. 2016). However, to keep pace with relative sea level rise and maintain integrity, marshes must be able to horizontally expand in the landward direction, which may cause issues in areas where marshes and human habitations co-exist (Field et al. 2016, Roman 2017). In addition, some marshes which are dependent on sediment inputs have been cut off due to extensive flood protection projects (Elsey-Quirk et al. 2019). Subsurface fluid extraction, such as for groundwater or oil, can result in subsidence which drowns marshes (Kennish 2001, Kolker et al. 2011). Oil spills can damage marshes through plant death from direct toxicity and through lingering toxic effects (Solomon et al. 2009, Lin and Mendelssohn 2012, Michel et al. 2013).

Oil spills can be deadly to flora and fauna from any ecosystem and leave long lasting impacts detectable decades later (Fleeger and Chandler 1983, DeLaune et al. 1984, Smith et al. 1984, Lin and Mendelssohn 1996). Marine and coastal ecosystems are especially at risk of oil pollution due to offshore oil production and marine oil transport (Teal and Howarth 1984). Recovery and environmental assessment efforts following major spills are unfortunately plagued by a lack of long-term baseline data on populations of organisms in affected ecosystems.

On September 16, 1969, the barge Florida ran aground near West Falmouth, Massachusetts, spilling 630 tons of No. 2 fuel oil into the bay (Teal and Howarth 1984). The next day, a storm caused the oil to mix into sediments and water. This mixing process created a water-oil emulsion and rapidly increased the rate of distribution of the oil into sediments and the water column, eventually oiling four miles of the primarily marsh coastline of Wild Harbor, nearby the wreck. Immediate effects included a near total kill of Sicrobenthic organisms and *Spartina* grasses in heavily oiled sites, as well as mass deaths of clams and fish in Wild Harbor (Souza 1970, Burns and Teal 1979). *Capitella* polychaetes, which are indicators of pollution, were found to dominate sediments over the next few months, while *Mytillus edulis* mussels in the area were found to be reproductively inactive over the next year (Sanders et al. 1980). Nearly two decades after the spill, trace amounts of hydrocarbons linked to the spill were still being found in crabs and sediments in the marshes of Wild Harbor (Teal et al. 1992). In 2005, a reduction in both above and belowground biomass of *Spartina* grasses was detected in association with elevated hydrocarbon residues in the soil at sites that were oiled in Wild Harbor over 35 years previously (Culbertson, Valiela, Pickart, et al. 2008). Fiddler crabs from previously oiled sites dug shallower burrows and showed slower escape responses than fiddler crabs from reference marshes (Culbertson et al. 2007). *Geukensia* mussels showed slowed growth and reproductive rates when transplanted into previously oiled sites from reference marshes (Culbertson, Valiela, Olsen, et al. 2008).

On December 15, 1976, the Argo Merchant tanker ran aground 29 nautical miles southeast of Nantucket Island, Massachusetts (Grose and Mattson 1977). Six days later this tanker broke in half under gale force wind conditions, spilling its cargo of 7 million gallons of No. 6 fuel oil into the Atlantic Ocean. No dispersants were used during this spill, and the majority of the oil stayed at the surface of the ocean, floating to the east of the spill site into open water (Teal and Howarth 1984). Benthic sediment contamination was discovered in the

area surrounding the wreck and may have extended to an area as large as 15 km². Fuel oil contamination was detected in zooplankton, fish, and shellfish populations in the spill area (Grose and Mattson 1977, Polak et al. 1978). Pollock and cod eggs suffered increased mortality with proximity to the spill site (Grose and Mattson 1977). Long term effects from this spill are undescribed ; but approximately seven months after the spill, benthic sediments and organisms were found to contain no petroleum hydrocarbons, excluding sediments from near the bow of the shipwreck (Hoffman and Quinn 1980). Contamination in sediments was either released into the water column leading to biodegradation or evaporation, or due to the mixing forces of the tides in Nantucket sound was buried or transported.

On June 3, 1979, the Ixtoc I oil well in the Bay of Campeche, Mexico underwent a catastrophic blow out, resulting in 3.4 million barrels of crude oil spilled over the next ten months (Soto et al. 2014). The circulation patterns of the southern Gulf of Mexico would carry some of the spilled oil to the Mexico and Texas coastlines, impacting a number of different tropical and subtropical coastal ecosystems (Jernelov and Linden 1981). The impacted ecosystems included sandy beaches, barrier islands, and the marshes and mud flats of coastal lagoons. Dispersants were sprayed at the surface, burning was applied at the well site, booms were used to protect the coastline, and mechanical recovery was applied at beaches (Jernelov and Linden 1981). Populations of benthic infauna in the intertidal and subtidal zones of the south Texas coast showed a reduction following oiling, but it was unclear whether this was the result of oiling or cleanup procedures enacted in the area (Thebeau et al. 1981). Hatchlings of Kemp's Ridley sea turtles, an endangered species which primarily nests within the Gulf of Mexico, were evacuated from monitored conservation beaches in Tamaulipas, Mexico, to offshore waters in order protect them from oiled beach sediments and nearshore waters (Fritts and McGehee 1982). Unusually large phytoplankton blooms were reported in the offshore region, possibly due to eutrophication or reduction zooplankton populations (Jernelov and Linden 1981). Over the next year, hydrocarbon signatures matching to Ixtoc I oil signatures were discovered in sediments and oysters (*Crassostrea virginica*) in the lagoons near Tabasco, Mexico (Botello et al. 1983). Ixtoc I oil, in combination with overexploitation, climate change, and hypoxia, may have reduced fish biodiversity and total biomass in the Bay of Campeche region over the long term (Soto et al. 2014). Similarly, the penaeid shrimp populations of the area have been in a declining trend since the late 1970's, possibly due to long term benthic contamination from the Ixtoc I spill (Soto et al. 2014). However, poor baseline data available before the incident prevent strong conclusions about long term declines related to the Ixtoc I spill from being drawn.

On March 24, 1989, the Exxon Valdez tanker struck the Bligh Reef in Prince William Sound. Approximately 10.8 million gallons of crude oil were spilled, eventually resulting in more than 2000 km of oiled coastline in Prince William Sound and the Gulf of Alaska (Neff et al. 1995, Paine et al. 1996). The immediate death toll on sea birds, marine mammals, fish, and invertebrates was massive (Shigenaka 2014). Despite the massive clean-up efforts launched, including application of dispersant, on site burning, booming, and aggressive shoreline cleaning, only 10% of the spilled oil was recovered or disposed of (Wolfe et al. 1994). The remaining 90% of the oil was naturally weathered or degraded. Unfortunately, the weathering process was slow due to low temperatures inhibiting biological breakdown of oil and a reduction in

weathering rates over time due to sequestration and physical burial (Hayes and Michel 1999). Chronic exposure to oil in sediments remained a source of mortality in fishes, sea ducks, and sea otters for years after the spill (Peterson et al. 2003). Small pockets of lingering oil from the Exxon Valdez spill were still being found on shorelines nearly 25 years after the spill (Shigenaka 2014). Indirect effects of the spill included trophic cascades due to losses of keystone predators such as sea otters and losses of habitat providing species such as the rockweed *Fucus gardneri* (Peterson et al. 2003). Again, baseline data on most species were lacking for this spill, but previous data on orcas allowed for the discovery of a major population decline and lack of recruitment in the two pods which inhabit Prince William Sound (Shigenaka 2014). Many of the sea birds, fishes, marine mammals, and marine invertebrates took decades to reach a recovered status, and some species still have not recovered (Barron et al. 2020).

On April 20, 2010, the Deepwater Horizon drilling rig exploded, resulting in an oil leak at the wellhead. This would result in nearly 4.9 million barrels of crude oil released into the Gulf of Mexico before the well was sealed 87 days later. Chemical dispersants were applied both at the wellhead and to surface oil, resulting in plumes of hydrocarbon contaminated water in the deep Gulf of Mexico (Beyer et al. 2016). The Deepwater Horizon oil spill (DHOS) was the worst marine oil spill in history in terms of volume spilled, and due to the location of the well, multiple distinct marine and coastal ecosystems were impacted. Nearly 2100 km of shoreline across the northern Gulf of Mexico was oiled including nearly 700 km of marsh shoreline (Michel et al. 2013). The majority of oiled marsh habitat was located in Louisiana, with the Barataria Bay area being oiled especially heavily (Michel et al. 2013). Heavily oiled marsh sites experienced rapid plant dieback, while a reduction in the photosynthetic rate of marsh plants was associated with plants at moderately oiled sites (Lin and Mendelssohn 2012). Long term effects on the marsh soil remained after the apparent recovery of most taxa, including a reduction of belowground biomass of marsh plants (Lin and Mendelssohn 2012). The reduction in belowground biomass led to a weakening of the strength of the marsh soil, causing enhanced erosion in heavily oiled areas (Silliman et al. 2012, McClenachan et al. 2013). Following Hurricane Isaac in 2012, marsh edge shearing was observed in areas that were previously heavily oiled during the DHOS, showing the compounding effects of multiple disturbances on the marsh (Ragoonwala et al. 2016). Biodegradation activity of polycyclic aromatic hydrocarbons and other hydrocarbons by the bacterial community was discovered in sediments across the northern Gulf of Mexico, with associated changes in bacterial composition (Atlas et al. 2015). A rapid, drastic change from metazoan dominated sediments to fungal dominated sediments was observed in the eukaryotic community of northern Gulf of Mexico shorelines using metabarcoding techniques following oiling (Bik et al. 2012). In addition, a morphological approach revealed a loss in the richness and diversity of nematodes present following oiling of sediments, with a shift of nematode genera to favor those with predatory and scavenging feeding strategies. The change in metazoan dominance to fungal dominance was reversed by one year after the spill in sites from Mobile Bay and Dauphin Island (Brannock et al. 2014). The density and community composition of salt marsh infauna and meiofauna populations was reduced following the spill, with distinct stages of recovery observed in heavily oiled sites compared to reference sites (Fleeger et al. 2015, 2018, 2019, 2020). The first stage of this recovery included the return of nematodes, copepods, and most annelids to the oiled sites

within 3 years (Fleeger et al. 2015). Following this, amphipods and juvenile bivalves approached reference densities at oil sites within 6 years (Fleeger et al. 2018). Finally, a group of specific taxa had not returned to reference densities in the oiled sites within 6 years. This group included the annelid *Manayunkia aestuarina*, the tanaid *Hargeria rapax*, the kinorhynch *Echinoderes coulli*, and ostracods (Fleeger et al. 2019, 2020). These taxa were found to be primarily associated with the reference locations which had higher belowground biomass and low total petroleum hydrocarbons, although these two factors can be inversely related to each other (Fleeger et al. 2019). The larvae of the horse fly *Tabanus nigrovittatus*, are key invertebrate predators in marsh soils, and the adult females are considered to be pests due to their blood-feeding. Following the spill, populations of both adult and larval *T. nigrovittatus* underwent a crash and genetic bottlenecks also were demonstrated. (Husseneder et al. 2016). This crash and bottlenecks of the population of adult horse flies was reversed at least partially by migration of individuals from non-oiled areas within six years (Husseneder et al. 2018). A failure in oyster (*Crassostrea virginica*) recruitment was observed in areas such as Barataria Bay, Black Bay, Breton Sound, and Mississippi Sound several years after the spill, though this effect was compounded by the release of freshwater in these areas (Barron et al. 2020). Several species of commercially important fish, including the Gulf menhaden, *Brevoortia patronus*, were found to have elevated concentrations of polycyclic aromatic hydrocarbons (Xia et al. 2012, Olson et al. 2016). Terrestrial birds, such as the seaside sparrow *Ammodramus maritimus*, were found to have incorporated oil via the food web which supports them (Bonisoli-Alquati et al. 2016). Estimations of sea bird deaths due to oiling exceeded half a million individuals (Haney et al. 2014), alongside an observed increase in sea turtle and marine mammal mortality (Antonio et al. 2011). Again, previously established baseline populations of organisms were lacking, limiting the conclusions that could be drawn about recovery trajectories despite the massive amount of research conducted.

1.4. Proposed solutions to combat global salt marsh losses

Actions that have been proposed to combat salt marsh loss are most frequently specific to the causes. In systems where the sediment source has been cut off due to human intervention, restoring the sediment source can help to reverse marsh loss. By reconnecting reclaimed marshes to the tidal redistribution of sediment, some marshes can be rebuilt with minimal human effort (Broome et al. 1988, Faber 2001, Warren et al. 2002, Teal and Weishar 2005, Wolters et al. 2005, Orescanin et al. 2018). In river dominated systems which have been cut off due to flood protection measures, sediment diversions can restore natural sediment inputs to marshes and create new land (Kearney et al. 2011, Elsey-Quirk et al. 2019). Sediment subsidy is another marsh restoration solution where sediment is directly added to marshes to induce vertical accretion and restore ecological function to submerged or subsiding marshes (Stagg and Mendelssohn 2010, Thorne et al. 2019). However, sediment subsidy must strike a delicate balance, as adding too much sediment to a marsh can bury it and impair ecological function. Another action to supplement sediment accretion in marshes is replanting, which can allow for enhanced trapping of sediment and recovery even after disturbances such as oil spills (Broome et al. 1988, Gundlach et al. 2003).

1.5. Louisiana specific issues

The marshes in Louisiana are estuarine in nature, and were built by yearly flood pulses of the Mississippi River over thousands of years (Russell 1940). However, marshes have been largely cut off from this sediment source because of manmade flood control structures along the Mississippi. Without the sediment input from the river, the redistribution of sediment caused by tides and by periodical tropical weather systems has been the only way that sediments have been moved onto marshes (Morton and Barras 2011). Tides in the northern Gulf of Mexico tend to have both a lower range (<0.5m) and frequency than other systems (diurnal), so tidal redistribution of sediments onto the marsh platform is lower in Gulf tidal marshes than in Atlantic marshes. Vertical accretion through organic material rather than through sediment is the primary way which Louisiana marshes build (Turner et al. 2005, Jankowski et al. 2017), resulting in marshes which are dependent on plant growth. Settlement of the sediment in much of Louisiana is occurring due to the recent (geologically speaking) deposition of the land, leading to subsidence in marshes (Jankowski et al. 2017). Louisiana marshes have been heavily modified by the oil and gas industry, leading to widespread dredging of canals with associated erosion (Day et al. 2000, Turner and McClenachan 2018). Historic extraction of oil and gas from Louisiana marshes also contributed to subsidence (Kolker et al. 2011). Louisiana has been subjected to hurricanes originating in the Gulf and Atlantic systems, leading to erosion from storm surge and loss of inland freshwater wetland due to saltwater intrusion (Sasser et al. 1986, Holm and Sasser 2001, Deis et al. 2019). All of these factors contributed to the loss of land across the system (Couvillion et al. 2017).

1.6. Proposed solutions to Louisiana issues

The Coastal Restoration and Protection Agency developed the Louisiana Coastal Master Plan in 2012 with a funding level of \$50 billion specifically focused on flood risk reduction and resilience of coastal communities in Louisiana during the subsequent 50 years (CPRA 2007, 2012, 2017, Peyronnin et al. 2013). The largest projects within the Coastal Master Plan revolve around reconnecting the Mississippi River to the marshes of Louisiana via sediment and freshwater diversions to the marshes that are currently isolated from the river due to flood control structures such as levees built during the previous century. Reconnecting the Mississippi River with the marshes would result in the addition of sediment to marshes and potentially increase the ability of marshes to accrete vertically. Despite the benefits to marshes, there will be many changes associated with an abrupt change in salinity. The vegetation types in Louisiana marshes are governed primarily by salinity, falling into three zones with increasing salinity: intermediate, brackish, and saline (Penfound and Hathaway 1938, Chabreck 1970, 1972); rapid salinity changes will change the distribution of marsh plants. Furthermore, intermediate marshes in Louisiana have a structurally weak zone in the soil due to the relatively shallow rooting depth of low salinity wetland plants (Howes et al. 2010), which can mean greater marsh edge shear during tropical weather patterns. Salinity also controls the distribution and density of numerous estuarine benthic infauna (Boesch et al. 1976). Meiofauna specifically are known to increase in density in salt marshes as salinity increases due to the invasion of marine species (Montagna and Kalke 1992). Commercial shrimp and crab production also may be affected by these changes, as prey and refuge areas change (Posey et

al. 2005, Rozas and Minello 2011). Baseline data on marsh communities are needed for future studies of community will changes in response to salinity and other environmental changes.

Baseline data on many species in the northern Gulf of Mexico were lacking following the DHOS. In an ideal situation, baseline data would be derived from long-term sampling programs of organisms in the areas where oiling could occur which would allow robust comparisons of healthy unoiled populations and the impacted oiled populations. Of course, continuous long term-data was unavailable for most studies following the DHOS. The solution to this issue was generally to sample nearby, unoiled reference sites or unaffected populations for comparisons, or to collect as many data points as possible after the spill occurred but before the oil reached sites. Of the numerous organisms present in these ecosystems, the commercially important species are probably the most well-known in terms of continuous long-term data. The Louisiana Department of Wildlife and Fisheries (LDWF) maintains stock assessments of major commercially and recreationally exploited species (Louisiana Department of Wildlife and Fisheries 2019), including black drum (*Pogonias cromis*), red drum (*Sciaenops ocellatus*), sheepshead (*Archosargus probatocephalus*), southern flounder (*Paralichthys lethostigma*), spotted seatrout (*Cynoscion nebulosus*), striped mullet (*Mugil cephalus*), blue crab (*Callinectes sapidus*), oyster (*C. virginica*) and the three species of penaeid shrimp which are commercially exploited in Louisiana: the white shrimp (*Litopenaeus setiferus*), the brown shrimp (*Farfantepenaeus aztecus*), and the seabob shrimp (*Xiphopenaeus kroyeri*). The National Oceanographic and Atmospheric Administration (NOAA) maintains stock assessments of marine mammals through stranding reports and radio tagging programs (Hayes et al. 2019). Terrestrial and benthic invertebrates have been well studied in marshes, but no coordinated long-term sampling programs were in place for these organisms when the DHOS occurred. Aker (2020) conducted a year-long sampling of insects using sweep-net techniques in intermediate, brackish, and saline tidal marshes in Louisiana to establish baseline population data and determine indicator taxa for the different marsh types. Indicator insects for intermediate marshes included members of the families Buprestidae, Cicadellidae, Coenagrionidae, Chironomidae, Derbidae, Coccinellidae, Clastopteridae, and Ceratopogonidae. Indicator insects for intermediate and brackish marshes included additional members of the Chironomidae and Buprestidae. Indicators of the brackish marshes included species from the families Phlaeothripidae, Ceratopogonidae, Cicadellidae, and Issidae. Indicators insects of the brackish and saline marshes included Mirids, Ulidiids, Ceratopogonids, and Clerids. Finally, indicators of the saline marsh included members of the Ulidiidae, Blissidae, Mordellidae, and Melyridae.

Soil meiofauna and macrofauna (collectively, infauna) have been studied for decades in marshes as indicators of health and recovery, and inventories are relatively complete for major taxa at the phylum level. In Gulf and Atlantic marsh systems, nematodes dominate the meiofauna, comprising as much as 89% of the individuals in samples (Bell 1979, Fleeger 1985). Copepods, typically harpacticoid copepods, are the next most abundant group, and may comprise as much as 15% of individuals. Polychaetes and oligochaetes are also commonly collected from marsh sites. Kinorhynchs, platyhelminthes, bryozoans, ostracods, juvenile amphipods, insect larvae, and mites are more rarely detected. Common macrofauna include polychaetes, oligochaetes, amphipods, ostracods, and hydrobiid snails (Kneib 1984). However, inventories of meiofauna or macrofauna over large geographic scales tend to be less common,

especially due to the effort required for meiofaunal identification. In addition, these studies tend to only identify meiofauna to major taxonomic levels, such as phylum, instead of species, so knowledge of species distributions is quite limited.

1.7. Meiofauna as a measure of marsh health and recovery

Infauna are a group of highly diverse sediment dwelling taxa found globally and are united solely by habitat rather than phylogenetic grouping. Infauna are generally split into two groups by size, the macrofauna and the meiofauna. Macrofauna are generally any soil dwelling taxa which are larger in size than 500µm, while meiofauna are taxa that range from 500µm to 45µm (Mare 1942, Coull and Chandler 2001, Giere 2009). Increases in the biodiversity of meiofauna have been linked to the ecological functions and efficiency of ecosystems by increasing the number of functional traits present in the ecosystem (Snelgrove 1997, Danovaro et al. 2008). Meiofauna are important prey items for commercial species and act as a link between the microbial and macrofaunal food webs (Bell 1980, Gee 1989, Coull 1990, Fantle et al. 1999). These meiofauna are often used as bioindicators in marshes, especially with regards to pollution responses (Fleeger and Chandler 1983, Semprucci et al. 2015, Fleeger et al. 2018). Nematodes, which tend to be more tolerant of pollution and disturbance, are often the first group of meiofauna to return to habitats after disturbance (Sherman and Coull 1980, Alves et al. 2013, Fleeger et al. 2015). Other groups of meiofauna return more slowly after disturbances, which makes them better for tracking long term effects and recovery. In particular, taxa which lack a pelagic larvae, such as the annelid *Manayunkia aestuarina* and oligochaetes, may take years to decades to return to disturbed sites (Craft and Sacco 2003, Fleeger et al. 2018). Meiofauna have been studied in both Gulf and Atlantic coastal marshes (Bell 1979, Coull and Bell 1979, Fleeger 1985), but meiofauna are poorly known at the species level (Snelgrove 1997). For nematodes alone, total species estimations range from 100 thousand to 1 million, but the current total number of described species is approximately 27 thousand (Coomans 2000, Hugot et al. 2001). The primary reason why meiofauna diversity is poorly known is due to how difficult they are to study. Due to their small size, meiofauna cannot be identified down to lower taxonomic levels without the use of a high magnification microscope and observation of complex morphological characters. In addition, the taxonomic experience gap is widening as experts retire and their positions are not replaced. Because of these difficulties, many studies are turning to DNA metabarcoding for rapid, cost-effective identification of meiofauna (Bik et al. 2012, Brannock and Halanach 2015, Creer et al. 2016).

1.8. DNA metabarcoding and associated analyses

DNA barcoding refers to the use of highly conserved segments of DNA with variable regions as “barcodes” to identify species or broader taxonomic groups without the need to sequence the organism’s entire genome (Arnot et al. 1993, Hebert et al. 2003). Several regions of the genome of eukaryotes have been proposed as barcoding targets, including the mitochondrial COX1 region and ribosomal 18S regions (Folmer et al. 1994, Creer et al. 2010, Jacquiod et al. 2016). The application of DNA barcoding to bulk environmental samples to determine species composition without using traditional identification methods is referred to as DNA metabarcoding (Creer et al. 2016). Metabarcoding has tremendous implications for environmental studies. As the cost of sequencing DNA has gone down with the advent of next

generation sequencing, these methods have been widely applied to various environments for a variety of purposes (Caporaso et al. 2012). Many metabarcoding studies have focused on the prokaryotic portion of the microbiome, but studies of eukaryote microbiomes are becoming more commonplace. Many metabarcoding studies focus on difficult to identify groups, such as flagellated soil eukaryotes (Venter et al. 2018), nematodes (Waeyenberge et al. 2019), or zooplankton (Schroeder et al. 2019). A number of studies are using environmental DNA (i.e. samples which do not isolate any target organisms but contain traces of DNA) to map invasive species (Deiner et al. 2017, Mychek-Londer et al. 2019, Ruppert et al. 2019). Bik et al. (2012) found that major shifts in eukaryote biodiversity in sediments occurred after oiling associated with the DHOS by using metabarcoding methods, including a shift from metazoan dominated samples to fungus dominated samples, though these shifts were short lived (Brannock et al. 2014). Bhalerao (2018) used taxa in the guts of tabanid larvae and surrounding marsh sediment discovered by metabarcoding methods to discover what portions of the meiofaunal food web support the larvae in oiled and unoiled sites. In addition, the groups Liliopsida, Maxillopoda, and Cyrtolophosidida had higher relative abundances in western Louisiana sites compared to eastern Louisiana sites, while the groups Alveolata and Rhizaria had higher relative abundances in the eastern sites compared to the western sites.

Despite the potential, metabarcoding methods are not without issues. Environmental sampling, DNA extraction, amplification, and sequencing can all introduce biases in biodiversity if not conducted properly (Leasi et al. 2018, Zinger et al. 2019). The datasets produced by metabarcoding are sparse (i.e., full of zeroes), high-dimensional, and compositional, which can cause issues with analysis and interpretation (Weiss et al. 2017). To deal with these issues, numerous specialized software programs have been developed. QIIME 2 is a microbiome bioinformatics platform which supports numerous methods for the analysis of sequencing data (Bolyen et al. 2019). This program allows for the input of raw sequencing data, the manipulation of that data, and the output of many different kinds of descriptive data, including tables of operational taxonomic units (OTUs) by sample, numerous biodiversity metrics, and multivariate analyses and ordinations. An OTU is defined as a cluster of sequences which all share a selected level of similarity (frequently 97%) and are treated as one unit as a stand-in for traditional species (Blaxter et al. 2005, Callahan et al. 2017). One of the methods packaged into the base QIIME 2 distribution is the DADA2 algorithm, which allows for quality control of sequencing data (Callahan et al. 2016). The primary method of taxonomic identification of OTUs is through an algorithm, such as the Basic Local Alignment Search Tool (BLAST+) (Camacho et al. 2009), matching the sequence of the OTU to a database of sequences. Numerous nucleotide databases with taxonomic assignments have been developed, such as SILVA (Quast et al. 2013) or GenBank (Benson et al. 2011). These databases are currently nowhere near complete databases of sequences for all life, but they continuously improve with the collection and submission of additional data through efforts of numerous research groups. As time passes, the insights to be gained from metabarcoding data will increase because database coverage will increase, allowing for more accurate taxonomic assignments. Following the generation of taxonomic identities for OTUs, a wide variety of biodiversity analyses can be applied to draw conclusions about different communities (Gotelli and Colwell 2001, Creer et al. 2016).

Chapter 2. A Comparison of Intertidal Metazoan Infauna Biodiversity between Previously Oiled Sheared and Intact Marsh Margins in Bay Jimmy, Louisiana, Using DNA Extraction of Whole Sediments

2.1. Introduction

Salt marshes are unique ecosystems that provide a number of important services such as acting as nursery grounds for commercially and recreationally important species (Zimmerman et al. 2002, Engle 2011). Wave attenuation properties of marshes protect inland human and wildlife communities from storm surge during hurricanes and other tropical weather systems (Möller and Spencer 2002, Tonelli et al. 2010). The carbon sequestration and storage abilities of salt marshes also make them valuable habitats for mitigation of carbon emissions (Chmura et al. 2003, Kirwan and Mudd 2012). Furthermore, salt marsh plants serve as important facilitators of denitrification microbes in coastal sediments (Hinshaw et al. 2017a).

In spite of the many benefits provided to humans, salt marsh ecosystems across the globe are in peril due to a wide variety of threats which are primarily anthropogenic in nature (Barbier et al. 2011). Oil and gas exploration alongside groundwater withdrawal can cause subsidence and inundation in marshes (Couvillion et al. 2017). Land reclamation for both human settlement and agriculture can replace land that was formerly salt marsh. Climate change induced sea-level rise is on track to outpace vertical marsh accretion of sediment and organic matter in some areas within the next century (Jankowski et al. 2017). The same hurricanes that marshes protect inland settlements from can rapidly accelerate marsh erosion (Palaseanu-Lovejoy et al. 2013, Deis et al. 2019). In addition, climate change stands to make hurricane events more frequent and extreme (Knutson et al. 2010).

During the past century, more than half of the area of all North American tidal salt marshes has been lost (Kennish 2001). Louisiana salt marshes make up nearly thirty percent of the coastal estuarine wetlands of the United States and are home to some of the most productive fisheries in the United States (Engle 2011). One quarter of Louisiana's wetland area was lost (approximately 4,833 km², an area nearly the size of Delaware) during the period from 1932 to 2016 (Couvillion et al. 2017). The Barataria Bay basin, the location of this study, lost the second most land area (approximately 1,120 km²) of all of the coastal basins of Louisiana during this same time period. These losses are due to numerous factors, including hurricanes, flood protection measures for local communities, sediment compaction, and oil exploration. Hurricanes can directly damage marshes through wind shear and storm surge, but may also deliver saltwater to freshwater marshes, causing additional damage (Palaseanu-Lovejoy et al. 2013). The marshes of Louisiana are dependent on the Mississippi River for sediment input, but the river has been thoroughly leveed to protect local communities from yearly floodwaters, limiting sediment inputs severely (Elsey-Quirk et al. 2019). The marshes of Louisiana were deposited by the Mississippi River geologically recently, since the beginning of the Holocene period approximately 10,000 years ago, and in some areas are still compacting, leading to subsidence (Meckel et al. 2006). Historic oil exploration in Louisiana marshes has also enhanced subsidence by removing subsurface fluids (Yuill et al. 2009). In addition, navigation channels cut

for marsh access largely for oil exploration have contributed to erosion in the region (Scaife et al. 1983, Turner and McClenachan 2018). Finally, oil associated with the 2010 Deepwater Horizon Oil Spill (DHOS) swept ashore in Louisiana marshes, causing large-scale marsh shoreline retreat due to plant dieback among many other effects (Rabalais and Turner 2016).

During the storm surge and high winds associated with hurricanes, marsh margins can be ripped away in an erosional process known as margin shearing. This process has been observed in Louisiana wetlands previously, and it is an effect of the damage occurring from hurricanes (Morton and Barras 2011). In Louisiana, marsh margin shearing has historically been greatest in brackish and fresh water marshes, which have lower soil tensile strength than salt marshes (Howes et al. 2010). Shearing leads to higher rates of erosion due to loss of the marsh grasses' roots which hold together the sediment. Salt marshes were less affected by shearing during events like Hurricane Katrina when compared to fresher, more inland marshes. However, the oiling associated with the DHOS in the Gulf of Mexico reduced belowground root biomass in affected salt marshes, lowering the tensile strength of the marsh and leaving it open to future shearing events (Lin and Mendelssohn 2012, McClenachan et al. 2013, Lin et al. 2016). The weakened salt marsh margins were then impacted by Hurricane Isaac in 2012, and shearing was detected via satellite analysis in Bay Jimmy, a heavily oiled marsh site (Michel et al. 2013, Ragoonwala et al. 2016).

Marshes are complex ecosystems due to the interaction of many factors including hydrology, geology, and environmental stressors, and there are many biological indicators of marsh health. A massive amount of research has been conducted in an attempt to understand how marshes are impacted by and recover from disturbances such as hurricanes and oil spills (Morton and Barras 2011, Deis et al. 2019, Hanley et al. 2020). A wide variety of studies were conducted in Gulf Coast marshes to determine impacts on and track recovery of marshes specifically following the DHOS. For example, studies documented the fate of oil (Turner et al. 2019), the role of bacteria in degrading oil and changes in the bacterial community (Beazley et al. 2012, Kimes et al. 2014, Zhang et al. 2018) as well as impact of oil on health and recovery of marsh plants (Lin and Mendelssohn 2012, Rabalais and Turner 2016). Species-level studies focused mostly on oil related decline and recovery of commercially important species (Fry and Anderson 2014, Grey et al. 2015, Beyer et al. 2016). In addition, invertebrate species native to the marsh such as horse flies were investigated as bioindicators of marsh health (Husseneder et al. 2016, 2018). Impact of oil at the community-level was documented by studies of eukaryote community (Bik et al. 2012), and infauna population changes (Brannock et al. 2014, Fleeger et al. 2015, 2018, 2019, 2020). Infauna abundance and diversity can be strong measures of the recovery and restoration of function of the marsh platform (Craft and Sacco 2003).

Soil infauna are a group of sediment dwelling invertebrates which show long-term responses to a wide variety of environmental stressors, including oiling (Fleeger and Chandler 1983). Infauna include phylogenetically diverse invertebrate organisms ranging from polychaete worms to nematodes and kinorhynchs to crustaceans. This group ranges widely in size, from near microscopic (such as nematodes) to those easily observed with the naked eye (such as fiddler crabs). Nematode populations in particular show functional and taxonomic differences reflecting local environmental factors, such as salinity and sediment grain size (Alves et al.

2013). The abundance and diversity of infauna are important to the food web of the marsh because they frequently occupy the niche of primary consumer (McClelland and Valiela 1998). The near microscopic portion of this community can serve as the linkage between the micro and the macro food webs, serving as prey for commercially important species (Tito de Moraes and Bodiou 1984, Gee 1989, Fantle et al. 1999, Hewitt et al. 2020). Following the DHOS, infauna abundance and diversity at moderately and heavily oiled sites in Barataria Bay which were reduced by oiling have largely recovered following the recovery of marsh plants, with exceptions of particular taxa, following previously observed trends of infauna recovery (Fleeger and Chandler 1983, Carman and Todaro 1996, Fleeger et al. 2015, 2018, 2019, 2020).

Since sheared sites erode at a more rapid rate than the surrounding marsh (Ragoonwala et al. 2016), it is important to understand what happens to the infauna communities in this environment. Previous plant removal manipulation experiments in salt marshes showed a reduction in species richness of infauna and changes in the densities of different taxa in the plant removal sites versus control sites (Whitcraft and Levin 2007). Previous studies of infauna in and around Bay Jimmy were conducted to determine if the populations had recovered following the DHOS (Fleeger et al. 2015, 2018), so the composition of the local infauna is well known. However, their study did not examine sheared sites in the area. Since sheared sites erode faster and lack live plants, they should have reduced infauna biodiversity when compared to intact sites.

Infauna communities are difficult to study because of the miniscule scale of some of the organisms and the time-consuming nature of identification. Identification of these organisms to a taxonomic level lower than order using traditional taxonomic methods also frequently requires considerable technical expertise. Alternatively, some studies of infauna have used metabarcoding as an identification tool (Bik et al. 2012, Brannock and Halanych 2015, Creer et al. 2016, Ruppert et al. 2019). Metabarcoding methods allow for the rapid assessment of biodiversity of understudied or difficult to identify groups such as bacteria, soil eukaryotes, fungi, or infauna. Metabarcoding functions by extracting and amplifying marker gene sequences from environmental samples, which can be used to separate taxa based upon previously reported marker gene sequences for different taxa. A number of different marker genes have been proposed for metabarcoding, but this study uses the 18S small ribosomal subunit gene as it selects for eukaryotes (Creer et al. 2016, Jacquiod et al. 2016). These techniques make it possible to study large numbers of diverse infauna samples in a more reasonable amount of time. The purpose of this study was to compare infauna communities in sediment samples collected from sheared and intact margins of the 3 different islands in Bay Jimmy to determine if sheared and intact sites support different communities.

2.2. Materials and Methods

Site determination:

Sample collection sites for this study were selected using previous shoreline satellite analysis (Ragoonwala et al. 2016). The shorelines of three marsh islands in Barataria Bay surrounding Bay Jimmy designated as “Dragon Island,” “Stingray Island,” and “Horseshoe Island” were the study locations. The three islands have been fully separated since at least the

early 1980's, with Dragon Island being separate from the others since the earliest available aerial photography of the area from 1956 (aerial photography single frame and Landsat 4-5 TM C1 Level-2 images courtesy of the U. S. Geological Survey). The southward facing portions of these shorelines experienced heavy oiling associated with the DHOS (Michel et al. 2013) and the shores of Dragon Island were heavily sampled for infauna as part of a long term study to track recovery from oiling (Fleeger et al. 2018, 2019). Following Hurricane Isaac in 2012, severe shoreline retreat due to shearing was detected (Ragoonwala et al. 2016). Sheared margins were still visible in 2017 (Fig. 2.1), when sampling for this study was conducted. Two sites per island, each with a visible sheared margin and nearby intact margins, were selected for investigation.

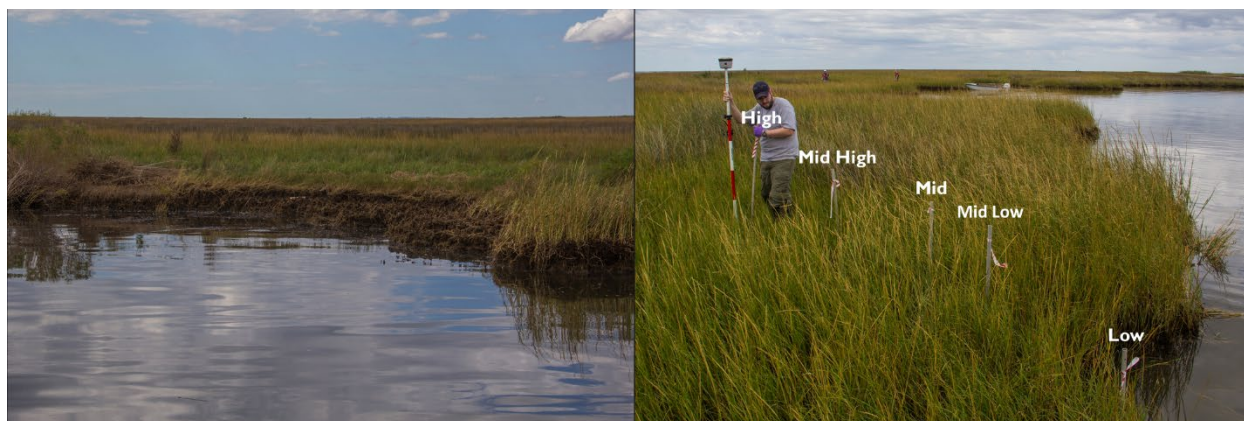


Fig. 2.1. Sheared and intact margins photo comparison. Left: a sheared margin site. Right: an intact margin site with a sample transect; each PVC pole depicts the site where one sample was taken, starting at the low sample at the water's edge and moving upwards in elevation to the high sample (Photographer: Claudia Husseneder).

Sample collection:

At each site, two sample transects were collected; one was within the sheared margin and the other was nearby in an intact portion of the marsh shoreline. For each transect, five samples were taken beginning at the water's edge and moving inward. A Trimble R2 GPS (Trimble, Sunnydale, California) was used to measure the elevation for each transect using the Height Above Ellipsoid (HAE) model. The ellipsoid of the HAE model refers to a theoretical model of the surface of the planet which is used to calculate elevations in a consistent manner even in areas where mean sea level is not available. Every time the elevation increased by 0.05m, another sample was taken until 5 cores total were collected. The samples were labeled as "Low", "MidLow", "Mid", "MidHigh", and "High" in order of ascending elevation for each transect. These cores were labelled by margin status and transect position. The average total transect distance (from the "Low" sample to the "High") was 7.57m.

Samples were collected using two methods. Initially, a 5.08 cm diameter 30.48 cm long PVC tube was used to collect soil cores from marsh sediments. The PVC cores were forced into marsh sediment until the top of the pipe was level with the marsh surface, then removed and

capped on both ends to retain sediment. Four transects on Dragon Island were collected using the PVC cores during August 2017, for a total of 20 samples. All transects after August 2017 were taken using a Barrett corer, for a total of 10 transects and 50 samples. One site (one sheared transect and one intact transect) on Dragon Island was a repeated collection with the Barrett device (Perret and Barrett 1971). The Barrett device uses a unidirectional ball valve attached to PVC pieces to hold suction on a removable 10.16 cm diameter x 30.48 cm long cylindrical acrylic core. Once the core had been collected, caps were added to each end of the core, and marked with the orientation of the core. There was a total of 14 transects (12 unique transects plus 2 repeat transects) and 70 samples. Aside from the core collection devices, there were no other differences in collection method. All cores were immediately placed into an ice chest containing ice packs for transport and then transferred into a -20°C freezer at the end of the day. Each sample was assigned metadata categories based on which island it was collected on, which elevation position it was collected from, which site it was collected from, and whether it was collected from a sheared or intact site.

Latitude, longitude, and elevation were recorded for each sample site using the Trimble R2 GPS and downloaded using the Trimble Terraflex software. Depth of the local anoxic layer for each transect was measured using a HI993310 direct soil activity probe (Hanna Instruments, Smithfield, Rhode Island); the depth at which soil conductivity (miliSiemens/centimeter) became less than -10 was recorded to ensure that eventual soil aliquots for DNA were collected from above the anoxic zone. All anoxic layer depths were between 4 and 6 cm with the exception of one at 32cm.

The initially collected PVC cores lacked sufficient soil volume for soil analysis in addition to DNA extraction; therefore, only samples collected with the Barrett device acrylic core were submitted for soil analyses. Approximately half of the sample volumes of all acrylic cores from the “Mid” and “High” elevation position of each transect were submitted to the LSU Agcenter Soil Testing and Plant Analysis lab for testing. The analyses performed on these 20 samples were Boron (ppm), Calcium (ppm), Chloride (ppm), Conductivity (dS/m), Magnesium (ppm), Salts (ppm), Sodium Adsorption Ratio (SAR), Sodium (ppm), Sulfur (ppm), Carbon (%), Nitrogen (%), Copper (ppm), Magnesium (ppm), pH, Phosphorus (ppm), Potassium (ppm), Sodium (ppm), Sulfur (ppm), Zinc (ppm), Iron (ppm), Percent Organic Matter (%), and Aluminum (ppm). Phosphorus, Potassium, Calcium, Sodium, Sulfur, Copper, Zinc, Chloride, Magnesium, SAR, Manganese, Iron, Aluminum, and Boron were analyzed using inductively coupled plasma optical emission spectroscopy (Baker and Amacher 1982, Barnhisel and Bertsch 1982, Bingham 1982, Rhoades 1982, Mehlich 1984). Soil pH was analyzed using a pH meter and electrode (McLean 1982). Organic Matter was analyzed using a dip probe colorimeter (Nelson and Sommers 1982). Soluble salts were analyzed using a conductivity probe (Rhoades 1982). Total Carbon and Total Nitrogen were analyzed on a LECO CN Analyzer using Dumas Dry-Combustion. Complete descriptions of the soil chemistry tests performed are available from https://www.lsuagcenter.com/portals/our_offices/departments/spess/servicelabs/soil_testing_lab/procedures/procedures-used-at-the-laboratory. Soil chemistry data were tested using the

aov function in the stats package in R, which performs a standard ANOVA (Chambers et al. 1992). The three factors used were the elevation position (High, Mid), margin status (Sheared, Intact), and island (Dragon, Horseshoe, and Stingray). Post hoc testing was performed using the TukeyHSD function in the stats package in R, which computes Tukey's Honest Significant Differences (Miller 1981, Yandell 1997).

DNA extraction from core subsamples, polymerase chain amplification and sequencing:

Six small (<5g) sections were cut from the top 5cm of each frozen core using a handsaw. To prevent cross contamination, all tools were cleaned in a 10% bleach solution in between samples. The six subsamples were placed together into storage bags and mixed. Three 0.25g soil aliquots from each sample bag were processed separately using DNeasy Powersoil kit (Qiagen, Hilden, Germany) according to the manufacturer's protocol. The three DNA extractions were performed on each sample in order to account for patchy small-scale distributions of certain infauna within samples (Coull 1990). Each sample was checked for DNA quantity (>10 ng) using the Nanodrop Spectrophotometer ND-1000 (Thermo Fisher Scientific, Wilmington, DE). Subsequently, the 210 DNA aliquots were shipped on ice to the University of New Hampshire Hubbard Center for Genome Studies for amplification and sequencing. DNA aliquots were amplified following the Earth Microbiome Project 18S PCR protocols (available from <https://press.igsb.anl.gov/earthmicrobiome/protocols-and-standards/18s/>) with primer constructs using the forward primer Illumina_Euk_1391f (Amaral-Zettler et al. 2009) and reverse primer Illumina_EukBr (Stoeck et al. 2010). PCR products from the amplification process were then sequenced on the Illumina HiSeq 2500 platform using the HiSeq Rapid SBS v2 kits (Illumina, San Diego, California) for sequencing preparation, producing 2x250 base pair forward and reverse raw FASTQ files for each sample (Caporaso et al. 2012). Sequence files and metadata are available in GenBank via the BioProject accession number PRJNA704031.

Analysis and Bioinformatics:

Bioinformatics steps were primarily performed in QIIME 2 (version 2020-2) (Bolyen et al. 2019). Raw FASTQ files containing the demultiplexed forward and reverse reads for each sample were first imported into QIIME 2 as a QIIME artifact file. Raw reads were examined using the q2-demux plugin and then subjected to rigorous quality control using the DADA2 algorithm (Callahan et al. 2016). As the 2x250 procedure on the Illumina HiSeq 2500 platform only reliably produces reads of 250 base pairs (bp) in length, anything longer than that was trimmed. In addition, the earliest bp position below 250 bp which showed a major drop and no recovery in Phred quality scores across a random subsampling of reads was chosen as a trimming point. For this dataset, these values were 150 bp for the forwards reads and 121 for the reverse reads. The DADA2 procedure output a table of merged paired end amplicon sequence variants (ASVs) associated with each sample and a representative sequence file containing all sequences for the ASVs. At this point the separate files for the three DNA extractions for each sample were merged using the group method of the q2-feature-table plugin, resulting in 70 samples in the ASV table. The SILVA 132 reference database and

taxonomy files were then imported as qza files (Quast et al. 2013). The BLAST algorithm was used on these database files to classify sequences to a 97% pairwise identity cutoff using the consensus method (Camacho et al. 2009). This step outputs a classification file which contains the matches to the database and taxonomy strings for all reads. Using this classification file, the ASV table was filtered using the filter-table method of the q2-taxa plugin to only allow ASV which contained the term “metazoa” but not “vertebrata” to separate metazoan infauna and to remove all vertebrates from the analysis. At this point, the taxonomy file was exported to examine the ASVs for any taxa which might be contaminants originating during the sample collection or processing. Any taxa determined to be a contaminant, such as any matching to *Demodex* sp., was filtered using the filter-table method of the q2-taxa plugin. Following filtering, ASVs were clustered into operational taxonomic units (OTUs) at a 97% identity threshold using the cluster-features-de-novo method of the q2-vsearch plugin (Rognes et al. 2016) to account for intraspecific variation in the barcode sequences as recommended to avoid inflating biodiversity (Bucklin et al. 2011, Brandt et al. 2019, Phillips et al. 2019). Sequences were aligned using the mafft method (Katoh et al. 2002) and masked (Lane 1991) in the q2-alignment plugin. Masked and aligned sequences were used to generate a midpoint-rooted phylogenetic tree using the q2-fasttree plugin (Price et al. 2010). A table of reads per OTU by sample with taxonomy and metadata was exported in the biom format from the QIIME 2 OTU table. This table was then imported to R using the biomformat package (McMurdie and Paulson 2016) and modified to turn read counts into OTU incidences (presence of individual OTUs in each sample), resulting in a binary table (0 = OTU not present, 1 = OTU present). “Incidences” in this text will refer to the presence of an OTU within a sample. Total incidences will refer to all the times an individual OTU was present in a sample in the dataset. Incidences were used because cell counts vary in metazoan individuals, and therefore read counts (which correspond to the number of cells and gene copies in environmental DNA in a sample) do not represent a realistic picture of the number of metazoan individuals in a sample.

Alpha rarefaction curves for OTU richness were generated using the original OTU table in the rarecurve method of the package vegan in R (Oksanen et al. 2018). The OTU incidence table was also input into the R package iNEXT and used to generate extrapolated sampling and coverage-based rarefaction curves (Chao et al. 2015). The package iNEXT relies on Hill numbers, which are “a mathematically unified family of diversity indices (differing among themselves only by an exponent q) that incorporate relative abundance and species richness” (Chao et al. 2014). The first three Hill numbers, $q = 0, 1$, and 2 , which are equivalent to species richness (number of observed species), the exponential of Shannon’s entropy index, and the inverse of Simpson’s index respectively, are used here. The values produced by the Hill number rarefaction calculations are effective diversity, or the number of species with equal numbers of incidences required to produce the value of the index. Because the input data was incidence-based (presence/absence of OTUs), the resultant indexes are the incidence-based extensions of the traditional abundance-based indexes. Sampling based rarefaction plots effective diversity of order q against the number of samples taken and extrapolates effective diversity values to

twice the number of samples collected. Coverage-based rarefaction plots effective diversity of order q against the estimated coverage of the dataset and extrapolates effective diversity to the estimated coverage of a dataset with double the number of samples. Estimated coverage is a comparison of values for richness and diversity metrics for the estimated actual community with the values for the observed community.

The OTU incidence table was input to SpadeR Online (Chao and Jost 2012, Chao et al. 2015) to calculate the basic diversity profile, number of shared OTUs between communities, and OTU richness estimations using the Homogenous, iChao, iChao2, and Incidence-based Coverage Estimator (ICE) models. The basic diversity profile for the dataset included observed total incidences, total number of observed OTUs, coverage estimate (CE), estimated Coefficient of Variation (CV), incidences and number of OTUs for the infrequent group. Total incidences are the total number of times all OTUs appear in the dataset. Coverage estimate is “an objective measure of sampling completeness” which represents the fraction of the actual community that was captured by the sampling effort (Chao et al. 2015). Samples rarely represent 100% of the community present in the environment, so estimations of how much of the actual community was collected are useful. The phrase “actual community” in this text will refer to the total community present in the environment including all species which were not observed during sampling. The CV represents the heterogeneity of OTU incidence in the dataset. A dataset with a $CV = 0$ would be totally homogenous (either all OTUs appear in all samples or no OTUs appear in all samples), and as heterogeneity increases the CV increases, with values above 2 considered highly heterogeneous. The infrequent group is a group of OTUs which appear in less than a selected number of samples and is Used in certain richness estimators such as ICE. In this study, the default setting of 10 samples was used as the cut off point for the infrequent group. Shared OTUs between communities collected from sheared and intact margins, from different elevation positions, and from different islands were also calculated. The OTU richness values for the actual community were estimated using 4 different models which were most appropriate for this dataset. The homogenous model estimates actual richness as if all OTUs have an equal probability of being detected. The Chao2 value estimates actual richness based on the number of OTUs which have up to two incidences in the dataset, and is an incidence based extension of the Chao1 estimator (Chao 1984). The iChao2 value is an improved version of Chao2 that takes into account OTUs which have up to four incidences, which is better than Chao2 for more heterogeneous datasets. The ICE value estimates actual richness based on the infrequent group (OTUs detected in 10 samples or less) and is an extension of the Abundance-based Coverage Estimator (Chao and Lee 1992).

The OTUs were organized by the phylum to which each was assigned, then plotted as percentages of total OTU incidences and total number of OTUs as pie charts in Microsoft Excel. In addition, OTUs were presented with phylum and order level assignment, total incidence, lowest level assignments from SILVA and GenBank, and incidence by metadata category (sheared or intact, island, and elevation position). Lowest level assignments were the most specific assignment given to an OTU, regardless of what level of taxonomy it was. Most OTUs

received a species level assignment, but an OTU which was ambiguous at the species level would have a lowest level assignment of genus.

Due to low resolution of some SILVA strings (where the string jumps directly from taxonomic order to ambiguous species) and some errors in the SILVA reference database (such as listing *Wolbachia* under the class Insecta), a more detailed taxonomic assignment was required. The sequences from all taxa were manually checked using the BLAST+ algorithm against the NCBI GenBank database (Benson et al. 2011). Each OTU was assigned an additional taxonomic identification based on the top BLAST hits (sorted by E-value) in order to . Nematode sequences specifically were given potential functional feeding group assignments (Hodda 2011). The taxonomic strings associated with GenBank assignments were checked for accuracy against the World Register of Marine Species database (WoRMS Editorial Board 2020).

The OTU incidence table was used to generate bar plots for each sample in R using the ggplot2 package. Each bar plot shows the number of OTUs assigned to each phylum as a relative percentage of the total number of observed OTUs within the sample.

Alpha and beta diversity measures for the dataset were obtained using several metrics and diversity indices. Alpha diversity is generally defined as the measure of diversity within samples, while beta diversity is generally defined as changes in diversity across samples within an environment (Whittaker 1972, Anderson et al. 2011, Chao et al. 2012). –Prior to calculating the alpha diversity values, the OTU table was rarefied with replacement to 200 reads, which was a number of reads that would allow more than 80% of samples to remain, using the rarefy method of the feature-table plugin in QIIME 2. Alpha diversity vectors were calculated in QIIME 2 using the alpha and alpha-phylogenetic methods of the q2-diversity plugin on the rarefied OTU table and the phylogenetic tree using the OTU richness and Faith’s Phylogenetic Diversity (PD) measures (Faith 1992). OTU richness consists of the number of OTUs found in individual samples. Faith’s PD consists of the total branch length of the phylogenetic tree of all OTUs within a sample. Each of these vectors were tested for differences across metadata categories (Margin, Island, and Elevation position) using Kruskal-Wallis tests in the q2-diversity plugin (Kruskal and Wallis 1952). OTU richness and Faith’s PD values were used to generate box plots in R using the ggpubr and ggplot2 packages with separate boxes per island by elevation position and separate plots for samples from sheared and intact margins.

The OTU incidence table was input to SpadeR Online (Chao and Jost 2012, Chao et al. 2015) to calculate similarity indices representing beta diversity for both the observed communities and the estimated actual communities based on Chao’s estimates of richness and incidence for the actual community (Chao et al. 2013). Given the likelihood of sampling not capturing the true richness present in the environment, it is likely that the empirical indices undershoot the actual similarity between the communities. Nevertheless, empirical indices are compared to the estimated values to assess how well the observations represent the actual community diversity. Indices were calculated to determine similarity of infauna community between samples from sheared and intact margins, from each position of elevation transects,

and from each island. The indices selected were Sørensen, Jaccard, Horn (equal-weighted), Morisita-Horn (relative), and Regional overlap (relative). Each of these indices was calculated for both the observed community and the estimated actual community. Additional indices calculated by the program were discarded due to being based on the absolute number of OTU incidences within each community because the absolute number of incidences was low, which may cause bias. All the indices calculated by SpadeR Online run from zero to one, with higher values representing higher similarity of richness and incidence. The Jaccard and Sørensen indices both compare the shared OTUs of both groups to the total OTUs of both groups, but Jaccard gives less weight to shared OTUs than Sørensen. In all following indices, which normally use abundance of species as part of the calculation of similarity, the relative proportion of the incidences of an OTU in a community with respect to the total number of incidences in that community was used as a proxy of abundance of that OTU. These indices also partition gamma diversity using alpha diversity to determine beta diversity. The Horn (equal-weighted) index is a measure of the overlap between the alpha and gamma Shannon diversity, using the relative proportion of incidences within each community instead of absolute numbers of incidence (Horn 1966). The “equal-weighted” portion of the name refers to the other version of the index, the Horn (size-weighted) index, which weighs the size of total community more heavily in the calculation than the Horn (equal-weighted) index does. The Morisita-Horn (relative) and regional overlap (relative) indices are measures of overlap between alpha and gamma Gini-Simpson diversity, using the relative proportion of incidences within each community instead of absolute numbers of incidence (Morisita 1961). Morisita-Horn gives more weight to gamma Gini-Simpson diversity, while regional overlap gives more weight to the alpha Gini-Simpson diversity.

A distance matrix of Sørensen index values was calculated from the original OTU table using the beta method of the q2-diversity plugin (Dice 1945, Sørensen 1948). This index was chosen because it sidesteps the issue of read counts not aligning with number of individuals in metazoan taxa by comparing the composition of OTUs in each sample with the composition of every other sample. The Sørensen index is quite similar to the Jaccard index, but gives higher weight to the number of shared species between two samples than the Jaccard index, resulting in higher index values between samples with more shared species. Sørensen index values for each set of two samples were computed by doubling the number of shared OTUs between two samples and dividing that by the sum of the total number of OTUs in both samples to obtain similarity, then subtracting the similarity from one to determine dissimilarity. The distance matrix is a matrix of the Sørensen index values for each set of two samples in the dataset. Non-metric MultiDimensional Scaling (NMDS) ordination was performed on the Sørensen distance matrix using the function metaMDS in the R package vegan (Oksanen et al. 2018). Ordination was started with 10 dimensions, with each subsequent run using the previous solution with 1 fewer dimension to reduce the stress of the ordination. Stress (goodness of fit of the regression of the original distance matrix values against the ordination distances) was plotted against the number of dimensions to determine the lowest number of dimensions with a stress below 0.1.

This process resulted in an ordination with 7 dimensions. The resulting ordination was plotted using the `ggordiplot` package to overlay the `vegan` package methods `ordihull`, `ordispider`, and `ordiellipse` over a figure produced by the package `ggplot`.

Distance matrices based on Sørensen dissimilarity indices were analyzed using the multifactorial Adonis method (Anderson 2001, Oksanen et al. 2018) in the `q2-diversity` plugin using the formula with the factors “Island*Margin*Elevation Position” with 10,000 permutations. The Adonis test is a multifactorial PERMANOVA test, which uses the sum of squares of the distances between the centroids of factors and the overall centroid in multivariate space to calculate F-ratios and permutations of the observations to determine significant differences. The multivariate space is the space in multiple dimensions (with each column of data in the distance matrix corresponding to one dimension) that the dataset occupies. The centroid of a factor is the geometric center of the group of samples which fall under that factor within the multivariate space, while the overall centroid is the geometric center of all samples within the multivariate space. The factor Island had three classes, Dragon (DI), Horseshoe (HI), and Stingray Island (SI), denoting the islands that the samples were collected on. The factor Margin had two classes, Sheared and Intact. The factor Elevation Position had five classes, High, MidHigh, Mid, MidLow, and Low. One of the assumptions of the PERMANOVA test is that the multivariate spread of each factor is homogenous, i.e., all of the samples are roughly equally distant from centroid of a factor. The distance matrix was tested for homogeneity of the multivariate spread of each factor using the PERMDISP procedure in the `q2-diversity` plugin to ensure the assumptions of the Adonis test were not violated. Following the Adonis test, a Benjamini-Hochberg correction procedure was performed on the resulting p-values using the `p.adjust` function in the `stats` package in R (Benjamini and Hochberg 1995a) to control the false discovery rate. The Benjamini-Hochberg procedure functions by ranking all p-values in order from smallest to largest p-value, then comparing them to a value computed by taking the assigned rank of each p-value, multiplying by the selected alpha (here, 0.05) and dividing by the number of hypothesis tests. The largest p-value that is lower than the calculated value is the largest p-value which is accepted, all larger p-values are considered false discoveries. Following the Adonis test, subsequent tests, and adjustments, the OTU table was split into three separate tables according to the factor Island, each containing only samples within each island that were then used to generate separate Sørensen distance matrices for each island. The matrices were then tested using the Adonis test with the formula “Margin*Elevation Position” with 10,000 permutations, followed by additional PERMDISP tests and Benjamini-Hochberg corrections. The NMDS ordination process was repeated with the separate island distance matrices, however, due to results from the Adonis test on the individual island datasets, the only ordination that was informative was the Stingray Island NMDS, which resulted in a NMDS with 4 dimensions.

Differential taxa abundances:

Taxa differentials were generated from the original OTU table using the q2-songbird plugin (Morton et al. 2019) with a differential prior of 0.01, an epoch value of 300,000, and a learning rate of 0.00001 using the model formula “Island + Margin + Elevation Position”. The differential prior option specifies the possible width of the differentials, and the epoch value specifies how long the model is allowed to run, which can impact whether the multinomial regression performed by the program reaches convergence. The model as specified above was compared with a null model (i.e., the same parameters but with the model set to “1” instead of the above formula) using the summarize-paired method in the Songbird plugin to generate a pseudo- Q^2 value, which gives an indication of how much more the model learns versus the null model. This pseudo- Q^2 value behaves like the R^2 value of a linear regression analysis, and ranges up to 1, with positive values indicating better learning in the test model than in the null model. The parameters were adjusted (differential prior reduced, epoch value extended, learning rate reduced) until the pseudo- Q^2 value no longer showed an increase when parameters were adjusted. The final pseudo- Q^2 value was 0.146, showing that the model gained some information from the dataset. Taxa differentials are the relative log-fold change in OTU abundance (read counts) across a metadata category. Positive differentials represent higher abundance (enrichment) of read counts of an OTU in samples from a category compared to those from another category, while negative values represent lower abundance.

2.3. Results

Soil chemistry analysis:

Of all the soil chemistry variables tested using ANOVA relative to elevation position, sheared margin status and island, only Carbon (%), Nitrogen (%), and Percent Organic Matter (POM) were significantly different across any factors (Tables 2.1, 2.2, 2.3). Numerous other variables had high standard deviation, though they were not significantly different across any factors according to ANOVA presumably due to the high variation not associated with any factors. These variables were Boron, Calcium, Chloride, Conductivity, Magnesium, Salts, Sodium, Sulfur, Phosphorus, and Potassium. Variability in the Chloride, Conductivity, Salts, and Sodium variables can potentially be explained by diurnal variability of local salinity of the area. The remaining variables tend to be high in salt marshes and did not exceed historic values (Palmisano Jr. 1970, Chabreck 1972, Brupbacher et al. 1973, Santschi et al. 2001, Bhattarai 2006)

For carbon percentage (Table 2.4), the interaction of Margin and Island ($F(2,8) = 16.70$, $p < 0.01$) was significant. All class combinations for these two factors were significantly different according to Tukey’s HSD (all $p < 0.01$). The carbon percentage of samples from sheared margins on Dragon Island was an extreme outlier, being more than double the percentage of any other margin and island class combination. Carbon percentage was higher in samples from sheared margins than in samples from intact margins ($F(1,8) = 23.26$, Intact mean = 9.96 ± 2.47 , Sheared mean = 14.09 ± 6.45 , $p < 0.01$), though this may be driven by the high values from the samples from sheared margins on Dragon Island. Carbon percentage in Dragon Island samples

was nearly double that of Stingray or Horseshoe samples, likely due to the outlier values of the samples from sheared margins on Dragon Island. The carbon percentage in Stingray Island samples was slightly higher than Horseshoe Island ($F(2,8) = 35.60$, Dragon mean = 19.14 ± 8.12 , Horseshoe mean = 9.59 ± 2.08 , Stingray mean = 10.90 ± 1.93 , $p < 0.01$). Samples from sheared margins had higher nitrogen percentage than samples from intact margins ($F(1,8) = 13.05$, Intact mean = 0.69 ± 0.07 , Sheared mean = 0.81 ± 0.11 , $p < 0.01$), possibly driven by higher nitrogen percentage from samples from sheared margins on Dragon Island (Table 2.5). However, the nitrogen percentage of all samples ranged from 0.5% to 1%. For Percent Organic Matter (POM), the interaction of Margin and Island was significant ($F(2,8) = 5.86$, $p = 0.03$), with samples from sheared margins on Dragon Island having higher POM than all other margin and island class combinations other than samples from intact margins on Stingray Island (Table 2.6). Percent Organic Matter was higher in Dragon Island samples than in Horseshoe Island samples, but neither were different from Stingray Island samples ($F(2,8) = 4.55$, Dragon mean = 9.81 ± 4.64 , Horseshoe mean = 6.62 ± 0.74 , Stingray mean = 7.86 ± 2.17 , $p = 0.05$, Dragon-Horseshoe $p = 0.04$). Carbon/Nitrogen (C/N) ratios were calculated using the percentages for carbon and nitrogen from each sample. These ratios were then tested using ANOVA and the same factors as above (Table 2.7). For C/N ratios, the interactions of Elevation Position and Margin ($F(1,8) = 10.49$, $p = 0.01$) and Island and Margin ($F(2,8) = 11.67$, $p < 0.01$) were both significant. Mid elevation position samples from sheared margins showed higher C/N ratios than Mid position samples from intact margins ($p < 0.01$, Tukey's HSD). Due to the high carbon percentage in samples from sheared margins on Dragon Island, those samples showed higher C/N ratios than all other margin and island class combinations (all $p < 0.01$, Tukey's HSD). For this same reason, samples from sheared margins had higher C/N ratios than samples from intact margins ($F(1,8) = 11.48$, Intact mean = 14.36 ± 2.59 , Sheared mean = 16.99 ± 5.59 , $p < 0.01$) and samples from Dragon Island had higher C/N ratios than samples from other islands. Samples from Stingray Island had higher C/N ratios than samples from Horseshoe Island, again tracking the carbon percentage ($F(2,8) = 35.61$, Dragon mean = 22.08 ± 5.90 , Horseshoe mean = 13.32 ± 1.75 , Stingray mean = 14.83 ± 2.28 , $p < 0.01$). Though values of carbon percentage, nitrogen percentage, percent organic matter, and C/N ratios were consistently higher in samples from sheared margins, it is unclear why the samples from sheared margins from Dragon Island had extremely high values for carbon percentage. However, the carbon percentage in these samples did not exceed historic values in marsh samples (Chabreck 1972, Brupbacher et al. 1973).

Table 2.1. Mean and standard deviation values for soil chemistry analyses of samples from sheared and intact margins across the islands surrounding Bay Jimmy, Louisiana from August 2017 to November 2017.

Island	Margin	Carbon (%) *	St Dev	Nitrogen (%) *	St Dev	C/N Ratio *	St Dev	Organic Matter (%) *	St Dev	Boron (ppm)	St Dev	Calcium (ppm)	St Dev	Chloride (ppm)	St Dev
Dragon	Sheared	26.06 ^A	1.83	0.96 ^A	0.12	27.12 ^A	1.41	12.94 ^A	5.04	18.29	11.44	536.97	352.03	8808.84	226.03
	Intact	12.23 ^B	1.85	0.72 ^B	0.07	17.04 ^B	0.86	6.68 ^{AB}	0.16	9.46	0.99	273.71	109.39	13390.25	2558.12
Horseshoe	Sheared	10.97 ^B	1.50	0.79 ^A	0.04	13.94 ^B	1.92	6.82 ^B	1.00	11.43	2.02	414.45	135.46	22509.68	11400.81
	Intact	8.20 ^B	1.66	0.64 ^B	0.07	12.70 ^B	1.56	6.42 ^B	0.42	10.05	0.62	639.08	62.73	32126.15	18825.55
Stingray	Sheared	11.22 ^B	1.45	0.75 ^A	0.09	14.98 ^B	1.80	7.44 ^B	0.99	12.15	1.13	524.85	302.19	21219.33	2172.70
	Intact	10.58 ^B	2.51	0.72 ^B	0.06	14.68 ^B	2.97	8.29 ^{AB}	3.09	11.42	1.72	593.34	74.00	22534.19	6647.78

Asterisks * indicate that values within columns were significantly different. Means in columns followed by the same letter are not significantly different ($P \geq 0.05$; Tukey HSD).

Table 2.2. Mean and standard deviation values for soil chemistry analyses of samples from sheared and intact margins across the islands surrounding Bay Jimmy, Louisiana from August 2017 to November 2017.

Island	Margin	Conductivity (dS/m)	St Dev	Magnesium (ppm)	St Dev	Salts (ppm)	St Dev	Sodium Adsorption Ratio	St Dev	Sodium (ppm)	St Dev	Sulfur (ppm)	St Dev
Dragon	Sheared	30.02	5.74	1327.84	462.97	19212.80	3674.69	2.52	0.56	461.83	6.08	606.12	60.29
	Intact	37.22	13.44	1234.53	496.89	23820.80	8598.42	2.68	0.64	452.30	14.65	476.19	99.71
Horseshoe	Sheared	45.17	16.60	1646.06	569.23	28908.80	10626.28	2.31	0.65	443.93	17.71	624.45	80.83
	Intact	64.15	4.11	2333.33	67.49	35488.00	2632.31	1.75	0.03	424.61	4.24	687.63	3.42
Stingray	Sheared	57.46	7.16	1890.93	816.74	36774.40	4580.74	1.81	0.27	385.88	89.44	488.82	156.91
	Intact	55.45	4.15	2064.96	211.22	35488.00	2656.62	1.90	0.12	434.36	20.85	677.07	18.30

Table 2.3. Mean and standard deviation values for soil chemistry analyses of samples from sheared and intact margins across the islands surrounding Bay Jimmy, Louisiana from August 2017 to November 2017.

Island	Margin	Copper (ppm)	St Dev	pH	St Dev	Phosphorus (ppm)	St Dev	Potassium (ppm)	St Dev	Zinc (ppm)	St Dev	Aluminum (ppm)	St Dev
Dragon	Sheared	1.05	1.12	6.21	0.20	67.95	29.83	1243.51	631.95	9.82	4.49	1.32	1.15
	Intact	3.41	1.05	6.45	0.25	88.05	10.46	1371.23	275.50	4.24	0.10	0.59	0.05
Horseshoe	Sheared	3.15	1.30	6.24	0.50	34.96	12.85	1392.85	118.69	8.28	2.13	0.60	0.06
	Intact	2.80	0.08	5.80	0.17	35.77	8.42	1522.03	35.25	9.02	2.87	0.70	0.05
Stingray	Sheared	2.18	1.42	6.24	0.41	38.29	7.47	1427.98	230.54	7.82	3.98	0.44	0.32
	Intact	1.99	0.48	5.88	0.30	36.83	10.00	1307.54	53.85	8.76	1.72	0.65	0.04

Table 2.4. ANOVA results for Carbon (%) in soil samples collected from marsh islands surrounding Bay Jimmy, Louisiana. Sampling occurred from August 2017 to November 2017.

Factor	Df	SumSq	MeanSq	F-value	p-value
ElevationPosition	1	0.88	0.88	0.241	0.636905
Margin	1	85.04	85.04	23.259	0.001317*
Island	2	260.36	130.18	35.604	0.000104*
ElevationPosition:Margin	1	7.26	7.26	1.986	0.196426
ElevationPosition:Island	2	5.99	3	0.819	0.4746
Margin:Island	2	122.15	61.07	16.704	0.001393*
ElevationPosition:Margin:Island	2	3.63	1.82	0.497	0.626176
Residuals	8	29.25	3.66		

Asterisks * indicate significant p-values (< 0.05).

Table 2.5. ANOVA results for Nitrogen (%) in soil samples collected from marsh islands surrounding Bay Jimmy, Louisiana. Sampling occurred from August 2017 to November 2017.

Factor	Df	SumSq	MeanSq	F-value	p-value
ElevationPosition	1	0.00627	0.00627	1.106	0.32364
Margin	1	0.07393	0.07393	13.053	0.00685*
Island	2	0.04325	0.02163	3.818	0.06852
ElevationPosition:Margin	1	0.00462	0.00462	0.816	0.3928
ElevationPosition:Island	2	0.01461	0.0073	1.29	0.327
Margin:Island	2	0.03252	0.01626	2.87	0.11491
ElevationPosition:Margin:Island	2	0.0064	0.0032	0.565	0.58937
Residuals	8	0.04531	0.00566		

Asterisks * indicate significant p-values (< 0.05).

Table 2.6. ANOVA results for Percent Organic Matter in soil samples collected from marsh islands surrounding Bay Jimmy, Louisiana. Sampling occurred from August 2017 to November 2017.

Factor	Df	SumSq	MeanSq	F-value	p-value
ElevationPosition	1	0.85	0.854	0.284	0.6085
Margin	1	5.71	5.705	1.897	0.2057
Island	2	27.34	13.672	4.547	0.048*
ElevationPosition:Margin	1	10.62	10.617	3.531	0.097
ElevationPosition:Island	2	18.45	9.225	3.068	0.1026
Margin:Island	2	35.25	17.626	5.862	0.0271*
ElevationPosition:Margin:Island	2	6.53	3.267	1.086	0.3825
Residuals	8	24.05	3.007		

Asterisks * indicate significant p-values (< 0.05).

Table 2.7. ANOVA results for C/N ratios in soil samples collected from marsh islands surrounding Bay Jimmy, Louisiana. Sampling occurred from August 2017 to November 2017.

Factor	Df	SumSq	MeanSq	F-value	p-value
ElevationPosition	1	0.23	0.23	0.076	0.790216
Margin	1	34.56	34.56	11.481	0.009523*
Island	2	214.41	107.21	35.614	0.000104*
ElevationPosition:Margin	1	31.57	31.57	10.486	0.01191*
ElevationPosition:Island	2	0.33	0.17	0.055	0.946714
Margin:Island	2	70.24	35.12	11.667	0.004249*
ElevationPosition:Margin:Island	2	1.07	0.53	0.177	0.840762
Residuals	8	24.08	3.01		

Asterisks * indicate significant p-values (< 0.05).

Preliminary evaluation of entire 18S rRNA gene sequence dataset:

The ASV table output from the DADA2 quality control algorithm contained approximately 15 million reads and 77,043 OTUs. A total of 74,619 of these ASVs were unassigned at any level of taxonomy leaving approximately 4 million reads and 2,424 ASVs which belonged to eukaryote taxa. These unassigned taxa may be the result of primer mismatch allowing for the amplification of prokaryotic taxa over eukaryotic taxa (Hadziavdic et

al. 2014). Because this study is focused on metazoan eukaryotes, it was justified to ignore these prokaryote taxa. The majority of the eukaryote ASVs were assigned at the sub-domain level to the SAR clade (Stramenopiles, Alveolates, and Rhizaria), followed by the Opisthokonta clade (Fungi, Metazoa, and related unicellular eukaryotes), Excavata (Flagellates), Archaeplastida (Algae and Plants), and Amoebazoa (Table 2.8). The Cryptophyceae, Incertae Sedis, Haptophyta and Picozoa groups all had very few ASVs (≤ 10) assigned to them. No clear or consistent patterns between samples from sheared and intact margins, from the different islands, or from the different elevation positions emerge at the sub-domain level of taxonomy (Fig. 2.2).

Twelve hundred and thirty-eight (51%) of the ASVs with taxonomical assignment produced an unclear assignment at the species level in the SILVA database (Table 2.8). Most of the sub-domain groups with >100 ASVs had high rates of unclear assignments similar to that of the entire dataset. However, the Metazoa within the Opisthokonta had a lower rate of unclear assignments (42%) than the sub-domain groups in the dataset (51%). All samples contained metazoa, and metazoa made up as much as 80% of the reads in certain samples. The Excavata, Amoebazoa, Cryptophyceae, Haptophyta, Incertae Sedis, Picozoa, and non-metazoan, non-fungi Opisthokonta were not present in all samples. Although ASVs in the SAR group and Excavata were more commonly detected in the dataset than metazoa, they are more poorly studied due to their microscopic size and difficult taxonomy, leading to recommendations of “taxonomy-free” studies (Apothélos-Perret-Gentil et al. 2017, Kelly 2019). Studies of benthic microalgae (including the SAR group) in marshes tend to focus on photosynthetic pigment analysis as a measure of differences between samples rather than the taxa present (Fleeger et al. 2015). Several metabarcoding studies on the Gulf Coast detected groups like SAR and Excavata but did not deal with them at lower levels of taxonomy (Bik et al. 2012, Brannock et al. 2014, Bhalerao 2018). Many groups of metazoa in marsh sediments were studied following the DHOS, including arthropods, annelids, nematodes, and mollusks (Fleeger et al. 2019), and have a long history of study in marsh sediments (Coull et al. 1982, Fleeger 1985, Coull 1990). Therefore, the metazoa contain more accessible information than the other groups.

Following filtering by the taxonomy term “metazoa” (excluding all matches to “vertebrata”), the dataset contained approximately 404,000 reads and 297 ASVs. After clustering sequences which were 97% similar to each other, the final number of metazoan OTUs was 157.

Table 2.8. Sub-Domain level taxonomy assignments from the SILVA database of the entire dataset of ASVs.

Taxon	Number of OTUs	Metagenome	Uncultured	Unidentified	Ambiguous Taxa	Percent Unclear Assignments
SAR	1080	20	106	4	396	48.70
Opisthokonta	695	4	62	0	311	54.24
Fungi	365	1	33	0	193	62.19
Metazoa	297	3	11	0	111	42.09
Excavata	302	2	26	0	122	49.67
Archaeplastida	189	0	9	0	91	52.91
Amoebazoa	114	22	6	0	28	49.12
Cryptophyceae	17	0	1	0	10	64.71
Incertae sedis	17	2	5	0	4	64.71
Haptophyta	8	0	3	0	2	62.5
Picozoa	1	0	0	0	1	100
Uncultured	1	0	1	0	0	100
Total	2424	50	219	4	965	51.07

The Metagenome column included all ASVs which were assigned as a metagenome without at least a genus level assignment; Uncultured, Unidentified, and Ambiguous Taxa columns have all ASVs assigned to those categories at the lowest level of taxonomy. The Percent Unclear Assignments is the percentage of the total ASVs for each row which were assigned as Metagenome, Uncultured, Unidentified, or Ambiguous Taxa. Fungi and Metazoa (shaded) fall under Opisthokonta, and should not be counted towards the total number of ASVs alongside the Opisthokonta totals.

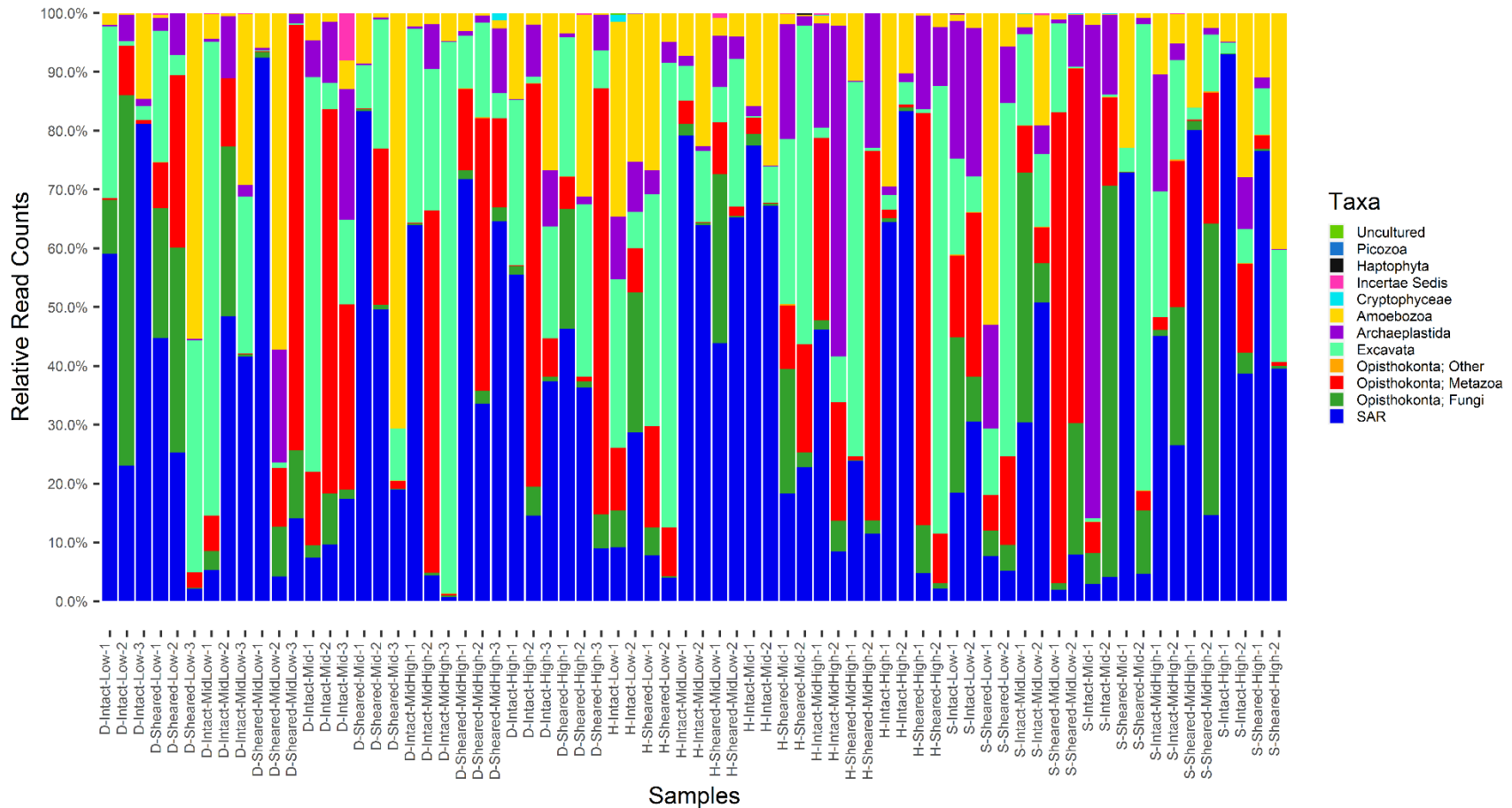


Fig. 2.2. Taxa bar plots for the full dataset of 70 samples collected from marsh islands surrounding Bay Jimmy, Louisiana from August 2017 to November 2017, with each colored section of the bar representing the relative proportion of the read counts assigned to different taxa at the taxonomic level below Domain (“Kingdom”) within that sample. The taxa are sorted within each bar by the overall lowest to highest number of ASVs from top to bottom. For the x-axis, samples are labeled as D (Dragon), H (Horseshoe), or S (Stingray) for the island, and Intact or Sheared for the margin type, as well as Low, MidLow, Mid, MidHigh, or High for the elevation position, followed by the transect number.

Alpha rarefaction curves:

Alpha rarefaction curves of metazoan OTU richness plotted against sequencing depth (Fig. 2.3) for all samples level off, indicating that sufficient sequencing depth to detect the majority of the taxa present in the community was achieved. Although there was a large variability in the number of OTUs detected in each sample as well as variability in the sequencing depth of each sample, higher sequencing depth did not lead to higher OTU richness, corroborating sufficient sequencing depth in the majority of samples. Samples from sheared and intact margins showed similarly wide range of OTU richness and sequencing depth.

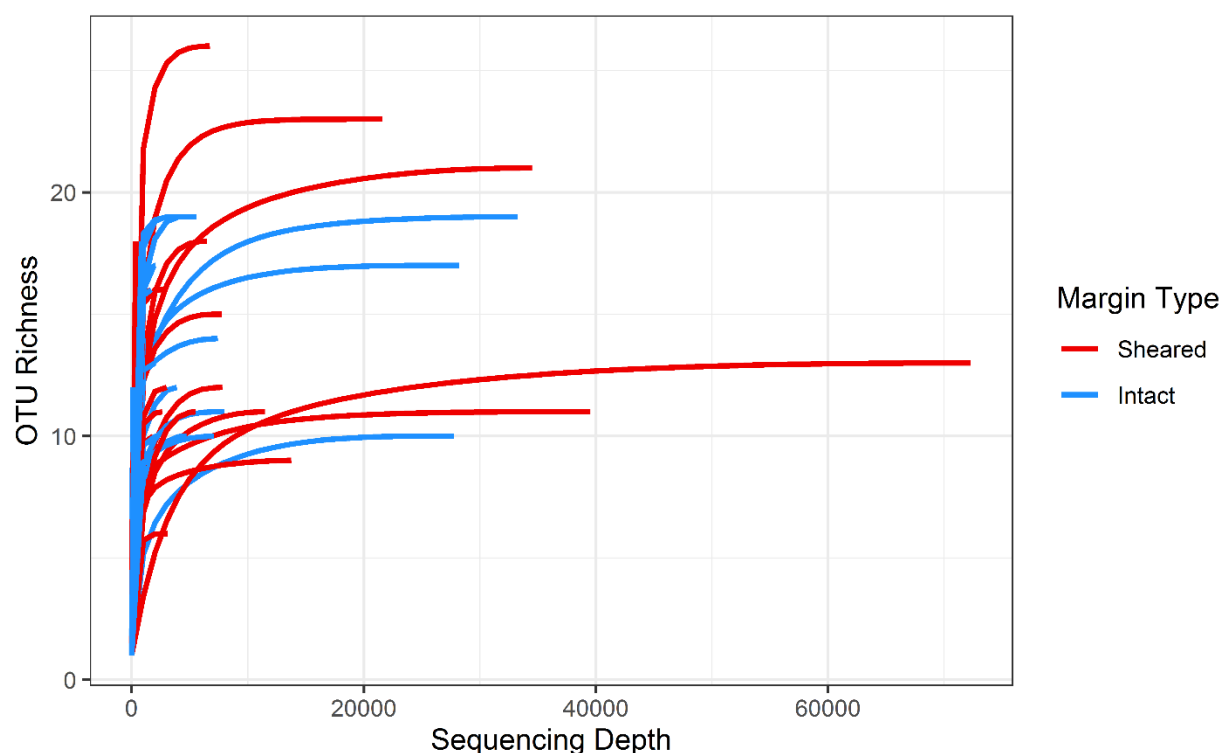


Fig. 2.3. Alpha rarefaction curves which show the number of OTUs detected when randomly sampling reads at each given sequencing depth. Each curve represents the summed sequences of the three DNA extractions from a single sample collected from marsh islands surrounding Bay Jimmy, Louisiana from August 2017 to November 2017.

Sample-based rarefaction curves:

The interpolated portion of the richness sample-based rarefaction curves (Fig. 2.4, 2.5, 2.6, 2.7) begin to level off, showing that there were enough samples collected to capture the majority of the OTU richness across the entire dataset, margin status, island, and elevation position communities. These plots feature effective diversity plotted against the number of samples collected. The solid portion of the curve is based on the input data, while the dashed portion of the curve is an extrapolation of additional sampling based on the collected samples.

The extrapolated portion of these richness curves show that doubling the number of samples taken could improve OTU richness from 25% to 50% of the currently captured richness across the elevation position communities. The curves for the samples from different elevation position samples (Fig. 2.7) are steeper than those for samples from sheared and intact margins (Fig. 2.5) and the different islands (Fig. 2.6) which is due to the division of the dataset into smaller parts. The Shannon and Simpson Inverse curves, which represent effective diversity, or the number of equally commonly detected OTUs required to achieve the value of the index at that point on the curve, are much flatter than the richness curves. Thus, additional captured OTUs would contribute more to richness than to the diversity metrics and would likely appear in very few samples.

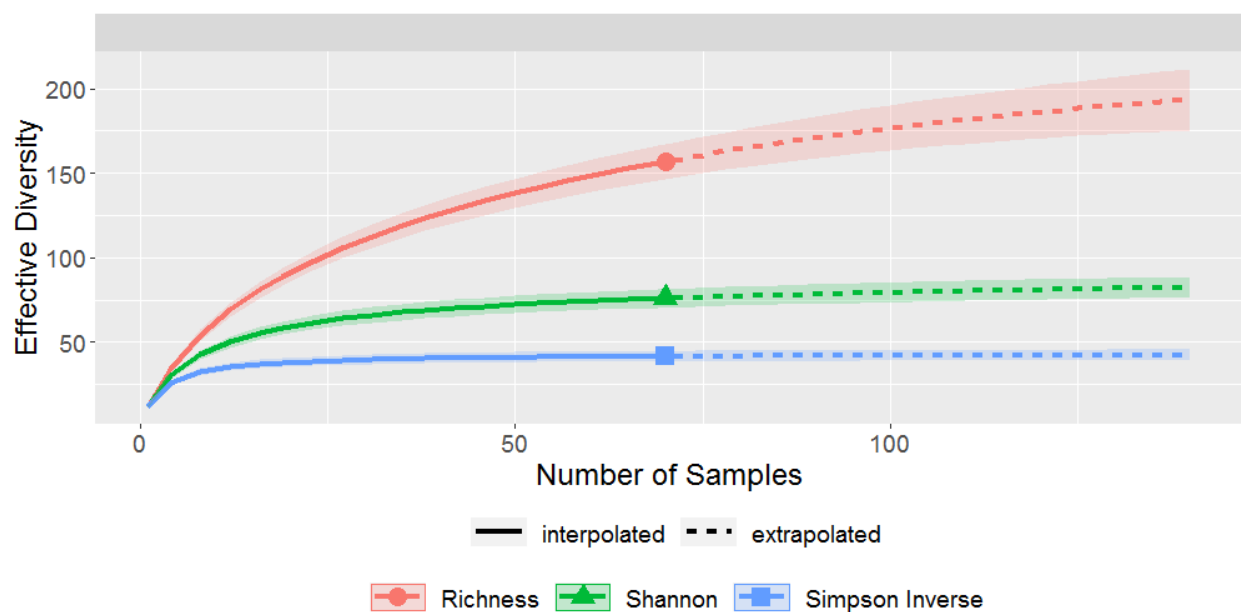


Fig. 2.4. Sample-based rarefaction curves for the full dataset with effective diversity for different metrics plotted against the number of samples collected from marsh islands surrounding Bay Jimmy, Louisiana from August 2017 to November 2017. Extrapolation extends out to twice the number of samples, and the shaded area around each curve represents the 95% confidence interval of the curve.

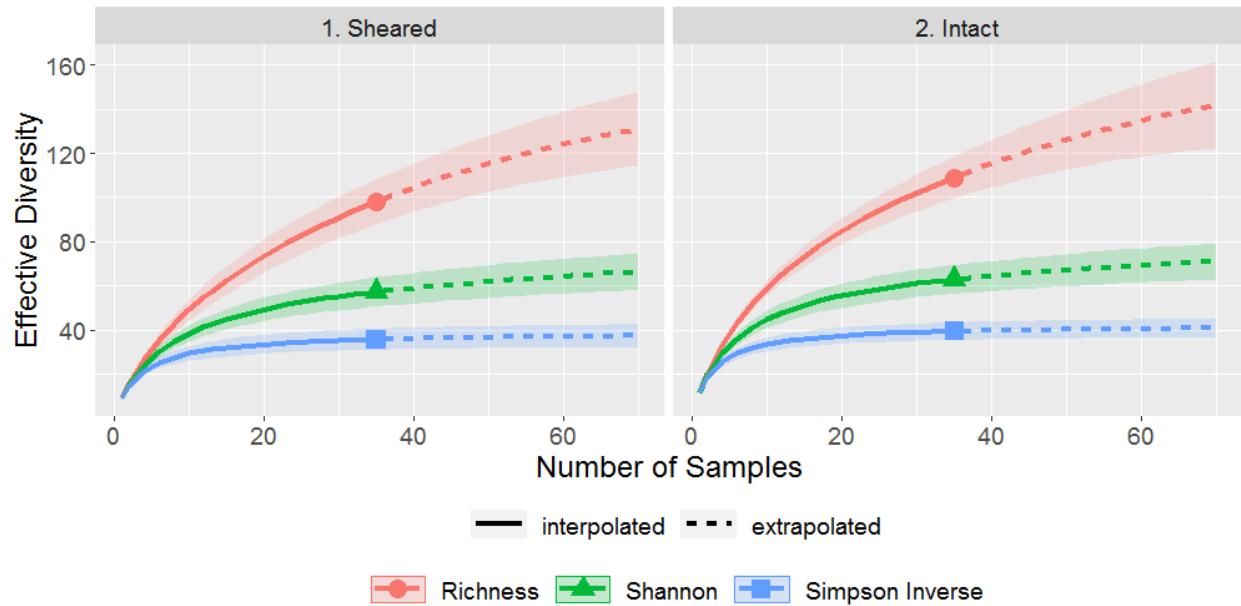


Fig. 2.5. Sample-based rarefaction curves for samples from sheared and intact marsh margins with effective diversity for different metrics plotted against the number of samples collected from marsh islands surrounding Bay Jimmy, Louisiana from August 2017 to November 2017. Extrapolation extends out to twice the number of samples, and the shaded area around each curve represents the 95% confidence interval of the curve.

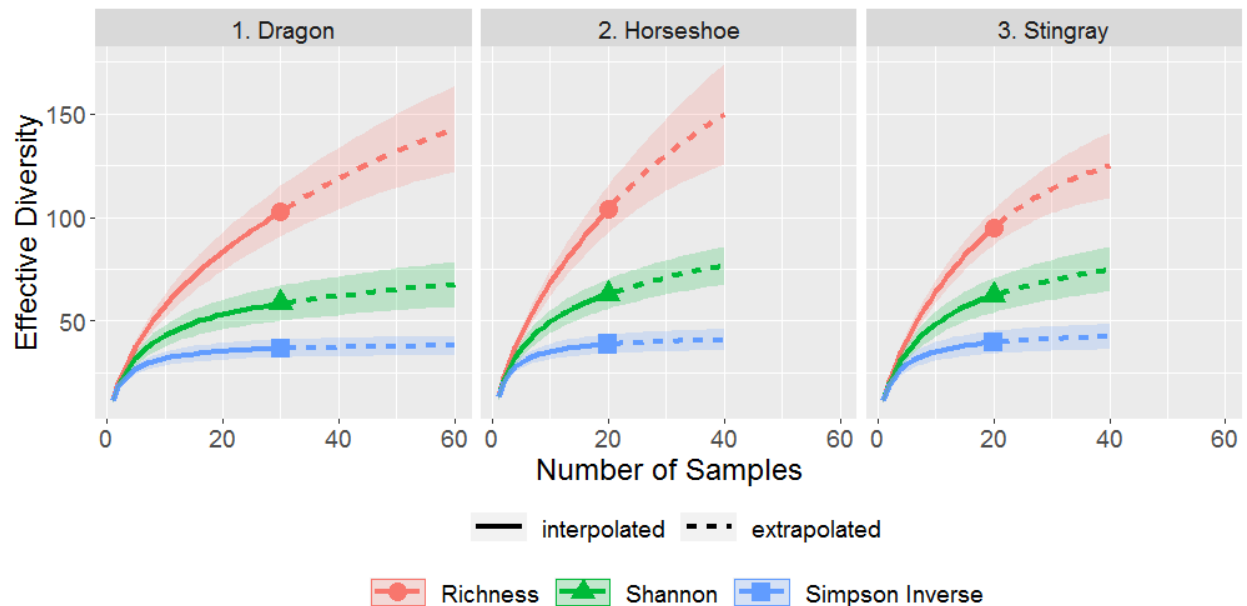


Fig. 2.6. Sample-based rarefaction curves for samples from the different islands with effective diversity for different metrics plotted against the number of samples collected from marsh islands surrounding Bay Jimmy, Louisiana from August 2017 to November 2017. Extrapolation extends out to twice the number of samples, and the shaded area around each curve represents the 95% confidence interval of the curve.

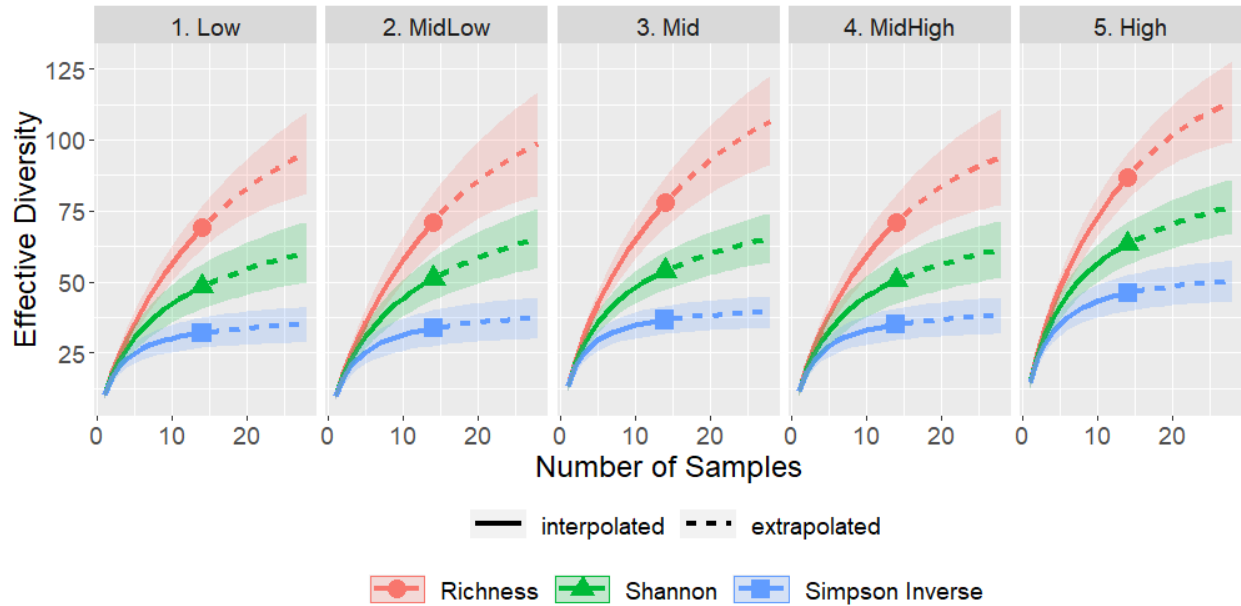


Fig. 2.7. Sample-based rarefaction curves for samples from the different elevation positions with effective diversity for different metrics plotted against the number of samples collected from marsh islands surrounding Bay Jimmy, Louisiana from August 2017 to November 2017. Extrapolation extends out to twice the number of samples, and the shaded area around each curve represents the 95% confidence interval of the curve.

Coverage-based rarefaction curves:

The interpolated portions of the coverage-based rarefaction curves (Fig. 2.8, 2.9, 2.10, 2.11) reach between 70% and 93% coverage of the estimated actual community. The extrapolated portion of the curves, which represent estimated coverage if the number of samples was doubled, extend between 5% and 10% past the interpolated coverage. The richness curves continue to increase in the extrapolated portion, indicating that more OTUs could be captured if the number of samples was doubled. However, the Shannon and Simpson Inverse curves do not have as steep of a slope as the richness curves. These two curves represent the effective diversity, or the number of equally frequently detected OTUs required to generate the values of the indices at that point on the curve. Because these two curves do not increase as much as the richness curve, therefore, the additional OTUs which may be captured would appear in few samples and contribute little to diversity metrics other than richness. The amount of additional sampling to achieve 100% coverage would be more than double the actual sampling and would achieve minimal gains in diversity metrics other than richness across most factors. The curves for the samples from different elevation positions show less estimated coverage and steeper extrapolated portions (Fig. 2.11), indicating that there may be additional diversity to capture, though this is likely a consequence of the smaller sample size due to subdivision into five individual elevation positions when compared to other factors with fewer categories.

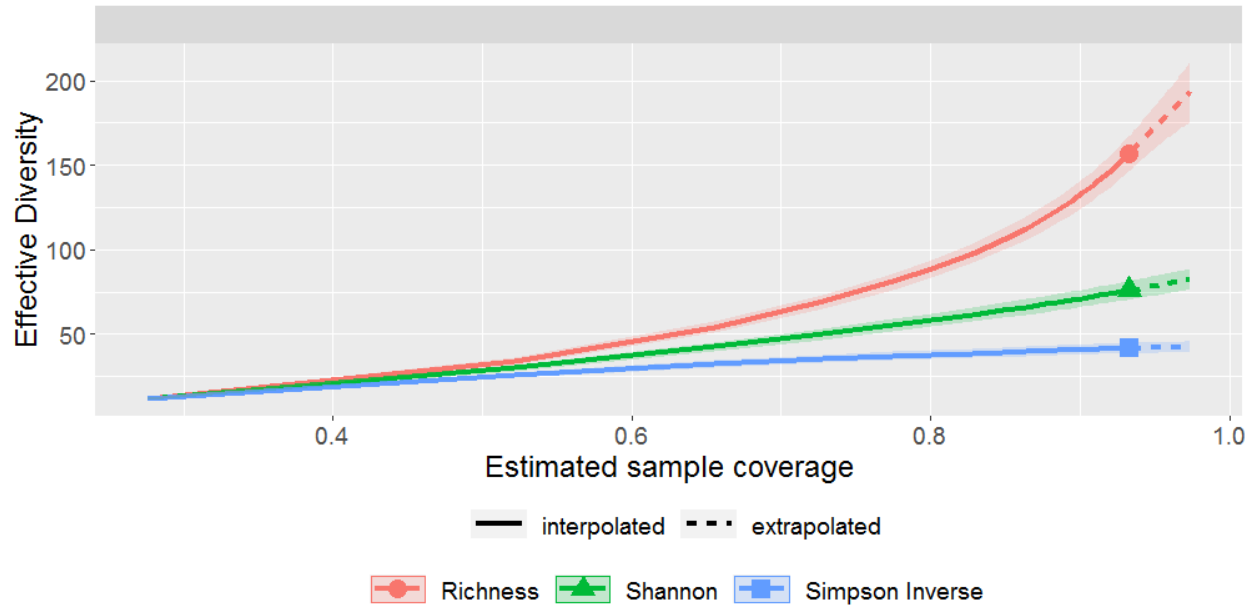


Fig. 2.8. Coverage-based rarefaction curves for the full dataset with effective diversity plotted for different metrics plotted against the number of samples collected from marsh islands surrounding Bay Jimmy, Louisiana from August 2017 to November 2017. Extrapolation extends out to the estimated coverage of twice the number of samples, and the shaded area around each curve represents the 95% confidence interval of the curve.

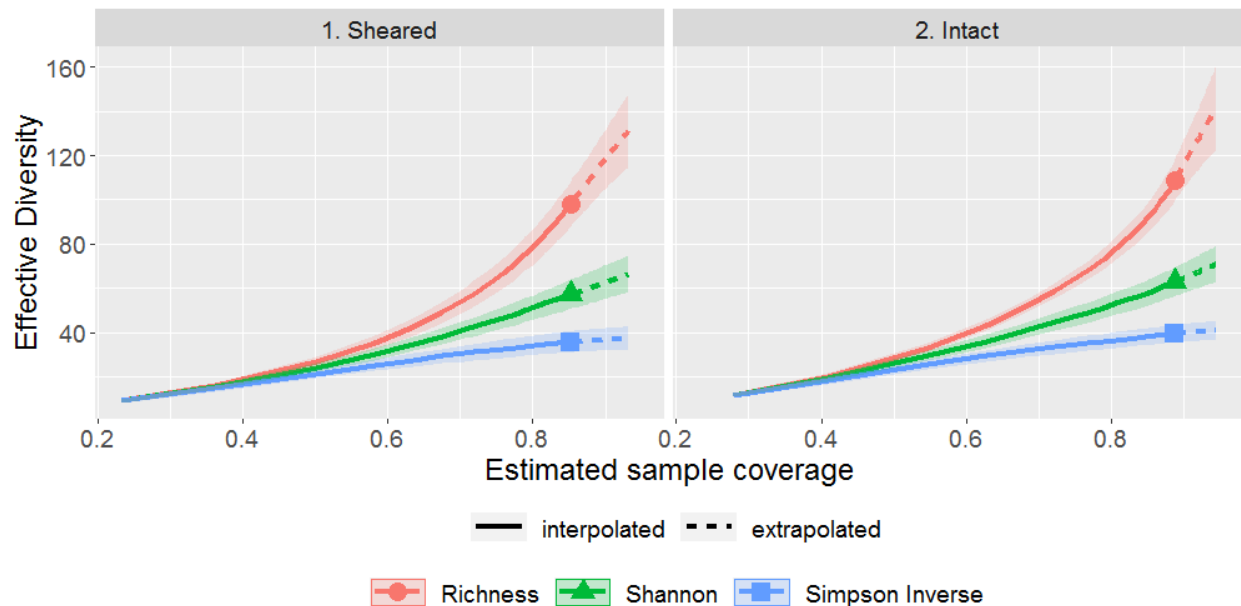


Fig. 2.9. Coverage-based rarefaction curves for samples from sheared and intact marsh margins with effective diversity for different metrics plotted against the number of samples collected from marsh islands surrounding Bay Jimmy, Louisiana from August 2017 to November 2017. Extrapolation extends out to the estimated coverage of twice the number of samples, and the shaded area around each curve represents the 95% confidence interval of the curve.

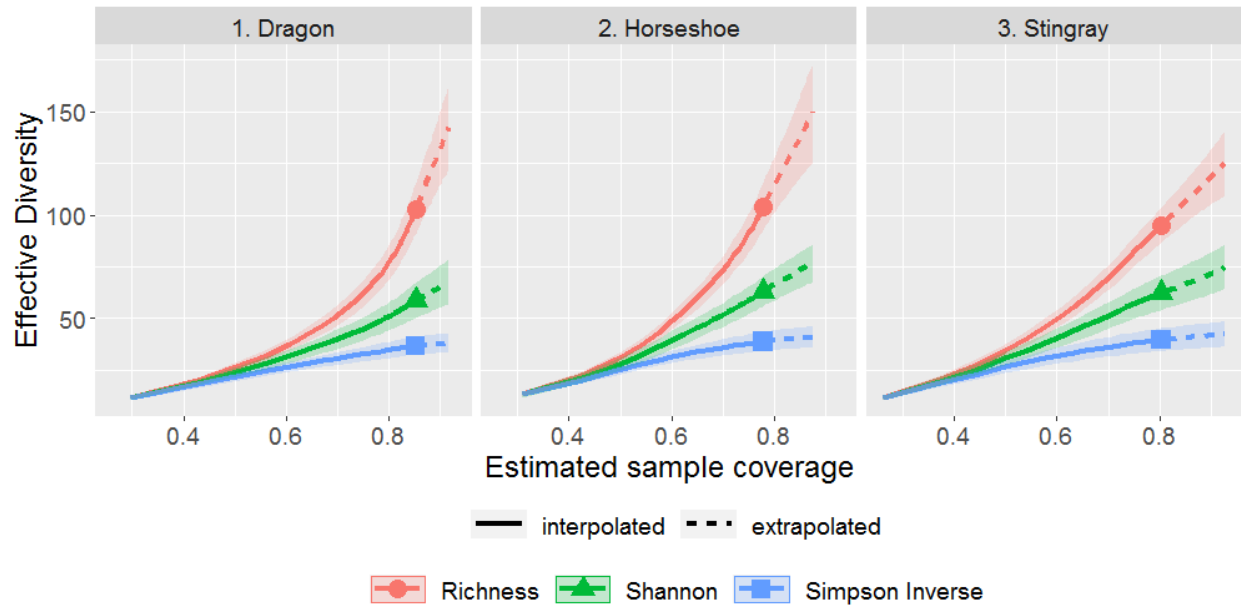


Fig. 2.10. Coverage-based rarefaction curves for samples from the different islands with effective diversity plotted for different metrics plotted against the number of samples collected from marsh islands surrounding Bay Jimmy, Louisiana from August 2017 to November 2017. Extrapolation extends out to the estimated coverage of twice the number of samples, and the shaded area around each curve represents the 95% confidence interval of the curve.

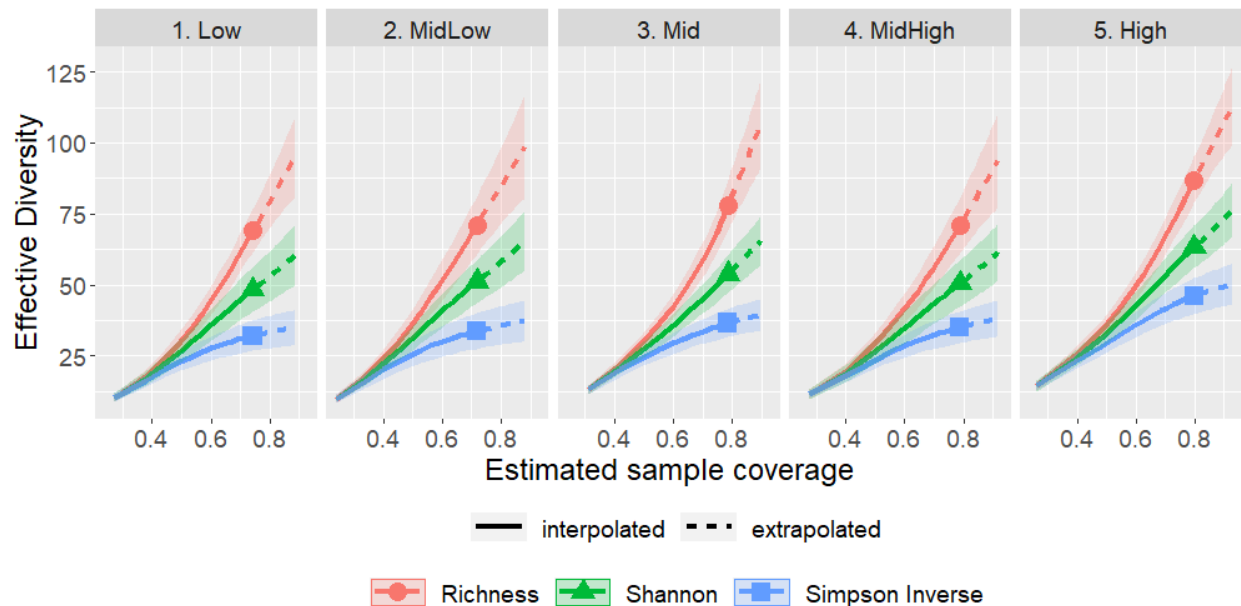


Fig. 2.11. Coverage-based rarefaction curves for samples from the different elevation positions with effective diversity for different metrics plotted against the number of samples collected from marsh islands surrounding Bay Jimmy, Louisiana from August 2017 to November 2017. Extrapolation extends out to the estimated coverage of twice the number of samples, and the shaded area around each curve represents the 95% confidence interval of the curve.

OTU diversity profile and richness estimations:

The coverage estimate (CE) for the whole dataset was high (93.4%) indicating that the majority of the taxa present in the actual community was likely detected (Table 2.9), matching the results from the coverage-based rarefaction (Fig. 2.8). However, estimated Coefficient of Variation (CV) was also moderately high (1.676, with a value of 2 or higher being considered extreme), indicating that the dataset was heterogeneous, with few OTUs appearing in most samples. This was likely because the majority of the taxa observed (139 of 157) fell into the infrequent group, which were taxa that are found in 10 samples or less. The 18 OTUs which did not fall into the infrequent group accounted for more than half of the total number of incidences in the dataset. The CE for the infrequent group was somewhat lower than the full dataset but still high (86%), indicating high coverage even for the infrequent group. The CV for this group was lower than the CV for the whole group, indicating a lower heterogeneity in the infrequent group.

Table 2.9. OTU diversity profile. Samples were collected from marsh islands surrounding Bay Jimmy, Louisiana from August 2017 to November 2017.

Observation/Estimation	Value
Number of samples	70
Total OTU Richness	157
Total number of incidences	835
Coverage estimate for entire dataset	0.93
Estimated coefficient of variation for entire dataset	1.70
Number of observed OTUs for frequent group	18
Total number for incidences in frequent group	438
Number of observed OTUs for infrequent group	139
Total number for incidences in infrequent group	397
Estimated sample coverage for infrequent group	0.86
Estimated coefficient of variation for infrequent group	0.73

The coverage estimate and coefficient of variation for the infrequent group ($n \leq 10$) are presented because they are used in the calculation of the Incidence-based Coverage Estimate (ICE) richness estimator model (Fig. 2.12).

The dataset was moderately heterogeneous but not extremely rich (fewer than 1000 OTUs according to Spade R manual); therefore, Chao2 (based on OTUs which appear in 2 samples or less), iChao2 (based on the OTUs which appear in 4 samples or less), and Incidence-based Coverage Estimator (ICE, based on the OTUs which appear in 10 samples or less) were likely the best estimators of the actual richness (Chao et al. 2015). In addition, the Homogenous

model, which estimates richness if all OTUs have an equal chance of being detected, is presented for comparison. The estimated actual richness falls into the range of 172 (lower bound of Homogenous model estimation) to 275 (upper bound of Chao2 model estimation) OTUs (Fig. 2.12). These estimations track with the richness curves of the sample-based rarefactions above (Fig. 2.4), which estimate that sampling twice as much could have captured over 200 OTUs. Comparing the Homogenous model, which estimates richness if all OTUs have an equal chance of being detected, with the other models, which base their estimations on the number of rarer OTUs in the dataset, showed that more OTUs were estimated when the rare OTUs were taken into consideration.

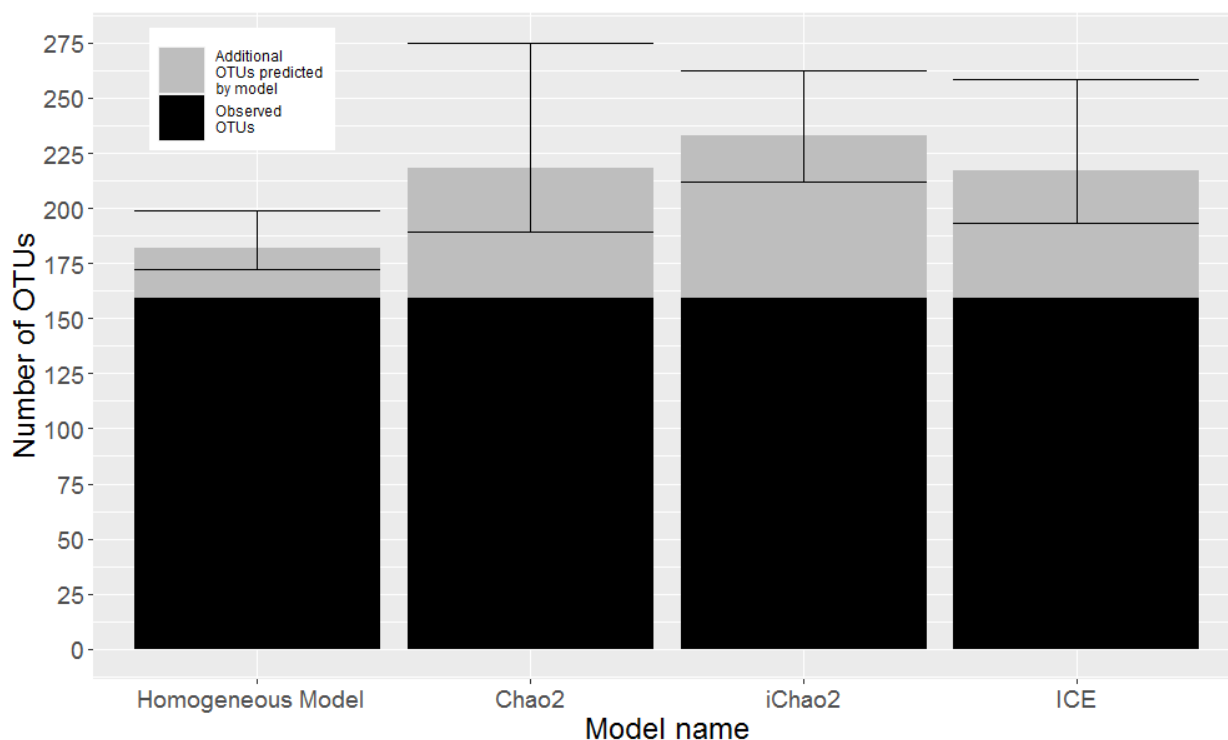


Fig. 2.12. Observed total OTU richness and incidence based OTU richness estimations from four estimator models. Samples were collected from marsh islands surrounding Bay Jimmy, Louisiana from August 2017 to November 2017. The lower portion of the columns in this chart is the observed OTU richness, while the upper portion of the columns represents additional OTU richness predicted by the different models. Error bars represent the 95% confidence interval of the estimate. The error bars represent the 95% confidence interval of the estimate.

Shared OTUs:

Seventy-eight of the 157 total detected OTUs were shared between the 109 OTUs for samples from sheared margins and the 126 OTUs for samples from intact margins (Table 2.10). All 18 OTUs of the frequent group (OTUs found in more than 10 samples, Table 2.13) were found in samples from both sheared and intact margins. Since only two classes are compared, the Chao2-shared estimate index can be used to estimate the number of shared species in the

actual community. Compared to the observed shared number of OTUs (78), the estimated number of shared OTUs in the actual community was nearly double (163 OTUs) with a wide 95% confidence interval ranging from 105 to 338 for the communities from sheared and intact margins. Given that this upper confidence interval is much higher than the estimated upper confidence interval of the number of OTUs in the dataset (Fig. 2.12), more than twice the number of samples collected would be required to reach observed richness equivalent to the estimated richness

Table 2.10. Shared and total number of OTUs for samples from sheared and intact margins which were collected from marsh islands surrounding Bay Jimmy, Louisiana from August 2017 to November 2017.

	Intact	Sheared
Intact	126 (18)	78 (18)
Sheared		109 (18)

The intersection of a single category (such as Sheared-Sheared) is the total number of OTUs for that elevation position, while the intersection of 2 categories (such as Sheared-Intact) is the number of OTUs shared between these two categories. Numbers in parenthesis are the number of frequent group OTUs in the category.

Island communities had an average of 99 OTUs with an average of 63 shared OTUs (Table 2.11), resulting in an average of 36 unique OTUs per island. In addition, 49 of the OTUs were shared between all three islands. On Dragon and Horseshoe Island, all 18 of the frequent group OTUs (Table 2.13) were present, while on Stingray Island 16 of the frequent group OTUs were present. Additionally, samples from Stingray Island had slightly fewer total OTUs than the samples from the other two Islands.

Table 2.11. Shared and total numbers of OTUs in the samples collected from different marsh island communities surrounding Bay Jimmy, Louisiana from August 2017 to November 2017.

	Dragon	Horseshoe	Stingray
Dragon	101 (18)	67 (18)	61 (16)
Horseshoe		102 (18)	60 (16)
Stingray			93 (16)

The intersection of a single category (such as Dragon-Dragon) is the total number of OTUs for that island, while the intersection of 2 categories (such as Dragon-Horseshoe) is the number of OTUs shared between these two categories. Numbers in parenthesis indicate the number of frequent group OTUs in the category.

Relative to elevation position, the average total of OTUs detected was 77 while the average of shared OTUs was 44 (Table 2.12), resulting in an average of 33 unique OTUs per elevation position. In Low, Mid, and High position samples, all 18 frequent group OTUs were present. In MidLow and MidHigh position samples, 17 of the frequent group OTUs were

present. Twenty-six of the OTUs were shared between all elevation positions. Samples from the Low elevation position had less total OTUs than the other elevations, and High position samples had the highest number of total OTUs. Samples from elevation positions which were closer together tended to share more OTUs.

Table 2.12. Shared and total numbers of OTUs in the samples from elevation position transect communities collected from marsh islands surrounding Bay Jimmy, Louisiana from August 2017 to November 2017.

	Low	MidLow	Mid	MidHigh	High
Low	69 (18)	43 (17)	41 (18)	43 (17)	39 (18)
MidLow		71 (17)	41 (17)	42 (16)	39 (17)
Mid			78 (18)	49 (17)	48 (18)
MidHigh				71 (17)	50 (17)
High					87 (18)

The intersection of a single category (such as High-High) is the total number of OTUs for that elevation position, while the intersection of 2 categories (such as High-MidHigh) is the number of OTUs shared between these two categories. Numbers in parenthesis indicate the number of frequent group OTUs in the category.

Taxa bar plots:

Nematoda were present in all samples, and Annelida, Arthropoda, and Mollusca were present in most samples (Fig. 2.13). The samples from Stingray Island were different than the other two islands at the phylum level with several samples lacking Mollusca and Arthropoda OTUs, especially in the MidHigh and High samples. Samples had an average of 6 ± 2 phyla, with a range of 2 to 11 phyla.

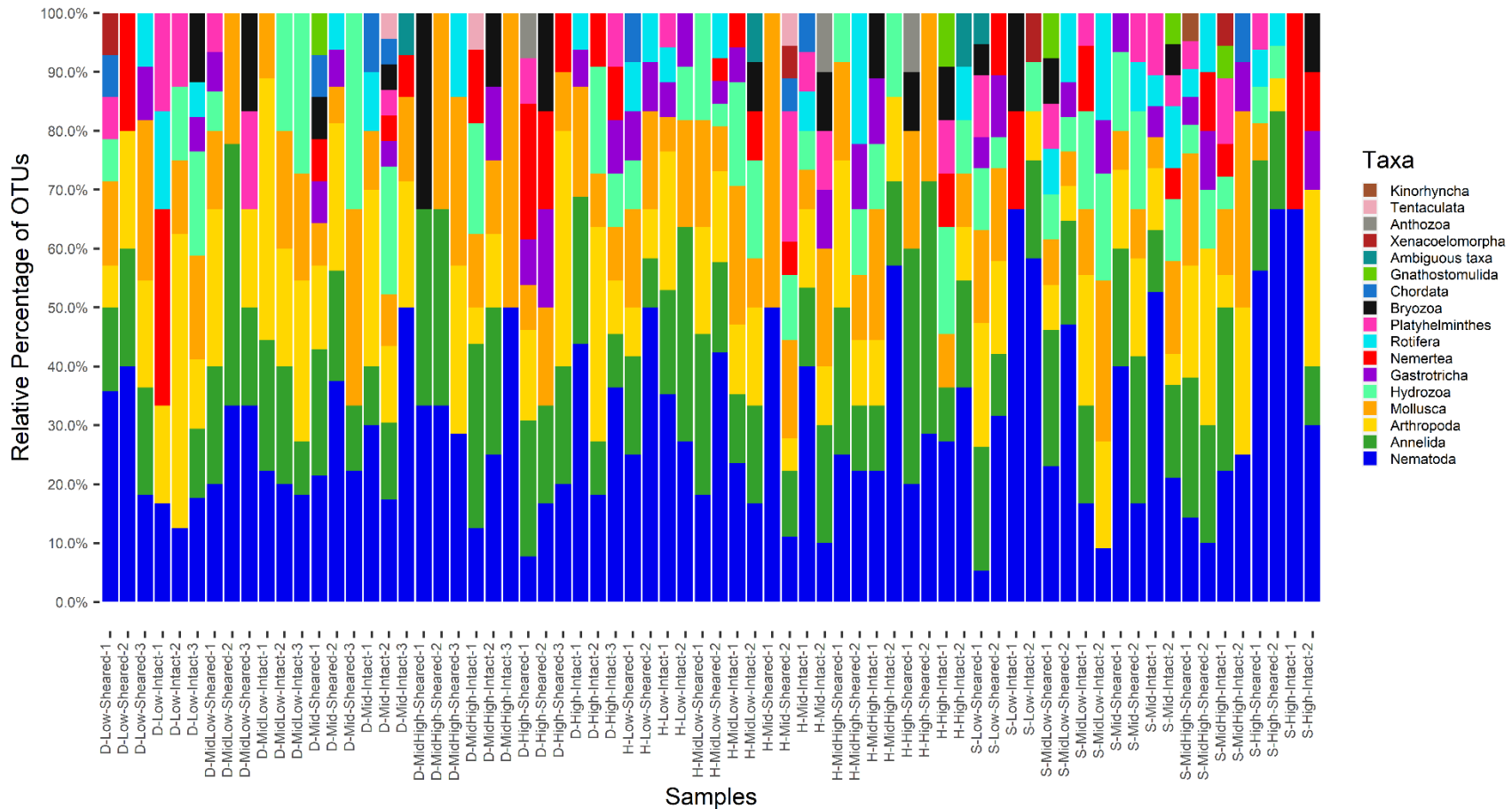


Fig. 2.13. Taxa bar plots of the 70 samples collected from marsh islands surrounding Bay Jimmy, Louisiana, from August 2017 to November 2017, with each colored section of the bar representing the relative proportion of the OTUs belonging to different phyla within that sample. Phyla are sorted within each bar by the overall highest to lowest relative percentage (from top to bottom). On the x-axis, Dragon (D), Horseshoe (H), and Stingray (S) represent the island which the sample is from, Low, MidLow, Mid, MidHigh, and High designate the elevation position, while Sheared and Intact indicate the margin type, and the number at the end of the sample designation on the x-axis represents the transect number.

Biodiversity within phyla

Phylum Nematoda made up the largest percentage of the 835 total incidences in the dataset, followed by Annelida, Arthropoda, Mollusca, and other phyla (Fig. 2.14), while Phylum Arthropoda made up the largest percentage of the total OTU richness of the dataset, followed by Nematoda, Annelida, Mollusca, and other groups (Fig. 2.15). Lowest level OTU assignments for metazoan OTUs ranged from the subkingdom clade “Bilateria” to the species level (Table 2.13). Accuracy of species level assignments is limited by both the resolution power of the 18S rRNA gene and by incomplete presence of taxa in databases, so closely related species have to be considered. The 18 OTUs which belonged to the frequent group were detected in a range of 11 to 64 samples. These OTUs consisted of 6 nematodes, 4 annelids, 2 arthropods, 2 hydrozoans, 2 mollusks, a gastrotrich, and a rotifer. The most commonly detected OTU was assigned to the nematode species *Thoracosoma trachygaster*, which appeared in 64 samples, followed by an OTU which was assigned to an ambiguous member of the superfamily Mytiloidea (phylum Mollusca) and appeared in 54 samples. The next two most common OTUs both were assigned to phylum Annelida, as *Polydora ciliata* in 49 samples and as *Alitta succinea* in 30 samples. Following these annelids, the next most common OTU was assigned to the genus *Heterolepidoderma* (phylum Gastrotricha) and appeared in 28 samples. The next two most common OTUs were both assigned to the phylum Nematoda, as an ambiguous member of the order Enoplida in 25 samples and an ambiguous member of the order Dorylaimida in 24 samples. Following these nematodes, the next most common OTU appeared in 22 samples and was assigned to the annelid species *Manayunkia aestuarina*. All four of the next most common OTUs were detected in 17 samples. These OTUs were assigned as *Helgicirrho cari* (phylum Hydrozoa), an ambiguous member of the order Siphonophorae (phylum Hydrozoa), *Nerita peloronta* (Mollusca), and an ambiguous member of the order Monhysterida (phylum Nematoda). The next two most common OTUs were both detected in 14 samples and were assigned to the arthropod *Cancrincola plumipes* and to an ambiguous member of the order Adinetida (phylum Rotifera). The next most common OTU was assigned to the nematode species *Pontonema vulgare* and was detected in 13 samples. The final three members of the frequent group were all detected in 11 samples, and were assigned as an ambiguous member of the annelid order Phyllodocida, the arthropod *Prorhinotermes simplex*, and the nematode *Diplolaimella dievengatensis*.

The assignments produced by GenBank and SILVA usually agreed, however, the taxonomic strings in GenBank were frequently more complete and were used to assign family level taxonomy to ambiguous lowest assignments from SILVA. Important taxa from the groups given new lowest or family level assignments included Naididae (Annelida, SILVA: ambiguous oligochaetes from several OTUs, present in 21.43% of 70 samples), Sipionidae (Annelida, SILVA: *Polydora ciliata*, present in 70% of samples) Leptosomatidae (Nematoda, SILVA: *Thoracosoma trachygaster*, present in 91.43% of samples), Mytilidae (Mollusca, SILVA: ambiguous Mytiloidea, present in 71.43% of samples), and *Reticulitermes flavipes* (Arthropoda, SILVA: *Prorhinotermes simplex*, present in 15.71% of samples). There were 18 *M. aestuarina* (Annelida) OTUs detected

in samples from Dragon Island, compared to four on Horseshoe and zero on Stingray. Conversely, Naididae (Annelida) OTUs were detected in samples from Stingray and Horseshoe Islands but not in samples from Dragon Island. Additionally, the Mytilidae (Mollusca) OTU (along with all mollusks) was absent from the several of the MidHigh and High samples from Stingray Island.

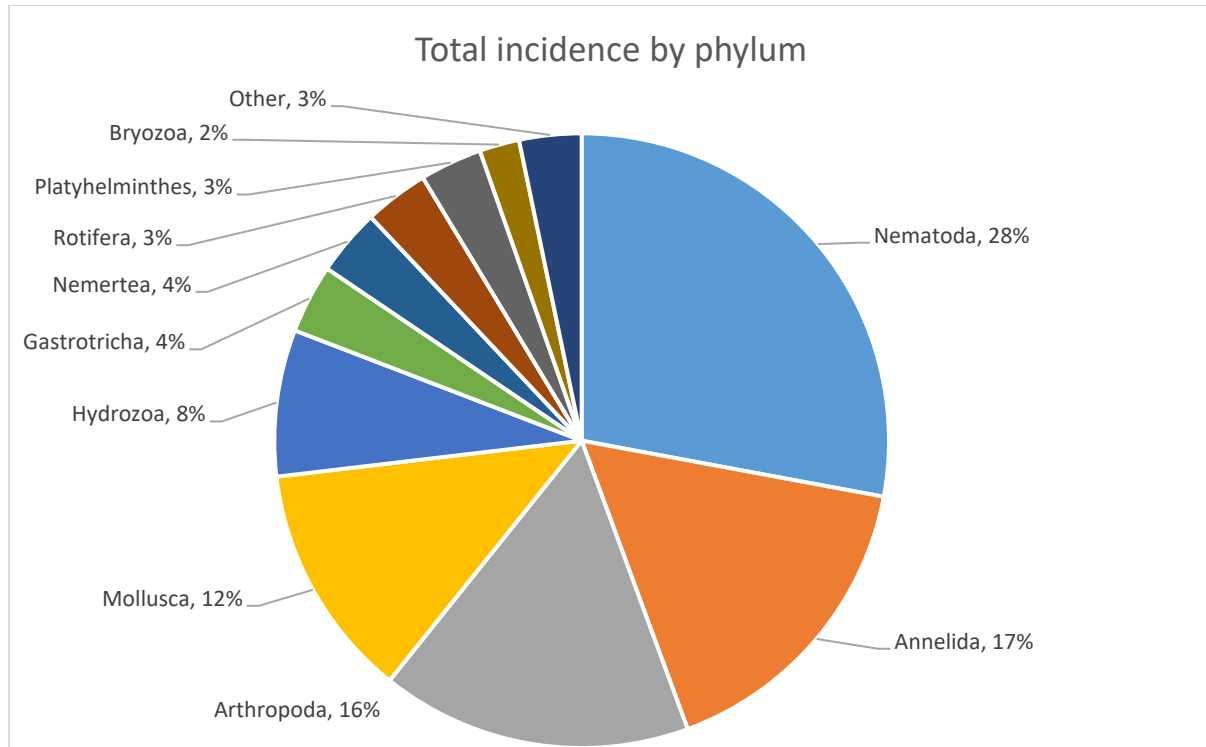


Fig. 2.14. Percentage of the 835 total OTU incidences by phylum level OTU assignment from samples collected from marsh islands surrounding Bay Jimmy, Louisiana, from August 2017 to November 2017. Phyla which individually made up less than 1% of the total incidence were combined into the “Other” category, which included Chordata, Gnathostomulida, Ambiguous taxa, Xenacoelomorpha, Anthozoa, Ctenophora, and Kinorhyncha in order of most to least percentage of the total incidence.

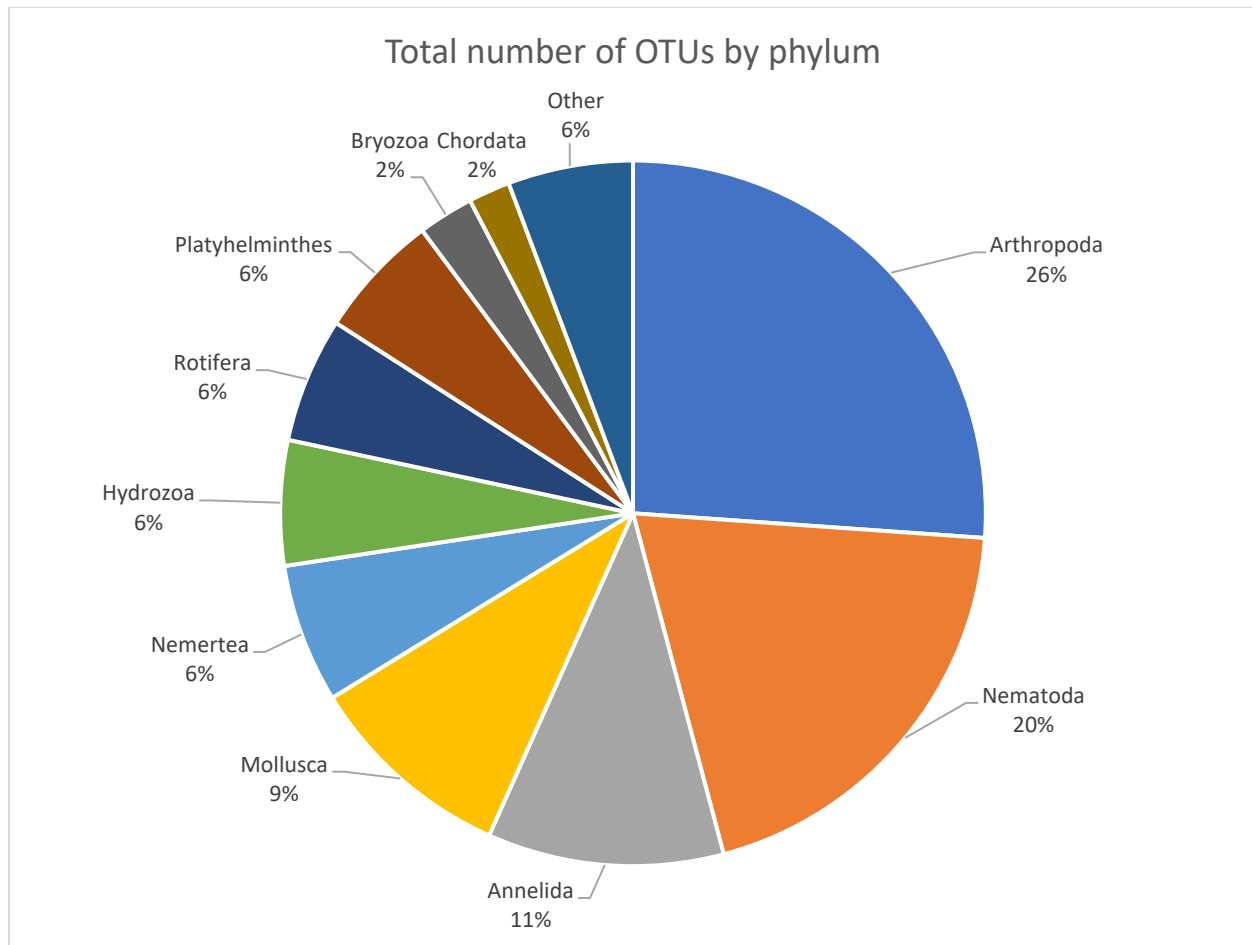


Fig. 2.15. Percentage of the 157 total OTUs per phylum assignment. Samples were collected from marsh islands surrounding Bay Jimmy, Louisiana from August 2017 to November 2017. Phyla which individually made up less than 1% of the total OTUs were combined into the “Other” category, which included Gastrotricha, Anthozoa, Gnathostomulida, Ambiguous taxa, Xenacoelomorpha, Ctenophora, and Kinorhyncha in order of most to least percentage of the total number of OTUs.

Table 2.13. Assignment of OTUs to phyla, orders and the lowest feasible level and OTU incidence. Samples were collected from marsh islands surrounding Bay Jimmy, Louisiana from August 2017 to November 2017.

Phylum	Order	OTU incidence	Lowest SILVA assignment	Top GenBank Match	Percent Identity	Accession	S	I	DI	HI	SI	L	ML	M	MH	H
Ambiguous taxa	-	4	Bilateria	<i>Macrostomum lignano</i> clone c100550_g1_i1	97.92%	KR132223.1	1	3	1	3	0	0	1	1	2	0
Annelida	Spionida	49	<i>Polydora ciliata</i>	<i>Polydora lingshuiensis</i>	99.31%	KF562236.1	26	23	20	15	14	11	7	11	11	9
	Phyllodocida	30	<i>Alitta succinea</i>	<i>Alitta succinea</i>	100.00%	AY210447.1	14	16	10	14	6	6	6	6	7	5
	Sabellida	22	<i>Manayunkia aestuarina</i>	<i>Manayunkia aestuarina</i>	97.71%	HM042108.1	11	11	18	4	0	4	3	5	4	6
	Polychaeta Incertae Sedis	11	Phyllodocida; metagenome	<i>Eteone longa</i>	97.67%	AF448155.1	6	5	4	6	1	2	0	3	2	4
	Haplotaxida	7	Haplotaxida	<i>Ainudrilus</i> sp. EKEH-2002	98.59%	AF411871.1	2	5	0	4	3	1	1	2	2	1
	Haplotaxida	5	Haplotaxida	<i>Lumbricillus dubius</i> isolate CE5221	97.22%	KU862790.1	2	3	0	0	5	0	0	1	2	2
	Polychaeta Incertae Sedis	3	<i>Polygordius jouinae</i>	<i>Polygordius jouinae</i>	96.53%	DQ153064.1	1	2	0	2	1	0	2	0	0	1
	Haplotaxida	2	<i>Olavius vacuus</i>	<i>Clitellio arenarius</i>	100.00%	AF411863.1	1	1	0	1	1	0	1	1	0	0
	Haplotaxida	2	Haplotaxida	<i>Enchytraeus albidus</i>	100.00%	GU453340.1	2	0	0	1	1	0	0	1	1	0
	Haplotaxida	2	Haplotaxida	<i>Olavius vacuus</i>	98.58%	AF411892.1	2	0	0	0	2	0	0	0	0	2
	Haplotaxida	2	Haplotaxida	Uncultured <i>Tubificina</i> clone Sey064	97.92%	AY605206.1	0	2	0	0	2	0	1	0	1	0
	Polychaeta Incertae Sedis	1	<i>Protodrilus hochbergi</i>	<i>Capitella</i> sp. FP-2009	97.92%	FN421417.1	0	1	1	0	0	0	0	0	0	1

(table cont'd.)

Phylum	Order	OTU incidence	Lowest SILVA assignment	Top GenBank Match	Percent Identity	Accession	S	I	DI	HI	SI	L	ML	M	MH	H
	Polychaeta Incertae Sedis	1	<i>Protodrilus</i> sp. 19 MDD-2014	<i>Glycinde armigera</i> isolate FS17	92.73%	KT989339.1	1	0	0	0	1	0	0	1	0	0
	Phyllodocida	1	<i>Namalycastis jaya</i>	<i>Notomastus hemipodus</i>	100.00%	HM746728.1	0	1	0	0	1	0	0	0	0	1
	Capitellida	1	Capitellida	<i>Phyllochaetopterus</i> sp. 2 KJO-2005	97.92%	DQ209216.1	1	0	0	0	1	0	1	0	0	0
	Phyllodocida	1	<i>Glycinde armigera</i>	<i>Protodrilus</i> sp. 19 MDD-2014	100.00%	KJ451219.1	1	0	0	1	0	0	1	0	0	0
	Capitellida	1	Capitellida	<i>Protodrilus</i> sp. 2 AM-2013	98.48%	JX402099.1	0	1	0	1	0	0	0	0	0	1
Total Annelida OTUs	17	141	-	-	-	-	70	71	53	49	39	24	23	31	30	33
Anthozoa	Actiniaria	2	Actiniaria	<i>Aiptasia pulchella</i>	100.00%	AY297437.1	1	1	1	0	1	0	1	0	1	0
	-	1	Ceriantharia	<i>Isarachnanthus maderensis</i> isolate SS33	100.00%	JX125657.1	0	1	0	0	1	1	0	0	0	0
Total Anthozoa OTUs	2	3	-	-	-	-	1	2	1	0	2	1	1	0	1	0
Arthropoda	Harpacticoida	14	<i>Cancrincola plumipes</i>	<i>Cancrincola plumipes</i>	97.24%	L81938.1	8	6	6	4	4	3	3	2	1	5
	Isoptera	11	<i>Prorhinotermes simplex</i>	<i>Reticulitermes flavipes</i>	97.93%	AY572861.1	5	6	5	2	4	2	3	3	0	3
	Tanaidacea	8	<i>Tanais dulongii</i>	<i>Tanais dulongii</i>	99.31%	AY781428.1	3	5	2	4	2	0	1	1	2	4
	Diptera	7	Diptera	<i>Bradysia hygida</i>	100.00%	JQ652461.1	4	3	1	4	2	3	1	0	2	1
	Podocopida	7	Podocopida	<i>Leptocythere lacertosa</i>	98.61%	AB076631.1	4	3	6	0	1	2	1	2	2	0

(table cont'd.)

Phylum	Order	OTU incidence	Lowest SILVA assignment	Top GenBank Match	Percent Identity	Accession	S	I	DI	HI	SI	L	ML	M	MH	H
	Sessilia	6	Sessilia	<i>Acropora granulosa</i>	100.00%	LT631075.1	4	2	3	2	1	1	1	1	1	2
	Podocopida	6	Podocopida; uncultured eukaryote	<i>Cythere lutea</i>	96.48%	AB076636.1	0	6	3	2	1	2	2	0	1	1
	Calanoida	5	Calanoida; uncultured eukaryote	<i>Formica exsecta</i>	99.31%	XR_003884956.1	3	2	2	1	2	1	1	1	1	1
	Hymenoptera	5	<i>Systropha curvicornis</i>	<i>Prorocentrum texanum</i>	99.32%	JQ390504.1	2	3	1	3	1	2	1	2	0	0
	Diptera	4	<i>Chrysops niger</i> (black deer fly)	<i>Chrysops niger</i>	98.78%	AF073889.1	2	2	2	1	1	1	0	2	1	0
	Eucarida	4	Eucarida	<i>Hemigrapsus takanoi</i>	98.62%	KC771054.1	3	1	4	0	0	0	0	2	1	1
	Blattodea	3	<i>Supella longipalpa</i> (brown-banded cockroach)	<i>Supella longipalpa</i>	100.00%	EF383467.1	2	1	1	1	1	2	1	0	0	0
	Hymenoptera	2	Hymenoptera	<i>Bulaea anceps</i> voucher BYU AG04	100.00%	FJ687667.1	1	1	1	1	0	1	1	0	0	0
	-	2	Collembola	<i>Chrysomya saffranae</i> voucher H2_ITS1	95.77%	MG594018.1	2	0	2	0	0	0	0	0	1	1
	Diptera	2	<i>Lipara lucens</i>	<i>Coquimba ishizakii</i>	97.92%	AB076645.1	0	2	0	1	1	0	1	0	1	0
	-	2	<i>Tetranychus urticae</i> (two-spotted spider mite)	<i>Tetranychus urticae</i>	100.00%	AF005458.1	2	0	1	1	0	1	0	0	0	1
	Zygentoma	2	<i>Lepisma</i> sp. GG-1997	<i>Lepisma</i> sp. GG-1997	96.91%	XR_003474831.1	0	2	1	1	0	0	0	1	1	0

(table cont'd.)

Phylum	Order	OTU incidence	Lowest SILVA assignment	Top GenBank Match	Percent Identity	Accession	S	I	DI	HI	SI	L	ML	M	MH	H
	Podocopida	2	<i>Coquimba ishizakii</i>	<i>Nasonia vitripennis</i>	98.58%	XR_004228347.1	0	2	1	1	0	0	1	0	1	0
	Sarcoptiformes	2	<i>Hemileius microclava</i>	<i>Tetranychus urticae</i>	98.61%	XR_003083727.1	1	1	1	0	1	0	0	1	0	1
	-	2	Acari	<i>Rostrozetes nebulosus</i>	99.30%	KR081633.1	1	1	0	1	1	0	0	1	0	1
	Hemiptera	2	Hemiptera	<i>Schizaphis graminum</i>	98.61%	AH003128.2	1	1	0	1	1	1	1	0	0	0
	Coleoptera	2	<i>Pristonema</i> sp. JAG-2009	<i>Stenacidia violacea</i> isolate 4A1a1_JC472	98.61%	KY230784.1	1	1	1	1	0	0	1	0	0	1
	Hemiptera	1	Hemiptera	<i>Acyrtosiphon pisum</i>	99.42%	AF487715.1	0	1	0	1	0	0	0	1	0	0
	Orthoptera	1	Orthoptera	<i>Blattella germanica</i>	98.63%	AF005243.2	1	0	0	0	1	0	1	0	0	0
	Psocoptera	1	<i>Liposcelis bostrychophila</i>	<i>Bombyx mori</i>	99.31%	DQ347470.1	0	1	1	0	0	1	0	0	0	0
	Hemiptera	1	Hemiptera	<i>Conocephalus longipennis</i> isolate gh242	99.29%	MH934186.1	1	0	0	1	0	1	0	0	0	0
	Diptera	1	<i>Drosophila sechellia</i>	<i>Conocephalus longipennis</i> isolate gh242	97.16%	MH934186.1	1	0	0	1	0	0	0	0	1	0
	Orthoptera	1	Orthoptera	<i>Eretmocerus</i> sp. WTT-2016 18S	98.58%	KX714966.1	1	0	0	1	0	0	0	0	0	1
	Dictyoptera	1	<i>Blattella germanica</i> (German cockroach)	<i>Friesia claviveta</i> isolate 8F1a1_JC360	98.57%	KY230727.1	0	1	0	1	0	0	0	0	0	1
	Lepidoptera	1	Lepidoptera	<i>Gryllus assimilis</i>	99.32%	KM853171.1	1	0	1	0	0	0	0	1	0	0
	-	1	Acari	<i>Laodelphax striatellus</i>	98.61%	AB085211.1	1	0	1	0	0	0	0	0	0	1

(table cont'd.)

Phylum	Order	OTU incidence	Lowest SILVA assignment	Top GenBank Match	Percent Identity	Accession	S	I	DI	HI	SI	L	ML	M	MH	H
	Hymenoptera	1	Hymenoptera	<i>Liposcelididae</i> sp. WH-21	98.60%	MK591059.1	0	1	1	0	0	1	0	0	0	0
	Poduromorpha	1	<i>Tetrodontophora bielanensis</i> (giant springtail)	<i>Litopenaeus setiferus</i> voucher KC6204	100.00%	JX403844.1	1	0	1	0	0	0	0	0	0	1
	-	1	Eucarida	<i>Malacotheirus monodactylus</i>	100.00%	KR081621.1	1	0	0	1	0	0	0	1	0	0
	-	1	Collembola; metagenome	<i>Parisotoma notabilis</i> isolate 2G1b1_JC436	99.28%	KY230771.1	0	1	0	0	1	0	1	0	0	0
	Hemiptera	1	<i>Acyrtosiphon pisum</i> (pea aphid)	<i>Podura aquatica</i>	97.22%	AF005452.1	1	0	0	1	0	0	1	0	0	0
	Poduromorpha	1	<i>Podura aquatica</i> (water springtail)	<i>Drosophila miranda</i>	99.31%	XR_004475045.1	0	1	0	1	0	0	0	0	0	1
	-	1	Acari	<i>R. nebulosa</i>	100.00%	X89495.1	1	0	0	0	1	0	0	1	0	0
	Diptera	1	Diptera	<i>Theridion californicum</i> isolate 2	100.00%	KX017248.1	0	1	0	1	0	0	0	1	0	0
	Araneae	1	<i>Triticum urartu</i>	<i>Trichocera brevicornis</i>	100.00%	KC177285.1	0	1	0	1	0	1	0	0	0	0
	Orthoptera	1	<i>Gryllus assimilis</i>	Uncultured eukaryote clone	98.61%	KY554502.1	0	1	1	0	0	1	0	0	0	0
Total Arthropoda OTUs	41	119	-	-	-	-	59	60	50	42	27	27	23	24	17	28
Bryozoa	Ctenostomatida	7	<i>Amathia verticillata</i>	<i>Amathia verticillata</i> voucher BRBRY-Z01	97.55%	KM373518.1	2	5	4	2	1	1	2	1	2	1
	Cheilostomatida	5	Cheilostomatida; uncultured eukaryote	<i>Adeona</i> sp. BLEED438	97.93%	MK894384.1	2	3	2	1	2	0	1	0	3	1

(table cont'd.)

Phylum	Order	OTU incidence	Lowest SILVA assignment	Top GenBank Match	Percent Identity	Accession	S	I	DI	HI	SI	L	ML	M	MH	H
	Cheilostomatida	5	<i>Smittoidea spinigera</i>	<i>Smittoidea spinigera</i>	97.93%	AF499746.1	1	4	0	2	3	3	1	0	1	0
	Cheilostomatida	1	<i>Electra pilosa</i>	Uncultured eukaryote clone	97.53%	FJ153776.2	0	1	1	0	0	1	0	0	0	0
Total Bryozoa OTUs	4	18	-	-	-	-	5	13	7	5	6	5	4	1	6	2
Chordata	Stolidobranchia	6	Stolidobranchia	<i>Molgula manhattensis</i>	100.00%	L12426.2	5	1	4	0	2	1	2	3	0	0
	Copelata	1	Oikopleuridae	Uncultured eukaryote clone	100.00%	KJ763355.1	0	1	0	1	0	0	0	0	0	1
	Copelata	1	Oikopleuridae; uncultured metazoan	Uncultured metazoan clone RS.12f.10m.381	100.00%	KC582967.1	0	1	0	0	1	1	0	0	0	0
Total Chordata OTUs	3	8	-	-	-	-	5	3	4	1	3	2	2	3	0	1
Ctenophora	-	3	Tentaculata	Uncultured eukaryote clone SGYP870	100.00%	KJ763915.1	3	0	1	1	1	0	2	1	0	0
Gastrotricha	Chaetonotida	28	<i>Heterolepidoderma</i> sp. 1 TK-2012	<i>Heterolepidoderma sinus</i> voucher ZH_1.79	98.55%	MK302474.1	13	15	13	8	7	5	3	8	5	7
	Macrodasyida	3	<i>Tetranchyroderma</i> sp. MVS-2005	<i>Tetranchyroderma</i> sp. MVS-2005	99.20%	DQ079911.1	1	2	0	2	1	0	2	0	1	0
Total Gastrotricha OTUs	2	31	-	-	-	-	14	17	13	10	8	5	5	8	6	7

(table cont'd.)

Phylum	Order	OTU incidence	Lowest SILVA assignment	Top GenBank Match	Percent Identity	Accession	S	I	DI	HI	SI	L	ML	M	MH	H
Gnathostomulida	Filospermoidea	5	<i>Haplognathia ruberrima</i>	<i>Haplognathia ruberrima</i>	100.00%	DQ079930.1	1	4	1	2	2	1	0	0	2	2
Hydrozoa	Leptothecata	17	<i>Helgicirra cari</i>	<i>Helgicirra cari</i> isolate MHNG-HYD-DNA1153	98.45%	KY363989.1	10	7	6	11	0	2	2	4	4	5
	Siphonophorae	17	Siphonophorae; uncultured eukaryote	Uncultured eukaryote clone SGYY874	100.00%	KJ757655.1	10	7	7	4	6	1	2	3	4	7
	Anthoathecata	9	Anthoathecata	<i>Moerisia</i> sp. AGC-2001	100.00%	AF358083.1	9	0	8	0	1	0	2	2	3	2
	Siphonophorae	9	Siphonophorae; uncultured eukaryote	Uncultured eukaryote clone SGYP774	100.00%	KJ763890.1	6	3	6	1	2	2	1	3	1	2
	Leptothecata	8	<i>Blackfordia virginica</i>	<i>Blackfordia virginica</i>	100.00%	AF358078.1	4	4	3	3	2	2	1	4	1	0
	Leptothecata	3	<i>Blackfordia virginica</i>	<i>Blackfordia virginica</i> voucher LEM m3x S42	100.00%	KT722387.1	2	1	2	1	0	1	2	0	0	0
	Leptothecata	1	Leptothecata	<i>Clytia</i> sp. AGC-2001	95.83%	AF358074.1	1	0	1	0	0	0	1	0	0	0
	Limnomedusae	1	Limnomedusae	<i>Maeotias marginata</i>	100.00%	AF358056.1	1	0	0	0	1	1	0	0	0	0
	Leptothecata	1	<i>Gonothyrea loveni</i>	<i>Gonothyrea loveni</i> voucher MZUSP:2803	97.40%	KX665455.1	1	0	0	1	0	1	0	0	0	0
Total Hydrozoa OTUs	9	66	-	-	-	-	44	22	33	21	12	10	11	16	13	16
Kinorhyncha	Echinorhagata	1	<i>Echinoderes hwiizaa</i>	<i>Echinoderes lanceolatus</i>	95.83%	GQ229038.1	1	0	0	1	0	0	0	0	0	1

(table cont'd.)

Phylum	Order	OTU incidence	Lowest SILVA assignment	Top GenBank Match	Percent Identity	Accession	S	I	DI	HI	SI	L	ML	M	MH	H
Mollusca	Mytiloida	54	Mytiloida	<i>Geukensia demissa</i>	100.00%	L33450.1	30	24	24	16	14	10	11	14	11	8
	Cycloneritida	17	<i>Nerita peloronta</i>	<i>Theodoxus fluviatilis</i>	100.00%	AF120515.1	7	10	5	11	1	4	3	4	3	3
	Veneroida	8	Veneroida	<i>Spisula subtruncata</i>	97.92%	L11271.1	5	3	7	1	0	2	1	2	2	1
	Veneroida	5	<i>Corbicula fluminea</i>	<i>Corbicula fluminea</i> clone CF046	99.30%	KT220186.1	2	3	2	1	2	0	2	1	0	2
	Siphonariida	4	<i>Siphonaria algesirae</i>	<i>Siphonaria japonica</i>	100.00%	KX529884.1	1	3	2	1	1	1	1	2	0	0
	Ostreida	3	Ostreoida	<i>Crassostrea gigas</i>	100.00%	AB064942.1	3	0	1	1	1	0	0	1	0	2
	Littorinimorpha	3	<i>Tectarius striatus</i>	<i>L. undulata</i>	97.93%	Y11756.1	1	2	1	2	0	0	0	0	1	2
	Stylommatophora	3	<i>Alinda biplicata</i>	<i>Systrophia</i> sp. sys	100.00%	MN022715.1	1	2	2	1	0	1	1	0	0	1
	Veneroida	2	Veneroida	<i>Cylichna cylindracea</i> isolate 2	99.29%	DQ923453.1	1	1	0	1	1	1	0	0	1	0
	-	2	Heterobranchia	<i>Soletellina diphos</i> clone 2	99.28%	KX495220.1	0	2	1	1	0	0	0	0	0	2
	Veneroida	1	Veneroida	<i>Cingulina</i> sp. EED-Phy-915	97.16%	GU331940.1	1	0	1	0	0	1	0	0	0	0
	Mytiloida	1	<i>Perna viridis</i>	<i>Melampus pulchellus</i> isolate PR1931	99.31%	KM280982.1	0	1	1	0	0	0	0	0	1	0
	-	1	<i>Cingulina</i> sp. EED-Phy-915	<i>Perna canaliculus</i> isolate N3	98.60%	MK419109.1	1	0	0	0	1	0	0	1	0	0
	Nudibranchia	1	<i>Notaeolidia depressa</i>	<i>Spisula subtruncata</i>	97.22%	L11271.1	0	1	0	1	0	0	0	0	0	1
	-	1	Heterobranchia	<i>Unidentia angelvaldesi</i> isolate SRR3726696	97.16%	MK088235.1	1	0	0	1	0	0	0	1	0	0

(table cont'd.)

Phylum	Order	OTU incidence	Lowest SILVA assignment	Top GenBank Match	Percent Identity	Accession	S	I	DI	HI	SI	L	ML	M	MH	H
Total Mollusca OTUs	15	106	-	-	-	-	54	52	47	38	21	20	19	26	19	22
Nematoda	Enoplida	64	<i>Thoracostoma trachygaster</i>	Leptosomatidae sp. 2 AAS-2018	97.16%	MK007581.1	33	31	26	19	19	13	13	13	12	13
	Enoplida	25	Enoplida	Uncultured eukaryote clone Pink_A05	100.00%	GQ483737.1	8	17	12	3	10	1	2	6	7	9
	Dorylaimida	24	Dorylaimida	<i>Tylencholaimus</i> sp. PDL-2005	97.86%	AJ966510.1	9	15	10	9	5	4	5	7	3	5
	Monhysterida	17	Monhysterida	<i>Daptonema</i> sp. 1255	100.00%	FJ040463.1	12	5	10	5	2	3	2	4	4	4
	Enoplida	13	<i>Pontonema vulgare</i>	Uncultured eukaryote clone Plate2-51-M13R_A06.ab1	97.24%	KU757347.1	5	8	4	3	6	4	3	2	2	2
	Monhysterida	11	<i>Diplolaimella dievengatensis</i>	<i>Diplolaimella dievengatensis</i>	99.24%	AJ966482.1	5	6	8	1	2	1	4	4	1	1
	Tylenchida	10	<i>Filenchus hamuliger</i>	<i>Filenchus</i> sp. 4 TJP-2012	100.00%	JQ814878.1	3	7	3	0	7	0	1	3	4	2
	Monhysterida	9	Monhysterida	<i>Daptonema</i> sp. PFN-2007	97.06%	EF436228.1	3	6	4	3	2	2	2	3	1	1
	Dorylaimida	8	Dorylaimida	Eimeriidae environmental sample clone Elev_18S_1534	100.00%	EF024986.1	4	4	1	4	3	0	0	2	2	4
	Araeolaimida	6	Araeolaimida	<i>Deontolaimus</i> sp. PaApSp	99.17%	FJ969132.1	1	5	3	1	2	0	1	3	1	1

(table cont'd.)

Phylum	Order	OTU incidence	Lowest SILVA assignment	Top GenBank Match	Percent Identity	Accession	S	I	DI	HI	SI	L	ML	M	MH	H
	Chromadorida	6	<i>Paracyatholaimus intermedius</i>	<i>Paracyatholaimus intermedius</i>	97.14%	AJ966495.1	3	3	1	2	3	0	0	2	3	1
	Monhysterida	6	<i>Diplolaimelloides</i> environmental sample	Uncultured <i>Diplolaimelloides</i> clone GD1D11P	100.00%	EF659925.1	4	2	1	1	4	0	0	2	2	2
	Tylenchida	5	<i>Aglenchus agricola</i>	<i>Aglenchus agricola</i> strain AgleAgr1	100.00%	FJ969113.1	4	1	1	1	3	1	0	1	1	2
	Monhysterida	5	Phrynidae environmental sample	Phrynidae environmental sample clone Amb_18S_868	97.12%	EF023624.1	5	0	2	1	2	0	0	1	2	2
	Dorylaimida	4	Dorylaimida	<i>Pungentus</i> sp. PDL-2005	97.14%	AJ966501.1	3	1	1	1	2	0	0	1	1	2
	Rhabditida	3	<i>Meloidogyne incognita</i> (southern root-knot nematode)	<i>Meloidogyne naasi</i> isolate 1014\3825\Sing\m\graminis\2	97.32%	EU910049.1	0	3	1	2	0	0	1	0	1	1
	Dorylaimida	3	Dorylaimida	<i>Tylencholaimus</i> sp. PDL-2005	97.14%	AJ966510.1	2	1	3	0	0	1	1	0	1	0
	Dorylaimida	2	Dorylaimida	<i>Ditylenchus persicus</i> isolate AA15_1	97.58%	KX463286.1	1	1	0	1	1	0	0	1	1	0
	Tylenchida	2	Tylenchida	<i>Helicotylenchus dihystra</i> isolate BH524	100.00%	JX207113.1	1	1	2	0	0	0	0	0	0	2
	Araeolaimida	2	Araeolaimida; metagenome	<i>Pellioditis mediterranea</i>	100.00%	AF083020.1	2	0	1	0	1	1	0	0	0	1
	Tylenchida	2	Tylenchida	<i>Pratylenchus hippeastri</i> isolate SD53	100.00%	KY424237.1	2	0	0	0	2	0	0	0	0	2

(table cont'd.)

Phylum	Order	OTU incidence	Lowest SILVA assignment	Top GenBank Match	Percent Identity	Accession	S	I	DI	HI	SI	L	ML	M	MH	H
	Rhabditida	2	Rhabditida	<i>Tylencholaimus</i> sp. PDL-2005	97.86%	AJ966510.1	1	1	1	0	1	0	0	1	1	0
	Tylenchida	2	Tylenchida	Uncultured eukaryote clone Ha2_mtz_A01	100.00%	FJ611061.1	2	0	0	0	2	0	0	0	0	2
	Tylenchida	1	<i>Parasitylenchus bifurcatus</i>	<i>Anguina obesa</i> isolate Female1	98.55%	KX385107.1	0	1	0	1	0	0	0	1	0	0
	Tylenchida	1	Tylenchida	<i>Mesodorylaimus japonicus</i>	97.14%	AJ966489.1	1	0	0	1	0	0	0	0	1	0
	Dorylaimida	1	Dorylaimida	<i>Panagrolaimus</i> cf. rigidus AF40	100.00%	DQ285636.1	1	0	0	0	1	0	0	0	0	1
	Dorylaimida	1	<i>Mesodorylaimus japonicus</i>	<i>Parasitylenchus bifurcatus</i>	100.00%	LT629307.1	1	0	0	1	0	0	0	1	0	0
	Triplonchida	1	Triplonchida	<i>Paratylenchus aculeatus</i> isolate HN55	98.56%	KR270603.1	1	0	0	0	1	0	0	0	0	1
	Rhabditida	1	<i>Panagrolaimus</i> cf. rigidus AF40	<i>Pungentus</i> sp. PDL-2005	99.29%	AJ966501.1	1	0	0	1	0	0	0	1	0	0
	Desmodorida	1	<i>Spirinia elongata</i>	<i>Spirinia elongata</i>	98.58%	EF527426.1	0	1	1	0	0	0	0	0	0	1
	Tylenchida	1	Tylenchida	Uncultured eukaryote clone Ha3_mtz25_G06	98.61%	EU740649.1	0	1	1	0	0	0	0	0	0	1
Total Nematoda OTUs	31	239	-	-	-	-	118	121	97	61	81	31	35	59	51	63
Nemertea	Monostilifera	8	Monostilifera	<i>Ototyphlonemertes pallida</i> sp. MCZ IZ 133745	98.44%	KF935329.1	1	7	2	2	4	1	2	1	1	3

(table cont'd.)

Phylum	Order	OTU incidence	Lowest SILVA assignment	Top GenBank Match	Percent Identity	Accession	S	I	DI	HI	SI	L	ML	M	MH	H
	-	4	<i>Cephalothrix</i> cf. alba MCZ IZ 45638	<i>Cephalothrix</i> cf. alba MCZ IZ 45638	100.00%	KP270792.1	4	0	1	1	2	0	1	2	0	1
	-	4	Palaeonemertea	<i>Carinoma</i> sp. SA-2011	99.22%	KF935278.1	3	1	2	2	0	0	1	2	0	1
	Heteronemertea	3	Heteronemertea	<i>Lineus sanguineus</i> isolate LINSa_veg_boat	100.00%	MK076334.1	1	2	1	1	1	1	0	0	2	0
	Monostilifera	3	Monostilifera	<i>Pantionemertes californiensis</i> isolate PROca_coos	100.00%	MK076307.1	1	2	2	0	1	2	1	0	0	0
	Monostilifera	3	Monostilifera	<i>Tetrastemma melanocephalum</i> isolate T20	97.22%	AY928365.1	2	1	1	2	0	0	0	0	1	2
	Anopla	2	<i>Cephalothrix queenslandica</i>	<i>Cephalothrix queenslandica</i>	97.92%	AY238989.1	2	0	1	1	0	0	2	0	0	0
	Monostilifera	1	Monostilifera	<i>Zygonemertes virescens</i> voucher MCZ DNA105575	100.00%	JF293016.1	1	0	0	0	1	0	1	0	0	0
	Monostilifera	1	<i>Ototyphlonemertes correae</i>	<i>Pantionemertes californiensis</i> isolate PROca_coos	95.77%	MK076307.1	1	0	0	0	1	0	1	0	0	0
	Monostilifera	1	<i>Prostoma eilhardi</i>	<i>Prostoma</i> cf. eilhardi EEZ-2018 isolate PROei_bost	100.00%	MK076304.1	1	0	0	1	0	0	0	1	0	0
Total Nemertea OTUs	10	30	-	-	-	-	17	13	10	10	10	4	9	6	4	7
Platyhelminthes	Neodalyellida	8	<i>Promesostoma</i> sp. WW-2004	<i>Promesostoma</i> sp. WW-2004	96.60%	AY775763.1	5	3	3	3	2	2	0	1	2	3

(table cont'd.)

Phylum	Order	OTU incidence	Lowest SILVA assignment	Top GenBank Match	Percent Identity	Accession	S	I	DI	HI	SI	L	ML	M	MH	H
	Rhabdocoela	5	<i>Litucivis serpens</i>	<i>Litucivis serpens</i>	96.58%	AY775758.1	1	4	1	3	1	0	0	1	1	3
	Macrostomida	3	Macrostomida	<i>Macrostomum hystricinum</i>	97.20%	AF051329.1	2	1	1	0	2	1	1	1	0	0
	Prolecithophora	3	<i>Plagiosomum ochroleucum</i>	<i>Plagiosomum ochroleucum</i>	97.06%	AF065419.1	1	2	1	1	1	0	0	1	1	1
	Rhabdocoela	3	<i>Phaenocora unipunctata</i>	<i>Phaenocora unipunctata</i>	100.00%	AY775762.1	1	2	2	0	1	0	0	1	0	2
	Polycladida	2	Polycladida	<i>Leptoplana tremellaris</i> isolate	97.74%	MN421937.1	1	1	1	1	0	1	1	0	0	0
	Rhabdocoela	2	<i>Placorhynchus dimorphus</i>	<i>Placorhynchus dimorphus</i> voucher EXT663	98.59%	KJ887409.1	2	0	1	0	1	0	0	2	0	0
	Rhabdocoela	1	<i>Typhlopolecystis</i> sp. TJ-2014	<i>Typhlopolecystis</i> sp. TJ-2014 voucher DNA035HAW	97.89%	KJ887427.1	0	1	1	0	0	1	0	0	0	0
	Polycladida	1	<i>Boninia divae</i>	Uncultured eukaryote clone 28a	96.60%	FJ153784.2	0	1	0	0	1	1	0	0	0	0
Total Platyhelminthes OTUs	9	28	-	-	-	-	13	15	11	8	9	6	2	7	4	9
Rotifera	-	14	Adinetida; metagenome	<i>Adineta vaga</i>	97.16%	GQ398061.1	4	10	6	2	6	2	1	4	3	4
	Flosculariacea	7	<i>Testudinella clypeata</i>	<i>Testudinella clypeata</i> isolate A758_T4	99.26%	KF561109.1	4	3	5	1	1	1	0	2	2	2
	Bdelloida	2	Adinetida; metagenome	Uncultured bacterium clone contig115446	97.89%	KP428754.1	2	0	0	2	0	0	1	1	0	0

(table cont'd.)

Phylum	Order	OTU incidence	Lowest SILVA assignment	Top GenBank Match	Percent Identity	Accession	S	I	DI	HI	SI	L	ML	M	MH	H
	Ploimida	1	Ploimida; invertebrate environmental sample	<i>Synchaeta</i> sp. YW-2019 isolate 4-3	97.22%	MK644612.1	1	0	1	0	0	0	1	0	0	0
	Flosculariacea	1	Flosculariacea	<i>Filinia terminalis</i> isolate 201	97.92%	MK352482.1	1	0	1	0	0	0	0	0	0	1
	Adinetida	1	Bdelloidea environmental sample	Uncultured bdelloid rotifer clone Rot_H_08A	99.22%	GQ922289.1	1	0	0	0	1	0	0	0	0	1
	Flosculariacea	1	<i>Ptygura libera</i>	<i>Filinia terminalis</i> isolate 201	96.25%	MK352482.1	1	0	1	0	0	0	0	0	1	0
	Ploimida	1	Ploimida	<i>Synchaeta</i> sp. YW-2019 isolate 4-3	96.88%	MK644612.1	0	1	1	0	0	0	0	0	0	1
	Ploimida	1	Ploimida	<i>Lecane inermis</i> isolate	99.31%	KY859765.1	1	0	0	1	0	0	0	0	0	1
Total Rotifera OTUs	9	29	-	-	-	-	15	14	15	6	8	3	3	7	6	10
Xenacoelom orpha	Acoela	4	<i>Atriofronta polyvacuola</i>	<i>Atriofronta polyvacuola</i>	97.24%	AF102895.1	3	1	1	1	2	1	0	1	1	1

Any OTU with a “-” in the order column was ambiguous at the order level for the SILVA taxonomy assignment. The OTUs in white are members of the frequent group of OTUs which appeared in more than 10 samples in the dataset, while the OTUs shaded in gray are part of the infrequent group which appeared in 10 samples or less. OTU incidence is further broken down by category, i.e., samples from Sheared (S) and Intact (I) margins, from Dragon (DI), Horseshoe (HI), and Stingray Island (SI), and at the Low (L), MidLow (ML), Mid (M), MidHigh (MH), and High (H) elevation transect positions.

Unique taxa of the different margin types and on the different islands:

Certain taxa were only detected in the samples from either the sheared or intact margins (Table 2.14) and thus have an impact on beta diversity indices which rely on the ratio of shared OTUs to total OTUs. The OTUs which were unique to the samples from intact margins included four arthropods, one annelid, one mollusk, and one nematode. The four arthropod OTUs were assigned to two ostracods (order Podocopida) and two hexapods, one in the order Diptera and one in the order Zygentoma. The lone annelid was assigned to a member of the order Haplotaxida in the subclass Oligochaeta, with the GenBank assignment indicating that it was likely a member of the family Naididae, which contains all of the former Tubificidae. The only mollusk OTU unique to this category was assigned to the subclass Heterobranchia, which falls under the class Gastropoda. Finally, the only nematode unique to this category was assigned to the genus *Meloidogyne*, which are plant parasites. The OTUs which were unique to the samples from sheared margins included four nematodes, two annelids, two arthropods, two nemerteans, one hydrozoan, one platyhelminthes, one rotifer, and one member of the Tentaculata. Two of the nematode OTUs were assigned to the order Tylenchida, while the other two were assigned to the orders Araeolaimida and Monhysterida. Both of the annelid OTUs were assigned to members of the order Haplotaxida. The two arthropod OTUs were assigned to a member of the order Collembola and a member of the subclass Acari. Both of the nemertean OTUs were assigned to members of the genus *Cephalothrix*. The lone hydrozoan OTU which unique to this category was assigned to the order Anthoathecata, while the lone mollusk OTU was assigned to the genus *Crassostrea*. The only member of Platyhelminthes which was unique to the samples from sheared margins was assigned to the genus *Placorhynchus*. The lone rotifer OTU was assigned to the order Bdelloida, and the only Tentaculata OTU had an ambiguous assignment bellow the phylum level.

Table 2.14. Unique OTUs in the samples from sheared and intact margins.

Phylum	Order	Lowest SILVA assignment	Top GenBank Match	S	I
Annelida	Haplotaxida	Haplotaxida	Uncultured Tubificina clone Sey064	0	2
Arthropoda	Diptera	Lipara lucens	Coquimba ishizakii	0	2
Arthropoda	Podocopida	Podocopida;uncultured eukaryote	Cythere lutea	0	6
Arthropoda	Podocopida	Coquimba ishizakii	Nasonia vitripennis	0	2
Arthropoda	Zygentoma	Lepisma sp. GG-1997	Lepisma sp. GG-1997	0	2
Mollusca	-	Heterobranchia	Soletellina diphos clone 2	0	2
Nematoda	Rhabditida	Meloidogyne incognita	Meloidogyne naasi isolate	0	3
Annelida	Haplotaxida	Haplotaxida	Enchytraeus albidus	2	0
Annelida	Haplotaxida	Haplotaxida	Olavius vacuus	2	0

(table cont'd.)

Phylum	Order	Lowest SILVA assignment	Top GenBank Match	S	I
Arthropoda	Collembola	Collembola	Chrysomya saffranae voucher H2 ITS1	2	0
Arthropoda	-	Tetranychus urticae	Tetranychus urticae	2	0
Ctenophora	-	Tentaculata	Uncultured eukaryote clone SGP870	3	0
Hydrozoa	Anthoathecata	Anthoathecata	Moerisia sp. AGC-2001	9	0
Mollusca	Ostreida	Ostreida	Crassostrea gigas	3	0
Nematoda	Araeolaimida	Araeolaimida;metagenome	Pellioiditis mediterranea	2	0
Nematoda	Monhysterida	Phrynidae environmental sample	Phrynidae environmental sample clone	5	0
Nematoda	Tylenchida	Tylenchida	Pratylenchus hippeastri isolate SD53	2	0
Nematoda	Tylenchida	Tylenchida	Uncultured eukaryote clone Ha2_mtz_A01	2	0
Nemertea	Anopla	Cephalothrix cf. alba MCZ IZ 45638	Cephalothrix cf. alba MCZ IZ 45638	4	0
Nemertea	Anopla	Cephalothrix queenslandica	Cephalothrix queenslandica	2	0
Platyhelminthes	Rhabdocoela	Placorhynchus dimorphus	Placorhynchus dimorphus voucher EXT663	2	0
Rotifera	Bdelloida	Adinetida;metagenome	Uncultured bacterium clone contig115446	2	0

All taxa presented in this table are those which were only detected in samples from either the sheared or intact margins, and were detected in at least two samples. The numbers under the S and I columns are the number of samples from sheared and intact margins that the OTUs were detected in.

Additionally, certain taxa were only detected on one or two of the islands, rather than all three (Table 2.15). Two arthropod and two nematode OTUs were unique to samples from Dragon Island. These two arthropods were members of the orders Collembola and Eucarida, respectively. The nematodes were assigned to the orders Dorylamida and Tylenchida. A single rotifer OTU (assigned to the order Bdelloida) was unique to Horseshoe Island. Three annelids and two nematodes were unique to Stingray Island. All three of these annelids were assigned to the order Haplotaxida, while both nematodes were assigned to the order Tylenchida. An annelid, a hydrozoan, and a nemertean OTU were only detected in Dragon and Horseshoe Island samples. This annelid OTU was assigned to the polychaete *Manayunkia aestuarina*, while the hydrozoan OTU was assigned to the species *Helgicirra cari*, and the nemertean was assigned to the class Palaeonemertea. A chordate and a nematode OTU were only detected in Dragon and Stingray Island samples. The chordate OTU was assigned to the order Stolidobranchia (under the subphylum Tunicata) and the nematode was assigned to the order Tylenchida. An annelid and a bryozoan OTU were unique to the Horseshoe and Stingray Island samples. This annelid was assigned to the order Haplotaxida and the bryozoan was assigned to the order Cheilostomatida.

Table 2.15. Unique OTUs in the samples from different islands.

Phylum	Order	Lowest SILVA assignment	Top GenBank Match	DI	HI	SI
Arthropoda	Collembola	Collembola	Chrysomya saffranae voucher H2 ITS1	2	0	0
Arthropoda	Eucarida	Eucarida	Hemigrapsus takanoi	4	0	0
Nematoda	Dorylaimida	Dorylaimida	Tylencholaimus sp. PDL-2005	3	0	0
Nematoda	Tylenchida	Tylenchida	Helicotylenchus dihystra isolate BH524	2	0	0
Annelida	Sabellida	Manayunkia aestuarina	Manayunkia aestuarina	18	4	0
Hydrozoa	Leptothecata	Helgicirrha cari	Helgicirrha cari isolate MHNG-HYD-DNA1153	6	11	0
Nemertea	-	Palaeonemertea	Carinoma sp. SA-2011	2	2	0
Chordata	Stolidobranchia	Stolidobranchia	Molgula manhattensis	4	0	2
Nematoda	Tylenchida	Filenchus hamuliger	Filenchus sp. 4 TJP-2012	3	0	7
Rotifera	Bdelloida	Adinetida;metagenome	Uncultured bacterium clone contig115446	0	2	0
Annelida	Haplotaxida	Haplotaxida	Ainudrilus sp. EKEH-2002	0	4	3
Bryozoa	Cheilostomatida	Smittoidea spinigera	Smittoidea spinigera	0	2	3
Annelida	Haplotaxida	Haplotaxida	Lumbricillus dubius isolate CE5221	0	0	5
Annelida	Haplotaxida	Haplotaxida	Olavius vacuus	0	0	2
Annelida	Haplotaxida	Haplotaxida	Uncultured Tubificina clone Sey064	0	0	2
Nematoda	Tylenchida	Tylenchida	Pratylenchus hippeastri isolate SD53	0	0	2
Nematoda	Tylenchida	Tylenchida	Uncultured eukaryote clone Ha2_mtz_A01	0	0	2

All OTUs presented in this table are those which were not detected in at least one of the island categories, and were detected in at least two samples on at least one island. The numbers under the DI, HI and SI columns are the number of samples from Dragon, Horseshoe, and Stingray Island that the OTUs were detected in.

Alpha diversity:

There were no significant differences in OTU richness ($\chi^2(1) = 1.5$, $p = 0.21$, Kruskal-Wallis test, Fig. 2.16) and Faith's Phylogenetic Diversity (PD) ($\chi^2(1) = 0.62$, $p = 0.43$, Kruskal-Wallis test, Fig. 2.17) between samples from sheared and intact margins, following rarefying. Faith's PD is tied to phylogenetic distance among OTUs and also OTU richness, as increasing the number of detected OTUs will raise the branch lengths of the phylogenetic tree. Given that total OTU richness (Table 2.9) and Faith's PD were not significantly different, it can be concluded that the phylogenetic distances of OTUs collected from sheared and intact margins were also similar.

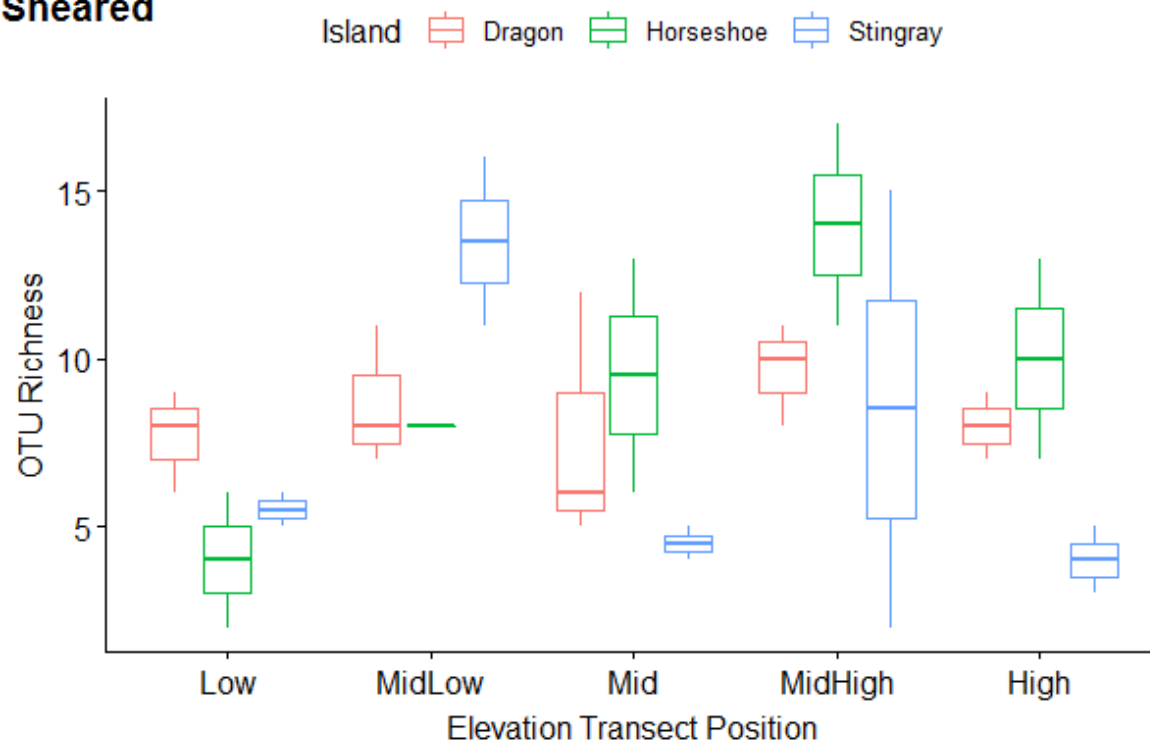
The OTU richness of samples from each island was not different from samples from other islands ($\chi^2(2) = 1.21$, $p = 0.55$, Kruskal-Wallis test, Fig. 2.16). However, one sample from

the Mid elevation position in a sheared margin on Horseshoe Island had the highest richness of any single sample at 17 OTUs. None of the groups of samples from each island were more phylogenetically diverse than the others (Faith's PD, $\chi^2(2) = 0.12$, $p = 0.92$, Kruskal-Wallis test, Fig. 2.17). Given that both the OTU richness and Faith's PD were not significantly different, the phylogenetic distances for the OTUs from the samples different islands were similar.

The communities from samples collected at each of the elevation position had similar OTU richness (Kruskal-Wallis test, $\chi^2(4) = 7.17$, $p = 0.12$). However, samples from the different elevation positions tended to be variable in OTU richness on different islands, especially in samples from intact margins (Fig. 2.16). Samples from each of the elevation positions also showed no difference in phylogenetic diversity (Faith's PD: Kruskal-Wallis test, $\chi^2(4) = 7.72$, $p = 0.10$). Again, because the richness and Faith's PD were not significantly different, the phylogenetic distances between the OTUs from the different elevation positions were not different.

In addition, OTU richness ($\chi^2(5) = 5.64$, $p = 0.34$, Kruskal-Wallis test, Fig. 2.16) and Faith's PD were not significantly different between the groups of samples from different margin types on different islands ($\chi^2(5) = 3.67$, $p = 0.60$, Kruskal-Wallis test, Fig. 2.17). None of the other combinations of factors were significantly different in OTU richness (Margin-Elevation position: $\chi^2(9) = 12.40$, $p = 0.19$, Kruskal-Wallis test, Island-Elevation position: $\chi^2(14) = 10.38$, $p = 0.73$, Kruskal-Wallis test, Margin-Island-Elevation position: $\chi^2(29) = 41.20$, $p = 0.07$, Kruskal-Wallis test, Fig. 2.16) or Faith's PD (Margin-Elevation position: $\chi^2(9) = 9.02$, $p = 0.44$, Kruskal-Wallis test, Island-Elevation position: $\chi^2(14) = 12.12$, $p = 0.60$, Kruskal-Wallis test, Margin-Island-Elevation position: $\chi^2(29) = 41.20$, $p = 0.07$, Kruskal-Wallis test, Fig. 2.17). However, richness and Faith's PD could be highly variable across the interaction of the three factors. The OTU richness was low in the Low positions from sheared margins in all three islands, in the High position samples from sheared margins on Stingray Island, and in the High position samples from intact margins on Dragon and Horseshoe Islands (Fig. 2.16). The OTU richness was high in the Low position samples from intact margins on Horseshoe and Stingray Islands and in the High position samples from intact margins on Stingray Island. These trends largely held true for the Faith's PD values, though the values for the Low position samples from sheared margins on all three islands were closer to the middle of the range of values.

Sheared



Intact

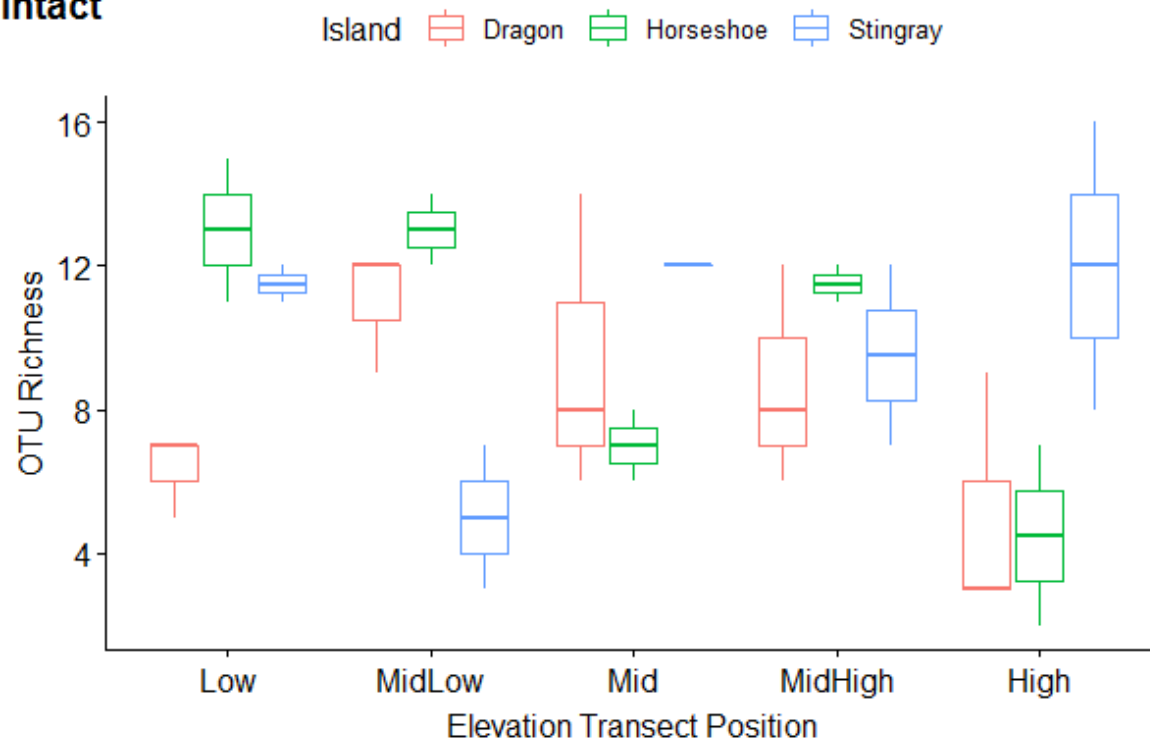
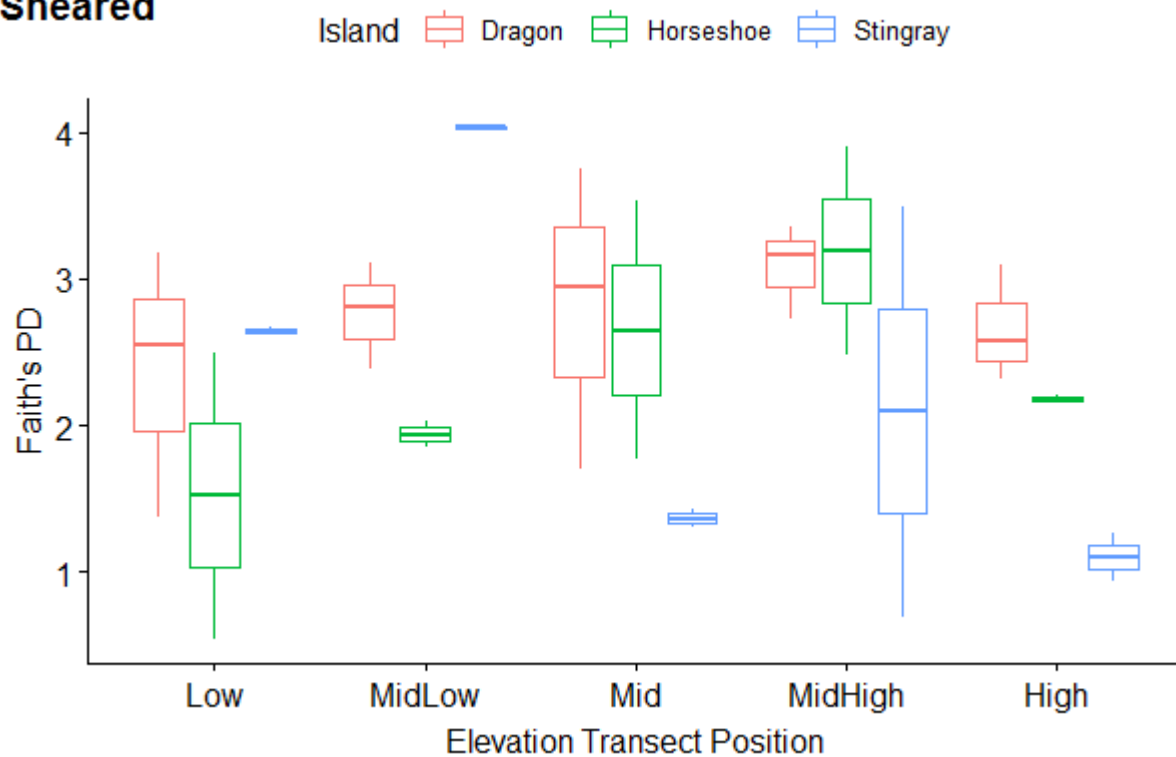


Fig. 2.16. The OTU richness for sheared and intact sites, split by island of origin. Samples were collected from marsh islands surrounding Bay Jimmy, Louisiana from August 2017 to November 2017.

Sheared



Intact

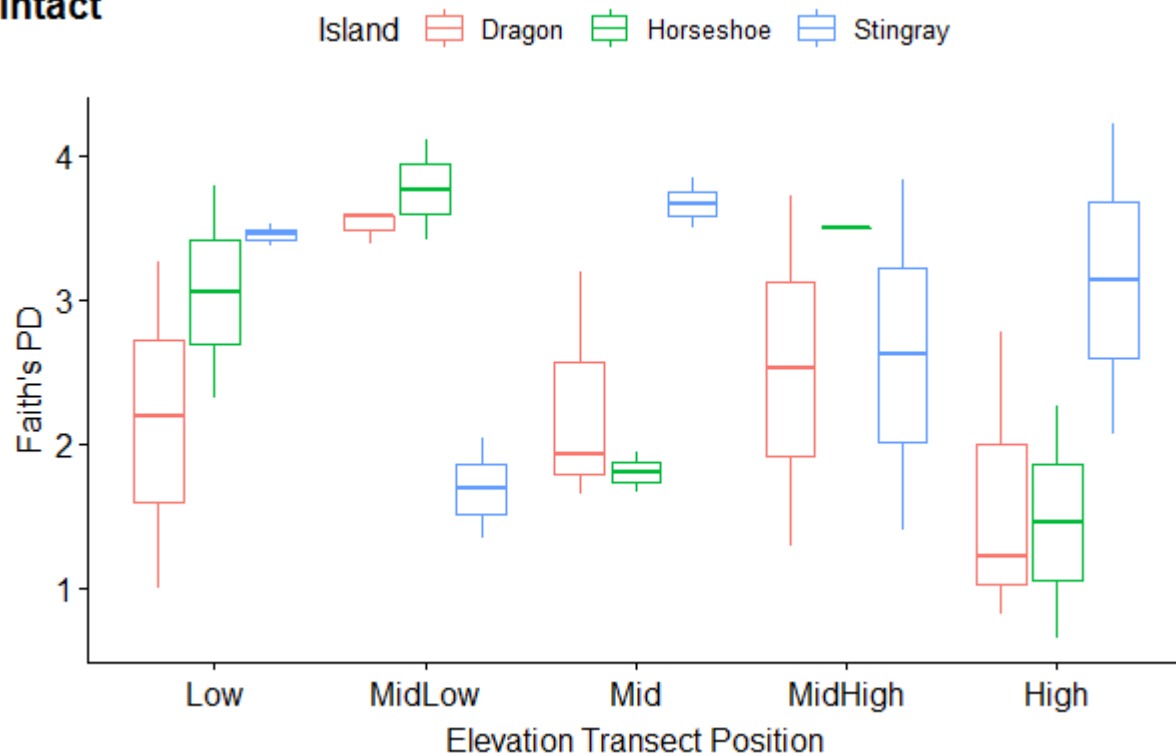


Fig. 2.17. Faith's PD for sheared and intact sites, split by island of origin. Samples were collected from marsh islands surrounding Bay Jimmy, Louisiana from August 2017 to November 2017.

Beta diversity group similarity indices:

Each of the beta diversity similarity indices generated using SpadeR Online returned a value from zero to one, with higher values indicating more similarities between groups. Both the empirical and estimated indices (Table 2.16) show similarity (index values >0.66) between the sheared and intact margin communities, except the empirical Jaccard index. The Jaccard index gives less weight to shared species, typically resulting in lower values than the Sørensen index. The richness-based indices (Sørensen, Jaccard) differ the most between the empirical and estimated results, matching the extrapolated sample-based rarefaction curves (Fig. 2.4) which estimated that more richness could be captured but diversity measures (Shannon and Simpson, which the other indices are based on) would not be increased very much.

Table 2.16. Empirical and estimated similarity indices between communities collected from different margins (sheared and intact), islands (Dragon, Horseshoe, Stingray) and elevation positions (Low, MidLow, Mid, MidHigh, High). Samples were collected from marsh islands surrounding Bay Jimmy, Louisiana from August 2017 to November 2017.

Factor	Index	Estimate	S.E.	95% Lower	95% Upper
Margin	Sørensen Empirical	0.6638	0.0292	0.6066	0.721
	Sørensen Estimated	0.8628	0.1663	0.5369	1
	Jaccard Empirical	0.4968	0.0284	0.4411	0.5525
	Jaccard Estimated	0.7587	0.2867	0.1968	1
	Horn (equal-weighted) Empirical	0.8092	0.0229	0.7642	0.8541
	Horn (equal-weighted) Estimated	0.9101	0.0472	0.8176	1
	Morisita-Horn (relative) Empirical	0.9062	0.0108	0.8851	0.9273
	Morisita-Horn (relative) Estimated	0.9991	0.1413	0.7222	1
	Regional overlap (relative) Empirical	0.9508	0.0057	0.9395	0.9621
	Regional overlap (relative) Estimated	0.9995	0.0627	0.8766	1
Island	Sørensen Empirical	0.7044	0.021	0.6633	0.7455
	Sørensen Estimated	0.9127	0.0722	0.7712	1
	Jaccard Empirical	0.4427	0.0239	0.3958	0.4896
	Jaccard Estimated	0.7769	0.1433	0.4961	1
	Horn (equal-weighted) Empirical	0.768	0.0111	0.7462	0.7898
	Horn (equal-weighted) Estimated	0.8369	0.0155	0.8065	0.8674

(table cont'd.)

Factor	Index	Estimate	S.E.	95% Lower	95% Upper
	Morisita-Horn (relative) Empirical	0.8209	0.0116	0.7982	0.8436
	Morisita-Horn (relative) Estimated	0.9477	0.0983	0.755	1
	Regional overlap (relative) Empirical	0.9322	0.0044	0.9237	0.9408
	Regional overlap (relative) Estimated	0.9819	0.0258	0.9314	1
Elevation Position	Sørensen Empirical	0.7281	0.0108	0.707	0.7491
	Sørensen Estimated	0.8128	0.0232	0.7674	0.8582
	Jaccard Empirical	0.3487	0.0194	0.3107	0.3867
	Jaccard Estimated	0.4648	0.0881	0.2922	0.6374
	Horn (equal-weighted) Empirical	0.7834	0.0095	0.7647	0.8021
	Horn (equal-weighted) Estimated	0.8307	0.0099	0.8113	0.85
	Morisita-Horn (relative) Empirical	0.8527	0.0118	0.8296	0.8758
	Morisita-Horn (relative) Estimated	1	0.1079	0.7884	1
	Regional overlap (relative) Empirical	0.9666	0.003	0.9608	0.9725
	Regional overlap (relative) Estimated	1	0.0137	0.9731	1

S.E. is standard error. 95% Lower and Upper are the values for the confidence intervals. Estimates range from zero to one, with higher values indicating higher similarity.

For the island communities, overall empirical similarity was high (>0.70) between the three island communities, excluding the Jaccard index (Table 2.16). The Jaccard index always returns lower values than the Sørensen, because the Jaccard index gives less weight to the shared species. Again, the richness based estimated indices (Sørensen and Jaccard) showed higher similarity, tracking the expected increase in richness but not the other diversity metrics with additional sampling from the extrapolated rarefaction curves (Fig. 2.6). In addition, estimated similarity indices were generated for each pair of elevation transect position categories to form a pairwise similarity matrix using the Sørensen index (Table 2.17). These show the highest similarity between samples from Horseshoe and Stingray Islands, followed by samples from Dragon and Horseshoe Islands, with the lowest similarity between samples from Dragon and Stingray Islands.

Table 2.17. Estimated pairwise similarity matrix for island communities, Sørensen index. Samples were collected from marsh islands surrounding Bay Jimmy, Louisiana from August 2017 to November 2017.

Community	Dragon	Horseshoe	Stingray
Dragon	1	0.882 (0.505,1.000)	0.637 (0.416,0.859)
Horseshoe		1	0.892 (0.405,1.000)
Stingray			1

Numbers in parenthesis for each pairwise similarity are the 95% confidence interval for that similarity.

With the exception of the Jaccard index, all indices showed high similarity (>0.70) between the five elevation position communities (Table 2.16). Again, the Jaccard index always returns a lower value than the Sørensen index due to the way it is calculated. The richness-based indices (Sørensen, Jaccard) only increased slightly when calculated for the estimated elevation position community, unlike the richness-based indices for the margin and island communities, which increased greatly. The pairwise Sørensen index values (Table 2.18) showed very high similarity between the communities from MidHigh and MidLow positions (0.89), and all other communities showed moderately high pairwise similarity (>0.5), with the lowest similarity between communities from the Mid and Low elevation position (0.51).

Table 2.18. Estimated pairwise similarity matrix for elevation transect communities, Sørensen index. Samples were collected from marsh islands surrounding Bay Jimmy, Louisiana from August 2017 to November 2017.

Community	Low	MidLow	Mid	MidHigh	High
Low	1	0.608 (0.356,0.860)	0.519 (0.375,0.662)	0.615 (0.380,0.850)	0.597 (0.281,0.914)
MidLow		1	0.564 (0.333,0.795)	0.893 (0.421,1.000)	0.683 (0.355,1.000)
Mid			1	0.703 (0.377,1.000)	0.561 (0.278,0.843)
MidHigh				1	0.627 (0.372,0.881)
High					1

Numbers in parenthesis for each pairwise similarity are the 95% confidence interval for that similarity.

Non-Metric Dimensional Scaling (NMDS):

Beta-diversity, i.e., differentiation among communities of samples from different margins, islands and elevation positions, was visualized using NMDS ordination. The distances between samples in NMDS ordination correspond to the ranking of similarity of communities among those samples in the distance matrix and separation of groups and group centroids would indicate differences in metazoan composition among different factors. In addition, NMDS plots also visualize the dispersion of the groups from the centroid. Plotting the Margin groups over the ordination (Fig. 2.18) revealed that the centroids of the Intact and Sheared groups were positioned close to each other, meaning that these groups were similar in composition. One sample in the group of samples from sheared margins was very distant from all other points, potentially affecting the location of the group centroid. However, the groups are similar in dispersion. Plotting the Island groups over the ordination (Fig. 2.19) leads to a similar conclusion as the Margin groups, with especially close centroids between the groups of samples from Horseshoe and Dragon Island. However, the Stingray Island centroid shows some separation from the other two, likely due to the sample that was most distant from all others falling into that group. Horseshoe Island showed a smaller dispersion than the other two island groups.

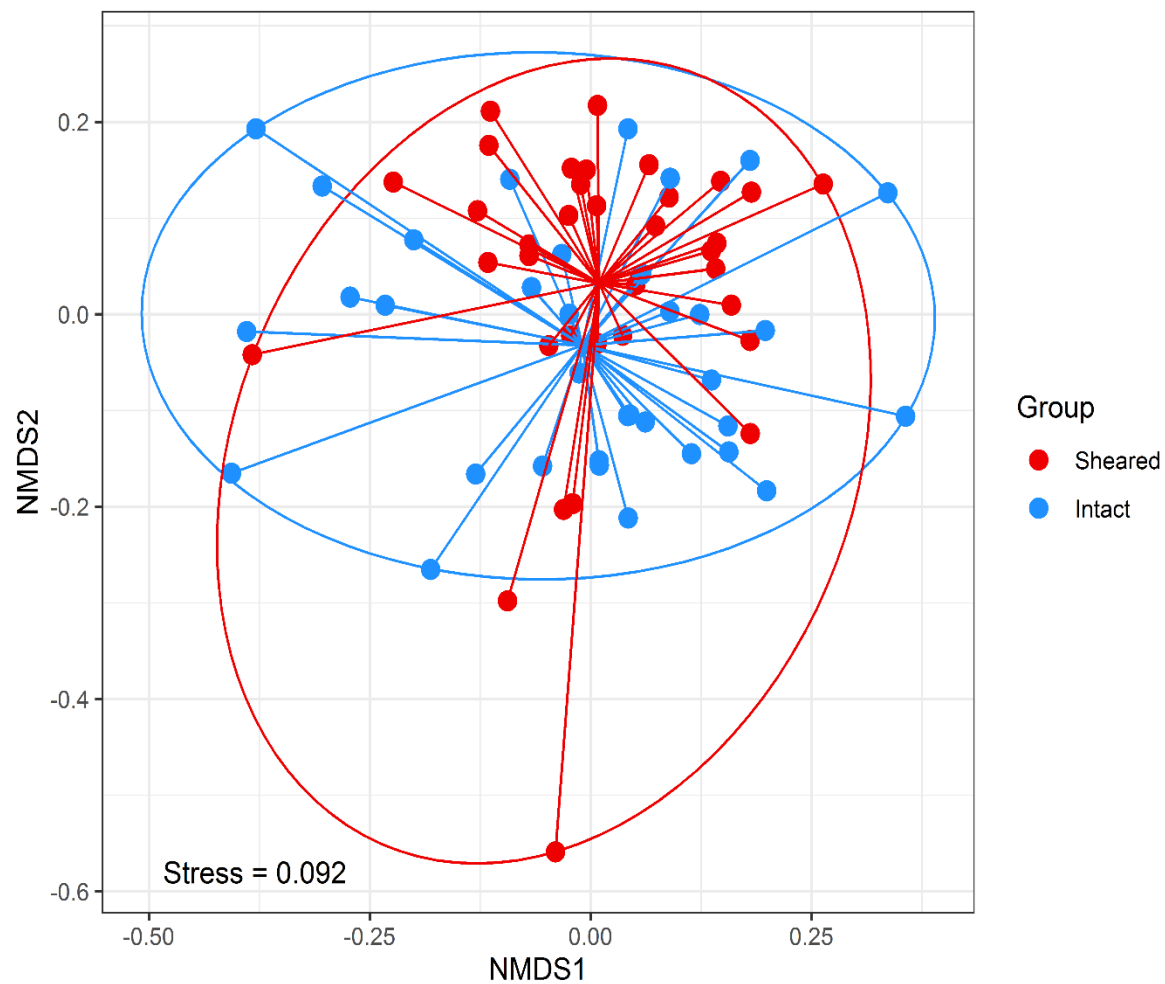


Fig. 2.18. Plot of the first two dimensions of the NMDS ordination of the Sørensen distance matrix. Samples were collected from marsh islands surrounding Bay Jimmy, Louisiana from August 2017 to November 2017. Small circles represent individual samples. Solid ellipses represent the elliptical hulls of the groups. Solid, straight lines connect a sample to the group centroid.

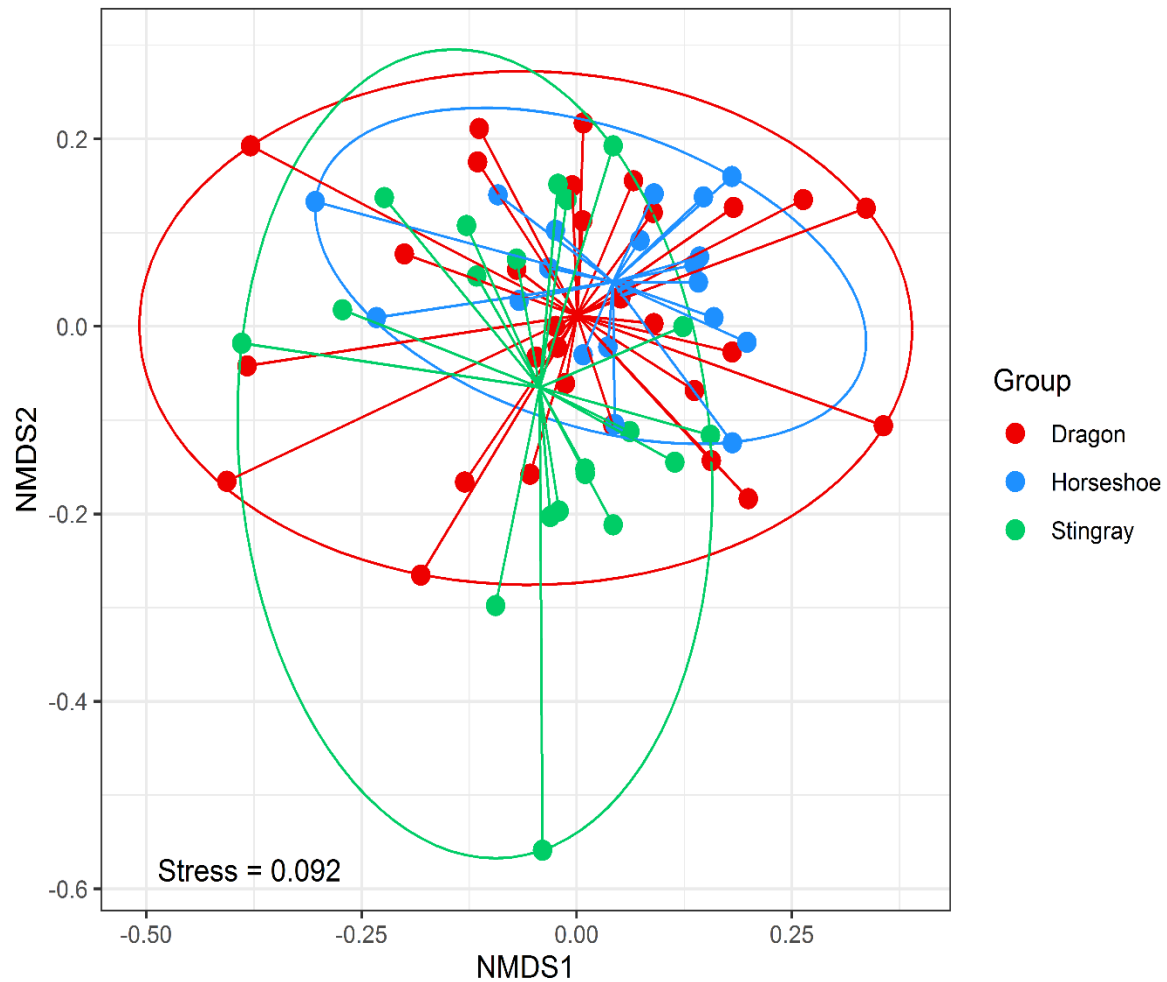


Fig. 2.19. Plot of the first two dimensions of the NMDS ordination of the Sørensen distance matrix. Samples were collected from marsh islands surrounding Bay Jimmy, Louisiana from August 2017 to November 2017. Small circles represent individual samples. Solid ellipses represent the elliptical hulls of the groups. Solid, straight lines connect a sample to the group centroid.

The effect of the interaction of the factors Island and Margin on community composition in the dataset was visualized by plotting the groups of samples belonging to each interaction of Island and Margin over the NMDS ordination (Fig. 2.20). Centroid locations show that there was more distance between the overall community compositions of the Dragon Island samples from sheared and intact margins than between the sheared and intact margins of the other islands. The samples from sheared margins on Horseshoe Island showed a distinct separation from the samples from sheared margins on Stingray Island, indicating a difference in community composition. The largest differences in the location of the groups of samples appear to be due to the location of several samples from sheared margins on Stingray Island. The lowest point on the figure, which is distant from all other samples, belongs to a sample from a sheared margin on Stingray Island in the MidHigh position with a low number of

metazoan OTUs (6 OTUs present). This sample also only contained one of the frequent group OTUs, meaning that the OTUs it does have are not common to most samples, leading to low compositional similarity and high distance from other samples. Otherwise, almost all samples fall inside of the largest group (samples from intact margins on Dragon Island). In addition, the group of samples from sheared margins on Horseshoe Island showed a much tighter distribution than other groups. These samples, because they have a tighter distribution, are more similar within their own group than the groups of samples from other island and margin status interactions.

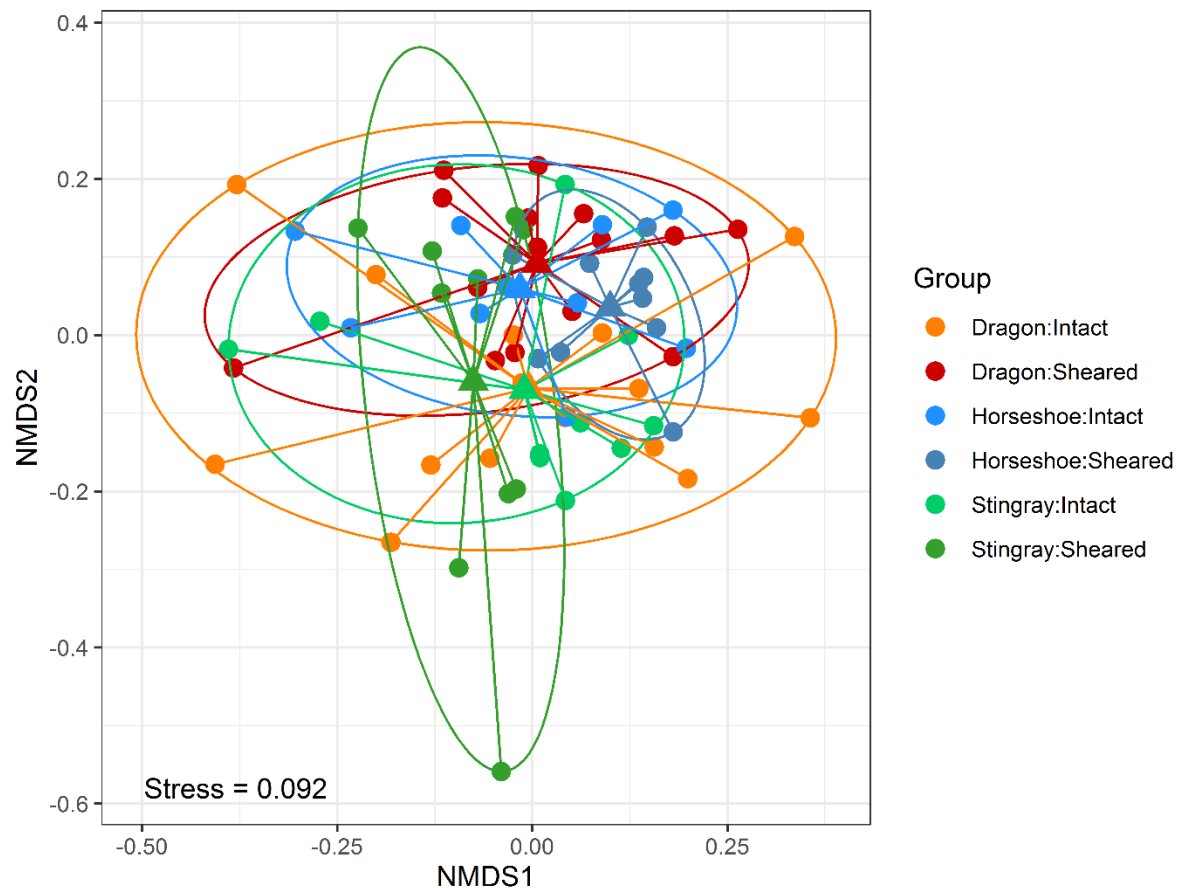


Fig. 2.20. Plot of the first two dimensions of the NMDS ordination of the Sørensen distance matrix. Samples were collected from marsh islands surrounding Bay Jimmy, Louisiana from August 2017 to November 2017. Small circles represent individual samples. Triangular points are the centroids for the interaction of factors indicated by the legend. The centroid point for the Dragon: Intact group of samples is plotted behind the centroid point for the Stingray: Intact group because they are nearly in the same location. Solid lines represent the ordination hulls of each interaction group.

Beta diversity distance matrix analysis:

Following the Benjamini-Hochberg correction of the Adonis test results, Margin ($F(1,69) = 1.81$, BH corrected $p = 0.02$) and Island ($F(2,69) = 2.64$, BH corrected $p < 0.01$) had significant effects on community similarity, while the factor Elevation Position did not (Table 2.19). Since the dispersion of these factors was homogeneous (PERMDISP tests based on Sørensen distance matrix, $p > 0.05$), these differences were based on community differences among samples from sheared and intact margins and from the three islands and not on the differences in community similarity of samples within categories. However, the effect size for these factors was low (R^2 values: 0.02 and 0.06, respectively), so they only explain a small amount of the variation in the data. The differences were also subject to interaction between the factors Margin, Island, and Elevation position ($F(8,69) = 1.42$, BH corrected $p < 0.01$), Margin and Island ($F(2,69) = 2.04$, BH corrected $p < 0.01$), and Island and Elevation position ($F(8,69) = 1.31$, BH corrected $p = 0.02$). The dispersion of these interactions was also homogenous (PERMDISP tests based on Sørensen distance matrix, BH corrected $p > 0.05$). The R^2 values for the interactions were also low, at 0.13, 0.05, and 0.12, respectively.

Table 2.19. Adonis test results. Samples were collected from marsh islands surrounding Bay Jimmy, Louisiana from August 2017 to November 2017.

Factor	Df	SumOfSqs	R2	F-value	p-value
Margin	1	0.4246	0.0222	1.8180	0.0150*
Island	2	1.2351	0.0646	2.6441	0.0001*
Elevation Position	4	1.1800	0.0617	1.2631	0.0641
Margin:Island	2	0.9527	0.0498	2.0396	0.0003*
Margin:Elevation Position	4	0.8906	0.0466	0.9533	0.5928
Island:Elevation Position	8	2.4508	0.1281	1.3117	0.0092*
Margin:Island:Elevation Position	8	2.6534	0.1387	1.4201	0.0010*
Residual	40	9.3423	0.4884		
Total	69	19.1296	1.0000		

Asterisks * indicate a p-value that remained significant after the Benjamini-Hochberg correction.

To analyze interactions regarding the factors Margin and Island, which both showed significant effects, additional Adonis tests were performed on subsets of the data containing only samples from each individual island (Tables 2.18, 2.19, 2.20). For Dragon Island, community composition of samples from sheared and intact margins was significantly different ($F(1,29) = 2.33$, BH corrected $p = 0.01$), regardless of elevation position. This result also had a very low R^2 value, at 0.07, but is supported by the distance between the centroids for the

samples from the sheared and intact margins on Dragon Island (Fig. 2.20). Samples from Horseshoe Island had no significant differences detected across the Margin or Elevation Position factors. This is consistent with the location of the centroids of the samples from sheared and intact margins on Horseshoe Island (Fig. 2.20). For Stingray Island, the factors Margin ($F(4,19) = 2.18$, BH corrected $p = 0.01$), and Elevation Position ($F(4,19) = 1.59$, BH corrected $p = 0.01$) and their interaction ($F(4,19) = 1.60$, BH corrected $p = 0.01$) were significantly different. The Margin factor result also had a very low R^2 value, at 0.08, but the Elevation Position and the interaction of Margin and Elevation position had R^2 values of 0.26. The interaction of Margin and Elevation was not significantly different in the whole dataset, so the significant result for the Stingray Island samples explains on which island the significant difference in the interaction of the three factors occurred. The samples from Stingray Island showed a closer grouping of the centroids from intact sites, regardless of elevation position, while each sheared centroid showed separation from the other sheared centroids, indicating more community differentiation among samples from sheared margins (Fig. 2.21). However, this differentiation in community similarity between margin types may be due to the small number of samples in each group of Elevation Position-Margin combinations (2 samples per group). This result may also be due in part to the low diversity sample which showed a large distance from the rest of the dataset in the overall NMDS figures (Figs. 2.18, 2.19, 2.20) and showed a large distance to all other samples in Stingray Island.

Table 2.20. Adonis test results for Dragon Island samples only. Samples were collected from marsh islands surrounding Bay Jimmy, Louisiana from August 2017 to November 2017.

Factor	Df	SumOfSqs	R2	F-value	p-value
Margin	1	0.5617	0.0739	2.3316	0.0037*
Elevation Position	4	1.0280	0.1353	1.0669	0.3521
Margin:Elevation Position	4	1.1907	0.1567	1.2357	0.1227
Residual	20	4.8178	0.6341		
Total	29	7.5981	1.0000		

Asterisks * indicates a p-value that remained significant after the Benjamini-Hochberg correction.

Table 2.21. Adonis test results for Horseshoe Island samples only. Samples were collected from marsh islands surrounding Bay Jimmy, Louisiana from August 2017 to November 2017.

Factor	Df	SumOfSqs	R2	F-value	p-value
Margin	1	0.3409	0.0719	1.5158	0.0546
Elevation Position	4	1.1536	0.2433	1.2824	0.0643
Margin:Elevation Position	4	0.9978	0.2105	1.1092	0.2520
Residual	10	2.2490	0.4743		
Total	19	4.7414	1.0000		

Asterisks * indicates a p-value that remained significant after the Benjamini-Hochberg correction.

Table 2.22. Adonis test results for Stingray Island samples only. Samples were collected from marsh islands surrounding Bay Jimmy, Louisiana from August 2017 to November 2017.

Factor	Df	SumOfSqs	R2	F-value	p-value
Margin	1	0.4737	0.0874	2.1802	0.0102*
Elevation Position	4	1.3825	0.2550	1.5909	0.0136*
Margin:Elevation Position	4	1.3927	0.2569	1.6026	0.0123*
Residual	10	2.1725	0.4007		
Total	19	5.4215	1.0000		

Asterisks * indicates a p-value that remained significant after the Benjamini-Hochberg correction.

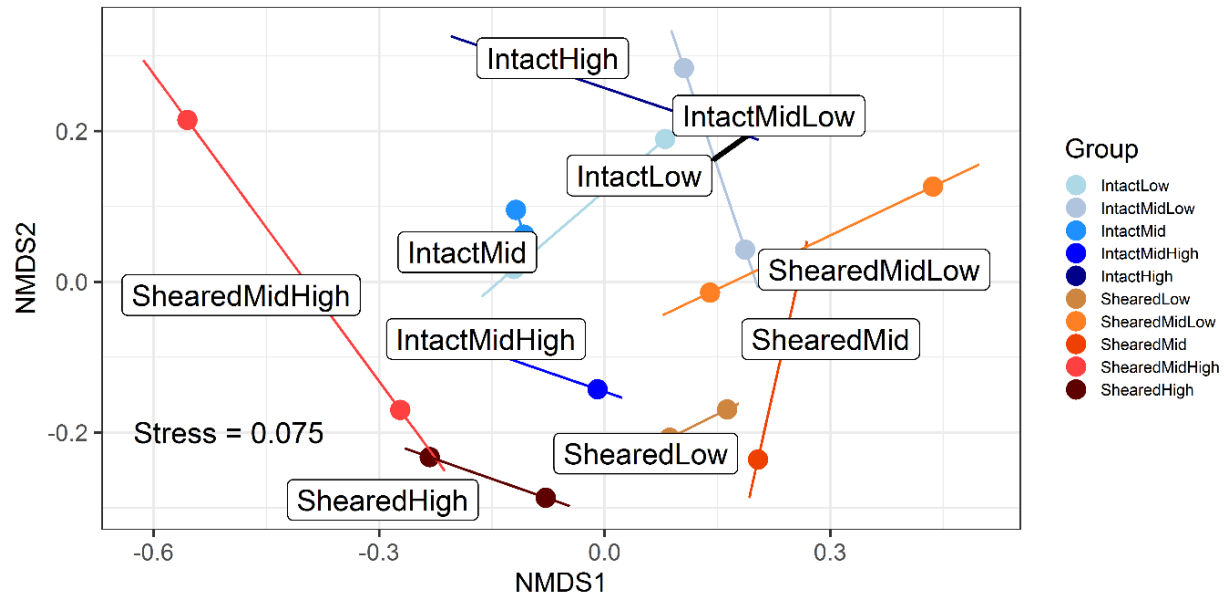


Fig. 2.21. Plot of the first two dimensions of the NMDS ordination of the Sørensen distance matrix for samples from Stingray Island. Samples were collected from marsh islands surrounding Bay Jimmy, Louisiana from August 2017 to November 2017. Small circles represent the samples. Labels are located near the centroid of the interaction group as indicated on the label. Solid lines represent the “hulls” for the interaction groups (here lines, due to the low number of samples in each group).

Differential abundance of OTUs:

Twelve OTUs were detected as having differential read count abundances across the categories of Margin, Island, and Elevation position (Table 2.23). Positive values of differentials indicate association with the class mentioned first in the column name, while negative values indicate association with the comparison class. Read counts, for metazoans, are not a substitute for counts of individuals, but the differential read count abundances are presented here as a measure of the difference in the number of cells. Of these, most were nematodes, including OTUs matching to *Thoracosoma trachygaster*, an ambiguous member of Monhysterida, an ambiguous member of Enoplida, and an ambiguous member of Dorylaimida. The remaining OTUs matched to three annelids (*Polydora ciliata*, *Alitta succinea*, and *Manayunkia aestuarina*), a gastrotrich (*Heterolepidoderma* sp.), a mollusk (ambiguous member of Mytiloida), a gastropod (*Nerita peloronta*, Mollusca), a harpacticoid copepod (*Cancrincola plumipes*, Arthropoda), and a hydrozoan (*Helgicirrhia cari*). It is important to note that differentials represent relative difference in read counts across a category and not absolute differences. From here, positive differentials in a category will be referred to as “enriched” in that category, while negative differentials will be referred to as “reduced”. The Songbird program produces differentials for the different categories selected in the model, which was “Island + Margin + Elevation Position”. The “Intercept” category represents the first class within each category, in

this case, Sheared for the Margin category, Dragon Island for the Island category, and Low for the Elevation position.

Positive differentials for the Sheared category showed read count enrichment in samples from sheared margins of the Monhysterida nematode, *T. trachygaster* (Nematoda), the Mytiloida mollusk, the gastrotrich, *A. succinea* (Annelida), and *H. cari* (Hydrozoa) compared to those from intact margins. Negative differentials in the Sheared column represent enrichment in samples from intact margins of the Enoplida nematode, *M. aestuarina* (Annelida), *N. peloronta* (Mollusca), *C. plumipes* (Arthropoda), *P. ciliata* (Annelida), and the Dorylamida nematode.

The following OTUs were enriched on both Horseshoe and Stingray Islands compared to Dragon Island: *N. peloronta* (Mollusca), *P. ciliate* (Annelida), and *A. succinea* (Annelida). Other OTUs which were enriched on Horseshoe Island compared to Dragon Island were *H. cari* (Hydrozoa) and the Dorylamida nematode. Positive differentials in the Stingray column showed read count enrichment of *T. trachygaster* (Nematoda) and the gastrotrich in samples from Stingray Island compared to samples from Dragon Island. The Monhysterida nematode, *C. plumipes* (Arthropoda), the Enoplida nematode, *M. aestuarina* (Annelida) and the Mytiloida mollusk all had negative differentials in the Horseshoe and Stingray columns, meaning that they were enriched in the samples from Dragon Island. Negative differentials unique to the Horseshoe column were the gastrotrich and *T. trachygaster*, meaning that these were enriched in Dragon Island samples compared to Horseshoe Island samples. The hydrozoan *H. cari* and the Dorylamida nematode showed enrichment in the Dragon Island samples compared to the Stingray Island samples.

For the samples from different Elevation Positions samples, the *C. plumipes* (Arthropoda) and *M. aestuarina* (Annelida) OTUs were enriched in a single Elevation Position category, in the Mid and High position samples respectively. The Mytiloida mollusk and *T. trachygaster* (Nematoda) were enriched in all Elevation Positions compared to the lowest elevation, while the gastrotrich and *H. cari* (Hydrozoa) were enriched in all Elevation Positions vs the Low position except for the Mid position. *Alitta succinea* (Annelida) was enriched in all Elevation Position columns except the MidHigh column. *Nerita peloronta* (Mollusca) was enriched in samples from both the MidLow and Mid positions, while the Monhysterida nematode was enriched in the MidLow and MidHigh. The final OTU which showed enrichment was the Enoplida nematode in the Mid and High position samples. Notably, the Dorylamida nematode was strongly reduced in the MidHigh and Mid positions compared to the Low position. *Cancrincola plumipes* (Arthropoda) was reduced in both the MidHigh and High positions compared to the Low position. Additional strongly negative differentials included the Monhysterida nematode in the High position, the Enoplida nematode in the MidLow position, and *H. cari* (Hydrozoa) in the Mid position, meaning that these OTUs were enriched in the Low position.

Table 2.23. Songbird differentials for the OTUs detected in samples from marsh islands surrounding Bay Jimmy collected from August 2017 to November 2017.

SILVA Taxonomy String	Intercept	Sheared Compared to Intact	Horseshoe Compared to Dragon	Stingray Compared to Dragon	MidLow Compared to Low	Mid Compared to Low	MidHigh Compared to Low	High Compared to Low
Nematoda Chromadorea Monhysterida Ambiguous taxa	0.5709	3.3277	-6.4437	-0.3027	0.3563	-1.6762	3.2470	-3.8739
Nematoda Enoplea Enoplia Enoplida Thoracostoma trachygaster	0.8201	2.0472	-0.3987	3.2469	1.4107	0.8933	1.8402	1.0554
Mollusca Bivalvia Pteriomorpha Mytiloidea Ambiguous taxa	0.3953	1.8248	-0.5922	-1.0522	1.6193	2.7692	2.7762	1.7039
Gastrotricha Chaetonotida Heterolepidoderma sp. 1 TK-2012	1.0163	1.2080	-2.4228	0.3248	1.5490	-1.1850	1.3031	1.5093
Hydrozoa Hydroidolina Leptothecata Helgicirrhia cari	-2.7055	0.8308	2.3393	-1.9540	1.4074	-2.2056	0.9976	0.9463
Annelida Polychaeta Palpata Phyllodocida Alitta succinea	-0.4328	0.4474	1.4064	0.9739	0.4657	0.6927	-0.2115	0.1505
Nematoda Enoplea Dorylaimia Dorylaimida Ambiguous taxa	1.7280	-1.2717	2.2529	-1.3346	-0.2179	-2.1611	-4.5604	-0.4655
Annelida Polychaeta Scolecida Spionida Polydora ciliata	-0.5820	-1.3694	2.8533	4.1954	-1.2272	1.1694	0.5002	-0.4630
Arthropoda Crustacea Maxillopoda Copepoda Harpacticoida Cancrincola plumipes	0.5743	-1.4777	-1.3802	-0.9628	-1.9930	1.7183	-2.7992	-2.9763

(table cont'd.)

SILVA Taxonomy String	Intercept	Sheared Compared to Intact	Horseshoe Compared to Dragon	Stingray Compared to Dragon	MidLow Compared to Low	Mid Compared to Low	MidHigh Compared to Low	High Compared to Low
Mollusca Gastropoda Neritimorpha Nerita peloronta	-2.2658	-1.4805	3.9351	0.8232	0.3917	0.1298	-1.9066	-1.4282
Annelida Polychaeta Palpata Sabellida Manayunkia aestuarina	0.0538	-1.6998	-0.1895	-2.9343	-1.4554	-1.0966	-1.1799	1.5222
Nematoda Enoplea Enoplia Enoplida Ambiguous taxa	0.8272	-2.3871	-1.3599	-1.0237	-2.3066	0.9517	-0.0069	2.3193

Columns are separated by vertical lines into metadata categories (Margin, Island, and Elevation Position). Higher positive values of differentials indicate higher relative abundance of reads in the metadata category of the column, while lower negative values indicate higher relative abundance of reads in the comparison class of the column. The intercept column represents the relative abundances of all comparison classes across all categories. The comparison class for Margin is the group of samples from intact margins. The comparison class for Island is the group of samples from Dragon Island. The comparison class for Elevation Position is the group of samples from the Low elevation position. Differentials are presented sorted by highest to lowest values for the Sheared column.

2.4. Discussion

There were differences in nitrogen, carbon, organic material, and C/N ratios detected between the sheared and intact sites as well as among the different islands (Tables 2.4, 2.5, 2.6, 2.7), but no significant differences were observed for all other measured soil chemistry concentrations (Tables 2.1, 2.2, and 2.3) which fell into normal ranges for salt marshes (Boyd and Walley 1972, Chabreck 1972, Brupbacher et al. 1973, Santschi et al. 2001, Bhattarai 2006). Salt marsh plants are known to facilitate denitrification microbes, and studies suggest that this function was not permanently impacted by the DHOS (Hinshaw et al. 2017b, Schutte et al. 2020). Because marsh plants are not present in sheared sites, the presence of soil microbes which perform denitrification may be diminished which would lead to nitrogen accumulation. The nitrogen percentage was higher in samples from sheared margins, but the total range of nitrogen percentage in the dataset was very small, between 0.5% and 1%. The highest total levels of both percent carbon and percent organic matter occurred on Dragon Island in the sheared margin sites. Consequently, the highest C/N ratios were also observed in the sheared margin sites on Dragon Island. C/N ratios are an indicator of the degree of decomposition of organic material in soils, with ratios higher than 10 indicating less decomposition than deposition (DeLaune et al. 1979). Though the ratios were highest for sheared sites on Dragon Island (Table 2.1), all ratios fell within historic value ranges for salt marsh soils (Brupbacher et al. 1973). All detected C/N ratios were above 10, indicating that these marsh sites accrete organic matter into the soil faster than it can be decomposed and returned to the atmosphere. The organic matter deposited into marsh sediment is critical to both marsh vertical accretion and carbon sequestration (Turner et al. 2005, Macreadie et al. 2013), as well as to the diets of

marsh organisms (Broome et al. 2000). Because the soil chemistry profiles fell within historic baselines and most variables were not significantly different across the dataset, it is unlikely that the soil chemistry variables were major factors in controlling the distribution of organisms across the study area. Both Horseshoe and Stingray Islands have evidence of industrial use on or nearby the island. Because the majority of the soil chemistry values were not significantly different, it is unlikely that the areas which were sampled were previously filled using dredged sediment, which might impact the infauna community (Johnston 1981, Wilber et al. 2008).

The clade SAR was the most frequently detected group in the dataset prior to filtering for metazoa, followed by the groups Opisthokonta, Excavata, Archaeplastida, and Amoebozoa (Fig. 2.2, Table 2.8). The remaining sub-domain groups (Incertae Sedis, Haptophyta, Picozoa and taxa assigned to uncultured eukaryotes) were rarely detected. No clear patterns across the different islands, margin types, or elevation positions were observed with regards to the detection of sub domain groups in the dataset, though the SAR clade usually dominated samples. The single celled eukaryotes which are not animals, fungi, or plants (the former kingdom Protista) tend to be the least studied of the eukaryotes even though they likely make up a large proportion of all eukaryote diversity (Sibbald and Archibald 2017, Burki et al. 2020). The SAR clade alone may contain half of all eukaryote species (del Campo et al. 2014). For example, in this study the non-metazoan groups received higher rates of unclear assignments than the metazoans (Table 2.8). Presumably, there is usable ecological information contained in the distribution and composition of the non-metazoan groups; and as databases become more complete, future research may return to these data to evaluate eukaryotic communities in a more holistic manner. Currently, the body of knowledge on metazoans (including more clearly resolved taxonomy, DNA sequences, and life cycle data from historic studies) does contain useful ecological data to draw conclusions from based on the distribution of organisms.

The sequencing depth of samples (including only metazoan sequences) primarily ranged between 300-5,000 sequences with a mean of approximately 5,000 sequences, although one sample reached over 70,000 sequences (Fig. 2.3). However, the samples with high sequencing depth did not necessarily have the highest OTU richness.

The extrapolated portion of the sample-based rarefaction curves for the full dataset continued to climb indicating that additional richness could be captured with additional sampling (Fig. 2.4). However, the extrapolated curves for the Shannon and Simpson Inverse effective diversity were almost completely flat which means that additional gains of richness would not impact the other diversity metrics; the potential additional richness gains from additional sampling would be comprised of rarely detected OTUs because the other two metrics are dependent on how many times OTUs are detected in the dataset. The majority of OTUs which would fall into the frequent group (detected in more than 10 samples) were collected by the sampling effort. Additional richness gains would only add to the infrequent group of OTUs. This result is supported by the higher estimated coverage of the full dataset than of the infrequent groups (Table 2.9). Since approximately all of the frequent OTUs were

captured by sampling, additional sampling would net limited gains in the diversity metrics even if richness increases. This result agrees with the OTU richness estimation models (Fig. 2.12), because the models with the highest predictions rely on the number of rarely detected OTUs to calculate an estimate. The end point of the extrapolated richness from the sample-based rarefaction curves falls within the range of estimated additional OTUs (between 15 and 118 additional OTUs, Fig. 2.12). Rare species should not be disregarded in ecological studies since they can have impacts on ecosystem services (Lyons et al. 2005, Dee et al. 2019a), but whether additional collected metazoan OTUs would actually represent additional species is questionable due to intraspecific variation (Brown et al. 2015, Phillips et al. 2019). The SpadeR program did not account for the measures used on this dataset to avoid artificially inflating biodiversity through multiple OTUs representing the same species. When the database was split by metadata categories for examination of the separate communities, the 95% confidence intervals increased and the Shannon and Simpson Inverse curves were steeper, due to lower sample sizes. The samples from the intact margins showed slightly higher observed and estimated richness than the samples from sheared margins, but the confidence intervals did overlap (Fig. 2.5). The confidence intervals for all three islands overlapped; Horseshoe Island samples had the highest observed and estimated richness while Stingray Island samples had the lowest (Fig. 2.6). The High elevation position samples had a higher observed and estimated richness than the other elevation positions, potentially indicating the detection of an inland community which is not present in the lower elevation positions (Fig. 2.7).

The coverage-based rarefaction curves indicated that the coverage of the full dataset was approximately 93% and that sampling twice as much could have improved coverage up to approximately 97% (Fig. 2.8). This result is supported by the overall coverage estimate of 93% (Table 2.9). Splitting the dataset by metadata category again had the sample size reduction effects as observed in the sample-based rarefactions. The samples from sheared margins showed slightly lower coverage (85%) than the samples from intact margins (89%, Fig. 2.9). Samples from Dragon Island showed higher coverage (85%) than the samples from the other two islands (80%), but this may have been an effect of the higher sample size of the Dragon Island samples (Fig. 2.10). The Mid, MidHigh, and High elevation position samples all had a coverage close to 80%, while the MidLow and Low position samples had coverage closer to 70% (Fig. 2.11). This may indicate a need for more intensive sampling in future studies at the Low and MidLow positions.

The 18 frequent group OTUs accounted for slightly more than half of all incidences of metazoan OTUs in the dataset (438/835 incidences, Table 2.9). Meanwhile, the other 139 OTUs accounted for slightly less than half of all incidences (397/835, Table 2.9). The distribution having few OTUs making up the majority of incidences would account for the moderately high (number) coefficient of variation (Table 2.9). Fourteen of the eighteen frequent group OTUs were detected on all islands, in both sheared and intact, and in each of the elevation positions. Because of this, the frequent group OTUs are probably not especially useful for differentiating

the communities present in these different categories, meaning that the focus of future studies should be on collecting enough samples to have good coverage of the infrequent group.

The groups of samples from sheared and intact margins shared 78 OTUs, including all of the OTUs from the frequent group (Table 2.10); more than half of the OTUs detected in each group were shared between sheared and intact. The group of samples from intact margins had slightly higher total number of OTUs than the group of samples from sheared margins, though the richness of individual samples in these categories was not significantly different (Fig. 2.16). This is likely because the commonly detected OTUs (i.e., the frequent group) were detected in both sheared and intact margins, meaning that most samples had the same few OTUs, with the unique OTUs from each type of margin being detected in fewer samples. Marsh margins are important habitats for commercial species (Peterson and Turner 1994), so more sampling to determine what OTUs are the most important in the sheared and intact margins is essential.

The groups of samples from the different islands shared more than half of the OTUs in each group with the other groups, and slightly less than that were shared between all three islands (Table 2.11). Samples from Horseshoe Island had the highest total of OTUs but this was only slightly more than the totals for the other two islands. However, the OTU richness of individual samples on the different islands was not significantly different (Fig. 2.16).

The OTU richness of individual samples within elevation replicates was not significantly different (Fig. 2.16). The groups of samples from the individual elevation positions each shared more than half of the OTUs with the other groups, excluding the combination of Low-High positions and MidLow-High positions (Table 2.12). The samples from the High position had the highest total number of OTUs, followed by the samples from the Mid position. The other three positions had similar total numbers of OTUs.

In this study, Nematodes were the group with the most OTUs present in any given sample (Fig. 2.13) and the most frequently occurring group of OTUs in the samples, followed by annelids, arthropods, and mollusks (Fig. 2.14). Nematode OTUs comprised 28.62% of all OTU incidences, followed by annelids at 16.88%, arthropods at 14.25%, and mollusks at 12.69% (Fig. 2.14). In terms of OTU richness, arthropods dominated with 26.11% of OTUs, followed by nematodes at 19.75% of OTUs, then annelids at 10.82% of OTUs, and mollusks at 9.55% of OTUs (Fig. 2.15). Nematodes being the most frequently detected group is consistent with other traditional taxonomic studies of salt marsh infauna (Fleeger and Chandler 1983, Alves et al. 2013). Nematodes were the most commonly collected taxa (by number of individuals collected) in previous, long term studies of the study area using traditional collection methods (Fleeger et al. 2018). However, many of these traditional studies lack coverage of the more soft bodied infauna (such as Platyhelminthes) due to poor preservation or destruction during sorting (Carugati et al. 2015).

Nematodes are important indicator organisms of soil biodiversity and ecosystem function because they respond rapidly to environmental stimuli but tend to have more stable

populations than bacteria (Ritz et al. 2009, Griffiths et al. 2016, Waeyenberge et al. 2019). However, nematodes also tend to recover quickly after disturbances, and returned rapidly in the study area after the DHOS (Fleeger et al. 2015). Nematodes are not colonial, but densities can reach high levels over small scales. Free living nematodes do not have pelagic larvae, instead having juveniles which resemble miniature adults (Barnes and Ruppert 1994). The most frequently detected OTU in the nematode community (detected in 91.43% of samples, Table 2.13) was assigned to the taxa *Thoracostoma trachygaster* in the SILVA taxonomy (GenBank: Leptosomatidae). Leptosomatid nematodes are microbivorous marine nematodes which are commonly recorded in intertidal environments (Hope 1967, Hodda 2011). Though the diversity of microbes in salt marsh soils can vary depending on local conditions, densities tend to remain high and are not likely to be a limiting factor for microbivore nematode populations (Rublee and Dornseif 1978, Klepac-Ceraj et al. 2004, Beazley et al. 2012). The next most frequently detected nematode OTU (35.71% of samples) was assigned to the order Enoplida (SILVA: Enoplida, ambiguous taxa, GenBank: Uncultured eukaryote clone). Order Enoplida includes nematodes which are often algal grazers or predators. Following this, the next most commonly detected nematode OTU (34.28% of samples) was assigned to the order Dorylaimida (SILVA: Dorylaimida, ambiguous taxa, GenBank: Uncultured eukaryote clone, Table 2.13). Members of the order Dorylaimida tend to be predatory terrestrial or aquatic nematodes (Hodda 2011). The distribution of these nematodes would then likely depend on prey availability. A nematode OTU assigned to the order Monhysterida (SILVA: Monhysterida, ambiguous taxa, GenBank: Daptonema sp.) was the next most commonly detected nematode OTU (24.29% of samples, Table 2.13). Nematodes from the order Monhysterida tend to be marine microbivores (Hodda 2011). The next most frequently detected nematode OTU (18.57% of samples) was assigned to the species *Pontonema vulgare* (SILVA: *Pontonema vulgare*, GenBank: Uncultured eukaryote clone, Table 2.13), which is in the order Enoplida. The final frequent group nematode OTU was assigned to the species *Diplolaimella dievengatensis* (SILVA: *Diplolaimella dievengatensis*, GenBank: *Diplolaimella dievengatensis*, Table 2.13), which is in the order Monhysterida. The other nematode OTUs (25/31 OTUs) were detected in 10 or fewer samples, and combined accounted for less than 10% of all incidences. This infrequently detected group included all detected nematodes which were assigned plant root feeders as a potential functional feeding group (Hodda 2011). Nematodes had reduced richness and abundances and shifted from evenly distributed functional feeding groups to a predator dominated community following the DHOS (Bik et al. 2012). In this study, most of the nematode OTUs were assigned to groups which are known to be microbivores, followed by a smaller group of plant root feeders and algal grazers, then an even smaller group of predators, though there was a group of nematode OTUs which did not receive a specific enough assignment to determine feeding mode.

Annelids were the second most commonly detected group of OTUs in the dataset after nematodes (Fig. 2.14). Some annelids have pelagic larvae, especially those in the class Polychaeta, which can influence distribution (Barnes and Ruppert 1994). An OTU assigned to the genus *Polydora* (SILVA: *Polydora ciliata*, GenBank: *Polydora lingshuiensis*) was detected in

70% of samples, making it the most frequently detected annelid OTU (Table 2.13). The second most frequently detected annelid OTU (42.85% of samples) was assigned to the taxa *Alitta succinea* in SILVA (GenBank: *Alitta succinea*, Table 2.13). This was followed by an OTU assigned to *M. aestuarina* (GenBank: *M. aestuarina*) at 31.43% of samples (Table 2.13). *M. aestuarina* OTUs were present in more than half of Dragon Island samples (18/30) and were only present in 4 other samples on Horseshoe Island. The last annelid member of the frequent group of OTUs was assigned to a metagenome sequence in the order Phyllodocida (SILVA: Phyllodocida, metagenome, GenBank: *Eteone longa*) and appeared in 15.71% of samples (Table 2.13). The remaining annelids (13/17 OTUs) were in the infrequent group and altogether accounted for 3.4% of the detections in the dataset (Table 2.13). However, all oligochaete OTUs were in the infrequent group (6 total OTUs, 4 of which assigned in GenBank to family Naididae) and combined to be detected in 21.43% of samples (Table 2.13). These OTUs were only detected in samples on Horseshoe (6/20) and Stingray Islands (9/20). Of the 7 remaining infrequent annelid OTUs, only one was detected on Dragon Island. Annelids make up a significant portion of the infauna community of a healthy salt marsh, with *M. aestuarina* alone comprising 5% of the total community in traditional sampling of the study area (Fleeger et al. 2018). *M. aestuarina* and oligochaetes are annelids which are used as indicators of salt marsh recovery from disturbance or the achievement of natural levels of diversity in created salt marshes (DeLaune et al. 1984, Craft and Sacco 2003) because they lack planktonic larvae and will only reach reference densities when conditions such as belowground biomass are sufficient.

The Arthropoda were the third most frequently detected group of OTUs (2.14). Arthropods can disperse via the water column as larvae or adults (e.g. crustaceans) or through flight as adults, such as insects (Barnes and Ruppert 1994). The largest number of OTUs of any phylum in the dataset were arthropods (26% of all OTUs, Fig. 2.15), but only two of these OTUs were in the frequent group. The most common OTU of these two was assigned to the species *Cancrincola plumipes* and was detected in 20% of samples. This harpacticoid copepod is a gill parasite of the purple marsh crab *Sesarma reticulatum* (Humes 1941). This marsh crab was not detected in this dataset, but an OTU assigned to the superorder Eucarida (which includes all decapod crustaceans) matched to the crab species *Hemigrapsus takanoi* in the GenBank assignment at 98.62% similarity (Table 2.13). This crab is in the same superfamily as the host crab *S. reticulatum* and therefore this OTU may represent *S. reticulatum* in the dataset. Another OTU was assigned to the superorder Eucarida in SILVA, but this OTU assigned to mite species *Malaconothrus monodactylus* in GenBank (Table 2.13). The OTU assigned to *H. takanoi* appeared only on Dragon Island in 4 samples from both sheared and intact margins. Another possibility exists that the OTU matching to *C. plumipes* represent a different harpacticoid copepod species; harpacticoid copepods are common members of the infauna community in the study area (Fleeger et al. 2018). The other arthropod frequent group OTU was assigned to the termite species *Prorhinotermes simplex* in SILVA and *Reticulitermes flavipes* in GenBank and appeared in 15.71% of samples (Table 2.13). Of the two species, only *R. flavipes* is found in Louisiana. However, the GenBank BLAST results returned 85 matches to termite sequences

from 79 species at 97% or higher, indicating that the 18S region used in this study may not be specific enough to determine species level assignments for this group. Of the remaining arthropod OTUs in the infrequent group, 25/39 were assigned to hexapods, including those from the Collembola and the insect orders Diptera, Hemiptera, Hymenoptera, Orthoptera, Blattodea, Zygentoma, Lepidoptera, Coleoptera, and Isoptera (Table 2.13). Of the thirty-nine infrequent arthropod OTUs, eight were assigned to members of the Crustacea, five were assigned to members of the Acari, and one was assigned as a member of the Araneae (Table 2.13). The crustaceans included the OTU assigned to the crab *H. takanoi*, ostracods, tanaid amphipods, copepods, and a barnacle.

The mollusks were the fourth most frequently detected phylum of OTUs (Fig. 2.14). This group included two members of the frequent group (Table 2.13). Many marine mollusks distribute themselves via planktonic larvae (Barnes and Ruppert 1994). An OTU assigned to *Geukensia demissa* in SILVA and GenBank was the most frequently detected mollusk OTU, appearing in 77.14% of samples (Table 2.13). *Geukensia* mussels have been found to facilitate primary production of *Spartina* plants by increasing soil nitrogen (Bertness 1984) and may enhance ecosystem functions (Christine et al. 2015). An OTU assigned to the family Neritidae (SILVA: *Nerita peloronta*, GenBank: *Theodoxus fluviatilis*) was the next most frequently detected mollusk OTU at 24.29% of samples. The infrequent group mollusk OTUs included members of the orders Veneroida, Siphonariida, Ostreoida, Littorinimorpha, Stylomatophora, Mytiloida, and Nudibranchia (Table 2.13). The OTU assigned to the order Ostreoida (SILVA: Ostreoida, GenBank: *Crassostrea gigas*) was detected in 3 samples. The eastern oyster, *Crassostrea virginica*, is known to inhabit the marshes of Louisiana, and the detection here of an Ostreoida OTU may indicate the presence of environmental DNA. An OTU assigned to the order Littorinimorpha (SILVA: *Tectarius striatus*, GenBank: *Littoraria undulata*) was detected in 3 samples (Table 2.13). Marsh periwinkles of the genus *Littoraria* are primarily associated with aboveground *Spartina* so logically this OTU would not be frequently detected in soil samples.

The Hydrozoa consisted of a total of 8% of the incidences and were the fifth most common phylum in the dataset (Fig. 2.14). The majority of hydrozoans have both a polyp (benthic) and a medusa (pelagic) life stage, with the polyps forming colonies (Barnes and Ruppert 1994). Two of these OTUs were in the frequent group and were assigned as *Helgicirrho cari* (GenBank: *Helgicirrho cari*) and an uncultured member of the order Siphonophorae (SILVA: Siphonophorae; uncultured eukaryote, GenBank: uncultured eukaryote, Table 2.13). Both of these OTUs were detected in 24.29% of the samples (Table 2.13). The Leptomedusa species *H. cari* is primarily known from Europe and Africa (Schuchert 2017). However, other Leptomedusa species, such as *Blackfordia virginica*, are known to be invasive in estuarine systems around the world (Genzano et al. 2006). The order Siphonophorae consists of colonial hydrozoans which are primarily pelagic, though some species are found in coastal waters (Mapstone 2014). However, members of the Siphonophorae lack a benthic life stage unlike most other cnidarians, developing instead as plankton.

A single gastrotrich OTU was included in the frequent group, although the gastrotrichs made up only 4% of the incidences in the dataset (Fig. 2.14). Gastrotrichs are common members of the interstitial meiofauna, but they are less studied than groups such as nematodes and arthropods due to their soft-bodied nature and do not have pelagic larvae (Barnes and Ruppert 1994). The single frequent group OTU in this group was assigned as a member of the genus *Heterolepidoderma* in both SILVA and GenBank and was detected in 40% of samples (Table 2.13). Gastrotrichs of the genus *Heterolepidoderma* have been found in freshwater, brackish, and saline environments from a variety of substrates across the world (Grilli et al. 2009, Garraffoni and Melchior 2015, Kolicka 2019).

Rotifera made up 3% of the total incidences in the dataset (Fig. 2.14). Many rotifers are free living members of planktonic communities, though some are benthic or colonial (Barnes and Ruppert 1994). One of these OTUs, which was assigned as a member of the order Adinetida (GenBank: *Adineta vaga*), was included in the frequent group and appeared in 20% of the samples (Table 2.13). The order Adinetida are under the class Bdelloidea, which are typically benthic rather than planktonic (Ricci and Balsamo 2000).

For comparisons of sheared vs intact, the similarity index estimates (Table 2.16), the OTU richness (Fig. 2.16), and Faith's PD results (Fig. 2.17) suggested that there was a high degree of similarity in the OTU composition, OTU richness, and phylogenetic diversity of the soil infauna community between samples from sheared and intact margins. The NMDS ordination (Fig. 2.18) showed a large overlap between the two groups of samples and therefore did not indicate a clear differentiation between the groups, though the centroids of the groups were separate. The Adonis test results (Table 2.19) indicated that there were significant differences in the soil community composition between sheared and intact sites, but that the type of marsh margin explained a minimal percentage of the variation in the dataset. The most common OTUs (*Thoracostoma trachygaster*, *Mytloida*, *Polydora ciliata*) in the dataset did not contribute much to the differentiation of samples because they were present in most samples. All of the frequent group OTUs were shared between the samples from intact and sheared margins (Table 2.10), so the differences in composition detected by the Adonis test were impacted by the OTUs which were less commonly detected and were unique to either group. The groups of OTUs which were unique to the sheared and intact margins were similar at the phylum level, with both groups containing unique Annelida, Arthropoda, Nematoda, and Mollusca OTUs (Table 2.14). Many of the OTUs that were unique to either sheared or intact margins were assigned to taxa which have limited dispersal, although some have pelagic larvae. All of the annelids which were unique to either margin type and were detected more than once were assigned to the order Haplotaxida, which is within the class Oligochaeta. Members of the Oligochaeta lack planktonic larvae, meaning that their distribution is limited. The arthropod OTUs which were unique to the intact margins included 2 ostracod OTUs. Ostracods lack a planktonic larval stage and juveniles resemble adults, so dispersion may be limited (Barnes and Ruppert 1994). However, another ostracod OTU was present in samples from both sheared and intact margins. The only mollusk that was detected at least twice and was unique to samples

from sheared margins was assigned to the order Ostreida, which have planktonic larvae. The only mollusk unique to the intact margins was a member of the gastropod subclass Heterobranchia, which includes snails and slugs and do not typically have planktonic larvae. The only nematode which was both unique to the intact margins and was detected more than once was assigned to a member of the genus *Meloidogyne*, which are known to be parasitic on plants. In addition to the common phyla, the samples from sheared margins also contained unique members of the Ctenophora (1 OTU detected in 3 samples), Hydrozoa (1 OTU detected in 9 samples), Nemertea (2 OTUs detected in a total of 6 samples), Platyhelminthes (1 OTU detected in 2 samples), and Rotifera (1 OTU detected in 2 samples). Ctenophora are typically members of offshore plankton communities, but the genus *Moerisia* (which the unique Ctenophora OTU was assigned to in GenBank) is known to be invasive in estuaries in Louisiana and across North America (Poirrier and Mulino 1977, Purcell et al. 1999). Notably, this was the only Ctenophora OTU detected in the dataset. Nemertea are predatory worms which are collected in salt marshes but are usually not especially abundant (Nordström et al. 2014, Qiu et al. 2019). Some nemerteans have a planktonic larvae which aids in distribution (Barnes and Ruppert 1994). The samples from sheared margins also contained the only Kinorhynch OTU, but this OTU only occurred in one sample. Kinorhynchs are commonly found in marshes with varying density by season (Higgins and Fleeger 1980), but were locally absent in the study area following the DHOS (Fleeger et al. 2015). The OTUs which were most strongly associated with sheared margins according to the Songbird differential read abundance analysis were an ambiguous member of the nematode order Monhysterida and the nematode *Thoracostoma trachygaster* (Table 2.19). Those OTUs most associated with intact sites were the annelid *Manayunkia aestuarina* and an ambiguous member of the nematode order Enoplida (Table 2.19). The primary physical differences between sheared and intact sites are the lack of plants and the reduced elevation compared to the surrounding marsh. Previous manipulation studies had shown losses in infauna species richness and changes in the densities of different groups upon removal of *Spartina* aboveground biomass, partially due to losses of plant associated infauna (Whitcraft and Levin 2007, Osenga and Coull 1983). Previous traditional studies of infauna in the study area found that the recovery of the majority of the infauna community in the microtidal intertidal zone following the DHOS closely tracked the recovery of foundation marsh species such as *Spartina* (Fleeger et al. 2019). Any primary consumers present in the sheared margins must be fully relying on benthic microalgae and planktonic primary production, the two remaining sources of primary production for this ecosystem (Odum 1971). However, many infauna rely on benthic microalgae as a primary food source to begin with (Galván et al. 2008), so perhaps the primary consumers consist of similar groups of taxa in shared and intact margins. As the sheared sites erode, the elevation of the site is reduced relative to the surrounding marsh, and the site transitions from an intertidal (periodically inundated) to a benthic (permanently inundated) environment. This transition in elevation may be driving succession to a group of organisms adapted to a new set of environmental conditions, rather than a difference totally due to the loss of *Spartina* in the site. However, there is a significant degree of overlap between benthic and intertidal communities (Fleeger et

al. 1984). The possibility of a transitional community is potentially supported by the Songbird differentials (Table 2.23), which indicate that *Manayunkia aestuarina* was enriched in intact sites. *M. aestuarina* is a filter feeder which is primarily associated with healthy marshes with high belowground biomass (Craft and Sacco 2003, Fleeger et al. 2018).

Differences in the communities present across the three islands were detected by the Adonis test (Table 2.19), although the Island variable only explains a minimal amount of the variation in the overall dataset. The island communities had high overall similarity (Table 2.18) but Stingray Island had lower pairwise similarity with the other two islands (Table 2.19). Alpha diversity metrics (OTU richness, Faith's PD) were not significantly different among the three islands (Fig. 2.16, Fig. 2.17). The NMDS ordination showed overlap between the groups of samples from different islands (Fig. 2.19). In addition, this ordination showed a short distance between the group centroids. All of the 18 frequent group OTUs were shared between Dragon and Horseshoe Islands, but two of these OTUs were not present on Stingray Island. These two OTUs were assigned as the annelid *Manayunkia aestuarina* and as the hydrozoan *Helgicirrhacari* (Table 2.13). The OTUs that were unique to Dragon Island and were detected more than once were 2 nematodes and 2 arthropods (Table 2.14). The only OTU which was unique to Horseshoe Island and was detected more than once was a rotifer (Table 2.14). The OTUs which were unique to Stingray Island and were detected more than once included 3 annelids and 2 nematodes. The three OTUs which were shared only between Dragon and Horseshoe Island and were detected more than once on both islands were assigned as the annelid *M. aestuarina*, the hydrozoan *H. cari*, and a nemertean. The two OTUs which were shared only between Dragon and Stingray Island and were detected more than once on each island were assigned as a chordate in the order Stolidobranchia (under the subphylum Tunicata) and a nematode. The two OTUs shared between only Horseshoe and Stingray Island and were detected more than once were assigned to an oligochaete annelid and a bryozoan. Bryozoans are colonial animals which have a planktonic stage to aid in dispersal (Barnes and Ruppert 1994). The OTUs most heavily associated with Dragon Island when compared to Horseshoe or Stingray Island in the Songbird differential read abundance analysis were assigned to the annelid *M. aestuarina*, the gastrotrich *Heterolepidoderma* sp., and an ambiguous member of the nematode order Monhysterida (Table 2.23). The OTUs most associated with Horseshoe Island compared to Dragon Island were assigned to the mollusk *Nerita peloronta*, the annelid *Polydora ciliata*, the hydrozoan *H. cari*, and an ambiguous member of the nematode order Dorylamida (Table 2.23). The OTUs most associated with Stingray Island compared to Dragon Island were assigned to the annelid *P. ciliata* and the nematode *Thoracostoma trachygaster* (Table 2.23). Additionally, mollusks were not as frequently detected on Stingray Island, especially in some of the MidHigh and High samples (Fig. 2.13). The most common mollusk OTU in the dataset was a filter feeder (assigned to the mussel genus *Geukensia*). The islands were assumed to be similar at the start of this study due to all sites falling in the Heavily Oiled category under the Shoreline Cleanup Assessment Technique crew assessments following the DHOS (Michel et al. 2013) and the total infauna community in the area was mostly considered to be recovered to pre-DHOS levels

(Fleeger et al. 2018, 2019). However, only Dragon Island was sampled to assess recovery of infauna following the DHOS, so no recent data on infauna for Stingray and Horseshoe Islands are available, leading to questions about conditions on those islands as a result of oiling associated with the DHOS.

No cleanup procedures were applied to oiled shorelines in Bay Jimmy following the DHOS (Duan et al. 2018). Oil residues (aromatics and alkanes) in sediments in Barataria Bay were monitored following the DHOS from 2010 to 2018 (Turner et al. 2019). Detected levels of oil residues in sediments were consistently higher than pre-spill reference levels. Analysis of sediment cores collected roughly 1.5 years after the DHOS indicated that the distribution of oil residues throughout locations within Barataria Bay was heterogeneous (Kirman et al. 2016). Later analysis indicated that certain infauna, including *M. aestuarina*, were negatively associated with PAHs in the sediment (Fleeger et al. 2019). The heterogeneous distribution of the oil may offer some explanation for the differences detected among the infauna communities on the different islands. The sites that this study sampled from were all described as heavily oiled by the SCAT analysis, but Dragon Island had more shoreline that was moderate or lightly oiled when compared to the more consistent heavy oiling of Horseshoe or Stingray Island (SCAT data available at <https://erma.noaa.gov/gulfofmexico/erma.html>).

OTUs matching to the sabellid polychaete *Manayunkia aestuarina* were detected on Dragon and Horseshoe Island but not on Stingray Island. This annelid is a tube dwelling suspension feeder with very limited dispersal ability (Craft and Sacco 2003) that was specified by Fleeger et al. 2018 as a taxa which had not recovered to reference site levels at the heavily oiled sites on Dragon Island. *M. aestuarina* is typically very abundant in healthy salt marshes, where it may be one of the most abundant single species in the annelid community (Johnson et al. 2007, Galván et al. 2008), but following oiling associated with the DHOS this annelid was locally absent (Fleeger et al. 2015). *M. aestuarina* has been shown to be associated with higher levels of belowground biomass and negatively associated with polyaromatic hydrocarbon (PAH) concentrations, (Craft and Sacco 2003, Fleeger et al. 2019). The increased levels of carbon and percent organic matter observed on Dragon Island may be related to the detection of this polychaete primarily on this island.

The family Naididae (which contains the former Tubificidae) is a group of oligochaetes that are well known and studied for tolerance to various types of pollution, and the species *Tubifex tubifex* in particular is frequently used as an indicator of pollution (Duguay 1997, Bhattacharyya et al. 2003, Smutná et al. 2008, Gerhardt 2009). OTUs assigned to this group were only detected in samples from Horseshoe (6/20 samples) and Stingray Islands (9/20 samples, Table 2.13). Oligochaetes are generally subsurface deposit feeders with limited dispersal ability, and in constructed salt marshes were shown to only reach density levels similar to reference marsh after 25 years (Craft and Sacco 2003). Following the DHOS, oligochaetes in general were only rarely collected and only in lightly oiled or reference sites (Fleeger et al. 2018). None of the sites where oligochaetes were detected in this dataset were

sampled by the Fleeger group according to the available data. When considering this information alongside the distribution of *M. aestuarina* (Table 2.14) there may be a local pollution pattern occurring within the annelid community, which may be driving the differences detected by the Adonis test (Table 2.19). However, the density of Naididae has been observed to be highly variable in repeated samplings of experimental plots in Louisiana salt marshes (DeLaune et al. 1984). In addition, it is possible that these annelids are also slowly recolonizing the area following the DHOS and have not reached Dragon Island yet. Dragon Island has been fully separated from the other marsh islands surrounding Bay Jimmy since at least 1956 (aerial photography single frame courtesy of the U. S. Geological Survey at <https://earthexplorer.usgs.gov/>), which may account for some of the differences in low dispersal organism differences across the islands.

The Adonis results indicated that there were significant differences in the community composition of the sheared and intact margin samples from the different islands (Table 2.19) and the additional Adonis tests on the individual island datasets indicated that these differences were primarily in Dragon and Stingray Island (Table 2.20, 2.22). The NMDS ordination showed a large amount of overlap between groups from different islands and margin types (Fig 2.20) though the low diversity sample from Stingray Island again fell outside of the group overlap. The OTU richness and Faith's PD metrics were not significantly different between any of the island-margin groups (Fig. 2.16, Fig. 2.17). The samples from both sheared and intact margins from Dragon Island contained all of the frequent group OTUs, while the samples from sheared and intact margins from Horseshoe and Stingray did not. The Horseshoe intact margin samples contained 15 of the 18 frequent group OTUs, while the sheared margin samples from that island contained 16 of the 18 OTUs. In the intact margin samples from Stingray Island, 16 of the 18 frequent group OTUs were detected, while only 11 were detected in the sheared margin samples from that island. This indicates more differentiation from the infrequent group OTUs in Dragon Island samples and more differentiation from the frequent group OTUs in Stingray Island samples.

In addition, the Stingray Island samples showed significant differences in composition between the elevation positions and the interaction of margin and elevation position (Table 2.22). The NMDS ordination indicates that the samples from the intact margins on this island were more similar to each other (clustered together) than to the samples from sheared margins (Fig 2.21). However, the low number of samples resulting from dividing up the dataset into the elevation positions from different margin types on a single island limit the available inferences to be made from the position of groups in an NMDS plot.

The marsh margin habitat has been shown to be quite important for both commercial and prey species (Minello et al. 1994, Peterson and Turner 1994), so further studies of the impacts of sheared marsh margins are required, potentially over a larger scale than in this dataset. This dataset could be used as part of a longer-term study of the interactions between the multiple disturbances of various hurricanes and the DHOS. The metazoan OTUs which were

infrequently detected in the dataset likely comprised the majority of the differences between the sheared and intact margins, so an increased number of samples may be important to collect a sufficient level of biodiversity for analysis. The unfiltered dataset (all detected eukaryotes) may contain insights which will become apparent as databases become more complete. In addition, the meiofaunal community (infauna which range from 500 to 45 μm in size) may hold additional insights into the differences in community composition between the sheared and intact margins. Meiofauna specifically tend towards nearly sessile lifestyles with low dispersal mechanisms, have high species diversity, and short generational time, making them ideal to determine impacts on marsh health (Kennedy and Jacoby 1999). This dataset might also be useful for comparisons in long-term studies of previously or recently oiled marshes in other systems. A potential long-term study of sheared marsh margins might be able to determine a successional community pattern from marsh platform fauna to benthic or mudflat fauna, especially if it includes sampling of non-marsh platform sites which are exposed at low tide for comparison.

Chapter 3. A Comparison of Intertidal Metazoan Meiofauna Biodiversity between Previously Oiled Sheared and Intact Marsh Margins in Bay Jimmy, Louisiana, Using DNA Extraction of the Organic Portion of Sediments

3.1. Introduction

Salt marshes are important ecosystems, which make up an estimated 5.5 million hectares of wetland in Europe, the USA, and Australia, and are estimated to be as much as 40 million hectares of wetland worldwide (Mcowen et al. 2017). These marshes provide a number of valuable ecosystem services, including protection from storm surge, acting as a nursery for commercial species, recreation, denitrification, and carbon sequestration (Barbier et al. 2011, Engle 2011, Hinshaw et al. 2017a). However, salt marshes across the globe are under threat. A wide variety of factors, including anthropogenic factors, are to blame for this decline. These factors include subsidence, erosion, land reclamation, mean sea level rise, pollution, and extreme weather events such as hurricanes (Kennish 2001).

The coastal region of the northern Gulf of Mexico contains more than half of the coastal wetlands of the contiguous USA (Engle 2011). Of these coastal wetlands, the marshes of Louisiana are suffering the greatest land loss rate of any state. These marshes lost a land area approximately the size of the state of Delaware (4,833 km²) during the period from 1932 to 2016 (Couvillion et al. 2017). The marshes in Louisiana, and the majority of the land in the southeast of the state, were primarily built by the Mississippi River over thousands of years (Russell 1940). Because these marshes were recently deposited, sediments are still compacting, leading to natural subsidence in some areas (Meckel et al. 2006).

The mechanism by which the elevation of marshes keep pace with subsidence and relative sea level rise due to climate change is vertical accretion (Kirwan and Megonigal 2013). In Louisiana marshes, vertical accretion primarily occurs through the accumulation of organic matter from plants, because the major sediment source of the Mississippi River has been cut off by flood control structures (Turner et al. 2005).

Anthropogenic factors have had major impacts on Louisiana marshes. Flood control structures now prevent the Mississippi River from delivering sediment to the majority of the marshes of Louisiana (Else-Quirk et al. 2019). Subsidence of marshes is enhanced by subsurface fluid extraction particularly oil extraction (Yuill et al. 2009). Erosion has been greatly increased by channels cut for navigation and oil exploration in Louisiana marshes (Couvillion et al. 2017, Turner and McClenachan 2018).

Hurricanes cause massive damage to marshes through both wind and storm surge, causing immediate loss of land (Palaseanu-Lovejoy et al. 2013). Hurricanes also force saltwater inland, impacting freshwater habitats by stressing and killing plants (Sasser et al. 1986). Storm surge can enhance erosion and tear away marsh margins during a process known as margin shearing, which has been recorded during multiple hurricanes affecting Louisiana marshes

(Morton and Barras 2011). Typically, this damage has been greater in brackish and freshwater marshes, due to lower tensile strength in the soils compared to salt marsh soils (Howes et al. 2010). Shearing can lead to long term increases in the erosion rate of a marsh edge due to the loss of plants, which hold the marsh sediment together with their roots.

Louisiana marshes are especially at risk for oil pollution due to historic industry use of marshes and near and offshore oil fields (Fleeger and Chandler 1983). The Deepwater Horizon oil spill (DHOS) in 2010 caused extensive oiling in coastal ecosystems in the northern Gulf of Mexico, with over 700 km of marsh shoreline impacted (Michel et al. 2013). Rapid dieback of marsh plants was observed in areas with heavy oiling, and a reduction in marsh plant belowground biomass was observed for years after the spill (Lin and Mendelssohn 2012, Lin et al. 2016). This reduction in belowground biomass lowered the tensile strength of the marsh, and margin shearing was detected via satellite analysis following Hurricane Isaac in 2012 in previously heavily oiled sites in Bay Jimmy, Louisiana (Michel et al. 2013, Ragoonwala et al. 2016).

Marshes are complex ecosystems, and numerous biological indicators of marsh health have been proposed. Since marshes are also impacted by environmental disturbances such as hurricanes and oil spills, a large body of research has been dedicated to studying the impacts and recovery from such disturbances (Morton and Barras 2011, Deis et al. 2019, Hanley et al. 2020). Numerous studies were conducted following the DHOS to determine impacts of and recovery from oil in northern Gulf of Mexico marshes. These studies included documenting the fate of oil (Turner et al. 2019), changes in the bacterial community following oiling and the role of bacteria in degrading oil (Beazley et al. 2012, Kimes et al. 2014, Zhang et al. 2018), and impacts of and recovery from oil on marsh plants (Lin and Mendelssohn 2012, Rabalais and Turner 2016). Invertebrate species native to marshes, such as horse flies, were shown to have experienced dramatic population crashes and genetic bottlenecks in oiled areas, followed by a recovery due to migration effects (Husseneder et al. 2016, 2018). Rapid changes in the sediment eukaryote community were observed, with a shift from metazoan dominated to fungal dominated sediments (Bik et al. 2012); however, this change was reversed by one year after the spill (Brannock et al. 2014). Exposure to non-lethal concentrations of oil led to a reduction in growth rates in penaeid shrimp (Rozas et al. 2014). Estuarine filter feeders such as the mussel *Geukensia demissa* were found to only minimally incorporate carbon from oil (Fry and Anderson 2014). The concentrations of polycyclic aromatic hydrocarbons (PAHs) were tracked in a variety of commercially important seafood species, including the Gulf menhaden, *Brevoortia patronus* (Xia et al. 2012, Olson et al. 2016). This tracking revealed that the concentration of PAHs in organisms decreased over time following a peak after the DHOS, though the PAH concentrations remained below levels which might impact public health. Estimates of offshore effects indicated that large proportions of Gulf of Mexico sea bird populations suffered mortality during the DHOS (Haney et al. 2014). Sea turtles and marine mammals both experienced an increase in mortality following the DHOS (Antonio et al. 2011).

The communities of marsh infauna, i.e. sediment dwelling macrofauna and meiofauna, were compared between oiled and reference sites to determine impacts and recovery after the DHOS (Fleeger et al. 2015, 2018, 2019). Meiofauna are a specific size class of infauna which range from 0.5 mm to 45 μ m (Coull and Chandler 2001, Giere 2009). These near microscopic organisms include representatives from 19 of the 34 metazoan phyla. Meiofauna serve as a link between the microbial and macro food webs, and can be prey to commercially important species (Tito de Moraes and Bodiou 1984, Gee 1989, McClelland and Valiela 1998, Fantle et al. 1999, Hewitt et al. 2020). The pattern of recovery of most marsh meiofauna communities after the DHOS followed previously observed trends of meiofauna recovery after experimental oiling (Fleeger and Chandler 1983, Carman and Todaro 1996), specifically tracking the recovery trajectories of marsh plants (Fleeger et al. 2018, 2019). Most taxa recovered within 6 years, but the annelid *Manayunkia aestuarina*, the tanaid *Hargeria rapax*, ostracods, and kinorhynchs failed to recover to reference values within 6 years of sampling. The studies of meiofauna following the DHOS were conducted in the same area where margin shearing was detected, making meiofauna a good candidate for study to determine effects of margin shearing.

However, meiofauna are difficult to study due to the small scale of the organisms, and taxonomic identification of meiofauna to the species level requires deep technical expertise for numerous groups. To circumvent these issues, some studies have turned to metabarcoding to taxonomically identify bulk samples of meiofauna (Bik et al. 2012, Brannock and Halanych 2015, Creer et al. 2016, Ruppert et al. 2019). Metabarcoding is based on sequencing marker genes that are universal across taxa from environmental samples and using these sequences to identify taxa by matching to previously reported reference sequences, such as GenBank (Benson et al. 2011) or SILVA (Quast et al. 2013). Several of these marker genes have been used to study a variety of taxa, including 16S, 18S, COI, trnL, and ITS (Drummond et al. 2015, Ruppert et al. 2019). This study uses the 18S small ribosomal subunit gene because it is specific for eukaryotes (Creer et al. 2016, Jacquiod et al. 2016). Other commonly used marker genes for eukaryotes, such as COI, may not contain suitably conserved regions to be applicable in studies focused on taxonomically diverse groups, such as meiofauna (Creer et al. 2010, Deagle et al. 2014). Metabarcoding techniques make it possible to gain deep diversity insights into samples in a reasonable amount of time and with relatively low amounts of effort.

In the results for chapter 2, the composition of infauna was found to be different between samples from sheared and intact margins and between samples from different islands. The purpose of this chapter is to reexamine the same samples and apply size exclusion and extraction techniques to determine if the sheared and intact margins support different meiofauna communities. The Ludox-based meiofauna extraction method used in this chapter allows for the isolation of the organic portion of the sample selected for size by sieving (Burgess 2001). This method allows for the extraction of DNA from a consistent mixture of only meiofauna from a larger volume of sample than direct extraction of the sample.

3.2. Materials and methods

Sample collection:

Samples used for this study were subsamples of the same as those used in chapter 2; therefore, all collection methods and dates were exactly the same (Section 2.2, Site determination and Sample collection). Briefly, the three marsh islands surrounding Bay Jimmy, Louisiana, which were designated as heavily oiled following the DHOS and were identified as having sheared sites following Hurricane Isaac, were selected as the study area (Ragoonwala et al. 2016). These three islands are referred to as “Dragon Island”, “Horseshoe Island”, and “Stingray Island”. Each soil sample transect consisted of five samples. The first sample of the transect was collected at the marsh edge and the four other samples in the transect were collected every time the elevation increased by 0.05 m along a line into the marsh. Elevation was measured using a Trimble R2 GPS (Trimble, Sunnydale, California). Samples were initially collected using PVC cores (4 transects on Dragon Island), but the rest of the samples were collected using a Barrett coring device with detachable acrylic cores (Perret and Barrett 1971). Each sample transect was paired, with one transect in a sheared marsh margin and another in the nearby intact marsh margin. Two sets of paired transects were taken on each island, with a repeated paired transect on Dragon Island, for a total of 7 paired transects, 14 transects total, and 70 total samples. Soil samples were stored at -20°C until the meiofauna extraction process.

Sample sieving and meiofauna extraction:

Each sample was subsampled into approximately 5 cm³ cubes using a handsaw. All tools were cleaned with a 10% bleach solution in between samples to prevent cross contamination. All acrylic cores (the 50 cores collected after August 2017) had enough material to do so. However, several of the PVC cores (the 20 cores collected during August 2017) did not have enough material remaining to produce a cube of this size. If this was the case, half of the remaining core was taken. Each cube produced was then placed into 95% ethanol and allowed to thaw in a 4°C refrigerator. Following the thawing period, the soil was sieved with water into a 500 µm sieve, and then into a 45 µm sieve. Material left in the 500 µm sieve was then placed on 95% ethanol at -20°C as voucher material. Material left in the 45 µm sieve was placed into 50 ml tubes in 15 ml aliquots. This produced an unequal number of tubes per sample, as the amount of material on the 45 µm sieve was inversely related to the amount of root mass and large organic detritus present in the original sample. The amount of root mass and large organic detritus in each sample was not consistent across samples, therefore the amount of material retained on the 45 µm sieve was not consistent. Each tube was then filled with ethanol to allow any organisms to release from the sediment for a minimum period of two hours. Material from tubes resulting from the same sample were then combined onto a 45 µm sieve and rinsed thoroughly of ethanol with water. This material was then again separated out into 50 ml tubes in 15 ml aliquots. Thirty ml of Ludox (Sigma-Aldrich, Munich, Germany) was added to each tube and vigorously mixed with the material, then allowed to stand for a minimum period of two hours. The tubes were then subjected to centrifugation for 15 minutes at 4500 rpm at 25°C. The

supernatant material for each set of tubes from a single sample was then rinsed of the Ludox on a 45 µm sieve and pooled into one tube (or more if a large quantity of material was produced). This supernatant material was the organic portion of the sample, including the meiofauna, while the precipitant material was the sediment portion of the sample. Ethanol (95%) was added to the tubes as a preservative, and then the tubes were stored at -20°C. The precipitant material for each set of tubes from the sample was also pooled and stored separately as voucher material in the same manner as the supernatant. Four of the PVC core samples resulted in no material following the soil floating process due to low soil input and were excluded from the DNA extraction process.

DNA extraction from floated meiofauna, polymerase chain amplification, and sequencing:

Total DNA was extracted from the supernatant material using the DNeasy Blood and Tissue kit (Qiagen, Hilden, Germany). Three 0.025g portions of each sample were extracted, resulting in a total of 201 DNA aliquots. Each aliquot was checked for DNA quantity (>10 ng) using the Invitrogen Qubit 4 Fluorometer (Thermo Fisher Scientific, Wilmington, DE). However, six samples failed to produce any DNA during the extraction process, even following repeated extractions, so they were excluded from the PCR process. This resulted in 183 DNA aliquots (from 61 samples) that were shipped on ice for amplification and sequencing at the Hubbard Center for Genome Studies at the University of New Hampshire. These aliquots were amplified using the Earth Microbiome Project 18S PCR protocols (available at <https://press.igsb.anl.gov/earthmicrobiome/protocols-and-standards/18s/>) with primer constructs using the forward primer Illumina_Euk_1391f (Amaral-Zettler et al. 2009) and reverse primer Illumina_EukBr (Stoeck et al. 2010). The PCR products were then sequenced on the Illumina HiSeq 2500 platform (Caporaso et al. 2012) using the HiSeq Rapid SBS v2 kits (Illumina, San Diego, California) for sequencing preparation, which produced 2x250 base pair forward and reverse FASTQ files for each aliquot. Sequence files and metadata are available in GenBank via the BioProject accession number PRJNA706428.

Analysis and Bioinformatics:

Raw demultiplexed FASTQ files were imported into QIIME 2 (version 2020-2) (Boyle et al. 2019) as a QIIME zipped artifact using the q2-tools plugin. Reads were examined using the q2-demux plugin, and Phred quality scores showed low quality for a random subsampling of base pairs (bp) after position 95 in the forward reads and for the reverse reads after position 63. The DADA2 algorithm (Callahan et al. 2016) was used to trim reads at these positions, however this resulted in poor overlap between forward and reverse reads due to the short length. Reads which do not overlap are dropped from the table and representative sequences files from DADA2, so the majority of reads were dropped during this process. To preserve the majority of reads and eliminate low quality reads from the reverse reads, DADA2 was run again (using a 95 bp cutoff) on only the forward reads. This process may waste some of the information contained in the reverse reads, but using only forward reads is generally acceptable (Soergel et al. 2012, Liu et al. 2020). This resulted in an amplicon sequence variant (ASV) by

sample table and a representative sequence file containing all sequences from the ASVs with unique feature IDs. An ASV is the exact sequence returned from the sequencing process, following quality control (Callahan et al. 2017). The separate entries in the table for the three DNA extractions for each sample were then merged using the group method of the q2-feature-table plugin, resulting in 61 samples in the ASV table. The SILVA 132 database and taxonomy files (Quast et al. 2013) were imported and used to classify sequences with the BLAST algorithm (Camacho et al. 2009) resulting in a taxonomy file with taxonomic strings for each ASV. The ASV table and the representative sequence file were then filtered using this taxonomy file with the filter-table method of the q2-taxa plugin to only allow non-vertebrate metazoan ASVs in the database. The resulting taxonomy file was then examined for taxonomic assignments which might be the result of contamination during sample processing or an error in the database. Any ASV considered to be a contaminant or an error was filtered from the table, again using the filter-table method of the q2-taxa plugin. The resulting ASVs were then clustered at a 97% identity threshold using the cluster-features-de-novo method of the q2-vsearch plugin (Rognes et al. 2016) to account for intraspecific genetic variation (Bucklin et al. 2011, Brandt et al. 2019, Phillips et al. 2019). This process resulted in a table of operational taxonomic units (OTUs) by sample. The mafft and mask methods of the q2 alignment plugin (Lane 1991, Katoh et al. 2002) were used to align and mask sequences so that they could be used to generate a midpoint-rooted phylogenetic tree in the q2-fasttree plugin (Price et al. 2010). The OTU table (with taxonomy and metadata) was exported in the .biom format and imported to R using the biomformat package (McMurdie and Paulson 2016). This table was then modified to turn the read counts into OTU incidences (presence of individual OTUs in each sample), resulting in a table of presence and absence (i.e., 0 = OTU not present, 1 = OTU present). In this text, the phrase “incidence” will refer to a single appearance of an OTU in a sample, while the phrase “total incidence” will refer to all appearances of an OTU in the dataset. Incidences were used in this analysis due to the mismatch between number of cells and number of individuals in metazoan taxa. Due to this mismatch, read counts do not represent the number of metazoan individuals per sample.

Alpha rarefaction curves featuring OTU richness plotted against sequencing depth were generated using the rarecurve method in the package vegan in R (Oksanen et al. 2018). The OTU incidence table was used to generate extrapolated sampling and coverage-based rarefaction curves in the R package iNEXT (Chao et al. 2015). This method relies on the concept of Hill numbers, a family of diversity indices which incorporate both abundance (or in this case, incidence) and species (or in this case, OTU) richness (Chao et al. 2014). The first three Hill numbers, $q = 0$, 1 , and 2 , are equivalent to OTU richness, the exponential of Shannon’s entropy index, and Simpson’s inverse index, respectively. Hill number rarefaction calculations produce effective diversity values, which are the number of equally abundant OTUs required to reach the index value. Sampling based rarefaction plots the effective diversity against the number of samples taken and extrapolates effective diversity for double the actual number of samples. Coverage-based rarefaction plots effective diversity against the estimated percentage captured

of the actual community, and extrapolates effective diversity out to the estimated coverage of twice as many samples. The phrase “actual community” refers to the total community estimated to be present in a sample, including all species which were not observed during sampling.

Basic diversity profile observations, shared OTUs between communities, and OTU richness estimations using Homogenous Model, Chao2, iChao2, and Incidence-based Coverage Estimator (ICE) estimation models were generated using the incidence table in SpadeR Online (Chao and Jost 2012, Chao et al. 2015). Basic diversity profile observations included total incidences, total number of OTUs, coverage estimate (CE), estimated coefficient of variation (CV), and the incidences and number of OTUs present in the infrequent group. The CE is an estimate of how much of the actual community the sampling effort collected (Chao et al. 2015). The CV is a measure of how heterogeneous the dataset is, with higher values representing higher heterogeneity. A dataset with a low CV (close to 0) would be nearly homogenous, with all OTUs appearing in all samples. The infrequent group is a group of OTUs which appear in fewer than 10 samples which are used for certain richness estimator models. Shared OTUs between sheared and intact margin communities, island communities, and elevation position communities were generated. The OTU richness estimations for the actual community were calculated using models which were appropriate for the properties of the dataset. The Homogenous model estimates actual richness if all OTUs have an equal chance of being detected. Chao2 estimates actual richness based on the number of OTUs which appear in one or two samples. The iChao2 model is an extension of Chao2 which estimates actual richness which takes into account OTUs that appear in up to 4 samples. The ICE model is an incidence-based extension of the Abundance-based Coverage Estimator, which estimates actual richness based on the infrequent group (Chao and Lee 1992).

The OTUs were plotted as percentages of total OTU incidence and total number of OTUs, organized by phylum in Microsoft Excel. The OTUs were also presented with phylum and order level assignment, total incidence, lowest level assignments from the SILVA database, and incidence by metadata category (sheared or intact margins, island, and elevation position). The lowest level assignment was the taxonomic level closest to species which had a definite assignment. An OTU which had an ambiguous assignment at the species level would have a lowest level assignment of genus.

Certain taxonomic issues with the SILVA database, including low resolution for some taxa, led to a need for more complete taxonomic strings for important taxa, so all OTUs were manually checked against the NCBI GenBank database using the BLAST+ algorithm (Benson et al. 2011). The top result from GenBank (sorted by e-value) for each OTU was presented alongside the SILVA assignment. Taxonomic strings for GenBank assignments were checked against the World Register of Marine Species database for accuracy (WoRMS Editorial Board 2020).

Bar plots for each sample were generated in the R package ggplot2 using the OTU incidence table. These plots show the relative percentage of the total incidences in each sample that each phylum of OTUs makes up.

Alpha diversity index values for samples were generated in Qiime2 using the alpha and alpha-phylogenetic methods of the q2-diversity plugin based on the OTU table and the phylogenetic tree. Before index calculation, the dataset was rarefied to 150 reads per sample with replacement using the feature-table plugin. The alpha diversity indexes included OTU richness and Faith's Phylogenetic Diversity (PD). The OTU richness is the number of OTUs detected in a sample, while Faith's PD is the total branch length of the phylogenetic tree of all OTUs within a sample. Both of these sets of values were tested for differences across the metadata categories of Margin, Island, and Elevation Position using Kruskal-Wallis tests in the q2-diversity plugin (Kruskal and Wallis 1952). For tests with multiple comparisons, the Benjamini-Hochberg correction was used to control the false discovery rate. These values were also used to generate boxplots using the R packages ggplot2 and ggpubr with separate boxes for each elevation position on each island and separate plots for samples from sheared and intact margins.

Beta diversity similarity indices for both the input data and the estimated actual community (based on Chao's estimates of the total community) were generated using SpadeR Online with the OTU incidence table (Chao et al. 2013). Empirical and estimated indices are presented together for comparison purposes. These indices were calculated to show the similarity between various communities in the dataset, including the sheared and intact communities, individual island communities, and elevation position communities. The indices included incidence-based extensions of the Sørensen, Jaccard, Horn (equal-weighted), Morisita-Horn (relative), and Regional overlap (relative). Other indices calculated by the program were discarded because they rely on absolute numbers of incidences rather than relative numbers of incidences, which may cause bias. All of these indices run from zero to one, with higher values indicating higher similarity of composition and incidence between communities. The Sørensen and Jaccard indices are richness based, and only take into account the similarity of composition of samples. These indices both compare the number of shared OTUs in both groups to the total OTUs of both groups, but the Sørensen index gives more weight to the shared species than the Jaccard index. All of the rest of the selected indices ordinarily use abundances to calculate similarity, but the versions used here use incidences as a proxy for abundance. The Horn (equal-weighted) index measures the overlap between the within community and total Shannon diversity of the dataset (Horn 1966). The "equal-weighted" part of the name indicates distinction from the other version of this index (size-weighted) which weighs the size of the total community higher than the within community size. The Morisita-Horn (relative) and regional overlap (relative) indices are both measures of the overlap between the within community and total Gini-Simpson diversity (Morisita 1961). The Morisita-Horn (relative) index gives more weight to the total diversity, but the regional overlap (relative) index gives more

weight to the within community diversity. All of the estimated indices were based on estimates of the richness and incidence of the actual community.

Non-metric Multidimensional Scaling (NMDS) from the metaMDS function in the R package *vegan* (Oksanen et al. 2018) was applied to the initial distance matrix. Ordination was started with 10 dimensions, with subsequent lower dimensional ordinations using previous solutions to reduce stress. Stress is the measure of goodness of fit of the regression of the distance matrix values against the ordination distances. The ordination with the lowest number of dimensions and a stress below 0.1 was selected as the best result. This process resulted in an ordination with 4 dimensions. This ordination was then plotted using the *ggordiplot* R package, available at <https://github.com/jfq3/ggordiplots>, with overlaid elliptical hulls and spider lines for metadata categories.

Sørensen index values for each pair of samples in the OTU table were calculated using the beta method of the *q2-diversity* plugin to form a distance matrix. The Sørensen index was chosen for this analysis because it uses composition instead of read counts to determine differences between the samples, and gives more weight to shared OTUs than the Jaccard index. Index values for each set of two samples were calculated by doubling the number of shared OTUs and dividing this by the total number of OTUs in both samples. This value (similarity) was then subtracted from one to determine the dissimilarity. An index value for each pair of samples in the dataset was calculated and compiled into a distance matrix. This matrix was tested for differences across metadata categories using the Adonis method in the *q2-diversity* plugin with the formula “Margin*Island*ElevationPosition” with 10000 permutations. The Adonis method is a multifactorial extension of the PERMANOVA test, which is a non-parametric permutational ANOVA method for multivariate datasets. The Margin factor had two classes, Sheared and Intact. The Island factor had three classes, Dragon, Horseshoe, and Stingray Island. The Elevation Position factor had five classes, Low, MidLow, Mid, MidHigh, and High. The PERMDISP procedure was used to test individual factors in the distance matrix for homogeneity of multivariate spread because non-homogenous multivariate spread can influence the results of the Adonis test. Additionally, the Benjamini-Hochberg correction (Benjamini and Hochberg 1995b) from the *p.adjust* function of the *stats* package in R was applied to p-values resulting from the Adonis test to control the false discovery rate. After initial testing, the OTU table was split into three tables containing samples from each island and a new Sørensen distance matrix was generated from each table. These matrices were also tested using the Adonis procedure with the formula “Sheared*ElevationPosition” and 10000 permutations, followed by PERMDISP and Benjamini-Hochberg corrections.

Relative differential abundances of OTUs based on read counts were calculated using the Songbird plugin in *Qiime2* through an iterative process of parameter adjustment with comparisons to a null model. The comparison to the null model generates a pseudo- Q^2 value, which functions similarly to the R^2 value of a linear regression. The parameters of the model were adjusted until the Q^2 value was positive. The model formula used was “Island + Margin +

Elevation Position". The final parameters of the model were 0.01 for the differential prior, a learning rate of $1e^{-6}$, and an epoch value of 700,000. In addition, the minimum sample count parameter, which controls how many samples an OTU must be detected in to be considered by the model, was adjusted from the default of 10 samples to 9 samples. This parameter was adjusted to add additional OTUs into consideration by the model because this dataset had fewer OTUs which appeared in more than 10 samples than the dataset of chapter 2. The final pseudo- Q^2 value was 0.048. The differentials calculated by this program are the relative log-fold change in read count abundance of OTUs in samples from a class within a metadata category compared to those from another class within that category. Positive differentials indicate enrichment of OTUs in the selected class, while negative differentials indicate enrichment in the comparison class.

3.3. Results

Preliminary 18s SRS sequence dataset evaluation:

The amplicon sequence variant (ASV) table contained approximately 1.8 million reads and 13,704 ASVs after the forward reads were subjected to quality control with the DADA2 algorithm. Following the removal of ASVs which did not match to the SILVA database, approximately 154 thousand reads and 677 ASVs remained. The largest group of these ASVs was the Opisthokonta group, which includes Metazoa and Fungi, followed by the SAR (Stramenopiles Alveolates and Rhizarians) clade. The Archaeplastida, Excavata, Amoebozoa, Cryptophyceae, Incertae sedis, and Haplophyta groups all had fewer ASVs. Three hundred and forty-eight of the 677 ASVs which were assigned as eukaryotes had a species level assignment which was unclear (Table 3.1). Most of the sub-domain groups had a rate of unclear assignment similar to or worse than the entire dataset, excluding Opisthokonta, Archaeplastida, and Excavata.

Metazoa dominated the dataset and were the most common group of ASVs in most samples (Fig. 3.1). In comparison to the chapter 2 dataset, metazoan reads were much more commonly detected (Fig. 2.2). However, samples from Horseshoe and Stingray Island had a higher number of reads per sample of Archaeplastida ASVs than samples from Dragon Island. The majority of these ASVs were assigned to the rush species *Juncus effusus*. While this species is not known to inhabit salt marshes in Louisiana, the related rush species *Juncus roemerianus* is commonly present (Greenberg and Maldonado 2006). An ASV which was assigned to *J. effusus* was also present in the dataset from chapter 2. This rush species was present at the sites on these islands, but it was unclear why other marsh plants, particularly the smooth cordgrass *Spartina alterniflora* (which was also present at the sites), were apparently not detected in the dataset. However, inspection of the SILVA database (during November 2020) revealed that *S. alterniflora* was not present, nor were any other members of the genus *Spartina*. There remains the possibility of primer biases or an assignment mismatch of *S. alterniflora* in the database, but the absence of this and related taxa in the database is the most likely culprit. In either case, because this study is focused on the differences between the intact (which have plants) and

sheared (which lack plants) marsh margins, the composition of the plants in the area is not directly relevant. Of course, plant composition can influence meiofauna composition, as shown during the recovery from the DHOS (Fleeger et al. 2019). In addition to the Archaeplastida ASVs, the SAR group showed a higher number of reads per sample in the samples from Dragon Island than in samples from Horseshoe or Stingray Island, though this effect was variable depending on the sample.

In addition to being the most common group of ASVs in the dataset, Metazoa also had a much lower rate of ambiguous or unclear assignments than other groups and was the only group present in every sample. While ASVs in the SAR group were more numerous than Metazoa, the SAR ASVs were not as commonly detected. In addition, members of SAR are more poorly studied, leading to “taxonomy-free” approaches in some studies (Apothélos-Perret-Gentil et al. 2017, Kelly 2019). Benthic microalgae (which include members of the SAR group) have been studied in marshes, but these studies focus on pigment composition and biomass instead of the community composition (Fleeger et al. 2015). Metazoan meiofauna were heavily sampled following the DHOS (Fleeger et al. 2018) and have been studied in marshes for decades (Fleeger 1985, Coull 1990). Given this information, reducing the dataset to just metazoan meiofauna for study is justified.

Approximately 80 thousand reads and 163 ASVs remained following filtering for metazoa, excluding vertebrates. These ASVs were further reduced to 116 OTUs by the clustering algorithm combining sequences with 97% similarity to avoid artificially inflating diversity due to intraspecific variation in metazoa (Brandt et al. 2019).

Table 3.1. Sub-Domain level taxonomy assignments of the entire dataset from the SILVA database. Samples were collected from the marsh islands surrounding Bay Jimmy, Louisiana from August to November 2017.

Taxon	Number of ASVs	Metagenome	Uncultured	Unidentified	Ambiguous Taxa	Percent Unclear Assignment
Opisthokonta	294	7	41	0	76	42.18
Metazoa	163	0	0	0	39	23.93
Fungi	126	7	41	0	36	66.67
SAR	260	17	85	1	72	67.31
Archaeplastida	66	0	5	0	21	39.39
Excavata	30	0	3	0	3	20.00
Amoebozoa	19	3	2	0	6	57.89
Cryptophyceae	3	0	2	0	1	100.00

(table cont'd.)

Incertae sedis	3	1	1	0	0	66.67
Haptophyta	2	0	0	0	1	50.00
Total	677	28	139	1	180	51.40

The Metagenome column included all amplicon sequence variants (ASVs) which were assigned as a metagenome without at least a genus level assignment; Uncultured, Unidentified, and Ambiguous Taxa columns all have ASVs assigned as any of those categories for the most specific level of taxonomy. The Percent Unclear Assignments column is the percentage of the total ASVs for each row which were assigned a Metagenome, Uncultured, Unidentified, or Ambiguous Taxa. Fungi and Metazoa (shaded) fall under Opisthokonta, and should not be counted towards the total number of ASVs alongside the Opisthokonta total.

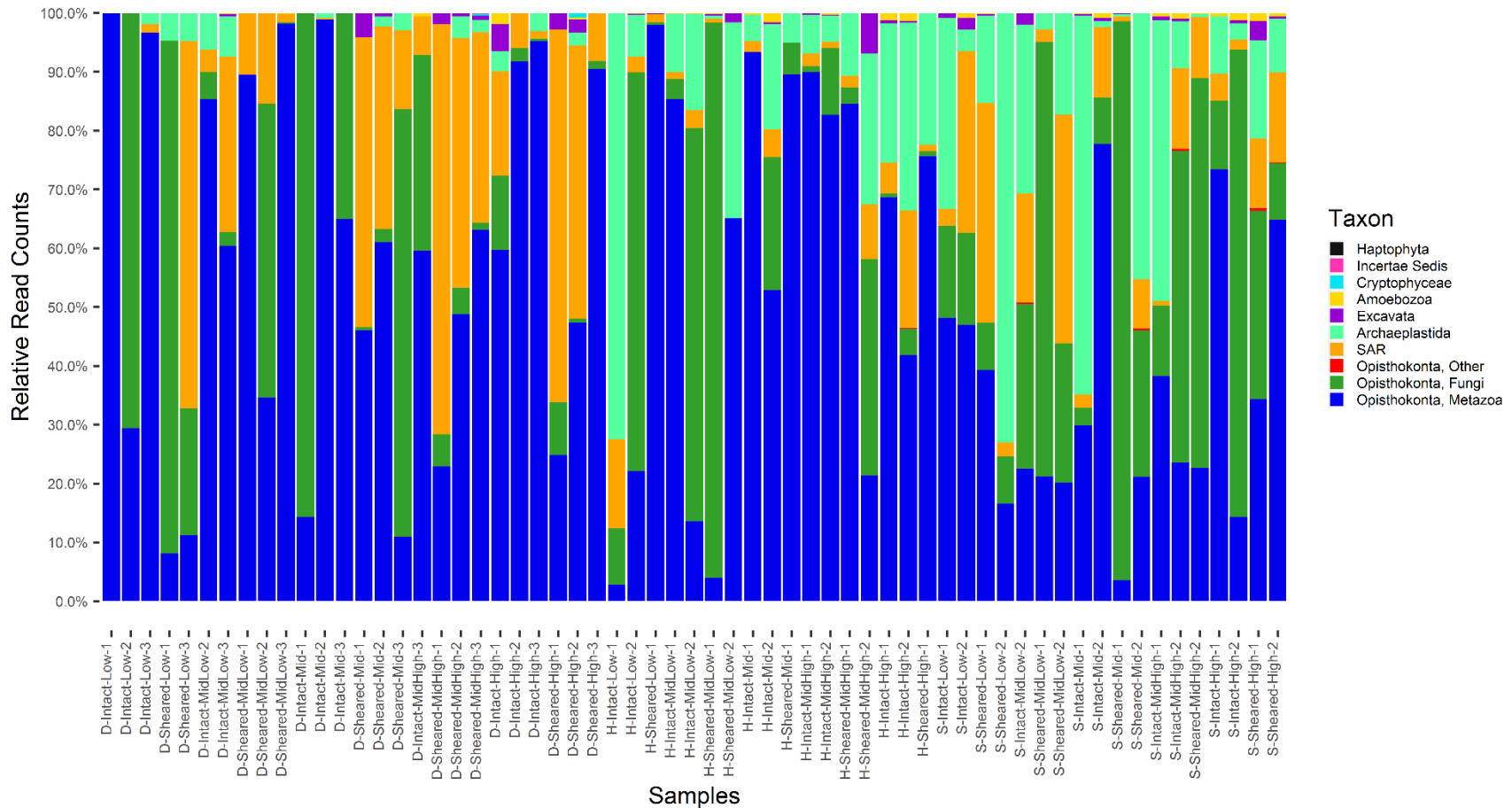


Fig. 3.1. Taxa bar plots for the full dataset of 70 samples collected from marsh islands surrounding Bay Jimmy, Louisiana from August 2017 to November 2017, with each colored section of the bar representing the relative proportion of the read counts assigned to different taxa within that sample. The taxa are sorted within each bar from the bottom to the top by the overall highest to lowest number of ASVs. For the x-axis, samples are labeled as D (Dragon), H (Horseshoe), or S (Stingray) for the island, and Intact or Sheared for the margin type, as well as Low, MidLow, Mid, MidHigh, or High for the elevation position, followed by the transect number.

Sequence-depth based alpha rarefaction:

Many of the alpha rarefaction curves (Fig. 3.2) of OTU richness plotted against sequencing depth leveled off, showing sufficient sequencing depth to capture the majority of the meiofauna community. However, some of the curves which show low richness began to flatten, but did not level off completely, indicating that some samples did not achieve enough sequencing depth to capture the majority of the meiofauna community. In addition, OTU richness was positively correlated to sequencing depth (Spearman's $\rho = 0.85$, $p < 0.01$). Among samples, there was also a wide range of the number of OTUs detected regardless of sequencing depth.

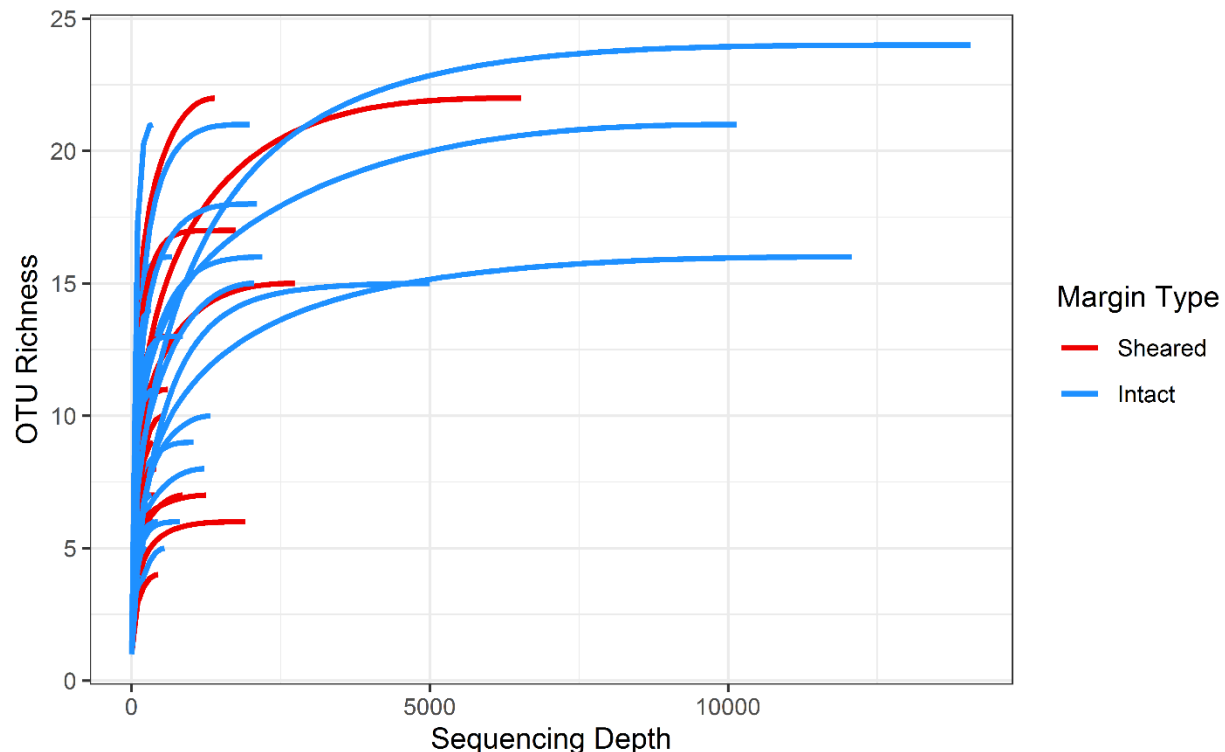


Fig. 3.2. Alpha rarefaction curves which show the number of metazoan OTUs detected when randomly sampling reads at a given sampling depth. Each line in the figure represents the metazoa detected in the summed sequences from the three extractions from each of the floated soil samples that were collected from the marsh islands surrounding Bay Jimmy, Louisiana from August 2017 to November 2017.

Sample-based rarefaction curves:

The interpolated portion of the sample-based rarefaction curves (Fig. 3.3, 3.4, 3.5, 3.6) begin to level off, indicating that the collected samples captured most of the OTU richness present in the actual communities in the samples from the whole dataset, different margin status, different island, and different elevation positions. The extrapolated portion of the richness curves indicate that doubling the number of samples could improve richness in the

total dataset from 116 to over 150 OTUs (Fig. 3.3). For the communities from different margin types, richness could be improved from approximately 80 to 110 OTUs (Fig. 3.4). Of the three communities from the different islands, the community from Stingray Island showed slightly higher richness than the Dragon or Horseshoe Island communities (Fig. 3.5). The richness of the communities from Dragon and Horseshoe Island could be improved from approximately 60 to 80 OTUs with additional sampling, while the richness of the Stingray Island community could be improved from approximately 75 to 95 (Fig. 3.5). The Shannon and Simpson Inverse curves, which represent the effective diversity, fully level off in the full dataset (Fig. 3.3) but continue to increase slightly in the community datasets from the different categories (Fig. 3.4, 3.5, 3.6). The disparity between the richness and diversity metrics curves indicates that though additional OTUs may be detected by additional sampling, these OTUs would not be detected often enough to influence the diversity metrics. Rare species should not be disregarded in ecological studies due to their potential impacts on ecosystem services (Lyons et al. 2005, Dee et al. 2019b), but it is not clear whether the rate at which additional OTUs are estimated would represent the actual rate, because nothing in the iNEXT software accounts for the OTU clustering process (Brown et al. 2015, Phillips et al. 2019).

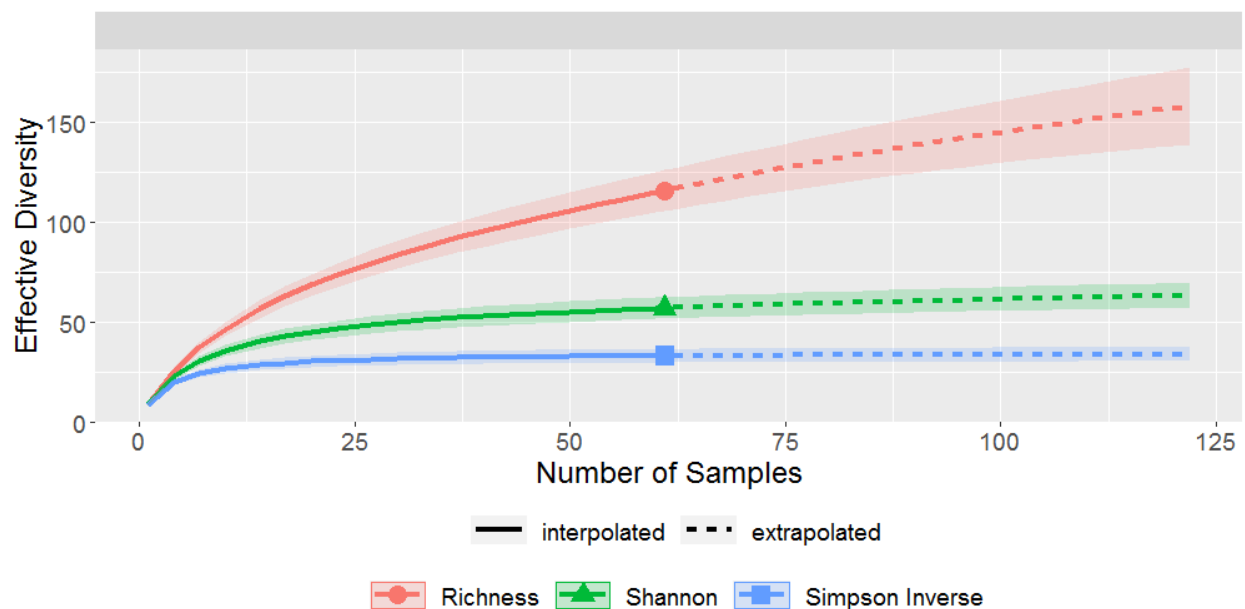


Fig. 3.3. Sample-based rarefaction curves for the full dataset with effective diversity for different metrics plotted against the number of samples collected from marsh islands surrounding Bay Jimmy, Louisiana from August 2017 to November 2017. Extrapolation of effective diversity extends to twice the number of samples, and the shaded area around the curves represents the 95% confidence interval for each curve.

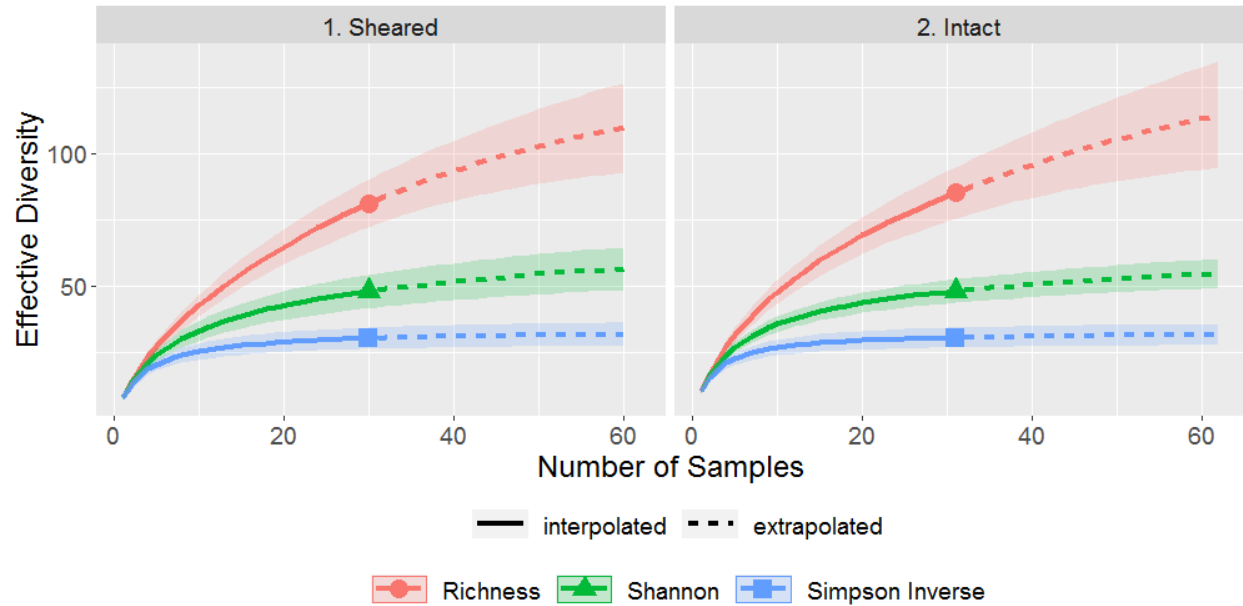


Fig. 3.4. Sample-based rarefaction curves for samples from sheared and intact margins with effective diversity for different metrics plotted against the number of samples collected from marsh islands surrounding Bay Jimmy, Louisiana from August 2017 to November 2017. Extrapolation of effective diversity extends to twice the number of samples, and the shaded area around the curves represents the 95% confidence interval for each curve.

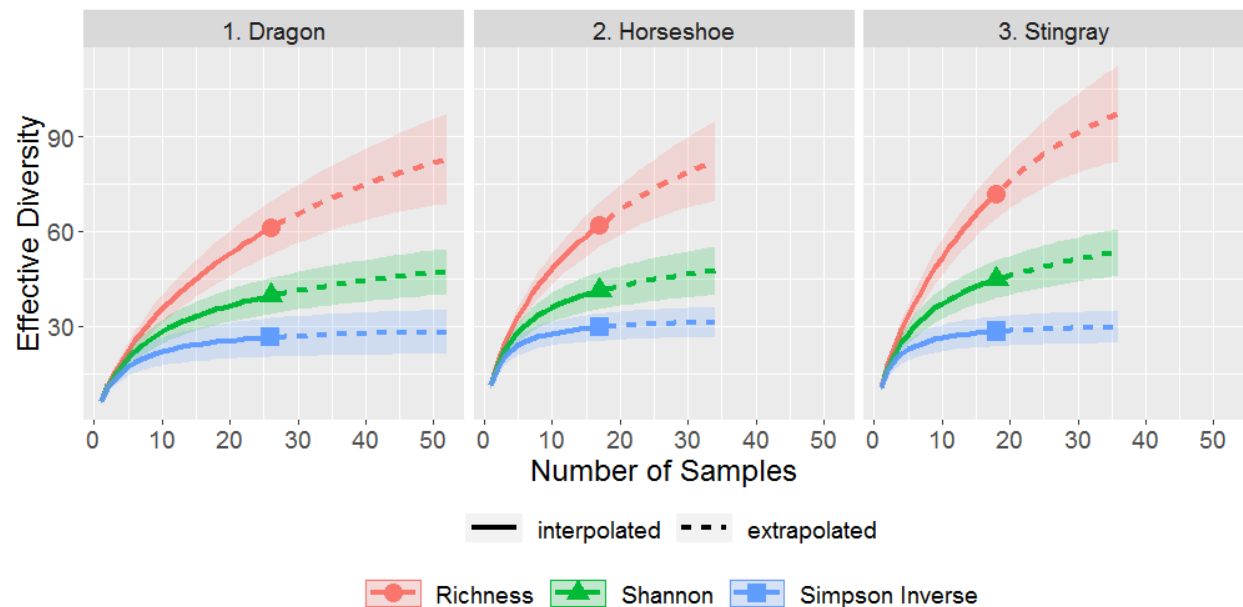


Fig. 3.5. Sample-based rarefaction curves for samples from the different islands with effective diversity for different metrics plotted against the number of samples collected from marsh islands surrounding Bay Jimmy, Louisiana from August 2017 to November 2017. Extrapolation of effective diversity extends to twice the number of samples, and the shaded area around the curves represents the 95% confidence interval for each curve.

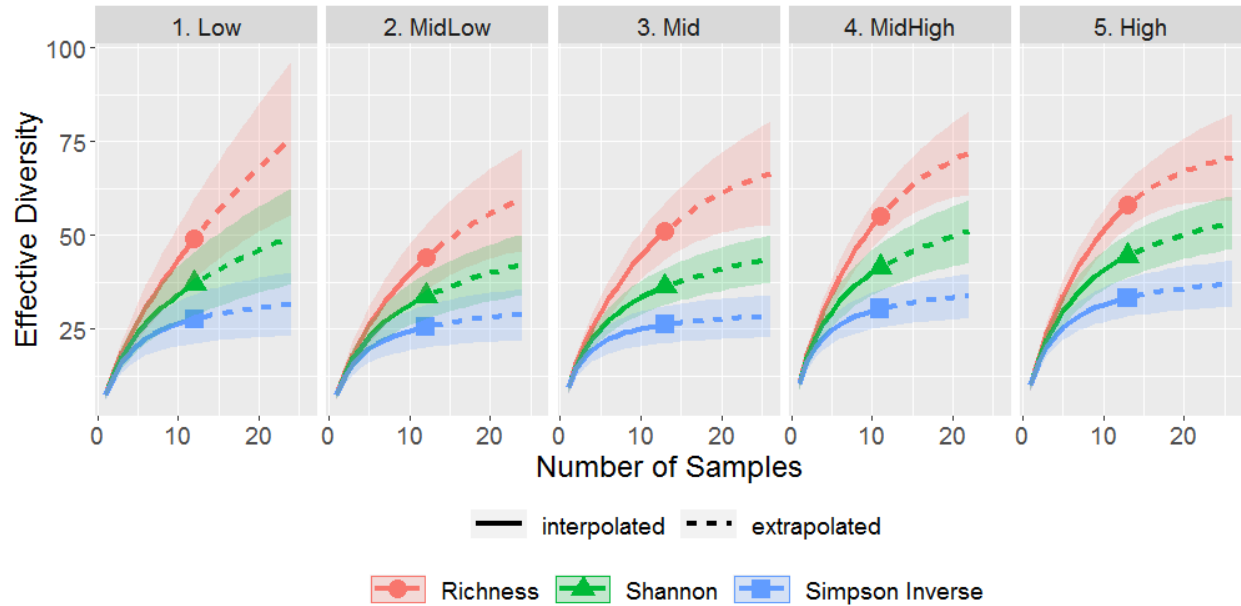


Fig. 3.6. Sample-based rarefaction curves for samples from the different elevation positions with effective diversity for different metrics plotted against the number of samples collected from marsh islands surrounding Bay Jimmy, Louisiana from August 2017 to November 2017. Extrapolation of effective diversity extends to twice the number of samples, and the shaded area around the curves represents the 95% confidence interval for each curve.

Coverage-based rarefaction curves:

The interpolated portion of the coverage-based rarefaction curves (Fig. 3.7, 3.8, 3.9, 3.10) reach between 65% and 90% of the estimated total community, with the lower coverage estimates belonging to the separate Elevation Position communities. The richness curves continue to climb in the extrapolated values for the full dataset, unlike the diversity metrics curves, which are nearly level in the extrapolated portion (Fig. 3.7), meaning that additional richness would not significantly increase the diversity metrics. The interpolated portion of the curves reach 90% coverage for the full dataset, and the extrapolated curves reach approximately 95% coverage, indicating that doubling the sampling effort would only achieve a 5% gain in coverage of the total community. However, for the split communities, the diversity metric curves are not level, and the separate diversity metric curves for the Elevation Position samples show a similar slope to the richness curves, likely due to the smaller sample size of the Elevation Position communities. In addition, there was a much lower level of coverage (60%) for Low Elevation Position samples than for the other Elevation Position Samples (approximately 80%).

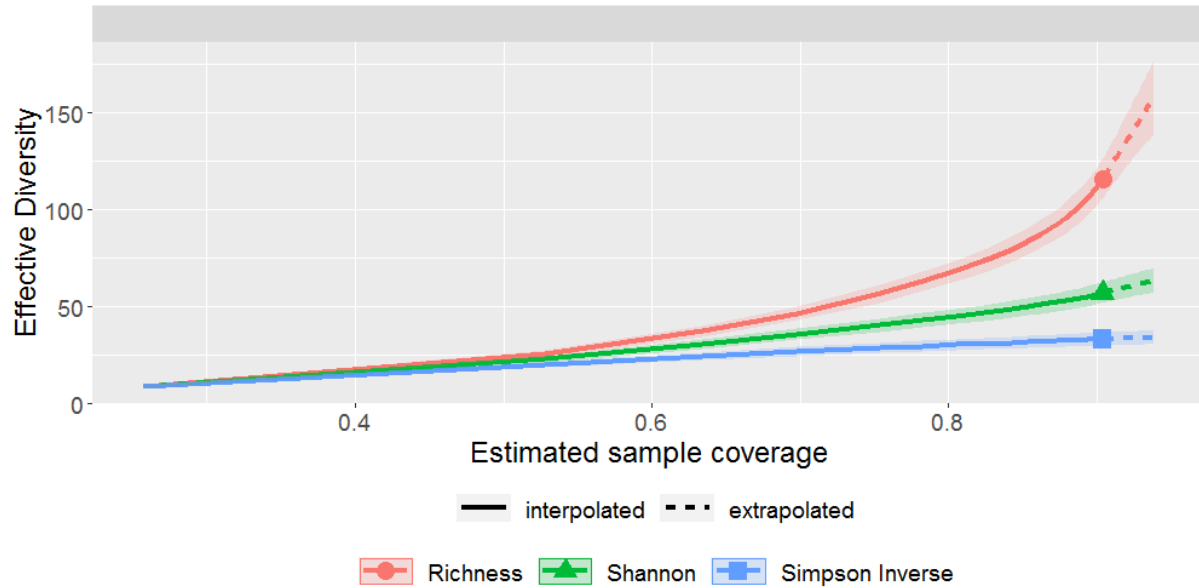


Fig. 3.7. Coverage-based rarefaction curves for the full dataset with effective diversity plotted for different metrics plotted against the number of samples collected from marsh islands surrounding Bay Jimmy, Louisiana from August 2017 to November 2017. Extrapolation extends out to the estimated coverage of twice the number of samples, and the shaded area around each curve represents the 95% confidence interval of the curve.

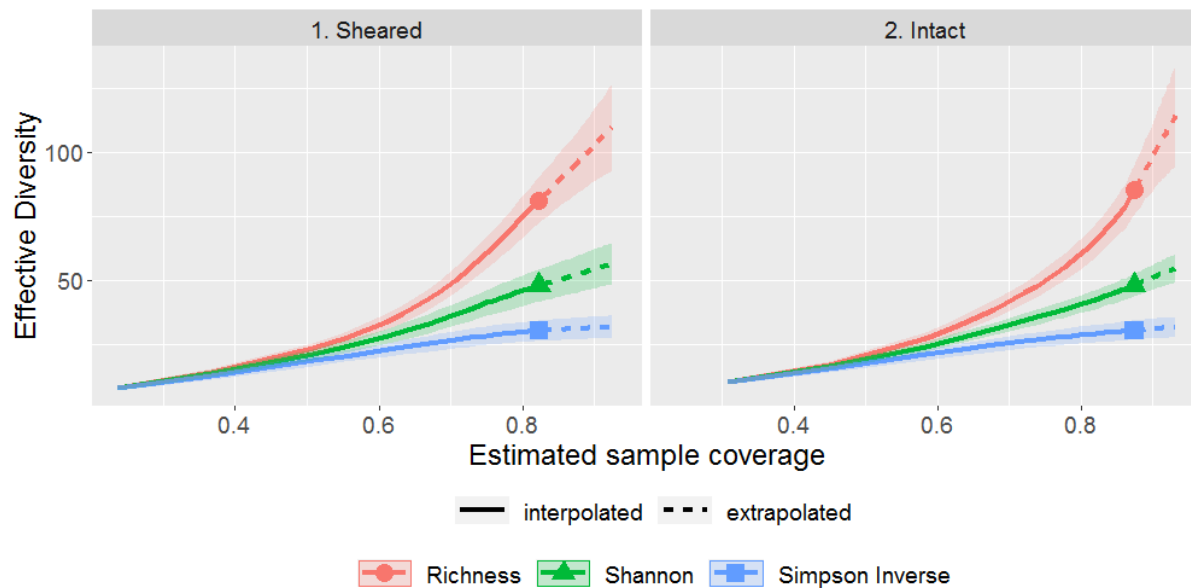


Fig. 3.8. Coverage-based rarefaction curves for samples from sheared and intact marsh margins with effective diversity plotted for different metrics plotted against the number of samples collected from marsh islands surrounding Bay Jimmy, Louisiana from August 2017 to November 2017. Extrapolation extends out to the estimated coverage of twice the number of samples, and the shaded area around each curve represents the 95% confidence interval of the curve.

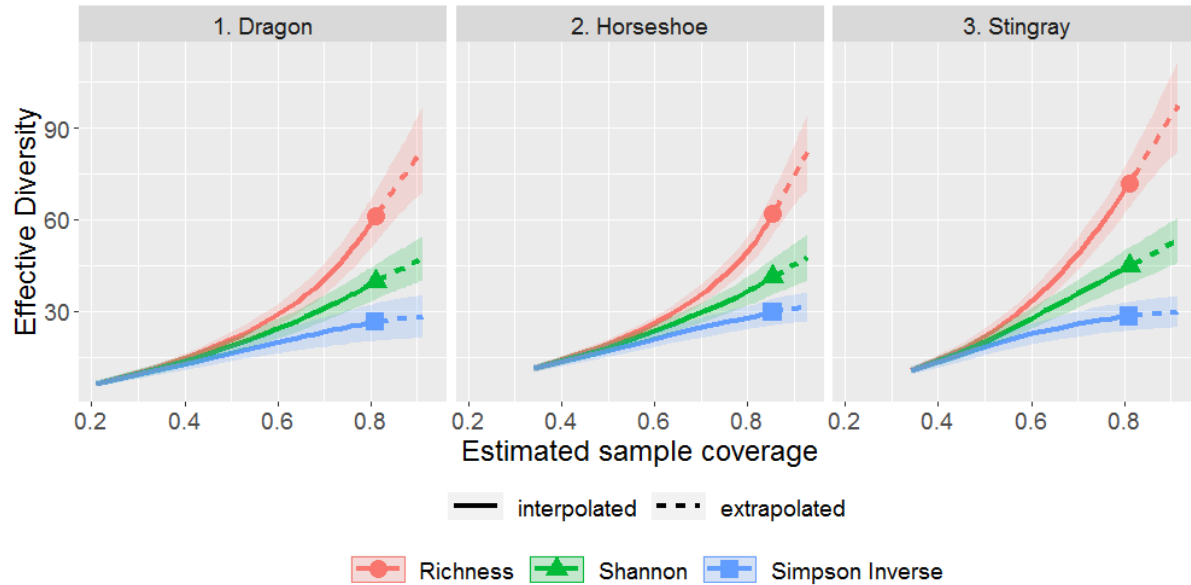


Fig. 3.9. Coverage-based rarefaction curves for samples from the different islands with effective diversity plotted for different metrics plotted against the number of samples collected from marsh islands surrounding Bay Jimmy, Louisiana from August 2017 to November 2017. Extrapolation extends out to the estimated coverage of twice the number of samples, and the shaded area around each curve represents the 95% confidence interval of the curve.

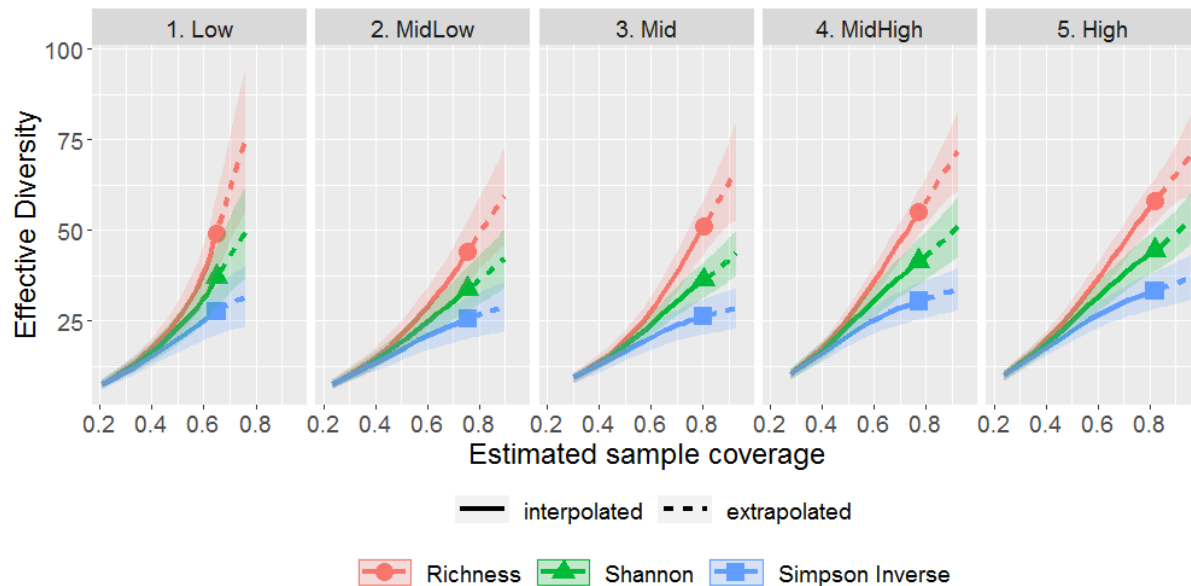


Fig. 3.10. Coverage-based rarefaction curves for samples from the different elevation positions with effective diversity plotted for different metrics plotted against the number of samples collected from marsh islands surrounding Bay Jimmy, Louisiana from August 2017 to November 2017. Extrapolation extends out to the estimated coverage of twice the number of samples, and the shaded area around each curve represents the 95% confidence interval of the curve.

OTU diversity profile and richness estimations:

The coverage estimate (CE) for the entire dataset was high (90.4%) and matched the estimations of coverage from the coverage-based rarefaction curves (Fig. 3.7), indicating good coverage of the estimated actual community (Table 3.2). The estimated Coefficient of Variation (CV) for the entire dataset was moderately high (1.63), indicating that most OTUs were not distributed evenly within the dataset. Only 12 of the 116 observed OTUs appeared in more than 10 of the samples (the frequent group), which likely explains the level of heterogeneity in the dataset. The CE for the infrequent group, where were the OTUs which appeared in 10 or less samples, was lower than that of the entire dataset (80.9%), indicating a slightly poorer coverage of that group, but the CV was also lower than that of the entire dataset (0.86), indicating more homogeneity in the infrequent group.

Table 3.2. OTU richness observations. All samples were collected from the marsh islands surrounding Bay Jimmy, Louisiana from August 2017 to November 2017.

Observation	Value
Number of samples	61
Total OTU Richness	116
Total number of incidences	547
Coverage estimate for entire dataset	0.904
Estimated coefficient of variation for entire dataset	1.639
Number of observed OTUs for frequent group	12
Total number for incidences in frequent group	272
Number of observed OTUs for infrequent group	104
Total number for incidences in infrequent group	275
Estimated sample coverage for infrequent group	0.809
Estimated coefficient of variation for infrequent group	0.855

The coverage estimate and coefficient of variation for the infrequent group are presented because they are used in the calculation of the Incidence-based Coverage Estimate (ICE) richness estimator model (Fig. 3.11). The frequent group of OTUs appeared in more than 10 samples, while the infrequent group appeared in 10 or less samples.

This dataset did not have extremely high OTU richness (less than 1000 OTUs) and was moderately heterogeneous, so the best estimators of actual richness were Chao2, iChao2, and ICE (Chao et al. 2015), with the Homogenous Model presented for comparison. The Homogenous model is an estimation of the actual community if all OTUs have an equal chance of being detected, the Chao2 estimator is based on OTUs which appear in 2 samples or less, the iChao2 estimator is based on the OTUs which appear in 4 samples or less, and Incidence-based

Coverage Estimator (ICE) is based on the OTUs which appear in 10 samples or less. The range of the estimated richness was 130 (lower bound of Homogenous Model estimation) to 365 (upper bound of Chao2 estimator) OTUs (Fig. 3.11). The upper bound of the richness estimates is much higher than the upper bounds for the richness curves from the sample and coverage-based rarefactions for the whole dataset (Fig. 3.3 and 3.7), which were around 175 OTUs. This means that even collecting twice as many samples would not have approached the amount of richness estimated for the whole dataset, tracking the interpolated coverage-based rarefactions.

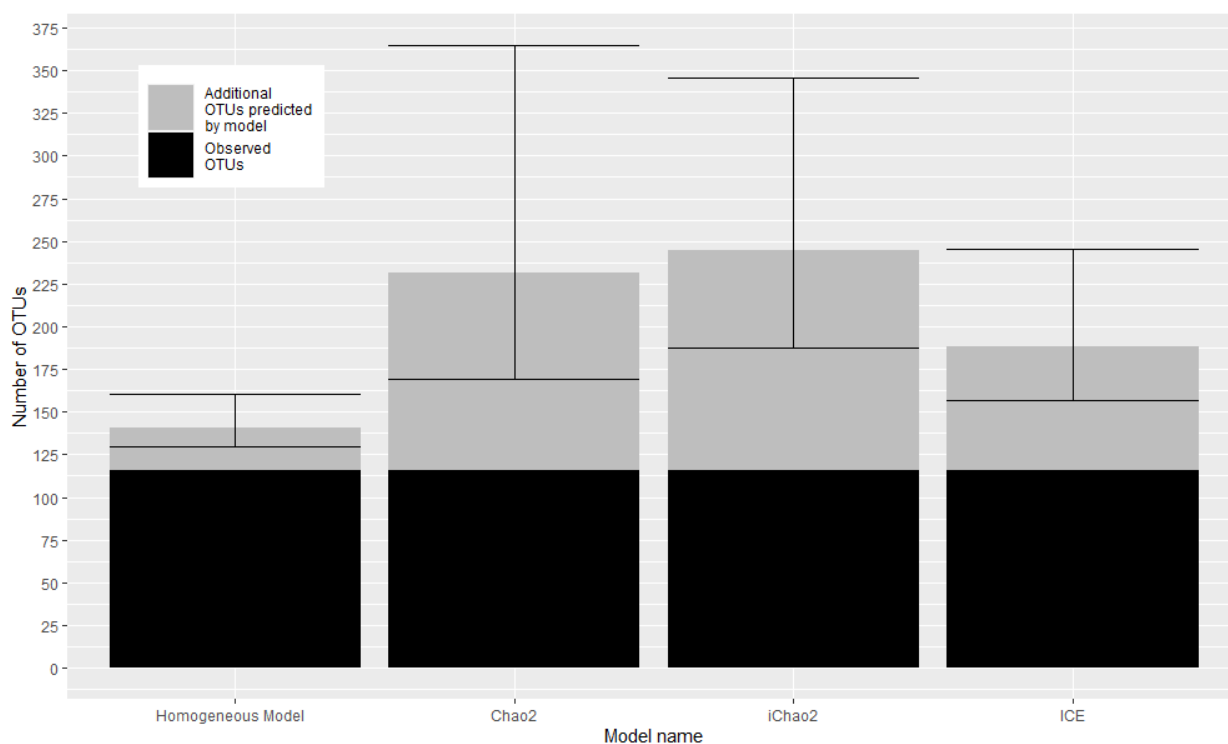


Fig. 3.11. Observed total OTU richness and incidence based OTU richness estimations from four estimator models. Samples were collected from marsh islands surrounding Bay Jimmy, Louisiana from August 2017 to November 2017. The lower portion of the columns in this chart is the observed number of OTUs (OTU richness of the entire dataset). The upper portion of the columns represents additional OTU numbers predicted by the different models, and the error bars represent the 95% confidence interval of the estimate.

Shared OTUs:

Fifty of the 116 observed OTUs were shared between sheared and intact margin samples, with 81 and 85 total OTUs in each community respectively (Table 3.3). Because only two communities are being compared, the Chao2-shared index can estimate the number of shared OTUs expected in the actual community between the samples from intact and sheared margins. This index produced a value of 72 for shared species between the estimated communities, with a 95% confidence interval of 58 to 108. The sheared and intact communities

both contained all 12 of the frequent group OTUs (Table 3.6). The bounds of this shared species estimate are well within the bounds of the richness estimates for the entire dataset.

Table 3.3. Shared and total number of OTUs for samples from sheared and intact margins which were collected from marsh islands surrounding Bay Jimmy, Louisiana from August 2017 to November 2017.

	Sheared	Intact
Sheared	81 (12)	50 (12)
Intact		85 (12)

The intersection of a single category (such as Sheared-Sheared) is the total number of OTUs for that elevation position, while the intersection of 2 categories (such as Sheared-Intact) is the number of OTUs shared between these two categories. Numbers in parenthesis are the number of the 12 frequent group OTUs in that total or shared number of OTUs.

Island OTU communities had an average total of 65 OTUs with an average of 35 OTUs shared between each (Table 3.4) and an average of 30 unique OTUs on each. Twenty-five OTUs were shared between all three islands. On Dragon and Horseshoe Island, all 12 of the frequent group OTUs (Table 3.6) were present, while on Stingray Island 11 frequent group OTUs were present. However, Stingray Island had the highest total number of OTUs, while Dragon and Horseshoe Islands had slightly less.

Table 3.4. Shared and total numbers of OTUs in the island communities which were collected from the marsh islands surrounding Bay Jimmy, Louisiana from August 2017 to November 2017.

	Dragon	Horseshoe	Stingray
Dragon	61 (12)	37 (12)	34 (11)
Horseshoe		62 (12)	33 (11)
Stingray			72 (11)

The intersection of a category, such as Horseshoe-Horseshoe, is the total number of OTUs for that category, while the intersection of two different categories, such as Dragon-Stingray, is the number of shared OTUs between those categories. Numbers in parenthesis are the number of the 12 frequent group OTUs in that total or shared number of OTUs.

Elevation position communities had an average of 53 OTUs with an average of 28 shared OTUs (Table 3.5) and an average of 24 unique OTUs. Fifteen of the OTUs were shared between all five elevation positions. All 12 of the frequent group OTUs (Table 3.6) were present in the High, MidHigh, and Mid communities, while 11 of these OTUs were present in the MidLow and Low communities. The High community had the highest total number of OTUs, while MidLow had the lowest.

Table 3.5. Shared and total numbers of OTUs in the elevation position communities which were collected from the marsh islands surrounding Bay Jimmy, Louisiana from August 2017 to November 2017.

	Low	MidLow	Mid	MidHigh	High
Low	49 (11)	20 (10)	27 (11)	26 (11)	28 (11)
MidLow		44 (11)	22 (11)	21 (11)	28 (11)
Mid			51 (12)	35 (12)	35 (12)
MidHigh				55 (12)	34 (12)
High					58 (12)

The intersection of a category, such as High-High, is the total number of OTUs for that category, while the intersection of two different categories, such as Low-Mid, is the number of shared OTUs between those categories. Numbers in parenthesis are the number of the 12 frequent group OTUs in that total or shared number of OTUs.

Taxa Bar Plots:

Arthropod OTUs were the most commonly detected in the dataset; they were present in 55 samples, followed by nematodes, which were present in 51 samples. Annelida were present in 44 samples, Platyhelminthes in 42 samples, and Mollusca in 41 samples. The samples from Dragon Island were less consistent in composition at the phylum level than the samples from Horseshoe or Stingray Island (Fig 3.12). Dragon Island samples more frequently contained Bryozoa OTUs than both Horseshoe and Stingray Island samples, and more frequently contained Hydrozoa and Gastrotricha OTUs than Stingray Island samples. Samples had an average of 5 ± 2 phyla, with a range of 1 to 12 phyla.

Four of the samples from Dragon Island and one of the samples from Horseshoe Island contained only one metazoan OTU (Fig 3.12). These samples contained very low diversity even in the unfiltered dataset (Fig 3.1), with ten or fewer additional OTUs captured alongside the single metazoan taxa compared to the unfiltered dataset average of 31 total OTUs per samples. The reason for the low diversity samples from Dragon and Horseshoe Island is unclear. Three of the samples from Dragon Island which showed low diversity were from the smaller PVC core samples which produced low amounts of material following the soil floating process, but one was from a larger acrylic core. Sequencing depth for these samples was very low in both the unfiltered dataset (<200 reads) and in the metazoa filtered dataset (<10 reads).

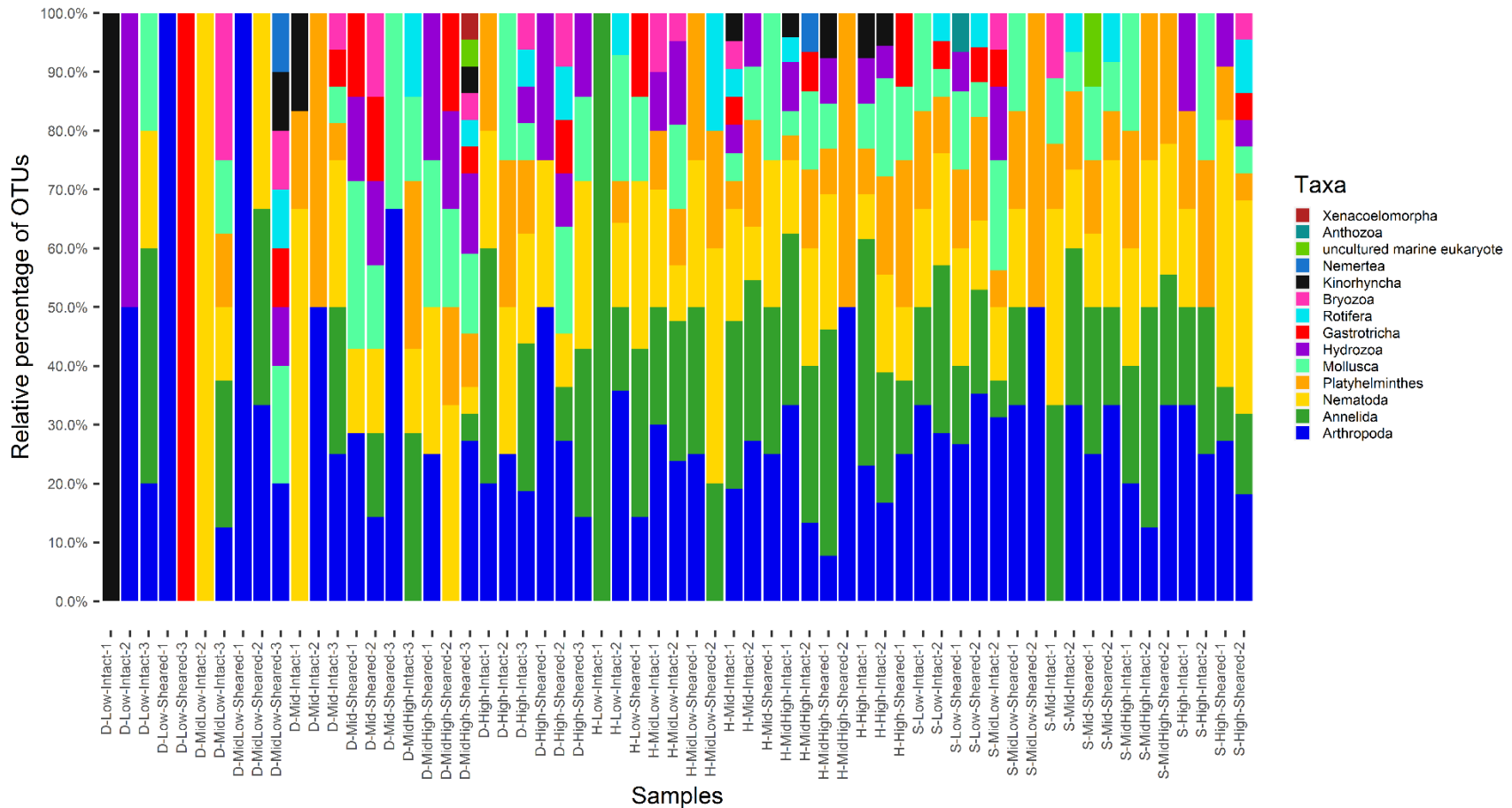


Fig. 3.12. Taxa bar plots of the 61 samples collected from marsh islands surrounding Bay Jimmy, Louisiana, from August 2017 to November 2017, with each colored section of the bar representing the relative proportion of the OTUs belonging to different phyla within that sample. Phyla are sorted within each bar by the overall highest to lowest relative percentage (from bottom to top). On the x-axis, Dragon (D), Horseshoe (H), and Stingray (S) represent the island which the sample is from, Low, MidLow, Mid, MidHigh, and High designate the elevation position, while Sheared and Intact indicate the margin type, and the number at the end of the sample designation on the x-axis represents the transect number.

Phylum level biodiversity:

Phylum Arthropoda had the highest percentage of the total incidences in the dataset, followed by Annelida, Nematoda, Platyhelminthes, Mollusca, and other phyla (Fig. 3.13). Phylum Arthropoda also contained the largest group of unique OTUs in the dataset, again followed by Annelida, Nematoda, Platyhelminthes, and other phyla (Fig. 3.14). Lowest level assignments for OTUs from the SILVA database ranged from the subkingdom clade “Bilateria” down to the species level (Table 3.6). Accuracy of species level assignments is limited by both the resolution of the 18S rRNA gene and by the presence of taxa in databases, so closely related species might not be adequately separated. Different OTUs with identical taxonomic assignments are either the result of high sequence variation in taxa exceeding 97% or the result of a lack of specificity within the marker gene sequence for the taxon the OTU was assigned to. Taxonomy assignments produced by the SILVA and GenBank databases generally agreed, but the GenBank assignments were usually more specific than the SILVA assignments. In this dataset, the arthropods and platyhelminthes were more commonly detected than in the chapter 2 dataset (Fig. 2.14).

The frequent group OTUs were detected in a range from 11 to 47 samples. This group of OTUs consisted of 3 annelids, 2 arthropods, 2 mollusks, 2 nematodes, a gastrotrich, a hydrozoan, and a platyhelminth (Table 3.6). An OTU which was assigned to an ambiguous member of the order Enoplida (Nematoda) was the most commonly detected OTU in the dataset, appearing in 47 samples. This OTU received a new assignment of *Adoncholaimus* sp. from the GenBank database, which agreed with the SILVA assignment but was more specific. The next most commonly detected OTU was assigned to an ambiguous member of the order Lecithoepitheliata (Platyhelminthes, GenBank: uncultured eukaryote) and appeared in 37 samples. Following this platyhelminth, the next most commonly detected OTU was assigned to the mollusk species *Brachidontes rodriguezii* (Mytiloida, GenBank: *Brachidontes mutabilis*) and was detected in 35 samples. The next most common OTU was present in 28 samples and was assigned to the phylum Annelida as an ambiguous member of the order Siponida. This OTU received a more specific assignment from the GenBank database as *Polydora lingshuiensis*. The next most common OTU was present in 24 samples and was assigned as the annelid *Alitta succinea* (Phyllodocida, GenBank: *Alitta succinea*). Following these annelids, the next most common OTU assigned to the arthropod *Haematopota pluvialis* (Diptera, GenBank: *Haematopota pluvialis*) and appeared in 23 samples. The next two most common OTUs were both detected in 15 samples, and were assigned to the annelid *Marionina coatesae* (Enchytraeida, GenBank: *Marionina coatesae*) and to the arthropod genus *Acarothrix* (Trombidiformes, GenBank: *Acarothrix* sp.). An OTU assigned to the gastrotrich genus *Heterolepidoderma* (Chaetonotida, GenBank: *Heterolepidoderma* sp.) was the next most common OTU, appearing in 14 samples. The next most common OTU was assigned to an ambiguous member of the mollusk subclass Neritimorpha which was detected in 12 samples. This OTU was assigned as the nerite species *Theodoxus fluviatilis* in the GenBank database. Both of the final members of the frequent group appeared in 11 samples, and were assigned to the

hydrozoan *Helgicirrha cari* (Leptothecata, GenBank: *Helgicirrha cari*) and an uncultured eukaryote belonging to the nematode order Enoplida (GenBank: uncultured eukaryote). Sixty-six percent of the frequent group OTUs in this chapter matched the frequent group OTUs from the dataset in chapter 2 at the order or species level, including *Polydora ciliata*, members of the Mytiloida, *Alitta succinea*, *Heterolepidoderma* sp., and *Helgicirrha cari* (Table 2.13).

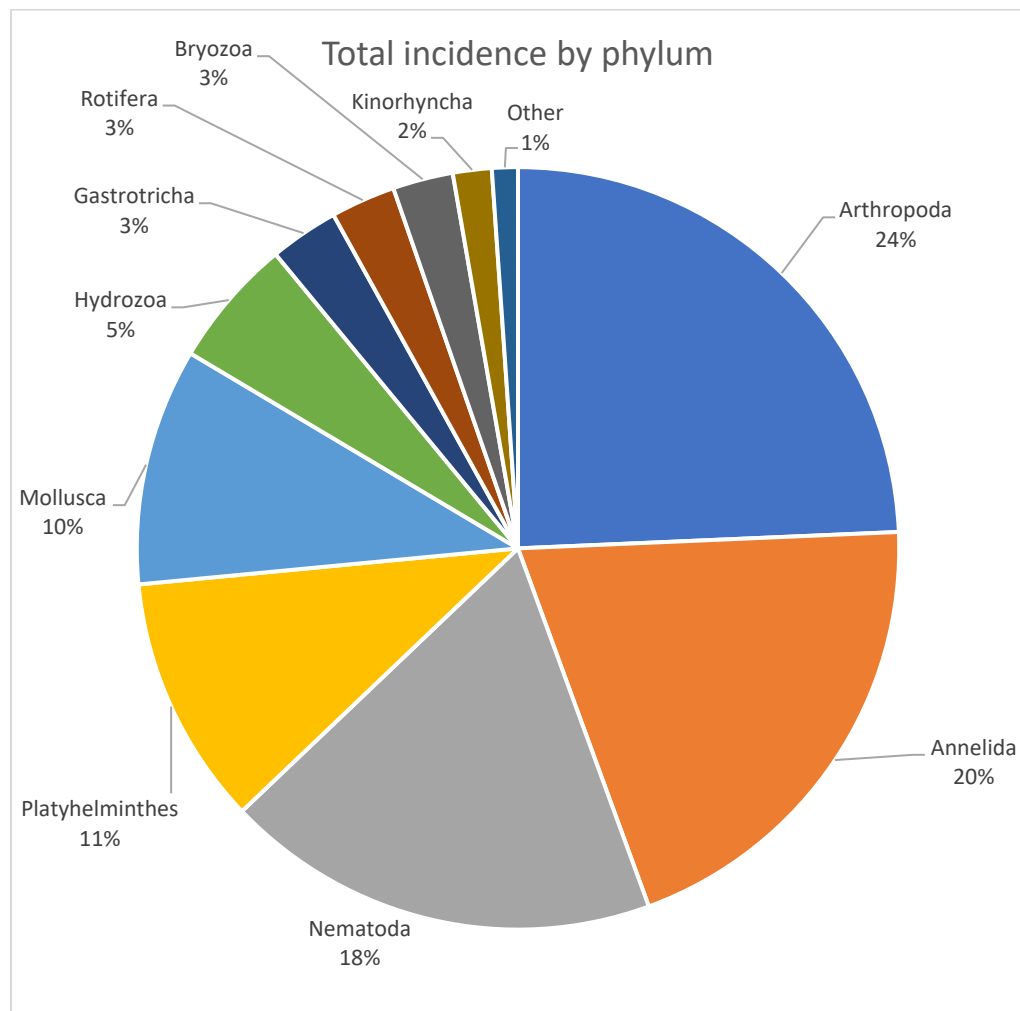


Fig. 3.13. Percentage of the 547 total OTU incidences by phylum level OTU assignment. All samples were collected from the marsh islands surrounding Bay Jimmy, Louisiana from August 2017 to November 2017. Phyla which individually made up less than 1% of the total incidences were combined into the “Other” category, which included Nemertea, Anthozoa, Xenocoelomorpha, and an OTU that was unassigned at the phylum level in order of most to least incidences.

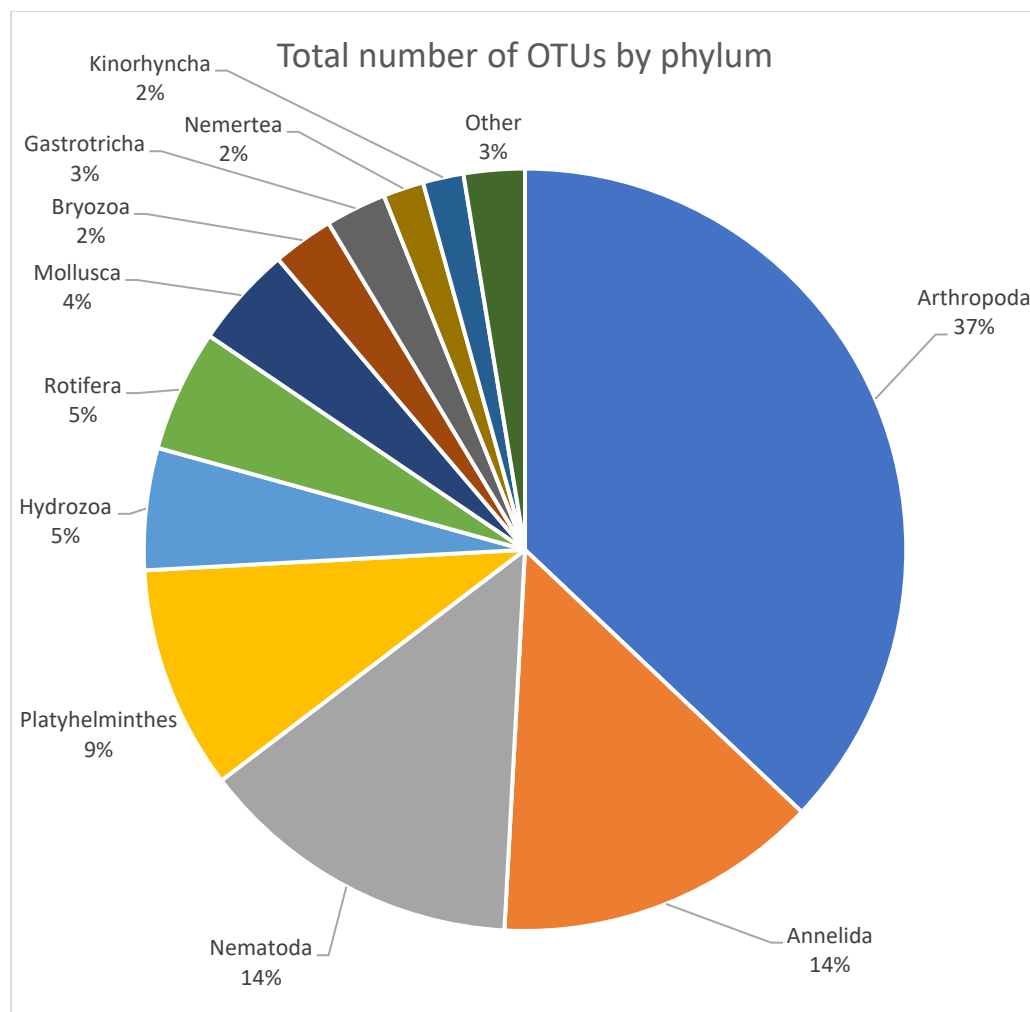


Fig. 3.14. Percentage of the 116 total OTUs per phylum assignment. All samples were collected from the marsh islands surrounding Bay Jimmy, Louisiana from August 2017 to November 2017. Phyla which individually made up less than 1% of the total OTUs were combined into the “Other” category, which included Anthozoa, Xenocoelomorpha, and an OTU that was unassigned at the phylum level in order of most to least incidences.

Table 3.6. Assignment of OTUs to phyla, orders, and lowest feasible level and OTU incidence. All samples were collected from the marsh islands surrounding Bay Jimmy, Louisiana from August 2017 to November 2017.

Phylum	Order	OTU Incidences	Lowest SILVA Assignment	Top GenBank Match	GenBank Percent Identity	GenBank Accession	S	I	DI	HI	SI	L	ML	M	MH	H
Annelida	Spionida	28	Spionida; Ambiguous taxa	<i>Polydora lingshuiensis</i> isolate Larvae-2	100.00%	MG767309.1	10	18	7	10	11	4	5	8	6	5
	Phyllodocida	24	<i>Alitta succinea</i>	<i>Alitta succinea</i>	100.00%	AY210447.1	9	15	4	14	6	8	4	5	3	4
	Enchytraeida	15	<i>Marionina coatesae</i>	<i>Marionina coatesae</i> isolate CE136	98.94%	GU901922.1	1	14	4	7	4	1	0	5	4	5
	Sabellida	10	<i>Manayunkia aestuarina</i>	<i>Manayunkia aestuarina</i>	100.00%	HM042108.1	2	8	4	4	2	0	2	3	3	2
	Phyllodocida	7	<i>Paranaitis kosteriensis</i>	<i>Eteone pacifica</i> voucher SMNH 124053	98.94%	MG254394.1	2	5	1	4	2	1	0	2	2	2
	Scolecida	5	<i>Heteromastus filiformis</i>	<i>Heteromastus filiformis</i>	97.87%	DQ790081.1	2	3	0	4	1	2	0	1	2	0
	Haplotaxida	4	Haplotaxida; Ambiguous taxa	<i>Ainudrilus</i> sp. EKEH-2002	98.94%	AF411871.1	3	1	1	1	2	1	2	0	0	1
	Enchytraeida	3	<i>Marionina tumulicola</i>	<i>Marionina tumulicola</i> clone CE571	97.87%	JN799891.1	2	1	0	0	3	0	0	0	2	1
	Haplotaxida	3	Haplotaxida; Ambiguous taxa	<i>Enchytraeus dicaetus</i> isolate CE24345	100.00%	MN248684.1	2	1	0	1	2	0	1	0	0	2
	Haplotaxida	3	<i>Aulodrilus acutus</i>	<i>Aulodrilus acutus</i> voucher CE1790	97.87%	KY636910.1	1	2	1	0	2	0	0	1	1	1
	Enchytraeida	2	<i>Marionina tumulicola</i>	<i>Marionina nothachaeta</i> clone LM225	98.94%	JN799906.1	0	2	0	2	0	0	0	0	2	0
	Haplotaxida	2	Haplotaxida; Ambiguous taxa	Lumbricidae sp. R50	100.00%	KY554641.1	0	2	0	2	0	0	1	0	0	1

(table cont'd.)

Phylum	Order	OTU Incidences	Lowest SILVA Assignment	Top GenBank Match	GenBank Percent Identity	GenBank Accession	S	I	DI	HI	SI	L	ML	M	MH	H
	Haplotaxida	1	Haplotaxida; Ambiguous taxa	<i>Olavius tenuissimus</i>	98.91%	KP943812.1	0	1	0	0	1	1	0	0	0	0
	Haplotaxida	1	Haplotaxida; Ambiguous taxa	Uncultured eukaryote clone SLV_3GJ1_30	100.00%	KT072115.1	0	1	0	0	1	0	0	0	0	1
	Haplotaxida	1	Haplotaxida; Ambiguous taxa	<i>Heronidrilus fastigatus</i> voucher CE236	96.30%	KY636912.1	0	1	0	1	0	0	0	1	0	0
	Phyllodocida	1	<i>Alitta succinea</i>	<i>Alitta succinea</i>	98.94%	AY210447.1	0	1	1	0	0	1	0	0	0	0
Total Annelida OTUs	16	110	-	-	-	-	34	76	23	50	37	19	15	26	25	25
Anthozoa	Actiniaria	1	<i>Nematostella vectensis</i>	<i>Nematostella vectensis</i>	100.00%	XR_004291954.1	1	0	0	0	1	1	0	0	0	0
Arthropoda	Diptera	23	<i>Haematopota pluvialis</i>	<i>Haematopota pluvialis</i>	98.94%	KC177294.1	11	12	4	7	12	3	6	3	6	5
	Trombidiformes	15	<i>Acarothrix</i> sp. ARP-2015	<i>Acarothrix</i> sp. ARP-2015 isolate	100.00%	KP276481.1	12	3	10	2	3	2	3	5	2	3
Arthropoda	Calanoida	10	<i>Acartia tonsa</i>	<i>Acartia tonsa</i> isolate ME-Atonsa1	100.00%	GU350741.1	6	4	0	3	7	4	3	1	1	1
	Harpacticoida	8	<i>Nitokra spinipes</i>	<i>Nitokra spinipes</i> strain CCUMP 40	97.47%	JQ315748.1	5	3	3	4	1	2	1	2	1	2
	Isoptera	7	Isoptera; Ambiguous taxa	<i>Reticulitermes flavipes</i>	100.00%	KX816795.1	4	3	0	0	7	1	0	2	2	2
	Decapoda	6	Eucarida; Ambiguous taxa	<i>Rhithropanopeus harrisii</i> voucher ULLZ 3995	100.00%	KF682856.1	4	2	2	3	1	2	0	1	2	1
	Tanaidacea	6	<i>Tanais dulongii</i>	<i>Tanais dulongii</i>	100.00%	AY781428.1	0	6	2	4	0	0	0	2	1	3
	Entomobryomorpha	5	<i>Orchesella cincta</i>	Katiannidae sp. R36	98.94%	KY554632.1	0	5	2	2	1	1	0	1	0	3

(table cont'd.)

Phylum	Order	OTU Incidences	Lowest SILVA Assignment	Top GenBank Match	GenBank Percent Identity	GenBank Accession	S	I	DI	HI	SI	L	ML	M	MH	H
-	-	4	Thecostraca; Ambiguous taxa	<i>Semibalanus balanoides</i> voucher WS834	100.00%	MK844693.1	1	3	1	3	0	2	0	1	1	0
-	-	4	Collembola; Ambiguous taxa	<i>Stenacidia violacea</i> isolate 4A1a1_JC472	98.94%	KY230784.1	1	3	2	1	1	1	0	1	1	1
Podocopida	Podocopida	4	Podocopida; Ambiguous taxa	<i>Leptocythere lacertosa</i>	100.00%	AB076631.1	1	3	2	2	0	0	0	2	2	0
Calanoida	Calanoida	3	<i>Centropages furcatus</i>	<i>Centropages furcatus</i>	97.83%	GU969158.1	0	3	0	2	1	1	1	1	0	0
Decapoda	Decapoda	3	<i>Eriocheir sinensis</i>	<i>Hemigrapsus takanoi</i>	98.91%	KC771054.1	2	1	2	1	0	0	1	0	0	2
Harpacticoida	Harpacticoida	3	<i>Leptocaris brevicornis</i>	<i>Leptocaris brevicornis</i>	100.00%	KR048734.1	1	2	2	1	0	0	2	1	0	0
Diptera	Diptera	2	<i>Culex quinquefasciatus</i>	<i>Culex modestus</i> isolate 1867	100.00%	KY887583.1	1	1	1	0	1	0	0	1	0	1
Diptera	Diptera	2	<i>Corynoptera saetistyla</i>	<i>Claustropyga abblanda</i>	100.00%	MG554134.1	1	1	0	0	2	0	1	0	0	1
Diptera	Diptera	2	Diptera; invertebrate environmental sample	<i>Culicoides imicola</i> sequence	98.94%	AF074019.1	1	1	0	1	1	1	0	0	1	0
-	-	1	Acari; Ambiguous taxa	<i>Tachornithoglyphus tachornis</i>	100.00%	KP406744.1	0	1	0	1	0	0	1	0	0	0
-	-	1	Acari; Ambiguous taxa	<i>Tyrophagus putrescentiae</i>	100.00%	MN545441.1	0	1	0	1	0	0	1	0	0	0
-	-	1	Collembola; Ambiguous taxa	<i>Dicyrtomina</i> cf. <i>minuta</i> 8G1a1_JC431	100.00%	KY230769.1	1	0	1	0	0	0	0	0	1	0
-	-	1	Collembola; metagenome	<i>Desoria trispinata</i> isolate 1G1b1_JC447	98.94%	KY230773.1	1	0	0	0	1	0	0	0	1	0

(table cont'd.)

Phylum	Order	OTU Incidences	Lowest SILVA Assignment	Top GenBank Match	GenBank Percent Identity	GenBank Accession	S	I	DI	HI	SI	L	ML	M	MH	H
Arthropoda	Araneae	1	<i>Alpaida alto</i>	<i>Zealaranea crassa</i>	100.00%	MK426169.1	1	0	0	0	1	1	0	0	0	0
	Astigmata	1	<i>Czenspinksia</i> sp. DL-2014	<i>Czenspinksia</i> sp. DL-2014 isolate MQ8	98.94%	KM277816.1	1	0	0	0	1	1	0	0	0	0
	Calanoida	1	<i>Parvocalanus crassirostris</i>	<i>Parvocalanus crassirostris</i>	97.85%	KU861810.1	0	1	0	1	0	0	0	1	0	0
	Calanoida	1	<i>Subeucalanus crassus</i>	<i>Subeucalanus pileatus</i>	100.00%	GU969188.1	0	1	0	1	0	1	0	0	0	0
	Coleoptera	1	<i>Stilbus testaceus</i>	<i>Stilbus testaceus</i> voucher UPOL002073	100.00%	EF209791.1	0	1	0	0	1	0	0	0	0	1
	Diptera	1	<i>Anopheles walkeri</i>	<i>Anopheles walkeri</i>	98.94%	AY988424.1	0	1	0	1	0	0	0	0	1	0
	Diptera	1	Diptera; uncultured eukaryote	Uncultured soil eukaryote clone a615	100.00%	MK946413.1	1	0	0	0	1	1	0	0	0	0
	Diptera	1	<i>Simulium sanctipauli</i>	<i>Simulium oblongum</i> voucher OB1961	100.00%	KP710739.1	0	1	0	0	1	0	1	0	0	0
	Diptera	1	<i>Nanexila argentiquadris</i>	<i>Patanothrix wilsoni</i>	97.89%	KM879014.1	0	1	1	0	0	0	0	0	0	1
	Diptera	1	<i>Drosophila biarmipes</i>	PREDICTED: <i>Drosophila innubila</i>	98.94%	XR_004618231.1	1	0	0	0	1	0	0	0	0	1
	Diptera	1	<i>Culicoides variipennis</i>	<i>Culicoides variipennis</i>	100.00%	LN484108.1	0	1	0	0	1	0	0	1	0	0
	Diptera	1	<i>Aedes albopictus</i>	<i>Aedes albopictus</i> clone Aealb_VU_VU1_1_4	100.00%	KF471544.1	0	1	0	0	1	1	0	0	0	0
	Diptera	1	Diptera; Ambiguous taxa	<i>Stomatosema obscurum</i> voucher JSC73	100.00%	MG684558.1	0	1	0	1	0	0	1	0	0	0
	Harpacticoida	1	<i>Cancrincola plumipes</i>	<i>Cancrincola plumipes</i>	97.87%	L81938.1	1	0	0	1	0	0	0	0	1	0

(table cont'd.)

Phylum	Order	OTU Incidences	Lowest SILVA Assignment	Top GenBank Match	GenBank Percent Identity	GenBank Accession	S	I	DI	HI	SI	L	ML	M	MH	H
	Hemiptera	1	Hemiptera; Ambiguous taxa	Corixidae sp. YW-2014	100.00%	KJ461264.1	0	1	0	0	1	1	0	0	0	0
	Lepidoptera	1	<i>Eudarcia simulatricella</i>	<i>Ostrinia furnacalis</i> haplotype 5	100.00%	MK987111.1	1	0	1	0	0	0	1	0	0	0
	Mesostigmata	1	<i>Lasioseius</i> sp. AL6866	PREDICTED: <i>Metaseiulus occidentalis</i>	98.94%	XR_003777136.1	0	1	0	0	1	1	0	0	0	0
	Podocopida	1	Cyprididae gen. sp. Mexico	<i>Manuelcypris tabascena</i> isolate 31	97.87%	KX940959.1	0	1	0	0	1	0	0	0	0	1
	Podocopida	1	<i>Cytheromorpha acupunctata</i>	<i>Cytheromorpha acupunctata</i>	98.94%	AB076630.1	1	0	1	0	0	0	0	1	0	0
	Podocopida	1	Podocopida; invertebrate environmental sample	<i>Physocypria kraepelini</i> voucher 1506303	97.87%	KY088231.1	0	1	0	0	1	0	0	1	0	0
	Sarcoptiformes	1	<i>Haplochthonius simplex</i>	<i>Haplochthonius simplex</i> voucher BMOC 07-0607-007 AD1124	100.00%	KP325062.1	1	0	1	0	0	0	0	1	0	0
	Zygentoma	1	<i>Lepisma</i> sp. GG-1997	<i>Ctenolepisma longicaudata</i>	100.00%	AY210811.1	0	1	0	0	1	0	1	0	0	0
Total Arthropoda OTUs	43	133	-	-	-	-	61	72	38	43	52	27	24	29	24	29
Bryozoa	Ctenostomatida	10	<i>Amathia</i> sp. n. 2 AW-2014	<i>Amathia verticillata</i> voucher BRBRY-Z01	96.84%	KM373518.1	3	7	6	3	1	0	3	4	1	2
	Cheilostomatida	3	<i>Smittoidea spinigera</i>	<i>Smittoidea spinigera</i>	97.87%	AF499746.1	1	2	1	0	2	0	2	0	0	1
	Plumatellida	1	<i>Plumatella casmiana</i>	<i>Plumatella casmiana</i>	100.00%	KT852567.1	1	0	1	0	0	0	1	0	0	0

(table cont'd.)

Phylum	Order	OTU Incidences	Lowest SILVA Assignment	Top GenBank Match	GenBank Percent Identity	GenBank Accession	S	I	DI	HI	SI	L	ML	M	MH	H
Total Bryozoa OTUs	3	14	-	-	-	-	5	9	8	3	3	0	6	4	1	3
Gastrotricha	Chaetonotida	14	<i>Heterolepidoderma</i> sp. 1 TK-2012	<i>Heterolepidoderma</i> sp. 1 TK-2012	100.00%	JQ798554.1	10	4	7	4	3	3	2	3	3	3
	-	1	Ambiguous taxa	<i>Chaetonotus persimilis</i> voucher GA_19.13	100.00%	MN496195.1	0	1	0	0	1	1	0	0	0	0
	Chaetonotida	1	<i>Halichaetonotus</i> sp. 2 TK-2012	<i>Halichaetonotus</i> sp. 2 TK-2012	98.94%	JQ798600.1	1	0	1	0	0	0	0	1	0	0
Total Gastrotricha OTUs	3	16	-	-	-	-	11	5	8	4	4	4	2	4	3	3
Hydrozoa	Leptothecata	11	<i>Helgicirra cari</i>	<i>Helgicirra cari</i> isolate MHNG-HYD-DNA1153	97.87%	KY363989.1	3	8	3	8	0	0	2	2	3	4
	Anthoathecata	8	Anthoathecata; Ambiguous taxa	<i>Moerisia inkermanica</i> voucher LEM m3x S41	100.00%	KT722408.1	6	2	7	1	0	1	1	2	2	2
	Leptothecata	5	<i>Blackfordia virginica</i>	<i>Blackfordia virginica</i>	100.00%	AF358078.1	2	3	2	1	2	0	2	0	2	1
	Limnomedusae	3	Limnomedusae; Ambiguous taxa	<i>Pennaria</i> sp. AMN-2009	100.00%	GQ424343.1	2	1	0	1	2	0	1	0	0	2
	Leptothecata	2	Leptothecata; Ambiguous taxa	<i>Clytia gracilis</i> voucher MZUSP:2774	100.00%	KX665411.1	1	1	0	0	2	1	1	0	0	0
	Leptothecata	1	<i>Blackfordia virginica</i>	<i>Blackfordia virginica</i> voucher LEM m3x S42	100.00%	KT722387.1	1	0	1	0	0	0	0	0	1	0
Total Hydrozoa OTUs	6	30	-	-	-	-	15	15	13	11	6	2	7	4	8	9
Kinorhyncha	Echinorhagata	7	<i>Echinoderes hwiizaa</i>	<i>Echinoderes hwiizaa</i>	98.94%	AB899167.1	1	6	2	5	0	1	0	2	2	2

(table cont'd.)

Phylum	Order	OTU Incidences	Lowest SILVA Assignment	Top GenBank Match	GenBank Percent Identity	GenBank Accession	S	I	DI	HI	SI	L	ML	M	MH	H
	Allomalorhagida	2	<i>Pycnophyes robustus</i>	<i>Pycnophyes flaveolatus</i>	100.00%	LC081129.1	2	0	2	0	0	0	1	0	1	0
Total Kinorhyncha OTUs	2	9	-	-	-	-	3	6	4	5	0	1	1	2	3	2
Mollusca	Mytilida	35	<i>Brachidontes rodriguezii</i>	<i>Brachidontes mutabilis</i> voucher MIEE2015-6HM1	100.00%	KY081328.1	16	19	14	11	10	6	4	9	8	8
	-	12	Neritimorpha; Ambiguous taxa	<i>Theodoxus fluviatilis</i>	100.00%	AF120515.1	6	6	4	5	3	3	2	2	2	3
	-	4	Heterobranchia; Ambiguous taxa	<i>Granulilimax</i> sp. KC9179	97.87%	LC508384.1	2	2	1	1	2	1	3	0	0	0
	Littorinimorpha	3	<i>Littoraria pallescens</i>	<i>Littoraria pallescens</i>	98.94%	AB611828.1	1	2	1	2	0	0	1	0	1	1
	Mytilida	1	<i>Perna viridis</i>	<i>Perna canaliculus</i> isolate N3	98.94%	MK419109.1	0	1	0	0	1	0	0	1	0	0
Total Mollusca OTUs	5	55	-	-	-	-	25	30	20	19	16	10	10	12	11	12
Nematoda	Enoplida	47	Enoplida; Ambiguous taxa	<i>Adoncholaimus</i> sp.	98.94%	AF036642.1	23	24	17	14	16	7	9	11	10	10
	Enoplida	11	Enoplida; uncultured eukaryote	Uncultured eukaryote clone Pink_A05	100.00%	GQ483737.1	2	9	3	4	4	1	1	4	3	2
	Chromadorida	7	<i>Ptycholaimellus</i> sp. 1092	<i>Ptycholaimellus</i> sp. 1092	98.94%	FJ040472.1	0	7	1	6	0	0	1	2	2	2
	Monhysterida	6	Monhysterida; Ambiguous taxa	<i>Daptonema</i> sp. 1255	100.00%	FJ040463.1	5	1	0	2	4	3	2	1	0	0
	Monhysterida	5	<i>Diplolaimella dievengatensis</i>	<i>Diplolaimella dievengatensis</i> isolate Diplo1	98.94%	MN072928.1	2	3	4	1	0	0	1	2	0	2

(table cont'd.)

Phylum	Order	OTU Incidences	Lowest SILVA Assignment	Top GenBank Match	GenBank Percent Identity	GenBank Accession	S	I	DI	HI	SI	L	ML	M	MH	H
	Dorylaimida	4	Dorylaimida; metagenome	Uncultured soil eukaryote clone y470	100.00%	MK946073.1	3	1	0	0	4	2	0	0	0	2
	Monhysterida	4	Diplolaimelloides environmental sample	Uncultured Diplolaimelloides clone GD1D53P	98.94%	EF659927.1	2	2	1	2	1	0	0	2	1	1
	Rhabditida	4	<i>Filenchus vulgaris</i>	<i>Filenchus</i> sp. 4 TJP-2012 isolate 21T16109	100.00%	JQ814878.1	1	3	0	1	3	0	0	2	1	1
	Enoplida	3	<i>Rhabdolaimus</i> cf. <i>terrestris</i> JH-2004	<i>Rhabdolaimus terrestris</i> strain RhDoTer1	97.87%	KJ636366.1	1	2	1	0	2	1	0	0	0	2
	Rhabditida	3	<i>Aglenchus agricola</i>	<i>Aglenchus agricola</i> strain AgleAgr1	100.00%	FJ969113.1	2	1	1	0	2	0	0	1	0	2
	Rhabditida	2	<i>Helicotylenchus digitiformis</i>	<i>Helicotylenchus pseudorobustus</i> strain HeliPse8	100.00%	KJ869399.1	2	0	0	0	2	0	0	0	0	2
	Enoplida	1	<i>Oncholaimus</i> sp. OUS2	Uncultured eukaryote clone Plate2-44-M13R_B05.ab1	100.00%	KU757379.1	1	0	0	0	1	0	0	0	1	0
	Enoplida	1	<i>Pontonema vulgare</i>	Uncultured eukaryote clone Plate2-51-M13R_A06.ab1	98.94%	KU757347.1	1	0	1	0	0	0	0	0	1	0
	Monhysterida	1	Monhysterida; uncultured eukaryote	Uncultured eukaryote	98.94%	LC150149.1	0	1	0	1	0	1	0	0	0	0
	Monhysterida	1	Monhysterida; Ambiguous taxa	Callipallenidae environmental sample clone Amb_185_445	98.94%	EF023156.1	1	0	0	0	1	0	0	0	0	1

(table cont'd.)

Phylum	Order	OTU Incidences	Lowest SILVA Assignment	Top GenBank Match	GenBank Percent Identity	GenBank Accession	S	I	DI	HI	SI	L	ML	M	MH	H
	Tylenchida	1	Tylenchida; Ambiguous taxa	<i>Pratylenchus</i> <i>hippeastri</i> isolate SD53	100.00%	KY424237.1	1	0	0	0	1	0	0	0	0	1
Total Nematoda OTUs	16	101	-	-	-	-	47	54	29	31	41	15	14	25	19	28
Nemertea	Archinemertea	1	<i>Cephalothrix</i> <i>hongkongiensis</i>	<i>Cephalothrix</i> sp. 1 AM-2014 voucher MNCN Ndes001	98.94%	KM230038.1	1	0	1	0	0	0	1	0	0	0
	Monostilifera	1	<i>Prostoma graecense</i>	<i>Prostoma</i> cf. <i>eilhardi</i> EEZ-2018 isolate PROei_bost	100.00%	MK076304.1	0	1	0	1	0	0	0	0	1	0
Total Nemertea OTUs	2	2	-	-	-	-	1	1	1	1	0	0	1	0	1	0
Platyhelminthes	Lecithoepitheliata	37	Lecithoepitheliata; uncultured eukaryote	Uncultured eukaryote	98.94%	LC150104.1	12	25	7	12	18	5	7	9	7	9
	Macrostomida	6	Macrostomida; Ambiguous taxa	<i>Macrostomum</i> <i>zhujiangensis</i> isolate 3	98.94%	KX771198.1	2	4	1	2	3	1	0	1	2	2
	Rhabdocoela	5	<i>Protoplanella simplex</i>	<i>Protoplanella</i> <i>simplex</i> isolate UH345.2	100.00%	KC529490.1	1	4	1	3	1	0	0	1	2	2
	Macrostomorpha	2	<i>Macrostomum clavituba</i>	<i>Macrostomum</i> <i>clavituba</i> voucher MTP LS 301	98.94%	FJ715304.1	0	2	1	0	1	1	1	0	0	0
	Prolecityophora	2	<i>Plagiosomum ochroleucum</i>	<i>Plagiosomum</i> <i>ochroleucum</i>	97.87%	AF065419.1	2	0	1	0	1	1	0	0	1	0
	Dolichomicrostomida	1	<i>Microstomum</i> sp. B TJ-2015	<i>Microstomum</i> sp. B TJ-2015 voucher MTP LS 524	97.87%	KP730505.1	1	0	1	0	0	0	0	0	1	0
	Polycladida	1	Polycladida; Ambiguous taxa	<i>Mirostylochus</i> <i>akkeshiensis</i> ICHUM:6022	98.94%	LC508173.1	1	0	1	0	0	0	0	0	1	0

(table cont'd.)

Phylum	Order	OTU Incidences	Lowest SILVA Assignment	Top GenBank Match	GenBank Percent Identity	GenBank Accession	S	I	DI	HI	SI	L	ML	M	MH	H
	Rhabdocoela	1	<i>Gieysztoria</i> sp. n. 5 'red'	<i>Gieysztoria dodgei</i> isolate UH358.2	100.00%	KC529479.1	1	0	0	1	0	0	0	0	1	0
	Rhabdocoela	1	<i>Olisthanella truncula</i>	<i>Olisthanella truncula</i> isolate UH76.3	100.00%	KC529494.1	1	0	0	1	0	0	0	0	0	1
	Rhabdocoela	1	<i>Gyratrix hermaphroditus</i>	<i>Gyratrix hermaphroditus</i> voucher DNA029SARIII	97.87%	KJ887459.1	1	0	0	0	1	1	0	0	0	0
	Tricladida	1	<i>Girardia tigrina</i>	<i>Girardia tigrina</i>	98.94%	AF013156.1	0	1	0	1	0	0	1	0	0	0
Total Platyhelminthes OTUs	11	58	-	-	-	-	22	36	13	20	25	9	9	11	15	14
Rotifera	Flosculariaceae	6	<i>Testudinella clypeata</i>	<i>Testudinella clypeata</i> isolate A758_T4	98.94%	KF561109.1	6	0	2	1	3	1	2	1	1	1
	Bdelloidea	4	<i>Rotaria sordida</i>	<i>Rotaria sordida</i> voucher A955_RS	97.87%	KM043269.1	0	4	2	0	2	1	0	1	1	1
	-	2	Bdelloidea environmental sample	Uncultured soil eukaryote clone b531	100.00%	MK946076.1	1	1	1	1	0	1	0	0	0	1
Rotifera	-	1	Bdelloidea; environmental sample	Uncultured bdelloid rotifer clone Rot_H_08A	98.94%	GQ922289.1	1	0	0	0	1	0	0	0	0	1
	Ploimida	1	Ploimida; Ambiguous taxa	<i>Notholca acuminata</i>	100.00%	AY218115.1	0	1	0	1	0	0	0	1	0	0
	Ploimida	1	Ploimida; metagenome	<i>Synchaeta pectinata</i> isolate ST_01I01	100.00%	KP875584.1	0	1	0	1	0	0	0	0	1	0
Total Rotifera OTUs	6	15	-	-	-	-	8	7	5	4	6	3	2	3	3	4

(table cont'd.)

Phylum	Order	OTU Incidences	Lowest SILVA Assignment	Top GenBank Match	GenBank Percent Identity	GenBank Accession	S	I	DI	HI	SI	L	ML	M	MH	H
uncultured marine eukaryote	-	2	-	uncultured marine eukaryote	100.00%	LR217397.1	2	0	1	0	1	0	0	1	1	0
Xenacoelomorpha	Acoela	1	<i>Philocelis brueggemanni</i>	<i>Philocelis robrochae</i> voucher MHSa	100.00%	FR837733.1	1	0	1	0	0	0	0	0	1	0

Any OTU with a “-” in the order column was ambiguous at the order level for the SILVA taxonomy assignment. The OTUs in white are members of the frequent group of OTUs, which appeared in more than 10 samples in the dataset. Taxa shaded in gray are part of the infrequent group which appeared in less than 10 samples in the dataset. OTU incidence is further separated by category, i.e., samples from Sheared (S) and Intact (I) margins, from Dragon (DI), Horseshoe (HI), and Stingray Island (SI), and at the Low (L), MidLow (ML), Mid (M), MidHigh (MH), and High (H) elevation transect positions. Rows with “Total Phylum OTUs” in the first cell have the number of total OTUs belonging to that phylum in the Order column and the total number of incidences of OTUs in that phylum in the OTU Incidences column. Similarly, the total incidences for each phylum in the categories are presented in the columns corresponding to the different categories. All phyla which had more than one OTU assigned received a “Total Phylum OTUs” row following the OTUs of that phylum.

Unique taxa:

Some of the OTUs in the dataset were only detected in either the samples from sheared or intact margins and were detected at least twice (Table 3.7). Both groups of OTUs contained members of the phyla Nematoda, Platyhelminthes, and Rotifera. The OTUs which were unique to the samples from intact margins also included two members of the Annelida and three members of the Arthropoda, while the OTUs unique to the sheared margins included a member of the Kinorhyncha and an uncultured marine eukaryote. Both of the annelids unique to the intact margins were assigned as oligochaetes, one as a member of the order Enchytraeida and the other as a member of the order Haplotaxida. One of the arthropod OTUs which was unique to the intact margins was assigned as a member of the crustacean order Tanaidacea, which lack a planktonic stage. The next arthropod OTU was assigned to the Entomobryomorpha, which is one of the orders contained within the Collembola. The last unique arthropod OTU was assigned to the Calanoida, as *Centropages furcatus*. Copepods of this genus are known to be members of zooplankton communities in the nearshore Gulf of Mexico (Park et al. 1989, Checkley Jr et al. 1992). The only nematode which was unique to the intact margins was assigned to the genus *Ptycholaimellus*, which is known to inhabit estuarine systems in North America (Eskin and Hopper 1985). The only member of the Platyhelminthes which was unique to the intact samples was assigned to the genus *Macrostomum*, which is a group of cosmopolitan free living flatworms (Adami and Damborenea 2020). The final member of the group of OTUs which were unique to the intact margins was assigned as a rotifer in the order Bdelloidea. The kinorhynch which was unique to the samples from sheared margins was assigned as a member of the genus *Pycnophyes*. Members of this genus are known from the continental shelf of the Gulf of Mexico (Landers et al. 2018). The only nematode unique to the sheared margins was assigned to the genus *Helicotylenchus* in the order Rhabditida. The platyhelminth OTU which was unique to this category was assigned as a member of the order Prolecithophora, which are typically interstitial dwelling, free living marine flatworms (Norén and Jondelius 1999). The last OTU in this category which received a meaningful assignment was a rotifer in the order Flosculariaceae.

Table 3.7. Unique taxa in the samples from sheared and intact margins.

Phylum	Order	OTU Incidences	Lowest SILVA Assignment	Top GenBank Match	S	I
Annelida	Enchytraeida	2	Marionina tumulicola	Marionina nothachaeta clone LM225	0	2
Annelida	Haplotaxida	2	Haplotaxida; Ambiguous taxa	Lumbricidae sp. R50	0	2
Arthropoda	Tanaidacea	6	Tanais dulongii	Tanais dulongii	0	6
Arthropoda	Entomobryomorpha	5	Orchesella cincta	Katiannidae sp. R36	0	5

(table cont'd.)

Phylum	Order	OTU Incidences	Lowest SILVA Assignment	Top GenBank Match	S	I
Arthropoda	Calanoida	3	<i>Centropages furcatus</i>	<i>Centropages furcatus</i>	0	3
Nematoda	Chromadorida	7	<i>Ptycholaimellus</i> sp. 1092	<i>Ptycholaimellus</i> sp. 1092	0	7
Platyhelminthes	Macrostomorpha	2	<i>Macrostomum clavituba</i>	<i>Macrostomum clavituba</i> voucher MTP LS 301	0	2
Rotifera	Bdelloidea	4	<i>Rotaria sordida</i>	<i>Rotaria sordida</i> voucher A955_RS	0	4
Kinorhyncha	Allomalorhagida	2	<i>Pycnophyes robustus</i>	<i>Pycnophyes flaveolatus</i>	2	0
Nematoda	Rhabditida	2	<i>Helicotylenchus digitiformis</i>	<i>Helicotylenchus pseudorobustus</i> strain HeliPse8	2	0
Platyhelminthes	Prolecithophora	2	<i>Plagiosomum ochroleucum</i>	<i>Plagiosomum ochroleucum</i>	2	0
Rotifera	Flosculariaceae	6	<i>Testudinella clypeata</i>	<i>Testudinella clypeata</i> isolate A758_T4	6	0
uncultured marine eukaryote	-	2	-	uncultured marine eukaryote	2	0

All taxa presented in this table are those which were only detected in samples from either the sheared or intact margins, and were detected at least twice.

Additionally, some of the OTUs were detected on only one or two of the islands (Table 3.8). A single OTU which was detected twice and only in Dragon Island samples was assigned as a kinorhynch in the genus *Pycnophyes*. Eleven OTUs were detected only in samples from Dragon and Horseshoe Islands, including five arthropods, two hydrozoans, two nematodes, one kinorhynch and one mollusk. All five of the arthropods were crustaceans, including a tanaid amphipod, an ostracod, a harpacticoid copepod, a decapod likely in the crab family Varunidae, and a barnacle. The two hydrozoans were an ambiguous member of the order Anthoathecata (GenBank: *Moerisia inkermanica*) and *Helgicirrha cari*, a member of the order Leptothecata. The two nematode OTUs were assigned to *Diplolaimella dievengatensis* and a member of the genus *Ptycholaimellus*. The kinorhynch OTU which was detected only in Dragon and Horseshoe Islands was assigned as a member of the genus *Echinoderes*, which is known from the study area (Fleeger et al. 2015). Finally, the mollusk which was unique to this group of samples was assigned to a member of the genus *Littoraria*, which is known to inhabit salt marshes across the Gulf and Atlantic coasts of North America (Gustafson et al. 2006). Five OTUs were detected only in samples from Dragon and Stingray Island. These consisted of two nematodes, an annelid, a bryozoan, and a rotifer. The two nematode OTUs were assigned to the orders Enoplida and Rhabditida, respectively. The sole annelid unique to Dragon and Stingray Island samples was assigned as a member of the order Haplotaxida in the genus *Aulodrilus*. This genus is a member

of the family Naididae. The bryozoan which was unique to this group of samples was in the order Cheilostomatida. Lastly, the rotifer which was unique to this group was assigned to the order Bdelloidea. Two annelid OTUs, both members of the Oligochaeta, were unique to the samples from Horseshoe Island. The first of these was assigned to the genus *Marionina*, which is known to inhabit the stems of *Spartina* plants in North American salt marshes (Healy and Walters 1994), while the other was an ambiguous member of the Haplotaxida. The group of OTUs which were only detected in samples from Horseshoe and Stingray Island consisted of two annelids, two arthropods, two nematodes, and a hydrozoan. The two annelids in this group were a polychaete (*Heteromastus filiformis*, family Capitellidae) and an ambiguous member of the oligochaete order Haplotaxida. Both of the arthropods were assigned to copepods in the order Calanoida. The nematode OTUs were assigned as members of the order Monhysterida and Rhabditida, respectively. Finally, the hydrozoan OTU in this group was assigned as an ambiguous member of the Limnomedusae. Six OTUs were unique to the samples from Stingray Island, including two arthropods, two nematodes, one annelid, and one hydrozoan. One of these arthropods was assigned to the insect order Isoptera, and the other was assigned to the insect order Diptera. The two nematode OTUs in this group were assigned as a member of the order Dorylamida and a member of the genus *Helicotylenchus*. Nematodes from this genus are known from agricultural sites in Louisiana and are considered a plant parasite (Bond et al. 2000). The lone annelid OTU in this group was assigned to the genus *Marionina*, though this was a different OTU than the one which was unique to the Horseshoe Island samples. Finally, the only hydrozoan in this group was assigned as an ambiguous member of the order Leptothecata.

Table 3.8. Unique taxa in the samples from different islands.

Phylum	Order	OTU Incidences	Lowest SILVA Assignment	Top GenBank Match	DI	HI	SI
Kinorhyncha	Allomalorhagida	2	Pycnophyes robustus	Pycnophyes flaveolatus	2	0	0
Arthropoda	Tanaidacea	6	Tanais dulongii	Tanais dulongii	2	4	0
Arthropoda	Podocopida	4	Podocopida; Ambiguous taxa	Leptocythere lacertosa	2	2	0
Arthropoda	Harpacticoida	3	Leptocaris brevicornis	Leptocaris brevicornis	2	1	0
Arthropoda	Decapoda	3	Eriocheir sinensis	Hemigrapsus takanoi	2	1	0
Arthropoda	-	4	Thecostraca; Ambiguous taxa	Semibalanus balanoides voucher WS834	1	3	0
Hydrozoa	Anthoathecata	8	Anthoathecata; Ambiguous taxa	Moerisia inkermanica voucher LEM m3x S41	7	1	0
Hydrozoa	Leptothecata	11	Helgicirrha cari	Helgicirrha cari isolate MHNG-HYD-DNA1153	3	8	0
Kinorhyncha	Echinorhagata	7	Echinoderes hwiizaa	Echinoderes hwiizaa	2	5	0

(table cont'd.)

Phylum	Order	OTU Incidences	Lowest SILVA Assignment	Top GenBank Match	DI	HI	SI
Mollusca	Littorinimorpha	3	Littoraria pallescens	Littoraria pallescens	1	2	0
Nematoda	Monhysterida	5	Diplolaimella dievengatensis	Diplolaimella dievengatensis isolate Diplo1	4	1	0
Nematoda	Chromadorida	7	Ptycholaimellus sp. 1092	Ptycholaimellus sp. 1092	1	6	0
Annelida	Haplotaxida	3	Aulodrilus acutus	Aulodrilus acutus voucher CE1790	1	0	2
Bryozoa	Cheilostomatida	3	Smittoidea spinigera	Smittoidea spinigera	1	0	2
Nematoda	Enoplida	3	Rhabdolaimus cf. terrestris JH-2004	Rhabdolaimus terrestris strain RhDoTer1	1	0	2
Nematoda	Rhabditida	3	Aglenchus agricola	Aglenchus agricola strain AgleAgr1	1	0	2
Rotifera	Bdelloidea	4	Rotaria sordida	Rotaria sordida voucher A955_RS	2	0	2
Annelida	Enchytraeida	2	Marionina tumulicola	Marionina nothachaeta clone LM225	0	2	0
Annelida	Haplotaxida	2	Haplotaxida; Ambiguous taxa	Lumbricidae sp. R50	0	2	0
Annelida	Scolecida	5	Heteromastus filiformis	Heteromastus filiformis	0	4	1
Annelida	Haplotaxida	3	Haplotaxida; Ambiguous taxa	Enchytraeus dicaetus isolate CE24345	0	1	2
Arthropoda	Calanoida	10	Acartia tonsa	Acartia tonsa isolate ME-Atonsa1	0	3	7
Arthropoda	Calanoida	3	Centropages furcatus	Centropages furcatus	0	2	1
Hydrozoa	Limnomedusae	3	Limnomedusae; Ambiguous taxa	Pennaria sp. AMN-2009	0	1	2
Nematoda	Monhysterida	6	Monhysterida; Ambiguous taxa	Daptonema sp. 1255	0	2	4
Nematoda	Rhabditida	4	Filenchus vulgaris	Filenchus sp. 4 TJP-2012 isolate 21T16I09	0	1	3
Annelida	Enchytraeida	3	Marionina tumulicola	Marionina tumulicola clone CE571	0	0	3
Arthropoda	Isoptera	7	Isoptera; Ambiguous taxa	Reticulitermes flavipes	0	0	7
Arthropoda	Diptera	2	Corynoptera saetistyla	Claustropyga abblanda	0	0	2
Hydrozoa	Leptothecata	2	Leptothecata; Ambiguous taxa	Clytia gracilis voucher MZUSP:2774	0	0	2
Nematoda	Dorylaimida	4	Dorylaimida; metagenome	Uncultured soil eukaryote clone y470	0	0	4
Nematoda	Rhabditida	2	Helicotylenchus digitiformis	Helicotylenchus pseudorobustus strain HeliPse8	0	0	2

All taxa presented in this table are those which were not detected in at least one of the island categories, and were detected at least twice on at least one island.

Alpha diversity:

No significant differences were detected between samples from sheared and intact margins in OTU richness (Kruskal-Wallis test, $\chi^2 (1) = 0.03$, $p = 0.86$, Fig. 3.15) and in Faith's Phylogenetic Diversity (PD) ($\chi^2 (1) = 0.48$, $p = 0.49$, Fig. 3.16) following rarefying. Given the similar total OTU richness of the samples from sheared and intact margins (Table 3.3, Fig. 3.4), the similarity of OTU richness of the samples from these groups is not an unexpected result. Because the OTUs richness and Faith's PD were not significantly different, the phylogenetic distances of OTUs collected from sheared and intact margins were similar.

A significant difference for OTU richness in the Island category was detected using the Kruskal-Wallis test ($\chi^2 (2) = 10.74$, $p < 0.01$), with the pairwise test indicating that samples from Dragon Island had reduced richness when compared to samples from Horseshoe or Stingray Island (Dragon-Horseshoe: $\chi^2 (1) = 4.89$, Benjamini-Hochberg corrected $p = 0.04$, Dragon-Stingray: $\chi^2 (1) = 9.89$, Benjamini-Hochberg corrected $p < 0.01$, Fig. 3.15). Five samples from Dragon Island showed very low richness, especially in the Low elevation position (Fig. 3.12). In addition, samples from Dragon Island showed lower richness than samples from the other two islands at nearly all elevation positions in both sheared and intact margins (Fig. 3.15). The Faith's PD values showed a significant difference between the groups of samples from the different islands (Kruskal-Wallis test, $\chi^2 (2) = 7.48$, $p = 0.02$, Fig. 3.16), with the pairwise test indicating that samples from Dragon Island had lower Faith's PD (Dragon-Stingray: $\chi^2 (1) = 7.18$, Benjamini-Hochberg corrected $p = 0.02$, Fig. 3.16). This result may have been influenced by the lower richness in Dragon Island samples as a whole or the result of more phylogenetic differences between the samples from different islands (Fig. 3.12).

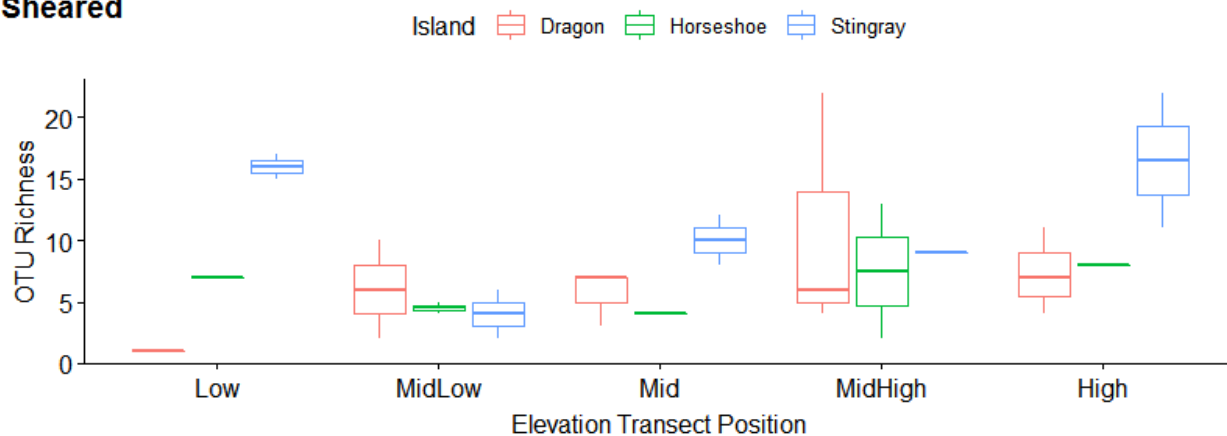
No significant differences in OTU richness (Kruskal-Wallis, $\chi^2 (4) = 3.4$, $p = 0.49$, Fig. 3.15) or Faith PD (Kruskal-Wallis, $\chi^2 (4) = 1.85$, $p = 0.76$, Fig. 3.16) between the samples from the different elevation positions were detected.

The interaction of Margin type and Island showed significant differences between groups overall (Kruskal-Wallis, $\chi^2 (5) = 15.53$, $p < 0.01$, Fig. 3.15) and the pairwise tests indicated that samples from intact margins on Dragon Island had lower richness than samples from intact margins on Horseshoe Island and from sheared margins on Stingray Island (Dragon Intact-Horseshoe Intact: $\chi^2 (1) = 7.39$, Benjamini-Hochberg corrected $p = 0.049$, Dragon Intact-Stingray Sheared: $\chi^2 (1) = 7.79$, Benjamini-Hochberg corrected $p = 0.049$, Fig. 3.15). The values for Faith's PD were significantly different overall (Kruskal-Wallis, $\chi^2 (5) = 14.44$, $p = 0.01$, Fig. 3.16) as well, but none of the pairwise comparisons remained significant after the Benjamini-Hochberg correction.

The interactions of all other categories were not significantly different in terms of richness (Kruskal-Wallis, Margin-Elevation Position, $\chi^2 (9) = 6.64$, $p = 0.67$, Island-Elevation Position, $\chi^2 (13) = 22.9$, $p = 0.06$, Margin-Island-Elevation Position, $\chi^2 (29) = 36.07$, $p = 0.17$) or

Faith's PD (Kruskal-Wallis, Margin-Elevation Position, χ^2 (9) = 6.00, p = 0.74, Island-Elevation Position, χ^2 (13) = 20.63, p = 0.11, Margin-Island-Elevation Position, χ^2 (29) = 36.87, p = 0.15). However, the variance of these values could be quite wide. Several trends are worth noting, even though the differences were not significant, likely due to low sample sizes after splitting the dataset into categories. Low and High samples had higher richness than other elevation positions in sheared margin samples on Stingray Island; Low elevation position samples in intact margins on Stingray Island also were higher than other positions (Fig. 3.15). This pattern held true for the Faith's PD values as well. The samples from intact margins on Horseshoe Island generally had higher richness than the samples from sheared margins on that island. This was also true for the Faith's PD values, excluding the MidHigh and High samples. The MidHigh samples from sheared margins on Dragon Island had a wide range of richness and Faith's PD values. The samples from Low and MidLow positions from intact margins on Stingray Island had high richness, which declined in the samples from Mid, MidHigh, and High samples. The richness values for the High position samples from sheared margins in this dataset were the opposite of what they were in the chapter 2 dataset, with higher richness in the Dragon and Horseshoe samples and low richness in the Stingray samples (Fig. 2.16).

Sheared



Intact

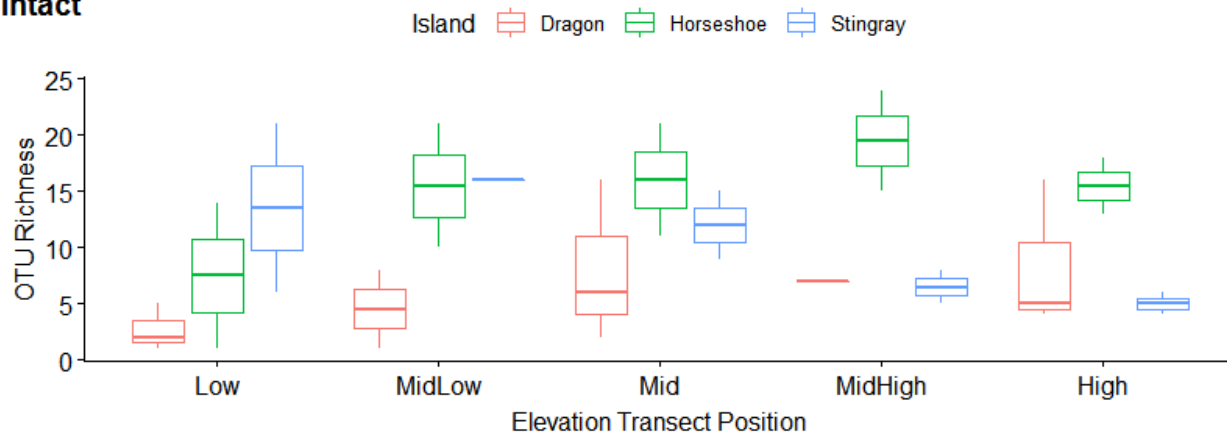


Fig. 3.15. The OTU richness values for sheared and intact sites, with individual box plots for

each island and elevation position. All samples were collected from the marsh islands surrounding Bay Jimmy, Louisiana from August 2017 to November 2017.

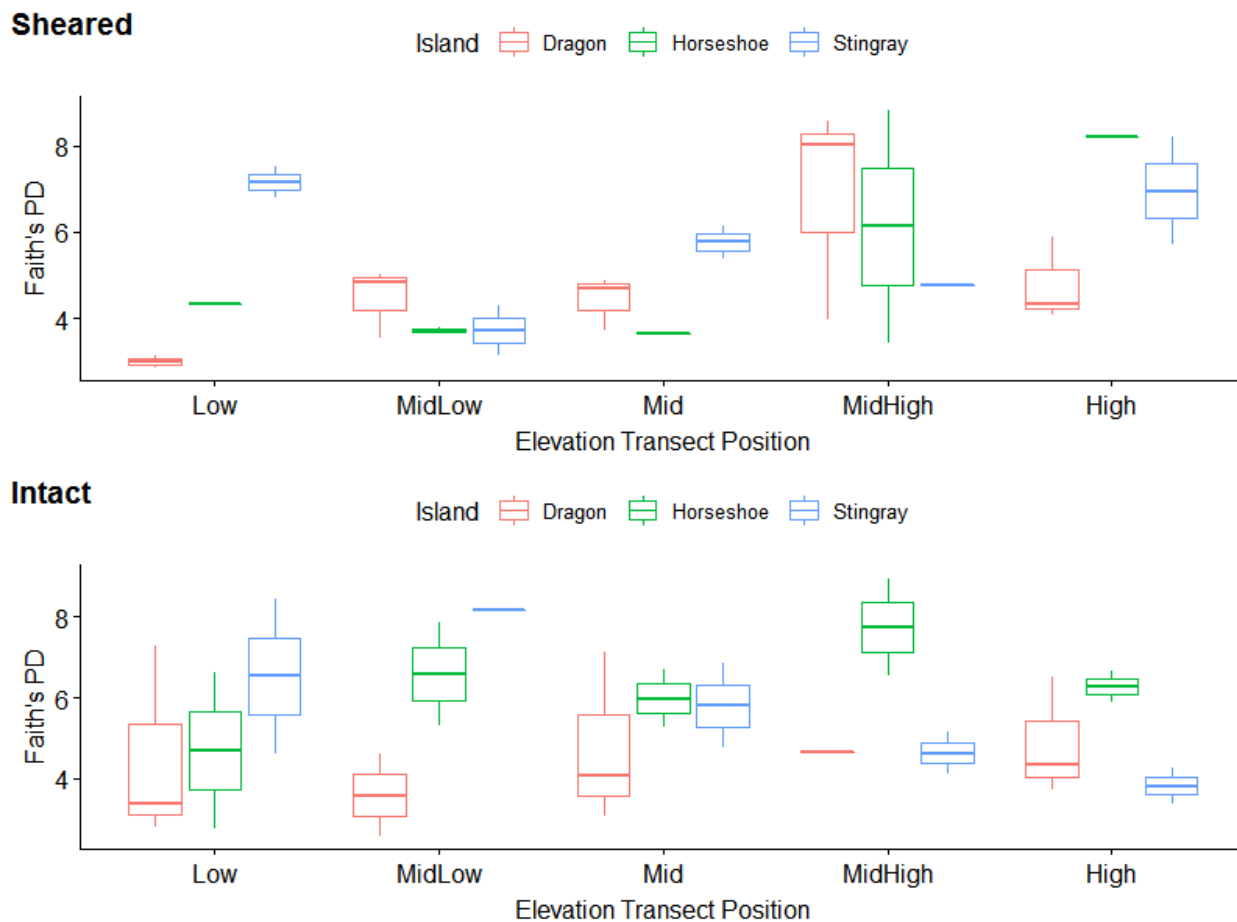


Fig. 3.16. Faith PD values for sheared and intact sites, with individual box plots for each island and elevation position. All samples were collected from the marsh islands surrounding Bay Jimmy, Louisiana from August 2017 to November 2017.

Beta diversity group similarity indices:

Beta diversity similarity indices run from zero to one, and values closer to one indicate more similarity of composition or incidence between groups. The similarity indices between the communities from sheared and intact margins (Table 3.9) generally showed high similarity (values > 0.6), excluding the Jaccard index. Indices based on estimates of the actual community returned higher values for the indices, excluding the two richness-based estimators, Sørensen and Jaccard, which showed lower estimated than empirical values. This was in contrast to the dataset from chapter 2, where the Sørensen and Jaccard indices returned higher estimated values (Table 2.16). The estimated version of the indices is based on an estimation of the actual

community. These two indices are the result of the shared OTUs divided by the total number of OTUs, though the Sørensen index gives more weight to the shared species than the Jaccard index, and will therefore always return a higher value. Because the estimated values for the richness-based indices are lower than the observed, the estimated actual community contains more unique OTUs in the samples from sheared and intact margins. However, because the estimated incidence-based indices were higher than the observed, the incidence of OTUs would continue to increase in similarity with additional sampling.

Table 3.9. Empirical and estimated similarity indices between communities collected from different margins (sheared and intact), islands (Dragon, Horseshoe, Stingray) and elevation positions (Low, MidLow, Mid, MidHigh, High). Samples were collected from marsh islands surrounding Bay Jimmy, Louisiana from August 2017 to November 2017.

Factor	Index	Estimate	S.E.	95% Lower	95% Upper
Margin	Sørensen Empirical	0.6024	0.0343	0.5352	0.6696
	Sørensen Estimated	0.5139	0.0975	0.3228	0.705
	Jaccard Empirical	0.431	0.0297	0.3728	0.4892
	Jaccard Estimated	0.3458	0.0905	0.1684	0.5232
	Horn (equal-weighted) Empirical	0.7401	0.0265	0.6881	0.792
	Horn (equal-weighted) Estimated	0.8296	0.0585	0.7151	0.9442
	Morisita-Horn (relative) Empirical	0.8159	0.0178	0.7811	0.8507
	Morisita-Horn (relative) Estimated	0.9161	0.2123	0.5	1
	Regional overlap (relative) Empirical	0.8986	0.0098	0.8795	0.9178
	Regional overlap (relative) Estimated	0.9562	0.0695	0.82	1
Island	Sørensen Empirical	0.6077	0.0295	0.5498	0.6656
	Sørensen Estimated	0.4338	0.0767	0.2835	0.584
	Jaccard Empirical	0.3405	0.0353	0.2713	0.4098
	Jaccard Estimated	0.2034	0.1594	0	0.5158
	Horn (equal-weighted) Empirical	0.7166	0.0194	0.6786	0.7546
	Horn (equal-weighted) Estimated	0.794	0.0214	0.7521	0.836
	Morisita-Horn (relative) Empirical	0.7669	0.0228	0.7222	0.8115

(table cont'd.)

Factor	Index	Estimate	S.E.	95% Lower	95% Upper
	Morisita-Horn (relative) Estimated	0.902	0.252	0.4081	1
	Regional overlap (relative) Empirical	0.908	0.0095	0.8894	0.9265
	Regional overlap (relative) Estimated	0.9651	0.0257	0.9147	1
Elevation Position	Sørensen Empirical	0.6858	0.0185	0.6496	0.722
	Sørensen Estimated	0.6003	0.0332	0.5352	0.6654
	Jaccard Empirical	0.3039	0.0181	0.2684	0.3393
	Jaccard Estimated	0.231	0.1225	0	0.4711
	Horn (equal-weighted) Empirical	0.7506	0.0148	0.7216	0.7795
	Horn (equal-weighted) Estimated	0.8005	0.0191	0.763	0.8379
	Morisita-Horn (relative) Empirical	0.8176	0.0223	0.7739	0.8614
	Morisita-Horn (relative) Estimated	1	0.1539	0.6984	1
	Regional overlap (relative) Empirical	0.9573	0.0065	0.9446	0.97
	Regional overlap (relative) Estimated	1	0.0162	0.9683	1

S.E. is standard error. 95% Lower and Upper are the values for the confidence intervals. Indices all run from 0 to 1, with higher values indicating higher similarity.

Similarity indices between the island communities were generally high (>0.6), excluding the Jaccard index (Table 3.9). However, the estimated Sørensen and Jaccard indices were again reduced compared to the empirical indices. Again, this means that the estimate of the actual community contains more unique OTUs for each island community than the observed community. This result may be partially due to the low richness observed in some Dragon and Horseshoe Island samples (Fig. 3.15), leading to lower overlap between the groups. However, samples from Dragon Island showed only a slightly lower estimated coverage than the samples from other islands (Fig 3.9). In addition, low similarity (<0.4) was observed in the estimated pairwise Sørensen index values between the Horseshoe and Stingray Island communities (Table 3.10).

Table 3.10. Estimated pairwise similarity matrix for island communities, Sørensen index. Samples were collected from marsh islands surrounding Bay Jimmy, Louisiana from August 2017 to November 2017

Community	Dragon	Horseshoe	Stingray
Dragon	1	0.498 (0.324,0.671)	0.542 (0.333,0.752)
Horseshoe		1	0.398 (0.229,0.567)
Stingray			1

Numbers in parenthesis for each pairwise similarity are the 95% confidence interval for that similarity estimate.

The similarity indices between the elevation position communities were generally high (>0.6, Table 3.9). The Sørensen and Jaccard index values were again lower for the estimated community, potentially as a result of lower coverage in the Low position samples (Fig. 3.6). Several of the pairwise Sørensen indices were quite low (<0.5), including the Low-MidLow, Low-MidHigh, MidLow-Mid, and MidLow-MidHigh comparisons (Table 3.11). This means that there were less shared OTUs compared to the total OTUs between these comparisons. Meanwhile, all of the pairwise indices for the High community were high (>0.5), meaning that there were more shared OTUs compared to the total OTUs than in the other pairwise comparisons. This is potentially because the High samples had the highest total richness of any of the elevation positions (Table 3.5). All of the pairwise similarity indices involving the MidLow position samples were much lower in this dataset than in the chapter 2 dataset, especially the MidLow-MidHigh index value, which was 0.893 in the chapter 2 (Table 2.18). Other indices which were much lower than the chapter 2 dataset included the Low-MidHigh (0.615 previously) and the Mid-MidHigh (0.703 previously, Table 2.18).

Table 3.11. Estimated pairwise similarity matrix for elevation transect communities, Sørensen index. Samples were collected from marsh islands surrounding Bay Jimmy, Louisiana from August 2017 to November 2017.

Community	Low	MidLow	Mid	MidHigh	High
Low	1	0.346 (0.104,0.588)	0.551 (0.095,1.000)	0.415 (0.180,0.650)	0.529 (0.180,0.650)
MidLow		1	0.363 (0.194,0.532)	0.371 (0.192,0.549)	0.549 (0.267,0.832)
Mid			1	0.599 (0.369,0.829)	0.589 (0.356,0.823)
MidHigh				1	0.589 (0.398,0.779)
High					1

Numbers in parenthesis for each pairwise similarity are the 95% confidence interval for that similarity estimate.

Non-Metric Dimensional Scaling:

Patterns of beta diversity (using the Sørensen index distance matrix) among the samples from sheared and intact margins and the different islands were visualized using NMDS ordination. The distance between samples in an NMDS plot represents the ranking of the distances between samples in a distance matrix, and separation of groups and group centroids indicates differences in the metazoan composition of groups of samples. NMDS plots can also visualize the dispersion of groups from the group centroid. The group centroids of the groups of samples from different margin types (intact, sheared) were positioned closely to each other, indicating similarity of composition between these two groups (Fig. 3.17). In addition, both groups showed a wide dispersion, largely due to a small number of low diversity samples from the Low position on Dragon Island. These samples were located furthest to the top left, and furthest to the right of the plot. The low diversity samples were evenly distributed between the samples from sheared and intact margins. Low diversity samples, especially samples which only contain one OTU, will show very high Sørensen dissimilarity from samples with an average level of diversity. This is because a sample with low diversity cannot have a large number of OTUs shared with a sample with average diversity compared to the number of total OTUs in both samples. Low numbers of shared OTUs result in low similarity between samples, increasing the distance between samples in the multivariate space. Plotting the Island groups over the ordination revealed centrally located centroids for all groups, but a very large difference in the spread between the Island groups (Fig. 3.18). Samples from Horseshoe and Stingray Island showed a much tighter distribution than samples from Dragon Island. Again, this was primarily driven by the position of the low diversity samples from Dragon Island, causing a much wider spread than Horseshoe or Stingray Island.

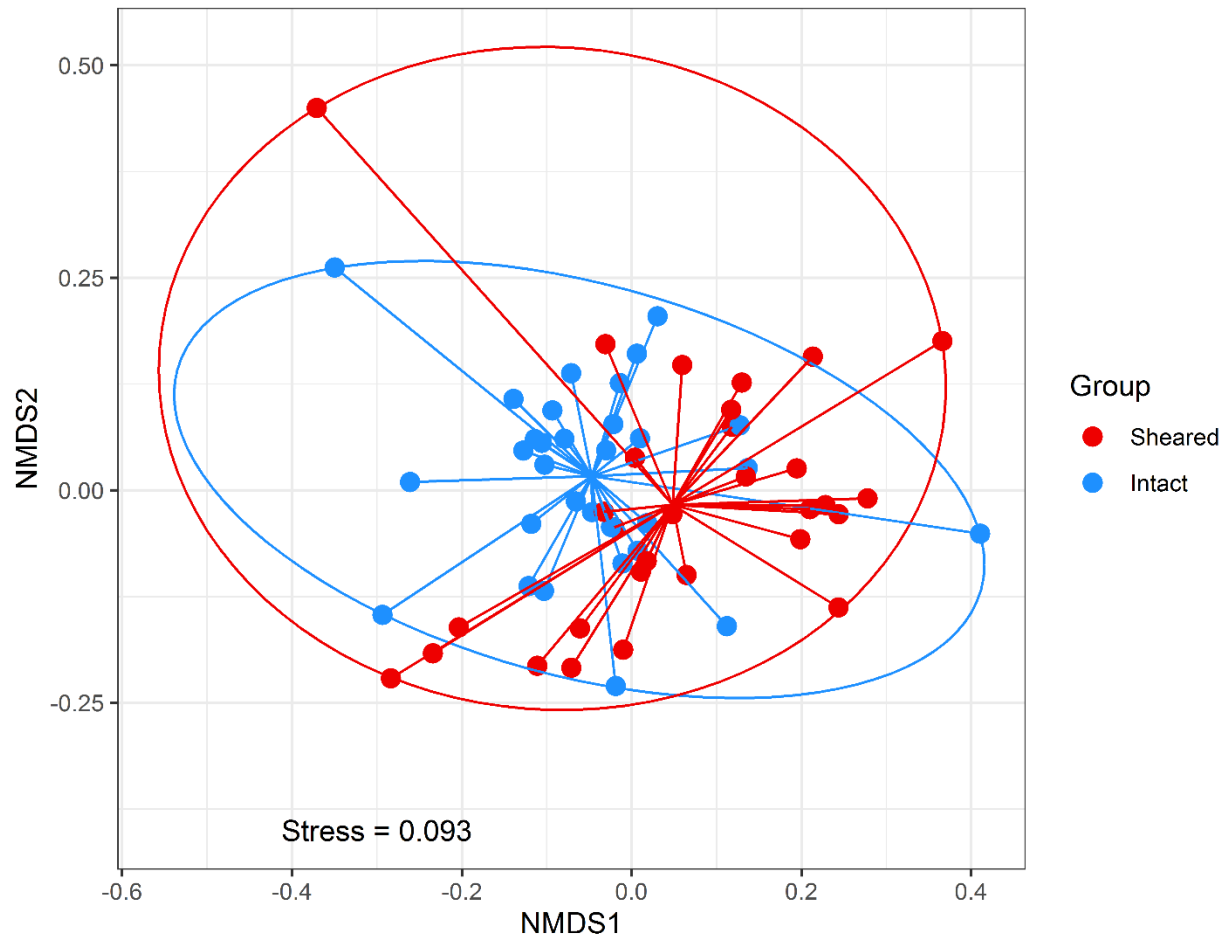


Fig. 3.17. Plot of the first two dimensions of the NMDS ordination of the Sørensen distance matrix. All samples were collected from the marsh islands surrounding Bay Jimmy, Louisiana from August 2017 to November 2017. Small circles represent individual samples. Ellipses represent the elliptical hulls of the groups. Straight lines connect a sample to the group centroid. The stress value is the goodness of fit of the regression of the original distances between samples in the original dataset to the distances between samples in NMDS ordination.

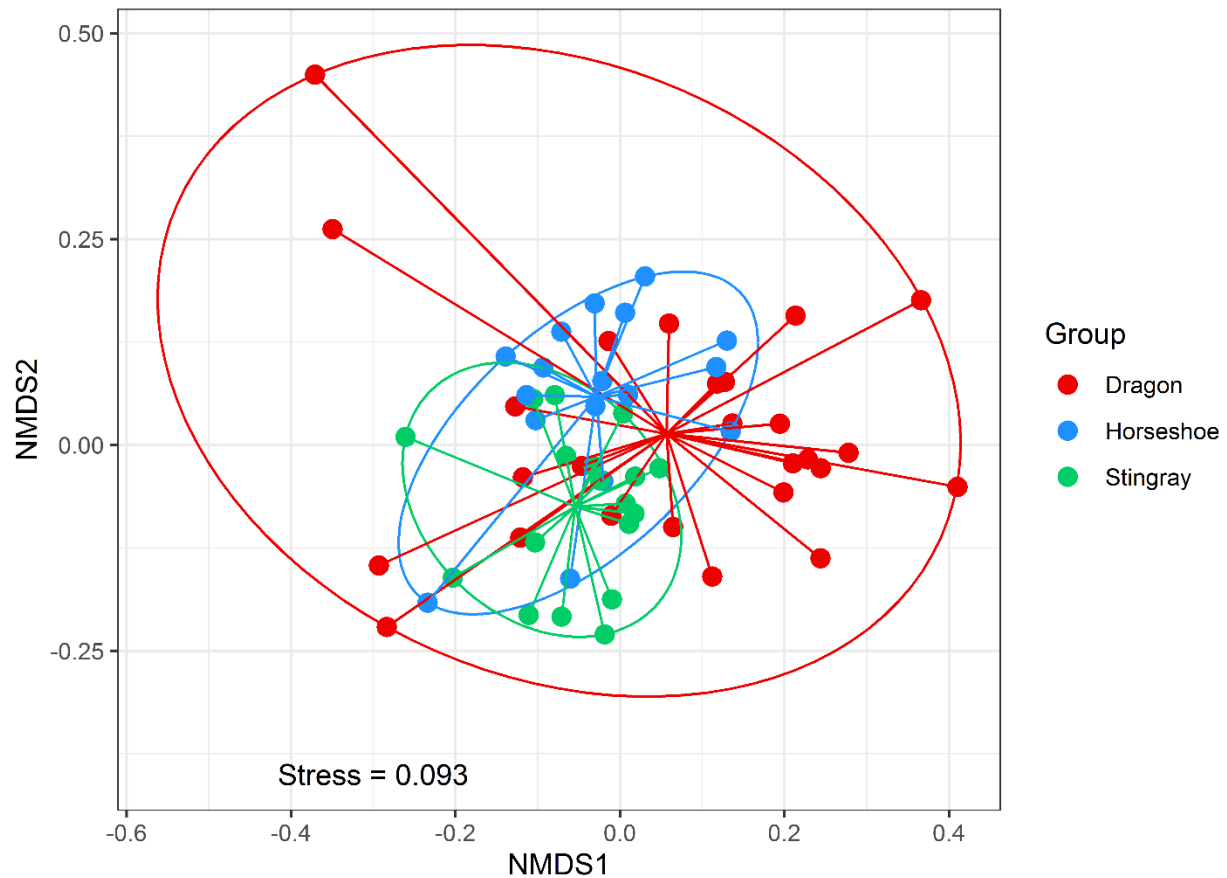


Fig. 3.18. Plot of the first two dimensions of the NMDS ordination of the Sørensen distance matrix. All samples were collected from the marsh islands surrounding Bay Jimmy, Louisiana from August 2017 to November 2017. Small circles represent individual samples. Ellipses represent the elliptical hulls of the groups. Straight lines connect a sample to the group centroid. The stress value is the goodness of fit of the regression of the original distances between samples in the original dataset to the distances between samples in NMDS ordination.

Patterns of community composition due to the interaction of the factors Island and Margin were visualized using NMDS ordination (Fig. 3.19). Samples from Dragon Island showed the wide dispersion previously observed (Fig. 3.18) in both sheared and intact margins. However, the group of samples from the sheared margins on Dragon Island had a cluster of samples to the right side of the ordination, meaning that the centroid of that group was much further to the right than the centroid of the samples from intact margins on Dragon Island. This cluster of samples includes samples from all of the elevation positions except for Low. The influence of this cluster of samples on the location of the Dragon-Sheared centroid is important to note, because it shifts that centroid away from the Dragon-Intact centroid. The locations of the centroids in multivariate space were used to test the differences in group composition in the Adonis test. Samples from Horseshoe and Stingray Islands had similar dispersion, excluding

the groups of samples from intact margins on Horseshoe Island, which had a smaller spread and therefore a greater within-group similarity. This was in contrast to the dataset from chapter 2, where the samples from sheared margins on Horseshoe Island had a smaller dispersion than the samples from intact margins on that island (Fig. 2.20).

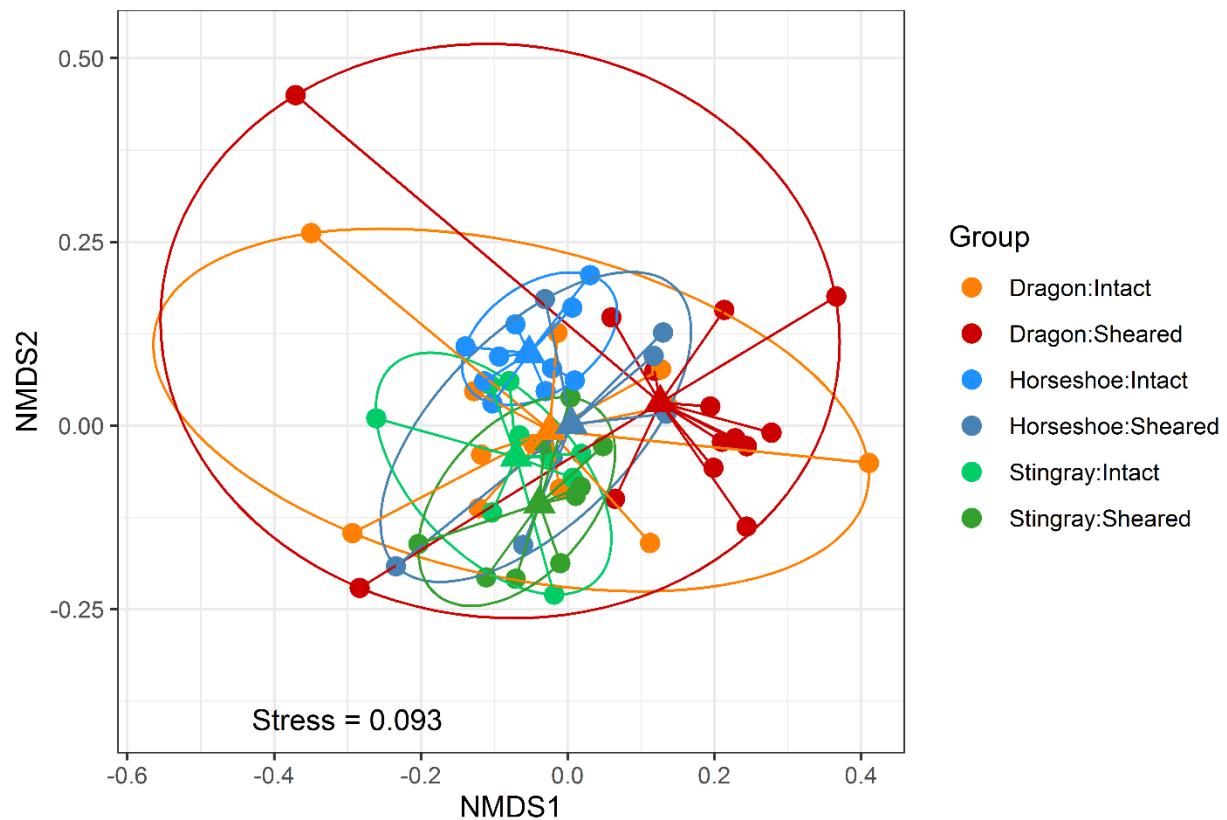


Fig. 3.19. Plot of the first two dimensions of the NMDS ordination of the Sørensen distance matrix. All samples were collected from the marsh islands surrounding Bay Jimmy, Louisiana from August 2017 to November 2017. Small circles represent individual samples. Ellipses represent the elliptical hulls of the groups. Straight lines connect a sample to the group centroid. Triangular points are the group centroid for the interaction of factors indicated by the legend. The stress value is the goodness of fit of the regression of the original distances between samples in the original dataset to the distances between samples in NMDS ordination.

Beta-diversity significance testing:

Following Benjamini-Hochberg correction, the Margin (Adonis test, $F(1,60) = 3.09$, $p < 0.01$) and Island (Adonis test, $F(2,60) = 3.37$, $p < 0.01$) factors had significant effects on the differentiation of community composition (Table 3.12). The factor Elevation Position and all interactions of factors did not significantly affect the group location following the BH correction. The dispersion of the groups in factor Margin was homogenous (PERMDISP test based on Sørensen distance matrix, BH corrected $p > 0.05$), so the differences between the samples from the two types of margins were based on the community differences between the two groups, rather than on the differences within the groups (i.e., dispersion). However, the Island factor was not homogenous in dispersion (PERMDISP test, overall: BH corrected $p = 0.01$, pairwise tests: Dragon-Horseshoe, BH corrected $p = 0.03$, Dragon-Stingray, BH corrected $p < 0.01$, Horseshoe-Stingray, BH corrected $p = 0.55$). This result was supported by the NMDS ordination (Fig. 3.18), which showed a much wider dispersion in the Dragon Island samples than in the samples from the other islands. The factors Margin and Island had low R^2 values, meaning that the factors explain a small amount of the variation in the data (0.05 and 0.10, respectively).

Table 3.12. Adonis test results. All samples were collected from the marsh islands surrounding Bay Jimmy, Louisiana from August 2017 to November 2017.

Factor	Df	SumOfSqs	R2	F-value	p-value
Margin	1	0.8293	0.0445	3.0873	0.0004*
Island	2	1.8141	0.0974	3.3766	0.0001*
Elevation Position	4	1.3540	0.0727	1.2601	0.1034
Margin:Island	2	0.7967	0.0428	1.4828	0.0556
Margin:Elevation Position	4	1.5206	0.0817	1.4151	0.0359
Island:Elevation Position	8	2.2766	0.1222	1.0594	0.3316
Margin:Island:Elevation Position	8	1.7038	0.0915	0.7928	0.9367
Residual	31	8.3275	0.4472		
Total	60	18.6226	1.0000		

Asterisks * indicate a p-value which remained significant following the Benjamini-Hochberg correction.

Additional Adonis tests were conducted on subsets of the data containing only samples from the individual islands to test the effects of the Margin and Elevation Position factors on the different islands. For the samples from Dragon Island, the factor Margin but not Elevation Position or their interaction had a significant effect on community composition ($F(2) = 2.36$, BH corrected $p = 0.01$, Table 3.13). The multivariate dispersion of the samples from sheared and

intact margins on Dragon Island was homogenous (PERMDISP test, $p > 0.05$), meaning that the differences in community composition were due to differences in community between the groups rather than within the groups. This factor also had a low R^2 value, at 0.09. This difference between samples from sheared and intact margins was also detected in chapter 2 (Table 2.20). For the Horseshoe and Stingray Island datasets, no factors were significantly different following the Benjamini Hochberg correction (Table 3.14, Table 3.15). This result indicates that the majority of the difference in the Margin factor for the whole dataset is due to the differences in community composition between samples from the two margin types on Dragon Island. This was different from the dataset in chapter 2, where the samples from Stingray Island also contributed to the differences between the sheared and intact margins (Table 2.22).

Table 3.13. Adonis test output for Dragon Island samples. All samples were collected from the marsh islands surrounding Bay Jimmy, Louisiana from August 2017 to November 2017.

Factor	Df	SumsOfSqs	R2	F-value	p-value
Margin	1	0.7762	0.0881	2.3606	0.0040*
Elevation Position	4	1.2844	0.1457	0.9766	0.5186
Margin:Elevation Position	4	1.4922	0.1693	1.1346	0.2575
Residuals	16	5.2607	0.5969		
Total	25	8.8134	1.0000		

Asterisks * indicate a p-value which remained significant following the Benjamini-Hochberg correction.

Table 3.14. Adonis test output for Horseshoe Island samples. All samples were collected from the marsh islands surrounding Bay Jimmy, Louisiana from August 2017 to November 2017.

Factor	Df	SumsOfSqs	R2	F-value	p-value
Margin	1	0.5204	0.1292	2.3712	0.0180
Elevation Position	4	1.1134	0.2763	1.2683	0.1859
Margin:Elevation Position	4	0.8594	0.2133	0.9789	0.5102
Residuals	7	1.5364	0.3813		
Total	16	4.0296	1.0000		

Table 3.15. Adonis test output for Stingray Island samples. All samples were collected from the marsh islands surrounding Bay Jimmy, Louisiana from August 2017 to November 2017.

Factor	Df	SumsOfSqs	R2	F-value	p-value
Margin	1	0.2313	0.0596	1.2091	0.2743
Elevation Position	4	1.1176	0.2879	1.4605	0.0390
Margin:Elevation Position	4	1.0021	0.2582	1.3095	0.1041
Residuals	8	1.5305	0.3943		
Total	17	3.8815	1.0000		

Differential abundance of OTUs:

Twelve OTUs had differential relative read count abundances across the Margin, Island and Elevation position categories detected by the Songbird plugin in QIIME 2 (Table 3.16). These differentials represent the relative log fold difference in reads between the comparison class and the class which the column is named for. Read counts are not equivalent to numbers of individuals in metazoan taxa, so differential abundances are presented here as the difference in cell counts between categories. A separate comparison class was selected for each metadata category, which were the Intact margin class for the Margin category, Dragon Island class for the Island category, and Low position class for the Elevation position category. Positive values indicate more enrichment in the samples from the class being compared to the comparison class, while negative values indicate more enrichment in the comparison class. The intercept column represents the differential abundance for all comparison classes. At the phylum level, the differential OTUs consisted of three Annelida, two Arthropoda, two Mollusca, two Nematoda, one Platyhelminthes, one Hydrozoa, and one Gastrotricha. The three annelid OTUs were assigned to the species *Marionina coatesae*, *Alitta succinea*, and an ambiguous member of the order Spionida. This ambiguous annelid received an alternative assignment of *Polydora lingshuiensis* from the GenBank database and will be referred to as such. The two arthropod OTUs were assigned to the horse fly *Haematopota pluvialis* and a member of the mite genus *Acarothrix*. The mollusk OTUs were assigned to the mussel *Brachidontes rodriguezii* and an ambiguous member of the subclass Neritimorpha. The ambiguous member of the Neritimorpha was given an alternate assignment in GenBank of *Theodoxus fluviatilis*. The two nematode OTUs were both assigned to Enopida, as an ambiguous taxon and as an uncultured eukaryote. The nematode assigned as an ambiguous member of Enoplida was assigned as *Adoncholaimus* sp. in GenBank and will be referred to as such to avoid confusion with the uncultured eukaryote in the order Enoplida. The hydrozoan OTU was assigned to the hydromedusa *Helgicirrha cari*, while the gastrotrich OTU was assigned to a member of the

genus *Heterolepidoderma*. Finally, the Platyhelminthes OTU was assigned to a member of the order Lecithoepitheliata.

In the Margin category, the OTU most enriched in the samples from sheared margins compared to the intact margins was assigned to the mite from the genus *Acarothrix*. (Table 3.16) The OTU assigned to the genus *Adoncholaimus* (Nematoda) was the next most enriched within the samples from the sheared margins. Following these OTUs, the next two most enriched OTUs in sheared compared to intact margins were assigned to the hydrozoan *Helgicirrha cari* and the horse fly *Haematopota pluvialis*, respectively. The final two OTUs which were more enriched in the sheared margins than in the intact margins were assigned to the gastrotrich genus *Heterolepidoderma* and the mussel *Brachidontes rodriguezii*. The OTU which was most enriched in the intact margins compared to the sheared margins was assigned to the oligochaete *Marionina coatesae*. The next most enriched OTU in intact margins was assigned to an uncultured eukaryote in the nematode order Enoplida. The next two OTUs which were more enriched in the intact margins than sheared margins were assigned to *Polydora lingshuiensis* (Annelida) and *Theodoxus fluviatilis* (Mollusca). The final two OTUs which were enriched in the intact margins were assigned as an uncultured eukaryote of the order Lecithoepitheliata (Platyhelminthes) and the polychaete *Alitta succinea* (Annelida).

In the Island category, the OTU which was most enriched in Horseshoe Island samples compared to Dragon Island samples was assigned to the oligochaete *Marionina coatesae* (Table 3.16). The next two most enriched OTUs for the Horseshoe Island samples were assigned to *Polydora lingshuiensis* (Annelida) and the genus *Adoncholaimus* (Nematoda), respectively. Following these two OTUs, the next two most enriched OTUs in Horseshoe Island samples were assigned to the mussel *Brachidontes rodriguezii* and the polychaete *Alitta succinea*. The last OTU which was more enriched in Horseshoe Island samples than Dragon Island samples was assigned to an uncultured eukaryote of the order Lecithoepitheliata (Platyhelminthes). The OTUs which were most enriched in Dragon Island samples compared to Horseshoe Island samples were assigned as the mite *Acarothrix* sp., the hydrozoan *Helgicirrha cari*, the gastrotrich *Heterolepidoderma* sp., the horse fly *Haematopota pluvialis*, an uncultured eukaryote in the nematode order Enoplida, and *Theodoxus fluviatilis*, in order of most to least enriched.

The OTU which was most enriched in the Stingray Island samples compared to Dragon Island samples was assigned to the horse fly *Haematopota pluvialis* (Table 3.16). Following this OTU, the next two OTUs that were most enriched in Stingray Island samples were assigned to the polychaete *Polydora lingshuiensis* and the oligochaete *Marionina coatesae*. The next two most enriched OTUs in this island were assigned to the mussel *Brachidontes rodriguezii* and an uncultured eukaryote of the order Lecithoepitheliata (Platyhelminthes). The final two OTUs which were more enriched in Stingray Island samples than in Dragon Island samples were both assigned to the nematode order Enoplida, as the genus *Adoncholaimus* and as an uncultured eukaryote, respectively. The OTUs which were most enriched in the Dragon Island samples

compared to the Stingray Island samples were assigned as the hydrozoan *Helgicirrha cari*, the nerite *Theodoxus fluviatilis*, the mite *Acarothrix* sp., the gastrotrich *Heterolepidoderma* sp., and the polychaete *Alitta succinea*, in order of most to least enriched.

The OTUs which were consistently more enriched in the Dragon Island samples (i.e., always had negative differentials in the Island category) were assigned as the mite *Acarothrix* sp., the hydromedusa *Helgicirrha cari* (Hydrozoa), a member of the genus *Heterolepidoderma* (Gastrotricha), and the nerite *Theodoxus fluviatilis* (Mollusca, Table 3.16).

For the Elevation position category, the OTU which was most enriched in the MidLow samples compared to Low samples was the mite *Acarothrix* sp. (Table 3.16) Six other OTUs were more enriched in MidLow samples than in Low samples. These OTUs were assigned to the polychaete *Polydora lingshuiensis* (Annelida), an uncultured eukaryote in the order Lecithoepitheliata (Platyhelminthes), a member of the genus *Heterolepidoderma* (Gastrotricha), the nerite *Theodoxus fluviatilis* (Mollusca), the horse fly *Haematopota pluvialis* (Arthropoda), and a member of the nematode genus *Adoncholaimus*. The five OTUs which were more enriched in Low samples than in MidLow samples were assigned to the hydromedusa *Helgicirrha cari* (Hydrozoa), the mussel *Brachidontes rodriguezii* (Mollusca), the oligochaete *Marionina coatesae* (Annelida), the polychaete *Alitta succinea* (Annelida), and an uncultured member of the order Enoplida (Nematoda), in order of most to least enriched.

In the Mid samples compared to Low samples column, the most enriched OTU was assigned to the oligochaete *Marionina coatesae* (Annelida, Table 3.16). Five other OTUs were more enriched in the Mid samples compared to the Low samples. These were assigned to the polychaete *Polydora lingshuiensis* (Annelida), a member of the nematode genus *Adoncholaimus* (Nematoda), an uncultured eukaryote in the order Lecithoepitheliata (Platyhelminthes), the polychaete *Alitta succinea* (Annelida), and a member of the genus *Heterolepidoderma* (Gastrotricha). Six OTUs were more enriched in Low samples than in the Mid samples. These were assigned to the horse fly *Haematopota pluvialis* (Arthropoda), the hydromedusa *Helgicirrha cari* (Hydrozoa), the nerite *Theodoxus fluviatilis* (Mollusca), the mussel *Brachidontes rodriguezii* (Mollusca), an uncultured member of the order Enoplida (Nematoda), and the mite *Acarothrix* sp., in order of most to least enriched.

The OTU which was most enriched in the MidHigh samples compared to the Low samples was assigned to the gastrotrich *Heterolepidoderma* sp. (Table 3.16). Seven more OTUs were more enriched in the MidHigh samples than in the Low samples. These were assigned to the polychaete *Alitta succinea* (Annelida), the hydromedusa *Helgicirrha cari* (Hydrozoa), the oligochaete *Marionina coatesae* (Annelida), the mussel *Brachidontes rodriguezii* (Mollusca), an uncultured eukaryote in the order Lecithoepitheliata (Platyhelminthes), the horse fly *Haematopota pluvialis* (Arthropoda), a member of the nematode genus *Adoncholaimus* (Nematoda). Four OTUs were more enriched in the Low compared to the MidHigh samples. These OTUs were assigned to an ambiguous member of the subclass Neritomorpha (Mollusca),

the mite *Acarothrix* sp., the polychaete *Polydora lingshuiensis* (Annelida), and an uncultured member of the order Enoplida (Nematoda), in order of most to least enriched.

The two most enriched OTUs in the High samples compared to Low samples were a member of the nematode genus *Adoncholaimus* and the gastrotrich *Heterolepidoderma* sp. (Table 3.16). Four more OTUs were more enriched in High compared to Low samples, these were assigned to the nerite *Theodoxus fluviatilis* (Mollusca), an uncultured eukaryote in the order Lecithoepitheliata (Platyhelminthes), the polychaete *Alitta succinea* (Annelida), and the horse fly *Haematopota pluvialis* (Arthropoda). Six OTUs were more enriched in Low samples than in High samples. These were assigned to the mussel *Brachidontes rodriguezii* (Mollusca), the hydromedusa *Helgicirra cari* (Hydrozoa), the polychaete *Polydora lingshuiensis* (Annelida), the oligochaete *Marionina coatesae* (Annelida), the mite *Acarothrix* sp., and an uncultured member of the order Enoplida (Nematoda).

The only OTU which was always more enriched in the Low samples (always negative in the Elevation position category) was assigned to an uncultured eukaryote in the order Enoplida (Nematoda, Table 3.16).

Table 3.16. Songbird differentials for the OTUs detected in samples from marsh islands surrounding Bay Jimmy collected from August 2017 to November 2017.

SILVA Taxonomy String	Intercept	Sheared compared to Intact	Horseshoe compared to Dragon	Stingray compared to Dragon	MidLow compared to Low	Mid compared to Low	MidHigh compared to Low	High compared to Low
Arthropoda Chelicerata Arachnida Acari <i>Acarothrix</i> sp. ARP-2015	0.9347	1.1173	-1.9796	-2.0122	1.8787	-0.1314	-1.5438	-0.8407
Nematoda Enoplea Enoplia Enoplida Ambiguous taxa *	0.6196	1.0698	1.3394	0.7975	0.0075	1.0286	0.2350	1.5458
Hydrozoa Hydroidolina Leptothecata <i>Helgicirra cari</i> *	0.1359	0.8145	-1.9199	-2.3397	-1.0772	-1.5543	0.7481	-1.4006
Arthropoda Hexapoda Insecta Pterygota Neoptera Diptera <i>Haematopota pluvialis</i>	-1.1435	0.6153	-1.0066	1.6624	0.0390	-2.2450	0.5144	0.1102

(table cont'd.)

SILVA Taxonomy String	Intercept	Sheared compared to Intact	Horseshoe compared to Dragon	Stingray compared to Dragon	MidLow compared to Low	Mid compared to Low	MidHigh compared to Low	High compared to Low
Gastrotricha Chaetodontida Heterolepidodermata sp. 1 TK-2012 *	-0.9723	0.5090	-1.2027	-0.6301	0.1500	0.3096	1.3617	1.5443
Mollusca Bivalvia Pteriomorpha Mytiloida Brachidontes rodriguezii *	0.8547	0.3364	1.1229	1.0503	-0.9608	-0.6357	0.6102	-1.4907
Annelida Polychaeta Palpata Phyllodoce Alitta succinea *	1.0508	-0.0515	0.2662	-0.1465	-0.6416	0.4015	1.2458	0.8001
Platyhelminthes Rhabditophora Lecithoepitheliata uncultured eukaryote	0.5006	-0.1459	0.0809	0.8816	0.6310	0.7417	0.5730	1.1386
Mollusca Gastropoda Neritimorpha Ambiguous taxa *	-0.7869	-0.5387	-0.0791	-2.0195	0.1037	-1.1674	-2.0094	1.2220
Annelida Polychaeta Scolecidia Spionida Ambiguous taxa *	0.4847	-0.9733	1.7628	1.4326	1.0925	1.6049	-1.4607	-1.3274
Nematoda Enoplea Enoplia Enoplida uncultured eukaryote *	-1.8370	-1.1467	-0.3241	0.0045	-0.5530	-0.1395	-0.8948	-0.2017
Annelida Clitellata Oligochaeta Haplotaxida Marionina coatesae	0.1587	-1.6063	1.9398	1.3190	-0.6698	1.7871	0.6204	-1.0999

Columns are separated by vertical lines into metadata categories (Margin, Island, and Elevation Position). Higher positive values of differentials indicate higher relative abundance of reads in the metadata category of the column, while lower negative values indicate higher relative abundance of reads in the comparison class of the column. The intercept column represents the relative abundances of all comparison classes across all categories. The comparison class for Margin is the group of samples from intact margins. The comparison class for Island is the group of samples from Dragon Island. The comparison class for Elevation Position is the group of samples from the Low elevation position. Differentials are presented sorted by highest to lowest values for the Sheared column. Taxa with asterisks were also members of the frequent group in chapter 2.

3.4. Discussion

Metazoan OTUs represented the largest percentage of the unfiltered dataset (Fig. 3.1) and had the second lowest percentage of unclear assignments in the dataset (Table 3.1). In

samples from Dragon Island, Fungi and the SAR clade made up the majority of the non-metazoan reads. However, in the samples from Horseshoe and Stingray Islands, the Archaeplastida largely replaced the SAR clade as one of the dominant non-metazoa groups, though Fungi generally remained the same. These Archaeplastida ASVs were primarily assigned to a species of *Juncus*, which is present in Louisiana marshes. However, the reason for this dominance of Archaeplastida ASVs may be because records for *Spartina* species are lacking in the SILVA database and not as a result of a lack of plants on Dragon Island. The groups Excavata, Amoebozoa, Cryptophyceae, Incertae Sedis, Haplophyta, and the non-metazoan, non-fungi members of the Opisthokonta collectively never made up more than 10% of any sample. The only group present in every sample was the metazoa; the SAR and Fungi were present in >85% of samples (Table 3.1). The total number of ASVs was lower in this chapter, and the percentage of ASVs in the dataset which matched to Excavata was lower compared to the chapter 2 dataset (~12% of ASVs in chapter 2, ~4% of ASVs in chapter 3). The other groups in this dataset made up similar percentages of the total ASVs in the dataset when compared to chapter 2, but the Opisthokonta and SAR groups swapped positions as the most numerous and second most numerous groups in this chapter compared to chapter 2. It is unclear how sample processing in this study could have reduced the amount of Excavata, perhaps they are more easily washed out of the sample or are more tightly attached to the sediment grains than other groups.

Sequencing depth for metazoan sequences in the dataset tended to be lower than in the chapter 2 dataset, with a mean sequencing depth of approximately 1300 reads and quartiles at 100 and 1200 (Fig. 3.2). For comparison, the mean sequencing depth of the samples in chapter 2 was approximately 5000 (Fig. 2.4). In addition, richness was correlated with sequencing depth, so rarefying was employed for the alpha diversity comparisons.

The sample-based rarefactions of the entire dataset indicated that additional richness could be detected if additional samples were collected (Fig. 3.3). However, the extrapolated portions of the Shannon and Simpson Inverse effective diversity were nearly flat, only increasing by ~10. Therefore, additional samples would collect new OTUs, but these OTUs would be rarely detected in the dataset and would contribute little to the Shannon and Simpson Inverse metrics. Although more of the infrequent group could potentially be collected, the sampling effort revealed the majority of OTUs from the frequent group. As the database was split into smaller groups to examine the trends within the different metadata categories, the range of the 95% confidence interval increased, and the curves for Shannon and Simpson Inverse started to increase more than in the full dataset. These are likely effects of the reduced sample size compared to the full dataset. However, several trends were evident outside of sample size reduction. One such trend was a higher total richness and extrapolated richness estimate observed on Stingray Island (Fig. 3.5). In addition, the MidLow elevation position showed slightly lower richness and extrapolated richness estimate when compared to the other elevation positions (Fig 3.6). In contrast, the Low position samples had the lowest richness and diversity curves compared to the other elevation position samples in chapter 2. However, the

sample-based rarefactions and extrapolations for the different margin types were very similar (Fig. 3.4).

The coverage-based rarefaction curves for the entire dataset indicated that approximately 90% of the actual community was collected (Fig. 3.7); doubling sampling only would reach a coverage level of approximately 95%. Splitting the database into the smaller groups showed the same trends as the split sample-based rarefactions, including lower estimated coverage, wider confidence intervals, and steeper slopes on the Shannon and Simpson Inverse curves than in the whole dataset. The samples from different margin types and different islands showed similar coverage estimates (80-85%, Fig. 3.8, 3.9), but the Low elevation position had a much lower estimated coverage (65%) than the other elevation positions (Fig. 3.10). It is not entirely clear why Low position samples had such a lower coverage value than the elevation positions, as these samples had the second lowest number of total OTUs (following MidLow position samples, Table 3.5) and had the same number of total incidences as the MidLow position samples (91 incidences, Table 3.6). Both of these elevation positions were missing a single member of the frequent group. However, the Low elevation position did have the lowest total incidences of the frequent group (43 incidences), though this was only slightly lower than the incidences of the frequent group in MidLow position samples (45 incidences). This potentially means that future studies on distribution of organisms in coastal islands should have increased sampling or sequencing efforts on the Low and MidLow positions.

The 12 frequent group OTUs accounted for nearly half of all incidences (272/547 incidences, Table 3.2). The infrequent group, which consisted of the remaining 104 OTUs, accounted for slightly more than half of all incidences (275/547 incidences, Table 3.2). This skewed distribution of OTU incidence explains the moderately high value (1.6, with a value of 2 being considered high) of the coefficient of variation of the dataset (Table 3.2).

The total richness of the actual community was estimated by the various models to be between 130 and 365 OTUs (Fig. 3.11). The end point of the sample-based rarefaction curve fell within the lower end of this range at approximately 160 OTUs (Fig. 3.3). The majority of these estimated additional OTUs would likely be rarely detected in the dataset because the other diversity metric curves level off.

A total of 50 of the OTUs detected in the groups of samples from sheared and intact margins were shared between these two categories, including all of the OTUs in the frequent group (Table 3.3). This was more than half of the total number of OTUs detected in each category. The group of samples from the intact margins had slightly higher total richness than the group of samples from sheared margins. However, the samples from these groups did not have significantly different OTU richness (Fig. 3.15).

The groups of samples from Dragon and Horseshoe Islands shared more than half of the total OTUs detected on each island, but the samples from Stingray Island shared slightly less

than half of the detected OTUs with the other islands (Table 3.4). the samples from Stingray Island also had a slightly higher total richness than the other two islands. The samples from Dragon Island were shown to have significantly lower richness than the samples from the other two islands (Fig. 3.15) which may have been caused by low richness samples from this island, especially from the Low and MidLow positions.

The groups of samples from the different elevation positions shared more than half of the total OTUs, excluding the Low and MidLow positions which shared less OTUs with the other elevation positions (Table 3.5). The Low and MidLow positions had lower OTU totals than the Mid, MidHigh, and High positions, with the High position having the highest total number of OTUs. Both the Low and MidLow positions were missing one of the frequent groups OTUs. For the Low position, this was the hydrozoan *Helgicirrho cari* while for the MidLow position, the missing OTU was the annelid *Marionina coatesae* (Table 3.6).

The richness-based beta diversity indices (Jaccard and Sørensen) in this dataset showed an interesting pattern, where the estimated index value was lower than the empirical value (Table 3.9). These lower estimates indicate that if more samples were taken or better coverage was achieved, more OTUs unique to each of the sheared and intact communities should be detected. This would decrease the number of shared OTUs compared to the total, and therefore reduce the value of the richness-based indices. However, because the incidence-based estimated indices (Horn, Morisita-Horn, and Regional overlap) showed higher values than the empirical indices, an increase sampling or coverage would show an increase in the similarity of the patterns of incidence. In other words, increased sampling would increase richness (including adding additional unique OTUs to each group), but also increase the incidence of the OTUs which were already observed in both groups, leading to higher incidence-based similarity, but lower richness-based similarity. This was not the case for chapter 2, where both the richness and incidence-based similarity indices had higher estimated values than empirical values (Table 2.16). The difference between chapters may indicate a need for additional sample collection if using the sample processing methods used here.

When the OTUs were broken down by phylum assignment, Arthropod OTUs were the both the most commonly detected OTUs (25.5% of all incidences, Fig. 3.13) and the most numerous OTUs (38.1% of all OTUs, Fig. 3.14) in the dataset. The next most commonly detected group of OTUs was the Annelida (19.8% of incidences), followed by the Nematoda (18.2%), Platyhelminthes (10.4%), and Mollusca (9.9%). Finally, the Gastrotricha (2.9% of incidences), Rotifera (2.7%), Bryozoa (2.5%), Kinorhyncha (1.6%), Nemertea (0.4%), an uncultured marine eukaryote (0.4%), Anthozoa (0.2%), and Xenocoelomorpha (0.2%) were rarely detected in the dataset. Annelida and Nematoda also followed Arthropoda in total number of OTUs (each making up 13.6% of the total number of OTUs), with Platyhelminthes (9.9%), Hydrozoa (5.1%), Rotifera (5.1%), and Mollusca (4.2%) following the annelids and nematodes. Bryozoa (2.5% of the total number of OTUs), Gastrotricha (2.5%), Nemertea (1.7%), Kinorhyncha (1.7%),

Anthozoa (0.8%), Xenocoelomorpha (0.8%), and an uncultured marine eukaryote (0.8%) each accounted for a very small number of the OTUs in the dataset.

Arthropod OTUs in this dataset were a larger proportion of incidences (25.5% of incidences, Fig. 3.13) than in the dataset from chapter 2 (14.3%, Fig. 2.14). The arthropod OTUs in the dataset included two members of the frequent group of OTUs, which were assigned as a member of the insect order Diptera (SILVA: *Haematopota pluvialis*, GenBank: *Haematopota pluvialis*, 37.7% of samples) and a member of the mite order Trombidiformes (SILVA: *Acarothrix* sp., GenBank: *Acarothrix*, 24.6%, Table 3.6), respectively. The tabanid horse fly *H. pluvialis* is not found in North America, but there are several species of tabanid horse fly known to native to Louisiana marshes, including the species *Tabanus nigrovittatus*, *T. hinellus*, , and *T. acutus* (Wilson 1963, Tidwell 1970). Though four Diptera OTUs were detected in the dataset of chapter 2, none were frequently detected and only one was a match for the family Tabanidae (assigned as *Chrysops niger*, Table 2.15). Eleven other OTUs were assigned to the Diptera in this dataset (Table 3.6), making the Diptera the largest group of OTUs within the arthropod OTUs, but none of the 11 other Diptera OTUs were detected in more than 2 samples. The mite genus *Acarothrix* falls within the family Halacaridae, which is a group of marine mites consisting of over 1000 species. The mites of this genus are found in brackish and marine benthic; representatives of the Halacaridae are found all over the world at all marine depths (Bartsch 2002). This mite OTU was detected primarily in samples from sheared margins (12 detections in sheared margins, 3 in intact margins). In addition, this OTU was primarily detected in samples from Dragon Island (10 detections on Dragon Island, 2 in Horseshoe, 3 in Stingray). Seven copepod OTUs were detected in the dataset, including 3 harpacticoids and 4 calanoids. This is in contrast to the dataset of chapter 2, where only 2 copepods were detected. Copepods are commonly collected meiofauna, and previous traditional studies of meiofauna in the area collected more than eight species of copepod on average in samples (Fleeger et al. 2018). Therefore, if copepods and other arthropods are a taxon of interest, processing samples to separate meiofauna should be made a priority.

The annelids were the second most detected group in this dataset with 19.8% of incidences which is similar to the detection rate for annelids in the dataset of chapter 2 (16.9% of incidences). Three annelid OTUs were members of the frequent group in this dataset, these were assigned in the SILVA database as an ambiguous member of the order Spionida (GenBank: *Polydora lingshuiensis*, 45.9% of samples, Table 3.6), as *Alitta succinea* (GenBank: *Alitta succinea* 39.3%, Table 3.6), and as *Marionina coatesae*, (GenBank: *Marionina coatesae*, 24.6%, Table 3.6). The polychaetes in the genus *Polydora* burrow into a wide variety of substrates, from soft muds to oyster shells. An OTU which matched to a *Polydora* species was also a member of the frequent group in chapter 2. The polychaete *A. succinea* is a macrofaunal, free living worm which preys on a variety of meiofauna groups. The oligochaetes in the genus *Marionina* are known to inhabit stems of *Spartina* plants in marshes in North America, and like most oligochaetes they lack a planktonic larva (Healy and Walters 1994) . The OTU which was assigned to *M. coatesae* was primarily detected in samples from intact margins (1 time in

sheared margins, 14 times in intact margins, Table 3.6) these annelids are known to inhabit plant stems. In addition, the majority of the incidences of annelid OTUs were in intact margins (34 incidences in sheared, 76 in intact, Table 3.6). The annelid OTUs were also more commonly detected in Horseshoe Island than in either of the other two islands (50 incidences in Horseshoe, 23 in Dragon, and 37 in Stingray, Table 3.6).

Nematode OTUs were the third most commonly detected group of metazoan OTUs. Though nematode OTUs were commonly detected in this dataset (18% of all incidences, Fig 3.13), their relative presence in this dataset was reduced from the dataset from chapter 2, where they were the most common group (28.2% of all incidences, Fig. 2.14). However, the most commonly detected OTU in the dataset (present in 77% of samples) was a nematode assigned as an ambiguous member of the order Enoplida (GenBank: *Adoncholaimus* sp., Table 3.6). Members of the genus *Adoncholaimus* are predators of other meiofauna (Hodda 2011). The only other nematode OTU which was included in the frequent group of OTUs was assigned to an uncultured eukaryote also belonging to the order Enoplida (GenBank: Uncultured eukaryote clone). The remainder of the nematodes in the dataset were either microbivores (4/16 OTUs), plant root or algal feeders (4/16 OTUs), predators (2/16 OTUs) or did not receive a specific enough assignment to determine likely feeding mode (4/16 OTUs). Nematode OTUs were most commonly detected on Stingray Island (41 detections, 29 on Dragon Island, 31 on Horseshoe), but this trend was not observed in chapter 2 (Table 2.13). In addition, nematodes were detected less often in the Low and MidLow positions than in the other positions (Table 3.6).

Platyhelminthes were the fourth most commonly detected group in the dataset. This group was much more commonly detected in the dataset (10% of incidences, Fig. 3.13) for this chapter than in the chapter 2 (3% of incidences, Fig. 2.14). The sample processing increased the amount of Platyhelminthes (whether whole or partial organisms) in the material which would be extracted. All of the OTUs which were assigned to the phylum Platyhelminthes were assigned to groups which are free-living. One of these OTUs was included in the frequent group and was assigned as a member of the order Lecithoepitheliata (GenBank: Uncultured eukaryote clone). This order of non-parasitic flatworms are found in both freshwater and marine sediments (Schockaert et al. 2008). This OTU was detected twice as often in samples from intact margins than in sheared margins (12 in sheared margins, 25 in intact) and was detected less often in samples from Dragon Island (7 in Dragon, 12 in Horseshoe, 18 in Stingray). Platyhelminthes in general were detected less often in the Low and MidLow position samples than in the MidHigh and High position samples (Table 3.6). The marine non-parasitic flatworms have been poorly studied even among meiofauna in the past due to their soft bodied nature but are recognized as important members of meiofaunal communities, acting as both algal grazers and predators of other meiofauna (Martens and Schockaert 1986, Boaden 1995). The advent of genetic methods such as metabarcoding makes this group much more accessible to ecologists and may be more diverse than previously indicated using traditional meiofaunal extraction methods (Mitsi et al. 2019). Fleeger et al (2015) previously did not collect members

of the Platyhelminthes in this study area, likely due to the preservation, sampling, or processing methods used. If collection of the Platyhelminthes is a priority, then DNA extraction from processed sediment material is highly recommended.

Mollusca were the fifth most commonly detected group in the dataset at 9.8% of all incidences (Fig 3.13) which is slightly lower than the incidence of mollusks in the dataset of chapter 2 at 12.7% of all incidences (Fig 2.14). Two mollusk OTUs were members of the frequent group of OTUs, these were assigned to the mussel *Brachidontes rodriguezii* (GenBank: *Brachidontes mutabilis*) and to an ambiguous member of the gastropod subclass Neritimorpha (GenBank: *Theodoxus fluviatilis*, Table 3.6). The OTU matching to *B. rodriguezii* is likely one of the mussels which inhabit Louisiana marshes, such as a species from the genus *Geukensia*, which was one of the frequent OTUs in chapter 2. Members of the Neritimorpha are not common to Louisiana marshes, but several other snails do occur, including the marsh periwinkle *Littoraria irrorata*, the pulmonate gastropod *Melampus bidentatus*, and members of the family Hydrobiidae (Kneib 1984).

The Hydrozoa were the sixth most commonly detected phylum in the dataset. The incidence of hydrozoans in the dataset in this chapter (5.4%, Fig 3.13) was similar to but slightly lower than that of chapter 2 (7.9%, Fig 2.14). However, in chapter 2 hydrozoans were more frequently detected in samples from sheared margins, while they were evenly distributed across both margin types in this dataset. A single OTU from this group was a member of the frequent group, this OTU was assigned as the hydrozoan *Helgicirra cari* (GenBank: *Helgicirra cari*, Table 3.6). This hydrozoan was also a member of the frequent group of OTUs in chapter 2. In both chapters, this OTU was not detected in any samples from Stingray Island, and in this chapter, it was not detected at the Low elevation position.

Gastrotricha were the seventh most commonly detected group of OTUs in the dataset, with 2.9% of all incidences (Fig. 3.13). This was similar to the incidence of gastrotrichs in chapter 2 (3.7%, Fig 2.14). One OTU assigned to this phylum was a member of the frequent group. This OTU was assigned as a member of the genus *Heterolepidoderma* (GenBank: *Heterolepidoderma* sp.), which was also the only gastrotrich member of the frequent group in chapter 2. Gastrotrich OTUs were detected twice as often in sheared margins than in intact samples and twice as often in Dragon Island samples than in samples from the other islands. This was almost entirely due to the *Heterolepidoderma* OTU, because the other two Gastrotrich OTUs were only detected one time each.

Many of the frequent group OTUs were the same or very similar for both this chapter and chapter 2 (Table 2.13, Table 3.6). The most common OTU in both chapters was assigned to a nematode in the order Enoplida, though these OTUs received a different assignment in both chapters (*Thoracostoma trachygaster* in chapter 2, *Adoncholaimus* sp. in this chapter). The most common mollusk OTU in both chapters was assigned as a member of the Mytiloida, likely a species of the genus *Geukensia*. In addition, the second most common mollusk OTU in both chapters received a GenBank assignment of *Theodoxus fluviatilis*, a member of the

Neritimorpha. The two most common annelids in both chapters were assigned as a *Polydora* sp. and as *Alitta succinea*. The most common gastrotrich OTU in both chapters was assigned to *Heterolepidoderma* sp., while the most common hydrozoan OTU was *Helgicirrha cari* in both chapters. From here, however, the frequent group in the two chapters were somewhat different. This chapter had a single member of the Platyhelminthes in the frequent group (uncultured Lecithoepitheliata), while chapter 2 had no members of the Platyhelminthes in the frequent group. Platyhelminthes were more commonly detected in general, so clearly the sample processing improved collection of these organisms, which are more rarely collected in traditional studies (Martens and Schockaert 1986, Leasi et al. 2018). The arthropod OTUs in chapter 2 consisted of a harpacticoid copepod and a member of the Isoptera, while in this chapter the frequent group arthropod OTUs were assigned to the horse fly *Haematopota pluvialis* and a mite in the genus *Acarothrix*. The termite is potentially a subterranean species, but the other arthropods likely reside at the surface. In chapter 2, 6 of the 18 frequent group OTUs were nematodes, while in this chapter, only 2 of the 12 frequent group OTUs were nematodes. A single rotifer was in the frequent group in chapter 2 (a member of the subclass Adinetida) but no rotifers were present in the frequent group in this chapter. Potentially, rotifers and nematodes may have been washed from the sample at a greater rate than other organisms due to their small size, even for meiofauna. Clearly the methods employed in these two chapters have a large amount of overlap in terms of the taxa detected, but are distinct enough to be complementary to each other.

The samples from sheared and intact margins had similar values for both richness and Faith's PD (Fig. 3.15, Fig. 3.16). Approximately 60% of the OTUs in the samples from sheared and intact margins were shared between both margin types (Table 3.4). All of the frequent group OTUs were detected in samples from both sheared and intact margins. The samples from sheared and intact margins showed high similarity (>0.5) in all indices excluding Jaccard, which always returns a lower value (Table 3.9). The NMDS ordination showed a high degree of overlap between the groups of samples from sheared and intact margins (Fig. 3.17). However, the Adonis test indicated that significant differences in community composition were present between the samples from intact and sheared margins; the margin factor explained only a small proportion of the variation in the dataset (Table 3.12). This result was similar to the results from chapter 2, where overall similarity was high due to the most common OTUs being shared between the sheared and intact margins, but a group of less common OTUs was unique to each group. In addition, when the samples from different islands were tested separately relative to margin type, the Dragon Island samples were the only group which showed significant differences between samples from sheared and intact margins (Table 3.13). This means that the majority of the differences between the sheared and intact margins were represented on Dragon Island. The most common OTU in the dataset (Enoplida; ambiguous taxa) did not contribute much to the differentiation of samples because it appeared in most samples. Of the frequent group OTUs, the ones which likely impacted the Sørensen index values the most were assigned to Lecithoepitheliata (Platyhelminthes), *Acarothrix* sp. (Arthropoda), *Marionina*

coatesae (Annelida), and *Heterolepidoderma* sp. (Gastrotricha). These OTUs appeared in more samples of one margin type than the other. The Lecithoepitheliata OTU appeared in 25 intact margin samples but only 12 sheared margin samples, while the *M. coatesae* OTU appeared in 14 intact margin samples but only a single sheared margin sample. The *Acarothrix* sp. OTU appeared in 12 sheared margin samples and 3 intact margin samples. The *Heterolepidoderma* sp. appeared in 10 sheared margin samples but only 4 intact margin samples. Samples from sheared margins had 31 unique OTUs, while samples from intact margins had 35 unique OTUs, which were all members of the infrequent group. The group of OTUs which were unique to samples from intact margins and were detected more than once were assigned as *Ptycholaimellus* sp. (Nematoda, Chromadorida), *Tanais dulongii* (Arthropoda, Tanaidacea), *Orchesella cincta* (Arthropoda, Collembola), *Rotaria sordida* (Rotifera, Bdelloidea), *Centropages furcatus* (Arthropoda, Calanoida), *Marionina tumulicola* (Annelida, Enchytraeida), an ambiguous member of the Haplotaxida (Annelida), and *Macrostomum clavituba* (Platyhelminthes, Macrostomorpha). Nematodes in the genus *Ptycholaimellus* are microbivores (Hodda 2011). Tanaid amphipods were one of the groups which had not recovered in previously heavily oiled sites in the study area (Fleeger et al. 2018), potentially indicating a more normal marsh community in the intact margins. Oligochaete annelids show reduction in population densities in sites which had marsh plants removed (Whitcraft and Levin 2007), and certain oligochaetes (especially those in the genus *Marionina*) have shown association with the microhabitats within *Spartina* stems (Healy and Walters 1994). Oligochaete annelids tend to lack pelagic larval stages, limiting their distribution throughout the marsh habitat. The group of OTUs which were unique to samples from sheared margins and were detected more than once were assigned as *Testudinella clypeata* (Rotifera, Flosculariaceae), *Helicotylenchus digitiformis* (Nematoda, Rhabditida), *Plagiostomum ochroleucum* (Platyhelminthes, Prolecithophora), *Pycnophyes robustus* (Kinorhyncha, Allomalorhagida), and an uncultured marine eukaryote. The genus *Pycnophyes* is known from offshore samples in the Gulf of Mexico, which may indicate a more benthic community in the sheared margins. Notably, there were no annelids within the group of OTUs which were unique to the sheared margin samples. This was likely because annelid OTUs were less frequently detected in samples from sheared margins (Table 3.6). The OTUs which were most enriched in the sheared margins were assigned to *Acarothrix* sp. (Arthropoda) and a member of the nematode genus *Adoncholaimus*, while the OTUs which were most enriched in intact margins were assigned to *Marionina coatesae* (Annelida) and an uncultured member of the nematode order Enoplida. The most important taxa to focus on for the differences between the sheared and intact margins appears to be the annelids, because they were more commonly detected in the intact margins, they had more unique OTUs in the intact margins than in sheared, and certain OTUs were more associated with the intact than the sheared. This is likely because the oligochaetes in this chapter made up a larger proportion of the annelid OTUs (50% compared to 35% in chapter 2). Oligochaetes lack a pelagic stage, potentially making them less suited to benthic habitats than other taxa, and the *Marionina* species are especially associated with plants, making them less likely to appear in sheared margins.

The samples from the Dragon Island were found to have lower richness than the samples from the other islands. Between 44 and 54% of the OTUs were shared between each of the groups of samples from each island, with 25 of the total OTUs being shared between all islands (Table 3.4). Overall similarity was high between the samples from the different islands in all indices excluding the Jaccard index (Table 3.9). The lowest pairwise Sørensen index values were observed between samples from Stingray and Horseshoe Island (Table 3.10). In contrast to the Chapter 2 dataset, the Dragon and Stingray Islands had the lowest pairwise similarity index (Table 2.17). The NMDS ordination showed a much wider dispersion in composition in Dragon Island samples than in samples from the other two islands (Fig. 3.18). The Adonis test indicated that significant differences in community composition were present between the groups of samples from different islands (Table 3.12), though this factor only explains a small proportion of the variation in the dataset. The frequent group OTUs which showed the most variation over the three islands included *Helgicirrha cari* (Hydrozoa), a member of the order Lecithoepitheliata (Platyhelminthes), *Alitta succinea* (Annelida), *Haematopota pluvialis* (Arthropoda), and *Acarothrix* sp. (Arthropoda, Table 3.6). The platyhelminth was detected 12 and 18 times in Horseshoe and Stingray Island samples respectively, but only 7 times in Dragon Island samples. The polychaete *A. succinea* was detected 14 times in Horseshoe Island samples, but only 4 and 6 times in Dragon and Stingray Island samples, respectively. The dipteran *H. pluvialis* was detected 12 times on Stingray Island but only 4 and 7 times on Dragon and Horseshoe Islands, respectively. The mite *Acarothrix* sp. was detected 10 times on Dragon Island but only 2 and 3 times on Horseshoe and Stingray Islands. Finally, the hydrozoan *H. cari* was never detected on Stingray Island. Samples from Stingray Island contained the most unique OTUs at 30, while Horseshoe had 17 and Dragon had 15. The majority of the OTUs unique to Stingray Island were arthropods (16/30 OTUs). The OTUs which were unique to Stingray Island and were detected more than once were assigned to an ambiguous member of the Isoptera (Arthropoda), a member of the order Dorylamida (Nematoda), *Marionina tumulicola* (Annelida), *Corynoptera saetistyla* (Arthropoda, Diptera), an ambiguous member of the Leptothecata (Hydrozoa), and *Helicotylenchus digitiformis* (Nematoda). The OTUs which were unique to Horseshoe Island and were detected more than once were assigned to *Marionina tumulicola* (Annelida, a different OTU than the one unique to Stingray Island samples) and an ambiguous member of the Haplotaxida (Annelida). The only OTU which was unique to Dragon Island and was detected more than once was assigned to *Pycnophyes robustus* (Kinorhyncha). The OTUs which were most enriched in the Horseshoe Island samples (compared to Dragon Island samples) were assigned to *Marionina coatesae* (Annelida), the polychaete *Polydora lingshuiensis* (Annelida), and a member of the genus *Adoncholaimus* (Nematoda, Table 3.16). The OTUs which were most enriched in the Stingray Island samples (compared to Dragon Island samples) were assigned to *H. pluvialis* (Arthropoda), *M. coatesae* (Annelida), and the polychaete *Polydora lingshuiensis* (Annelida, Table 3.16). The OTUs which were most enriched in Dragon Island samples (compared to Horseshoe and Stingray) were assigned to *H. cari* (Hydrozoa), the nerite *Theodoxus fluviatilis* (Mollusca), and *Acarothrix* sp. (Arthropoda, Table 3.16).

In chapter 2, patterns of the location of selected OTUs were discussed with comparisons including annelids from the family Naididae and the sabellid polychaete *M. aestuarina*. The Naididae OTUs were detected on Horseshoe and Stingray Islands, while *M. aestuarina* OTUs were detected on Dragon and Horseshoe Islands (Table 2.15). However, in the floated samples, the Naididae and *M. aestuarina* OTUs were detected on all islands, both margin types, and all elevation positions, excluding *M. aestuarina* in the Low position samples. In addition, the OTU assigned as *M. aestuarina* did not fall into the frequent group in this chapter compared chapter 2, but was detected in exactly 10 samples while the frequent group was the group of OTUs detected in more than 10 sample. The loss of a pattern of detection may mean that the effort expended in generating the dataset from chapter 2 did not capture the entirety of OTUs present in all samples. Differences in sample processing such as the size filtering of organisms for this chapter influenced the difference in composition of detected organisms when compared to chapter 2, although it is not clear how the flotation method would affect partial organisms (environmental DNA) in the samples. Furthermore,, the samples from this chapter were extracted in the organic portion of a larger volume of sample indicating that the patchy small-scale variation of meiofauna may be better accounted for in this chapter than in chapter 2.

In this chapter, none of the interactions of the factors (margin, island, and position) were significantly different according to the Adonis test (Table 3.12). In chapter 2, the interaction of margin and island, the interaction of island and elevation, and the interaction of all three factors were all significant, though each of these had low R^2 values (Table 2.19). The samples from the different margin types on Dragon Island were significantly different from each other, but there were no significant differences between margin type or elevation positions for the other two islands. Although the majority of the detectable differences in composition between the samples from sheared and intact margins were present in Dragon Island samples for this chapter, there were significant differences between margin, elevation position, and the interaction of those two factors for Stingray Island in chapter 2 (Table 2.22). The NMDS ordination for the separate groups of samples from sheared and intact samples on Dragon Island did overlap (Fig. 3.19), but the centroids were separated. Values of the alpha diversity metrics between the samples from different islands, margins, and elevations were not significantly different, though they could vary considerably between the different elevation positions (Fig. 3.15, Fig. 3.16). in comparison of the sheared or intact margins on Dragon Island, the frequent group OTUs which were absent from the sheared margins were assigned as an ambiguous member of the Lecithoepitheliata (Platyhelminthes), *Marionina coatesae* (Annelida), and an ambiguous member of the Enoplida (Nematoda). The only frequent group OTU which was missing from the intact margins of Dragon Island was an ambiguous member of the Neritimorpha (Mollusca), but the OTUs which matched to a member of the genus *Acarothrix* (Arthropoda) and the genus *Heterolepidoderma* (Gastrotricha) were more commonly detected in sheared than intact margins (8 sheared margin samples to 2 intact margin samples, 6 sheared

to 1 intact, respectively). These are some of the same OTUs for which their occurrence likely drives the differences in the overall dataset.

This dataset could potentially hold additional insights for future research if the full dataset, including the non-metazoan eukaryotes, was reexamined. As databases improve, new taxa could be identified in this dataset, potentially leading to new conclusions about the state of biodiversity in the shared and intact marsh margins of Bay Jimmy. This dataset also could be used for comparisons in future studies of the impacts of hurricanes on previously oiled marshes. If a long-term study on meiofauna in sheared margins was initiated, insights about how marsh meiofauna communities change as sheared margins erode and become open water could be gained. Longitudinal studies could track which taxa are outcompeted by benthic fauna and are lost from the community, as well as tracking which taxa invade from the surrounding benthos and become established. The role of metabarcoding in future long term environmental monitoring should be important given the limited and shrinking number of authorities on metazoan taxonomy (Creer et al. 2016).

Chapter 4. A Comparison of Intertidal Metazoan Biodiversity among Three Different Salinity Zones and Two Different Bays in the Marshes of Louisiana

4.1. Introduction

Salt marshes are highly productive coastal ecosystems found primarily in temperate zones across the world, located between marine and terrestrial ecosystems (Odum 1971, Mcowen et al. 2017). These marshes provide a number of ecosystem services which are valuable to humans, including coastal protection from storms, carbon sequestration, and denitrification (Barbier et al. 2011). These habitats also act as nurseries for commercially and recreationally important species (Zimmerman et al. 2002, Engle 2011).

However, salt marshes across the globe are in decline due to a variety of factors (Barbier et al. 2011). Depending on the individual marsh habitat, these detrimental factors may include storm damage, pollution, subsidence, relative sea level rise, the encroachment of human structures or agriculture, or human modifications which limit the ability of the marsh to vertically accrete (Kennish 2001, Gedan et al. 2009, Crosby et al. 2016). Vertical accretion is the primary mechanism that keeps marshes above permanent flooding due to relative sea level rise (DeLaune et al. 2003, Jankowski et al. 2017).

More than half of the land area of marshes in North America has been lost over the past century (Kennish 2001), for example, the marshes of Louisiana have lost an area the size of the state of Delaware since 1932 (Couvillion et al. 2017). The marshes of Louisiana were initially built by yearly flooding of the Mississippi River over thousands of years (Russell 1940). However, flood control structures now prevent these floods, and the sediments which they contain, from reaching the marshes which limits the ability of marshes to accrete via sediment. The primary manner in which these marshes accrete vertically is through plant growth and the deposition of organic matter (Turner et al. 2005). The low density soils of coastal marshes may consist of only 5-15% sediment and organic matter, with the remainder of the soil volume made up of pore water and trapped gasses (Nyman et al. 1990). Because these soils are low density, they compact readily, leading to subsidence. In some areas of Louisiana marsh, subsidence may exceed 1 cm per year, which is among the highest rates of subsidence along the Gulf Coast (Penland and Ramsey 1990). Subsidence can lead to plant drowning and associated losses in marsh area (Day et al. 2000, DeLaune et al. 2003, Yuill et al. 2009). In addition, erosion may cause losses in plants by undercutting bank areas and increasing plant stresses (Nyman et al. 1994). Disturbances, such as hurricanes or oil spills can also be drivers of plant death and marsh loss (Palaseanu-Lovejoy et al. 2013, Rabalais and Turner 2016).

Numerous solutions have been proposed to counteract the alarming rate of loss of Louisiana marshes. Many of these proposals have been combined by the Coastal Resource Management Agency into the Louisiana Coastal Master Plan, a comprehensive plan outlining coastal restoration projects through the next half century (CPRA 2012, 2017, Peyronnin et al.

2013). This plan includes 79 restoration projects, 13 structural protection projects, and 32 nonstructural risk reduction projects across the coast of Louisiana. Included in these projects are several sediment diversions planned to divert flow from the Mississippi River into the marshes, restoring sediment and freshwater inputs and reducing saltwater intrusion into historically freshwater marshes (Zhang et al. 2012, Nyman 2014, Elsey-Quirk et al. 2019). The first of these major sediment diversions is the Mid-Barataria Sediment Diversion, which is currently slated to begin construction in 2022, following environmental impact studies and the permitting process. Because salinity is one of the dominant environmental variables in salt marshes, restoring freshwater inputs will have an effect on the distributions of organisms, especially marsh plants like the *Spartina* species which dominate brackish and salt marshes in Louisiana (Elsey-Quirk et al. 2019). When salt tolerant plant species are exposed to freshwater conditions, they can be outcompeted by plants which are less salt tolerant, resulting in changes in ecosystem dynamics (Greiner La Peyre et al. 2001, Elsey-Quirk et al. 2019). Changes in salt marsh plant communities due to competition may take a period of 2-3 years before the outcomes are fully observable (Bertness 1991b). Potentially, changes in invertebrate communities could provide more rapid information on the changes caused by salinity shifts when compared to plant communities; therefore, meiofauna taxa were selected for this study.

Meiofauna are sediment-dwelling taxa which are united by a size range from 500 to 45 μm (Giere 2009). This group acts as a linkage between microbe and macrofauna food webs and between benthic and pelagic food webs (Coull 1999). This group of organisms shows responses of both diversity and abundance of major taxa to changes in environmental variables, including salinity (Montagna et al. 2002, Cai et al. 2012, Ngo et al. 2013, Zeppilli et al. 2015). The intergenerational time of many groups of meiofauna is quite short, with multiple generations per year, meaning that the response to environmental changes is more rapid than other groups (Warwick 1981, Kennedy and Jacoby 1999). Studies of meiofauna in Louisiana estuaries have tended to focus on pollution effects (Fleeger and Chandler 1983, Fleeger et al. 2007, 2015, 2018) especially in the wake of the Deepwater Horizon oil spill, but colonization and field manipulation studies also have been conducted (Fleeger et al. 1981, Chandler and Fleeger 1983, Fleeger 1985).

While meiofauna have been studied both in Louisiana estuaries and with regards to salinity all over the world, studies tend to identify meiofauna to major taxonomic groups such as nematodes, harpacticoid copepods, oligochaetes, etc. (Kennedy and Jacoby 1999). This is largely due to the effort and technical experience required to identify meiofauna to the species level. Traditional studies of meiofauna also are limited in their capture of certain groups, especially the smaller, soft bodied organisms such as the Platyhelminthes, Rotifera, and Gastrotricha, due to sampling bias and preservation issues (Kennedy and Jacoby 1999, Carugati et al. 2015, Leasi et al. 2018). Some studies on meiofauna are now using metabarcoding methods for rapid, cost effective identification of meiofauna over traditional methods (Bik et al. 2012, Brannock and Halanych 2015, Creer et al. 2016).

Metabarcoding is the use of DNA sequences from previously identified organisms to assign taxonomic information to sequenced DNA from environmental samples. Generally, these sequences are short sections of DNA which contain both highly conserved and variable sequences, often referred to as marker genes. A number of these marker genes have been proposed with specificity for different groups, but this study uses a sequence from the 18S small ribosomal subunit gene which selects for eukaryotes (Creer et al. 2016, Jacquioud et al. 2016). Other marker genes which also select for eukaryotes, such as the COI gene, may not be appropriate for a widely taxonomically diverse group such as meiofauna (Deagle et al. 2014, Collins et al. 2019). Metabarcoding techniques reduce the need for time consuming advanced microscopy techniques and allow for the rapid study of large numbers of samples.

This study was designed to provide baseline data for what the changes in meiofaunal communities caused by diversion projects might be by using extant communities in different salinity zones and bays in Louisiana marshes. These communities were selected from multiple salinity zones in two areas in Louisiana marshes, Barataria Bay and Caillou Bay. Before the construction of manmade flood control structures, Barataria Bay was connected to the Mississippi River by annual flood pulses. However, Barataria Bay is now largely cut off from river inputs and has lost 1,120 km² of land area since 1932 (Couvillion et al. 2017). Meanwhile, Caillou Bay is situated closer to the mouth of the Atchafalaya River, which captures a portion of the flow of the Mississippi River and has contributed to the creation of new land since the 1970s in the Wax Lake Delta (Couvillion et al. 2017). These sites were initially selected for the collection of baseline insect community data across the salinity zones in these marshes (Aker 2020). The purpose of this study was to examine meiofaunal community diversity at different salinity zones in different Louisiana estuaries with the primary intention of generating baseline data for comparison of future salinity changes within these salinity zones due to proposed freshwater and sediment diversions.

4.2. Materials and Methods

Site determination:

Sampling sites were selected from two major Louisiana estuaries: Caillou Bay and Barataria Bay. Caillou Bay is to the southwest of the mouth of the Atchafalaya River, and Barataria Bay is to the east of the mouth of the Mississippi River. Three salinity zones (low, mid, and high) for each bay were determined using monthly salinity data from 2014 until the end of 2017 from six different Coastal Reference Monitoring Stations (CRMS, <http://cims.coastal.louisiana.gov>). Data were analyzed using a Welch test ($F_{(5, 126.26)} = 61.99$, $p < 2.2e^{-16}$) and multiple t tests with corrections for multiple testing (Fig. 4.1). The results of this test showed significant differences between low, mid and high salinity zones but no differences between zones of the same category between bays. Each area also was checked against Deepwater Horizon oil landing data from the Environmental Response Management Application (<https://erma.noaa.gov/gulfofmexico/>) to ensure no oiling had been observed at collection sites. Within each zone in each bay, three replicate sites were selected by

accessibility and proximity to the CRMS station used to determine local salinity. The sites in Barataria Bay were also selected for proximity to the proposed Mid-Barataria Sediment Diversion project.

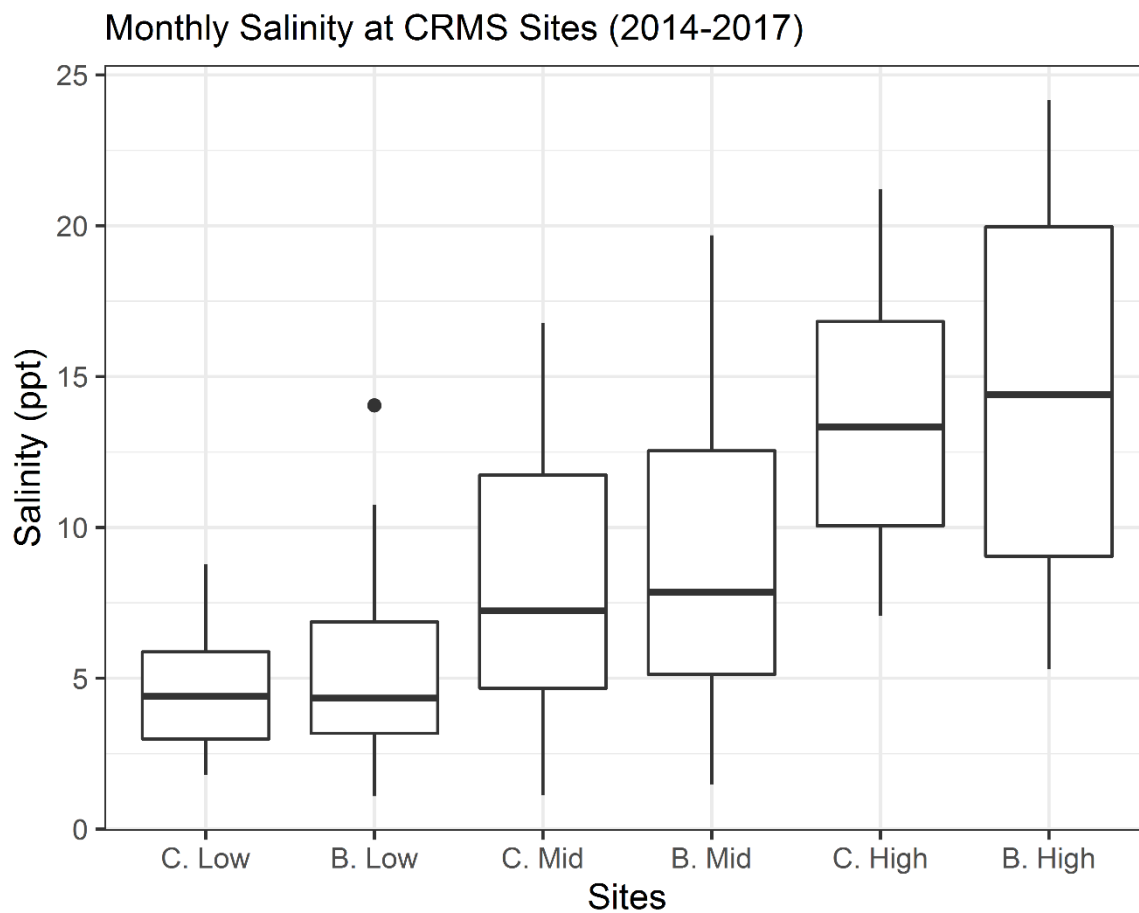


Fig. 4.1. Average monthly salinity recorded at CRMS sites in Barataria and Caillou Bays over the four years prior to the initiation of the study. Figure adapted from Aker (2020).

Sample collection:

One sample transect was collected at each of the three replicate sites in each salinity zone in each bay, for a total of 18 transects. Each transect consisted of 4 soil samples, taken at 0, 1, 5, and 10 m into the marsh, resulting in 72 individual samples. The starting point of transects (0m into the marsh) was defined as the edge of the marsh, where the outermost plants begin to appear. Soil samples were collected using a Barrett coring device with removable 10.16 cm diameter x 30.48 cm long cylindrical acrylic cores (Perret and Barrett 1971). Once the soil sample was collected, it was immediately capped and placed into a cooler with ice for transport. Soil cores were stored in a -20°C freezer upon return from the marsh sites until processing.

Soil chemistry and analysis:

Each of the samples collected 5 and 10m from the marsh edge were selected for chemistry analysis. Half of the collected soil volume of each of these 36 samples was submitted to the LSU Agcenter Soil Testing and Plant Analysis lab for testing. Analyses conducted were Carbon (%), Nitrogen (%), Percent Organic Matter (%), Aluminum (ppm), Boron (ppm), Calcium (ppm), Chloride (ppm), Conductivity (dS/m), Copper (ppm), Iron (ppm), Magnesium (ppm), Manganese (ppm), pH, Phosphorus (ppm), Potassium (ppm), Salts (ppm), Sodium (ppm), Sodium Adsorption Ratio (SAR), Sulfur (ppm), and Zinc (ppm). Additionally, carbon/nitrogen (C/N) ratios were determined by dividing values for carbon (%) were divided by values for nitrogen (%) for each sample. Inductively coupled plasma optical emission spectroscopy was used to determine the values for Aluminum, Boron, Calcium, Chloride, Copper, Iron, Magnesium, Manganese, Phosphorus, Potassium, Sodium, SAR, Sulfur, and Zinc (Baker and Amacher 1982, Barnhisel and Bertsch 1982, Bingham 1982, Rhoades 1982, Mehlich 1984). A pH meter and electrode were used to determine pH values (McClean 1982). A conductivity probe was used to analyze soluble salts present in the samples (Rhoades 1982). A dip probe colorimeter was used to determine the amount of organic matter in the samples (Nelson and Sommers 1982). A LECO CN Analyzer using the Dumas Dry-Combustion method was used to analyze the amount of carbon and nitrogen in the samples. Full descriptions of all tests are available at

https://www.lsuagcenter.com/portals/our_offices/departments/spess/servicelabs/soil_testing_lab/procedures/procedures-used-at-the-laboratory. All soil chemistry data were tested for significant differences across the salinity zones, the different bays, and the different distances from the marsh edge using a standard ANOVA in the aov function in the stats package in R (Chambers et al. 1992). The TukeyHSD method in R, which computes Tukey's Honest Significant Differences (Miller 1981, Yandell 1997), was used to perform post hoc testing on all analyses.

Sample processing:

Frozen soil cores were removed from the acrylic cores and an approximately 5 cm³ section was cut from each core using a handsaw. All tools were cleaned in a 10% bleach solution in between samples to prevent cross contamination. The cut sections were thawed in 95% ethanol in a 4°C refrigerator, then drained and rinsed through a 500 µm sieve onto a 45 µm sieve. The portion of the sample retained on the 500 µm sieve was reserved and placed in 95% ethanol at -20°C as voucher material. The portion of the sample retained on the 45 µm sieve was placed into 50 ml tubes with 95% ethanol for several hours to allow organisms to release from the sediment. Following this, the sample material was placed onto the 45 µm sieve, thoroughly rinsed of ethanol, and returned to the 50 ml tubes in 15 ml increments per tube. These tubes were then filled to the 45 ml mark with Ludox (Sigma-Aldrich, Munich, Germany), thoroughly mixed by agitation, and allowed to stand for 1 hour. They were then centrifuged at 45000 rpm for 15 minutes at 25°C. The supernatants from each tube from a single sample were collected onto a 45 µm sieve and thoroughly rinsed of the Ludox. This

supernatant was the organic portion of the sample, while the precipitate was the sediment portion. The supernatants were collected into one or more 50 ml tubes filled with 95% ethanol and then retained at 4°C until DNA extraction.

DNA extraction from floated material, polymerase chain amplification, and sequencing:

DNA extractions were performed on the processed organic material from each sample using DNeasy Powersoil kits (Qiagen, Hilden, Germany) according to the manufacturer's protocol. Extractions were performed on three 0.25 g portions of the organic portion of each sample, resulting in a total of 216 DNA aliquots. All aliquots were checked for DNA concentration (>10 ng/ μ L) using the Invitrogen Qubit 4 Fluorometer (Thermo Fisher Scientific, Wilmington, DE) with the Qubit dsDNA BR Assay Kit. All extractions produced sufficient DNA to continue with the polymerase chain reaction (PCR) process. The primer constructs used for this study were the NF1/18Sr2b primer set (Porazinska et al. 2009, 2010), with NextEra Illumina adapter sequences. The PCR mix consisted of 10.5 μ L Taq polymerase master mix (New England BioLabs), 0.5 μ L (at 5 μ M concentration) of each of the forward and reverse primer construct, 1 μ L extracted sample DNA (at 10 ng/ μ L), and 12.5 μ L DNA-ase free water for a total of 25 μ L for each reaction. All PCR products were shipped on ice to the University of New Hampshire Hubbard Center for Genomic Studies for sequencing. All sequencing was performed on the Illumina Hiseq 2500 platform (Caporaso et al. 2012), using NextEra DNA Flex Library Prep kits (Illumina, San Diego, California). For all DNA aliquots, 2x250 base pair forward and reverse FASTQ files were produced. Sequence files and metadata are available in GenBank via the BioProject accession number PRJNA706429.

Bioinformatics and analysis:

Initial bioinformatics steps were performed in QIIME 2 (version 2020-2, Bolyen et al. 2019). The raw FASTQ files from sequencing, which contained demultiplexed forward and reversed reads, were imported to the qza format using the q2-tools plugin. These reads were then examined for average Phred quality scores at each base pair position using the q2-demux plugin. Using the DADA2 algorithm (Callahan et al. 2016), all reads were subjected to rigorous quality control including chimera removal, denoising, dereplication, and removal of sequences with more than expected errors. Though the Illumina Hiseq 2500 platform produces reads up to 250 bp in length, reads after base pair position 158 in the forward reads and position 147 in the reverse reads were trimmed due to the long lower whiskers on the Phred quality score boxplots after those points, which indicate low minimum quality scores. The DADA2 procedure output an amplicon sequence variant (ASV) by sample table and a representative sequences file, which shows the sequences for each ASV. The database and taxonomy files for the SILVA 132 database (Quast et al. 2013) were imported and used to classify ASV sequences with the BLAST algorithm (Camacho et al. 2009). At this point, the list of ASVs (along with taxonomic assignments) which survived and quality control process was examined. Few ASVs were retained (1,442 ASVs), and fewer still were assigned to any eukaryote taxa (131 ASVs). The DADA2 procedure was repeated only using the forward reads (again using position 158 as a

quality cut off point), and much more diversity, metazoan and otherwise, was recovered (11620 ASVs total, with 3813 ASVs assigned to eukaryote taxa). The separate entries in the ASV table for each DNA aliquot were then merged into a single entry per sample using the q2-feature-table plugin. All ASVs were filtered to remove non-metazoa taxa, vertebrate metazoa, and any taxa which might be contaminants using the filter-table method of the q2-taxa plugin. After filtering, the ASVs were clustered at 97% using the cluster-features-de-novo method in the q2-vsearch plugin to account for the intraspecific variation present in metazoans and to avoid artificially inflating biodiversity (Bucklin et al. 2011, Brandt et al. 2019, Phillips et al. 2019). This produced a table of operational taxonomic units (OTUs) by sample. From this point, the sequences were aligned using the mafft method (Katoh et al. 2002) and masked (Lane 1991) in the q2-alignment plugin. Aligned sequences were then used to create a mid-point rooted phylogenetic tree in the q2-fasttree plugin (Price et al. 2010). The OTU table was exported from the qiime format to the biom format for use in R with the biomformat package (McMurdie and Paulson 2016). This table was manipulated to turn read counts per sample into incidence (presence of OTUs) per sample, resulting in a binary table (0 when an OTU is not present in a sample, and 1 when an OTU is present). The phrase “incidence” in this text will refer to the presence of an OTU in a sample, and the phrase “total incidences” is used to refer to all the times an OTU was detected in the dataset. Incidences were used over read counts because cell counts vary in metazoan individuals; thus, read counts do not represent an accurate estimate of the number of individuals in the metazoan community.

The method rarecurve in the R package vegan (Oksanen et al. 2018) was used to generate alpha rarefaction curves from the original OTU table. These curves feature OTU richness plotted against sequencing depth for each sample. Additional sample and coverage-based rarefaction curves were generated in the R package iNEXT (Hsieh et al. 2016) using the incidence table. These curves feature effective diversity for three metrics by either number of samples or estimated coverage for the entire dataset and for the groups within the dataset. The three metrics are richness, the exponential of Shannon’s entropy index, and the inverse of Simpson’s index. Effective diversity is the number of equally abundant species (or OTUs) required to reach the value of the metric at the number of samples or estimated coverage.

The online version of the R package SpadeR (Chao and Jost 2012, Chao et al. 2015) was used to calculate basic diversity profiles, shared OTUs between communities and OTU richness estimations using the OTU incidence table. The diversity profile contains observed total incidences, total richness, coverage estimate (CE), estimated coefficient of variation (CV), incidences and total OTUS for both the frequent and infrequent groups of OTUs. The coverage estimate is a measure of sampling completeness, which estimates the percentage of the actual community present in the environment that the sampling captured. The phrase “actual community” in this text will refer to the entire community present in the environment, including all taxa which were not captured by the sampling. Any sampling effort will rarely collect 100% of the actual community, so estimates of the sampling completeness are useful. The coefficient of variation is the measure of heterogeneity in the dataset. A dataset with a CV

of 0 would be completely homogenous, and all OTUs would appear in all samples. As heterogeneity increases, the CV increases, and a dataset with a CV over 2 would be considered extremely heterogeneous. The infrequent group is a group of OTUs found in less than 10 samples (default setting for the infrequent group); this group is used for estimations of richness (especially the incidence-based coverage estimator model). Conversely, the frequent group is any OTU which appeared in more than 10 samples. Shared OTUs between communities from the different bays, salinity zones, and distances from the marsh edge were calculated. Richness values for the actual community were estimated using the homogenous model, the Chao2 model, the iChao2 model, and the incidence-based coverage estimator (ICE) model. The homogenous model estimates richness as though all OTUs have an equal chance of being detected. The Chao2 model uses the group of OTUs detected in one or two samples to estimate actual richness. The iChao2 model uses the group of OTUs detected in four or less samples to estimate actual richness, and is less biased than the Chao2 model for more heterogeneous datasets. The ICE model uses the infrequent group of OTUs to estimate OTUs, and is an incidence based version of the abundance-based coverage estimator (Chao and Lee 1992).

All OTUs were organized by phylum and plotted as percentages of total OTU incidence and richness in Microsoft Excel. All OTUs were also presented with phylum and order level assignment, total incidence, lowest level assignments from SILVA and GenBank, and incidence by metadata category (bay, salinity zone, and distance from marsh edge). The lowest level assignment was the most specific assignment given to an OTU, regardless of the taxonomic level the assignment. The majority of the metazoan OTUs received a species level assignment, but an OTU which was ambiguous at the species level would have a lowest level of genus.

However, some of the assignments from the SILVA had low resolution (i.e. the taxonomic string states a phylum or order and is ambiguous after that), so all OTUs were manually checked using the BLAST+ algorithm against the NCBI GenBank database (Benson et al. 2011). All OTUs were given additional assignments based on the top BLAST hit, sorted by E-value. All taxonomic strings were checked for accuracy against the World Register of Marine Species database (WoRMS Editorial Board 2020).

Taxa bar plots were created using the OTU incidence table in the R package ggplot2. These plots feature the number of incidences for each phylum within each sample as a relative percentage of the total incidences in the sample. Separate plots were created for each salinity zone.

Alpha and beta diversity metrics were calculated using several methods. Alpha diversity is usually defined as the diversity within samples, while beta diversity is the change in diversity across samples (Whittaker 1972, Anderson et al. 2011, Chao et al. 2012). Alpha diversity values, using the OTU richness and Faith's Phylogenetic Diversity (PD) measures, were calculated in the q2-alpha plugin. OTU richness is the number of OTUs in a sample, while the Faith's PD value is the total branch length of the phylogenetic tree of all OTUs within a sample (Faith 1992). Both of these values were tested for differences across the salinity zones, bays, and distances from

the marsh's edge using a Kruskal-Wallis procedure in the q2-diversity plugin (Kruskal and Wallis 1952). These values were also used to create boxplots in the ggplot2 package in R.

Beta diversity similarity indices were calculated in SpadeR Online (Chao and Jost 2012, Chao et al. 2015) using the incidence table of OTUs; these similarity indices were calculated for comparisons of communities between bays and among different salinity zones and distances from marsh edge. Indices were also calculated for both the observed and estimated richness and incidence values of the community, based on Chao's estimates of the actual community (Chao et al. 2013). Estimated indices were calculated because the observed data often undershoots actual similarity between communities. The indices selected for use were the Sørensen, Jaccard, Horn (equal-weighted), Morisita-Horn (relative), and Regional overlap (relative). The Sørensen and Jaccard indices are both based on the similarity of the composition of communities, but the Sørensen index gives more weight to the shared portions of the communities. The Horn (equal-weighted) index is a measure of the overlap between the total and within community values for Shannon diversity. The Morisita-Horn (relative) and regional overlap (relative) indices are both measures of the overlap between the within community and total values for the Gini-Simpson diversity (Morisita 1961). Morisita-Horn gives more weight to total Gini-Simpson diversity, while regional overlap gives more weight to the within community Gini-Simpson diversity.

A distance matrix of Sørensen index values for each pair of samples in the dataset was created using the q2-diversity plugin (Dice 1945, Sørensen 1948). This index was chosen because it uses the composition of samples, rather than read counts, which avoids the issue of individual numbers not corresponding to read counts in metazoan taxa. The Sørensen index provides measures of differences between samples by dividing twice the number of shared OTUs between two samples by the total number of OTUs in both samples (thus obtaining the similarity between the two samples), then subtracting that number from 1 (thus obtaining dissimilarity, or distance between the two samples).

Non-metric MultiDimensional Scaling (NMDS) ordination was used to explore the distance between groups of samples from different metadata categories (salinity zone, bay, and distance from marsh edge) in the distance matrix in a reduced number of dimensions using the metaMDS method in the R package vegan (Oksanen et al. 2018). The ordination process was begun with 10 dimensions, with each subsequent run reducing the number of dimensions by 1, using the previous run as a starting point for the new run. Stress (goodness of fit of the regression of the original distance matrix values against the ordination distances) of the ordination was plotted against the number of dimensions, and the ordination with the lowest number of dimensions to have a stress below 0.1 was selected for plotting. For this dataset, the number of dimensions was 5, with the first two presented. The metaMDS method automatically sorts the axis scores by maximum scatter, to reduce overlap between points and present the most informative ordination in the first two dimensions. The ordination was plotted using the R package ggordiplot, available at <https://github.com/jfq3/ggordiplots>, which uses

the package ggplot to make publication quality versions of the plots available in the ordiplot method in vegan. This ordination is presented several times with different metadata categories and the ordination hulls, spiders, and centroids of those categories overlaid. The centroid of a metadata category is the geometric center of the points within that group, while a spider is a set of lines linking all points to the centroid of the group.

The distance matrix was then tested using the Adonis procedure in the q2-diversity plugin, with the formula “Salinity Zone*Bay*Distance from marsh edge” and 10,000 permutations. The Adonis procedure is a multifactorial PERMANOVA test, which uses the sum of squares of the distances between centroids of groups of samples belonging to each factor and the overall centroid to calculate F-ratios and permutations of observations to determine significant differences. The multivariate space of the dataset is the space in multiple dimensions (with each column of the distance matrix corresponding to one dimension) which the dataset occupies. The factor Salinity Zone had three classes, Low, Mid, and High. The factor Bay had two classes, Barataria and Caillou. The Distance from marsh edge factor had four classes, 0m, 1m, 5m, and 10m. An assumption of the PERMANOVA test is that all groups have similar spread in the multivariate space. A PERMDISP test was used to determine the spread of these groups. Following all tests, p-values were corrected to account for the false discovery rate using the p.adjust function in the stats package in R (Benjamini and Hochberg 1995b).

Differential taxa abundance:

The q2-songbird plugin (Morton et al. 2019) was used to calculate taxa differentials with the following parameters: a formula of “Salinity Zone + Bay”, a differential prior of 0.0001, a learning rate of $1e^{-7}$, and an epoch value of 4000000. The minimum sample and feature counts were left as defaults. These parameters, excluding the formula, were also used to create a null model to calculate a pseudo- Q^2 value. The pseudo- Q^2 value behaves like the R^2 value of a classical regression, in that the closer it is to 1, the higher the predictive accuracy of the model. The pseudo- Q^2 value was 0.04 for this dataset. Parameters were adjusted numerous times in attempts to improve the pseudo- Q^2 value to no avail. Initially, the formula “Salinity Zone + Bay+ Distance from Marsh Edge” was used, but this formula never produced a positive pseudo- Q^2 value, likely due to model overfitting and low predictive accuracy. In addition, the different factors in the model were tested separately and the “Distance” factor never produced a positive pseudo- Q^2 value. The taxa differentials are the relative log-fold change in OTU abundance (as represented by read counts) across a metadata category. Positive differential values represent higher abundance in samples from a category compared to the reference category, while negative differentials represent lower abundance in samples from a category compared to the reference.

4.3. Results

Soil chemistry analyses:

Almost all of the soil chemistry variables were significantly different across the interaction of the bay and salinity zone factors, or across Bay or salinity zone (Tables 4.1, 4.2, 4.3). Phosphorus was the only variable that was different across the distance from edge factor. The majority of the soil chemistry variables fell within historic ranges for marshes (Table 4.2). Differences across bays were expected due to different sources of sediment and water, and differences across the salinity zones were expected due to the influence of saltwater on local soil chemical variables.

Table 4.1. Mean and standard deviation values for soil chemistry analyses of samples collected from different salinity zones in Barataria and Caillou Bays in Louisiana marshes during July 2018.

Bay Salinity zone	Barataria			Caillou		
	Low	Mid	High	Low	Mid	High
Carbon (%)	15.55 ^A	11.72 ^A	6.42 ^B	10.64 ^B	7.23 ^B	6.85 ^B
St Dev	2.02	3.24	1.65	1.68	2.1	2.94
Nitrogen (%)	1.19 ^A	0.97 ^A	0.46 ^B	0.81 ^C	0.48 ^{BC}	0.50 ^{BC}
St Dev	0.1	0.28	0.11	0.2	0.08	0.19
Organic Matter (%)	8.35 ^A	10.63 ^{BC}	8.93 ^{AC}	9.43 ^{AC}	8.79 ^A	8.23 ^A
St Dev	1.45	1.42	0.6	1.09	0.33	0.29
CN ratio	13.1	12.11	14.08	13.5	14.9	13.73
St Dev	0.91	0.91	1.7	2	2.4	1.77
Aluminum (ppm)	0.29 ^{AB}	0.84 ^A	0.17 ^B	0.31 ^{AB}	0.26 ^A	0.23 ^A
St Dev	0.07	0.66	0.03	0.1	0.18	0.12
Boron (ppm)	12.66 ^A	99.05 ^B	53.54 ^{AB}	8.65 ^A	7.27 ^A	20.53 ^A
St Dev	9.74	74.05	34.79	4.27	6.66	26.12
Calcium (ppm)	1972.68 ^{AB}	2411.29 ^{AB}	1830.69 ^{AB}	2289.14 ^A	1371.92 ^B	1580.43 ^{AB}
St Dev	208.59	625.13	419.23	403.6	89.02	764.1
Chloride (ppm)	1381.52 ^{AB}	993.94 ^{AB}	628.76 ^{AB}	530.57 ^A	1603.91 ^B	1395.35 ^{AB}
St Dev	336.44	1076.1	519.34	117.64	133.95	389.14
Conductivity dS m	14.77 ^A	21.10 ^{BC}	19.21 ^{AC}	2.86 ^D	8.95 ^E	15.50 ^A
St Dev	1.8	4.97	2.26	0.66	1.74	2.72
Copper (ppm)	3.59	2.48	4.32	5.22	4.56	2.71
St Dev	0.87	0.45	3.57	3.85	4.04	0.75
Iron (ppm)	137.67 ^{AC}	76.31 ^A	41.10 ^A	219.89 ^{BC}	146.96 ^B	102.43 ^B
St Dev	103.57	37.19	15.44	89.55	40.9	73.49
Magnesium (ppm)	3459.59 ^A	3532.78 ^A	2561.98 ^B	2541.65 ^B	2140.60 ^B	2436.21 ^B
St Dev	199.52	616.2	359.12	204.56	90.5	430.85
Manganese (ppm)	38.04 ^A	10.86 ^B	17.14 ^B	58.45 ^C	17.95 ^B	8.92 ^B
St Dev	14.54	1.11	4.86	23.56	6.98	1.98
pH 1:1 Water	6.58 ^A	6.95 ^A	6.88 ^A	6.18 ^B	5.95 ^B	6.22 ^B
St Dev	0.55	0.24	0.36	0.22	0.33	0.61

Bay Salinity zone	Barataria			Caillou		
	Low	Mid	High	Low	Mid	High
Phosphorus (ppm)	80.91 ^A	93.73 ^A	42.32 ^B	60.53 ^A	70.21 ^A	47.88 ^B
St Dev	30.16	25.92	3.61	22.04	16.27	10.46
Potassium (ppm)	1083.33 ^A	1443.24 ^B	1201.63 ^{AB}	683.58 ^C	1000.15 ^{AC}	1239.61 ^{ABC}
St Dev	98.66	83.82	248.42	114.93	120.32	248.76
(table cont'd.)						
Salts (ppm)	9452.80 ^A	13501.87 ^B	12292.27 ^{AB}	1828.48 ^C	5728.00 ^D	9917.87 ^A
St Dev	1154.72	3179.8	1443.77	421.51	1113.7	1739.79
SAR	2.66 ^A	2.23 ^A	2.34 ^A	5.38 ^B	3.84 ^C	2.63 ^A
St Dev	0.48	0.46	0.24	0.7	0.64	0.35
Sulfur (ppm)	7027.96 ^A	9381.88 ^B	7643.57 ^{AB}	1581.79 ^C	4281.30 ^D	6973.84 ^A
St Dev	675.45	1700.69	1540.01	309.68	531.16	1236.14
Sodium (ppm)	392.99 ^A	566.41 ^{AC}	441.89 ^{AC}	220.39 ^B	354.72 ^{BC}	460.38 ^{BC}
St Dev	183.66	152.04	190.03	120.68	63.76	74
Zinc (ppm)	13.11 ^A	5.59 ^B	10.42 ^{AB}	9.54 ^{AB}	7.04 ^B	6.93 ^B
St Dev	4.51	1.27	2.78	2.71	1.77	1.68

Means in rows followed by the same letter are not significantly different ($p \geq 0.05$; Tukey HSD).

Table 4.2. Historic data ranges for soil chemical analyses in Gulf Coast marshes.

Chemical analysis	Collected Data Range		Historic Data Range		Source
Carbon %	3.16	18.42	1	40	Chabreck 1972
Nitrogen %	0.25	1.31	0.09	2.27	Brupbacher et al. 1973
CN ratio	11.02	17.62	8	28.2	Brupbacher et al. 1973
Organic matter %	7.72	12.02	5	66	Brupbacher et al. 1973
Aluminum (ppm)	0.13	1.53	1000	80000	Santschi et al. 2001
Boron (ppm)	1.74	247.53	0	600	Boyd et al 1972
Calcium (ppm)	1053.69	3428.12	296	11333	Brupbacher et al. 1973
Chloride (ppm)	6.03	2874.23	56	16218	Brupbacher et al. 1973
Copper (ppm)	1.21	20.34	0	72.08	Bhattarai 2006
Iron (ppm)	21.77	308.37	370.96	27990	Bhattarai 2006
Magnesium (ppm)	1876.31	4532.29	100	12430	Brupbacher et al. 1973
pH	5.44	7.63	4.1	7.5	Brupbacher et al. 1973
Phosphorus (ppm)	34.25	138.64	5	386	Brupbacher et al. 1973
Potassium (ppm)	549.72	1572.74	24	719	Brupbacher et al. 1973
Salts (ppm)	1062.40	19033.60	550	29570	Brupbacher et al. 1973
Sodium (ppm)	997.31	12268.67	120	56800	Brupbacher et al. 1973
Sulfur (ppm)	31.33	392.77	6	285	Chambers & Pederson 2006
Zinc (ppm)	2.92	18.01	0	249	Bhattarai 2006

Historic data for conductivity, Manganese (ppm), and SAR were unavailable.

Carbon percentage was different across the bay and salinity interaction (ANOVA, $F(2,24) = 4.35$, $p = 0.02$), across the salinity factor (ANOVA, $F(2,24) = 20.64$, $p < 0.01$), and across the bay factor (ANOVA, $F(1,24) = 13.24$, $p < 0.01$). Barataria was higher in carbon percentage than Caillou at both the Low and Mid salinity zones (Tukey's HSD, $p < 0.05$), but the High zones were similar in each bay (Tukey's HSD, $p = 0.99$). The Low and Mid salinity zones in Barataria bay both had significantly higher percentage of carbon than the High salinity zone in that bay (Tukey's HSD, $p < 0.05$). Additionally, the percentage of carbon was not different among the different salinity zones in Caillou Bay (Tukey's HSD, $p > 0.05$). Carbon percentage in this study fell within historic ranges (Table 4.2)

Nitrogen percentage was different across the bay and salinity interaction (ANOVA, $F(2,24) = 6.67$, $p < 0.01$), salinity (ANOVA, $F(2,24) = 23.00$, $p < 0.01$), and the bay factor (ANOVA, $F(1,24) = 19.47$, $p < 0.01$). The nitrogen percentage of samples followed a similar pattern to the carbon percentage of samples, with Barataria having higher percentages of nitrogen in the Low and Mid salinity zones than Caillou (Tukey's HSD, $p < 0.05$), but having no difference in the nitrogen percentage of the High sites in both bays (Tukey's HSD, $p = 0.99$). Additionally, the salinity zones in Caillou were not significantly different in nitrogen percentage. Nitrogen percentage in this study fell within historic ranges (Table 4.2)

The organic matter percentage was different across the interaction of bay and salinity zone (ANOVA, $F(2,24) = 6.54$, $p < 0.01$), and across the salinity zones (ANOVA, $F(2,24) = 4.16$, $p = 0.03$). Again, this variable showed a similar pattern to the carbon percentage, with one major exception. Instead of the High salinity zone in Barataria having the highest average organic matter percentage (as would be expected from the high carbon percentage in those samples), it had the lowest averages in the dataset, with one outlier at a higher percentage. The Mid salinity zone in Barataria had the highest organic matter percentage in the dataset, which was significantly higher than the High salinity zone in Barataria and the Low and Mid salinity zones in Caillou (Tukey's HSD, $p < 0.05$). Organic matter percentage in this study fell within historic ranges (Table 4.2)

The C/N ratios were not significantly different across any of the factors or interactions of factors. High nitrogen percentages aligned with high carbon percentages in the dataset, leading to ratio values which were similar across all samples. However, samples from Caillou Bay tended to have larger ranges of values for C/N ratios. The C/N ratios in this study did not fall outside of historic ranges (Table 4.2)

Aluminum (ppm) was different across the bay and salinity zone interaction (ANOVA, $F(2,24) = 3.98$, $p = 0.03$) and the salinity zone factor (ANOVA, $F(2,24) = 4.07$, $p = 0.03$). This is likely due to the relatively large range in values detected in samples from the Mid salinity zone in Barataria Bay. These samples had higher aluminum (ppm) than samples from the High salinity zone in Barataria Bay, and samples from the Mid and High salinity zones in Caillou Bay (Tukey's HSD, $p < 0.05$). Aluminum values can be variable in Barataria Bay as a result of long

term industrial activity in the area (Powell and Alexander 2003). Aluminum (ppm) in this study was much lower than historic ranges (Table 4.2)

Boron (ppm) was significantly different across the bay and salinity zone interaction (ANOVA, $F(2,24) = 4.58$, $p = 0.02$), salinity (ANOVA, $F(2,24) = 4.22$, $p = 0.02$), and bay (ANOVA, $F(1,24) = 12.67$, $p < 0.01$). Mid salinity zone samples in Barataria Bay were significantly higher in boron (ppm) than Low salinity zone samples in that bay and all salinity zone samples in Caillou Bay (Tukey's HSD, $p < 0.05$). Boron (ppm) fell within historic ranges (Table 4.2).

Calcium (ppm) was different across the interaction of bay and salinity zone (ANOVA, $F(2,24) = 6.85$, $p < 0.01$) and the bay factor (ANOVA, $F(1,24) = 4.67$, $p = 0.04$). The samples from the Low salinity zone in Caillou Bay were higher in calcium (ppm) than the Mid salinity zone samples in both bays in Caillou Bay (Tukey's HSD, $p < 0.05$). Additionally, the samples from the Mid salinity zone in Barataria Bay were higher in calcium than the samples from the High salinity zone in Caillou Bay (Tukey's HSD, $p = 0.04$). The calcium values for the soil samples fell within historically recorded ranges (Table 4.2).

Chloride (ppm) was different across the interaction of the bay and salinity zone factors (ANOVA, $F(2,24) = 7.98$, $p < 0.01$). The samples from the Mid salinity zone in Caillou Bay were higher in chloride (ppm) than the samples from the Low salinity zone in Caillou Bay (Tukey's HSD, $p = 0.03$), but all other groups of samples were similar. Chloride (ppm) values from samples in this study fell within historic ranges (Table 4.2).

Conductivity (dS/m) was different across the interaction of the bay and salinity zone factors (ANOVA, $F(2,24) = 9.23$, $p < 0.01$), the bay factor (ANOVA, $F(1,24) = 102.75$, $p < 0.01$), and the salinity zone factor (ANOVA, $F(2,24) = 31.15$, $p < 0.01$). Samples from the Low salinity zone in Caillou Bay were lower in conductivity (dS/m) than all other salinity zones in each bay (Tukey's HSD, $p < 0.05$). Samples from the Mid salinity zone in Caillou Bay were also lower in conductivity (dS/m) than all other salinity zones in each bay, excluding the samples from the Low salinity zone in Caillou Bay (Tukey's HSD, $p < 0.05$). In addition, samples from the High salinity zone in Caillou Bay were lower in conductivity (dS/m) than samples from the Mid salinity zone in Barataria Bay (Tukey's HSD, $p = 0.01$).

Copper (ppm) was not significantly different across any factor or interaction of factors. However, samples from the Low salinity zone in Caillou Bay showed a large range of values which was not observed in any other salinity zone from either bay, excluding outliers in the Mid salinity zone samples from Caillou Bay and the High salinity zone samples from Barataria Bay. Copper (ppm) values fell within historic ranges (Table 4.2).

Iron (ppm) was significantly different across both the bay (ANOVA, $F(1,24) = 8.53$, $p < 0.01$) and salinity zone factors (ANOVA, $F(2,24) = 6.78$, $p < 0.01$). Samples from Caillou Bay had significantly higher iron (ppm) than samples from Barataria Bay (Tukey's HSD, $p < 0.01$). The samples from Low salinity zones had higher iron (ppm) than samples from the High salinity zones (Tukey's HSD, $p < 0.01$). Iron (ppm) fell within historic ranges (Table 4.2).

Magnesium (ppm) was different across the bay and salinity interaction (ANOVA, $F(2,24) = 8.52$, $p < 0.01$), salinity zone factor (ANOVA, $F(2,24) = 5.44$, $p = 0.01$), and the bay factor (ANOVA, $F(1,24) = 41.15$, $p < 0.01$). The samples from the Low and Mid salinity zones in Barataria Bay were higher in magnesium (ppm) than the High salinity sites from Barataria and all three salinity zones from Caillou Bay (Tukey's HSD, $p < 0.05$). Magnesium (ppm) values for this study fell within historic ranges (Table 4.2).

Manganese (ppm) was different across the interaction of bay and salinity zone (ANOVA, $F(2,24) = 3.98$, $p = 0.03$) and the salinity zone factor (ANOVA, $F(2,24) = 6.78$, $p < 0.01$). The samples from Low salinity zones in both bays were higher in manganese (ppm) than the samples from Mid and High salinity zones in both bays (Tukey's HSD, $p < 0.05$). However, the samples from the Low salinity zone in Caillou Bay were higher in manganese than the Low salinity zone samples from Barataria Bay (Tukey's HSD, $p = 0.03$).

The soil pH was closer to neutral in samples from Barataria Bay than in samples from Caillou Bay (ANOVA, $F(1,24) = 24.18$, $p < 0.01$), which were slightly acidic. Historically, marsh soils in Louisiana tend to range between somewhat acidic and neutral (Table 4.2).

Phosphorus (ppm) was different across both the distance from edge (ANOVA, $F(1,24) = 5.01$, $p = 0.03$) and salinity zone factors (ANOVA, $F(2,24) = 11.67$, $p < 0.01$). Samples that were collected 5m from the edge of the marsh had lower phosphorus (ppm) than samples that were collected 10m from the edge of the marsh (Fig. 4.2). Additionally, samples from the Low and Mid salinity zones had higher phosphorus (ppm) than samples from the High salinity zones (Tukey's HSD, $p < 0.05$). Phosphorus (ppm) values fell within historic ranges (Table 4.2).

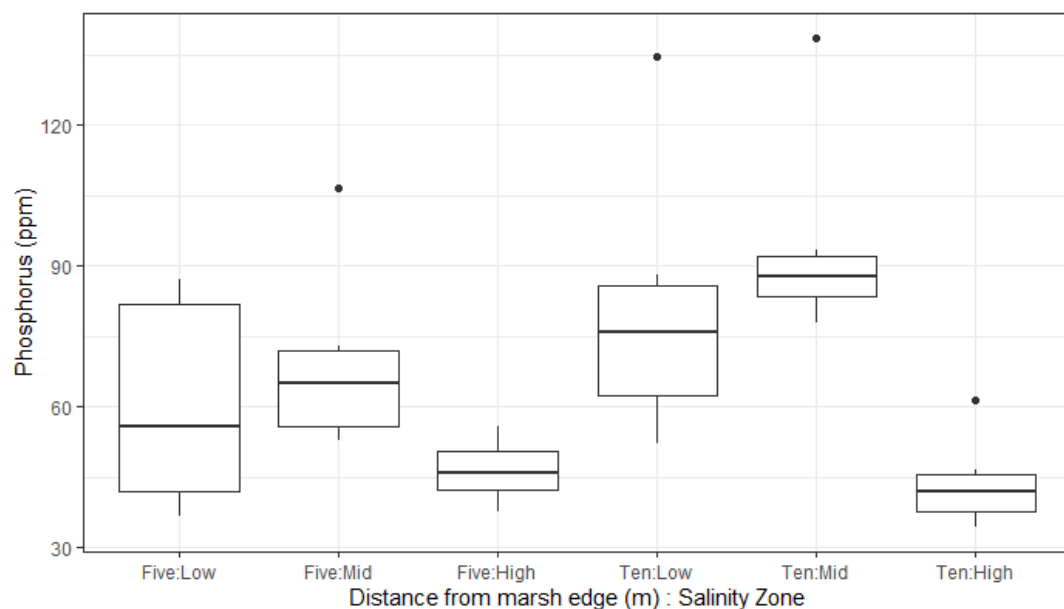


Fig. 4.2. Soil phosphorus boxplots, by distance from marsh edge and salinity zone of sample collected in July 2018 from sites in Barataria and Caillou Bays, Louisiana. Points indicate outliers, while the vertical lines indicate the top and bottom quartiles.

Potassium (ppm) was different across the interaction of the bay and salinity zone factors (ANOVA, $F(2,24) = 6.68$, $p < 0.01$), the bay factor (ANOVA, $F(1,24) = 20.36$, $p < 0.01$), and the salinity zone factor (ANOVA, $F(2,24) = 14.34$, $p < 0.01$). Samples from the Low salinity zone in Caillou Bay were lower in potassium (ppm) than samples from all other salinity zones in each bay (Tukey's HSD, $p < 0.05$), excluding the samples from the Mid salinity zone in Caillou Bay. Additionally, samples from the Mid salinity zone in Caillou Bay and samples from the Low salinity zone in Barataria were lower in potassium (ppm) than the samples from the Mid salinity zone in Barataria Bay (Tukey's HSD, $p < 0.05$). Potassium (ppm) values fell within historic ranges for Louisiana marshes (Table 4.2).

Salts (ppm) closely followed the pattern of results for conductivity (dS/m) and were different across the interaction of the bay and salinity zone factors (ANOVA, $F(2,24) = 9.23$, $p < 0.01$), the bay factor (ANOVA, $F(1,24) = 102.75$, $p < 0.01$), and the salinity zone factor (ANOVA, $F(2,24) = 31.15$, $p < 0.01$). Samples from the Low salinity zone in Caillou Bay were lower in salts (ppm) than all other salinity zones in each bay (Tukey's HSD, $p < 0.05$). Samples from the Mid salinity zone in Caillou Bay were also lower in salts (ppm) than all other salinity zones in each bay, excluding the samples from the Low salinity zone in Caillou Bay (Tukey's HSD, $p < 0.05$). In addition, samples from the High salinity zone in Caillou Bay were lower in salts (ppm) than samples from the Mid salinity zone in Barataria Bay (Tukey's HSD, $p < 0.05$). Total salts (ppm) did not exceed historic ranges for Louisiana marshes (Table 4.2).

The sodium adsorption ratio (SAR) was different across the interaction of the bay and salinity zone factors (ANOVA, $F(2,24) = 18.83$, $p < 0.01$), the bay factor (ANOVA, $F(1,24) = 90.89$, $p < 0.01$), and the salinity zone factor (ANOVA, $F(2,24) = 31.00$, $p < 0.01$). Samples from the Low salinity zone in Caillou Bay had higher SAR values than samples from any other salinity zone in either bay (Tukey's HSD, $p < 0.05$). Samples from the Mid salinity zone in Caillou Bay had higher SAR values than samples from any other salinity zone in either bay, excluding samples from the Low salinity zone in Caillou Bay (Tukey's HSD, $p < 0.05$).

Sodium (ppm) was different across the interaction of the bay and salinity zone factors (ANOVA, $F(2,24) = 14.56$, $p < 0.01$), the bay factor (ANOVA, $F(1,24) = 86.04$, $p < 0.01$), and the salinity zone factor (ANOVA, $F(2,24) = 21.39$, $p < 0.01$). The samples from the Low salinity zone in Caillou Bay were lower in sodium (ppm) than samples from all other salinity zones in each bay (Tukey's HSD, $p < 0.05$). In addition, the samples from the Mid salinity zone in Barataria Bay were higher in sodium than all samples from other salinity zones in each bay, excluding the samples from the High salinity zone in Barataria Bay (Tukey's HSD, $p < 0.05$). The sodium content (ppm) of samples fell within historic ranges (Table 4.2).

Sulfur (ppm) was different across both the bay factor (ANOVA, $F(1,24) = 6.31$, $p = 0.02$) and the salinity zone factor (ANOVA, $F(2,24) = 4.21$, $p = 0.03$). The samples from Barataria Bay were higher in sulfur (ppm) than the samples from Caillou Bay (Tukey's HSD, $p = 0.02$). Additionally, the samples from the Low salinity zones were lower in sulfur (ppm) than the samples from the Mid salinity zones (Tukey's HSD, $p = 0.04$). Sulfur (ppm) did exceed historic ranges for marshes, though these ranges were for south Florida sites (Table 4.2).

Zinc (ppm) was significantly different across the different salinity zones (ANOVA, $F(2,24) = 5.10$, $p = 0.01$). Samples from the Low salinity zones were higher in zinc (ppm) than the samples from the Mid salinity zones (Tukey's HSD, $p = 0.01$), but neither of these zones were different in zinc content from the samples from the High salinity zones. Zinc (ppm) fell within historic ranges for Louisiana marshes (Table 4.2).

Preliminary evaluation of 18S sequence dataset:

Following quality control from the DADA2 algorithm, the ASV table contained 11,620 OTUs and approximately 15 million reads. After the removal of all ASVs which did not gain an assignment from the SILVA database, 3,810 OTUs and approximately 8 million reads remained. The OTUs which did not receive assignments from the SILVA database were potentially the result of mismatches of the primer pair to prokaryote sequences (Hadziavdic et al. 2014). The majority of the ASVs which did receive assignments (1,861 ASVs) were assigned to the clade Opisthokonta (Metazoa, Fungi, and related eukaryotes) at the sub-domain level (Table 4.3), followed by the Stramenopiles, Alveolates, and Rhizaria (SAR) clade (1,326 ASVs), Archaeplastida (445 ASVs), Amoebozoa (86 ASVs), Incertae Sedis (50 ASVs), Haptophyta (13 ASVs), Excavata (11 ASVs), Centrohelida (9 ASVs), and Cryptophyceae (9 ASVs). Overall, Metazoa dominated the database, making up the majority of the reads in most samples (Fig. 4.3). Fungi were more common in samples from Caillou Bay, while some of the Mid and High salinity zone samples from this bay had lower numbers of SAR clade reads.

Approximately 53% of the assigned ASVs in the dataset were given an unclear assignment at the species level from the SILVA database (Table 4.3). The SAR group had a higher rate of unclear assignments than the total dataset, at 66%, while Opisthokonta and Archaeplastida both had lower rates of unclear assignments, at 46% and 37%, respectively. Amoebozoa and Haptophyta both also had lower rates of unclear assignments than the whole dataset, at 47% and 46%, respectively. The rest of the sub-domain groups all had similar or higher rates of unclear assignments to the entire dataset. Metazoa, which fall under the Opisthokonta clade, had a very low rate of unclear assignments at 29%, while the Fungi had a high rate of unclear assignments (61%). Only the groups Metazoa, Fungi, and Archaeplastida were present in all samples. The taxonomy of groups such as SAR and Excavata is poorly described, leading to recommendations of "taxonomy free" studies (Apothéoz-Perret-Gentil et al. 2017, Kelly 2019) for these groups. Typically, studies of benthic microalgae (including the SAR group) in marshes have used photosynthetic pigments and biomass as measures of difference between samples (Fleeger et al. 2015). Certain groups of soil metazoa have been well studied in coastal marshes (Coull et al. 1982, Fleeger 1985, Coull 1990, Fleeger et al. 2018,

and see the previous chapters of this thesis). Therefore, not only is the rate of clear assignments in the group Metazoa better than in the whole dataset, the information contained within this group is more readily accessible.

After filtering the dataset for only non-vertebrate metazoa, approximately 4 million reads and 893 ASVs remained. Following clustering ASVs which were 97% similar to each other to control for intraspecific variation, the final total of OTUs was 312.

Table 4.3. Sub-Domain level taxonomy assignments from the SILVA database of the entire dataset of ASVs. Samples were collected from different salinity zones in Barataria and Caillou Bays in Louisiana marshes during July 2018.

Taxon	Number of ASVs	Metagenome	Uncultured	Unidentified	Ambiguous Taxa	Percent Unclear Assignments
Opisthokonta	1861	106	299	0	464	46.70
Metazoa	893	13	23	0	228	29.56
Fungi	887	80	236	0	231	61.67
SAR	1326	101	457	0	328	66.82
Archaeplastida	445	1	45	2	117	37.08
Amoebozoa	86	13	13	0	15	47.67
Incertae Sedis	50	5	30	0	3	76.00
Haptophyta	13	0	2	0	4	46.15
Excavata	11	2	3	0	1	54.55
Centrohelida	9	1	4	0	1	66.67
Cryptophyceae	9	0	3	0	5	88.89
Total	3810	229	856	2	938	53.15

The Metagenome column included all ASVs which were assigned as a metagenome without at least a genus level assignment; Uncultured, Unidentified, and Ambiguous Taxa columns have all ASVs assigned to those categories at the most specific level of assigned taxonomy. The Percent Unclear Assignments is the percentage of the total ASVs for each row which were assigned as Metagenome, Uncultured, Unidentified, or Ambiguous Taxa. Fungi and Metazoa (shaded) fall under Opisthokonta, and should not be counted towards the total number of ASVs alongside the Opisthokonta totals.

Alpha rarefaction of metazoan dataset:

Rarefaction curves of OTU richness versus sequencing depth for all samples leveled off, indicating that sufficient sampling depth was achieved for all samples to collect all OTUs present (Fig. 4.4). In addition, though a wide range of both richness and sampling depth was detected, higher sequencing depth did not lead to higher OTU richness. High and Mid salinity zone samples consistently had a wide range of OTU richness, but the Low salinity zone samples had a notably narrower and higher range of OTU richness.

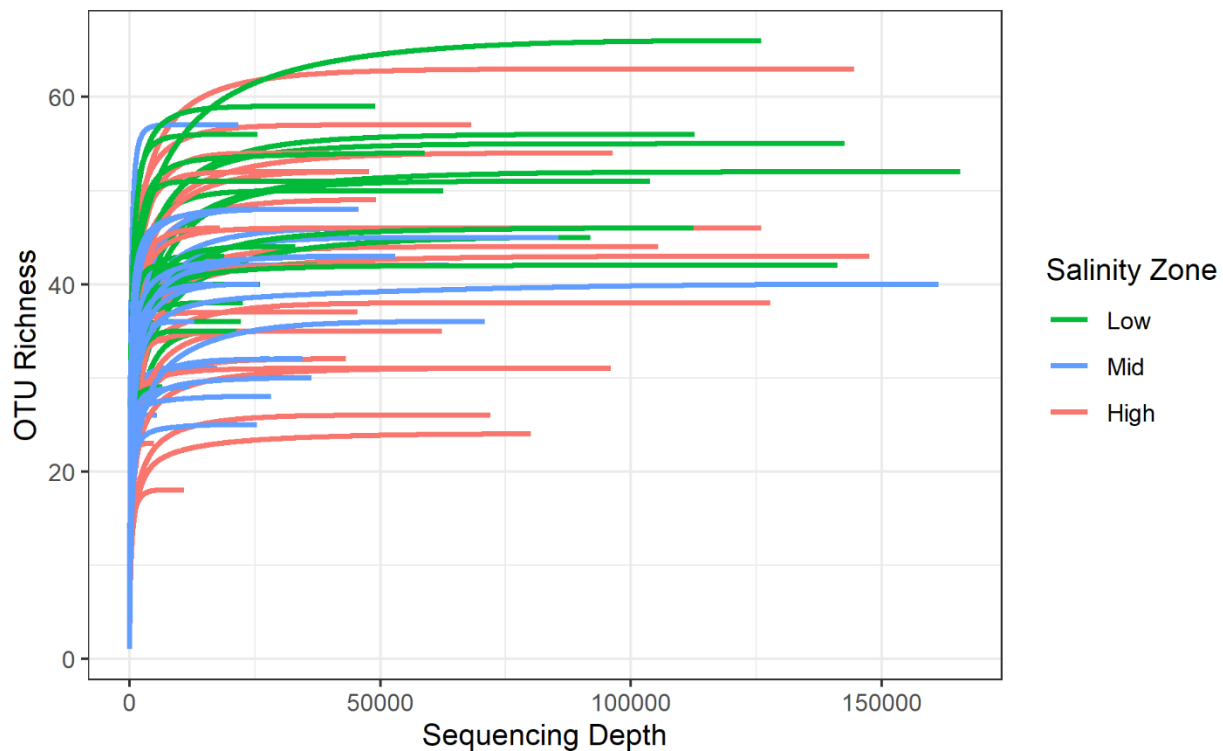


Fig. 4.4. Alpha rarefaction curves show the number of OTUs detected when randomly sampling reads at each given sequencing depth. Each curve represents the summed sequences of the three DNA extractions from a single sample collected during July 2018 from marsh sites in Barataria and Caillou Bays.

Sample-based rarefaction:

The interpolated portion of the sample-based rarefaction curves for the whole dataset begin to level off, showing that a large portion of the richness and effective diversity was captured (Fig. 4.5). The extrapolated portion of the richness curve for the full dataset continues to increase with additional samples, but the curves for the effective diversity of the Shannon and Simpson Inverse indices barely increase (Fig. 4.5). The effective diversity is the number of OTUs with equivalent numbers of incidences required to reach the value of the index, so the flatness of these curves indicates that all common OTUs within the actual community were

collected. For the curves from the different bays (Fig. 4.6), the results were similar, but the curves from samples from Barataria Bay reached higher values than the samples from Caillou Bay, indicating both higher richness and incidence. In the different salinity zones (Fig. 4.7), higher richness and incidence were observed in the curves from the Low salinity zone. For the different distance from marsh edge categories (Fig. 4.8), slightly higher richness and incidence were observed in the zero and one meter from marsh edge samples. The different distance from marsh edge curves also showed steeper slopes than the total dataset, due to the further division of the dataset resulting in smaller sample sizes for each group.

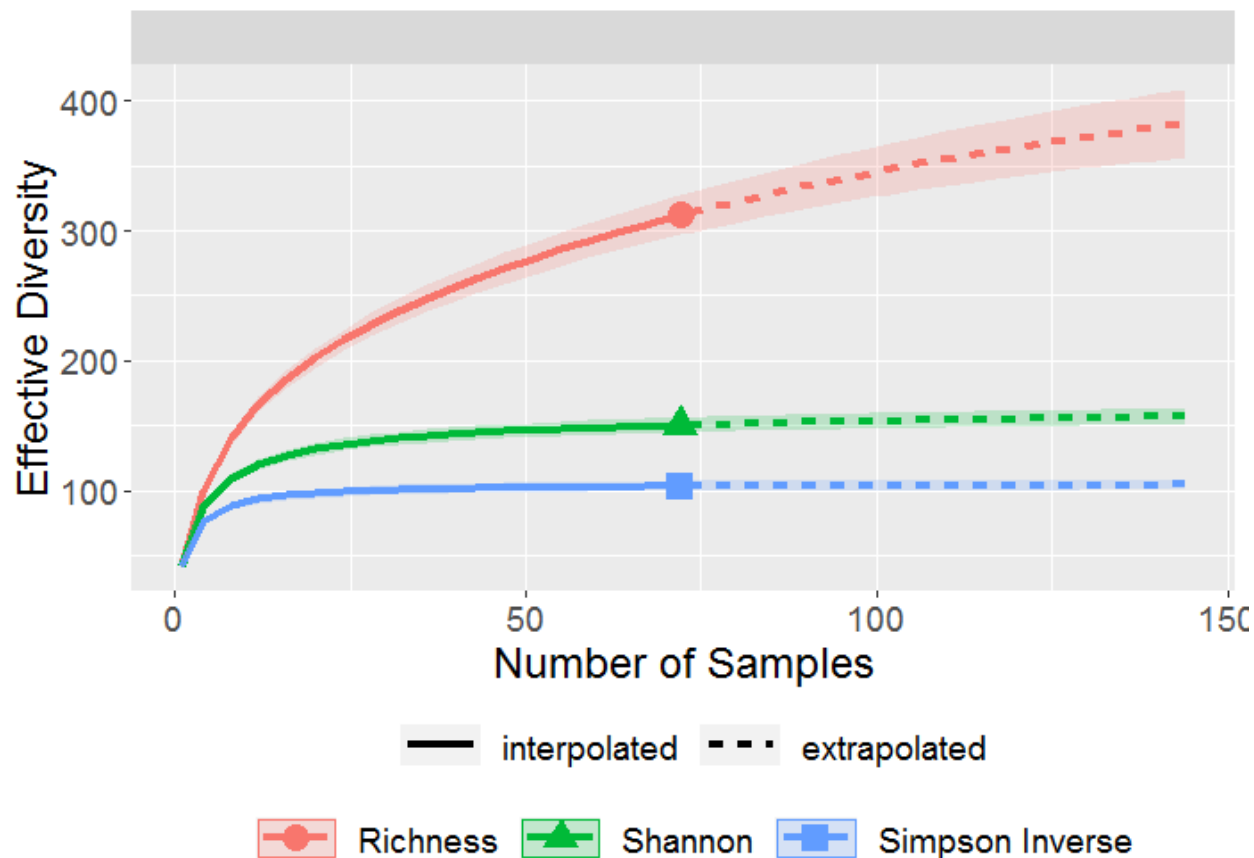


Fig. 4.5. Sample-based rarefaction curves for the full dataset with effective diversity for different metrics plotted against the number of samples collected from marsh sites in Barataria and Caillou Bays during July 2018. Extrapolation extends out to twice the number of samples, and the shaded area around each curve represents the 95% confidence interval of the curve.

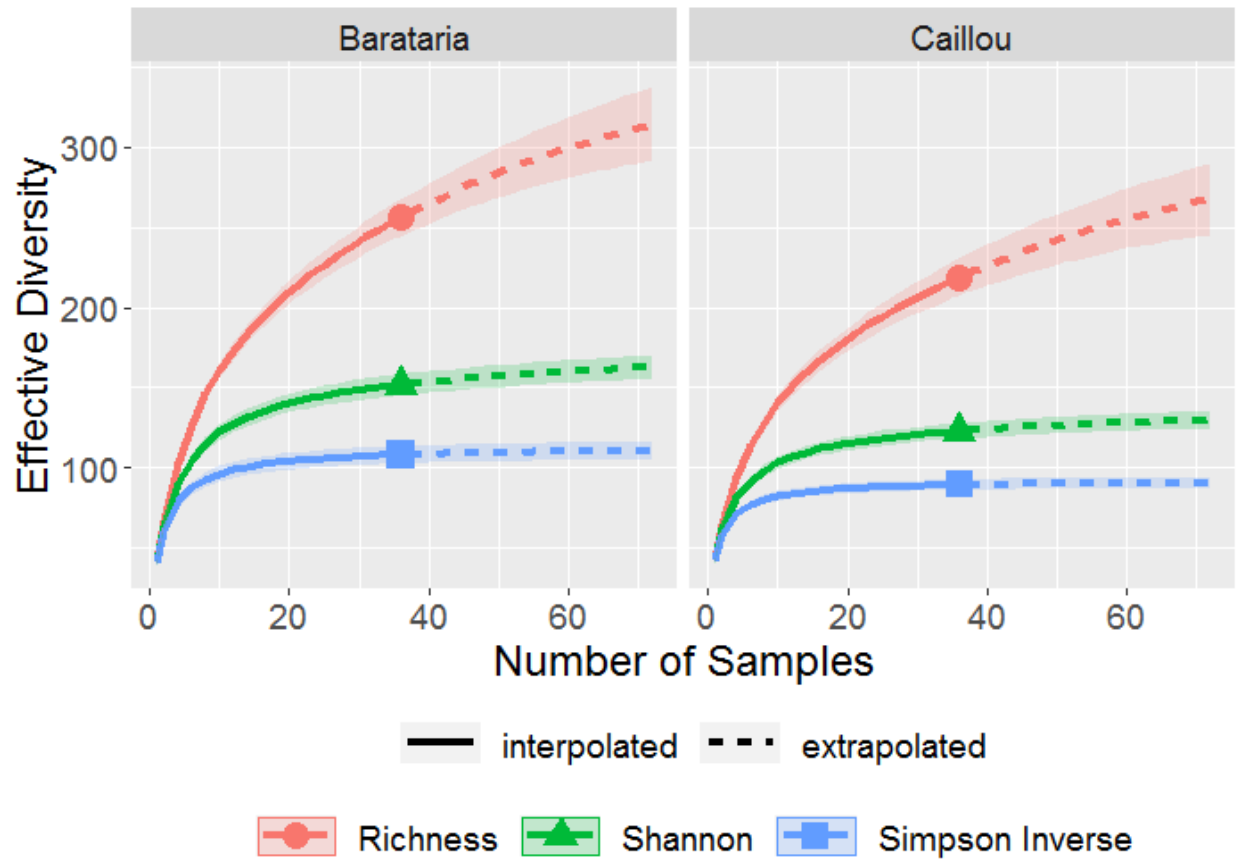


Fig. 4.6. Sample-based rarefaction curves for the samples collected from the different bays with effective diversity for different metrics plotted against the number of samples collected from marsh sites in Barataria and Caillou Bays during July 2018. Extrapolation extends out to twice the number of samples, and the shaded area around each curve represents the 95% confidence interval of the curve.

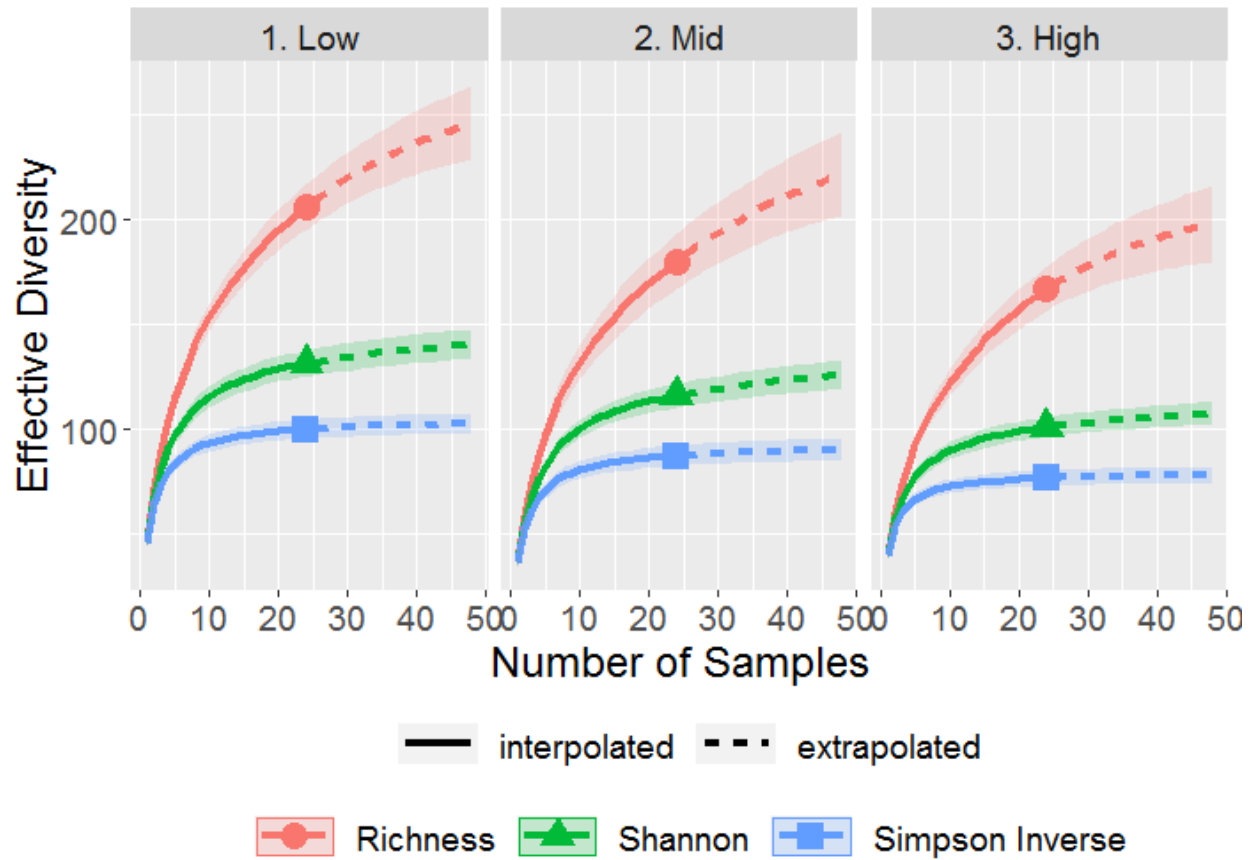


Fig. 4.7. Sample-based rarefaction curves for the samples collected from the different salinity zones with effective diversity for different metrics plotted against the number of samples collected from marsh sites in Barataria and Caillou Bays during July 2018. Extrapolation extends out to twice the number of samples, and the shaded area around each curve represents the 95% confidence interval of the curve.

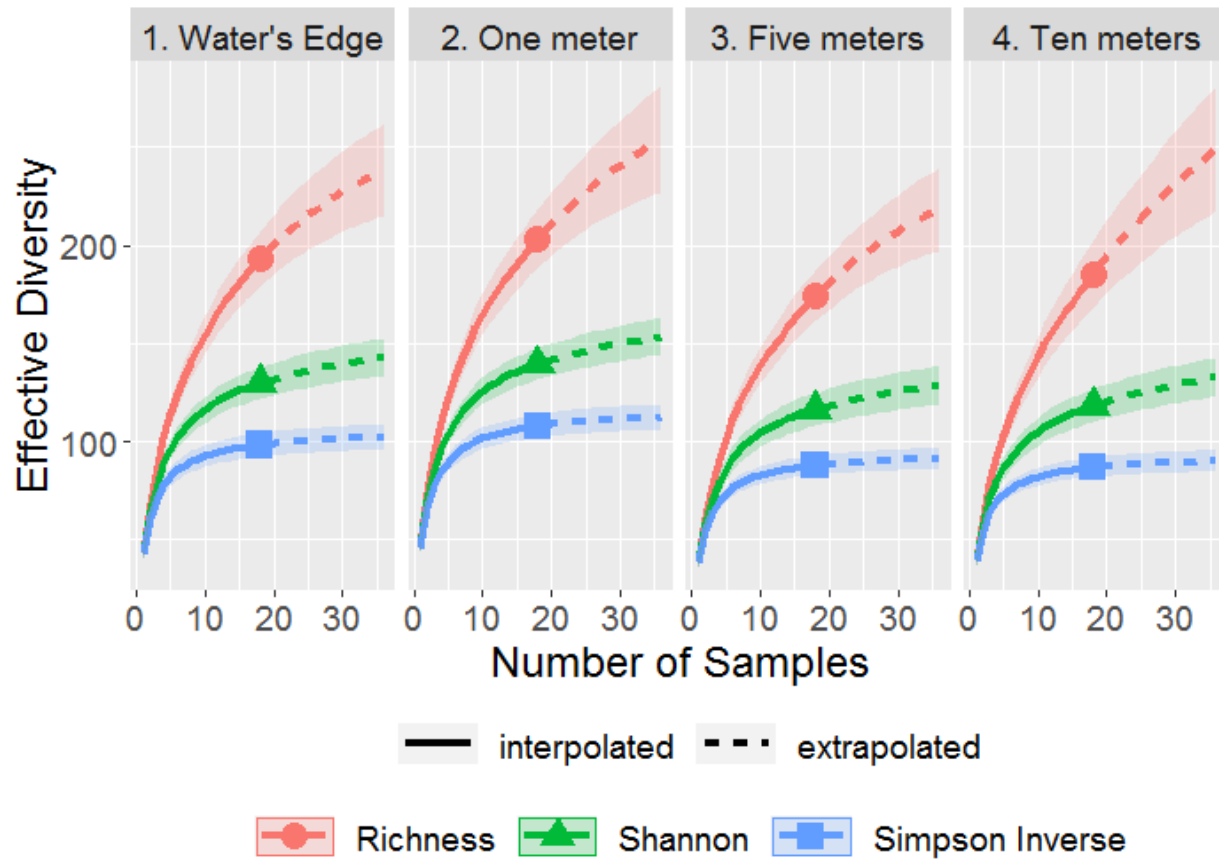


Fig. 4.8. Sample-based rarefaction curves for the samples from the different distances from the marsh edge with effective diversity plotted against the number of samples collected from marsh sites in Barataria and Caillou Bays during July 2018. Extrapolation extends out to twice the number of samples, and the shaded area around each curve represents the 95% confidence interval of the curve.

Coverage-based rarefaction:

The interpolated portions of the coverage-based rarefaction curves for the full dataset extended to approximately 97% coverage (Fig. 4.9). The extrapolated portions, which estimate coverage if the number of samples collected was doubled, reach approximately 98%. Thus, the current number of samples collected represents the vast majority of richness in the actual community, and that even doubling the number of samples would only marginally increase the coverage of the dataset. The extrapolated portion of the richness curves continued to increase, but the Shannon and Simpson Inverse extrapolated curves did not which showed that while additional richness could still be collected, the majority of the common OTUs were collected. These trends also held true for the curves for the separate communities in the different bays (Fig. 4.10), salinity zones (Fig. 4.11), and distances from the marsh edge (Fig. 4.12). The communities from the different bays and the different salinity zones reached approximately 94% coverage while the communities from the different distances from the marsh edge reached approximately 90% coverage.

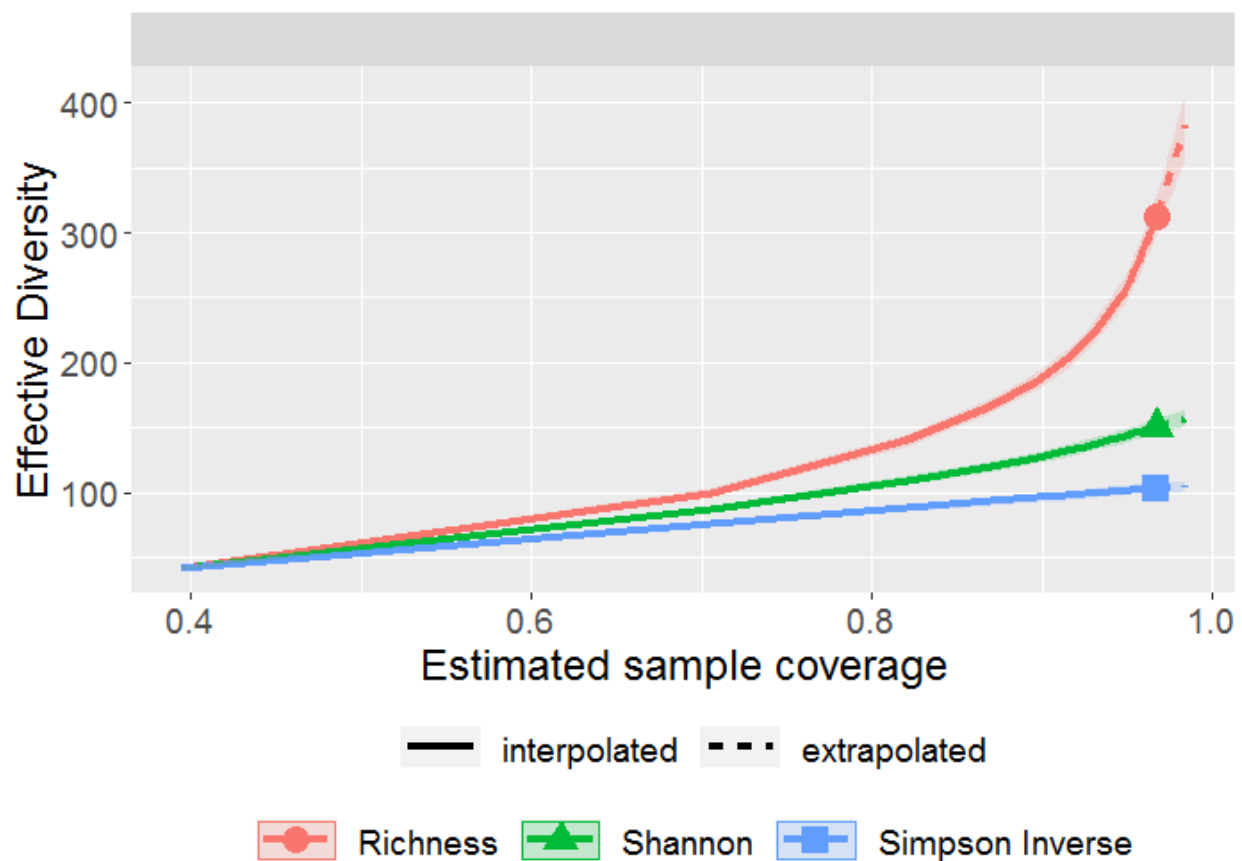


Fig. 4.9. Coverage-based rarefaction for the full dataset with effective diversity for different metrics plotted against the estimated coverage of the actual community in samples collected from marsh sites in Barataria and Caillou Bays during July 2018. Extrapolation extends out to the estimated coverage of twice the number of samples, and the shaded area around each curve represents the 95% confidence interval of the curve.

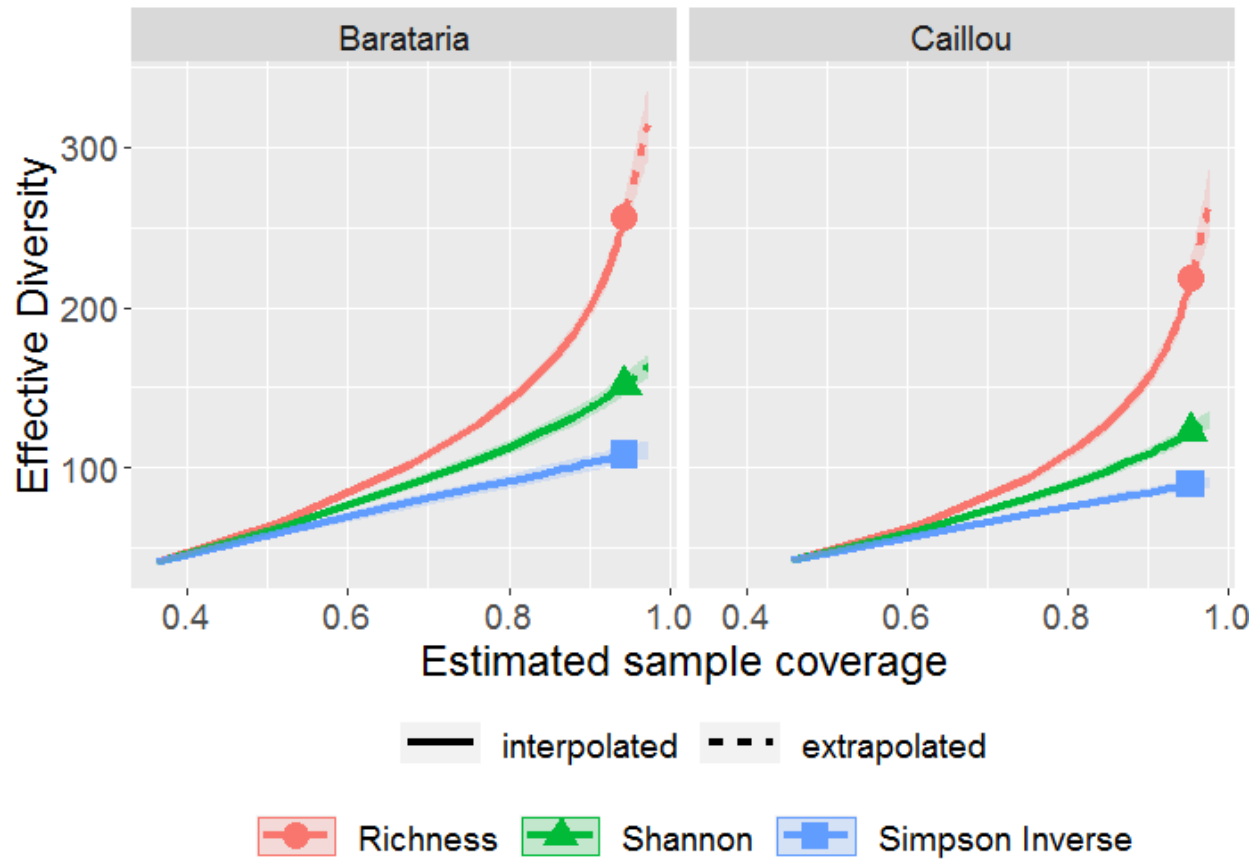


Fig. 4.10. Coverage-based rarefaction for the communities from different bays with effective diversity for different metrics plotted against the estimated coverage of the actual community in samples collected from marsh sites in Barataria and Caillou Bays during July 2018. Extrapolation extends out to the estimated coverage of twice the number of samples, and the shaded area around each curve represents the 95% confidence interval of the curve.

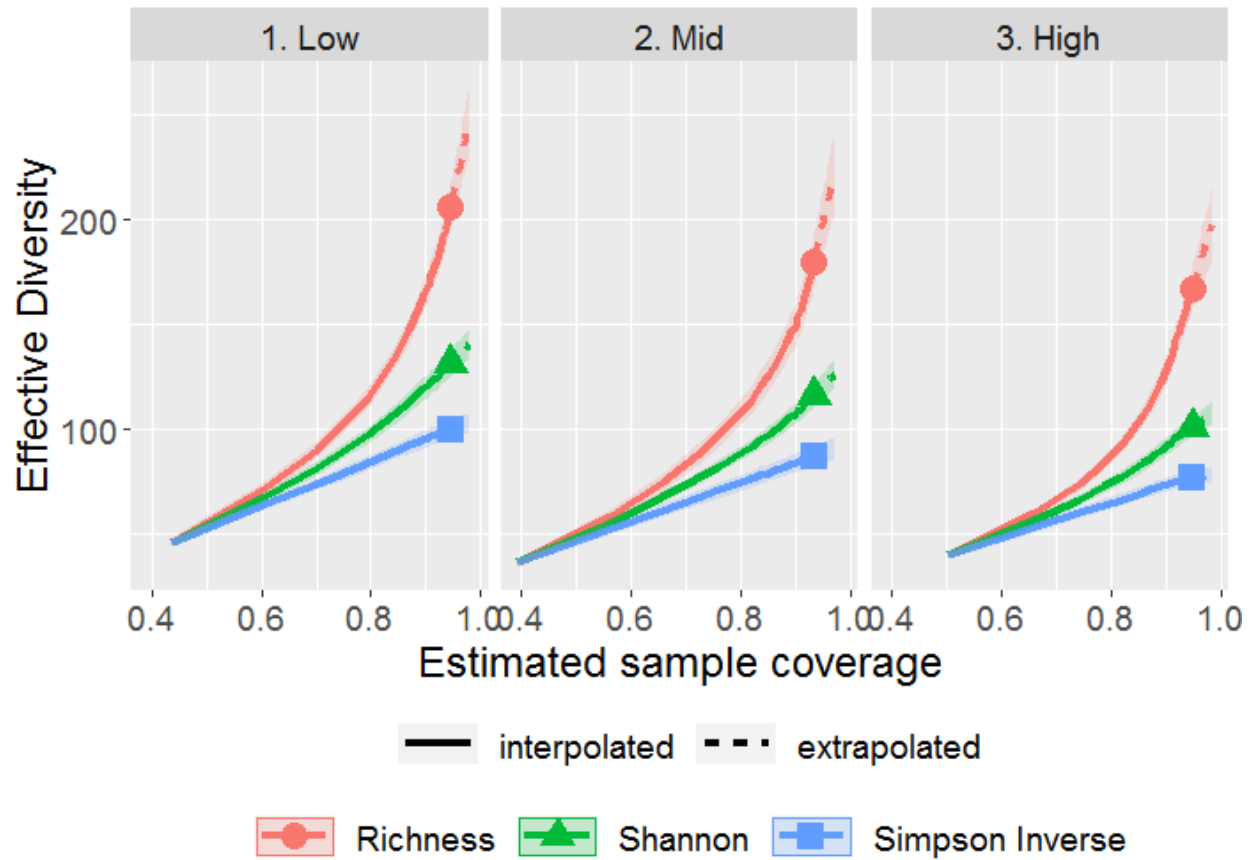


Fig. 4.11. Coverage-based rarefaction for the communities from different salinity zones with effective diversity for different metrics plotted against the estimated coverage of the actual community in samples collected from marsh sites in Barataria and Caillou Bays during July 2018. Extrapolation extends out to the estimated coverage of twice the number of samples, and the shaded area around each curve represents the 95% confidence interval of the curve.

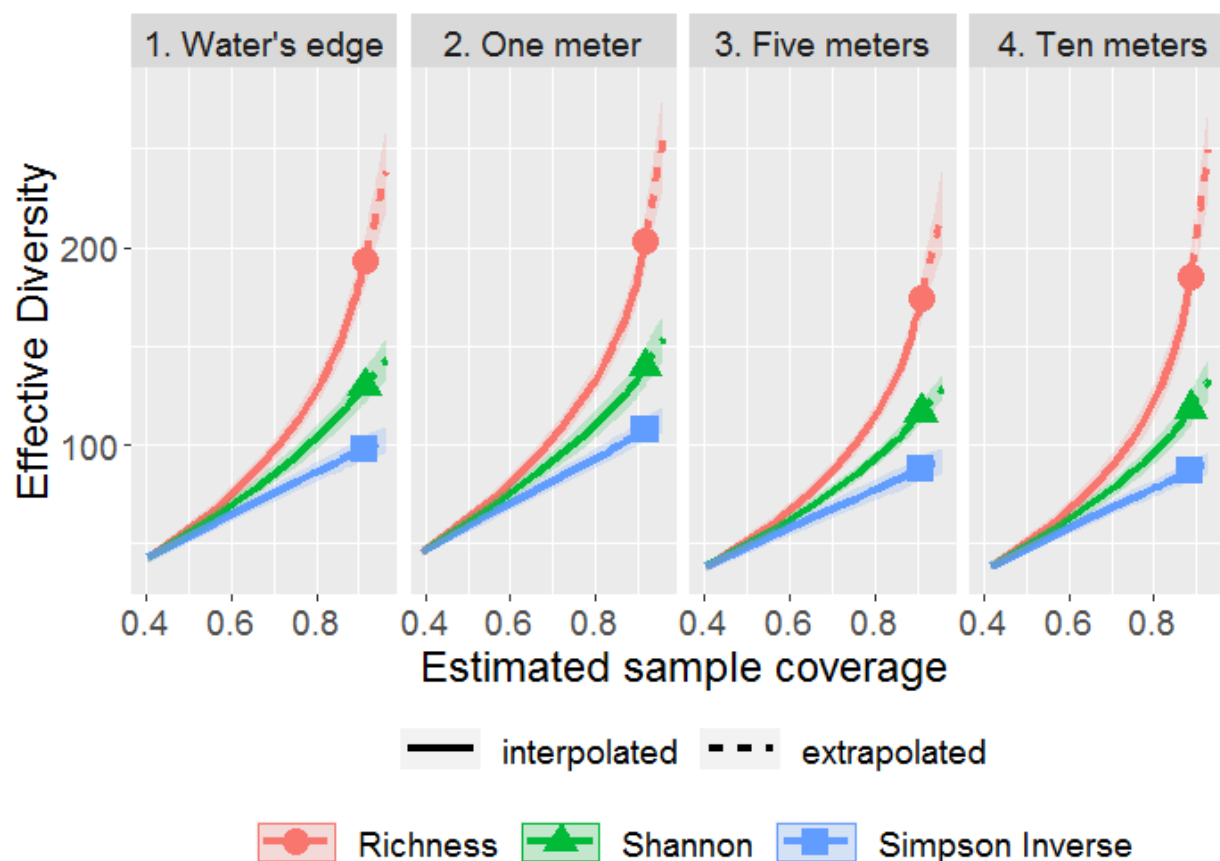


Fig. 4.12. Coverage-based rarefaction for the communities from different distances from the marsh edge with effective diversity for different metrics plotted against the estimated coverage of the actual community in samples collected from marsh sites in Barataria and Caillou Bays during July 2018. Extrapolation extends out to the estimated coverage of twice the number of samples, and the shaded area around each curve represents the 95% confidence interval of the curve.

Diversity Profile and Richness Estimations:

The coverage estimate (CE) for the entire dataset was high (Table 4.4, 96.7%), indicating that the vast majority of OTUs present in the actual community were collected, which matched the results from the coverage-based rarefaction curves (Fig 4.9). The Coefficient of Variation (CV) of the dataset was somewhat high (1.4, with a value of 2 considered extreme), indicating that the dataset was heterogeneous, with few OTUs making up the majority of the incidences in the dataset. This heterogeneity was illustrated by the frequent group observations, i.e., the OTUs which appeared in more than 10 samples. These OTUs were just 88 of the 312 OTUs but made up 2,345 of the 2,993 incidences. Meanwhile, the remaining 224 OTUs (the infrequent group, which appeared in 10 samples or less) only accounted for 648 incidences. The infrequent group had a lower coverage estimate at 84.6%, and also was much less heterogeneous than the whole dataset, with a CV of 0.838.

Table 4.4. OTU diversity profile of the dataset. Samples were collected from marsh sites in Barataria and Caillou Bays during July 2018.

Observation	Value
Number of samples	72
Total OTU Richness	312
Total number of incidences	2993
Coverage estimate for entire dataset	0.967
CV for entire dataset	1.437
Number of observed OTUs for frequent group	88
Total number for incidences in frequent group	2345
Number of observed OTUs for infrequent group	224
Total number for incidences in infrequent group	648
Estimated coverage for infrequent group	0.846
Estimated CV for infrequent group	0.838

The coverage estimate and coefficient of variation for the infrequent group (≤ 10 samples) are presented because they are used in the calculation of the ICE richness estimator model.

Estimated richness:

Richness of the actual community was estimated using the Homogenous model (all OTUs have an equal chance of being detected), Chao2 estimator (based on OTUs which appear in 2 samples or less), iChao2 estimator (based on the OTUs which appear in 4 samples or less), and Incidence-based Coverage Estimator (ICE, based on the OTUs which appear in 10 samples or less). These models are better suited to data such as this, which is neither extremely rich (fewer than 1000 OTUs) nor extremely heterogeneous (CV lower than 2), than the other models available in SpadeR Online (Chao et al. 2015). Among all the models, the range of the OTU richness was 339 OTUs (lower bound of the Homogenous Model) to 535 OTUs (upper bound of the Chao2 model, Fig. 4.13). The upper bound of richness of the actual community in the sample-based rarefaction curves for the total dataset was approximately 400 OTUs, falling into the range estimated by these models. Because the Homogenous model estimates richness if all OTUs have an equal chance of being detected, it had a lower value than the other models, which estimate additional richness based on the number of rare OTUs.

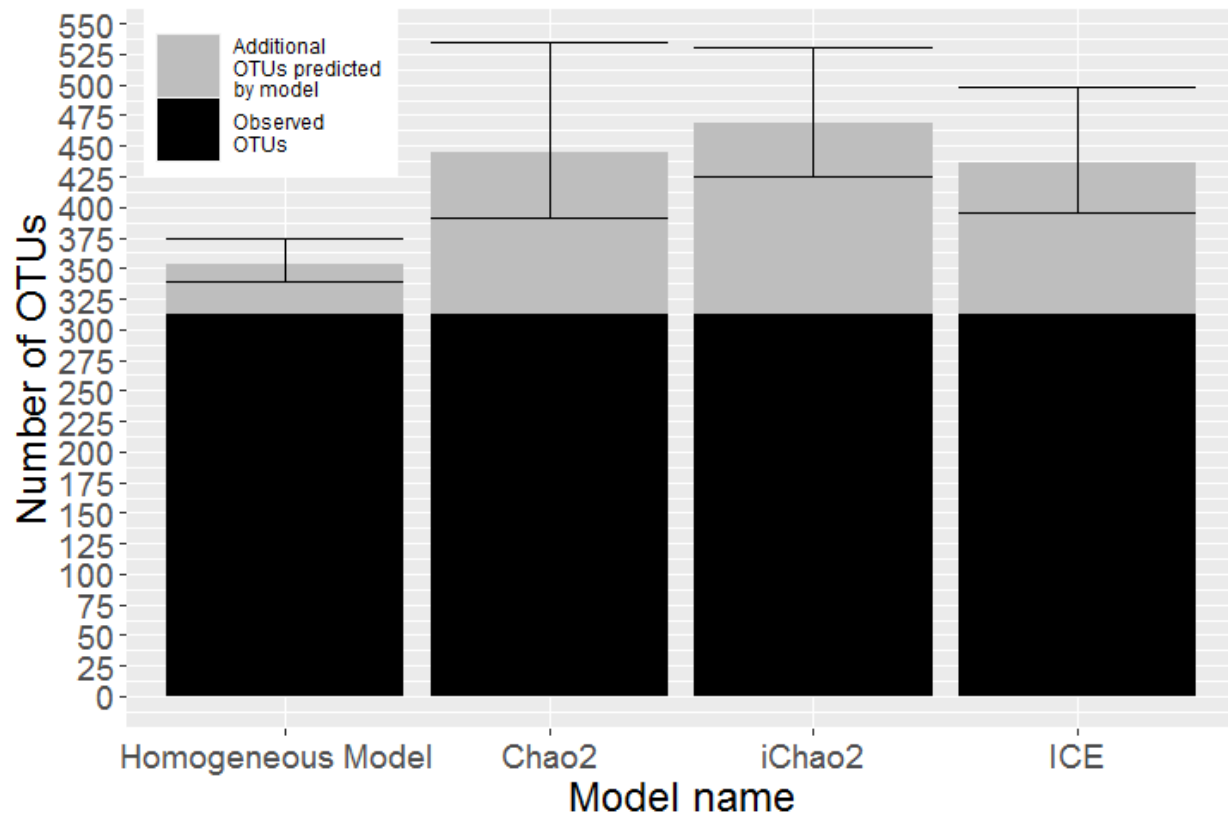


Fig. 4.13. Observed total OTU richness and incidence based OTU richness estimations from four estimator models. All samples were collected in July 2018 at marsh sites in Barataria and Caillou Bays. The lower portion of the columns in this chart is the observed OTU richness, while the upper portion of the columns represents additional OTU richness predicted by the different models. Error bars represent the 95% confidence interval of the estimate.

Shared OTUs:

One hundred and sixty-three OTUs were shared between the Barataria and Caillou Bay samples (Table 4.5), which was more than half of the OTUs detected in each bay. All 88 of the frequent group OTUs (OTUs found in more than 10 samples, Table 4.8) were detected in samples from each of the two bays. Because only two classes are being compared, the Chao2-shared index can be used to estimate the number of shared OTUs. For the two bays, the estimated number of shared OTUs in the actual community was 221 OTUs, with a 95% confidence interval of 187 to 302. This range falls well within the estimate of total OTUs from the richness estimates (Fig. 4.13)

Table 4.5. Shared and total number of OTUs for samples from marsh sites in Barataria and Caillou Bays during July 2018.

	Caillou	Barataria
Caillou	256	163
Barataria		219

The intersection of a single category (such as Barataria-Barataria) is the total number of OTUs for that bay, while the intersection of 2 categories (such as Barataria-Caillou) is the number of OTUs shared between these two categories.

The salinity zone communities had an average of 184 OTUs detected, with an average of 108 OTUs shared between the different zones and an average of 76 unique OTUs in each zone (Table 4.6). The Low salinity zone samples had the highest total number of detected OTUs at 206, followed by Mid salinity zone samples at 180 and finally High salinity zone samples at 167. Low and Mid salinity zone samples shared the most OTUs between them at 115, followed by Mid and High at 113. Low and High salinity zone samples shared the least OTUs at 97. Of the 88 frequent group OTUs, 79 were present at the Low salinity zone sites, 82 were present at the Mid salinity zone sites, and 75 were present at the High salinity zone sites (Table 4.8).

Table 4.6. Shared and total number of OTUs for samples collected from the different salinity zones in Barataria and Caillou Bays during July 2018.

	Low	Mid	High
Low	206	115	97
Mid		180	113
High			167

The intersection of a single category (such as Low-Low) is the total number of OTUs for that bay, while the intersection of 2 categories (such as Low-Mid) is the number of OTUs shared between these two categories.

The communities in the different distance from marsh edge samples had an average of 189 OTUs, with an average of 132 shared OTUs and 57 unique OTUs. Samples from the 1m from marsh edge category had the highest number of detected OTUs at 203, followed by the 0m samples at 193 and the 10m samples at 185 (Table 4.7). The 5m from marsh edge samples had the lowest number of OTUs of the four distance categories at 174. The lowest number of shared OTUs was between the 0m and 5m samples at 119 OTUs, followed by those shared between the 0m and 10m samples at 122 OTUs. The highest number of shared OTUs was between the 0m and 1m samples at 145 OTUs, followed by the OTUs shared between the 1m and 10m samples at 137 OTUs. The 0m samples contained 87 of the 88 frequent group OTUs, while the 1m samples contained all 88 of these OTUs (Table 4.8). The 5m and 10m samples contained 85 and 86 of the frequent group OTUs, respectively.

Table 4.7. Shared and total number of OTUs for samples from the different distances from the marsh edge (meters). All samples were collected from marsh sites in Barataria and Caillou Bays during July 2018.

	Zero	One	Five	Ten
Zero	193	145	119	122
One		203	139	137
Five			174	130
Ten				185

The intersection of a single category (such as Zero-Zero) is the total number of OTUs for that bay, while the intersection of 2 categories (such as Zero-One) is the number of OTUs shared between these two categories.

Taxa Bar Plots:

Because the only OTU that was given an ambiguous assignment at the phylum level in the SILVA database was given an assignment of Platyhelminthes at the phylum level in the GenBank database, this OTU was grouped with the other Platyhelminthes for the taxa bar plots. Nematodes, arthropods, and annelids were present in all samples in the dataset (Fig. 4.14). Platyhelminthes, rotifers, and mollusks were present in nearly all samples. Gastrotrichs and bryozoans were more commonly detected in the Low salinity zone samples than in the Mid or High, while kinorhynchans were entirely absent from the Low salinity zone samples and were most commonly detected in the High salinity zone samples. Members of the phyla Nemertea, Tardigrada, Xenacoelomorpha, and Calcinea were rarely detected in samples. Samples contained an average of 8 ± 1 phyla, with a range of 5 to 10 phyla.

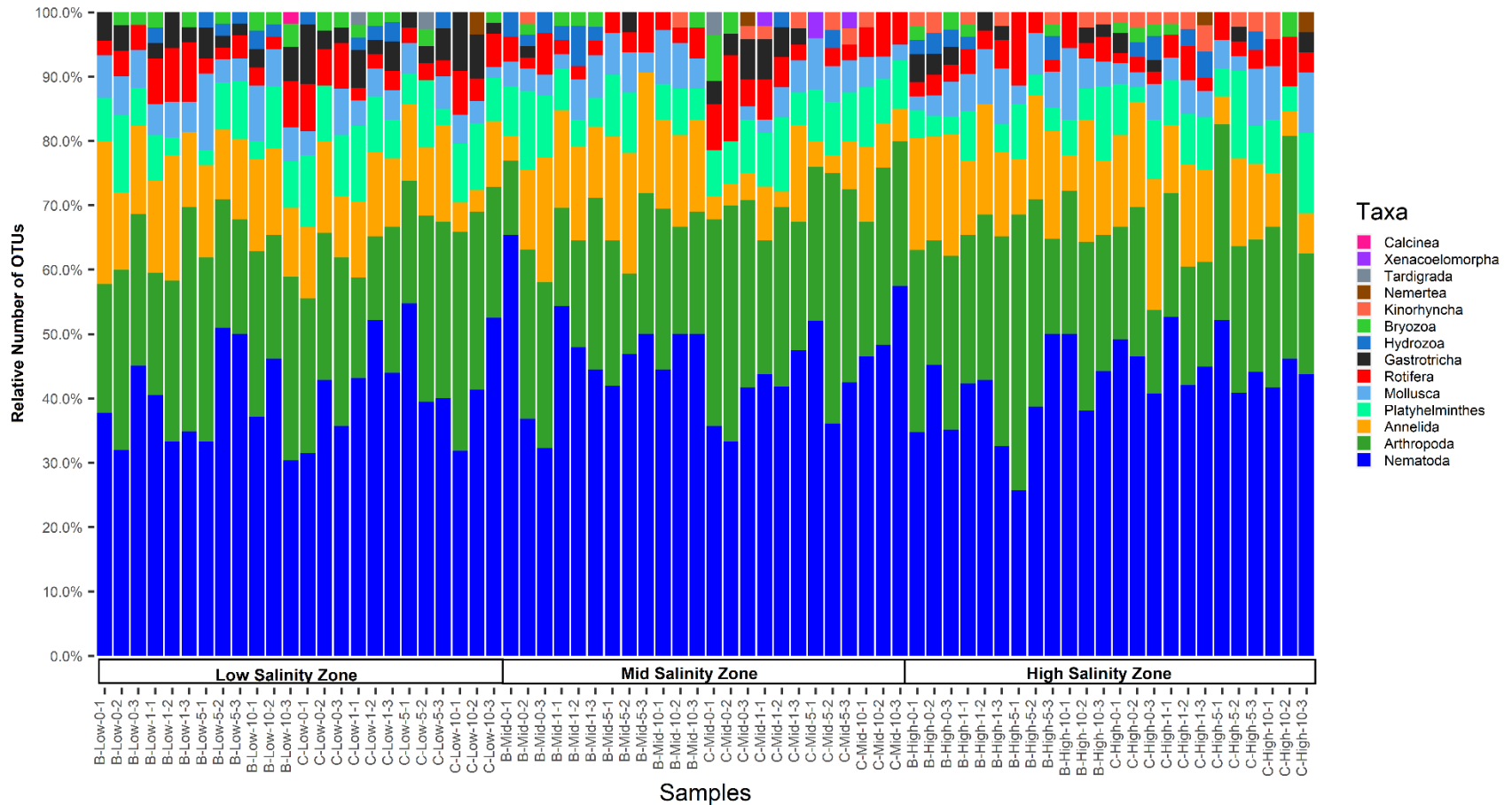


Fig. 4.14. Taxa bar plots of the 72 samples collected from the salinity zones of Barataria and Caillou Bays during July 2018, with each colored section of the bar representing the relative proportion of the OTUs belonging to different phyla within that sample. Phyla are sorted within each bar by the overall highest to lowest relative percentage (from top to bottom). All samples were collected in July 2018 from marsh sites. For the x axis, samples are labelled as B (Barataria) or C (Caillou), and Low, Mid, and High for the salinity zones. The number following the salinity zone designation indicates the distance from the edge of the marsh, designated as 0, 1, 5, or 10 meters, followed by the transect replicate number.

Biodiversity within phyla:

The phylum Nematoda made up the largest percentage of the 2993 incidences in the dataset, followed by Arthropoda, Annelida, Platyhelminthes, Mollusca, Rotifera, Gastrotricha, and other taxa (Fig. 4.14). Nematoda also made up the largest percentage of the OTU richness in the dataset, followed by Arthropods, Annelida, Platyhelminthes, Gastrotricha, Mollusca, Rotifera, and other taxa (Fig. 4.15). Lowest level assignments for metazoan OTUs from the SILVA database ranged from ambiguous at the sub-kingdom level to species level assignments (Table 4.8). Accuracy of species level assignments is limited by both the resolution power of the 18S rRNA gene and by the presence of taxa from this environment in databases, so closely related species should be considered when looking at the species level assignment. The most common OTU in the dataset was assigned in the SILVA database to the rotifer *Octotrocha speciosa* (detected in 99% of samples), followed by an OTU assigned to the arthropod *Chrysops niger* (96% of samples) and an OTU assigned to the nematode *Spirinia parasitifera* (94% of samples). The 88 frequent group OTUs, which were detected in more than 10 samples, were detected in a range of 11 to 71 samples. Of these 88 OTUs, 38 belonged to phylum Nematoda, 19 were Arthropoda, 12 were Annelida, 7 were Platyhelminthes, 3 were Mollusca, 2 each belonged to Bryozoa, Gastrotricha, and Rotifera, and 1 each belonged to Hydrozoa, Kinorhyncha, and Ambiguous taxa. Of the 38 nematode OTUs in the frequent group, 9 were assigned to the order Enoplida, 8 were assigned to the order Monhysterida, 7 were assigned to the order Tylenchida, 4 each were assigned to the orders Chromadorida and Dorylamida, 2 each were assigned to the orders Desmodorida and Plectida, and 1 each was assigned to the orders Areolamida and Rhabditida. Nine of the arthropod frequent group OTUs belonged to the crustacean orders Podocopida, Harpacticoida, Decapoda, and Tanaidacea, 5 belonged to the insect order Diptera, 3 OTUs belonged to the Collembola orders Symphypleona and Entomobryomorpha, with an additional ambiguous Collembola OTU, and a final OTU was assigned an ambiguous member of the Acari. Of the 12 annelid OTUs in the frequent group, half were assigned as the oligochaete order Haplotaxida, 3 were assigned as the polychaete order Phyllodocida, and a final 3 were assigned as the polychaete order Spionida. The 7 Platyhelminthes OTUs which were in the frequent group were mostly assigned to the order Rhabdocoela, with one OTU assigned to the order Macrostomida and one assigned to the class Catenulida. Both of the frequent group Gastrotrich OTUs were assigned to the order Chaetonotida. The two Bryozoa OTUs in the frequent group were assigned to the orders Ctenostomatida and Plumatellida. The two OTUs in the frequent group which fell under Rotifera were assigned to the orders Flosculariaceae and Ploimida. The only hydrozoan in the frequent group was assigned to the order Limnomedusae, while the only kinorhynch OTU in the frequent group was assigned to the order Cyclorhagida. The final OTU in the frequent group was unassigned at the phylum level in the SILVA database.

The SILVA and GenBank assignments usually agreed, but the GenBank assignments frequently were more specific in terms of taxonomic level than the SILVA assignments. Twenty-three of the 88 frequent group OTUs received a more specific assignment from the GenBank database. Notably, the only OTU which received an ambiguous assignment at the sub-kingdom level was both common in the dataset (appeared in 63% of samples) and was assigned to a genus in the phylum Platyhelminthes using the GenBank database. This genus, *Macrostomum*, was assigned to another common OTU in the dataset, so it is unclear why this OTU did not receive the same assignment using the SILVA database. This OTU matched to 27 GenBank entries for the genus *Macrostomum* at 100% query coverage and percent identity, which may indicate an issue with the ability of the 18S gene at the location specified by the primers to differentiate between species in this genus. Three of the frequent group OTUs were unique to the Low salinity zone samples, including OTUs assigned to an ambiguous member of the nematode order Enoplida (GenBank: *Prismatolaimus* sp.), the nematode *Eumonhystera filiformis* (GenBank: *Eumonhystera filiformis*), and the Platyhelminthes species *Rhynchoscolex simplex* (GenBank: *Rhynchoscolex simplex*). None of the frequent group OTUs were unique to the Mid or High salinity zone samples, nor were any of the frequent group OTUs unique in either of the bays or in any of the distance from marsh edge categories. However, of the nine frequent group OTUs which were absent from the Low salinity zone, five were twice as likely to appear in High salinity zone samples as Mid salinity zone samples. These OTUs included an OTU assigned to the nematode *Meloidogyne spartinae* (GenBank: *Meloidogyne spartinae*), a nematode assigned to the genus *Prochaetosoma* (GenBank: *Prochaetosoma* sp.), an OTU assigned to an ambiguous kinorhynch (GenBank: *Echinoderes* sp.), an OTU assigned the annelid *Alitta succinea* (GenBank: *Alitta succinea*), and an OTU assigned to the platyhelminth *Macrostomum kepneri* (GenBank: *Macrostomum kepneri*). In addition, 75 of the infrequent group OTUs were unique to the Low salinity zone samples, followed by 35 OTUs unique to the Mid salinity zone samples and 41 OTUs unique to the High salinity zone samples.

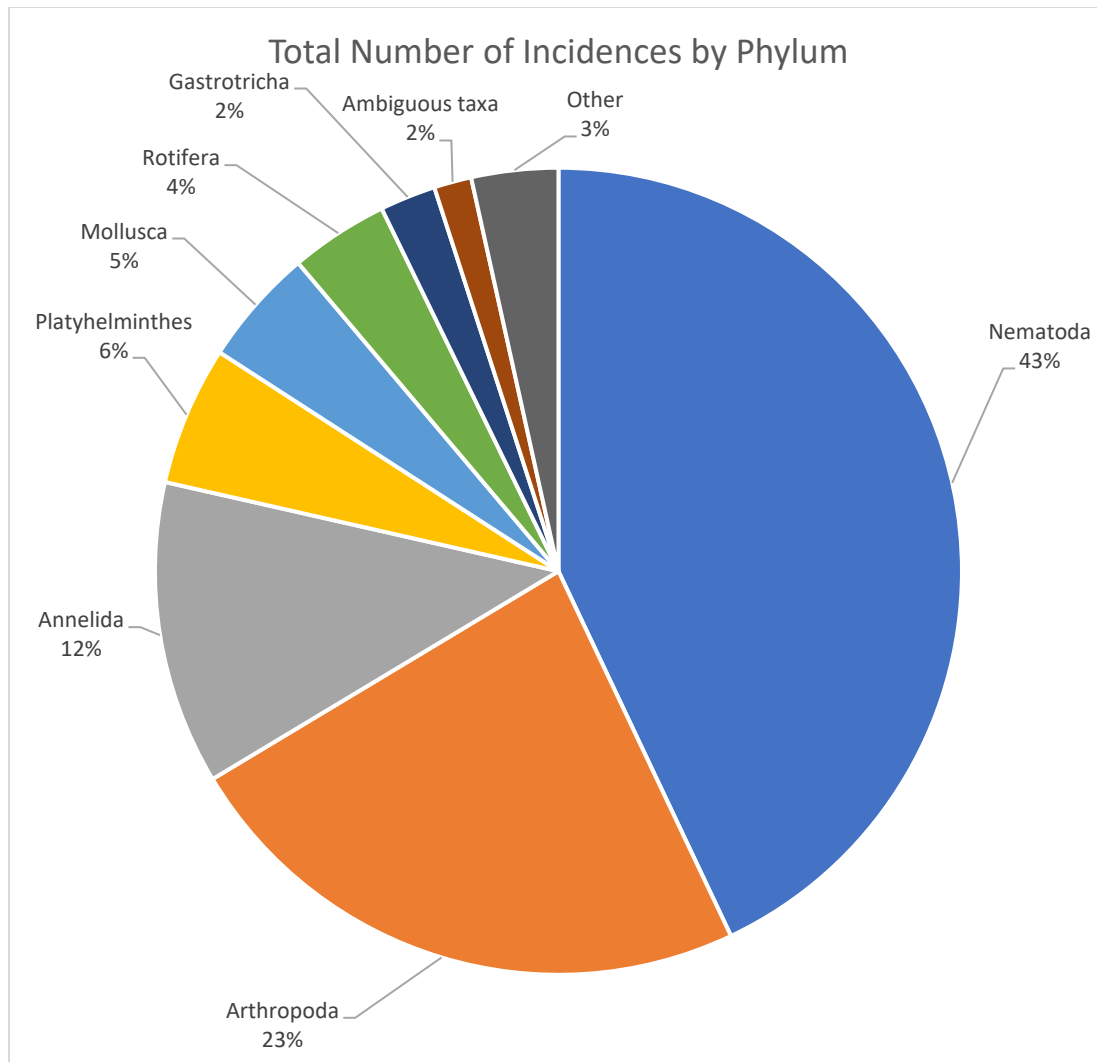


Fig. 4.15. Percentage of the 2,993 total OTU incidences by phylum level OTU assignment in samples collected from marsh sites in Barataria and Caillou Bays during July 2018. Phyla which individually made up less than 1% of the total incidence were combined into the “Other” category, which included the phyla Hydrozoa, Bryozoa, Kinorhyncha, Nemertea, Tardigrada, Xenacoelomorpha, and Calcinea.

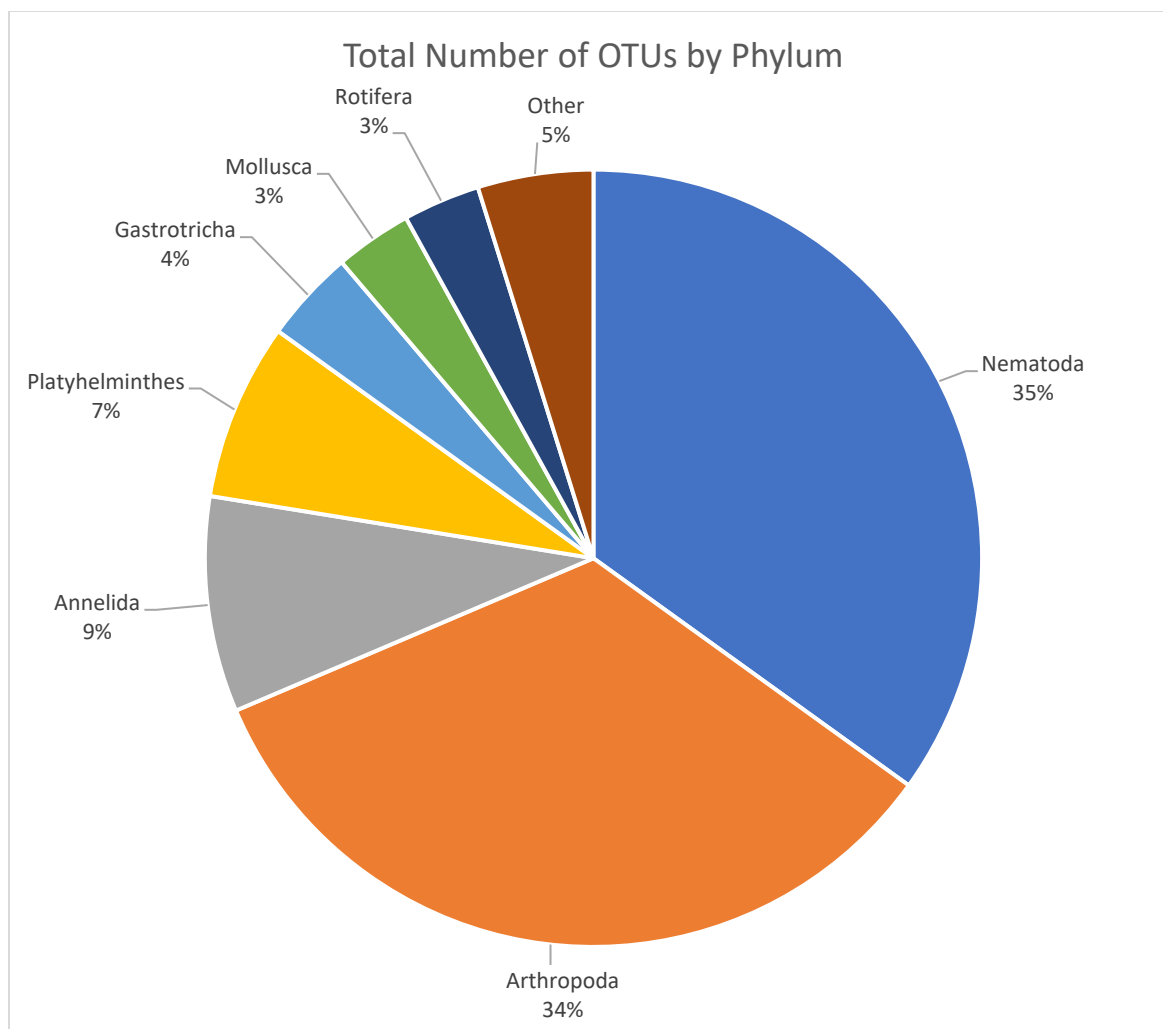


Fig. 4.16. Percentage of the 312 total OTUs per phylum assignment in samples collected from marsh sites in Barataria and Caillou Bays during July 2018. Phyla which individually made up less than 1% of the total OTUs were combined into the “Other” category, which included Hydrozoa, Nemertea, Bryozoa, Kinorhyncha, Xenacoelomorpha, Ambiguous taxa, Calcinea, and Tardigrada.

Table 4.8. Assignment of OTUs to phyla, orders and the lowest feasible level and OTU incidence for the SILVA taxonomic assignment (97% similarity minimum), sorted by the total incidence in each phylum. All samples were collected from marsh sites in Barataria and Caillou Bays during July 2018.

Phylum	Order	Total Incidence	Lowest SILVA assignment	Top GenBank Match	Percent Identity	Accession	C	B	L	M	H	0m	1m	5m	10m
Ambiguous taxa	-	45	Ambiguous metazoan	<i>Macrostromum lignano</i> isolate Egger et al. 2015	100.00%	MN421938.1	27	18	13	15	17	10	12	11	12
Annelida	Haplotaxida	63	<i>Monopylephorus rubroniveus</i>	<i>Monopylephorus rubroniveus</i>	100.00%	GQ355436.1	31	32	22	18	23	13	15	17	18
Annelida	Spionida	43	<i>Paraprionospio patiens</i>	<i>Streblospio benedicti</i> isolate StBe-01	100.00%	KC686673.1	14	29	9	17	17	15	11	11	6
Annelida	Haplotaxida	37	<i>Marionina sublitoralis</i>	<i>Marionina sublitoralis</i>	98.68%	AY365458.1	5	32	14	12	11	6	11	10	10
Annelida	Haplotaxida	36	<i>Marionina coatesae</i>	<i>Marionina coatesae</i> isolate CE136	100.00%	GU901922.1	10	26	13	12	11	10	11	6	9
Annelida	Haplotaxida	34	Haplotaxida; Ambiguous_taxa	<i>Thalassodrilides ineri</i>	100.00%	AF411905.1	18	16	12	7	15	12	13	5	4
Annelida	Haplotaxida	24	<i>Paranaeis litoralis</i>	<i>Paranaeis litoralis</i> isolate PARIHBMD	100.00%	MK076299.1	13	11	18	2	4	6	6	7	5
Annelida	Spionida	18	<i>Boccardiella hamata</i>	<i>Boccardiella hamata</i> isolate NIBRIV0000866080	98.69%	MT482712.1	7	11	3	4	11	7	6	2	3
Annelida	Spionida	16	<i>Polydora brevipalpa</i>	<i>Polydora lingshuiensis</i> isolate	99.34%	MG767309.1	5	11	2	5	9	9	3	3	1
Annelida	Phyllodocida	14	<i>Alitta succinea</i>	<i>Alitta succinea</i> isolate AISu-02	100.00%	KC686631.1	6	8	0	1	13	6	5	2	1
Annelida	Haplotaxida	13	<i>Marionina southerni</i>	<i>Marionina nothachaeta</i> clone LM225	99.34%	JN799906.1	8	5	9	4	0	2	3	3	5
Annelida	Phyllodocida	11	<i>Dendronereis aestuarina</i>	<i>Dendronereis aestuarina</i> isolate dea184	97.39%	KT900288.1	5	6	10	1	0	1	4	3	3
Annelida	Phyllodocida	11	<i>Namalycastis jaya</i>	<i>Namalycastis abiuma</i> isolate naa185	100.00%	KT900289.1	4	7	0	6	5	2	3	3	3
Annelida	Haplotaxida	9	<i>Enchytraeus japonensis</i>	<i>Enchytraeus japonensis</i> isolate CE881	100.00%	GU901875.1	5	4	5	3	1	1	6	2	0
Annelida	Haplotaxida	7	<i>Rheomorpha neiswestonovae</i>	<i>Rheomorpha neiswestonovae</i>	99.34%	AY527049.1	4	3	6	1	0	2	1	2	2
Annelida	Spionida	5	Spionida; uncultured metazoan	<i>Eteone pacifica</i> voucher SMNH 124053	100.00%	MG254394.1	2	3	1	2	2	2	2	1	0
Annelida	Haplotaxida	4	<i>Tubifex</i> sp	<i>Limnodrilus udekemianus</i> voucher CE2127	100.00%	KY636908.1	1	3	4	0	0	0	0	1	3
Annelida	Polychaeta incertae sedis	4	<i>Mesonerilla roscovita</i>	<i>Mesonerilla</i> cf. fagei kw291	97.39%	MK579424.1	0	4	4	0	0	3	1	0	0
Annelida	Haplotaxida	2	Haplotaxida; Ambiguous_taxa	<i>Inanidrilus exumae</i> isolate CE73	99.34%	MF991275.1	2	0	0	0	2	1	1	0	0

(table cont'd.)

Phylum	Order	Total Incidence	Lowest SILVA assignment	Top GenBank Match	Percent Identity	Accession	C	B	L	M	H	0m	1m	5m	10m
Annelida	Haplotaxida	2	<i>Paranais litoralis</i>	<i>Paranais litoralis</i> isolate PARIHBMD	97.32%	MK076299.1	1	1	1	0	1	0	0	2	0
Annelida	Sabellida	2	<i>Manayunkia aestuarina</i>	<i>Manayunkia aestuarina</i>	98.60%	HM042108.1	1	1	0	0	2	0	1	1	0
Annelida	Scolecida	2	<i>Barantolla lepte</i>	<i>Notomastus sunae</i> voucher TIO-BTS-Poly 118	98.03%	MT055861.1	1	1	0	0	2	2	0	0	0
Annelida	Haplotaxida	1	<i>Gordiodrilus elegans</i>	<i>Gordiodrilus elegans</i>	99.34%	HQ728879.1	1	0	1	0	0	0	0	1	0
Annelida	Haplotaxida	1	<i>Limnodriloides barnardi</i>	<i>Alexandrovina onegensis</i> voucher CE4913	100.00%	KY636909.1	1	0	1	0	0	0	1	0	0
Annelida	Haplotaxida	1	<i>Marionina sublitoralis</i>	<i>Marionina sublitoralis</i>	97.37%	AY365458.1	0	1	0	1	0	0	0	1	0
Annelida	Haplotaxida	1	<i>Monopylephorus rubroniveus</i>	<i>Monopylephorus rubroniveus</i>	100.00%	GQ355436.1	1	0	0	0	1	1	0	0	0
Annelida	Haplotaxida	1	<i>Tubificoides heterochaetus</i>	<i>Tubificoides heterochaetus</i> isolate CE2447	100.00%	HM460009.1	1	0	1	0	0	1	0	0	0
Annelida	Sabellida	1	<i>Manayunkia aestuarina</i>	<i>Manayunkia aestuarina</i>	97.37%	HM042108.1	1	0	0	0	1	0	0	1	0
Annelida	Spionida	1	<i>Boccardiella hamata</i>	<i>Boccardiella hamata</i> isolate NIBRIV0000866080	98.43%	MT482712.1	1	0	0	0	1	1	0	0	0
Total Annelida OTUS	28	364	-	-	-	-	149	215	136	96	132	103	104	84	73
Arthropoda	Diptera	69	<i>Chrysops niger</i> (black deer fly)	<i>Chrysops niger</i>	98.03%	AF073889.1	33	36	24	23	22	18	16	17	18
Arthropoda	Diptera	57	<i>Haematopota pluvialis</i>	<i>Haematopota pluvialis</i>	98.03%	KC177294.1	28	29	19	19	19	15	12	15	15
Arthropoda	Diptera	45	<i>Hermetia illucens</i>	<i>Tabanus</i> sp. CP2_1	96.03%	MK714120.1	20	25	17	14	14	12	11	12	10
Arthropoda	Diptera	39	<i>Haematopota pluvialis</i>	<i>Tabanus nigrovittatus</i>	100.00%	KU321600.1	20	19	10	14	15	12	9	6	12
Arthropoda	Symphyleon a	34	<i>Sminthurides aquaticus</i>	Katiannidae sp. R36	100.00%	KY554632.1	17	17	8	6	20	6	7	9	12
Arthropoda	-	31	Acari; Ambiguous_taxa	<i>Neoribates aurantiacus</i> voucher BMOC 17-0901-037	99.34%	MK014977.1	13	18	13	7	11	8	9	9	5
Arthropoda	Harpacticoida	31	<i>Nitokra hibernica</i>	<i>Nitokra hibernica</i>	98.04%	EU380305.1	14	17	16	11	4	5	9	7	10
Arthropoda	Harpacticoida	30	<i>Leptocaris brevicornis</i>	<i>Leptocaris brevicornis</i> voucher LEGO-HAR017	98.03%	KR048734.1	14	16	7	12	11	10	9	6	5
Arthropoda	Symphyleon a	23	<i>Sminthurides aquaticus</i>	<i>Sminthurides schoetti</i> isolate 5G1b1_JC463	97.39%	KY230781.1	9	14	8	12	3	6	7	6	4
Arthropoda	Podocopida	19	<i>Howeina</i> sp SN004	<i>Howeina</i> sp. SN004	98.68%	AB076626.1	10	9	2	5	12	7	6	4	2
Arthropoda	Podocopida	16	<i>Cytheromorpha acupunctata</i>	<i>Cytheromorpha acupunctata</i>	98.03%	AB076630.1	10	6	2	6	8	3	4	6	3
Arthropoda	Podocopida	15	Cyprididae gen sp Mexico	<i>Cypridopsis</i> sp. Ca1 isolate CYD_SMA1	100.00%	MF076784.1	1	14	10	5	0	4	4	4	3

(table cont'd.)

Phylum	Order	Total Incidence	Lowest SILVA assignment	Top GenBank Match	Percent Identity	Accession	C	B	L	M	H	0m	1m	5m	10m
Arthropoda	Entomobryomorpha	14	<i>Cryptopygus sverdrupi</i>	<i>Isotoma viridis</i> isolate 6G1a1_JC448	100.00%	KY230774.1	8	6	10	4	0	2	4	4	4
Arthropoda	-	13	Collembola; Ambiguous_taxa	Dicyrtomidae sp. R3	99.34%	KY554638.1	6	7	8	5	0	1	5	5	2
Arthropoda	Decapoda	13	<i>Carcinus maenas</i> (green crab)	<i>Inachus aguiarii</i> voucher ULLZ 11667	100.00%	MK285641.1	6	7	3	1	9	3	3	4	3
Arthropoda	Podocopida	12	<i>Cypria</i> sp QY-2003	<i>Physocypria</i> cf. <i>biwaensis</i> 32 IK-2017	98.03%	KX940960.1	3	9	9	3	0	6	1	1	4
Arthropoda	Tanaidacea	12	<i>Tanais dulongii</i>	<i>Tanais dulongii</i>	100.00%	AY781428.1	7	5	2	3	7	6	5	0	1
Arthropoda	Diptera	11	Diptera; Ambiguous_taxa	<i>Camptodiplosis auriculariae</i> voucher JSC52	100.00%	MG684576.1	4	7	4	4	3	6	1	1	3
Arthropoda	Harpacticoida	11	<i>Leptocaris brevicornis</i>	<i>Leptocaris brevicornis</i> voucher LEGO-HAR017	98.68%	KR048734.1	3	8	3	3	5	3	3	4	1
Arthropoda	Diptera	10	Diptera; invertebrate environmental sample	<i>Culicoides scoticus</i>	95.39%	FN263322.1	7	3	0	4	6	2	0	5	3
Arthropoda	Trombidiformes	10	Eupodidae sp AMUENV025	Eupodidae sp. AMUENV025	97.37%	GQ864273.1	2	8	3	6	1	2	3	2	3
Arthropoda	Hemiptera	9	<i>Paraliburnia adela</i>	<i>Nilaparvata lugens</i>	100.00%	XR_002606755.1	6	3	4	3	2	1	1	3	4
Arthropoda	Mesostigmata	8	<i>Gamasellodes adrianae</i>	<i>Blattisocius keegani</i>	99.34%	MH916618.1	5	3	2	4	2	0	4	3	1
Arthropoda	Isoptera	7	Isoptera; Ambiguous_taxa	Uncultured eukaryote clone PUDS-432	100.00%	JN147503.1	4	3	4	2	1	3	3	1	0
Arthropoda	Podocopida	7	<i>Cypridopsis vidua</i>	<i>Cypridopsis</i> sp. Ca3 isolate CYP_EXP	100.00%	MF076771.1	7	0	6	1	0	3	3	1	0
Arthropoda	-	6	Collembola; Ambiguous_taxa	<i>Micranurida pygmaea</i> isolate 5F1a1_JC352	99.34%	KY230723.1	2	4	2	4	0	2	3	1	0
Arthropoda	Podocopida	6	Podocopida; Ambiguous_taxa	<i>Darwinula</i> sp. QY-2003	100.00%	AY191456.1	4	2	4	0	2	0	3	1	2
Arthropoda	Poduromorpha	6	<i>Xenylla grisea</i>	<i>Xenylla boernerii</i> isolate 2F1a1_JC361	100.00%	KY230728.1	6	0	1	2	3	0	3	2	1
Arthropoda	Ephemeroptera	5	Ephemeroptera; Ambiguous_taxa	<i>Clypeocaenis</i> sp. BYU IGCEP131	100.00%	GQ118265.1	1	4	3	0	2	0	2	2	1
Arthropoda	Trombidiformes	5	<i>Acarothrix</i> sp ARP-2015	<i>Acarothrix</i> sp. ARP-2015 isolate AC22	100.00%	KP276481.1	2	3	2	1	2	3	1	0	1
Arthropoda	-	4	Acari; Ambiguous_taxa	<i>Sancassania berleseii</i>	100.00%	GQ864331.1	2	2	3	0	1	2	0	1	1
Arthropoda	Diptera	4	<i>Culex chidesteri</i>	<i>Culex renatoi</i> partial	100.00%	HE600020.1	3	1	2	1	1	1	3	0	0
Arthropoda	Diptera	4	<i>Megaselia scalaris</i>	<i>Megaselia scalaris</i>	100.00%	KC177299.1	4	0	0	2	2	1	1	1	1
Arthropoda	Diptera	4	<i>Minettia flaveola</i>	Uncultured eukaryote	93.42%	LN576160.1	2	2	0	1	3	2	0	1	1
Arthropoda	Diptera	4	<i>Thaumatomyia notata</i>	<i>Thaumatomyia notata</i>	98.03%	KC177306.1	2	2	0	2	2	0	1	2	1

(table cont'd.)

Phylum	Order	Total Incidence	Lowest SILVA assignment	Top GenBank Match	Percent Identity	Accession	C	B	L	M	H	0m	1m	5m	10m
Arthropoda	Cyclopoida	3	<i>Macrocyclus albidus</i>	<i>Macrocyclus albidus</i> voucher N381DZMB	100.00%	MK370209.1	3	0	3	0	0	2	0	0	1
Arthropoda	Diptera	3	Diptera; Ambiguous_taxa	<i>Camptodiplosis auriculariae</i> voucher JSC52	98.41%	MG684576.1	0	3	1	0	2	1	1	1	0
Arthropoda	Diptera	3	Diptera; Ambiguous_taxa	<i>Psorophora ferox</i>	98.68%	AY988442.1	2	1	2	1	0	1	1	0	1
Arthropoda	Diptera	3	<i>Culex brethesi</i>	<i>Culex brethesi</i> partial	99.34%	HE600017.1	0	3	0	1	2	0	2	1	0
Arthropoda	Entomobryomorpha	3	<i>Isotomurus</i> sp cei5	<i>Isotomurus</i> sp. cei5	100.00%	KX351376.1	0	3	2	1	0	0	0	2	1
Arthropoda	Harpacticoida	3	<i>Bradya</i> sp Greenland-RJH-2004	Harpacticoida sp. 8641009	98.03%	KX070241.1	2	1	3	0	0	0	0	0	3
Arthropoda	Lepidoptera	3	Ambiguous_taxa	<i>Ostrinia furnacalis</i> haplotype 11	100.00%	MK987117.1	1	2	2	0	1	1	1	0	1
Arthropoda	Podocopida	3	Ambiguous_taxa	<i>Leptocythere lacertosa</i>	100.00%	AB076631.1	2	1	0	0	3	1	1	1	0
Arthropoda	Sarcoptiformes	3	<i>Pheroliodes</i> sp PP-2016	<i>Masthermannia</i> sp. AD1256 voucher UMMZ BMOC 08-0515-049 AD1256	100.00%	KY922217.1	3	0	3	0	0	0	2	1	0
Arthropoda	Sarcoptiformes	3	<i>Sellea</i> sp AD658	<i>Sellea</i> sp. AD658	100.00%	JQ000060.1	1	2	0	2	1	0	1	1	1
Arthropoda	Symphyleon	3	<i>Papirinus prodigiosus</i>	<i>Bourletiella hortensis</i> isolate 4A1a1_JC284	100.00%	KY230700.1	3	0	3	0	0	0	0	0	3
Arthropoda	Trombidiformes	3	<i>Haplochthonius simplex</i>	<i>Haplochthonius simplex</i> voucher BMOC 07-0607-007	99.34%	KP325062.1	1	2	1	2	0	1	1	0	1
Arthropoda	Coleoptera	2	Coleoptera; Ambiguous_taxa	<i>Carpelimus pusillus</i> voucher BMNH:742887	100.00%	JN619339.1	1	1	0	1	1	2	0	0	0
Arthropoda	Cyclopoida	2	Cyclopoida	<i>Acanthocyclops americanus</i> isolate AG08	99.34%	KP772919.1	1	1	1	0	1	0	0	0	2
Arthropoda	Cyclopoida	2	Cyclopoida; uncultured eukaryote	<i>Microcyclops anceps</i> voucher USNM:1139167	97.37%	HQ008762.1	2	0	2	0	0	1	0	0	1
Arthropoda	Diptera	2	<i>Culicoides variipennis</i>	<i>Culicoides sonorensis</i>	100.00%	LN484108.1	1	1	1	1	0	2	0	0	0
Arthropoda	Diptera	2	<i>Haematopota pluvialis</i>	<i>Tabanus</i> sp. CP2_1	98.48%	MK714120.1	1	1	2	0	0	1	1	0	0
Arthropoda	Diptera	2	Diptera; invertebrate environmental sample	<i>Culicoides scoticus</i>	94.74%	FN263322.1	1	1	0	0	2	1	0	1	0
Arthropoda	Harpacticoida	2	<i>Leptocaris brevicornis</i>	<i>Leptocaris brevicornis</i> voucher LEGO-HAR017	97.39%	KR048734.1	1	1	2	0	0	0	0	1	1
Arthropoda	Oribatida	2	<i>Phauloppia lucorum</i>	<i>Phauloppia lucorum</i>	100.00%	EU432198.1	0	2	1	1	0	0	0	1	1
Arthropoda	Pseudoscorpiones	2	<i>Chelifer cancroides</i>	<i>Chelifer cancroides</i> voucher WAMT130755	100.00%	KT354350.1	1	1	0	1	1	0	0	2	0

(table cont'd.)

Phylum	Order	Total Incidence	Lowest SILVA assignment	Top GenBank Match	Percent Identity	Accession	C	B	L	M	H	0m	1m	5m	10m
Arthropoda	Sarcoptiformes	2	<i>Oulenziella bakeri</i>	<i>Oulenziella bakeri</i> isolate MQ4	99.34%	KM277810.1	1	1	0	1	1	0	0	2	0
Arthropoda	Sarcoptiformes	2	<i>Schusteria littorea</i>	<i>Fortuynia churaumi</i> voucher JP76_F_07	100.00%	MN372433.1	1	1	0	1	1	1	1	0	0
Arthropoda	Trombidiformes	2	<i>Rhombognathus levigatoides</i>	<i>Rhombognathus</i> sp. UFMG 173954	100.00%	MK014993.1	2	0	0	2	0	1	1	0	0
Arthropoda	Trombidiformes	2	<i>Tetranychus okinawanus</i>	<i>Tetranychus okinawanus</i>	100.00%	AB926305.1	2	0	2	0	0	0	1	0	1
Arthropoda	-	1	Acari; Ambiguous_taxa	<i>Eotetranychus quercifoliae</i> strain: Eotque0507	97.78%	AB926267.1	1	0	0	0	1	0	0	0	1
Arthropoda	-	1	Acari; Ambiguous_taxa	<i>Pergalumna</i> cf. <i>nervosa</i> BMOC 17-0901-036	100.00%	MK014976.1	0	1	0	1	0	0	1	0	0
Arthropoda	-	1	Acari; uncultured eukaryote	<i>Punctoribates punctum</i>	99.34%	MH198175.1	0	1	0	1	0	0	1	0	0
Arthropoda	Acarida	1	<i>Czenspinksia</i> sp DL-2014	<i>Czenspinksia</i> sp. DL-2014 isolate MQ8	100.00%	KM277816.1	0	1	1	0	0	0	0	1	0
Arthropoda	Coleoptera	1	Coleoptera; Ambiguous_taxa	Heterocerinae sp. UPOL RK0661	98.05%	KX093031.1	0	1	0	0	1	0	0	1	0
Arthropoda	Coleoptera	1	<i>Hydrochara affinis</i>	<i>Enochrus ochraceus</i> isolate SLE0248	100.00%	KC935036.1	0	1	1	0	0	0	0	0	1
Arthropoda	Coleoptera	1	<i>Lissorhoptrus</i> sp DDM-2009	<i>Oophthalmus</i> sp. BMNH668165	98.68%	DQ337154.1	1	0	1	0	0	0	0	0	1
Arthropoda	Coleoptera	1	<i>Melanophthalma</i> sp 1 NPL-2007	<i>Melanophthalma</i> sp. 1 NPL-2007	98.03%	EU164632.1	1	0	1	0	0	0	0	1	0
Arthropoda	Cyclopoida	1	<i>Apocyclops borneoensis</i>	<i>Apocyclops panamensis</i> voucher N386DZMB	99.34%	MK370202.1	0	1	1	0	0	1	0	0	0
Arthropoda	Decapoda	1	<i>Carcinus maenas</i> (green crab)	Eriphiidae sp. BPX-2007	96.71%	EU284155.1	1	0	0	0	1	1	0	0	0
Arthropoda	Diptera	1	Diptera; Ambiguous_taxa	<i>Ochlerotatus sollicitans</i>	100.00%	AY988435.1	1	0	0	0	1	0	0	0	1
Arthropoda	Diptera	1	<i>Chrysops niger</i> (black deer fly)	<i>Chrysops niger</i>	100.00%	AF073889.1	0	1	0	0	1	0	1	0	0
Arthropoda	Diptera	1	<i>Coquillettidia perturbans</i>	<i>Culiseta melanura</i>	95.10%	AY988453.1	1	0	1	0	0	0	0	0	1
Arthropoda	Diptera	1	<i>Haematopota pluvialis</i>	<i>Tabanus</i> sp. CP2_1	99.34%	MK714120.1	0	1	0	0	1	1	0	0	0
Arthropoda	Diptera	1	<i>Haematopota pluvialis</i>	<i>Tabanus</i> sp. CP2_1	100.00%	MK714120.1	1	0	0	1	0	0	0	1	0
Arthropoda	Diptera	1	<i>Haematopota pluvialis</i>	<i>Tabanus</i> sp. CP2_1	99.29%	MK714120.1	1	0	0	1	0	1	0	0	0
Arthropoda	Diptera	1	Diptera; invertebrate environmental sample	<i>Culicoides pulicaris</i> partial isolate	96.05%	FN263323.1	1	0	1	0	0	0	0	1	0
Arthropoda	Entelegynae	1	<i>Pardosa pseudoannulata</i>	<i>Varacosa gosiuta</i> isolate ARAPS000119	100.00%	KY016531.1	1	0	1	0	0	0	1	0	0

(table cont'd.)

Phylum	Order	Total Incidence	Lowest SILVA assignment	Top GenBank Match	Percent Identity	Accession	C	B	L	M	H	0m	1m	5m	10m
Arthropoda	Entelegynae	1	<i>Pteroneta</i> cf saltans MR368	<i>Pteroneta</i> cf. saltans MR368 isolate ARAMR000368	99.34%	KY016345.1	1	0	0	1	0	0	0	1	0
Arthropoda	Entelegynae	1	<i>Scotinella</i> sp SP94	<i>Scotinella</i> sp. SP94 isolate ARASP000094	97.37%	KY016616.1	0	1	1	0	0	0	1	0	0
Arthropoda	Entomobryomorpha	1	<i>Cyphoderus javanus</i>	<i>Tetracanthella</i> sp. YB-2012 voucher Gao 0903	98.04%	JN981025.1	1	0	0	0	1	1	0	0	0
Arthropoda	Entomobryomorpha	1	<i>Lepidocyrtus</i> sp 2 FZ-2013	<i>Lepidocyrtus</i> sp. 2 FZ-2013	100.00%	KC236249.1	1	0	1	0	0	0	0	1	0
Arthropoda	Harpacticoida	1	<i>Lourinia armata</i>	<i>Lourinia armata</i> voucher LEGO-HAR030	97.79%	KR048739.1	0	1	0	0	1	0	1	0	0
Arthropoda	Harpacticoida	1	<i>Nitokra spinipes</i>	<i>Nitokra spinipes</i> strain CCUMP 40	100.00%	JQ315748.1	1	0	0	0	1	1	0	0	0
Arthropoda	Harpacticoida	1	<i>Paramenophia</i> sp New Caledonia-RJH-2007	<i>Paramenophia</i> sp. New Caledonia-RJH-2007	98.68%	EU380300.1	1	0	0	1	0	1	0	0	0
Arthropoda	Hemiptera	1	<i>Cedusa</i> sp JMU-2006	<i>Cedusa</i> sp. JMU-2006 isolate DER02	100.00%	DQ532518.1	1	0	1	0	0	1	0	0	0
Arthropoda	Hemiptera	1	<i>Mesoveliidae</i> sp YW-2014	<i>Mesoveliidae</i> sp. YW-2014	99.34%	KJ461234.1	0	1	0	1	0	0	1	0	0
Arthropoda	Hemiptera	1	<i>Onymcoris izzardi</i>	<i>Dalpada</i> sp. SY-2015	100.00%	KJ535892.1	0	1	0	0	1	0	1	0	0
Arthropoda	Hymenoptera	1	Hymenoptera; Ambiguous_taxa	<i>Nylanderia fulva</i>	100.00%	XR_003822572.1	1	0	0	1	0	0	0	0	1
Arthropoda	Hymenoptera	1	<i>Cynipencyrtus</i> sp D2655	<i>Cynipencyrtus</i> sp. D2655 voucher UCRC_ENT	97.37%	JN623500.1	0	1	1	0	0	0	0	0	1
Arthropoda	Isoptera	1	Isoptera; Ambiguous_taxa	Uncultured eukaryote clone PUDS-432	97.35%	JN147503.1	1	0	1	0	0	0	0	0	1
Arthropoda	Odonata	1	Odonata; Ambiguous_taxa	<i>Pseudagrion</i> sp. BOLD:ACG1528 voucher MDFRC_OD0007	100.00%	KP697661.1	1	0	1	0	0	1	0	0	0
Arthropoda	Orthoptera	1	Batrachideidae gen sp	<i>Batrachideidae</i> sp. nuclear (partial)	100.00%	Z97631.1	0	1	1	0	0	0	0	1	0
Arthropoda	Podocopida	1	Podocopida; environmental sample	<i>Krithe</i> sp. 1 HY-2019 voucher Kuril03 Fe	98.43%	MK584861.1	1	0	0	1	0	1	0	0	0
Arthropoda	Podocopida	1	<i>Mungava</i> sp SH-2016	<i>Mungava</i> sp. SH-2016	100.00%	LC169518.1	1	0	0	1	0	1	0	0	0
Arthropoda	Podocopida	1	<i>Paracypria</i> sp SH-2014b	<i>Paracypria plumosa</i>	98.68%	AB920551.1	1	0	1	0	0	1	0	0	0
Arthropoda	Poduromorpha	1	<i>Xenylla grisea</i>	<i>Xenylla grisea</i>	97.37%	AY555517.1	1	0	0	0	1	0	1	0	0
Arthropoda	Psocoptera	1	<i>Liposcelis bostrychophila</i>	<i>Liposcelidae</i> sp. B1763	97.37%	AY900135.1	1	0	0	0	1	0	0	1	0
Arthropoda	Sarcoptiformes	1	<i>Aleuroglyphus ovatus</i> (brown legged grain mite)	<i>Aleuroglyphus ovatus</i> voucher UMMZ BMOC 05-0918-003 AD613	100.00%	JQ000109.1	0	1	0	0	1	0	0	0	1
Arthropoda	Sarcoptiformes	1	<i>Crabrovidia</i> sp AD610	<i>Crabrovidia</i> sp. AD610	97.37%	JQ000073.1	1	0	0	0	1	0	0	1	0

(table cont'd.)

Phylum	Order	Total Incidence	Lowest SILVA assignment	Top GenBank Match	Percent Identity	Accession	C	B	L	M	H	0m	1m	5m	10m
Arthropoda	Symphyleon a	1	<i>Sminthurus viridis</i>	<i>Sminthurus viridis</i> isolate 1G1a1_JC293	100.00%	KY230701.1	1	0	0	1	0	0	0	0	1
Arthropoda	Thysanoptera	1	Thysanoptera; Ambiguous_taxa	<i>Frankliniella tritici</i> voucher TH97	100.00%	KC512960.1	1	0	1	0	0	0	0	0	1
Arthropoda	Trombidiform es	1	<i>Cheletomimus</i> <i>wellsi</i>	<i>Cheletomimus wellsii</i> voucher MZSPAC 00024	99.34%	HM070363.1	1	0	0	1	0	0	0	0	1
Arthropoda	Trombidiform es	1	<i>Microtrombidium</i> <i>cooki</i>	<i>Microtrombidium cooki</i> isolate HKP35	100.00%	KM100935.1	0	1	1	0	0	1	0	0	0
Arthropoda	Trombidiform es	1	<i>Recifella</i> sp AP- 2010	<i>Recifella</i> sp. AP-2010 voucher MZSPAC 00008	98.68%	HM070347.1	1	0	1	0	0	0	1	0	0
Total Arthropoda OTUs	105	701	-	-	-	-	347	354	261	217	223	184	180	170	167
Bryozoa	Plumatellida	22	<i>Plumatella</i> <i>casmiana</i>	<i>Plumatella casmiana</i>	100.00%	KT852566.1	11	11	15	5	2	8	6	2	6
Bryozoa	Ctenostomati da	11	<i>Amathia</i> sp n 1 AW- 2014	<i>Amathia</i> sp. n. 1 AW-2016	100.00%	JN680939.1	4	7	1	3	7	5	4	1	1
Total Bryozoa OTUs	2	33	-	-	-	-	15	18	16	8	9	13	10	3	7
Calcinea	Murrayonida	1	<i>Murrayona</i> <i>phanolepis</i>	<i>Lelapiella incrustans</i> specimen voucher G313914	98.03%	AM180969.1	0	1	1	0	0	0	0	0	1
Gastrotricha	Chaetonotida	16	<i>Chaetonotus</i> cf novenarius TK151	<i>Haltidytes pseudosquamosus</i> voucher HA1	99.34%	MN959459.1	10	6	15	0	1	4	4	5	3
Gastrotricha	Chaetonotida	16	<i>Heterolepidoderma</i> sp 1 TK-2012	<i>Heterolepidoderma</i> sp. 1 TK- 2012 voucher TK124	98.03%	JQ798554.1	8	8	5	3	8	6	6	1	3
Gastrotricha	Chaetonotida	8	Chaetonotida; Ambiguous_taxa	<i>Chaetonotus</i> aff. <i>euhystris</i> MK- 2019 voucher TR_8.37	100.00%	MN496214.1	6	2	8	0	0	2	2	1	3
Gastrotricha	Chaetonotida	7	Chaetonotida; Ambiguous_taxa	<i>Dasydytes papaveri</i> voucher TK149	98.68%	JQ798564.1	6	1	1	6	0	3	2	1	1
Gastrotricha	Chaetonotida	5	Chaetonotida; Ambiguous_taxa	<i>Aspidiophorus</i> sp. n. 2 MK-2019 voucher GA_10.5	98.04%	MN496168.1	5	0	1	2	2	4	1	0	0
Gastrotricha	Chaetonotida	4	<i>Heterolepidoderma</i> sp 1 TK-2012	<i>Heterolepidoderma</i> sinus voucher ZH_1.79	98.68%	MK302474.1	2	2	3	1	0	0	3	0	1
Gastrotricha	Chaetonotida	3	Chaetonotida; Ambiguous_taxa	<i>Chaetonotus</i> sp. TK25	98.68%	JQ798593.1	0	3	3	0	0	1	1	1	0
Gastrotricha	Chaetonotida	2	Chaetonotida; Ambiguous_taxa	<i>Chaetonotus</i> aff. <i>subtilis</i> MK- 2019 voucher HA_30.1	98.03%	MN496228.1	2	0	1	0	1	2	0	0	0
Gastrotricha	Chaetonotida	2	Chaetonotida; Ambiguous_taxa	<i>Aspidiophorus</i> sp. n. 2 MK-2019 voucher GA_10.5	98.03%	MN496168.1	0	2	2	0	0	0	0	1	1
Gastrotricha	Chaetonotida	2	<i>Halichaetonotus</i> <i>paradoxus</i>	<i>Halichaetonotus paradoxus</i> voucher TK79	97.40%	JQ798599.1	1	1	1	1	0	1	0	0	1
Gastrotricha	Chaetonotida	1	Chaetonotida; Ambiguous_taxa	Uncultured metazoan clone Ma29_3E_17	98.68%	HM103490.1	1	0	1	0	0	1	0	0	0

(table cont'd.)

Phylum	Order	Total Incidence	Lowest SILVA assignment	Top GenBank Match	Percent Identity	Accession	C	B	L	M	H	0m	1m	5m	10m
Gastrotricha	Chaetonotida	1	Chaetonotida; uncultured eukaryote	<i>Chaetonotus</i> sp. A MK-2019	96.75%	MH425551.1	0	1	0	0	1	0	0	0	1
Total Gastrotricha OTUs	12	67	-	-	-	-	41	26	41	13	13	24	19	10	14
Hydrozoa	Limnomedusae	20	Limnomedusae; Ambiguous_taxa	<i>Pennaria</i> sp. AMN-2009	100.00%	GQ424343.1	9	11	11	4	5	2	9	7	2
Hydrozoa	Leptothecata	10	<i>Helgicirrha cari</i>	<i>Helgicirrha cari</i> isolate MHNG-HYD-DNA1153	100.00%	KY363989.1	4	6	0	2	8	6	3	1	0
Hydrozoa	Anthoathecata	5	Anthoathecata; Ambiguous_taxa	<i>Moerisia inkermanica</i> voucher LEM m3x S41	100.00%	KT722408.1	2	3	1	4	0	2	3	0	0
Total Hydrozoa OTUs	3	35	-	-	-	-	15	20	12	10	13	10	15	8	2
Kinorhyncha	-	24	Cyclorhagida; Ambiguous_taxa	<i>Echinoderes</i> sp. MVS2014	98.65%	LC007048.1	15	9	0	8	16	7	7	5	5
Kinorhyncha	-	1	Cyclorhagida; Ambiguous_taxa	<i>Echinoderes</i> sp. MVS2014	98.43%	LC007048.1	1	0	0	0	1	0	1	0	0
Total Kinorhyncha OTUs	2	25	-	-	-	-	16	9	0	8	17	7	8	5	5
Mollusca	Littorinimorpha	47	<i>Tectarius spinulosus</i>	<i>Diffalaba opiniosa</i> voucher WAM:S103111	99.34%	MN119725.1	22	25	12	17	18	14	13	8	12
Mollusca	-	41	Caenogastropoda; Ambiguous_taxa	<i>Cantharus cecillei</i> isolate LSGB23208	99.34%	HQ834018.1	11	30	13	12	16	7	7	14	13
Mollusca	Veneroida	29	<i>Cyrenoida floridana</i>	<i>Geloina</i> sp. Aceh Besar clone III	100.00%	MG946720.1	11	18	19	5	5	4	10	6	9
Mollusca	-	9	Heterobranchia; Ambiguous_taxa	<i>Melampus pulchellus</i> isolate PR1931	100.00%	KM280982.1	5	4	6	3	0	0	5	2	2
Mollusca	Cycloneritida	6	<i>Neritina virginea</i>	<i>Smaragdia viridis</i> voucher MCZ:Mala:378748	100.00%	FJ977657.1	5	1	2	2	2	3	1	2	0
Mollusca	Ostreida	4	Ostreoida; Ambiguous_taxa	<i>Crassostrea virginica</i> isolate Cv_A3	100.00%	KM460896.1	3	1	0	0	4	1	3	0	0
Mollusca	Veneroida	2	Veneroida; Ambiguous_taxa	<i>Rangia cuneata</i> voucher BivAToL-280	99.34%	KC429401.1	0	2	0	0	2	0	1	1	0
Mollusca	-	1	Caenogastropoda; Ambiguous_taxa	<i>Cantharus cecillei</i> isolate LSGB23208	97.83%	HQ834018.1	0	1	1	0	0	0	0	1	0
Mollusca	Veneroida	1	Veneroida; Ambiguous_taxa	<i>Mytilopsis leucophaeata</i> voucher BivAToL-9	100.00%	KX713323.1	1	0	0	1	0	0	1	0	0
Mollusca	Veneroida	1	<i>Strigilla euronion</i>	<i>Semele purpurascens</i> voucher BivAToL-55	100.00%	KX713345.1	0	1	0	0	1	0	0	1	0
Total Mollusca OTUs	10	141	-	-	-	-	58	83	53	40	48	29	41	35	36
Nematoda	Desmodorida	68	<i>Spirinia parasitifera</i>	<i>Spirinia parasitifera</i>	98.68%	AY854217.1	33	35	22	22	24	18	17	16	17

(table cont'd.)

Phylum	Order	Total Incidence	Lowest SILVA assignment	Top GenBank Match	Percent Identity	Accession	C	B	L	M	H	0m	1m	5m	10m
Nematoda	Monhysterida	63	<i>Terschellingia longicaudata</i>	<i>Terschellingia longicaudata</i>	97.37%	AY854230.1	31	32	19	23	21	16	17	15	15
Nematoda	Enoplida	52	<i>Rhabdolaimus</i> cf <i>terrestris</i> JH-2004	<i>Rhabdolaimus terrestris</i> strain RhDoTer1	100.00%	KJ636366.1	28	24	21	18	13	11	12	15	14
Nematoda	Monhysterida	52	<i>Diplolaimella dievengatensis</i>	<i>Diplolaimella dievengatensis</i>	97.37%	AJ966482.1	26	26	11	18	23	14	12	14	12
Nematoda	Rhabditida	50	<i>Poikilolaimus</i> sp NKTW41	<i>Poikilolaimus</i> sp. NKTW41	97.37%	AB535568.1	22	28	8	20	22	10	14	14	12
Nematoda	Dorylaimida	47	Dorylaimida; environmental sample	<i>Mesodorylaimus</i> sp. 1 WJW-2018 clone 2	100.00%	MG921252.1	24	23	22	16	9	8	13	12	14
Nematoda	Tylenchida	41	<i>Filenchus hamuliger</i>	<i>Tylenchus arcuatus</i> isolate fafu02	100.00%	MN542210.1	21	20	16	17	8	8	10	13	10
Nematoda	Enoplida	40	Enoplida; Ambiguous_taxa	<i>Metoncholaimus albidus</i> isolate Ra2	100.00%	MH587715.1	9	31	14	12	14	12	11	8	9
Nematoda	Chromadorida	38	<i>Paracyatholaimus intermedius</i>	<i>Paracyatholaimus intermedius</i> isolate PCyalnt2	100.00%	JQ957907.1	18	20	18	13	7	9	10	8	11
Nematoda	Monhysterida	38	Monhysterida; Ambiguous_taxa	<i>Daptonema</i> sp. PFN-2007	100.00%	EF436228.1	16	22	6	9	23	10	10	10	8
Nematoda	Enoplida	37	Enoplida; Ambiguous_taxa	<i>Oncholaimidae</i> sp. TCR69	98.68%	HM564640.1	11	26	12	10	15	11	11	7	8
Nematoda	Monhysterida	33	<i>Diplolaimelloides</i> environmental sample	Uncultured <i>Diplolaimelloides</i> clone GN23NB23	98.03%	EF659931.1	16	17	6	15	12	6	8	8	11
Nematoda	Chromadorida	32	<i>Ptycholaimellus</i> sp 1092	<i>Ptycholaimellus</i> sp. 1092	98.68%	FJ040472.1	15	17	5	9	18	11	9	8	4
Nematoda	Tylenchida	32	Tylenchida; Ambiguous_taxa	<i>Hirschmanniella santarosae</i> voucher ITD266	100.00%	EF029855.1	21	11	3	10	19	7	9	7	9
Nematoda	Araeolaimida	28	Araeolaimida; Ambiguous_taxa	<i>Deontolaimus</i> sp. PaApSp	100.00%	FJ969132.1	13	15	9	10	9	7	5	8	8
Nematoda	Plectida	27	<i>Paraphanolaimus behningi</i>	<i>Paraphanolaimus behningi</i> strain PaAPBeh3	97.39%	KJ636381.1	16	11	11	9	7	5	11	7	4
Nematoda	Plectida	26	<i>Chronogaster typica</i>	<i>Chronogaster</i> sp. JH-2004 isolate ChGaSp2	97.37%	AY284709.1	18	8	11	9	6	3	6	8	9
Nematoda	Tylenchida	24	<i>Filenchus vulgaris</i>	<i>Filenchus vulgaris</i> strain FileVul3	98.03%	KJ869335.1	12	12	8	10	6	3	8	7	6
Nematoda	Enoplida	22	Triplonchida; Ambiguous_taxa	<i>Prismatolaimus</i> sp. MCB2	98.03%	LC186858.1	13	9	18	4	0	3	6	5	8
Nematoda	Tylenchida	20	<i>Meloidogyne spartinae</i>	<i>Meloidogyne spartinae</i>	100.00%	EF189177.1	11	9	0	2	18	4	7	5	4
Nematoda	Desmodorida	19	<i>Prochaetosoma</i> sp 3 HSR-2009	<i>Prochaetosoma</i> sp. OK-2015 isolate t2	98.03%	KR259342.1	10	9	0	1	18	5	5	4	5
Nematoda	Dorylaimida	19	Dorylaimida; Ambiguous_taxa	<i>Clavicaudoides</i> sp. PGM-2004	100.00%	AY552967.1	8	11	11	6	2	4	5	3	7
Nematoda	Enoplida	19	<i>Anoplostoma</i> sp 1093	<i>Anoplostoma</i> sp. 1093	97.37%	FJ040492.1	5	14	10	9	0	2	6	6	5

(table cont'd.)

Phylum	Order	Total Incidence	Lowest SILVA assignment	Top GenBank Match	Percent Identity	Accession	C	B	L	M	H	0m	1m	5m	10m
Nematoda	Tylenchida	18	<i>Aglenchus agricola</i>	<i>Aglenchus geraerti</i> isolate NFP01	100.00%	MK639388.1	8	10	11	6	1	1	7	3	7
Nematoda	Monhysterida	17	<i>Diplolaimella dievengatensis</i>	<i>Diplolaimella dievengatensis</i> isolate Diplo1	98.68%	MN072928.1	5	12	5	8	4	2	5	5	5
Nematoda	Enoplida	16	Triplonchida; Ambiguous_taxa	<i>Prismatolaimus</i> sp. MCB6	99.34%	LC186861.1	12	4	16	0	0	3	3	6	4
Nematoda	Monhysterida	16	Monhysterida; Ambiguous_taxa	<i>Daptonema</i> sp. 1255	99.34%	FJ040463.1	10	6	2	9	5	5	5	5	1
Nematoda	Monhysterida	16	<i>Diplolaimelloides</i> environmental sample	Uncultured <i>Diplolaimelloides</i> clone GN11N5	99.34%	EF659911.1	12	4	2	2	12	3	5	5	3
Nematoda	Dorylaimida	15	Dorylaimida; Ambiguous_taxa	<i>Mesodorylaimus</i> sp. 2 WJW-2018	98.03%	MG921256.1	3	12	6	7	2	1	4	6	4
Nematoda	Enoplida	15	<i>Halalaimus</i> sp 1034	<i>Halalaimus</i> sp. 1034	99.34%	FJ040501.1	5	10	0	6	9	5	7	1	2
Nematoda	Tylenchida	14	Tylenchida; Ambiguous_taxa	<i>Gracilacus paralatescens</i>	100.00%	MH200615.1	6	8	3	8	3	4	4	4	2
Nematoda	Tylenchida	14	<i>Ditylenchus</i> sp 2 JH-2014	<i>Anguina tritici</i> strain AnguTri2	100.00%	KJ636412.1	5	9	4	3	7	1	5	4	4
Nematoda	Chromadorida	13	<i>Dichromadora</i> sp 2 JH-2014	Cf. <i>Dichromadora</i> sp. 2 JH-2014	98.68%	KJ636253.1	6	7	0	7	6	1	5	4	3
Nematoda	Dorylaimida	12	<i>Prodorylaimus</i> sp HHBM-2007a	<i>Prodorylaimus</i> sp. HHBM-2007a	98.03%	EF207246.1	10	2	10	2	0	5	2	3	2
Nematoda	Enoplida	12	Enoplida; Ambiguous_taxa	Uncultured eukaryote clone CRDS_188	99.34%	JN142461.1	3	9	4	6	2	7	4	0	1
Nematoda	Enoplida	12	<i>Halalaimus</i> sp BCA25	<i>Halalaimus</i> sp. BCA25	98.03%	HM564490.1	6	6	2	4	6	5	5	0	2
Nematoda	Chromadorida	11	Chromadorida; Ambiguous_taxa	<i>Chromadorina</i> sp. 1971	100.00%	FJ040471.1	4	7	3	1	7	9	1	1	0
Nematoda	Monhysterida	11	<i>Eumonhystera filiformis</i>	<i>Eumonhystera filiformis</i> strain EumoFil2 829+830	100.00%	AY593937.1	7	4	11	0	0	1	4	3	3
Nematoda	Desmoscolecida	10	<i>Desmoscolex</i> sp ITDL-2011	<i>Desmoscolex</i> sp. 5 TJP-2019 voucher Nem.291	98.68%	MN250118.1	5	5	0	5	5	3	4	1	2
Nematoda	Desmodorida	9	Epsilonematidae sp Epsifamil1	Epsilonematidae sp. Epsifamil1	99.34%	EF591340.1	0	9	0	7	2	0	3	2	4
Nematoda	Desmodorida	9	<i>Laxus</i> sp 'heron 1'	<i>Laxus</i> sp. 'heron 1' isolate HX1W911	98.68%	KP943959.1	8	1	1	6	2	5	4	0	0
Nematoda	Dorylaimida	9	<i>Dorylaimellus montenegricus</i>	<i>Dorylaimellus parvulus</i> isolate Barger 2	100.00%	AY911968.1	8	1	8	1	0	1	3	2	3
Nematoda	Enoplida	9	Enoplida; environmental sample	<i>Alaimus</i> sp. SSU1_19	99.34%	MG993561.1	8	1	9	0	0	2	3	3	1
Nematoda	Monhysterida	9	<i>Diplolaimelloides</i> sp BCG-2008	<i>Diplolaimelloides</i> sp. BCG-2008	99.34%	EU551671.1	7	2	0	3	6	1	2	4	2
Nematoda	Desmodorida	8	<i>Spirinia elongata</i>	<i>Spirinia elongata</i>	99.34%	EF527426.1	2	6	3	4	1	7	1	0	0

(table cont'd.)

Phylum	Order	Total Incidence	Lowest SILVA assignment	Top GenBank Match	Percent Identity	Accession	C	B	L	M	H	0m	1m	5m	10m
Nematoda	Tylenchida	8	<i>Dolichodorus</i> sp WY-2006	<i>Dolichodorus</i> sp. WY-2006	98.03%	DQ912918.1	8	0	8	0	0	2	2	2	2
Nematoda	Desmodorida	7	<i>Desmodora</i> sp DL-2016	<i>Desmodora</i> sp. DL-2016	98.03%	KX077910.1	2	5	0	0	7	3	1	2	1
Nematoda	Dorylaimida	7	Dorylaimida; uncultured eukaryote	<i>Colpoda</i> sp. clone wx2	98.68%	MK801290.1	4	3	4	1	2	0	2	4	1
Nematoda	Enoplida	7	<i>Alaimus</i> sp 1247	<i>Alaimus</i> sp. GSt19	97.37%	LC186627.1	3	4	7	0	0	0	2	2	3
Nematoda	Monhysterida	7	<i>Sabatieria punctata</i>	<i>Sabatieria</i> sp. 4 TJP-2019 voucher NPRB.50	100.00%	MN250141.1	4	3	0	4	3	3	3	0	1
Nematoda	Plectida	7	<i>Chronogaster</i> sp JH-2004	<i>Chronogaster</i> sp. JH-2004 isolate ChGaSp1	98.03%	AY284708.1	5	2	7	0	0	1	3	2	1
Nematoda	Plectida	7	Haliplectidae; Ambiguous_taxa	<i>Haliplectus</i> cf. <i>dorsalis</i> HaPIDorZ2	97.37%	FJ969123.1	2	5	0	7	0	0	3	0	4
Nematoda	Rhabditida	7	Rhabditida; Ambiguous_taxa	<i>Euteratocephalus</i> sp. 803L-008	100.00%	EU880036.1	6	1	6	0	1	0	2	3	2
Nematoda	Tylenchida	7	<i>Aphelenchoides besseyi</i>	<i>Aphelenchoides pseudogoodeyi</i> isolate 40	100.00%	MK291494.1	3	4	3	3	1	1	2	3	1
Nematoda	Araeolaimida	6	Araeolaimida; Ambiguous_taxa	<i>Onchium</i> sp. San Elijo	99.34%	JX678601.1	2	4	2	0	4	2	2	1	1
Nematoda	Tylenchida	6	Tylenchida; Ambiguous_taxa	<i>Pratylenchus hippeastri</i> isolate 40196	99.34%	KJ001716.1	5	1	3	2	1	0	2	1	3
Nematoda	Enoplida	5	Enoplida; Ambiguous_taxa	<i>Oxystomina</i> sp. NUS3	99.34%	HM564440.1	1	4	4	1	0	5	0	0	0
Nematoda	Plectida	5	<i>Paraphanolaimus behningi</i>	<i>Paraphanolaimus behningi</i> strain PaAPBeh4	98.04%	KJ636380.1	5	0	3	0	2	1	2	0	2
Nematoda	Rhabditida	5	<i>Acrobeloides buetschlii</i>	<i>Plectus</i> sp. MCT11	100.00%	LC186814.1	3	2	4	1	0	0	1	3	1
Nematoda	Desmodorida	4	<i>Calomicrolaimus parahonestus</i>	Microlaimidae sp. 3 TJP-2019 voucher NPRB.45	99.34%	MN250137.1	4	0	0	4	0	3	1	0	0
Nematoda	Desmodorida	4	Desmodorida; uncultured metazoan	<i>Metachromadora</i> sp. MAchSp1	98.68%	EF591339.1	2	2	0	0	4	1	1	1	1
Nematoda	Dorylaimida	4	<i>Dorylaimellus virginianus</i>	<i>Dorylaimellus virginianus</i> isolate 9 Mile 9-22 LP2-26	100.00%	AY552969.1	3	1	4	0	0	0	2	1	1
Nematoda	Dorylaimida	4	<i>Isomermis lairdi</i>	<i>Isomermis lairdi</i> partial isolate	97.37%	FN400900.1	3	1	3	1	0	3	0	0	1
Nematoda	Monhysterida	4	Monhysterida; uncultured eukaryote	<i>Daptonema normadicum</i>	97.37%	AY854224.1	2	2	0	2	2	3	1	0	0
Nematoda	Plectida	4	<i>Chronogaster</i> sp JH-2004	<i>Chronogaster</i> sp. JH-2004 isolate ChGaSp2	99.34%	AY284709.1	4	0	0	4	0	0	2	1	1
Nematoda	Tylenchida	4	<i>Hirschmanniella</i> sp Yuma	<i>Hirschmanniella</i> sp. Yuma	100.00%	EF029857.1	1	3	3	1	0	2	2	0	0
Nematoda	Enoplida	3	<i>Pseudoncholaimus</i> sp AS89	<i>Pseudoncholaimus</i> sp. AS89	97.37%	KR265048.1	1	2	3	0	0	2	0	0	1

(table cont'd.)

Phylum	Order	Total Incidence	Lowest SILVA assignment	Top GenBank Match	Percent Identity	Accession	C	B	L	M	H	0m	1m	5m	10m
Nematoda	Monhysterida	3	<i>Diplolaimella dievengatensis</i>	<i>Diplolaimella dievengatensis</i>	98.69%	AJ966482.1	1	2	0	1	2	1	1	0	1
Nematoda	Monhysterida	3	Monhysterida; uncultured eukaryote	Uncultured eukaryote clone: B21_ek_33	99.34%	LC150171.1	1	2	2	1	0	0	0	2	1
Nematoda	Rhabditida	3	Rhabditida; Ambiguous_taxa	<i>Acrobeloides varius</i> strain LKC27	100.00%	MK636581.1	3	0	3	0	0	0	1	1	1
Nematoda	Rhabditida	3	<i>Daubaylia potomaca</i>	<i>Daubaylia potomaca</i>	98.03%	KU180669.1	1	2	3	0	0	0	0	2	1
Nematoda	Tylenchida	3	<i>Mesocriconema</i> sp YZ-2014a	<i>Mesocriconema</i> sp. N570	99.34%	MF094894.1	3	0	3	0	0	0	2	0	1
Nematoda	Desmodorida	2	<i>Spirinia parasitifera</i>	<i>Spirinia parasitifera</i>	97.64%	AY854217.1	0	2	1	0	1	0	0	0	2
Nematoda	Dorylaimida	2	<i>Limnomermis</i> sp 1 JH-2014	<i>Limnomermis</i> sp. 1 JH-2014	100.00%	KJ636371.1	2	0	2	0	0	2	0	0	0
Nematoda	Dorylaimida	2	<i>Mermis nigrescens</i>	<i>Mermis nigrescens</i> voucher VT046NM01-1	98.68%	MG182373.1	2	0	2	0	0	0	1	0	1
Nematoda	Enoplida	2	<i>Oncholaimus</i> sp OUS2	<i>Oncholaimus</i> sp. OUS2	100.00%	HM564450.1	2	0	0	2	0	2	0	0	0
Nematoda	Enoplida	2	<i>Oxystomina</i> sp HCL32	<i>Oxystomina</i> sp. HCL20	98.68%	HM564562.1	2	0	0	0	2	1	1	0	0
Nematoda	Monhysterida	2	<i>Geomonhystera</i> sp ZQZ-2010a	Monhysteridae environmental sample isolate: 003-034B-2.26	100.00%	AB614352.1	2	0	2	0	0	0	0	1	1
Nematoda	Plectida	2	<i>Aphanolaimus aquaticus</i>	<i>Aphanolaimus aquaticus</i> strain AphaAqu3	97.37%	KJ636362.1	2	0	0	2	0	1	1	0	0
Nematoda	Plectida	2	<i>Paraphanolaimus behningi</i>	<i>Paraphanolaimus behningi</i> strain PaAPBeh3	97.39%	KJ636381.1	2	0	0	2	0	1	1	0	0
Nematoda	Tylenchida	2	<i>Ditylenchus dipsaci</i>	<i>Ditylenchus</i> sp. 85C1	98.03%	MK292126.1	1	1	1	1	0	0	1	0	1
Nematoda	Tylenchida	2	<i>Helicotylenchus digitiformis</i>	<i>Helicotylenchus dihystra</i> isolate T35 11 29935	100.00%	KJ934127.1	1	1	2	0	0	0	2	0	0
Nematoda	Chromadorid a	1	<i>Paracyatholaimus intermedius</i>	<i>Paracyatholaimus intermedius</i> isolate PCyalnt2	98.45%	JQ957907.1	0	1	0	1	0	0	1	0	0
Nematoda	Chromadorid a	1	<i>Ptycholaimellus</i> sp 1092	<i>Ptycholaimellus</i> sp. 1092	97.73%	FJ040472.1	0	1	0	0	1	0	0	1	0
Nematoda	Chromadorid a	1	Chromadorida; uncultured eukaryote	Chromadorina sp. 1971	96.71%	FJ040471.1	0	1	0	0	1	1	0	0	0
Nematoda	Desmodorida	1	<i>Spirinia parasitifera</i>	<i>Spirinia parasitifera</i>	98.52%	AY854217.1	1	0	0	1	0	0	1	0	0
Nematoda	Desmodorida	1	<i>Spirinia parasitifera</i>	<i>Spirinia parasitifera</i>	98.40%	AY854217.1	1	0	0	0	1	0	1	0	0
Nematoda	Desmodorida	1	<i>Spirinia parasitifera</i>	<i>Spirinia parasitifera</i>	98.50%	AY854217.1	0	1	1	0	0	1	0	0	0
Nematoda	Dorylaimida	1	Dorylaimida; Ambiguous_taxa	<i>Eudorylaimus</i> environmental sample isolate: 005-020B-2.380	100.00%	AB614327.1	1	0	1	0	0	0	1	0	0
Nematoda	Dorylaimida	1	Dorylaimida; Ambiguous_taxa	<i>Tylencholaimellus striatus</i> isolate Konza IAD-128	96.92%	AY146530.1	1	0	0	1	0	0	0	0	1

(table cont'd.)

Phylum	Order	Total Incidence	Lowest SILVA assignment	Top GenBank Match	Percent Identity	Accession	C	B	L	M	H	0m	1m	5m	10m
Nematoda	Dorylaimida	1	Dorylaimida; Ambiguous_taxa	Dorylaimina environmental sample isolate: 005-023B-4.392	100.00%	AB614298.1	1	0	1	0	0	0	0	0	1
Nematoda	Dorylaimida	1	<i>Leptonchus granulosus</i>	<i>Leptonchus granulosus</i> isolate Kouhdasht	97.37%	KR184128.1	0	1	1	0	0	0	1	0	0
Nematoda	Dorylaimida	1	Dorylaimida; metagenome	<i>Lenonchium zanjanense</i>	100.00%	MK089266.1	1	0	0	1	0	0	0	0	1
Nematoda	Dorylaimida	1	Dorylaimida; uncultured eukaryote	<i>Colpoda</i> sp. clone wx2	98.03%	MK801290.1	0	1	0	1	0	0	1	0	0
Nematoda	Dorylaimida	1	<i>Limnomermis</i> sp 1 JH-2014	<i>Limnomermis</i> sp. 1 JH-2014	97.90%	KJ636371.1	1	0	1	0	0	1	0	0	0
Nematoda	Enoplida	1	Enoplida; Ambiguous_taxa	<i>Tripyloides</i> sp. AUK45	100.00%	HM564476.1	0	1	1	0	0	1	0	0	0
Nematoda	Enoplida	1	Enoplida; Ambiguous_taxa	Uncultured eukaryote clone CRDS_97	99.22%	JN142464.1	0	1	1	0	0	1	0	0	0
Nematoda	Enoplida	1	<i>Oncholaimus</i> sp DS-2015	<i>Oncholaimus</i> sp. ESC003	99.22%	KY792443.1	1	0	0	0	1	1	0	0	0
Nematoda	Monhysterida	1	<i>Diplolaimella dievengatensis</i>	<i>Diplolaimella dievengatensis</i>	98.03%	AJ966482.1	0	1	0	1	0	1	0	0	0
Nematoda	Monhysterida	1	<i>Diplolaimelloides</i> sp BCG-2008	<i>Diplolaimelloides</i> sp. BCG-2008	99.20%	EU551671.1	1	0	0	0	1	0	1	0	0
Nematoda	Monhysterida	1	<i>Diplolaimelloides</i> sp BCG-2008	<i>Diplolaimelloides</i> sp. BCG-2008	97.18%	EU551671.1	1	0	0	0	1	0	0	1	0
Nematoda	Monhysterida	1	<i>Theristus agilis</i>	<i>Theristus</i> sp. ESC032	98.68%	KY792465.1	1	0	0	1	0	0	1	0	0
Nematoda	Monhysterida	1	<i>Theristus</i> sp 1268	<i>Theristus</i> sp. 1268	98.36%	FJ040464.1	1	0	1	0	0	1	0	0	0
Nematoda	Plectida	1	<i>Aphanolaimus aquaticus</i>	<i>Aphanolaimus aquaticus</i> strain AphaAqu3	97.37%	KJ636362.1	1	0	0	1	0	0	1	0	0
Nematoda	Rhabditida	1	<i>Pseudacrobeles variabilis</i>	Cf. <i>Cephalobus</i> sp. Konza IDD-93	98.68%	AY911937.1	1	0	1	0	0	0	0	0	1
Nematoda	Tylenchida	1	Tylenchida; Ambiguous_taxa	<i>Meloidogyne aegracyper</i> isolate	100.00%	MN037410.1	1	0	0	1	0	0	0	0	1
Nematoda	Tylenchida	1	<i>Basiria</i> sp 2 JH-2014	<i>Basiria</i> sp. 2 JH-2014	99.34%	KJ869354.1	1	0	1	0	0	0	0	0	1
Nematoda	Tylenchida	1	<i>Ditylenchus adasi</i>	<i>Ditylenchus adasi</i> strain DityAda2	98.68%	KJ636375.1	1	0	0	0	1	0	1	0	0
Nematoda	Tylenchida	1	<i>Filenchus discrepans</i>	<i>Filenchus discrepans</i> voucher C172	100.00%	KX156295.1	1	0	1	0	0	0	0	0	1
Total Nematoda OTUs	109	1286	-	-	-	-	653	633	457	416	413	307	365	304	310
Nemertea	-	2	Palaeonemertea; Ambiguous_taxa	<i>Carinoma</i> sp. SA-2011	99.34%	KF935278.1	2	0	0	1	1	1	1	0	0
Nemertea	Archinemertea	1	<i>Cephalothrix rufifrons</i>	<i>Cephalothrix rufifrons</i> isolate CEPsi_nzsi2	100.00%	MK076300.1	1	0	0	0	1	0	0	0	1

(table cont'd.)

Phylum	Order	Total Incidence	Lowest SILVA assignment	Top GenBank Match	Percent Identity	Accession	C	B	L	M	H	0m	1m	5m	10m
Nemertea	Monostilifera	1	<i>Prostoma graecense</i>	<i>Prostoma</i> cf. <i>eilhardi</i> EEZ-2018 isolate PROei_bost	100.00%	MK076304.1	1	0	1	0	0	0	0	0	1
Total Nemertea OTUs	3	4	-	-	-	-	4	0	1	1	2	1	1	0	2
Platyhelminthes	Rhabdocoela	31	Kalyptorhynchia; Ambiguous_taxa	<i>Lagenopolycystis</i> sp. n. 2 TJ-2014 voucher DNA526ZAF	97.37%	KJ887441.1	13	18	11	9	11	12	8	6	5
Platyhelminthes	Rhabdocoela	22	<i>Gyratrix hermaphroditus</i>	<i>Gyratrix hermaphroditus</i> partial	100.00%	AJ012510.1	9	13	9	11	2	4	5	7	6
Platyhelminthes	Rhabdocoela	18	<i>Olisthaneella truncula</i>	<i>Olisthaneella truncula</i>	99.34%	AY775761.1	11	7	12	6	0	4	2	5	7
Platyhelminthes	Macrostomida	15	<i>Macrostomum kepneri</i>	<i>Macrostomum kepneri</i> voucher MTP LS 285	98.68%	FJ715307.1	11	4	0	5	10	0	3	4	8
Platyhelminthes	Rhabdocoela	14	<i>Baicalellia canadensis</i>	<i>Baicalellia canadensis</i>	98.68%	KC869833.1	8	6	10	3	1	8	5	1	0
Platyhelminthes	Rhabdocoela	13	<i>Mesorhynchus terminostylis</i>	<i>Itaipusa sinensis</i> isolate YTP3	98.03%	MF443161.1	5	8	0	4	9	2	4	4	3
Platyhelminthes	-	11	<i>Rhynchoscolex simplex</i>	<i>Rhynchoscolex simplex</i> isolate K05_04	100.00%	FJ384817.1	8	3	11	0	0	3	2	2	4
Platyhelminthes	Rhabdocoela	10	<i>Placorhynchus</i> sp. 1 JPS-2015	<i>Placorhynchus</i> sp. 1 JPS-2015 isolate PMAG_001	97.37%	KR339034.1	6	4	1	6	3	5	3	1	1
Platyhelminthes	Proseriata	6	<i>Monocelis fusca</i>	<i>Monocelis fusca</i>	100.00%	KC869814.1	3	3	0	1	5	3	1	0	2
Platyhelminthes	Thalassiosphaerales	5	<i>Catenula</i> sp. KL-2009	<i>Catenula</i> sp. KL-2009	100.00%	FJ196321.1	5	0	5	0	0	1	3	0	1
Platyhelminthes	Rhabdocoela	3	<i>Prognathorhynchus busheki</i>	<i>Prognathorhynchus busheki</i> isolate EGPKS_002	100.00%	KR339035.1	0	3	0	3	0	2	0	1	0
Platyhelminthes	Rhabdocoela	3	<i>Gieysztoria infundibuliformis</i>	<i>Gieysztoria pavimentata</i> isolate UH235.3	98.68%	KC529472.1	3	0	3	0	0	0	1	1	1
Platyhelminthes	Macrostomida	2	<i>Microstomum papillosum</i>	<i>Microstomum westbladi</i> isolate S114	99.34%	MK504553.1	2	0	0	2	0	1	1	0	0
Platyhelminthes	Rhabdocoela	2	Dalyellioida; Ambiguous_taxa	<i>Canetellia beauchampi</i> isolate W19ss	99.34%	KC529504.1	1	1	2	0	0	1	0	0	1
Platyhelminthes	Rhabdocoela	2	<i>Zonorhynchus tvaerminnensis</i>	<i>Zonorhynchus tvaerminnensis</i> voucher EXT665	100.00%	KJ887455.1	2	0	0	1	1	0	1	1	0
Platyhelminthes	Rhabdocoela	2	Neodalyelliida; Ambiguous_taxa	<i>Beklemischeviella angustior</i> isolate UH77.6	100.00%	KC529412.1	0	2	2	0	0	2	0	0	0
Platyhelminthes	Rhabdocoela	2	<i>Ptychopera</i> sp. NVS-2013	<i>Ptychopera</i> sp. NVS-2013 isolate UH294.10	100.00%	KC529420.1	1	1	0	0	2	0	1	1	0
Platyhelminthes	Polycladida	1	<i>Notoplana australis</i>	<i>Koinostylochus elongatus</i> ICHUM:6014	99.34%	LC508171.1	1	0	0	0	1	1	0	0	0
Platyhelminthes	Rhabdocoela	1	Kalyptorhynchia; Ambiguous_taxa	<i>Lagenopolycystis</i> sp. n. 2 TJ-2014 voucher DNA526ZAF	97.73%	KJ887441.1	0	1	1	0	0	0	0	0	1
Platyhelminthes	Rhabdocoela	1	<i>Gyratrix</i> sp. n. TJ-2014	<i>Gyratrix</i> sp. n. TJ-2014 voucher DNA23PAN	100.00%	KJ887436.1	1	0	0	1	0	0	1	0	0

(table cont'd.)

Phylum	Order	Total Incidence	Lowest SILVA assignment	Top GenBank Match	Percent Identity	Accession	C	B	L	M	H	0m	1m	5m	10m
Platyhelminthes	Rhabdocoela	1	<i>Mesorhynchus terminostylis</i>	<i>Itaipusa sinensis</i> isolate YTP3	98.68%	MF443161.1	1	0	0	1	0	0	0	1	0
Platyhelminthes	Rhabdocoela	1	<i>Placorhynchus dimorphus</i>	<i>Placorhynchus dimorphus</i> voucher EXT663	98.68%	KJ887409.1	0	1	0	0	1	0	0	0	1
Platyhelminthes	Tricladida	1	<i>Pentacoelum kazukolinda</i>	<i>Pentacoelum kazukolinda</i> isolate Val14	100.00%	KM200926.1	1	0	1	0	0	1	0	0	0
Total Platyhelminthes OTUs	23	167	-	-	-	-	92	75	68	53	46	50	41	35	41
Rotifera	Flosculariacea	71	<i>Octotrocha speciosa</i>	<i>Ptygura longicornis</i> isolate R15	100.00%	KM873603.1	35	36	24	23	24	18	18	17	18
Rotifera	Ploimida	25	Ploimida; metagenome	<i>Notholca acuminata</i>	100.00%	AY218115.1	15	10	9	11	5	8	7	2	8
Rotifera	Flosculariacea	8	<i>Filinia longiseta</i>	<i>Filinia terminalis</i> isolate 201	100.00%	MK352482.1	1	7	5	1	2	1	4	2	1
Rotifera	Ploimida	8	Ploimida; uncultured metazoan	<i>Conochilus coenobasis</i> isolate R91	98.68%	KM873590.1	5	3	4	2	2	3	2	1	2
Rotifera	-	1	Bdelloidea; Ambiguous_taxa	Uncultured bdelloid rotifer clone Rot_T1T2_03D	99.34%	GQ922321.1	1	0	1	0	0	0	0	0	1
Rotifera	Flosculariacea	1	Flosculariacea; Ambiguous_taxa	<i>Sinantherina socialis</i> isolate R90	100.00%	KM873606.1	0	1	1	0	0	0	1	0	0
Rotifera	Flosculariacea	1	<i>Testudinella clypeata</i>	<i>Brachionus calyciflorus</i> isolate 404	98.03%	MK271750.1	1	0	1	0	0	1	0	0	0
Rotifera	Ploimida	1	Ploimida; metagenome	Flosculariacea environmental sample clone KRN_S7d3	99.34%	MK499386.1	0	1	1	0	0	0	1	0	0
Rotifera	Ploimida	1	<i>Trifolium pratense</i>	<i>Varichaetadrilus</i> sp. YL-2017 voucher CE3621	98.03%	KY636922.1	1	0	1	0	0	0	0	0	1
Rotifera	Ploimida	1	<i>Trifolium pratense</i>	<i>Nais communis</i> isolate NAlco_IUCB	98.03%	MK076298.1	1	0	1	0	0	1	0	0	0
Total Rotifera OTUs	10	118	-	-	-	-	60	58	48	37	33	32	33	22	31
Tardigrada	Parachela	3	<i>Thulinus stephaniae</i>	<i>Thulinus stephaniae</i> clone 8	100.00%	GQ925701.1	3	0	2	1	0	1	1	1	0
Xenacoelomorpha	Acoela	2	<i>Paedomecynostomum bruneum</i>	<i>Paedomecynostomum bruneum</i> partial specimen voucher AWK05-47	98.03%	FR837720.1	2	0	0	2	0	0	1	1	0
Xenacoelomorpha	Acoela	1	Acoela; Ambiguous_taxa	<i>Praeconvoluta tigrina</i> partial specimen voucher MHMa6	100.00%	FR837740.1	1	0	0	1	0	0	0	1	0
Total Xenacoelomorpha OTUs	2	3	-	-	-	-	3	0	0	3	0	0	1	2	0

Any OTU with a “-” in the order column was ambiguous at the order level for the SILVA taxonomy assignment. The OTUs in white are members of the frequent group of OTUs which appeared in more than 10 samples in the dataset, while the OTUs shaded in gray are part of the infrequent group which appeared in 10 samples or less. OTU incidence is further broken down by category, i.e., samples from Caillou (C) and Barataria (B) Bays, from the Low (L), Mid (M), and High (H) salinity zones, and at 0m, 1m, 5m, and 10m from the marsh edge.

Unique Taxa from the two bays and the three salinity zones:

Certain OTUs from the infrequent group only were detected in the samples from either Barataria Bay or Caillou Bay. The group of OTUs which were unique to Barataria Bay included 4 Arthropoda, 2 Gastrotricha, 2 Nematoda, 2 Platyhelminthes, 1 Annelida, and 1 Mollusca. The arthropods that were unique to BB included 2 members of the insect order Diptera, a member of the Collembola order Entomobryomorpha, and a member of the mite order Oribatida. The two Gastrotrich OTUs in this group were both assigned to the order Chaetonotida. The two nematode OTUs were assigned to the order Desmodorida. The two Platyhelminthes OTUs were assigned to the order Rhabdocoela. The sole annelid OTU in this group was assigned to the family Nerillidae, while the sole mollusk OTU was assigned to the order Venerioda as the species *Rangia cuneata*, a benthic filter feeding clam common in the Gulf of Mexico (Wong et al. 2010). The OTUs that were unique to Caillou Bay consisted of 13 Nematoda, 9 Arthropoda, 4 Platyhelminthes, 2 Gastrotricha, 1 Annelida, 1 Nemertea, 1 Tardigrada, and 1 Xenocoelomorpha. Of the 13 nematodes, 4 were assigned to the order Plectida, 2 were assigned to the Dorylaimida, 2 were assigned to the Enoplida, 2 were assigned to the Tylenchida, 1 was assigned to the Desmodorida, 1 was assigned to the Monhysterida, and 1 was assigned to the Rhabditida.

Table 4.9. Unique OTUs in the sediment samples collected from Barataria and Caillou Bays in July 2018.

Phylum	Order	Total Incidence	Lowest SILVA assignment	Top GenBank Match	C	B
Annelida	Polychaeta incertae sedis	4	<i>Mesonerilla roscovita</i>	<i>Mesonerilla</i> cf. fagei kw291	0	4
Arthropoda	Diptera	3	Diptera; Ambiguous_taxa	<i>Camptodiplosis auriculariae</i> voucher JSC52	0	3
Arthropoda	Diptera	3	<i>Culex brethesi</i>	<i>Culex brethesi</i> partial	0	3
Arthropoda	Entomobryomorpha	3	<i>Isotomurus</i> sp cei5	<i>Isotomurus</i> sp. cei5	0	3
Arthropoda	Oribatida	2	<i>Phauloppia lucorum</i>	<i>Phauloppia lucorum</i>	0	2
Gastrotricha	Chaetonotida	3	Chaetonotida; Ambiguous_taxa	<i>Chaetonotus</i> sp. TK25	0	3
Gastrotricha	Chaetonotida	2	Chaetonotida; Ambiguous_taxa	<i>Aspidiophorus</i> sp. n. 2 MK-2019 voucher GA_10.5	0	2
Mollusca	Veneroida	2	Veneroida; Ambiguous_taxa	<i>Rangia cuneata</i> voucher BivAToL-280	0	2
Nematoda	Desmodorida	9	Epsilonematidae sp Epsifamil1	Epsilonematidae sp. Epsifamil1	0	9
Nematoda	Desmodorida	2	<i>Spirinia parasitifera</i>	<i>Spirinia parasitifera</i>	0	2
Platyhelminthes	Rhabdocoela	3	<i>Prognathorhynchus busheki</i>	<i>Prognathorhynchus busheki</i> isolate EGPKS_002	0	3
Platyhelminthes	Rhabdocoela	2	Neodalyellida; Ambiguous_taxa	<i>Beklemischeviella angustior</i> isolate UH77.6	0	2
Annelida	Haplotaxida	2	Haplotaxida; Ambiguous_taxa	<i>Inanidrilus exumae</i> isolate CE73	2	0
Arthropoda	Podocopa	7	<i>Cypridopsis vidua</i>	<i>Cypridopsis</i> sp. Ca3 isolate CYP_EXP	7	0
Arthropoda	Poduromorpha	6	<i>Xenylla grisea</i>	<i>Xenylla boernerii</i> isolate 2F1a1_JC361	6	0
Arthropoda	Diptera	4	<i>Megaselia scalaris</i>	<i>Megaselia scalaris</i>	4	0

(table cont'd.)

Phylum	Order	Total Incidence	Lowest SILVA assignment	Top GenBank Match	C	B
Arthropoda	Cyclopoida	3	<i>Macrocyclus albidus</i>	<i>Macrocyclus albidus</i> voucher N381DZMB	3	0
Arthropoda	Sarcoptiformes	3	<i>Pheroliodes</i> sp PP-2016	<i>Masthermannia</i> sp. AD1256 voucher UMMZ BMOC 08-0515-049 AD1256	3	0
Arthropoda	Symphyleona	3	<i>Papirinus prodigiosus</i>	<i>Bourletiella hortensis</i> isolate 4A1a1_JC284	3	0
Arthropoda	Cyclopoida	2	Cyclopoida; uncultured eukaryote	<i>Microcyclus anceps</i> voucher USNM:1139167	2	0
Arthropoda	Trombidiformes	2	<i>Rhombognathus levigatooides</i>	<i>Rhombognathus</i> sp. UFMG 173954	2	0
Arthropoda	Trombidiformes	2	<i>Tetranychus okinawanus</i>	<i>Tetranychus okinawanus</i>	2	0
Gastrotricha	Chaetonotida	5	Chaetonotida; Ambiguous_taxa	<i>Aspidiophorus</i> sp. n. 2 MK-2019 voucher GA_10.5	5	0
Gastrotricha	Chaetonotida	2	Chaetonotida; Ambiguous_taxa	<i>Chaetonotus</i> aff. subtilis MK-2019 voucher HA_30.1	2	0
Nematoda	Tylenchida	8	<i>Dolichodorus</i> sp WY-2006	<i>Dolichodorus</i> sp. WY-2006	8	0
Nematoda	Plectida	5	<i>Paraphanolaimus behningi</i>	<i>Paraphanolaimus behningi</i> strain PaAPBeh4	5	0
Nematoda	Desmodorida	4	<i>Calomicrolaimus parahonestus</i>	Microaimidae sp. 3 TJP-2019 voucher NPRB.45	4	0
Nematoda	Plectida	4	<i>Chronogaster</i> sp JH-2004	<i>Chronogaster</i> sp. JH-2004 isolate ChGaSp2	4	0
Nematoda	Rhabditida	3	Rhabditida; Ambiguous_taxa	<i>Acroboloides varius</i> strain LK27	3	0
Nematoda	Tylenchida	3	<i>Mesocriconema</i> sp YZ-2014a	<i>Mesocriconema</i> sp. N570	3	0
Nematoda	Dorylaimida	2	<i>Limnomermis</i> sp 1 JH-2014	<i>Limnomermis</i> sp. 1 JH-2014	2	0
Nematoda	Dorylaimida	2	<i>Mermis nigrescens</i>	<i>Mermis nigrescens</i> voucher VT046NM01-1	2	0
Nematoda	Enoplida	2	<i>Oncholaimus</i> sp OUS2	<i>Oncholaimus</i> sp. OUS2	2	0
Nematoda	Enoplida	2	<i>Oxystomina</i> sp HCL32	<i>Oxystomina</i> sp. HCL20	2	0
Nematoda	Monhysterida	2	<i>Geomonhystera</i> sp ZQZ-2010a	Monhysteridae environmental sample isolate: 003-034B-2.26	2	0
Nematoda	Plectida	2	<i>Aphanolaimus aquaticus</i>	<i>Aphanolaimus aquaticus</i> strain AphaAqu3	2	0
Nematoda	Plectida	2	<i>Paraphanolaimus behningi</i>	<i>Paraphanolaimus behningi</i> strain PaAPBeh3	2	0
Nemertea	-	2	Palaeonemertea; Ambiguous_taxa	<i>Carinoma</i> sp. SA-2011	2	0
Platyhelminthes	Thalassiophysales	5	<i>Catenula</i> sp KL-2009	<i>Catenula</i> sp. KL-2009	5	0
Platyhelminthes	Rhabdocoela	3	<i>Gieysztoria infundibuliformis</i>	<i>Gieysztoria pavimentata</i> isolate UH235.3	3	0
Platyhelminthes	Macrostomida	2	<i>Microstomum papillosum</i>	<i>Microstomum westbladi</i> isolate S114	2	0
Platyhelminthes	Rhabdocoela	2	<i>Zonorhynchus tvaerminensis</i>	<i>Zonorhynchus tvaerminensis</i> voucher EXT665	2	0
Tardigrada	Parachela	3	<i>Thulinus stephaniae</i>	<i>Thulinus stephaniae</i> clone 8	3	0
Xenacoelomorpha	Acoela	2	<i>Paedomecynostomum bruneum</i>	<i>Paedomecynostomum bruneum</i> partial specimen voucher AWK05-47	2	0

All taxa presented in this table are those which were only detected in samples from either Barataria or Caillou Bay, and were detected at least twice.

A large number of OTUs (113) were either unique to one of the salinity zones (and were detected at least twice) or were absent from one of the salinity zones (and were detected at least twice in one of the zones where it was present). Of the 113 total OTUs that were unique to the salinity zones, 23 were members of the frequent group which were detected in more than 10 samples. Thirty-three of the total OTUs were unique to the Low salinity zone, 10 were unique to the Mid salinity zone, and 11 were unique to the High salinity zone (Table 4.10). In

addition, 27 OTUs were present only in the Low and Mid zones, 9 OTUs were present only in the Low and High, and 23 were present only Mid and High. The OTUs that were unique to the Low salinity zone consisted of 15 Nematoda, 8 Arthropoda, 5 Platyhelminthes, 3 Gastrotricha, and 2 Annelida. These 15 nematode OTUs consisted of 4 Enoplida, 3 Dorylamida, 3 Tylenchida, 2 Monhysterida, 2 Rhabditida, and 1 Plectida. The nine arthropods consisted of 4 copepods (2 Harpacticoida and 2 Cyclopoida), 2 mites (1 Sarcoptiformes and 1 Trombidiformes), 1 member of the Diptera, and 1 member of the Collembola (order Symphypleona). The five Platyhelminthes OTUs included 3 OTUs assigned to the order Rhabdocoela, one OTU assigned to the order Thalassiophysales, and one OTU assigned to the family Stenostomidae (genus *Rhynchoscolex*). All three of the gastrotrich OTUs were assigned as members of the order Chaetonotida. Lastly, the two annelid OTUs were assigned as a member of the family Nerillidae and a member of the order Haplotaxida, respectively. Of these OTUs, 2 nematodes (1 assigned to Enoplida and 1 assigned to Monhysterida) and 1 platyhelminth (family Stenostomidae) were members of the frequent group.

The OTUs that were detected only in the Low and Mid salinity zones included 9 Arthropoda, 9 Nematoda, 3 Annelida, 2 Gastrotricha, 1 Hydrozoa, 1 Mollusca, 1 Platyhelminthes, and 1 Tardigrada (Table 4.10). The 9 arthropod OTUs consisted of 4 Collembola OTUs (2 Entomobryomorpha and 2 unassigned), 3 Ostracoda OTUs (Podocopida), 1 Diptera OTU, and 1 Acari OTU (Trombidiformes). The 9 nematodes consisted of 3 Dorylaimida, 3 Enoplida, and 1 each of Monhysterida, Rhabditida, and Tylenchida. Two of the three annelid OTUs were assigned to members of the Haplotaxida, while the last annelid was assigned to a member of the Phyllodocida. Both of the gastrotrich OTUs were assigned to the order Chaetonotida. The only hydrozoan in this group was assigned to a member of the genus *Moerisia* in the order Anthoathecata, while the only mollusk was assigned as a member of the Heterobranchia. The only Platyhelminth OTU was assigned to the order Rhabdocoela. In addition, the only tardigrade OTU was assigned to the order Parachela. In this group, 4 arthropod OTUs (2 Ostracoda and 2 Collembola), 3 nematode OTUs (2 Enoplida and 1 Dorylaimida), 2 annelid OTUs (1 Haplotaxida and 1 Phyllodocida), and 1 platyhelminth OTU (Rhabdocoela) were members of the frequent group.

The group of OTUs that were only detected in the Low and High zones consisted of 5 Arthropoda, 3 Nematoda, and 1 Gastrotrich (Table 4.10). The arthropods in this group consisted of 3 insects (1 in order Ephemeroptera, 1 in order Lepidoptera, and 1 in order Diptera), 1 ostracod (Podocopida), and 1 ambiguous member of the Acari. The 3 nematodes included 1 member each of the orders Rhabditida, Plectida, and Araeolamida. The lone gastrotrich OTU was assigned to the order Chaetonotida. Of these OTUs, the gastrotrich (Chaetonotida) was the only member of the frequent group.

Those OTUs that were unique to the Mid salinity zone included 6 Nematoda, 2 Platyhelminthes, 1 Arthropoda, and 1 Xenocoelomorpha. The nematodes in this group consisted of 4 OTUs assigned to the order Plectida, 1 OTU assigned to the order Desmodorida,

and 1 OTU assigned to the order Enoplida. One of the Platyhelminthes OTUs was assigned to the order Macrostomida while the other was assigned to the order Rhabdocoela. The only arthropod unique to this salinity zone was assigned to a mite in the order Trombidiformes. Lastly, the only Xenocoelomorpha OTU in this group was assigned to the order Acoela. None of the OTUs which were unique to the Mid salinity zone were members of the frequent group, as all were detected in fewer than 10 samples.

The OTUs that were only detected in the Mid and High zones included 10 Nematoda, 6 Arthropoda, 3 Platyhelminthes, 2 Annelida, 1 Hydrozoa, and 1 Kinorhynch (Table 4.10). The 10 nematode OTUs included 4 OTUs assigned to the order Monhysterida, 2 OTUs assigned to the order Desmodorida, and 1 OTU each assigned to the orders Chromadorida, Desmoscolecida, Enoplida, and Tylenchida. The arthropods in this group consisted of 5 Diptera OTUs and 1 mite OTU (Sarcoptiformes). The three Platyhelminthes OTUs included a single member of each of these orders: Macrostomida, Proseriata, and Rhabdocoela. The two annelids in this group were both assigned to the order Phyllodocida. The only Hydrozoa OTU in this group was assigned as a member of the order Leptothecata, while the only Kinorhyncha OTU in this group was assigned as an ambiguous member of the class Cyclorhagia. Nine members of this group were included in the frequent group, these consisted of 4 Nematodes (1 Chromadorida, 1 Desmodorida, 1 Enoplida, and 1 Tylenchida), 2 Platyhelminthes (1 Macrostomida and 1 Rhabdocoela), 1 Annelida (Phyllodocida), and 1 Kinorhyncha (Cyclorhagia).

Finally, the group of OTUs that only were detected in the High salinity zone consisted of 3 Annelida, 3 Nematoda, 2 Arthropods, 2 Mollusca, and 1 Platyhelminthes (Table 4.10). The three annelids in this group were assigned to members of the orders Haplotaxida, Sabellida, and Scolecida. The three Nematoda OTUs included 2 members of the order Desmodorida and 1 member of the order Enoplida. The arthropods which were unique to the High salinity zone included a member of the Diptera and a member of the Podocopida. The mollusks in this group were assigned to a member of the Ostreoida and a member of the Veneroida. Lastly, the sole member of the Platyhelminthes that was unique to the High salinity zone was assigned to the order Rhabdocoela. None of the OTUs in this group were also members of the frequent group.

Table 4.10. Unique OTUs in the samples from the different salinity zones.

Phylum	Order	Total Incidence	Lowest SILVA assignment	Top GenBank Match	L	M	H
Low Unique							
Annelida	Polychaeta incertae sedis	4	Mesonerilla roscovita	Mesonerilla cf. fagei kw291	4	0	0
Annelida	Haplotaxida	4	Tubifex sp	Limnodrilus udekemianus voucher CE2127	4	0	0
Arthropoda	Harpacticoida	3	Bradya sp Greenland-RJH-2004	Harpacticoida sp. 8641009	3	0	0

(table cont'd.)

	Phylum	Order	Total Incidence	Lowest SILVA assignment	Top GenBank Match	L	M	H
	Arthropoda	Cyclopoida	3	Macrocyclus albidus	Macrocyclus albidus voucher N381DZMB	3	0	0
	Arthropoda	Sarcoptiformes	3	Pheroliodes sp PP-2016	Masthermannia sp. AD1256 voucher UMMZ BMOC 08-0515-049 AD1256	3	0	0
	Arthropoda	Symphyleona	3	Papirinus prodigiosus	Bourletiella hortensis isolate 4A1a1_JC284	3	0	0
	Arthropoda	Diptera	2	Haematopota pluvialis	Tabanus sp. CP2_1	2	0	0
	Arthropoda	Harpacticoida	2	Leptocaris brevicornis	Leptocaris brevicornis voucher LEGO-HAR017	2	0	0
	Arthropoda	Cyclopoida	2	Cyclopoida; uncultured eukaryote	Microcyclus anceps voucher USNM:1139167	2	0	0
	Arthropoda	Trombidiformes	2	Tetranychus okinawanus	Tetranychus okinawanus	2	0	0
	Gastrotricha	Chaetonotida	8	Chaetonotida; Ambiguous_taxa	Chaetonotus aff. euhystrix MK-2019 voucher TR_8.37	8	0	0
	Gastrotricha	Chaetonotida	3	Chaetonotida; Ambiguous_taxa	Chaetonotus sp. TK25	3	0	0
	Gastrotricha	Chaetonotida	2	Chaetonotida; Ambiguous_taxa	Aspidiophorus sp. n. 2 MK-2019 voucher GA_10.5	2	0	0
	Nematoda	Enoplida	16	Triplonchida; Ambiguous_taxa	Prismatolaimus sp. MCB6	16	0	0
	Nematoda	Monhysterida	11	Eumonhystera filiformis	Eumonhystera filiformis strain EumoFil2 829+830	11	0	0
	Nematoda	Enoplida	9	Enoplida; environmental sample	Alaimus sp. SSU1_19	9	0	0
	Nematoda	Tylenchida	8	Dolichodorus sp WY-2006	Dolichodorus sp. WY-2006	8	0	0
	Nematoda	Enoplida	7	Alaimus sp 1247	Alaimus sp. GSt19	7	0	0
	Nematoda	Plectida	7	Chronogaster sp JH-2004	Chronogaster sp. JH-2004 isolate ChGaSp1	7	0	0
	Nematoda	Dorylaimida	4	Dorylaimellus virginianus	Dorylaimellus virginianus isolate 9 Mile 9-22 LP2-26	4	0	0
	Nematoda	Enoplida	3	Pseudoncholaimus sp AS89	Pseudoncholaimus sp. AS89	3	0	0
	Nematoda	Rhabditida	3	Daubaylia potomaca	Daubaylia potomaca	3	0	0
	Nematoda	Rhabditida	3	Rhabditida; Ambiguous_taxa	Acrobeloides varius strain LKC27	3	0	0
	Nematoda	Tylenchida	3	Mesocriconema sp YZ-2014a	Mesocriconema sp. N570	3	0	0
	Nematoda	Tylenchida	2	Helicotylenchus digitiformis	Helicotylenchus dihystra isolate T35 11 29935	2	0	0
	Nematoda	Dorylaimida	2	Limnomermis sp 1 JH-2014	Limnomermis sp. 1 JH-2014	2	0	0
	Nematoda	Dorylaimida	2	Mermis nigrescens	Mermis nigrescens voucher VT046NM01-1	2	0	0
	Nematoda	Monhysterida	2	Geomonhystera sp ZQZ-2010a	Monhysteridae environmental sample isolate: 003-034B-2.26	2	0	0

(table cont'd.)

Phylum	Order	Total Incidence	Lowest SILVA assignment	Top GenBank Match	L	M	H
Platyhelminthes	-	11	Rhynchoscolex simplex	Rhynchoscolex simplex isolate K05_04	11	0	0
Platyhelminthes	Thalassiphysales	5	Catenula sp KL-2009	Catenula sp. KL-2009	5	0	0
Platyhelminthes	Rhabdocoela	3	Gieysztoria infundibuliformis	Gieysztoria pavementata isolate UH235.3	3	0	0
Platyhelminthes	Rhabdocoela	2	Neodalyellida; Ambiguous_taxa	Beklemischeviella angustior isolate UH77.6	2	0	0
Platyhelminthes	Rhabdocoela	2	Dalyellioida; Ambiguous_taxa	Canetellia beauchampi isolate W19ss	2	0	0

Low/Mid

Annelida	Haplotaxida	13	Marionina southerni	Marionina nothachaeta clone LM225	9	4	0
Annelida	Phyllodocida	11	Dendronereis aestuarina	Dendronereis aestuarina isolate dea184	10	1	0
Annelida	Haplotaxida	7	Rheomorpha neiswestonovae	Rheomorpha neiswestonovae	6	1	0
Arthropoda	Podocopida	15	Cyprididae gen sp Mexico	Cypridopsis sp. Ca1 isolate CYD_SMA1	10	5	0
Arthropoda	-	13	Collembola; Ambiguous_taxa	Dicyrtomidae sp. R3	8	5	0
Arthropoda	Entomobryomorpha	14	Cryptopygus sverdrupi	Isotoma viridis isolate 6G1a1_JC448	10	4	0
Arthropoda	-	6	Collembola; Ambiguous_taxa	Micranurida pygmaea isolate 5F1a1_JC352	2	4	0
Arthropoda	Podocopida	12	Cypria sp QY-2003	Physocypria cf. biwaensis 32 IK-2017	9	3	0
Arthropoda	Trombidiformes	3	Haplochthonius simplex	Haplochthonius simplex voucher BMOC 07-0607-007	1	2	0
Arthropoda	Podocopida	7	Cypridopsis vidua	Cypridopsis sp. Ca3 isolate CYP_EXP	6	1	0
Arthropoda	Entomobryomorpha	3	Isotomurus sp cei5	Isotomurus sp. cei5	2	1	0
Arthropoda	Diptera	3	Diptera; Ambiguous_taxa	Psorophora ferox	2	1	0
Gastrotricha	Chaetonotida	7	Chaetonotida; Ambiguous_taxa	Dasydytes papaveroi voucher TK149	1	6	0
Gastrotricha	Chaetonotida	4	Heterolepidoderma sp 1 TK-2012	Heterolepidoderma sinus voucher ZH_1.79	3	1	0
Hydrozoa	Anthoathecata	5	Anthoathecata; Ambiguous_taxa	Moerisia inkermanica voucher LEM m3x S41	1	4	0
Mollusca	-	9	Heterobranchia; Ambiguous_taxa	Melampus pulchellus isolate PR1931	6	3	0
Nematoda	Enoplida	22	Triplonchida; Ambiguous_taxa	Prismatolaimus sp. MCB2	18	4	0
Nematoda	Enoplida	19	Anoplostoma sp 1093	Anoplostoma sp. 1093	10	9	0
Nematoda	Dorylaimida	12	Prodorylaimus sp HHBM-2007a	Prodorylaimus sp. HHBM-2007a	10	2	0
Nematoda	Dorylaimida	9	Dorylaimellus montenegricus	Dorylaimellus parvulus isolate Barger 2	8	1	0
Nematoda	Rhabditida	5	Acrobeloides buetschlii	Plectus sp. MCT11	4	1	0

(table cont'd.)

	Phylum	Order	Total Incidence	Lowest SILVA assignment	Top GenBank Match	L	M	H
	Nematoda	Enoplida	5	Enoplida; Ambiguous_taxa	Oxystomina sp. NUS3	4	1	0
	Nematoda	Tylenchida	4	Hirschmanniella sp Yuma	Hirschmanniella sp. Yuma	3	1	0
	Nematoda	Dorylaimida	4	Isomermis lairdi	Isomermis lairdi partial isolate	3	1	0
	Nematoda	Monhysterida	3	Monhysterida; uncultured eukaryote	Uncultured eukaryote clone: B21_ek_33	2	1	0
	Platyhelminthes	Rhabdoceola	18	Olisthanella truncula	Olisthanella truncula	12	6	0
	Tardigrada	Parachela	3	Thulinus stephaniae	Thulinus stephaniae clone 8	2	1	0
Low/High								
	Arthropoda	Podocopida	6	Podocopida; Ambiguous_taxa	Darwinula sp. QY-2003	4	0	2
	Arthropoda	Ephemeroptera	5	Ephemeroptera; Ambiguous_taxa	Clypeocaenis sp. BYU IGCEP131	3	0	2
	Arthropoda	-	4	Acari; Ambiguous_taxa	Sancassania berlesei	3	0	1
	Arthropoda	Lepidoptera	3	Ambiguous_taxa	Ostrinia furnacalis haplotype 11	2	0	1
	Arthropoda	Diptera	3	Diptera; Ambiguous_taxa	Camptodiplosis auriculariae voucher JSC52	1	0	2
	Gastrotricha	Chaetonotida	16	Chaetonotus cf novenarius TK151	Haltidytes pseudosquamosus voucher HA1	15	0	1
	Nematoda	Rhabditida	7	Rhabditida; Ambiguous_taxa	Euteratocephalus sp. 803L-008	6	0	1
	Nematoda	Plectida	5	Paraphanolaimus behningi	Paraphanolaimus behningi strain PaAPBeh4	3	0	2
	Nematoda	Araeolaimida	6	Araeolaimida; Ambiguous_taxa	Onchium sp. San Elijo	2	0	4
Mid Unique								
	Arthropoda	Trombidiformes	2	Rhombognathus levigatoides	Rhombognathus sp. UFMG 173954	0	2	0
	Nematoda	Plectida	7	Haliplectidae; Ambiguous_taxa	Haliplectus cf. dorsalis HaPIDor22	0	7	0
	Nematoda	Desmodorida	4	Calomicrolaimus parahonestus	Microlaimidae sp. 3 TJP-2019 voucher NPRB.45	0	4	0
	Nematoda	Plectida	4	Chronogaster sp JH-2004	Chronogaster sp. JH-2004 isolate ChGaSp2	0	4	0
	Nematoda	Enoplida	2	Oncholaimus sp OUS2	Oncholaimus sp. OUS2	0	2	0
	Nematoda	Plectida	2	Aphanolaimus aquaticus	Aphanolaimus aquaticus strain AphaAqu3	0	2	0
	Nematoda	Plectida	2	Paraphanolaimus behningi	Paraphanolaimus behningi strain PaAPBeh3	0	2	0
	Platyhelminthes	Rhabdoceola	3	Prognathorhynchus busheki	Prognathorhynchus busheki isolate EGPKS_002	0	3	0
	Platyhelminthes	Macrostomida	2	Microstomum papillosum	Microstomum westbladi isolate S114	0	2	0
	Xenacoelomorpha	Acoela	2	Paedomecynostomum bruneum	Paedomecynostomum bruneum partial specimen voucher AWK05-47	0	2	0

(table cont'd.)

	Phylum	Order	Total Incidence	Lowest SILVA assignment	Top GenBank Match	L	M	H
Mid/High								
	Annelida	Phyllodocida	14	Alitta succinea	Alitta succinea isolate AISu-02	0	1	13
	Annelida	Phyllodocida	11	Namalycastis jaya	Namalycastis abiuma isolate naa185	0	6	5
	Arthropoda	Diptera	10	Diptera; invertebrate environmental sample	Culicoides scoticus	0	4	6
	Arthropoda	Diptera	4	Minettia flaveola	Uncultured eukaryote	0	1	3
	Arthropoda	Diptera	4	Thaumatomyia notata	Thaumatomyia notata	0	2	2
	Arthropoda	Diptera	4	Megaselia scalaris	Megaselia scalaris	0	2	2
	Arthropoda	Diptera	3	Culex brethesi	Culex brethesi partial	0	1	2
	Arthropoda	Sarcoptiformes	3	Sellea sp AD658	Sellea sp. AD658	0	2	1
	Hydrozoa	Leptothecata	10	Helgicirrha cari	Helgicirrha cari isolate MHNG-HYD-DNA1153	0	2	8
	Kinorhyncha	-	24	Cyclorhagida; Ambiguous_taxa	Echinoderes sp. MVS2014	0	8	16
	Nematoda	Tylenchida	20	Meloidogyne spartinae	Meloidogyne spartinae	0	2	18
	Nematoda	Desmodorida	19	Prochaetosoma sp 3 HSR-2009	Prochaetosoma sp. OK-2015 isolate t2	0	1	18
	Nematoda	Enoplida	15	Halalaimus sp 1034	Halalaimus sp. 1034	0	6	9
	Nematoda	Chromadorida	13	Dichromadora sp 2 JH-2014	Cf. Dichromadora sp. 2 JH-2014	0	7	6
	Nematoda	Monhysterida	9	Diplolaimelloides sp BCG-2008	Diplolaimelloides sp. BCG-2008	0	3	6
	Nematoda	Desmoscolecida	10	Desmoscolex sp ITDL-2011	Desmoscolex sp. 5 TJP-2019 voucher Nem.291	0	5	5
	Nematoda	Monhysterida	7	Sabatieria punctata	Sabatieria sp. 4 TJP-2019 voucher NPRB.50	0	4	3
	Nematoda	Desmodorida	9	Epsilonematidae sp Epsifamil1	Epsilonematidae sp. Epsifamil1	0	7	2
	Nematoda	Monhysterida	4	Monhysterida; uncultured eukaryote	Daptonema normadicum	0	2	2
	Nematoda	Monhysterida	3	Diplolaimella dievangatensis	Diplolaimella dievangatensis	0	1	2
	Platyhelminthes	Macrostomida	15	Macrostomum kepleri	Macrostomum kepleri voucher MTP LS 285	0	5	10
	Platyhelminthes	Rhabdocoela	13	Mesorhynchus terminostylis	Itaipusa sinensis isolate YTP3	0	4	9
	Platyhelminthes	Proseriata	6	Monocelis fusca	Monocelis fusca	0	1	5
High Unique								
	Annelida	Sabellida	2	Manayunkia aestuarina	Manayunkia aestuarina	0	0	2
	Annelida	Scolecida	2	Barantolla lepte	Notomastus sunae voucher TIO-BTS-Poly 118	0	0	2
	Annelida	Haplotaxida	2	Haplotaxida; Ambiguous_taxa	Inanidrilus exumae isolate CE73	0	0	2
	Arthropoda	Podocopida	3	Ambiguous_taxa	Leptocythere lacertosa	0	0	3
	Arthropoda	Diptera	2	Diptera; invertebrate environmental sample	Culicoides scoticus	0	0	2
	Mollusca	Ostreida	4	Ostreoida; Ambiguous_taxa	Crassostrea virginica isolate Cv_A3	0	0	4

(table cont'd.)

	Phylum	Order	Total Incidence	Lowest SILVA assignment	Top GenBank Match	L	M	H
	Mollusca	Veneroida	2	Veneroida; Ambiguous_taxa	Rangia cuneata voucher BivAToL-280	0	0	2
	Nematoda	Desmodorida	7	Desmodora sp DL-2016	Desmodora sp. DL-2016	0	0	7
	Nematoda	Desmodorida	4	Desmodorida; uncultured metazoan	Metachromadora sp. MAchSp1	0	0	4
	Nematoda	Enoplida	2	Oxystomina sp HCL32	Oxystomina sp. HCL20	0	0	2
	Platyhelminthes	Rhabdocoela	2	Ptychopera sp NVS-2013	Ptychopera sp. NVS-2013 isolate UH294.10	0	0	2

All OTUs presented in this table are those which were not detected in at least one of the salinity zones, and were detected at least twice in at least one salinity zone.

Alpha diversity:

No significant differences in OTU richness were detected for the samples from the two bays (Kruskal-Wallis test, $\chi^2(1) = 0.02$, $p = 0.90$), though the OTU richness reached higher values in Caillou Bay (Fig 4.17). In addition, no difference in Faith's Phylogenetic Diversity (PD) was detected between samples from the two bays (Kruskal-Wallis test, $\chi^2(1) = 0.16$, $p = 0.69$, Fig. 4.18).

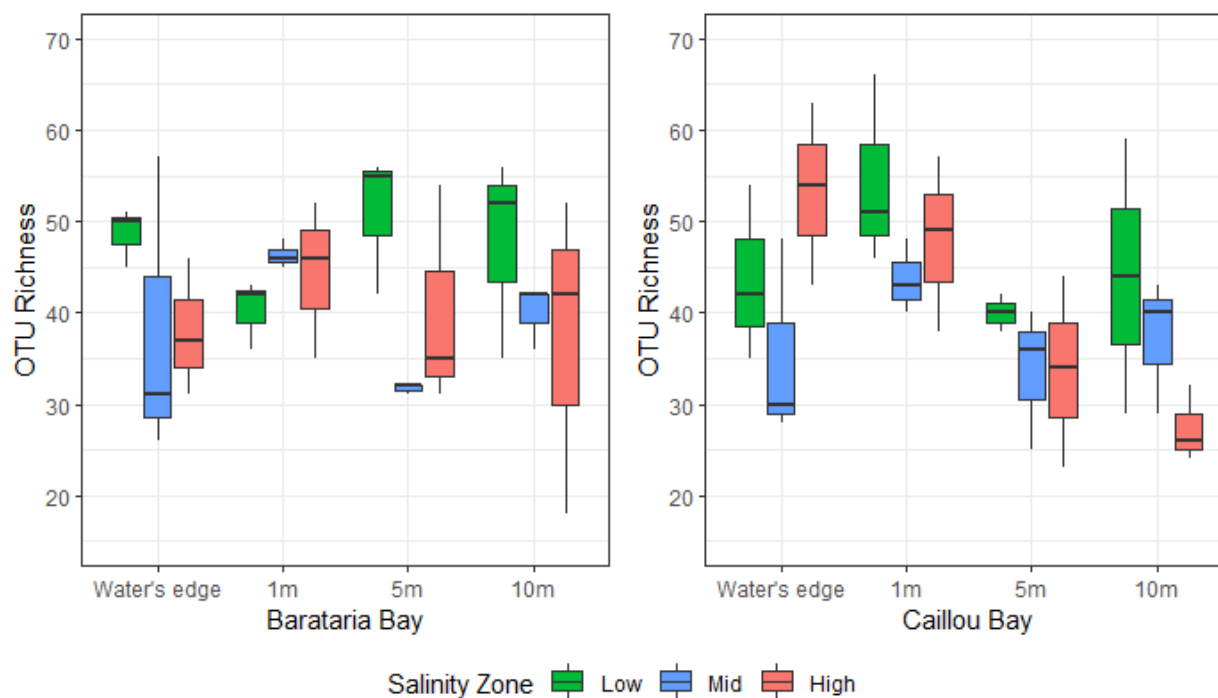


Fig. 4.17. Boxplot of OTU richness values, divided by bay, salinity zone, and distance from marsh edge. All samples were collected from marsh sites in Barataria and Caillou Bays during July 2018.

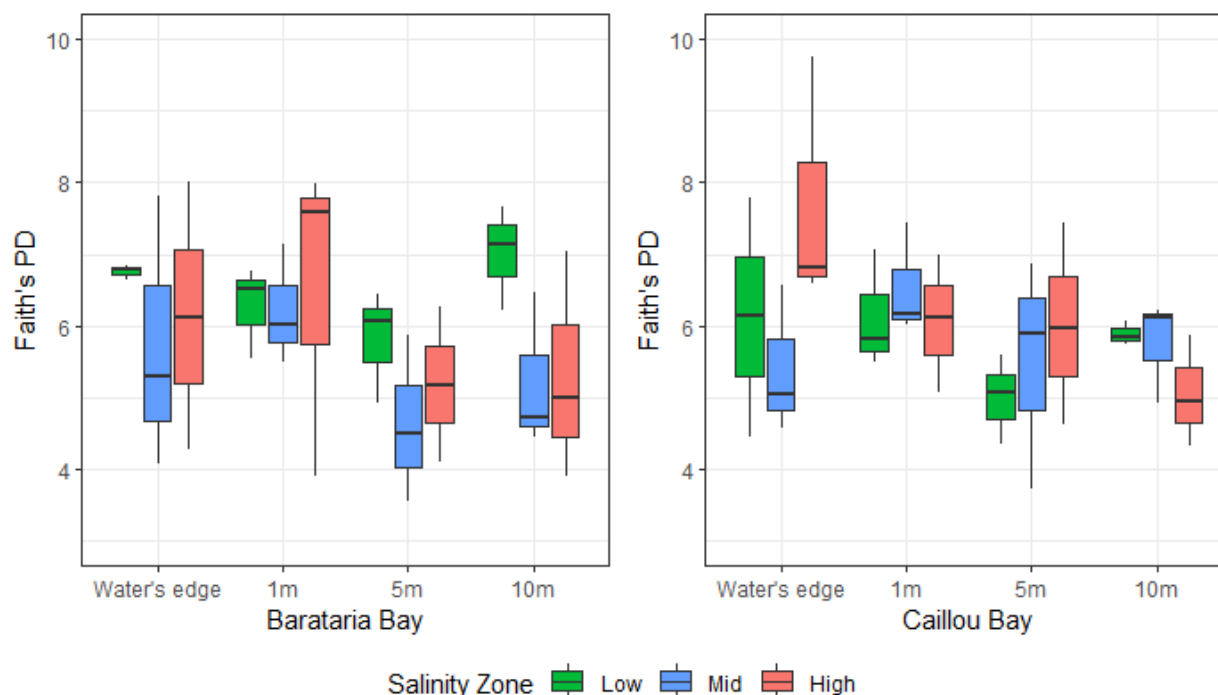


Fig. 4.18. Boxplot of Faith's Phylogenetic Diversity values in the samples from the different bays. All samples were collected from marsh sites in Barataria and Caillou Bays during July 2018.

The OTU richness was significantly higher in the Low salinity zone samples than in the Mid salinity zone samples (Kruskal-Wallis pairwise test, $\chi^2(2) = 9.16$, Benjamini Hochberg corrected $p < 0.01$, Fig. 4.17). Faith's PD was not significantly different across the three salinity zones (Kruskal-Wallis test, $\chi^2(2) = 2.10$, $p = 0.35$), meaning that the additional richness in Low zone samples did not come from widely phylogenetically different taxa. However, the High salinity zone samples had a larger range of PD values than the other two salinity zones (Fig. 4.18).

The OTU richness was not significantly different among any of the groups of samples from the different distance from marsh edge categories (Kruskal-Wallis pairwise test, $\chi^2(3) = 6.47$, $p = 0.09$, Fig 4.17). In addition, Faith's PD values were not significantly different across the distance from marsh edge factor ($\chi^2(3) = 5.46$, $p = 0.14$, Fig 4.18).

The OTU richness was not significantly different across the interaction of the Bay and Salinity zone factors ($\chi^2(5) = 8.96$, $p = 0.11$, Fig 4.17). The Faith's PD values for this interaction were also not significantly different ($\chi^2(5) = 4.51$, $p = 0.48$, Fig 4.18).

The OTU richness was not significantly different for the interaction of the Bay and distance from marsh edge factors ($\chi^2(7) = 9.08$, $p = 0.24$, Fig 4.17). In addition, the Faith's PD values for this interaction were not significantly different ($\chi^2(7) = 6.00$, $p = 0.54$, Fig 4.18).

The OTU richness was significantly different for the interaction of the Salinity zone and distance from marsh edge factors (χ^2 (11) = 21.88, p = 0.03, Fig 4.17), but none of the pairwise tests remained significantly different following the Benjamini-Hochberg correction (all p > 0.05). However, the Faith's PD values for this interaction of those factors were not significantly different (χ^2 (11) = 11.70, p = 0.39, Fig 4.18).

The OTU richness was not significantly different for the interaction of all three factors (χ^2 (23) = 27.80, p = 0.22, Fig 4.17). In addition, the Faith's PD values were not significantly different for the interaction of all three factors (χ^2 (23) = 17.73, p = 0.77, Fig 4.18).

Beta diversity group similarity indices:

All beta diversity similarity indices calculated in SpadeR Online returned a value from zero to one, with values closer to one indicating more similarities in composition and incidence of OTUs between the groups being compared (Table 4.11). For the samples from the different bays, all of the empirical incidence-based indices (Horn, Morisita-Horn, and Regional overlap) showed very high values (>0.8), while the empirical richness-based indices (Sørensen and Jaccard) showed moderately high values (>0.5). The estimated incidence-based indices all were higher than the empirical incidence-based indices, while the estimated richness-based indices were slightly lower than the empirical. Thus, with additional sampling, additional richness could be collected which might increase differences in composition between the samples from the bays. However, this additional richness would not change patterns of incidence in the dataset.

Table 4.11. Empirical and estimated similarity indices between communities collected from different bays (Barataria and Caillou), salinity zones (Low, Mid, and High) and distances from the marsh edge (0m, 1m, 5m, and 10m). All samples were collected during July 2018 at marsh sites in Barataria and Caillou Bays.

Factor	Index	Estimate	S.E.	95% Lower	95% Upper
Bay	Sørensen Empirical	0.6863	0.0186	0.6498	0.7228
	Sørensen Estimated	0.656	0.0558	0.5466	0.7654
	Jaccard Empirical	0.5224	0.0207	0.4818	0.563
	Jaccard Estimated	0.4881	0.0633	0.364	0.6122
	Horn (equal-weighted) Empirical	0.8601	0.0083	0.8438	0.8764
	Horn (equal-weighted) Estimated	0.8941	0.0147	0.8653	0.9229
	Morisita-Horn (relative) Empirical	0.8931	0.0038	0.8857	0.9005
	Morisita-Horn (relative) Estimated	0.9549	0.0566	0.844	1
	Regional overlap (relative) Empirical	0.9435	0.002	0.9397	0.9474
	Regional overlap (relative) Estimated	0.9769	0.029	0.92	1
Salinity Zone	Sørensen Empirical	0.6537	0.0099	0.6343	0.6731
	Sørensen Estimated	0.605	0.0268	0.5525	0.6576
	Jaccard Empirical	0.3862	0.0187	0.3495	0.4229

(table cont'd.)

Factor	Index	Estimate	S.E.	95% Lower	95% Upper
	Jaccard Estimated	0.338	0.0672	0.2063	0.4697
	Horn (equal-weighted) Empirical	0.7639	0.004	0.7561	0.7717
	Horn (equal-weighted) Estimated	0.8377	0.0044	0.8291	0.8462
	Morisita-Horn (relative) Empirical	0.773	0.004	0.7652	0.7807
	Morisita-Horn (relative) Estimated	0.8479	0.0318	0.7856	0.9101
	Regional overlap (relative) Empirical	0.9108	0.0014	0.9081	0.9136
	Regional overlap (relative) Estimated	0.9436	0.0173	0.9096	0.9775
Distance from Marsh Edge	Sørensen Empirical	0.7823	0.0084	0.7659	0.7988
	Sørensen Estimated	0.8397	0.0173	0.8058	0.8737
	Jaccard Empirical	0.4733	0.018	0.4381	0.5085
	Jaccard Estimated	0.5671	0.0551	0.459	0.6752
	Horn (equal-weighted) Empirical	0.8736	0.0043	0.8652	0.8819
	Horn (equal-weighted) Estimated	0.8971	0.0042	0.8888	0.9054
	Morisita-Horn (relative) Empirical	0.8952	0.0041	0.8871	0.9032
	Morisita-Horn (relative) Estimated	1	0.0362	0.9291	1
	Regional overlap (relative) Empirical	0.9716	0.0011	0.9693	0.9738
	Regional overlap (relative) Estimated	1	0.0097	0.9811	1

S.E. = standard error. 95% Lower and Upper are the range for the confidence interval. Estimates range from zero to one, with higher values indicating higher similarity.

The empirical indices for the similarity among salinity zone communities all returned values above 0.6, excluding the Jaccard index, which returned a low value of 0.38 (Table 4.11). The Jaccard index gives less weight to shared species between groups, so it always produces a lower value than the Sørensen index. The same pattern observed in the estimated indices for the different bay communities was observed in the estimated indices for the salinity zone communities, where the estimated richness-based indices were lower than the empirical while the incidence-based indices were higher than the empirical indices. Therefore, if additional OTUs were captured by increased sampling, the differences in composition between the salinity zones might increase, but this additional richness would not change the patterns of incidence. Estimated pairwise Sørensen index values (Table 4.12) indicated that the Low and High communities had the lowest similarity of any pair of the salinity zone communities because they shared the lowest number of OTUs (Table 4.6).

Table 4.12. Estimated pairwise similarity matrix for salinity zone communities, Sørensen index. All samples were collected in July 2018 from marsh sites in Barataria and Caillou Bays.

Community	Low	Mid	High
Low	1	0.548 (0.453,0.643)	0.456 (0.368,0.544)
Mid		1	0.559 (0.471,0.647)
High			1

Numbers in parenthesis for each pairwise similarity value are the 95% confidence interval for that similarity.

For the communities in the samples from different distances from the marsh edge, all empirical indices were quite high (>0.7), again excluding the Jaccard index (Table 4.11). All of the estimated indices were higher than the empirical indices, with several estimated index values reaching 1. This increase indicates that additional sampling would only increase the similarity of composition and incidence of the four communities. Pairwise estimated Sørensen index values showed that the most similar of these four communities were the communities from samples collected 0 and 1 meter from the marsh edge, while the least similar were those collected 0 and 10 meters from the marsh edge (Table 4.13). However, all of the pairwise indices showed similarity (>0.5) due to the high numbers of shared species between the different transect positions (Table 4.7).

Table 4.13. Estimated pairwise similarity matrix for the distance from marsh edge communities, Sørensen index. All samples were collected in July 2018 from marsh sites in Barataria and Caillou Bays.

Community	Zero	One	Five	Ten
Zero	1	0.836 (0.646,1.000)	0.612 (0.502,0.722)	0.592 (0.435,0.749)
One		1	0.723 (0.570,0.875)	0.615 (0.492,0.737)
Five			1	0.691 (0.517,0.865)
Ten				1

Numbers in parenthesis for each pairwise similarity value are the 95% confidence interval for that similarity.

Non-Metric Dimensional Scaling (NMDS):

Beta diversity (differentiation of the composition of samples using the Sørensen index) of the samples from the different salinity zones, bays, and the different distance from marsh edge categories was visualized using NMDS ordination. Plotting the salinity zone groups over the samples in the ordination revealed a distinct separation of samples from the Low and High salinity zones, with samples from the Mid salinity zone falling roughly between them (Fig. 4.19). However, the group of samples from the Mid salinity zone was much more widely dispersed than the other two groups. When separated by bay of origin, groups of samples from different

bays tended to overlap with the samples from the same salinity zone, but samples from the Mid salinity zone samples from Caillou Bay had a much wider dispersion than other groups (Fig. 4.20). Plotting the samples by the distance from the marsh edge, salinity, and bay reveals the reason for the dispersion of the Mid salinity zone from Caillou Bay: the 0 and 1m samples from that group showed a large separation from the 5 and 10m samples (Fig. 4.21). The 5m samples from the Mid salinity zone of Caillou Bay were closer to the groups of samples from the Mid salinity zone of Barataria Bay, while the 10m samples from the Mid salinity zone of Caillou Bay were closer to the Low salinity zone of Barataria Bay. For all other bay and salinity zone groups, the samples from different distances from the marsh edge grouped more closely together, with the High salinity zones from both bays grouping especially closely.

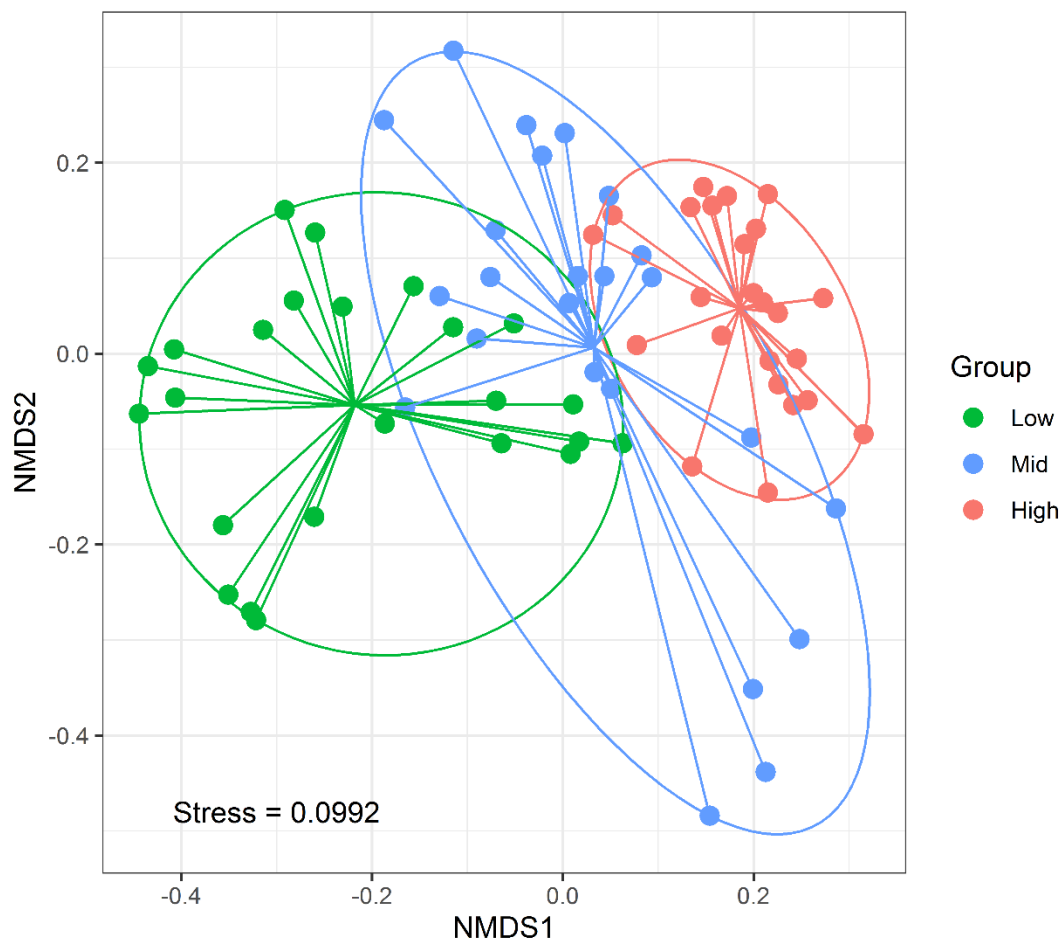


Fig. 4.19. Plot of the first two dimensions of the NMDS ordination of the Sørensen distance matrix, with salinity zone groups plotted as ellipses around the sample points. Samples were collected in July 2018 from marsh sites in Barataria and Caillou Bays. Small circles represent individual samples. Solid ellipses represent the elliptical hulls of the group. Solid, straight lines connect a sample to the group centroid.

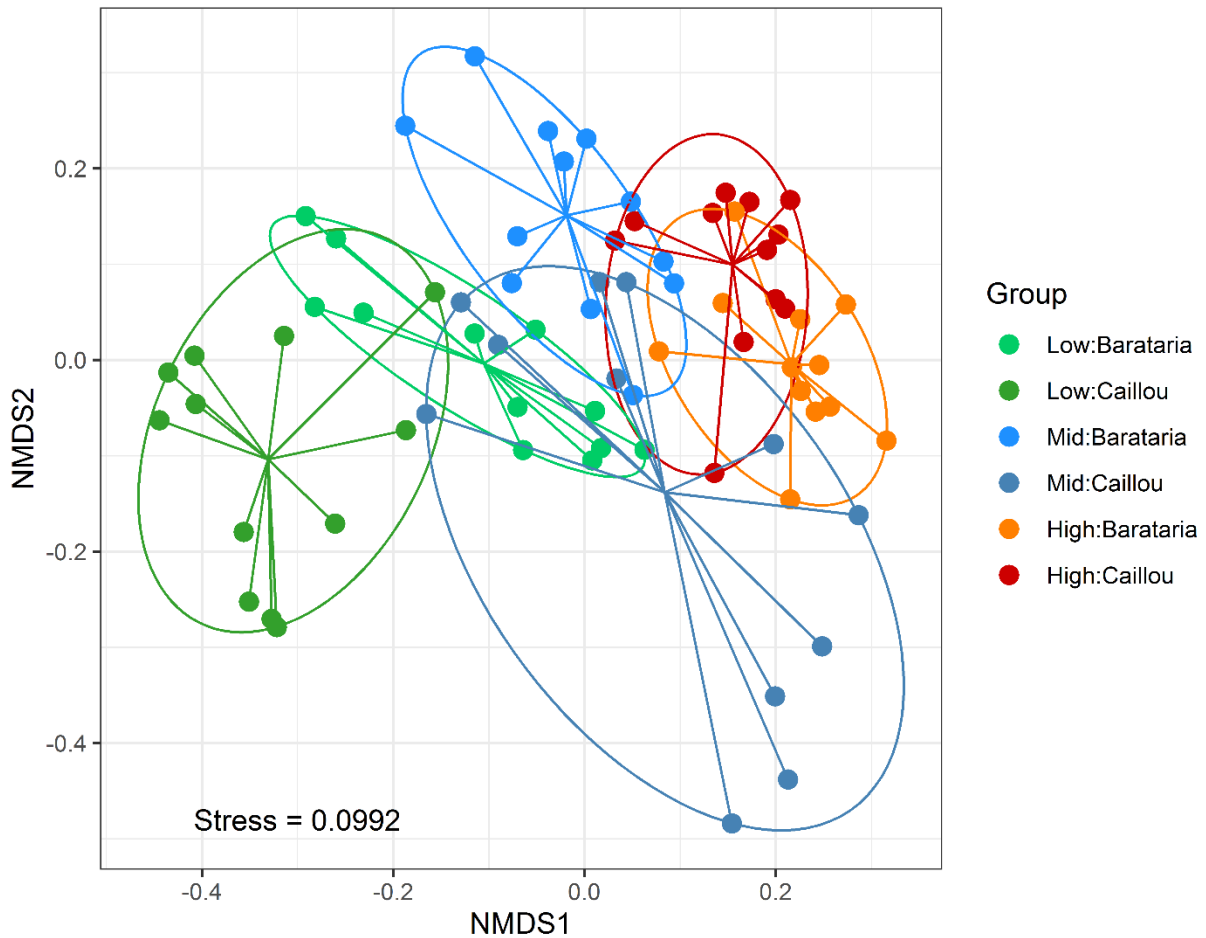


Fig. 4.20. Plot of the first two dimensions of the NMDS ordination of the Sørensen distance matrix, with salinity zone groups from each bay plotted as ellipses around the sample points. Samples were collected in July 2018 from marsh sites in Barataria and Caillou Bays. Labels for each group overlay the group centroid. Small circles represent individual samples. Solid ellipses represent the elliptical hulls of the group. Solid, straight lines connect a sample to the group centroid.

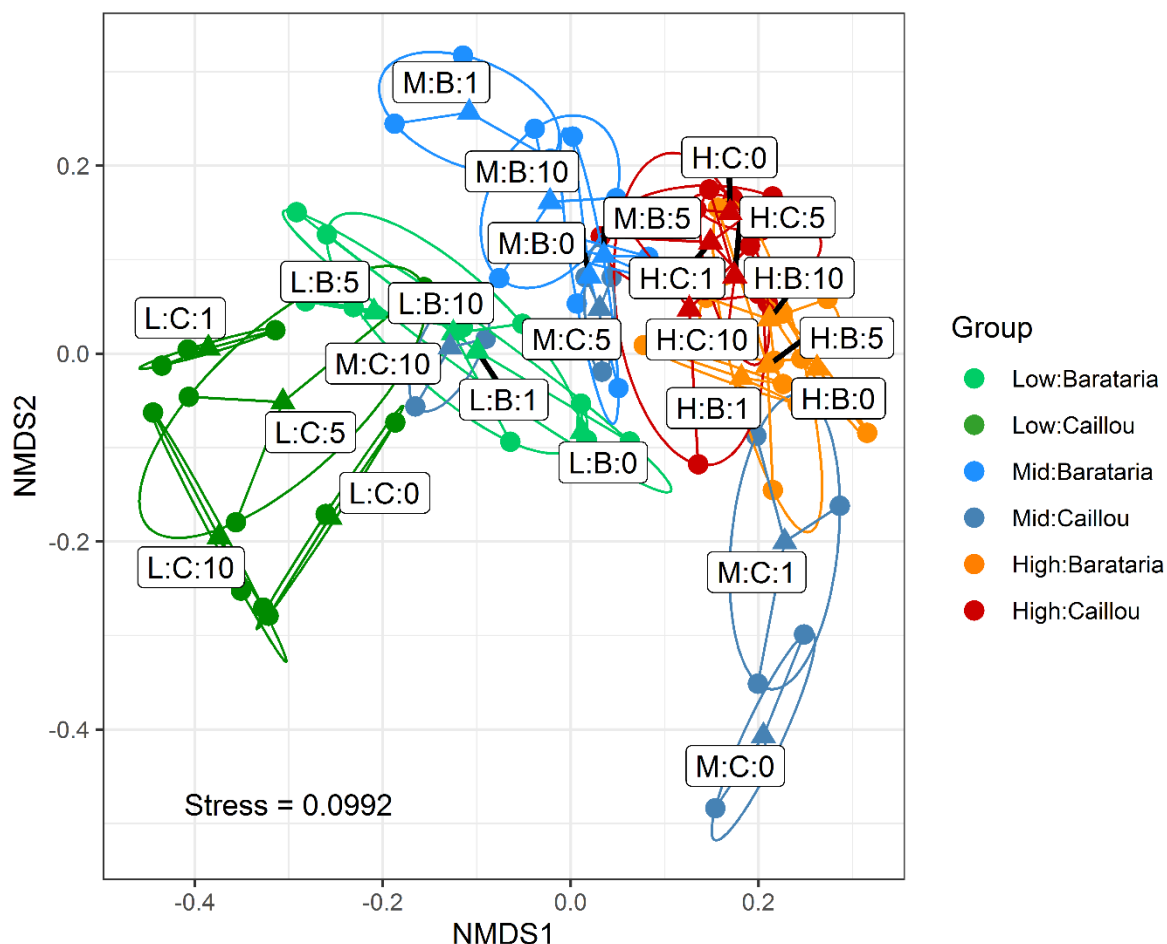


Fig. 4.21. Plot of the first two dimensions of the NMDS ordination of the Sørensen distance matrix, with salinity zone groups for each bay plotted as ellipses around the samples. Samples were collected in July 2018 from marsh sites in Barataria and Caillou Bays. Labels for each group are next to the group centroid, indicated by a triangular point. An “L”, “M”, or “H” represents a group from the Low, Mid or High salinity zones, respectively, while “C” indicates a group of samples from Caillou Bay, and “B” indicates a group of samples from Barataria Bay. The number at the end of a group label represents the distance from the marsh edge in meters. Small circles represent individual samples. Solid ellipses represent the elliptical hulls of samples.

Adonis test:

All factors (bay, distance from marsh edge, and salinity zone) and all factor interactions tested using the Adonis procedure (following Benjamini-Hochberg correction) had significant effects on the differentiation of composition of samples in the dataset (Table 4.14). However, following Benjamini-Hochberg correction, results from the PERMDISP procedure indicated that all factors and all interactions of factors (excluding the distance from marsh edge factor and the interaction of bay and distance from marsh edge) had non-homogenous multivariate spread. This means that differences detected by Adonis within the factors and interactions with

significant PERMDISP results may be due to differences in the multivariate spread of the groups, instead of or in addition to the differences in the location of the groups in the multivariate space. In the salinity zone factor, the groups of samples from Low and Mid zones had larger multivariate spread than the group of samples from the High zone (pairwise PERMDISP, Benjamini Hochberg corrected p-values <0.05). This is supported by the spread of these groups in the NMDS ordination (Fig. 4.19); but given the separation of the group centroids in the ordination (especially of the Low and High salinity zone centroids), there is likely also a location effect on top of the dispersion effect. However, when the salinity zones were split by bay, the samples from the Mid salinity zone in Caillou Bay had a significantly different multivariate spread from all other groups except for the samples from the Low salinity zone in Caillou Bay. This observation is supported by the spread observed in the NMDS ordination (Fig. 4.20).

The salinity zone factor had the highest R^2 value in the Adonis test, at 0.2, indicating that the salinity zone factor explained more variation in the dataset than any other factor or interactions (Table 4.14). All other factors and interactions had low R^2 values (<0.1).

Table 4.14. Adonis test results. All samples were collected in July 2018 from marsh sites in Barataria and Caillou Bays.

Factor	Df	SumOfSqs	R2	F	p
Bay	1	0.814162	0.059896	7.602378	1.00E-04*
Distance	3	0.971054	0.071438	3.022461	1.00E-04*
Salinity Zone	2	2.714158	0.199674	12.67196	1.00E-04*
Bay:Distance	3	0.591387	0.043507	1.840726	0.002*
Bay:Salinity Zone	2	1.12116	0.082481	5.234514	1.00E-04*
Distance:Salinity Zone	6	1.087835	0.080029	1.692976	0.0011*
Bay:Distance:Salinity Zone	6	1.152727	0.084803	1.793965	0.0003*
Residual	48	5.140466	0.378171		
Total	71	13.59295	1		

An asterisk * indicates a p-value which remained significant after the Benjamini-Hochberg correction.

Differential abundance:

Initially, the Songbird program was run using the formula “Salinity zone + Bay +Distance from marsh edge”. However, this formula resulted in negative pseudo- Q^2 values no matter what the parameters were adjusted to. With the differential prior set to 0.001, the learning rate set to $1e^{-6}$, the minimum samples and feature counts set to the defaults, and the epochs set to ,000,000, this formula achieved a Q^2 value of -0.13. The Q^2 values function similarly to the R^2 values of a regression, and negative Q^2 values indicate poor predictive accuracy and potential overfitting of the model. The program was then run again using models based on the individual factors, and the Distance from marsh edge factor did not result in a positive Q^2 value. The Distance from marsh edge factor was then dropped from the formula to determine if simplifying the formula could produce a positive Q^2 value. The new formula, “Salinity zone +

Bay", with the differential prior set to 0.0001, the learning rate set to $1e^{-7}$, and the epochs set to 4,000,000, achieved a Q^2 value of 0.04.

Eighty-eight OTUs were detected as having differential read count abundance across the salinity zone and bay categories (Table 4.15). These OTUs matched to the frequent group of OTUs because the minimum sample count was set to 10, which is the same as the minimum number of samples to be in the frequent group. Because read counts of metazoa do not necessarily reflect abundances of OTUs, the differentials should be interpreted as a measure of the relative difference in cell counts across categories. These 88 OTUs consisted of 38 Nematoda, 19 Arthropoda, 12 Annelida, 7 Platyhelminthes, 3 Mollusca, 2 Bryozoa, 2 Gastrotricha, 2 Rotifera, 1 Hydrozoa, 1 Kinorhyncha, and 1 ambiguous taxon (which matched in GenBank to Platyhelminthes). Due to the sheer number of differentials, only the highest and lowest 10%, i.e., the differentials showing the most difference between the categories, for each comparison category will be discussed in the text, while all of the differentials are presented in table format (Table 4.15). Positive values indicate association with the class that the column is named for, while negative values indicate association with the comparison class. More extreme values of the differential indicate stronger association, whether positive or negative.

For the Mid compared to Low salinity zone category, the OTU assigned to the annelid *Polydora brevipalpa* had the largest positive differential (i.e., most associated with the Mid salinity zone when compared to the Low salinity zone). The next three largest positive differentials for this category belonged to OTUs assigned to *Mesorhynchus terminostylis* (Platyhelminthes), an ambiguous nematode (matched to *Daptonema* sp. in GenBank), and the arthropod *Sminthurides aquaticus* (Collembola). The next three largest positive differentials were assigned to three annelids, *Marionina sublitoralis* (Oligochaeta), *Paraprionospio patiens* (Polychaeta), and *Monopylephorus rubroniveus* (Oligochaeta). The final OTU in the highest 10% of the positive differentials was assigned to an ambiguous nematode (matched to *Daptonema* sp. in GenBank). The first two of the lowest 10% of the differentials (i.e., those taxa most associated with the Low salinity zone when compared to the Mid salinity zone) were *Eumonhystra filiformis* (Nematoda) and *Alitta succinea* (Annelida, Polychaeta). The next two lowest differentials were both assigned to nematodes, *Meloidogyne spartinae*, and an ambiguous nematode (matched to *Prismatolaimus* sp. in GenBank). The next two of the lowest 10% of differentials in this category were assigned to *Rhynchoscolex simplex* (Platyhelminthes) and *Dendronereis aestuarina* (Annelida, Polychaeta). The two lowest differentials in this category were both assigned to ambiguous nematodes (matched to *Clavicaudoides* sp. and *Prismatolaimus* sp. in GenBank, respectively).

The largest positive differential in the High compared to Low salinity zone category was an OTU assigned to a nematode environmental sample (matched to *Mesodorylaimus* sp. in GenBank). The next two differentials in this category were the annelids *Namalycastis jaya* (Polychaeta) and *Monopylephorus rubroniveus* (Oligochaeta). The next highest differential was *Mesorhynchus terminostylis* (Platyhelminthes). Following this, the next two differentials were

an annelid and an arthropod, *Marionina coatesae* (Oligochaeta) and *Sminthurides aquaticus* (Collembola). The final two differentials in the highest 10% of the High to Low category were both ambiguous nematodes, which matched in GenBank to *Hirschmanniella santarosae* and a *Daptonema* sp. The first of the lowest 10% of the differentials for this category was an arthropod assigned to the genus *Cypria* (Ostracoda). The next two lowest differentials were both nematodes, an ambiguous nematode (matched to *Prismatolaimus* sp. in GenBank) and *Anoplostoma* sp. The next lowest differential was *Rhynchoscolex simplex*, a nematode, followed by two ambiguous arthropods, a member of the ostracod family Cyprididae (matched to *Cypridopsis* sp. in GenBank) and a member of the hexapod order Collembola (matched to family Dicyrtomidae in GenBank). The final two lowest differentials for the High to Low category were an ambiguous hydrozoan (matched to *Pennaria* sp. in GenBank) and a nematode belonging to the genus *Ditylenchus*.

In the Barataria compared to Caillou category, the highest positive differential was the nematode *Diplolaimella dievengatensis*, followed by an ambiguous nematode (matched to *Metoncholaimus albidus* in GenBank). The next highest differential in this category was the annelid *Dendronereis aestuarina* (Polychaeta). The next two differentials were an ambiguous member of the Platyhelminthes (matched to *Lagenopolycystis* sp. in GenBank) and the annelid *Marionina sublitoralis* (Polychaeta). Following these, the final three differentials of the highest 10% in this category were an ambiguous nematode (matched to *Chromadorina* sp. in GenBank), the rotifer *Octotrocha speciosa*, and another ambiguous nematode (matched to *Daptonema* sp. in GenBank). The first of the lowest 10% of the differentials in the Barataria compared to Caillou category was the nematode *Meloidogyne spartinae*, followed by the nematode *Chronogaster typica*. The next lowest differential was the annelid *Namalycastis jaya* (Polychaeta). This differential was followed by two nematodes, which matched to *Prodorylaimus* sp. and *Halalaimus* sp. in SILVA, respectively. The next two differentials belonged to a member of the phylum Platyhelminthes, *Rhynchoscolex simplex*, and a member of the phylum Mollusca, *Tectarius spinulosus*. The lowest differential for the Barataria compared to Caillou category was the annelid *Marionina southerni* (Oligochaeta).

Table 4.15. Songbird differentials for the OTUs detected in samples from marsh sites in Barataria and Caillou Bays during July 2018.

SILVA Taxonomy String	Intercept	Mid Compared to Low	High Compared to Low	Barataria Compared to Caillou
Annelida; Clitellata; Oligochaeta; Haplotaxida; Ambiguous taxa	1.5548	0.9041	1.1524	-0.5370
Annelida; Clitellata; Oligochaeta; Haplotaxida; <i>Marionina coatesae</i>	1.3283	1.3443	1.8708	0.6717
Annelida; Clitellata; Oligochaeta; Haplotaxida; <i>Marionina southerni</i>	1.5388	-0.2627	-1.5668	-1.9705
Annelida; Clitellata; Oligochaeta; Haplotaxida; <i>Marionina sublitoralis</i>	-0.8304	1.8596	-0.2929	1.6819
Annelida; Clitellata; Oligochaeta; Haplotaxida; <i>Monopylephorus rubroniveus</i>	1.5956	1.6997	2.3606	0.9214
Annelida; Clitellata; Oligochaeta; Haplotaxida; <i>Paranais litoralis</i>	-0.3538	-1.3238	0.7900	0.4731

(table cont'd.)

SILVA Taxonomy String	Intercept	Mid Compared to Low	High Compared to Low	Barataria Compared to Caillou
Annelida; Polychaeta; Palpata; Phyllodocida; <i>Alitta succinea</i>	0.3908	-1.3258	0.9604	0.1946
Annelida; Polychaeta; Palpata; Phyllodocida; <i>Dendronereis aestuarina</i>	-0.0330	-1.3295	-1.5699	2.0107
Annelida; Polychaeta; Palpata; Phyllodocida; <i>Namalycastis jaya</i>	2.4116	-0.3650	2.7042	-1.5702
Annelida; Polychaeta; Scolecida; Spionida; <i>Boccardiella hamata</i>	1.1706	-0.0547	1.6312	-0.7827
Annelida; Polychaeta; Scolecida; Spionida; <i>Paraprionospio patiens</i>	1.3881	1.7161	0.9746	-0.7462
Annelida; Polychaeta; Scolecida; Spionida; <i>Polydora brevipalpa</i>	-2.0706	4.4868	1.6078	-1.4460
Arthropoda; Chelicerata; Arachnida; Acari; Ambiguous taxa	0.3617	0.9181	0.7090	-0.8219
Arthropoda; Crustacea; Malacostraca; Eumalacostraca; Eucarida; <i>Carcinus maenas</i> (green crab)	1.2981	-1.3230	-0.9618	-1.0264
Arthropoda; Crustacea; Malacostraca; Eumalacostraca; Peracarida; <i>Tanais dulongii</i>	-2.4045	0.2181	1.3010	-0.6344
Arthropoda; Crustacea; Maxillopoda; Copepoda; Harpacticoida; <i>Leptocaris brevicornis</i>	1.4749	-0.5014	0.7127	0.0860
Arthropoda; Crustacea; Maxillopoda; Copepoda; Harpacticoida; <i>Leptocaris brevicornis</i>	-1.2438	-0.3221	-0.5667	-0.5664
Arthropoda; Crustacea; Maxillopoda; Copepoda; Harpacticoida; <i>Nitokra hibernica</i>	1.7077	0.3326	-1.5664	0.4641
Arthropoda; Crustacea; Ostracoda; Podocopa; Podocopida; <i>Cypria</i> sp. QY-2003	-0.8368	-0.4603	-1.5715	0.5065
Arthropoda; Crustacea; Ostracoda; Podocopa; Podocopida; Cyprididae gen. sp. Mexico	-0.7699	0.1310	-1.5722	0.7870
Arthropoda; Crustacea; Ostracoda; Podocopa; Podocopida; <i>Cytheromorpha acupunctata</i>	-1.0534	0.4568	0.5668	0.5868
Arthropoda; Crustacea; Ostracoda; Podocopa; Podocopida; <i>Howeina</i> sp. SN004	-0.8334	0.0050	0.4920	0.2370
Arthropoda; Hexapoda; Ellipura; Collembola; Ambiguous taxa	0.7457	-0.4797	-1.5723	-0.6205
Arthropoda; Hexapoda; Ellipura; Collembola; <i>Cryptopygus sverdrupi</i>	0.4651	0.7863	-1.5689	-1.1673
Arthropoda; Hexapoda; Ellipura; Collembola; <i>Sminthurides aquaticus</i>	1.3991	-1.0207	1.8683	0.6860
Arthropoda; Hexapoda; Ellipura; Collembola; <i>Sminthurides aquaticus</i>	0.8710	1.9294	0.2384	0.8320
Arthropoda; Hexapoda; Insecta; Pterygota; Neoptera; Diptera; Ambiguous taxa	-1.5518	-0.4429	-0.4872	0.4522
Arthropoda; Hexapoda; Insecta; Pterygota; Neoptera; Diptera; <i>Chrysops niger</i> (black deer fly)	0.3249	0.6775	0.4345	0.4302
Arthropoda; Hexapoda; Insecta; Pterygota; Neoptera; Diptera; <i>Haematopota pluvialis</i>	0.0832	-0.0541	0.0042	-0.9474
Arthropoda; Hexapoda; Insecta; Pterygota; Neoptera; Diptera; <i>Haematopota pluvialis</i>	0.6355	-0.2036	-0.0647	-0.5385
Arthropoda; Hexapoda; Insecta; Pterygota; Neoptera; Diptera; <i>Hermetia illucens</i>	-1.6956	0.5369	0.5376	0.2781
Bilateria; Ambiguous taxa	-0.1749	0.7986	1.0066	0.0379
Bryozoa; Gymnolaemata; Ctenostomatida; <i>Amathia</i> sp. n. 1 AW-2014	-1.6753	-0.8229	0.1333	-0.4602
Bryozoa; Phylactolaemata; Plumatellida; <i>Plumatella casmiana</i>	-0.1604	-1.1457	-1.5696	0.3842
Cnidaria; Hydrozoa; Trachylinae; Limnomedusae; Ambiguous taxa	-0.2005	-0.9046	-2.0764	0.2570
Gastrotricha; Chaetonotida; <i>Chaetonotus</i> cf. <i>novenarius</i> TK151	-0.1586	-1.3253	-1.5703	-1.3929
Gastrotricha; Chaetonotida; <i>Heterolepidoderma</i> sp. 1 TK-2012	-0.7259	-0.8207	0.8119	0.5049
Kinorhyncha; Cyclorhagida; Ambiguous taxa	0.7224	-1.0137	1.1253	0.8464
Mollusca; Bivalvia; Heteroconchia; Veneroidea; <i>Cyrenoida floridana</i>	-1.8945	-1.0778	-0.9242	1.3473
Mollusca; Gastropoda; Caenogastropoda; Ambiguous taxa	2.6717	-0.3828	-0.7328	-0.6636
Mollusca; Gastropoda; Caenogastropoda; <i>Tectarius spinulosus</i>	0.8396	0.5539	1.5902	-1.7269
Nematoda; Chromadorea; Araeolaimida; Ambiguous taxa	-1.5835	-0.4139	-0.9303	-0.9313
Nematoda; Chromadorea; Araeolaimida; <i>Chronogaster typica</i>	-1.2271	0.2458	-0.9154	-1.5700

(table cont'd.)

SILVA Taxonomy String	Intercept	Mid Compared to Low	High Compared to Low	Barataria Compared to Caillou
Nematoda; Chromadorea; Araeolaimida; <i>Paraphanolaimus behningi</i>	-1.1571	-1.3225	-1.2545	-0.9299
Nematoda; Chromadorea; Chromadorida; Ambiguous taxa	-0.1561	-1.3244	1.2575	1.6430
Nematoda; Chromadorea; Chromadorida; cf. <i>Dichromadora</i> sp. 2 JH-2014	-1.6757	0.1092	-0.1685	-0.2660
Nematoda; Chromadorea; Chromadorida; <i>Paracyatholaimus intermedius</i>	-0.1526	0.9664	-1.2859	0.9169
Nematoda; Chromadorea; Chromadorida; <i>Ptycholaimellus</i> sp. 1092	0.2497	-0.4400	1.4566	1.0858
Nematoda; Chromadorea; Desmodorida; <i>Prochaetosoma</i> sp. 3 HSR-2009	0.2605	-1.3242	1.5371	1.0639
Nematoda; Chromadorea; Desmodorida; <i>Spirinia parasitifera</i>	2.0692	0.5289	1.1586	0.1278
Nematoda; Chromadorea; Monhysterida; Ambiguous taxa	0.2254	2.6929	1.7581	1.4668
Nematoda; Chromadorea; Monhysterida; Ambiguous taxa	0.1758	1.5765	0.1822	-0.5775
Nematoda; Chromadorea; Monhysterida; <i>Diplolaimella dievengatensis</i>	-0.6795	0.4204	1.1355	2.4487
Nematoda; Chromadorea; Monhysterida; <i>Diplolaimella dievengatensis</i>	-1.6779	0.2526	-0.2303	-0.9114
Nematoda; Chromadorea; Monhysterida; Diplolaimelloides environmental sample	-1.3919	0.7299	1.0953	0.7832
Nematoda; Chromadorea; Monhysterida; Diplolaimelloides environmental sample	-1.6751	-1.2489	0.6057	-0.7501
Nematoda; Chromadorea; Monhysterida; <i>Eumonhystera filiformis</i>	-0.2307	-1.3255	-1.5676	-0.7770
Nematoda; Chromadorea; Monhysterida; <i>Terschellingia longicaudata</i>	0.6057	0.4383	1.5867	0.7051
Nematoda; Chromadorea; Rhabditida; <i>Poikilolaimus</i> sp. NKTW41	0.7614	0.0039	1.2234	0.8597
Nematoda; Chromadorea; Tylenchida; <i>Aglenchus agricola</i>	-1.1230	1.1597	-1.5682	-0.8655
Nematoda; Chromadorea; Tylenchida; Ambiguous taxa	0.0424	0.6680	1.8133	-0.5027
Nematoda; Chromadorea; Tylenchida; Ambiguous taxa	0.8976	1.5118	-0.8745	1.3046
Nematoda; Chromadorea; Tylenchida; <i>Ditylenchus</i> sp. 2 JH-2014	-1.6752	-1.1144	-2.2381	-0.9741
Nematoda; Chromadorea; Tylenchida; <i>Filenchus hamuliger</i>	0.4924	0.5111	-0.4109	-0.4159
Nematoda; Chromadorea; Tylenchida; <i>Filenchus vulgaris</i>	-1.1868	-0.5873	-0.7208	-1.1219
Nematoda; Chromadorea; Tylenchida; <i>Meloidogyne spartinae</i>	2.4364	-1.3262	-0.4093	-1.4671
Nematoda; Enoplea; Dorylaimia; Dorylaimida; Ambiguous taxa	-1.1433	0.8436	-1.3828	0.6603
Nematoda; Enoplea; Dorylaimia; Dorylaimida; Ambiguous taxa	-0.0869	-1.3633	-1.5700	-0.1004
Nematoda; Enoplea; Dorylaimia; Dorylaimida; Nematoda environmental sample	-0.2339	0.6149	2.9536	-0.5895
Nematoda; Enoplea; Dorylaimia; Dorylaimida; <i>Prodorylaimus</i> sp. HHBM-2007a	-0.5218	-1.1378	-1.5707	-1.5702
Nematoda; Enoplea; Enoplia; Enoplida; Ambiguous taxa	1.0326	-0.3239	1.5313	0.3705
Nematoda; Enoplea; Enoplia; Enoplida; Ambiguous taxa	0.3553	-0.7184	-0.0154	2.2577
Nematoda; Enoplea; Enoplia; Enoplida; Ambiguous taxa	1.6930	-0.4307	-0.0415	0.7133
Nematoda; Enoplea; Enoplia; Enoplida; <i>Anoplostoma</i> sp. 1093	0.9179	-0.6513	-1.5719	0.9155
Nematoda; Enoplea; Enoplia; Enoplida; <i>Halalaimus</i> sp. 1034	0.0589	0.1421	-0.6329	-0.2440
Nematoda; Enoplea; Enoplia; Enoplida; <i>Halalaimus</i> sp. BCA25	-1.2143	-0.0327	0.4571	-1.5709
Nematoda; Enoplea; Enoplia; Enoplida; <i>Rhabdolaimus</i> cf. <i>terrestris</i> JH-2004	0.3667	0.4045	1.6927	-0.4492
Nematoda; Enoplea; Enoplia; Triplonchida; Ambiguous taxa	1.1369	-1.3268	-1.5684	0.3780
Nematoda; Enoplea; Enoplia; Triplonchida; Ambiguous taxa	0.8761	-2.1589	-1.5716	-0.7269
Platyhelminthes; Catenulida; Stenostomidae; <i>Rhynchoscolex simplex</i>	-1.6051	-1.3285	-1.5719	-1.5711
Platyhelminthes; Rhabditophora; Macrostromida; <i>Macrostromum kepneri</i>	-0.6659	-0.3384	1.4265	-0.1487
Platyhelminthes; Rhabditophora; Rhabdocoela; Dalyellioida; <i>Baicalellia canadensis</i>	0.6945	-0.5198	-1.5669	-0.8439

(table cont'd.)

SILVA Taxonomy String	Intercept	Mid Compared to Low	High Compared to Low	Barataria Compared to Caillou
Platyhelminthes; Rhabditophora; Rhabdocoela; Kalyptorhynchia; Ambiguous taxa	1.2675	0.2672	0.4297	1.7314
Platyhelminthes; Rhabditophora; Rhabdocoela; Kalyptorhynchia; <i>Gyratrix hermaphroditus</i>	-0.0081	1.0394	-0.5446	0.9129
Platyhelminthes; Rhabditophora; Rhabdocoela; Kalyptorhynchia; <i>Mesorhynchus terminostylis</i>	-1.3095	2.8043	2.0886	0.5304
Platyhelminthes; Rhabditophora; Rhabdocoela; Neodalyellida; <i>Olisthanella truncula</i>	-0.8575	0.4079	-1.5682	0.6441
Rotifera; Monogononta; Flosculariacea; <i>Octotrocha speciosa</i>	1.0998	-0.3713	-1.4220	1.5255
Rotifera; Monogononta; Ploimida; metagenome	-0.7895	0.3978	-1.5655	-0.2286

Columns are separated by vertical lines into metadata categories (Salinity zone and Bay). The intercept column represents the comparison of classes across all categories. Positive values indicate increased relative abundance of read counts in the class that the column is named for, while negative values indicate increased relative abundance in the comparison class. The comparison class for the Salinity zone category is the Low salinity zone, while the comparison class for the Bay category is Caillou Bay. Differentials are sorted by the phylum which the OTU was assigned to using the SILVA database. The OTUs shaded in light gray are the OTUs which appeared in the highest 10% of the differentials of that category. The OTUs shaded in dark gray are the OTUs which appeared in the lowest 10% of the differentials of that category.

4.4. Discussion

The majority of the measured soil chemistry variables were significantly different across the different bays and salinity zones (Table 4.1). The chemical properties of soils in estuaries are dominated by the source of the sediments, in this case, the source for the whole study area is the Mississippi River, though in Caillou Bay this is partially by way of the Atchafalaya River (Bianchi 2007). Notably, the sediments in Barataria Bay are largely cut off from inputs from the Mississippi and may be more influenced by the local water chemistry. The chemical composition of the marine environment, especially with regards to salts and trace metals, tends to be largely stable across the globe (Bianchi 2007), and thus the High salinity zones are under the same influence in both bays. However, the disconnect of the Mississippi from Barataria means that sites in that bay are less influenced by the Mississippi than the sites in Caillou Bay are influenced by the Atchafalaya. This is likely the source of the differences in soil chemistry between the two bays and the three salinity zones. In addition, because the majority of these chemical variables were different across these factors but also did not fall outside of normal values (Table 4.2), differences in the composition of OTUs across these factors are likely less influenced by soil chemistry and more influenced by the salinity.

The eukaryote ASVs in this chapter were primarily composed of Opisthokonta ASVs (49% of ASVs), followed by SAR ASVs (35%), then Archaeplastida ASVs (11.26%, Table 4.3). The Metazoa ASVs made up the majority of the reads in most samples, followed by Fungi, Archaeplastida, and SAR ASVs (Fig 4.3). Notably, the samples from Caillou Bay were more likely to contain a large percentage of Fungi reads (Fig. 4.3).

Following the clustering of the metazoan OTUs, the alpha rarefaction curves showed that the majority of samples contained more than 20 OTUs (Fig. 4.4). In addition, all curves leveled off, indicating that the majority of samples were sequenced to an appropriate depth.

The mean sequencing depth for samples was approximately 56,000, and the majority of samples had a sequencing depth between 25,000 and 75,000.

The richness portion of the sample-based rarefaction curves for the full dataset did not level off in the interpolated portion, indicating that more OTUs could be collected (Fig. 4.5). The extrapolated portion of this richness curve indicated that up to 100 additional OTUs could be collected if twice as many samples were collected. However, the Shannon and Simpson Inverse curves leveled off, indicating that any additional OTUs would not be detected often enough to impact those metrics. When the dataset was split by the bay, salinity zone, or distance from edge factors, the richness curves were much steeper and the diversity metric curves were slightly steeper (Fig. 4.6, 4.7, 4.8). This is likely due to the splitting of the dataset resulting in lower sample sizes than the full dataset. However, several trends were evident aside from the sample size reduction effects. The samples from Caillou Bay had a lower total and extrapolated richness than the samples from Barataria Bay (Fig. 4.6). Similarly, the samples from the Low salinity zone had a higher total and extrapolated richness than the samples from the High salinity zone, with the Mid salinity zone samples falling between them (Fig. 4.7). Plant populations in salt marshes trend towards lower diversity as salinity increases (Chapman 1977, Greenberg and Maldonado 2006). Densities and diversity of macrofauna have showed enhancement when exposed to freshwater inputs, while densities of meiofauna have shown enhancement when exposed to higher salinities (Montagna and Kalke 1992, Montagna et al. 2002). Of the four distance from marsh edge categories, the 5 meters from edge category had the lowest observed richness (Fig. 4.8). Marsh infauna of different groups have shown distinct relationships with the distance from the marsh edge, such as crustaceans being more common at the 1m and oligochaetes being more common at the 5m and 10m (Whaley and Minello 2002).

The coverage-based rarefaction curves for the whole dataset reached an estimated coverage value of approximately 96% (Fig. 4.9). This matches the estimated coverage for the entire dataset of 96.7% (Table 4.4). Doubling the number of samples would result in an estimated increase in coverage of approximately 1-2%. When split by factor as the sample-based rarefactions were, the coverage-based rarefactions achieved coverage levels of 90-95% (Fig. 4.10, 4.11, 4.12). Taken as a whole, these rarefaction results indicate sufficient sequencing depth, capture of the majority of the common OTUs, and good coverage of the estimated actual community (Colwell et al. 2012).

The frequent group of OTUs, which were the OTUs which were detected in more than 10 samples, accounted for less than 30% of the OTUs in the dataset. However, this group accounted for more than 75% of the incidences in the dataset. This distribution, with a minority of OTUs accounting for a majority of incidences, explains the moderately high (1.4, with 2 being extremely high) coefficient of variation of the dataset (Table 4.4). The frequent group in this chapter (88 OTUs) was much larger than in chapter 2 (18 OTUs) or 3 (12 OTUs) and made up a larger proportion of number of OTUs in the dataset (28%) than in chapter 2 (11%) or 3 (10%, Table 4.8, Table 2.13, Table 3.6). This may be because the samples were from a more geographically wide area than the other two, leading to the collection of multiple communities

(and the associated frequent group members) along the salinity gradient. In addition, the locations in chapters 2 and 3 were known to be impacted by the Deepwater Horizon oil spill, which reduced meiofaunal diversity and left long-lasting impacts (Fleeger et al. 2015, 2018).

The richness values for the estimated actual community ranged from 339 OTUs to 535 OTUs (Fig. 4.13). This range contained the endpoint of the extrapolated richness curve, which represents the estimated richness of a dataset with twice the number of samples (Fig. 4.5). The models used to estimate the richness values rely on the number of OTUs which were rarely detected, meaning that the majority of the additional OTUs rarely would be detected in the dataset.

Of the two bays, the group of samples from Caillou Bay had a larger total richness than samples from Barataria Bay (Table 4.5). The groups from the two bays shared 163 of the 312 total OTUs, with 93 unique OTUs in Caillou samples and 56 unique OTUs in Barataria samples. The additional OTUs detected in Caillou Bay consisted primarily of 18 arthropod and 20 nematode OTUs that were not detected in Barataria Bay, the majority of which were only detected a single time in the dataset (Table 4.8, Table 4.9). This additional richness may be the result of the Atchafalaya River's influence on Caillou Bay. Meanwhile, the influence of the Mississippi on Barataria Bay is limited by flood control structures. However, the richness of samples from the different bays was not significantly different (Fig. 4.17).

The samples from the Low salinity zone had the largest total of OTUs at 206, followed by the Mid salinity zone at 180 and the High salinity zone at 167 (Table 4.6). The Low and High salinity zones shared the least OTUs of any two of the groups, with the Low-Mid and Mid-High shared OTUs being roughly equal. In addition, the samples from the Low salinity zone had significantly higher richness than the samples from the Mid salinity zone (Fig. 4.17). Salinity drives the distribution and resource use of many species, including meiofauna, macrofauna and commercial species (Odum 1988, Jones et al. 2002, Broman et al. 2019).

Samples that were collected 1m from the marsh edge had the highest total richness of any of the different distances from the marsh edge, at 203 OTUs, while the samples collected 5m from the marsh edge had the lowest, at 174 OTUs (Table 4.7). In addition, the samples collected from the marsh edge (0m) had the lowest number of shared OTUs with the samples collected 5m from the marsh edge (119), followed by the samples collected 10m from the marsh edge (122). However, the samples from the different distances from the marsh edge did not have significantly different richness (Fig. 4.17). If the number of samples is a concern, a future study might do best with a focus on the marsh near the edge (0m or 1m from the edge) and the marsh far from edge (10m), as these contain the majority of taxa within the dataset. These distance categories have also shown distinct categories of infauna in Texas salt marshes, with crustaceans and polychaete annelids near the edge and oligochaetes further into the marsh (Whaley and Minello 2002).

The largest group of OTUs in this dataset in terms of both number of OTUs (35% of OTUs) and number of incidences (43% of incidences) were assigned to the phylum Nematoda

(Fig. 4.16, 4.17). The next largest groups were Arthropoda (34% of OTUs), Annelida (9%), Platyhelminthes (7%), Gastrotricha (4%), Mollusca (3%), Rotifera (3%), Hydrozoa (1%), Nemertea (1%), Bryozoa (0.6%), Kinorhyncha (0.6%), Xenocoelomorpha (0.6%), Calcinea (0.3%), and Tardigrada (0.1%, 0.1%). Nematodes are typically considered to be the most abundant phylum of multicellular life on earth and are found in every environment (Barnes and Ruppert 1994). In traditional studies of marsh meiofauna, nematodes are typically the most commonly collected group (Fleeger 1985, Alves et al. 2013). However, these studies often have collection, preservation, or processing biases which prevent the identification of soft bodied taxa, such as the Platyhelminthes (Fonseca et al. 2010, Carugati et al. 2015). Future studies should seek to incorporate metagenomic methods and find a common ground between the two types of methods.

Nematodes were both the largest group in the dataset (35% of OTUs) and the largest group in the frequent group of OTUs, with 38 members of the 88 OTUs in the frequent group assigned to the phylum Nematoda (Table 4.8). Nematodes were also typically the largest group of OTUs in a sample (Fig. 4.14). Nematode incidences were roughly evenly distributed among the samples from the different bays, salinity zones, and distances from the marsh edge, with the Caillou Bay samples, the Low salinity samples and the 1m from marsh edge samples having the highest numbers of incidences in their respective categories (Table 4.8). The frequent group nematodes consisted of 9 members of the order Enoplida, 8 members of the Monhysterida, 7 members of the Tylenchida, 4 members of the Chromadorida, 4 members of the Dorylamida, 2 members of the Desmodorida, 2 members of the Plectida, 1 member of the Araeolaimida, and 1 member of the Rhabditida. The most common nematode OTU (detected in 94% of samples) was assigned to the species *Spirinia parasitifera*, a marine microbivore in the family Desmodoridae which is commonly found in European estuaries (Soetaert et al. 1997, Hodda 2011). Following the Deepwater Horizon oil spill in 2010, nematodes in Louisiana marshes were found to recover to reference levels quickly, making them one of the most resilient meiofauna groups studied (Fleeger et al. 2015). Five nematode members of the frequent group were never detected in samples from the High salinity zone, including two ambiguous members of the Triplonchida, *Anoplostoma* sp., *Prodorylaimus* sp., and *Eumonhystera filiformis*. If the study area was sampled again following the opening of the Mid-Barataria freshwater diversion, these OTUs might have expanded their range into the sites currently designated as the High salinity zone. Therefore, this group of nematode OTUs are potential indicators of reduced salinity in future studies of the area.

Arthropods were the 2nd most numerous (34% of OTUs) and 2nd most commonly detected group of OTUs (23% of incidences) in the dataset after the nematodes. Similar to the distribution of nematodes, arthropod incidences were roughly evenly distributed across the different bays, salinity zones, and distances from marsh edges. Arthropods were more commonly detected in the Low salinity zone than in the other salinity zones (37% of incidences in Low, 31% of incidences in Mid, and 32% in High, Table 4.8). Insects of the coastal marshes of Louisiana were surveyed by Aker (2020) using sweep nets at the same sites that were sampled for this study. Aker (2020) found that as salinity increased, the diversity of insects decreased, matching the reduction in arthropod incidence in this study. The DNA present in sediments

represents a broader timescale than an individual sweep net transect, though the exact length of DNA persistence in sediments is dependent on numerous factors, including oxygenation and decay rates (Harrison et al. 2019, Sakata et al. 2020). The families of insect detected in both studies included Staphylinidae (Coleoptera), Latridiidae (Coleoptera), Chloropidae (Diptera), Ceratopogonidae (Diptera), Culicidae (Diptera), Tabanidae (Diptera), Lauxaniidae (Diptera), Delphacidae (Hemiptera), Derbidae (Hemiptera), Formicidae (Hymenoptera), Coenagrionidae (Odonata), and Thripidae (Thysanoptera). Unfortunately, the comparisons that can be drawn between these studies are somewhat limited due to the differences in methodology, as sweep netting typically captures adult insects living on or in plants, while the metabarcoding of soil meiofauna will be biased heavily towards those insects and arthropods which have a soil dwelling stage, such as the Tabanidae, harpacticoid copepods, Collembola, Ostracoda, or Acari. Of the 27 OTUs assigned to insect families which were detected in this study and the sweep net study, just 4 were detected in more than 10 samples in this study, all of which were assigned to members of the Tabanidae. Tabanids were collected only 11 times in sweep nets over a year-long period (Aker 2020). Studies which focus on adult tabanids typically involve a baited trap because tabanids are drawn to the specific visual and chemical cues of the traps (Hribar et al. 1991). After the Deepwater Horizon oil spill, adult tabanid populations (specifically those of the greenhead horse fly, *Tabanus nigrovittatus*) crashed and underwent a genetic bottlenecking event but showed signs of recovery within five years (Husseneder et al. 2016, 2018). The larvae of *T. nigrovittatus* serve as top invertebrate predators in marsh soils, and are therefore important members of the invertebrate infauna in coastal marshes (Hansens 1979, Magnarelli and Stoffolano 1980).

Nineteen of the arthropod OTUs were members of the frequent group. These frequent group members were primarily hexapods and crustaceans, with a single member of this group assigned as an ambiguous Acari. The hexapod OTUs in this group included 5 Diptera OTUs and 4 Collembola OTUs in several orders, including Entomobryomorpha and Symphypleona. The crustacean OTUs consisted of 4 ostracod OTUs in the order Podocopida, 3 copepod OTUs in the order Harpacticoida, a single OTU in the order Tanaidacea, and a single OTU in the order Decapoda. The four most commonly detected arthropod OTUs (detected in 96%, 79%, 63%, and 54% of samples, respectively) were all assigned as members of the family Tabanidae in the order Diptera. These OTUs were assigned as the species *Chrysops niger* (GenBank: *Chrysops niger*), *Haematopota pluvialis* (GenBank: *Haematopota pluvialis*), *Hermetia illucens* (GenBank: *Tabanus* sp.), and *Haematopota pluvialis* (GenBank: *Tabanus nigrovittatus*). Unfortunately, the short region of the 18S gene which was amplified by the primers used in this study may not be suited for species identification within the Tabanidae apart (D. Davis, personal communication), but the *H. pluvialis* OTUs are most likely members of the genus *Tabanus*, as *H. pluvialis* is not known from North America and the next matches in GenBank are to *Tabanus*. Several of the frequent group arthropod OTUs were never detected in samples from the High salinity, these included two members of the Podocopida (Ostracoda, assigned as Cyprididae sp. and Cypria sp.) and two members of the Collembola (assigned as *Cryptopygus sverdrupi* and an ambiguous Collembola). These are groups which might expand their range as the proposed Mid-Barataria diversion opens.

Annelids were the 3rd most numerous group; approximately 60% of the annelid incidences were from Caillou Bay while the remaining 40% from Barataria Bay. The Low and High salinity zones had similar numbers of annelid incidence (~37% of the total annelid incidence each) while the Mid salinity zone had much lower numbers of annelid incidence (26%, Table 4.8). Annelids were more commonly detected in the marsh edge and 1m from marsh edge samples (accounting for 28% of the incidences each) when compared to the two internal distance categories (23% and 20% of the incidences for the 5m and 10m, respectively, Table 4.8). The frequent group of OTUs contained 12 annelid OTUs, which were comprised of 6 members of the oligochaete order Haplotaxida, 3 members of the polychaete order Phyllodocida, and 3 members of the polychaete order Spionida. The 6 Haplotaxida OTUs included 3 OTUs assigned to the family Naididae, including the most commonly detected annelid OTU in the dataset (detected in 88% of samples), assigned to the species *Monopylephorus rubroniveus*. The 3 remaining Haplotaxida OTUs were all assigned to members of the genus *Marionina* in the family Enchytraeidae. All three of the Spionida OTUs were assigned to members of various genera in the family Spionidae, while the Phyllodocida OTUs were assigned to the family Nereididae. The frequent group OTUs that were assigned to the annelid species *Marionina southerni* and *Dendronereis aestuarina* were never detected in the High salinity zone samples. The organisms that these OTUs represent could experience range expansions associated with decreased salinity as a result of the Mid Barataria freshwater diversion in the future.

The Platyhelminthes were the 4th most commonly detected and numerous group of OTUs. The Platyhelminthes are not commonly detected or reported in traditional studies of meiofauna (Fleeger et al. 2018) presumably since traditional sampling and extraction methodology causes destruction of the more soft bodied members of the meiofauna such as the Platyhelminthes (Carugati et al. 2015). The Platyhelminthes OTUs were most commonly detected in Caillou Bay samples in the bay category (55% of incidences in Caillou, 45% of incidences in Barataria), in the Low salinity zone in the salinity category (38% in Low, 33% in Mid, and 29% in High), and in the marsh edge samples in the distance from marsh edge category (28%, 25%, 21%, 25% for each of the distance from marsh edge categories, Table 4.8). The frequent group OTUs which were assigned to the Platyhelminthes included 5 members of the order Rhabdocoela, 2 members of the order Macrostomida, and 1 member of the subphylum Catenulida (Table 4.8). The most commonly detected Platyhelminthes OTU (detected in 63% of samples) was initially assigned to an ambiguous metazoan, but received a GenBank assignment of *Macrostomum lignano*, which is in the order Macrostomida. The flatworm *M. lignano* was initially collected from the intertidal zone of a lagoon in northern Italy and has been proposed as a model organism for a number of research topics, including aging, bioadhesion, regeneration, stem cells, and sexual selection (Ladurner et al. 2005, Schärer et al. 2020). Two of the Platyhelminthes frequent group OTUs were never detected in the High salinity zone, these were *Olisthanella truncula* and *Rhynchoscolex simplex*. These OTUs might be able to expand into the areas currently designated as High salinity when the Mid-Barataria freshwater diversion opens. An additional two frequent group Platyhelminthes OTUs (both assigned to members of the genus *Macrostomum*) were never detected in the Low salinity zone. These OTUs are potential candidates for indicators of saltwater intrusion.

The gastrotrichs were the 5th most numerous group, but they were the 7th most commonly detected group in the dataset. Gastrotrich OTUs were more commonly detected in the Caillou Bay samples (61% of incidences) than in the Barataria Bay samples (39%), in the Low zone samples (61%) than in the other two salinity zones (19.5% in each), and in the marsh edge samples (35%) than in the other distances from the marsh edge (28%, 14% and 21% for 1m, 5m, and 10m, respectively). Two of the twelve OTUs assigned to this phylum were members of the frequent group. Both of these OTUs were assigned to the order Chaetonotida, as *Chaetonotus* sp. (GenBank: *Haltidytes* sp.) and *Heterolepidoderma* sp. (GenBank: *Heterolepidoderma* sp.), respectively. The *Chaetonotus* OTU was detected a single time in High salinity zone samples, was detected zero times in the Mid, and was detected 15 times in the Low salinity zone samples, meaning that this OTU might experience a range expansion into areas which are currently High or Mid salinity when the Mid-Barataria diversion opens.

The Mollusca were the 6th most numerous group of OTUs and the 5th most commonly detected. Mollusk OTUs were much more commonly detected in the Barataria Bay samples (59% of incidences in Barataria Bay and 40% in Caillou, Table 4.8). These OTUs were roughly evenly distributed across the three salinity zones, though they were more commonly detected in the Low salinity zone (37% of incidences) than the others (28% in Mid, 34% in High, Table 4.8). These OTUs were less commonly detected in the marsh edge samples than the other distances from the marsh edge. Three mollusk OTUs were members of the frequent group, which were assigned as *Tectarius spinulosus* (GenBank: *Diffalaba opiniosa*), an ambiguous member of the Caenogastropoda (GenBank: *Cantharus cecillei*), and *Cyrenoida floridana* (GenBank: *Geloina* sp.). The OTU assigned to *C. floridana* was most commonly detected in the Low salinity zone (66% of the incidences of this OTU, with 17% in each of the other zones, Table 4.8) while the other two mollusk frequent group OTUs were roughly evenly distributed across the salinity zones. Oysters (SILVA: *Ostreoida* sp., GenBank: *Crassostrea virginica*) were detected only in the High salinity zone and only in the marsh edge and 1m distance categories, though they were only detected four times in the dataset. Oysters in Louisiana marshes typically do not live within the marsh platform itself, instead, they construct reefs in shallow water in estuarine systems which often also contain marshes. However, they do have planktonic larvae, which may explain their detection within the marsh platform. Salinities below 5 parts per thousand over extended periods of time can lead to mass mortalities in oysters, leading to concern over the impacts of the Mid-Barataria diversion on the commercial fishery in Barataria Bay (Hofmann and Powell 1998, Das et al. 2012, La Peyre et al. 2013).

The OTUs assigned to the phylum Rotifera were the 7th most numerous group but the 6th most common. Rotifers were most commonly found in the Low salinity zone (41% of incidences, 31% in Mid, and 28% in High), but were evenly distributed across the different bays and distances from the marsh edge. The frequent group of OTUs included 2 members of the Rotifera, which were assigned as *Octotrocha speciosa* (GenBank: *Ptygura longicornis*) and an ambiguous member of the order Plomida (GenBank: *Notholca acuminata*), respectively. These two rotifers were evenly distributed across the different bays, salinity zones, and distances from the marsh edge. However, the eight infrequent group OTUs in this phylum were most

commonly detected in the Low salinity zone (68% of the incidences of these OTUs, Table 4.8). Six of these infrequent group OTUs were only detected in one sample.

The phylum Hydrozoa had only 3 OTUs assigned to it, but one of these OTUs was a member of the frequent group. Hydrozoan OTUs were detected fairly evenly across the different bays and salinity zones, but were more common in samples from the marsh edge and 1m from the marsh edge. The lone frequent group OTU in this phylum was assigned as an ambiguous member of the Limnomedusae (GenBank: *Pennaria* sp.). This OTU was more commonly detected in the Low salinity zone than in the other zones. One of the infrequently detected OTUs was assigned to the hydrozoan *Helgicirrha cari*. This OTU was only detected in the Mid and High salinity zone, with 80% of those incidences being in the High salinity zone. An OTU assigned to *H. cari* was one of the frequent group OTUs in the datasets from chapters 2 and 3. The samples from chapters 2 and 3 were collected from a location in Barataria Bay (Bay Jimmy) that is closer to the High salinity sites and the open areas of Barataria Bay than to the Mid or Low salinity zones. In chapters 2 and 3, the OTU assigned to *H. cari* was most associated with the sheared margins in Bay Jimmy (Table 2.23, Table 3.16). The association of this OTU with sheared margins, as well as its detection only in the Mid and High salinity zones, may indicate that this taxon is an indicator of marine benthic environments.

The OTUs that were assigned to the phylum Kinorhyncha made up less than 1% of the total OTUs. However, one of the two OTUs assigned to this phylum was a member of the frequent group. Both of the OTUs in this phylum were assigned as ambiguous members of the class Cyclorhagida, but received GenBank assignments of *Echinoderes* sp. Kinorhynchs belonging to the genus *Echinoderes* were collected in unoiled reference sites in Louisiana salt marshes following the Deepwater Horizon oil spill, though they were absent from the heavily oiled marsh sites (Fleeger et al. 2015, 2018). Kinorhynchs were more commonly detected in Caillou Bay (64% of incidences) than in Barataria Bay (36%), but were evenly distributed across the different distances from the marsh edge (Table 4.8). These OTUs were never detected in the Low salinity zone, and were more commonly detected in the High (68% of incidences) than in the Mid salinity zone (32%, Table 4.8). Therefore, kinorhynchs may be a taxon which would be pushed out of the area impacted by the Mid-Barataria freshwater diversion, making them a potential candidate for an indicator of saltwater intrusion.

The largest differences in composition of samples were associated with the different salinity zones. The Low salinity zone samples had the highest total number of OTUs and had significantly higher richness values than those samples from the Mid salinity zone, though the richness of the samples from the Mid and Low zones was not significantly different from the High salinity zone samples (Fig. 4.17). The majority of the beta diversity similarity indices showed high similarity (> 0.6) excluding the Jaccard index, which always returns a lower value (Table 4.11). The Jaccard index uses shared members of the groups divided by the total members of groups to determine similarity. A low index value indicates a low number of shared OTUs among the three salinity zones compared to the total, which was the case (84 of the 312 OTUs). Among the pairwise Sørensen indices, the Low and High salinity zones had the lowest similarity (0.45, Table 4.12). The groups of samples from the Low and High salinity zone were

distinctly separated by the NMDS ordination, with the Mid salinity zone samples falling between them (Fig. 4.19). Lastly, the Adonis test indicated that the differences in composition between the samples from different salinity zones accounted for approximately 20% of the variation in the dataset (Table 4.14). These differences can be seen in the total incidences of several groups, including the Annelida, Gastrotricha, Kinorhyncha, Arthropoda, Nematoda, Platyhelminthes, and Rotifera (Table 4.8). Annelids had fewer incidences in the Mid salinity zone than in either the Low or High zones (26% of incidences in Mid, 37% in Low and High, Table 4.8). Gastrotrichs had a much larger number of incidences in the Low salinity zone than either of the others (61% of incidences in Low, 19% of incidences in each of the other salinity zones, Table 4.8), and the most common gastrotrich OTU (*Chaetonotus* sp.) was only detected 1 time outside of the Low zone while still remaining a member of the frequent group. Arthropods were more commonly detected in the Low salinity zone (37% in Low, 31% in Mid, 32% in High, Table 4.8), as were nematodes (36% in Low, 32% in both Mid and High, Table 4.8). The incidence of both Platyhelminthes and Rotifera OTUs had a gradual reduction of incidences as the salinity increased (for Platyhelminthes: 38% in Low, 32% in Mid, 30% in High, for Rotifera: 41%, 31%, 28%, Table 4.8). The OTUs assigned to the phylum Kinorhyncha (both assigned to *Echinoderes* sp.) were never detected in the Low salinity zone, and were detected half as often in the Mid zone as in the High (Table 4.8, Table 4.10). The OTUs which were unique to the different salinity zones also showed a few points of interest (Table 4.10). In general, the Low salinity zone had many more unique OTUs (33) than the other two zones (10 and 11 for Mid and High, respectively, Table 4.10). Specifically, three members of the frequent group were only detected in the Low salinity zone. These OTUs were assigned as two nematodes (ambiguous member of the Triplonchida and *Eumonhysterida filiformis*) and a member of the Platyhelminthes (*Rhynchoscolex simplex*). Another ten members of the frequent group were never detected in samples from the High salinity zone, including 4 Arthropoda (an ambiguous ostracod in the family Cyprididae, an ambiguous member of the Collembola, *Cryptopygus sverdrupi*, and *Cypria* sp.), 3 Nematoda (an ambiguous member of the Triplonchida, *Anoplostoma* sp., and *Prodorylaimus* sp.), 2 Annelida (*Marionina southerni* and *Dendronereis aestuarina*), and 1 Platyhelminthes (*Olisthanella truncula*). These thirteen OTUs may represent species which would expand their range into the previously high salinity zone following a salinity regime change, and could be considered indicators of long-term salinity change. A single member of the Platyhelminthes (*Chaetonotus* sp.) was the only frequent group member to never be detected in a Mid salinity zone sample. However, this OTU was detected a single time in the High salinity zone, with the remaining incidences in the Low salinity zone, so it is more likely to be found in the Low zone with the thirteen OTUs above. Meanwhile, none of the frequent group members were detected only in the Mid or High zones, but nine were never detected in Low salinity zones. These nine OTUs consisted of 4 Nematoda (*Meloidogyne spartinae*, *Prochaetosoma* sp., *Halalaimus* sp., and *Dichromadora* sp.), 2 Annelida (*Alitta succinea* and *Namalycastis jaya*), 2 Platyhelminthes (*Macrostomum kepneri* and *Mesorhynchus terminostylis*), and 1 Kinorhyncha (*Echinoderes* sp., Table 4.10). These OTUs represent the species which would be excluded from the habitat as salinity decreases, and their absence could be considered potential indicators of long-term salinity change in the region. The data presented in this study represent a single sampling event, and do not take into account the seasonal variability of meiofauna (Rutledge and Fleeger 1993). Aside from the OTUs which were

detected in all salinity zones (65 of the 88 frequent group members and 19 of the 224 infrequent group members), the communities detected in the Low and High salinity zones represent communities which do not share many members, i.e., freshwater and marine communities with low overlap. Meanwhile, the community detected in the Mid salinity zone likely represents a much less rich community which is adapted to brackish conditions, alongside those species from the fresh or marine sides which can tolerate the brackish salinity levels. In addition, many of the OTUs which were detected in all three salinity zones were more commonly detected in one or two of the salinity zones. These OTUs were either most common in the Low or High while being rare in the other two zones, or if common in two and rare in one, they were most common in the Low and Mid or Mid and High. The pattern of a limited number of species appearing only in the brackish zones of estuaries, with additional species from freshwater and marine environments overlapping into the brackish zone, has been observed frequently in estuarine systems across the globe (Odum 1988, Attrill 2002). This pattern has been hypothesized to occur because successful physiological adaptation to brackish water is rare due to the range of conditions that species must evolve to tolerate (Deaton and Greenberg 1986). The groups of OTUs which were excluded from the High or Low salinities could be useful starting points for future studies investigating the impacts of salinity on meiofauna in these regions and across other systems.

The OTUs that were most associated with the Mid salinity zone compared to the Low included 4 annelids (*Polydora brevipalpa*, *Marionina sublitoralis*, *Paraprionospio patiens*, and *Monopylephorus rubroniveus*), 2 nematodes (both ambiguous members of the Monhysterida), an arthropod (*Sminthurides aquaticus*), and a platyhelminth (*Mesorhynchus terminostylis*, Table 4.15). The annelid *P. patiens* was detected almost twice as often in Mid and High salinity zone samples than in the Low salinity zone samples (Table 4.8). The platyhelminth *M. terminostylis* was never detected in any Low salinity samples. The OTUs which were most associated with the Low compared to the Mid included 5 nematodes (*Eumonhystera filiformis*, *Meloidogyne spartinae*, an ambiguous member of the Doryamida, and 2 ambiguous members of the Triplonchida), 2 annelids (*Alitta succinea* and *Dendronereis aestuarina*), and a platyhelminth (*Rhynchoscolex simplex*, Table 4.15). The nematode *E. filiformis* and the platyhelminth *R. simplex* were only detected in the Low salinity zone samples (Table 4.10). The annelid *D. aestuarina* was much more commonly detected in the Low than in the Mid zone (Table 4.8). The OTUs which were most associated with the High compared to the Low included 3 annelids (*Namalycastis jaya*, *Monopylephorus rubroniveus*, and *Marionina coatesae*), 3 nematodes (ambiguous members of the Dorylaimida, Tylenchida, and Monhysterida), an arthropod (*Sminthurides aquaticus*, a different OTU than the one which was associated with the Mid salinity zone), and a platyhelminth (*Mesorhynchus terminostylis*). The annelid *N. jaya* was not detected in the Low salinity zone samples (Table 4.10). The OTU assigned to the collembolan *S. aquaticus* was detected more than twice as often in High salinity samples than in the Mid or Low. Those which were most associated with the Low compared to the High included 3 arthropods (*Cypria* sp, ambiguous member of the Cyprididae, and ambiguous member of the Collembola), 3 nematodes (ambiguous member of the Triplonchida, *Anoplostoma* sp., and *Ditylenchus* sp.), a hydrozoan (ambiguous member of the Limnomedusae), and a platyhelminth (*Rhynchoscolex simplex*, Table 4.15). The *Cypria* sp. OTU, the Cyprididae OTU, and the

Anoplostoma sp. OTU were never detected in the High salinity zone samples, while the *R. simplex* OTU was only detected in the Low samples (Table 4.10). Long term environmental monitoring studies using barcoding methods could build on this dataset in the future.

The differences in community composition between the two bays were less overt than the differences observed between the different salinity zones, although the Caillou Bay samples had a greater number of OTUs (Table 4.5). The alpha diversity values were not significantly different between samples from the two bays (Fig. 4.17, Fig. 4.18), All of the beta diversity indices returned values above 0.5 for the Bay comparison (Table 4.11). The NMDS ordination showed some separation between the Low and Mid salinity zone samples from Barataria and Caillou Bays, but less separation between the High salinity zone samples from those bays (Fig. 4.20). The Adonis test detected a significant difference in the composition of the samples from the two bays, but the Bay factor only accounted for around 6% of the variation of beta diversity in the dataset (Table 4.14). Annelid and mollusk OTUs were much more commonly detected in samples from Barataria Bay, while gastrotrichs, kinorhynchs, and platyhelminthes were more commonly detected in the Caillou Bay samples (Table 4.8). Of the annelids, the two frequent group OTUs which were assigned to *Marionina sublitoralis* and *Marionina coatesae* were much more commonly detected in the Barataria Bay samples (86% of incidences in Barataria, 72% of incidences in Barataria, for these two annelids, respectively, Table 4.8). Annelids in the genus *Marionina* are known to inhabit salt marshes in North America; they are particularly associated with the plant stem habitat linking to differences in distribution based on plant species (Healy and Walters 1994). The mollusk OTUs which were more common in the Barataria samples included the ambiguous member of the Caenogastropoda and *Cyrenoida floridana*, which were both in the frequent group (73% of incidences in Barataria, 62% of incidences in Barataria, for these two mollusks, respectively, Table 4.8). The marsh clam *C. floridana* occurs in the fresh and brackish portions of marshes along the Gulf Coast (Abbott and Morris 1995). Conditions for this clam may be better in areas which receive more inundation from freshwater, such as in Caillou Bay. Five gastrotrich OTUS, including one of the frequent group OTUs, were more common in the Caillou Bay samples, resulting in 61% of the overall gastrotrich incidences occurring in Caillou Bay samples (Table 4.8). Sixty-four percent of the kinorhynch incidences were in Caillou Bay samples (Table 4.8). Kinorhynchs were one of the taxa identified as slowly recovering from impacts of the Deepwater Horizon in Barataria Bay, potentially indicating that these organisms are still recovering in Barataria Bay (Fleeger et al. 2018). Two of the frequent group members of the Platyhelminthes, assigned as *Olisthanella truncula* and *Macrostomum kepneri*, were more common in Caillou samples. The Caillou Bay samples also had a larger number of unique OTUs than Barataria Bay samples (Table 4.9). The differential abundance results showed that the 8 OTUs which were most associated with Barataria Bay samples included 4 nematodes (ambiguous members of the Chromadorida, Monhysterida, and Enoplida, and *Diplolaimella dievengatensis*), 2 annelids (*Marionina sublitoralis* and *Dendronereis aestuarina*), a platyhelminth (ambiguous member of the Kalyptorhynchia) and a rotifer (*Octotrocha speciosa*, Table 4.15). The OTUs which were most associated with the Caillou Bay samples compared to the Barataria Bay samples included 4 nematodes (*Chronogaster typica*, *Meloidogyne spartinae*, *Prodorylaimus* sp., *Halalaimus* sp.), 2 annelids (*Marionina southerni*, *Namalycastis jaya*), a mollusk (*Tectarius spinulosus*) and a platyhelminth (*Rhynchoscolex simplex*, Table 4.15). The

majority of these OTUs were detected more frequently in the category which they were more associated. Both Caillou and Barataria Bays were originally built up by the deltaic processes of the Mississippi River, but Caillou Bay is near the mouth of the Atchafalaya River which is building new land, while Barataria Bay is nearly cut off from the Mississippi due to man-made flood control structures built over the last century (Roberts and Coleman 1996). These different freshwater inputs may influence what meiofauna can occur in the different bays. In addition, Barataria Bay was more heavily impacted by the Deepwater Horizon oil spill than Caillou Bay (Michel et al. 2013) and therefore certain meiofauna in Barataria Bay may still be suppressed by lingering impacts (Fleeger et al. 2018, 2019).

The samples which were collected at different distances from the marsh edge showed some differences in composition at the different distances. Neither of the alpha diversity metrics were significantly different for this category (Fig. 4.17, Fig. 4.18). The 1m from marsh edge samples had the highest total number of OTUs. With the exception of the Jaccard index, all of the beta diversity indices were quite high (>0.75 , Table 4.11). The marsh edge and 10m from marsh edge had the lowest pairwise index value, while the marsh edge and 1m from marsh edge had the highest (Table 4.13). The groups of samples from the different distances from the marsh edge showed separation on the NMDS ordination plot only when split by salinity zone and bay of origin (Fig 4.21). The Adonis test indicated that the distance from marsh edge accounted for ~7% of the variation in the dataset. Annelids, gastrotrichs, and hydrozoans were more commonly detected in the marsh edge and 1m from marsh edge samples, while mollusks and nematodes were more commonly detected in the 1m from marsh edge samples.

The sampling strategies varied slightly among the three research chapters in this document. Approximately 70 samples were collected for each of the chapters, resulting in good coverage for the overall dataset ($>90\%$ of the estimated actual community) in all chapters (Table 2.9, Table 3.2, Table 4.4). Chapter 3 had the lowest number of samples (due to losses in sample material before the sequencing process) and the lowest coverage, though 90% coverage was still achieved. Chapter 2 involved methods of direct DNA extraction from unprocessed sediment samples, while chapters 3 and 4 involved sample processing techniques to size restrict and extract the organic portion of the sample before DNA extraction was performed. The impact of processing soil samples was important in terms of the groups of taxa detected. When compared to chapter 2 results, a reduced proportion of Nematode OTUs but an increased proportion of Platyhelminthes and Arthropoda OTUs detected was described in chapter 3 (Fig. 2.15, Fig. 3.14). In this chapter both a high proportion of Nematode OTUs like chapter 2 and a high proportion of Platyhelminthes OTUs like chapter 3 was detected (Fig. 4.15). Sample processing in the manner used in chapters 3 and 4 is recommended in order to account for patchy small scale distributions of meiofauna (Creer et al. 2016). The chapter 3 and 4 datasets indicate that sample processing to extract the organic portion of soils before extracting DNA can result in adequate coverage and richness values for analysis. Although chapter 3 had a lower total number of OTUs than chapter 2, the results of chapter 4 had nearly twice as many OTUs as either of the other chapters. However, sampling in chapter 4 took place over a wider geographic region than the other two chapters and collected from multiple distinct communities within the salinity gradient, leading to an increased richness. None of the

three sampling efforts achieved total richness saturation, but the effective diversity curves of the Shannon and Simpson Inverse metrics indicated that the only richness left to gain would be OTUs which appear in single samples (Fig. 2.4, Fig. 3.3, Fig. 4.5). Individual transects from chapter 2 and 3 relied on elevation to delineate sample locations within a transect while chapter 4 relied on distance from the marsh edge. A reduced number of samples per transect combined with more transects are likely able to capture the diversity present in sites, as the elevation and distance from marsh edge factors never showed significant differences in alpha diversity values and accounted for only small amounts of the variation in beta diversity values. If a sampling project like the ones in this document was in the planning stages, 2 samples per transect (one at either extreme end of the transects used in this document) would allow for an increased number of transects, which might be a better use of resources. The 18S primers recommended by the Earth Microbiome Project (Gilbert et al. 2014) were used for both chapter 2 and 3, while a different set of 18S primers (Porazinska et al. 2009, 2010), were used in this chapter, which may have impacted the sequences which were amplified and eventually sequenced. A few cases of potentially inflated biodiversity (i.e., OTUs which receive the same taxonomic assignment while remaining separate entries in the OTU table) are still present in this chapter, even after clustering the ASVs into OTUs with 97% similarity, which may be a result of the primer used (i.e., the region amplified by the primer had too much variation in the species in question). A sampling project which followed the methodology of chapter 4 in particular, with a reduction in the number of samples per transect, could be a cost effective and robust method for monitoring meiofauna in marshes or other environments. The primers for potential future projects should be carefully considered based on the groups of organisms in question.

This research has shown significant variation in the composition of meiofauna between areas of differing average salinity, indicating that when the Mid-Barataria diversion is completed, it will have a major impact on the marsh community as a whole (Das et al. 2012). Meiofauna are prey to numerous other organisms, including commercial species, so these impacts will be important to monitor (Coull 1990). Future research should consider a year-round sampling program at these sites because meiofauna are known to have seasonal cycles (Rutledge and Fleeger 1993). Even if changes in densities of meiofauna cannot yet be reliably observed with metabarcoding methods, differences in composition may be informative, and a long-term sampling program would mean a better understanding of what species are present at which times of the year. Of course, a single sampling point of the DNA contained within sediments represents more than the biodiversity of a single timepoint due to preserved DNA (Harrison et al. 2019, Sakata et al. 2020) but the timeline for DNA degradation is variable and increased sampling could shed light on changes through time. A seasonal sampling program would give a more complete picture of what marsh meiofauna communities look like at the different salinity zones and potentially give more insight on how the communities might change with the changing salinity regime (Rutledge and Fleeger 1993, Elsey-Quirk et al. 2019).

Summary and Conclusions

The methods for chapter 2 involved direct extraction of DNA from sediment samples collected from sheared and intact margins in Bay Jimmy. The methods for chapter 3 involved these same samples and applied size filtering and organic extraction methods before additional DNA extraction. The methods for chapter 4 involved the same methods (size filtering, organic extraction) for soil sample processing applied to samples from different salinity zones in both Caillou and Barataria Bays. In addition, the primers selected for chapter 2 and 3 were the 18S primers recommended by the Earth Microbiome Project (Gilbert et al. 2014) while the primers selected for chapter 4 were a different set of 18S primers (Porazinska et al. 2009, 2010).

The datasets from all three research chapters produced robust coverage estimates of the sampled communities (>90% of the estimated communities in each chapter). The richness rarefaction curves for each chapter did not flatten out, indicating that additional OTUs could be collected. However, the effective diversity metrics curves did level off, indicating that any additional OTUs would be rarely collected and would not impact diversity metrics.

In both chapter 2 and 3, the sheared and intact margins shared a core group of frequent OTUs, while having unique, rare taxa. The dataset from chapter 2 contained a greater percentage of nematode incidences (28%) than chapter 3 (18%), while chapter 3 contained a greater percentage of arthropod (24%) and platyhelminth incidences (11%) than chapter 2 (16%, 3%, respectively). The different methods employed by each of these chapters (i.e., direct sediment DNA extraction and meiofauna extraction from sediment followed by DNA extraction) are complementary, and both methods collect environmental DNA effectively. However, the methods from chapter 3 collect a greater proportion of taxa which are often underrepresented in traditional studies, such as the Platyhelminthes.

In chapter 4, distinct communities were detected in the Low and High salinity zones, with the Mid salinity zone having few unique OTUs. The majority of the OTUs present in the Mid salinity zone represent organisms which are typically marine or freshwater but can tolerate some degree of salinity fluctuation. A number of OTUs were identified as potential bioindicators of freshwater discharge into typically saline marshes because they were unique to the Low salinity zone, including two nematodes (ambiguous member of Triplonchida and *Eumonhysterida filiformis*) and a member of the Platyhelminthes (*Rhynchoscolex simplex*). To a lesser extent, the OTUs which were never detected in the High salinity zone could also be used as bioindicators of freshwater disturbance. These OTUs included four arthropods (Cyprididae sp., Collembola sp., *Cryptopygus sverdrupi*, and *Cypria* sp.), three nematodes (Triplonchida sp., *Anoplostoma* sp., and *Prodorylaimus* sp.), two annelids (*Marionina southerni* and *Dendronereis aestuarina*), and a platyhelminth (*Olisthanella truncula*). The OTUs which were identified as potential indicators of saltwater intrusion included four nematodes (*Meloidogyne spartinae*, *Prochaetosoma* sp., *Halalaimus* sp., and *Dichromadora* sp.), two polychaete annelids (*Alitta succinea* and *Namalycastis jaya*), two platyhelminths (*Macrostomum kepneri* and *Mesorhynchus terminostylis*), and a kinorhynch (*Echinoderes* sp.). Together, these OTUs provide

a baseline of knowledge about the composition of different meiofauna communities in the different salinity zones. This baseline could be compared to future research targeting the same areas to determine impacts on the community from freshwater diversions, or in areas where saltwater intrusion is occurring.

Glossary

Abundance. The number of times a taxon appears in a sample (Whittaker 1972).

Actual Community. The community present in the environment, rather than the community collected in samples. The community collected in samples represents some portion of the actual community, but likely not 100%. The actual community can be estimated, allowing for coverage estimates to be generated (Chao and Lee 1992, Chao and Jost 2012).

Adonis Test. A multiple PERMANOVA, which is a permutation-based ANOVA. This method is non-parametric, allowing for the analysis of datasets which do not follow normal distributions (Anderson 2001, 2017).

Alpha Diversity. The diversity present in a given sample (Whittaker 1972).

Amplicon Sequence Variant (ASV). Each of these are an exact sequence returned from the sequencing process, following the application of the DADA2 quality filtering algorithm (Callahan et al. 2016).

Beta Diversity. The measure of diversity across samples. Frequently calculated as a comparison of the diversity in two samples for every set of two samples in a dataset, resulting in a distance matrix (Whittaker 1972, Anderson 2001, 2017).

Diversity Index. A measure of diversity. May incorporate measures of richness and abundance or incidence to condense information about a sample or samples into a single measure (Whittaker 1972).

DNA Barcoding. The use of short, specific sections of the genome to identify organisms. Typically, this is done by extracting the DNA of organisms and amplifying DNA by PCR with primers for the specific section of the genome (Hebert et al. 2003).

DNA Sequencing. One of several methods for determining the sequence of DNA in an organism's genome. These include Sanger, Roche 454, and Illumina Sequencing, among others (Caporaso et al. 2012).

Faith's Phylogenetic Diversity (PD). A measure of diversity in a sample, using the branch lengths of the phylogenetic tree of all taxa detected in that sample (Faith 1992).

Incidence. The presence of a taxon in a sample. Total incidence is the total number of times a taxon appeared in all samples in a dataset (Chao et al. 2014).

Infauna. Any sediment dwelling organism (Giere 2009).

Macroinfauna. Any infauna which is larger than 500 μm . Almost exclusively multicellular (Giere 2009).

Meiofauna. Any infauna smaller than 500 μm but larger than 45 μm . A mix of small multicellular and large single celled organisms (Mare 1942, Giere 2009).

Metabarcoding. The use of DNA barcoding to identify organisms from bulk environmental samples without separating individual organisms for DNA extraction (Creer et al. 2016).

Microfauna. Any infauna smaller than 45 μm . Almost exclusively single celled organisms (Giere 2009).

Non-Metric Dimensional Scaling (NMDS). A method for the ordination of distance matrices. This method uses random starts and an iterative process to represent the high dimensional data in a distance matrix in as few dimensions as possible (Legendre P 1998).

Operational Taxonomic Unit (OTU). These are groups of ASVs, clustered by a similarity percentage and treated as a single unit. These are used to reduce artificial inflation of biodiversity as a result of multiple ASVs representing the same taxon due to intraspecific variation (Blaxter et al. 2005).

Polymerase Chain Reaction (PCR). A method for producing copies of DNA, allowing for the amplification of few strands of DNA into many strands (Saiki et al. 1988).

Richness. The number of taxa present in a given sample or group of samples (Whittaker 1972).

Sørensen Index. One of many diversity indices. Calculated by taking two times the number of shared taxa between two samples divided by the number of total number of taxa in both samples (Sørensen 1948).

Literature Cited

- Abbott, R. T., and P. A. Morris. 1995.** A Field Guide to Shells: Atlantic and Gulf Coasts and the West Indies, Fourth Edi. ed. Houghton Mifflin Company, Boston, MA.
- Adami, M., and C. Damborenea. 2020.** Life history of the freshwater microturbellarian *Macrostomum velastylum* (Macrostomorpha) in the Neotropical region. *Stud. Neotrop. Fauna Environ.* 1–6.
- Aker, B. G. 2020.** The Collection of Baseline Data on Insect and Plant Communities Across Multiple Salinity Zones Within Louisiana’s Tidal Marshes.
- Alves, A. S., H. Adão, T. J. Ferrero, J. C. Marques, M. J. Costa, and J. Patrício. 2013.** Benthic meiofauna as indicator of ecological changes in estuarine ecosystems: The use of nematodes in ecological quality assessment. *Ecol. Indic.* 24: 462–475.
- Amaral-Zettler, L. A., E. A. McCliment, H. W. Ducklow, and S. M. Huse. 2009.** A Method for Studying Protistan Diversity Using Massively Parallel Sequencing of V9 Hypervariable Regions of Small-Subunit Ribosomal RNA Genes. *PLoS One.* 4: e6372.
- Anderson, M. J. 2001.** A new method for non-parametric multivariate analysis of variance. 26: 32–46.
- Anderson, M. J. 2017.** Permutational Multivariate Analysis of Variance (PERMANOVA), pp. 1–15. *In* Wiley StatsRef Stat. Ref. Online. John Wiley & Sons, Ltd, Chichester, UK.
- Anderson, M. J., T. O. Crist, J. M. Chase, M. Vellend, B. D. Inouye, A. L. Freestone, N. J. Sanders, H. V. Cornell, L. S. Comita, K. F. Davies, S. P. Harrison, K. N. J. B., J. C. Stegen, and N. G. Swenson. 2011.** Navigating the multiple meanings of β diversity: a roadmap for the practicing ecologist. *Ecol. Lett.* 14: 19–28.
- Antonio, F. J., R. S. Mendes, and S. M. Thomaz. 2011.** Identifying and modeling patterns of tetrapod vertebrate mortality rates in the Gulf of Mexico oil spill. *Aquat. Toxicol.* 105: 177–179.
- Apothéloz-Perret-Gentil, L., A. Cordonier, F. Straub, J. Iseli, P. Esling, and J. Pawlowski. 2017.** Taxonomy-free molecular diatom index for high-throughput eDNA biomonitoring. *Mol. Ecol. Resour.* 17: 1231–1242.
- Arnot, D. E., C. Roper, and R. A. L. Bayoumi. 1993.** Digital codes from hypervariable tandemly repeated DNA sequences in the *Plasmodium falciparum* circumsporozoite gene can genetically barcode isolates. *Mol. Biochem. Parasitol.* 61: 15–24.
- Atlas, R. M., D. M. Stoeckel, S. A. Faith, A. Minard-Smith, J. R. Thorn, and M. J. Benotti. 2015.** Oil Biodegradation and Oil-Degrading Microbial Populations in Marsh Sediments Impacted by Oil from the Deepwater Horizon Well Blowout. *Environ. Sci. Technol.* 49: 8356–8366.
- Attrill, M. J. 2002.** A testable linear model for diversity trends in estuaries. *J. Anim. Ecol.* 71: 262–269.

- Baker, D. E., and M. C. Amacher. 1982.** Nickel, Copper, Zinc, and Cadmium, pp. 323–336. *In* Methods Soil Anal. Part 2. Chem. Microbiol. Prop.
- Barbier, E. B., S. D. Hacker, C. Kennedy, E. W. Koch, A. C. Stier, and B. R. Silliman. 2011.** The value of estuarine and coastal ecosystem services. *Ecol. Monogr.*
- Barnes, R. G., and E. E. Ruppert. 1994.** Invertebrate Zoology, 6th ed. Saunders College Publishing, Fort Worth.
- Barnhisel, R., and P. M. Bertsch. 1982.** Aluminum, pp. 275–300. *In* Methods Soil Anal. Part 2. Chem. Microbiol. Prop.
- Barras, J. A. 2009.** Land Area Change and Overview of Major Hurricane Impacts in Coastal Louisiana, 2004-08. 1–11.
- Barron, M. G., D. N. Vivian, R. A. Heintz, and U. H. Yim. 2020.** Long-Term Ecological Impacts from Oil Spills: Comparison of Exxon Valdez, Hebei Spirit, and Deepwater Horizon. *Environ. Sci. Technol.* 54: 6456–6467.
- Bartsch, I. 2002.** Geographical and ecological distribution of marine halacarid genera and species (Acari: Halacaridae). *Exp. Appl. Acarol.* 34: 37–58.
- Beazley, M. J., R. J. Martinez, S. Rajan, J. Powell, Y. M. Piceno, L. M. Tom, G. L. Andersen, T. C. Hazen, J. D. Van Nostrand, J. Zhou, B. Mortazavi, and P. A. Sobecky. 2012.** Microbial Community Analysis of a Coastal Salt Marsh Affected by the Deepwater Horizon Oil Spill. *PLoS One.* 7: e41305.
- Beck, M. W., K. L. Heck, K. W. Able, D. L. Childers, D. B. Eggleston, B. M. Gillanders, B. Halpern, C. G. Hays, K. Hoshino, T. J. Minello, R. J. Orth, P. F. Sheidan, and M. P. Weinstein. 2001.** The identification, conservation, and management of estuarine and marine nurseries for fish and invertebrates. *Bioscience.* 51: 633–641.
- Bell, F. W. 1997.** The economic valuation of saltwater marsh supporting marine recreational fishing in the southeastern United States. *Ecol. Econ.* 21: 243–254.
- Bell, S. S. 1979.** Short- and long-term variation in a high marsh meiofauna community. *Estuar. Coast. Mar. Sci.* 9: 331–350.
- Bell, S. S. 1980.** Meiofauna-Macrofauna Interactions in a High Salt Marsh Habitat. *Ecol. Monogr.* 50: 487–505.
- Benjamini, Y., and Y. Hochberg. 1995a.** Controlling the False Discovery Rate: A Practical and Powerful Approach to Multiple Testing. *J. R. Stat. Soc. Ser. B.* 57: 289–300.
- Benjamini, Y., and Y. Hochberg. 1995b.** Controlling the False Discovery Rate: A Practical and Powerful Approach to Multiple Testing. *J. R. Stat. Soc. Ser. B.* 57: 289–300.
- Benson, D. A., I. Karsch-Mizrachi, D. J. Lipman, J. Ostell, and E. W. Sayers. 2011.** GenBank. *Nucleic Acids Res.* 39: D32–D37.
- Bertness, M. D. 1984.** Ribbed mussels and *Spartina alterniflora* production in a New England

- salt marsh. *Ecology*. 65: 1794–1807.
- Bertness, M. D. 1991a.** Interspecific interactions among high marsh perennials in a New England salt marsh. *Ecology*. 72: 125–137.
- Bertness, M. D. 1991b.** Zonation of *Spartina patens* and *Spartina alterniflora* in a New England salt marsh. *Ecology*. 72: 138–148.
- Beyer, J., H. C. Trannum, T. Bakke, P. V. Hodson, and T. K. Collier. 2016.** Environmental effects of the Deepwater Horizon oil spill: A review. *Mar. Pollut. Bull.*
- Bhalerao, D. R. 2018.** Determining bioindicators for the impact of oil spills using the food web of larvae of the greenhead horse fly (*Tabanus nigrovittatus*).
- Bhattacharyya, S., P. L. Klerks, and J. A. Nyman. 2003.** Toxicity to freshwater organisms from oils and oil spill chemical treatments in laboratory microcosms. *Environ. Pollut.* 122: 205–215.
- Bhattarai, S. 2006.** Spatial distribution of heavy metals in Louisiana sediments and study of factors impacting the concentrations.
- Bianchi, T. S. 2007.** Biogeochemistry of Estuaries. Oxford University Press, New York.
- Bik, H. M., K. M. Halanych, J. Sharma, and W. K. Thomas. 2012.** Dramatic Shifts in Benthic Microbial Eukaryote Communities following the Deepwater Horizon Oil Spill. *PLoS One*. 7: e38550.
- Bingham, F. T. 1982.** Boron, pp. 431–447. *In* Methods Soil Anal. Part 2. Chem. Microbiol. Prop.
- Blaxter, M., J. Mann, T. Chapman, F. Thomas, C. Whitton, R. Floyd, and E. Abebe. 2005.** Defining operational taxonomic units using DNA barcode data. *Philos. Trans. R. Soc. B Biol. Sci.* 360: 1935–1943.
- Blum, M. D., and H. H. Roberts. 2009.** Drowning of the Mississippi Delta due to insufficient sediment supply and global sea-level rise. *Nat. Geosci.* 2: 488–491.
- Boaden, P. J. S. 1995.** Where Turbellaria? Concerning knowledge and ignorance of marine turbellarian ecology. *Hydrobiol. Int. J. Aquat. Sci.* 305: 91–99.
- Board, W. E. 2020.** World Register of Marine Species. (<http://www.marinespecies.org>).
- Boesch, D. F., R. J. Diaz, and R. W. Virnstein. 1976.** Effects of Tropical Storm Agnes on soft-bottom macrobenthic communities of the James and York estuaries and the lower Chesapeake Bay. *Chesap. Sci.* 17: 246–259.
- Boesch, D. F., and R. E. Turner. 1984.** Dependence of fishery species on salt marshes: The role of food and refuge. *Estuaries*. 7: 460–468.
- Bolyen, E., M. Dillon, N. Bokulich, C. Abnet, G. Al-Ghalith, H. Alexander, E. Alm, M. Arumugam, F. Asnicar, Y. Bai, J. Bisanz, K. Bittinger, A. Brejnrod, C. Brislawn, T. Brown, B. Callahan, J. Chase, E. Cope, P. Dorrestein, G. Douglas, D. Durall, C. Duvallet, C.**

- Edwardson, M. Ernst, M. Estaki, J. Fouquier, J. Gauglitz, D. Gibson, A. Gonzalez, K. Gorlick, J. Guo, B. Hillmann, S. Holmes, H. Holste, C. Huttenhower, G. Huttley, S. Janssen, A. Jarmusch, L. Jiang, B. Kaehler, C. Keefe, P. Keim, S. Kelley, D. Knights, I. Koester, T. Kosciulek, J. Kreps, J. Lee, R. Ley, Y.-X. Liu, E. Loftfield, C. Lozupone, M. Maher, C. Marotz, B. Martin, D. McDonald, L. McIver, A. Melnik, J. Metcalf, S. Morgan, J. Morton, J. Navas-Molina, S. Orchanian, T. Pearson, S. Peoples, D. Petras, E. Priesse, A. Rivers, M. Robeson, P. Rosenthal, N. Segata, M. Shaffer, A. Shiffer, R. Sinha, J. Spear, A. Swafford, L. Thompson, P. Torres, P. Trinh, A. Tripathi, P. Turnbaugh, S. Ul-Hasan, F. Vargas, E. Vogtmann, W. Walters, Y. Wan, M. Wang, J. Warren, K. Weber, A. Willis, J. Zaneveld, Y. Zhang, Q. Zhu, R. Knight, and G. Caporaso. 2019. QIIME 2: Reproducible, interactive, scalable, and extensible microbiome data science. *Nat. Biotechnol.* 1.
- Bond, J. P., E. C. McGawley, and J. W. Hoy. 2000. Distribution of plant-parasitic nematodes on sugarcane in Louisiana and efficacy of nematicides. *J. Nematol.* 32: 493–501.
- Bonisoli-Alquati, A., P. C. Stouffer, R. E. Turner, S. Woltmann, and S. S. Taylor. 2016. Incorporation of Deepwater Horizon oil in a terrestrial bird. *Environ. Res. Lett.* 11: 114023.
- Botello, A. V., J. A. Goñi, and S. A. Castro. 1983. Levels of organic pollution in coastal lagoons of Tabasco state, Mexico; I: Petroleum hydrocarbons. *Bull. Environ. Contam. Toxicol.* 31: 271–277.
- Boyd, C. E., and W. W. Walley. 1972. Studies of the Biogeochemistry of Boron. I. Concentrations in Surface Waters, Rainfall and Aquatic Plants. *Am. Midl. Nat.* 88: 1.
- Brandt, M. I., B. Trouche, L. Quintric, P. Wincker, J. Poulain, and S. Arnaud-Haond. 2019. A flexible pipeline combining bioinformatic correction tools for prokaryotic and eukaryotic metabarcoding. *bioRxiv* [Preprint]. 717355.
- Brannock, P. M., and K. M. Halanych. 2015. Meiofaunal community analysis by high-throughput sequencing: Comparison of extraction, quality filtering, and clustering methods. *Mar. Genomics.* 23: 67–75.
- Brannock, P. M., D. S. Waits, J. Sharma, and K. M. Halanych. 2014. High-throughput sequencing characterizes intertidal meiofaunal communities in northern Gulf of Mexico (Dauphin Island and Mobile Bay, Alabama). *Biol. Bull.* 227: 161–74.
- Bridgham, S. D., J. P. Megonigal, J. K. Keller, N. B. Bliss, and C. Trettin. 2006. The carbon balance of North American wetlands. *Wetlands.* 26: 889–916.
- Broman, E., C. Raymond, C. Sommer, J. S. Gunnarsson, S. Creer, and F. J. A. Nascimento. 2019. Salinity drives meiofaunal community structure dynamics across the Baltic ecosystem. *Mol. Ecol.* 28: 3813–3829.
- Broome, S. W., C. B. Craft, and W. A. Toomey. 2000. Soil Organic Matter (SOM) Effects on Infaunal Community Structure in Restored and Created Tidal Marshes BT - Concepts and Controversies in Tidal Marsh Ecology, pp. 737–747. *In* Weinstein, M.P., Kreeger, D.A. (eds.), *Concepts Controv. Tidal Marsh Ecol.* Springer Netherlands, Dordrecht.

- Broome, S. W., E. D. Seneca, and W. W. Woodhouse. 1988.** Tidal salt marsh restoration. *Aquat. Bot.* 32: 1–22.
- Brown, E. A., F. J. J. Chain, T. J. Crease, H. J. Macisaac, and M. E. Cristescu. 2015.** Divergence thresholds and divergent biodiversity estimates: Can metabarcoding reliably describe zooplankton communities? *Ecol. Evol.* 5: 2234–2251.
- Brupbacher, R. H., J. E. Sedberry Jr., and W. H. Willis. 1973.** The coastal marshlands of Louisiana: chemical properties of the soil materials, *Ag Exp Bull.*
- Bucklin, A., D. Steinke, and L. Blanco-Bercial. 2011.** DNA Barcoding of Marine Metazoa. *Ann. Rev. Mar. Sci.* 3: 471–508.
- Burgess, R. 2001.** An improved protocol for separating meiofauna from sediments using colloidal silica sols. *Mar. Ecol. Prog. Ser.* 214: 161–165.
- Burki, F., A. J. Roger, M. W. Brown, and A. G. B. Simpson. 2020.** The New Tree of Eukaryotes. *Trends Ecol. Evol.*
- Burns, K. A., and J. M. Teal. 1979.** The West Falmouth oil spill: Hydrocarbons in the salt marsh ecosystem. *Estuar. Coast. Mar. Sci.* 8: 349–360.
- Cai, L., S. Fu, J. Yang, and X. Zhou. 2012.** Distribution of meiofaunal abundance in relation to environmental factors in Beibu Gulf, South China Sea. *Acta Oceanol. Sin.* 31: 92–103.
- Callahan, B. J., P. J. McMurdie, and S. P. Holmes. 2017.** Exact sequence variants should replace operational taxonomic units in marker-gene data analysis. *ISME J.* 11: 2639–2643.
- Callahan, B. J., P. J. McMurdie, M. J. Rosen, A. W. Han, A. J. A. Johnson, and S. P. Holmes. 2016.** DADA2: High-resolution sample inference from Illumina amplicon data. *Nat. Methods.* 13: 581–583.
- Camacho, C., G. Coulouris, V. Avagyan, N. Ma, J. Papadopoulos, K. Bealer, and T. L. Madden. 2009.** BLAST+: Architecture and applications. *BMC Bioinformatics.* 10: 1–9.
- Del Campo, J., M. E. Sieracki, R. Molestina, P. Keeling, R. Massana, and I. Ruiz-Trillo. 2014.** The others: Our biased perspective of eukaryotic genomes. *Trends Ecol. Evol.*
- Caporaso, J. G., C. L. Lauber, W. A. Walters, D. Berg-Lyons, J. Huntley, N. Fierer, S. M. Owens, J. Betley, L. Fraser, M. Bauer, N. Gormley, J. A. Gilbert, G. Smith, and R. Knight. 2012.** Ultra-high-throughput microbial community analysis on the Illumina HiSeq and MiSeq platforms. *Isme J.* 6: 1621.
- Carman, K. R., and M. A. Todaro. 1996.** Influence of polycyclic aromatic hydrocarbons on the meiobenthic- copepod community of a Louisiana salt marsh. *J. Exp. Mar. Bio. Ecol.* 198: 37–54.
- Carugati, L., C. Corinaldesi, and A. Dell’Anno. 2015.** Metagenetic tools for the census of marine meiofaunal biodiversity: An overview. *Mar. Genomics.* 24: 11–20.
- Chabreck, R. H. 1970.** Marsh zones and vegetative types in the Louisiana coastal marshes.

- Chabreck, R. H. 1972.** Vegetation, water and soil characteristics of the Louisiana coastal region.
- Chambers, J. M., A. Freeny, and R. M. Heiberger. 1992.** Analysis of variance; designed experiments. *In* Chambers, J.M., Hastie, T.J. (eds.), Stat. Model. S. Wadsworth & Brooks/Cole.
- Chandler, G. T., and J. W. Fleeger. 1983.** Meiofaunal colonization of azoic estuarine sediment in Louisiana: Mechanisms of dispersal. *J. Exp. Mar. Bio. Ecol.* 69: 175–188.
- Chao, A. 1984.** Nonparametric Estimation of the Number of Classes in a Population. *Scand. J. Stat.* 11: 265–270.
- Chao, A., C.-H. Chiu, and T. C. Hsieh. 2012.** Proposing a resolution to debates on diversity partitioning. *Ecology*. 93: 2037–2051.
- Chao, A., N. J. Gotelli, T. C. Hsieh, E. L. Sander, K. H. Ma, R. K. Colwell, and A. M. Ellison. 2014.** Rarefaction and extrapolation with Hill numbers: A framework for sampling and estimation in species diversity studies. *Ecol. Monogr.* 84: 45–67.
- Chao, A., and L. Jost. 2012.** Coverage-based rarefaction and extrapolation: Standardizing samples by completeness rather than size. *Ecology*. 93: 2533–2547.
- Chao, A., and S. M. Lee. 1992.** Estimating the number of classes via sample coverage. *J. Am. Stat. Assoc.* 87: 210–217.
- Chao, A., K. H. Ma, T. C. Hsieh, and C. H. Chiu. 2015.** Online Program SpadeR (Species-richness Prediction And Diversity Estimation in R). Program and User's Guide published at http://chao.stat.nthu.edu.tw/wordpress/software_download/. (http://chao.stat.nthu.edu.tw/wordpress/software_download/).
- Chao, A., Y. T. Wang, and L. Jost. 2013.** Entropy and the species accumulation curve: a novel entropy estimator via discovery rates of new species. *Methods Ecol. Evol.* 4: 1091–1100.
- Chapman, V. J. 1977.** Wet Coastal Ecosystems, Ecosystems of the World. Elsevier Scientific Pub. Co., Amsterdam.
- Checkley Jr, D. M., M. J. Dagg, and S. Uye. 1992.** Feeding, excretion and egg production by individuals and populations of the marine, planktonic copepods, *Acartia* spp. and *Centropages furcatus*. *J. Plankton Res.* 14: 71–96.
- Chesney, E. J., D. M. Baltz, and R. G. Thomas. 2000.** Louisiana estuarine and coastal fisheries and habitats: Perspectives from a fish's eye view. *Ecol. Appl.*
- Chmura, G. L., S. C. Anisfeld, D. R. Cahoon, and J. C. Lynch. 2003.** Global carbon sequestration in tidal, saline wetland soils. *Global Biogeochem. Cycles*. 17: n/a-n/a.
- Christine, A., van der H. Tjisse, G. J. N., M. J. P., D.-H. Marlous, L. L. P. M., S. A. J. P., and S. B. R. 2015.** Foundation species' overlap enhances biodiversity and multifunctionality from the patch to landscape scale in southeastern United States salt marshes. *Proc. R. Soc. B Biol. Sci.* 282: 20150421.

- Coen, L., R. Brumbaugh, D. Bushek, R. Grizzle, M. Luckenbach, M. Posey, S. Powers, and S. Tolley. 2007.** Ecosystem services related to oyster restoration. *Mar. Ecol. Prog. Ser.* 341: 303–307.
- Collins, R. A., J. Bakker, O. S. Wangensteen, A. Z. Soto, L. Corrigan, D. W. Sims, M. J. Genner, and S. Mariani. 2019.** Non-specific amplification compromises environmental DNA metabarcoding with COI. *Methods Ecol. Evol.* 2041–210X.13276.
- Colwell, R. K., A. Chao, N. J. Gotelli, S.-Y. Lin, C. X. Mao, R. L. Chazdon, and J. T. Longino. 2012.** Models and estimators linking individual-based and sample-based rarefaction, extrapolation and comparison of assemblages. *J. Plant Ecol.* 5: 3–21.
- Coomans, A. 2000.** Nematode systematics: Past, present and future, pp. 3–7. *In* *Nematology*. Brill Academic Publishers.
- Costanza, R., O. Pérez-Maqueo, M. L. Martinez, P. Sutton, S. J. Anderson, and K. Mulder. 2008.** The value of coastal wetlands for hurricane protection. *Ambio.* 37: 241–248.
- Coull, B. C. 1990.** Are Members of the Meiofauna Food for Higher Trophic Levels? *Trans. Am. Microsc. Soc.* 109: 233.
- Coull, B. C. 1999.** Role of meiofauna in estuarine soft-bottom habitats*. *Austral Ecol.* 24: 327–343.
- Coull, B. C., and S. S. Bell. 1979.** Perspectives of Marine Meiofaunal Ecology, pp. 189–216. *In* *Ecol. Process. Coast. Mar. Syst.* Springer US, Boston, MA.
- Coull, B. C., and G. T. Chandler. 2001.** Meiobenthos, pp. 726–731. *In* *Encycl. Ocean Sci.* Second Ed. Elsevier Inc.
- Coull, B. C., Z. Zo, J. H. Tietjen, and B. S. Williams. 1982.** Meiofauna of the southeastern United States continental shelf. *Bull. Mar. Sci.* 32: 139–150.
- Couvillion, B. R., H. Beck, D. Schoolmaster, and M. Fischer. 2017.** Land Area Change in Coastal Louisiana (1932 to 2016) Scientific Investigations Map 3381, U.S. Geol. Surv. Sci. Investig. Map 3381.
- CPRA. 2007.** Integrated Ecosystem Restoration and Hurricane Protection: Louisiana’s Comprehensive Masterplan for a Sustainable Coast. Coast. Prot. Restor. Auth.
- CPRA. 2012.** Louisiana’s Comprehensive Master Plan for a Sustainable Coast. Coast. Prot. Restor. Auth.
- CPRA. 2017.** Louisiana’s Comprehensive Master Plan for a Sustainable Coast. Coast. Prot. Restor. Auth.
- Craft, C., and J. Sacco. 2003.** Long-term succession of benthic infauna communities on constructed *Spartina alterniflora* marshes. *Mar. Ecol. Prog. Ser.* 257: 45–58.
- Cragg, S. M., D. A. Friess, L. G. Gillis, S. M. Trevathan-Tackett, O. M. Terrett, J. E. M. Watts, D. L. Distel, and P. Dupree. 2020.** Vascular Plants Are Globally Significant Contributors to

- Marine Carbon Fluxes and Sinks. *Ann. Rev. Mar. Sci.* 12: annurev-marine-010318-095333.
- Creer, S., K. Deiner, S. Frey, D. Porazinska, P. Taberlet, W. K. Thomas, C. Potter, and H. M. Bik. 2016.** The ecologist's field guide to sequence-based identification of biodiversity. *Methods Ecol. Evol.* 7: 1008–1018.
- Creer, S., V. G. Fonseca, D. L. Porazinska, R. M. Giblin-Davis, W. Sung, D. M. Power, M. Packer, G. R. Carvalho, M. L. Blaxter, P. J. D. Lamshead, and W. K. Thomas. 2010.** Ultrasequencing of the meiofaunal biosphere: Practice, pitfalls and promises. *Mol. Ecol.* 19: 4–20.
- Crosby, S. C., D. F. Sax, M. E. Palmer, H. S. Booth, L. A. Deegan, M. D. Bertness, and H. M. Leslie. 2016.** Salt marsh persistence is threatened by predicted sea-level rise. *Estuar. Coast. Shelf Sci.* 181: 93–99.
- Culbertson, J. B., I. Valiela, Y. S. Olsen, and C. M. Reddy. 2008.** Effect of field exposure to 38-year-old residual petroleum hydrocarbons on growth, condition index, and filtration rate of the ribbed mussel, *Geukensia demissa*. *Environ. Pollut.* 154: 312–319.
- Culbertson, J. B., I. Valiela, E. E. Peacock, C. M. Reddy, A. Carter, and R. VanderKruik. 2007.** Long-term biological effects of petroleum residues on fiddler crabs in salt marshes. *Mar. Pollut. Bull.* 54: 955–962.
- Culbertson, J. B., I. Valiela, M. Pickart, E. E. Peacock, and C. M. Reddy. 2008.** Long-term consequences of residual petroleum on salt marsh grass. *J. Appl. Ecol.* 45: 1284–1292.
- Danovaro, R., C. Gambi, A. Dell'Anno, C. Corinaldesi, S. Fraschetti, A. Vanreusel, M. Vincx, and A. J. Gooday. 2008.** Exponential Decline of Deep-Sea Ecosystem Functioning Linked to Benthic Biodiversity Loss. *Curr. Biol.* 18: 1–8.
- Das, A., D. Justic, M. Inoue, A. Hoda, H. Huang, and D. Park. 2012.** Impacts of Mississippi River diversions on salinity gradients in a deltaic Louisiana estuary: Ecological and management implications. *Estuar. Coast. Shelf Sci.* 111: 17–26.
- Day, J. W., L. D. Britsch, S. R. Hawes, G. P. Shaffer, D. J. Reed, and D. Cahoon. 2000.** Pattern and process of land loss in the Mississippi Delta: A spatial and temporal analysis of wetland habitat change. *Estuaries.* 23: 425–438.
- Deagle, B. E., S. N. Jarman, E. Coissac, F. Pompanon, and P. Taberlet. 2014.** DNA metabarcoding and the cytochrome c oxidase subunit I marker: Not a perfect match. *Biol. Lett.* 10: 20140562.
- Deaton, L. E., and M. J. Greenberg. 1986.** There is no horohalinicum. *Estuaries.* 9: 20–30.
- Dee, L. E., J. Cowles, F. Isbell, S. Pau, S. D. Gaines, and P. B. Reich. 2019a.** When do Ecosystem Services depend on rare species? *Trends Ecol. Evol.* xx: 1–37.
- Dee, L. E., J. Cowles, F. Isbell, S. Pau, S. D. Gaines, and P. B. Reich. 2019b.** When Do Ecosystem Services Depend on Rare Species? *Trends Ecol. Evol.*

- Deiner, K., H. M. Bik, E. Mächler, M. Seymour, A. Lacoursière-Roussel, F. Altermatt, S. Creer, I. Bista, D. M. Lodge, N. de Vere, M. E. Pfrender, and L. Bernatchez. 2017.** Environmental DNA metabarcoding: Transforming how we survey animal and plant communities. *Mol. Ecol.*
- Deis, D. R., I. A. Mendelssohn, J. W. Fleeger, S. M. Bourgoïn, and Q. Lin. 2019.** Legacy effects of Hurricane Katrina influenced marsh shoreline erosion following the Deepwater Horizon oil spill. *Sci. Total Environ.* 672: 456–467.
- DeLaune, R. D., R. J. Buresh, and W. H. Patrick. 1979.** Relationship of soil properties to standing crop biomass of *Spartina alterniflora* in a Louisiana marsh. *Estuar. Coast. Mar. Sci.* 8: 477–487.
- DeLaune, R. D., A. Jugsujinda, G. W. Peterson, and W. H. Patrick. 2003.** Impact of Mississippi River freshwater reintroduction on enhancing marsh accretionary processes in a Louisiana estuary. *Estuar. Coast. Shelf Sci.* 58: 653–662.
- DeLaune, R. D., C. J. Smith, W. H. Patrick, J. W. Fleeger, and M. D. Tolley. 1984.** Effect of oil on salt marsh biota: Methods for restoration. *Environ. Pollution. Ser. A, Ecol. Biol.* 36: 207–227.
- Dice, L. R. 1945.** Measures of the Amount of Ecologic Association Between Species. *Ecology.* 26: 297–302.
- Drummond, A. J., R. D. Newcomb, T. R. Buckley, D. Xie, A. Dopheide, B. C. Potter, J. Heled, H. A. Ross, L. Tooman, S. Grosser, D. Park, N. J. Demetras, M. I. Stevens, J. C. Russell, S. H. Anderson, A. Carter, and N. Nelson. 2015.** Evaluating a multigene environmental DNA approach for biodiversity assessment. *Gigascience.* 4: 46.
- Duan, J., W. Liu, X. Zhao, Y. Han, S. E. O'Reilly, and D. Zhao. 2018.** Study of residual oil in Bay Jimmy sediment 5 years after the Deepwater Horizon oil spill: Persistence of sediment retained oil hydrocarbons and effect of dispersants on desorption. *Sci. Total Environ.* 618: 1244–1253.
- Duguay, A. M. M. 1997.** The Ecotoxicology of Oil Sands Tailings on the Freshwater Leech, *Nepheleopsis obscura* and the Oligochaete Worm, *Tubifex tubifex*.
- Elsey-Quirk, T., S. A. Graham, I. A. Mendelssohn, G. Snedden, J. W. Day, R. R. Twilley, G. Shaffer, L. A. Sharp, J. Pahl, and R. R. Lane. 2019.** Mississippi river sediment diversions and coastal wetland sustainability: Synthesis of responses to freshwater, sediment, and nutrient inputs. *Estuar. Coast. Shelf Sci.* 221: 170–183.
- Engle, V. D. 2011.** Estimating the provision of ecosystem services by Gulf of Mexico coastal wetlands. *Wetlands.* 31: 179–193.
- Eskin, R. A., and B. E. Hopper. 1985.** Population Dynamics and Description of *Ptycholaimellus hibernus* n. sp. (Nematoda: Chromadoridae). *J. Nematol.* 17: 38–45.
- Faber, P. W. and P. 2001.** Salt Marsh Restoration Experience in San Francisco Bay. *J. Coast. Res.*

27: 203–211.

Faith, D. P. 1992. Conservation evaluation and phylogenetic diversity. *Biol. Conserv.* 61: 1–10.

Fantle, M. S., A. I. Dittel, S. M. Schwalm, C. E. Epifanio, and M. L. Fogel. 1999. A food web analysis of the juvenile blue crab, *Callinectes sapidus*, using stable isotopes in whole animals and individual amino acids. *Oecologia*. 120: 416–426.

Feagin, R. A., S. M. Lozada-Bernard, T. M. Ravens, I. Möller, K. M. Yeager, and A. H. Baird. 2009. Does vegetation prevent wave erosion of salt marsh edges? *Proc. Natl. Acad. Sci. U. S. A.* 106: 10109–10113.

Field, C. R., C. Gjerdrum, and C. S. Elphick. 2016. Forest resistance to sea-level rise prevents landward migration of tidal marsh. *Biol. Conserv.* 201: 363–369.

Fleeger, J., G. Chandler, G. Fitzhugh, and F. Phillips. 1984. Effects of tidal currents on meiofauna densities in vegetated salt marsh sediments. *Mar. Ecol. Prog. Ser.* 19: 49–53.

Fleeger, J. W. 1985. Meiofaunal Densities and Copepod Species Composition in a Louisiana , U . S . A ., Estuary. *Trans. Am. Microsc. Soc.* 104: 321–332.

Fleeger, J. W., K. R. Carman, M. R. Riggio, I. A. Mendelssohn, Q. X. Lin, A. Hou, D. R. Deis, and S. Zengel. 2015. Recovery of salt marsh benthic microalgae and meiofauna following the Deepwater Horizon oil spill linked to recovery of *Spartina alterniflora*. *Mar. Ecol. Prog. Ser.* 536: 39–54.

Fleeger, J. W., and G. T. Chandler. 1983. Meiofauna responses to an experimental oil spill in a Louisiana salt marsh. *Mar. Ecol. - Prog. Ser. Vol.* 11: 257–264.

Fleeger, J. W., K. A. Gust, S. J. Marlborough, and G. Tita. 2007. Mixtures of metals and polynuclear aromatic hydrocarbons elicit complex, nonadditive toxicological interactions in meiobenthic copepods. *Environ. Toxicol. Chem.* 26: 1677–1685.

Fleeger, J. W., D. S. Johnson, S. Zengel, I. A. Mendelssohn, D. R. Deis, S. A. Graham, Q. Lin, M. C. Christman, M. R. Riggio, and M. Pant. 2020. Macroinfauna responses and recovery trajectories after an oil spill differ from those following saltmarsh restoration. *Mar. Environ. Res.* 155: 104881.

Fleeger, J. W., M. R. Riggio, I. A. Mendelssohn, Q. Lin, D. R. Deis, D. S. Johnson, K. R. Carman, and S. A. Graham. 2019. What Promotes the Recovery of Salt Marsh Infauna After Oil Spills ? *Estuaries and Coasts.* 42: 204–217.

Fleeger, J. W., M. R. Riggio, I. A. Mendelssohn, Q. Lin, A. Hou, and D. R. Deis. 2018. Recovery of saltmarsh meiofauna six years after the Deepwater Horizon oil spill. *J. Exp. Mar. Bio. Ecol.* 502: 182–190.

Fleeger, J. W., S. A. Whipple, and L. L. Cook. 1981. Field manipulations of tidal flushing, light exposure and natant macrofauna in a Louisiana salt marsh: Effects on the meiofauna. *J. Exp. Mar. Bio. Ecol.* 56: 87–100.

- Folmer, O., M. Black, W. Hoeh, R. Lutz, and R. Vrijenhoek. 1994.** DNA primers for amplification of mitochondrial cytochrome c oxidase subunit I from diverse metazoan invertebrates. *Mol. Mar. Biol. Biotechnol.* 3: 294–9.
- Fonseca, V. G., G. R. Carvalho, W. Sung, H. F. Johnson, D. M. Power, S. P. Neill, M. Packer, M. L. Blaxter, P. J. D. Lamshead, W. K. Thomas, and S. Creer. 2010.** Second-generation environmental sequencing unmasks marine metazoan biodiversity. *Nat. Commun.* 1.
- Fritts, T. H., and M. A. McGehee. 1982.** Effects of Petroleum on the Development and Survival of Marine Turtle Embryos. Belle Chasse, LA.
- Fry, B., and L. C. Anderson. 2014.** Minimal incorporation of Deepwater Horizon oil by estuarine filter feeders. *Mar. Pollut. Bull.* 80: 282–287.
- Galván, K., J. Fleeger, and B. Fry. 2008.** Stable isotope addition reveals dietary importance of phytoplankton and microphytobenthos to saltmarsh infauna. *Mar. Ecol. Prog. Ser.* 359: 37–49.
- Garraffoni, A. R. S., and M. P. Melchior. 2015.** New species and new records of freshwater Heterolepidoderma (Gastrotricha: Chaetonotidae) from Brazil with an identification key to the genus. *Zootaxa.* 4057: 551–568.
- Gedan, K. B., M. L. Kirwan, E. Wolanski, E. B. Barbier, B. R. Silliman, K. B. Gedan, M. L. Kirwan, E. Wolanski, E. B. Barbier, and B. R. Silliman. 2011.** The present and future role of coastal wetland vegetation in protecting shorelines: answering recent challenges to the paradigm. *Clim. Change.* 106: 7–29.
- Gedan, K. B., B. R. Silliman, and M. D. Bertness. 2009.** Centuries of human-driven change in salt marsh ecosystems. *Ann. Rev. Mar. Sci.*
- Gee, J. M. 1989.** An ecological and economic review of meiofauna as food for fish. *Zool. J. Linn. Soc.* 96: 243–261.
- Genzano, G., H. Mianzan, E. M. Acha, and E. Gaitán. 2006.** First record of the invasive medusa *Blackfordia virginica* (Hydrozoa: Leptomedusae) in the Río de la Plata estuary, Argentina-Uruguay. *Rev. Chil. Hist. Nat.* 79: 257–261.
- Gerhardt, A. 2009.** Screening the toxicity of Ni, Cd, Cu, ivermectin, and imidacloprid in a short-term automated behavioral toxicity test with *tubifex tubifex* (muller 1774) (Oligochaeta). *Hum. Ecol. Risk Assess.* 15: 27–40.
- Giere, O. 2009.** Meiobenthology: The Microscopic Motile Fauna of Aquatic Sediments. Springer-Verlag, Berlin.
- Gilbert, J. A., J. K. Jansson, and R. Knight. 2014.** The Earth Microbiome project: successes and aspirations. *BMC Biol.* 12: 69.
- Gotelli, N. J., and R. K. Colwell. 2001.** Quantifying biodiversity: procedures and pitfalls in the measurement and comparison of species richness. *Ecol. Lett.* 4: 379–391.

- Greenberg, R., and J. E. Maldonado. 2006.** Diversity and endemism in tidal-marsh vertebrates. *Stud. Avian Biol.* 32–53.
- Greiner La Peyre, M. K., J. B. Grace, E. Hahn, and I. A. Mendelssohn. 2001.** The importance of competition in regulating plant species abundance along a salinity gradient. *Ecology*. 82: 62–69.
- Grey, E. K., S. C. Chiasson, H. G. Williams, V. J. Troeger, and C. M. Taylor. 2015.** Evaluation of Blue Crab, *Callinectes sapidus*, Megalopal Settlement and Condition during the Deepwater Horizon Oil Spill. *PLoS One*. 10: e0135791.
- Griffiths, B. S., J. Römbke, R. M. Schmelz, A. Scheffczyk, J. H. Faber, J. Bloem, G. Pérès, D. Cluzeau, A. Chabbi, M. Suhadolc, J. P. Sousa, P. Martins Da Silva, F. Carvalho, S. Mendes, P. Morais, R. Francisco, C. Pereira, M. Bonkowski, S. Geisen, R. D. Bardgett, F. T. De Vries, T. Bolger, T. Dirilgen, O. Schmidt, A. Winding, N. B. Hendriksen, A. Johansen, L. Philippot, P. Plassart, D. Bru, B. Thomson, R. I. Griffiths, M. J. Bailey, A. Keith, M. Rutgers, C. Mulder, S. E. Hannula, R. Creamer, and D. Stone. 2016.** Selecting cost effective and policy-relevant biological indicators for European monitoring of soil biodiversity and ecosystem function. *Ecol. Indic.* 69: 213–223.
- Grilli, P., R. M. Kristensen, and M. Balsamo. 2009.** *Heterolepidoderma caudosquamatum* (Gastrotricha: Chaetonotida), a new species from brackish waters of Denmark. *Zootaxa*. 2173: 49–54.
- Grose, P. L., and J. S. Mattson. 1977.** The Argo Merchant Oil Spill: a Preliminary Scientific Report.
- Gundlach, E. R., B. Baca, and D. C. Barry. 2003.** Emergency Marsh Restoration as Part of Response to the Swanson Creek (Maryland) Oil Spill. *Int. Oil Spill Conf. Proc.* 2003: 135–143.
- Gustafson, D. J., J. Kilheffer, and B. R. Silliman. 2006.** Relative effects of *Littoraria irrorata* and *Prokelisia marginata* on *Spartina alterniflora*. *Estuaries and Coasts*. 29: 639–644.
- Hadziavdic, K., K. Lekang, A. Lanzen, I. Jonassen, E. M. Thompson, and C. Troedsson. 2014.** Characterization of the 18s rRNA gene for designing universal eukaryote specific primers. *PLoS One*. 9.
- Haney, J., H. Geiger, and J. Short. 2014.** Bird mortality from the Deepwater Horizon oil spill. II. Carcass sampling and exposure probability in the coastal Gulf of Mexico. *Mar. Ecol. Prog. Ser.* 513: 239–252.
- Hanley, M. E., T. J. Bouma, and H. L. Mossman. 2020.** The gathering storm: Optimizing management of coastal ecosystems in the face of a climate-driven threat. *Ann. Bot.*
- Hansens, E. J. 1979.** Review: Tabanidae of the East Coast as an Economic Problem. *J. New York Entomol. Soc.* 87: 312–318.
- Harrison, J. B., J. M. Sunday, and S. M. Rogers. 2019.** Predicting the fate of eDNA in the

- environment and implications for studying biodiversity. *Proc. R. Soc. B Biol. Sci.* 286.
- Hayes, M. O., and J. Michel. 1999.** Factors determining the long-term persistence of Exxon Valdez oil in gravel beaches. *Mar. Pollut. Bull.* 38: 92–101.
- Hayes, S. A., E. Josephson, K. Maze-Foley, P. E. Rosel, B. Byrd, S. Chavez-Rosales, T. Vn Cole, L. P. Garrison, J. Hatch, A. Henry, S. C. Horstman, J. Litz, M. C. Lyssikatos, K. D. Mullin, C. Orphanides, R. M. Pace, D. L. Palka, J. Powell, F. W. Wenzel, W. L. Ross, N. Jacobs, and C. Oliver. 2019.** US Atlantic and Gulf of Mexico Marine Mammal Stock Assessments-2018.
- Healy, B., and K. Walters. 1994.** Oligochaeta in *Spartina* stems: the microdistribution of Enchytraeidae and Tubificidae in a salt marsh, Sapelo Island, USA BT - Aquatic Oligochaete Biology V, pp. 111–123. *In* Reynoldson, T.B., Coates, K.A. (eds.), . Springer Netherlands, Dordrecht.
- Hebert, P. D. N., A. Cywinska, S. L. Ball, and J. R. deWaard. 2003.** Biological identifications through DNA barcodes. *Proceedings. Biol. Sci.* 270: 313–21.
- Hewitt, D. E., T. M. Smith, V. Raoult, M. D. Taylor, and T. F. Gaston. 2020.** Stable isotopes reveal the importance of saltmarsh-derived nutrition for two exploited penaeid prawn species in a seagrass dominated system. *Estuar. Coast. Shelf Sci.* 236: 106622.
- Higgins, R. P., and J. W. Fleeger. 1980.** Seasonal changes in the population structure of *Echinoderes coulli* (Kinorhyncha). *Estuar. Coast. Mar. Sci.* 10: 495–505.
- Hinshaw, S. E., C. Tatariw, N. Flournoy, A. Kleinhuizen, C. Taylor, P. A. Sobecky, and B. Mortazavi. 2017a.** Vegetation Loss Decreases Salt Marsh Denitrification Capacity: Implications for Marsh Erosion. *Environ. Sci. Technol.* 51: 8245–8253.
- Hinshaw, S. E., C. Tatariw, N. Flournoy, A. Kleinhuizen, C. Taylor, P. A. Sobecky, and B. Mortazavi. 2017b.** Vegetation Loss Decreases Salt Marsh Denitrification Capacity: Implications for Marsh Erosion. *Environ. Sci. Technol.* 51: 8245–8253.
- Hodda, M. 2011.** “Phylum Nematoda Cobb 1932. *In*: Zhang, Z.-Q. (Ed.) *Animal biodiversity: An outline of higher-level classification and survey of taxonomic richness*. *Zootaxa*. 3148: 63.
- Hoffman, E., and J. G. Quinn. 1980.** The Argo Merchant oil spill and the sediments of Nantucket shoals, pp. 185–218. *In* Baker, R.A. (ed.), *Contam. Sediments*. Ann Arbor Science, Ann Arbor, MI.
- Hofmann, E. E., and T. M. Powell. 1998.** Environmental variability effects on marine fisheries: Four case histories. *Ecol. Appl.* 8: 23–32.
- Holm, G. O., and C. E. Sasser. 2001.** Differential salinity response between two Mississippi River subdeltas: Implications for changes in plant composition. *Estuaries*. 24: 78–89.
- Hope, W. D. 1967.** Free-Living Marine Nematodes of the Genera *Pseudocella* Filipjev, 1927, *Thoracostoma* Marion, 1870, and *Deontostoma* Filipjev, 1916 (Nematoda: Leptosomatidae) from the West Coast of North America. *Trans. Am. Microsc. Soc.* 86: 307.

- Hopkinson, C. S., and A. E. Giblin. 2008.** Nitrogen Dynamics of Coastal Salt Marshes, pp. 991–1036. *In* Nitrogen Mar. Environ. Elsevier Inc.
- Horn, H. S. 1966.** Measurement of “Overlap” in Comparative Ecological Studies. *Am. Nat.* 100: 419–424.
- Howes, N. C., J. A. Barras, J. M. Smith, I. Y. Georgiou, M. D. Miner, M. A. Kulp, D. M. FitzGerald, and Z. J. Hughes. 2010.** Hurricane-induced failure of low salinity wetlands. *Proc. Natl. Acad. Sci.* 107: 14014–14019.
- Hribar, L. J., D. J. Leprince, and L. D. Foil. 1991.** Design for a canopy trap for collecting horse flies (Diptera: Tabanidae). *J. Am. Mosq. Control Assoc.* 7: 657–659.
- Hsieh, T. C., K. H. Ma, and A. Chao. 2016.** iNEXT: an R package for rarefaction and extrapolation of species diversity (Hill numbers). *Methods Ecol. Evol.* 7: 1451–1456.
- Hugot, J. P., P. Baujard, and S. Morand. 2001.** Biodiversity in helminths and nematodes as a field of study: An overview. *Nematology.* 3: 199–208.
- Husseneder, C., J. R. Donaldson, and L. D. Foil. 2016.** Impact of the 2010 Deepwater Horizon oil spill on population size and genetic structure of horse flies in Louisiana marshes. *Sci. Rep.* 6: 18968.
- Husseneder, C., J. S. Park, and L. D. Foil. 2018.** Recovery of horse fly populations in Louisiana marshes following the Deepwater Horizon oil spill. *Sci. Rep.* 8: 1–10.
- Jacquioud, S., J. Stenbæk, S. S. Santos, A. Winding, S. J. Sørensen, and A. Priemé. 2016.** Metagenomes provide valuable comparative information on soil microeukaryotes. *Res. Microbiol.* 167: 436–450.
- Jankowski, K. L., T. E. Törnqvist, and A. M. Fernandes. 2017.** Vulnerability of Louisiana’s coastal wetlands to present-day rates of relative sea-level rise. *Nat. Commun.* 8: 14792.
- Jernelov, A., and O. Linden. 1981.** Ixtoc I: A case study of the world’s largest oil spill. *Ambio.* 10: 299–306.
- Johnson, D. S., J. W. Fleeger, K. A. Galván, and E. B. Moser. 2007.** Worm holes and their space-time continuum: Spatial and temporal variability of macroinfaunal annelids in a northern New England salt marsh. *Estuaries and Coasts.* 30: 226–237.
- Johnston, S. A. 1981.** Estuarine dredge and fill activities: A review of impacts. *Environ. Manage.* 5: 427–440.
- Jones, R. F., D. M. Baltz, and R. L. Allen. 2002.** Patterns of resource use by fishes and macroinvertebrates in Barataria Bay, Louisiana. *Mar. Ecol. Prog. Ser.* 237: 271–289.
- Katoh, K., K. Misawa, K. Kuma, and T. Miyata. 2002.** MAFFT: a novel method for rapid multiple sequence alignment based on fast Fourier transform. *Nucleic Acids Res.* 30: 3059–3066.
- Kearney, M. S., J. C. A. Riter, and R. E. Turner. 2011.** Freshwater river diversions for marsh restoration in Louisiana: Twenty-six years of changing vegetative cover and marsh area.

Geophys. Res. Lett. 38: n/a-n/a.

- Kelly, M. 2019.** Adapting the (fast-moving) world of molecular ecology to the (slow-moving) world of environmental regulation : lessons from the UK diatom metabarcoding exercise. *Metabarcoding and Metagenomics*. 3: 127–135.
- Kennedy, A. D., and C. A. Jacoby. 1999.** Biological Indicators of Marine Environmental Health: Meiofauna – A Neglected Benthic Component? *Environ. Monit. Assess.* 54: 47–68.
- Kennish, M. J. 2001.** Coastal Salt Marsh Systems in the U.S.: A Review of Anthropogenic Impacts. *J. Coast. Res.* 17: 731–748.
- Kimes, N. E., A. V. Callaghan, J. M. Suflita, and P. J. Morris. 2014.** Microbial transformation of the deepwater horizon oil spill-past, present, and future perspectives. *Front. Microbiol.*
- Kirman, Z. D., J. L. Sericano, T. L. Wade, T. S. Bianchi, F. Marcantonio, and A. S. Kolker. 2016.** Composition and depth distribution of hydrocarbons in Barataria Bay marsh sediments after the Deepwater Horizon oil spill. *Environ. Pollut.* 214: 101–113.
- Kirwan, M. L., and J. P. Megonigal. 2013.** Tidal wetland stability in the face of human impacts and sea-level rise. *Nature*.
- Kirwan, M. L., and S. M. Mudd. 2012.** Response of salt-marsh carbon accumulation to climate change. *Nature*.
- Kirwan, M. L., S. Temmerman, E. E. Skeehan, G. R. Guntenspergen, and S. Fagherazzi. 2016.** Overestimation of marsh vulnerability to sea level rise. *Nat. Clim. Chang.* 6: 253–260.
- Klepac-Ceraj, V., M. Bahr, B. C. Crump, A. P. Teske, J. E. Hobbie, and M. F. Polz. 2004.** High overall diversity and dominance of microdiverse relationship in salt marsh sulphate-reducing bacteria. *Environ. Microbiol.* 6: 686–698.
- Kneib, R. T. 1984.** Patterns of invertebrate distribution and abundance in the intertidal salt marsh: Causes and questions. *Estuaries*. 7: 392–412.
- Knutson, T. R., J. L. McBride, K. Emanuel, G. Holland, C. Landsea, I. Held, J. P. Kossin, A. K. Srivastava, and M. Sugi. 2010.** Tropical Cyclones and Climate Change. *Nat. Geosci.* 3: 157–163.
- Kolicka, M. 2019.** From saline to salty? *Heterolepidoderma sinus* (Chaetonotida, Chaetonotidae) from subsaline coal mine settling ponds. *Zootaxa*. 4559: 568–572.
- Kolker, A. S., M. A. Allison, and S. Hameed. 2011.** An evaluation of subsidence rates and sea-level variability in the northern Gulf of Mexico. *Geophys. Res. Lett.* 38: n/a-n/a.
- Kruskal, W. H., and W. A. Wallis. 1952.** Use of Ranks in One-Criterion Variance Analysis. *J. Am. Stat. Assoc.* 47: 583.
- Ladurner, P., L. Schärer, W. Salvenmoser, and R. M. Rieger. 2005.** A new model organism among the lower Bilateria and the use of digital microscopy in taxonomy of meiobenthic Platyhelminthes: *Macrostomum lignano*, n. sp. (Rhabditophora, Macrostomorpha). *J. Zool.*

Syst. Evol. Res. 43: 114–126.

- Landers, S. C., M. V Sørensen, K. R. Beaton, C. M. Jones, J. M. Miller, and P. M. Stewart. 2018.** Kinorhynch assemblages in the Gulf of Mexico continental shelf collected during a two-year survey. *J. Exp. Mar. Bio. Ecol.* 502: 81–90.
- Lane, D. J. 1991.** 16S/23S rRNA Sequencing, pp. 115–175. *In* Stackebrandt, E., Goodfellow, M. (eds.), *Nucleic Acid Tech. Bact. Syst.* John Wiley & Sons, Ltd, New York, NY, USA.
- Leasi, F., J. L. Sevigny, E. M. Laflamme, T. Artois, M. Curini-Galletti, A. de Jesus Navarrete, M. Di Domenico, F. Goetz, J. A. Hall, R. Hochberg, K. M. Jörger, U. Jondelius, M. A. Todaro, H. H. Wirshing, J. L. Norenburg, and W. K. Thomas. 2018.** Biodiversity estimates and ecological interpretations of meiofaunal communities are biased by the taxonomic approach. *Commun. Biol.* 1: 112.
- Legendre P, L. L. 1998.** *Numerical Ecology*, 2nd ed. Elsevier, Amsterdam.
- Lemasson, A. J., S. Fletcher, J. M. Hall-Spencer, and A. M. Knights. 2017.** Linking the biological impacts of ocean acidification on oysters to changes in ecosystem services: A review. *J. Exp. Mar. Bio. Ecol.*
- Lin, Q., and I. A. Mendelssohn. 1996.** A Comparative Investigation of the Effects of South Louisiana Crude Oil on the Vegetation of Fresh, Brackish and Salt Marshes. *Mar. Pollut. Bull.* Vol 32: 202–209.
- Lin, Q., and I. A. Mendelssohn. 2012.** Impacts and Recovery of the Deepwater Horizon Oil Spill on Vegetation Structure and Function of Coastal Salt Marshes in the Northern Gulf of Mexico. *Environ. Sci. Technol.* 46: 3737–3743.
- Lin, Q., I. A. Mendelssohn, S. A. Graham, A. Hou, J. W. Fleeger, and D. R. Deis. 2016.** Response of salt marshes to oiling from the Deepwater Horizon spill: Implications for plant growth, soil surface-erosion, and shoreline stability. *Sci. Total Environ.* 557–558: 369–377.
- Liu, T., C. Y. Chen, A. Chen-Deng, Y. L. Chen, J. Y. Wang, Y. I. Hou, and M. C. Lin. 2020.** Joining Illumina paired-end reads for classifying phylogenetic marker sequences. *BMC Bioinformatics.* 21: 105.
- Louisiana Department of Wildlife and Fisheries. 2019.** Louisiana Department of Wildlife and Fisheries 2018-2019 Annual Report. Baton Rouge, LA.
- Lyons, K. G., C. A. Brigham, B. H. Traut, and M. W. Schwartz. 2005.** Rare species and ecosystem functioning. *Conserv. Biol.*
- Macreadie, P. I., A. R. Hughes, and D. L. Kimbro. 2013.** Loss of “Blue Carbon” from Coastal Salt Marshes Following Habitat Disturbance. *PLoS One.* 8.
- Magnarelli, L. A., and J. G. Stoffolano. 1980.** Blood Feeding, Oögenesis, and Oviposition by *Tabanus nigrovittatus*1 in the Laboratory. *Ann. Entomol. Soc. Am.* 73: 14–17.
- Mapstone, G. M. 2014.** Global Diversity and Review of Siphonophorae (Cnidaria: Hydrozoa).

PLoS One. 9: e87737.

- Mare, M. F. 1942.** A study of a marine benthic community with special reference to the micro-organisms. *J. Mar. Biol. Assoc. United Kingdom*. 25: 517–554.
- Martens, P. M., and E. R. Schockaert. 1986.** The importance of turbellarians in the marine meiobenthos: a review. *Hydrobiologia*. 132: 295–303.
- McClelland, J. W., and I. Valiela. 1998.** Changes in food web structure under the influence of increased anthropogenic nitrogen inputs to estuaries. *Mar. Ecol. Prog. Ser.* 168: 259–271.
- McClenachan, G., R. Eugene Turner, and A. W. Tweel. 2013.** Effects of oil on the rate and trajectory of Louisiana marsh shoreline erosion. *Environ. Res. Lett.* 8.
- McGranahan, G., D. Balk, and B. Anderson. 2007.** The rising tide: assessing the risks of climate change and human settlements in low elevation coastal zones. *Environ. Urban.* 19: 17–37.
- McKee, K. L., I. A. Mendelssohn, and M. D. Materne. 2004.** Acute salt marsh dieback in the Mississippi River deltaic plain: A drought-induced phenomenon? *Glob. Ecol. Biogeogr.* 13: 65–73.
- McLean, E. O. 1982.** Soil pH and Lime Requirement, pp. 199–224. *In* *Methods Soil Anal. Part 2. Chem. Microbiol. Prop.*
- McMurdie, P. J., and J. N. Paulson. 2016.** biomformat: An interface package for the BIOM file format.
- Mcowen, C. J., L. V. Weatherdon, J. W. Van Bochove, E. Sullivan, S. Blyth, C. Zockler, D. Stanwell-Smith, N. Kingston, C. S. Martin, M. Spalding, and S. Fletcher. 2017.** A global map of saltmarshes. *Biodivers. Data J.* 5: 11764.
- Meckel, T. A., U. S. ten Brink, and S. J. Williams. 2006.** Current subsidence rates due to compaction of Holocene sediments in southern Louisiana. *Geophys. Res. Lett.* 33: L11403.
- Mehlich, A. 1984.** Mehlich 3 Soil Test Extractant: A Modification of Mehlich 2 Extractant. *Commun. Soil Sci. Plant Anal.* 15: 1409–1416.
- Mendelssohn, I. A., and K. L. McKee. 1988.** *Spartina Alterniflora* Die-Back in Louisiana: Time-Course Investigation of Soil Waterlogging Effects. *J. Ecol.* 76: 509.
- Michel, J., E. H. Owens, S. Zengel, A. Graham, Z. Nixon, T. Allard, W. Holton, P. D. Reimer, A. Lamarche, M. White, N. Rutherford, C. Childs, G. Mauseth, G. Challenger, and E. Taylor. 2013.** Extent and Degree of Shoreline Oiling: Deepwater Horizon Oil Spill, Gulf of Mexico, USA. *PLoS One*. 8: 1–9.
- Miller, R. G. 1981.** *Simultaneous Statistical Inference*. Springer New York.
- Minello, T. J., R. J. Zimmerman, and R. Medina. 1994.** THE IMPORTANCE OF EDGE FOR NATANT MACROFAUNA IN A CREATED SALT MARSH. *Wetlands*. 14: 184–198.
- Mitsi, K., A. S. Arroyo, and I. Ruiz-Trillo. 2019.** A global metabarcoding analysis expands

- molecular diversity of Platyhelminthes and reveals novel early-branching clades. *Biol. Lett.* 15: 20190182.
- Möller, I., and T. Spencer. 2002.** Wave dissipation over macro-tidal saltmarshes: Effects of marsh edge typology and vegetation change. *J. Coast. Res.* 36: 506–521.
- Montagna, P. A., and R. D. Kalke. 1992.** The Effect of Freshwater Inflow on Meiofaunal and Macrofaunal Populations in the Guadalupe and Nueces Estuaries, Texas 1.
- Montagna, P. A., R. D. Kalke, and C. Ritter. 2002.** Effect of restored freshwater inflow on macrofauna and meiofauna in upper Rincon Bayou, Texas, USA. *Estuaries.* 25: 1436–1447.
- Morisita, M. 1961.** Measuring of interspecific association and similarity between communities.
- Morton, J. T., C. Marotz, A. Washburne, J. Silverman, L. S. Zaramela, A. Edlund, K. Zengler, and R. Knight. 2019.** Establishing microbial composition measurement standards with reference frames. *Nat. Commun.* 10: 1–11.
- Morton, R. A., and J. A. Barras. 2011.** Hurricane Impacts on Coastal Wetlands: A Half-Century Record of Storm-Generated Features from Southern Louisiana. *J. Coast. Res.* 275: 27–43.
- Mychek-Londer, J. G., K. D. Balasingham, and D. D. Heath. 2019.** Using environmental DNA metabarcoding to map invasive and native invertebrates in two Great Lakes tributaries. *Environ. DNA.* edn3.56.
- Neff, J. M., E. H. Owens, S. W. Stoker, and D. M. McCormick. 1995.** Shoreline Oiling Conditions in Prince William Sound Following the *Exxon Valdez* Oil Spill, pp. 312–346. *In* Wells, P.G., Butler, J.N., Hughes, J.S. (eds.), *Exxon Vald. Oil Spill Fate Eff. Alaskan Waters*. ASTM International, West Conshohocken, PA.
- Nelson, D. W., and L. E. Sommers. 1982.** Total Carbon, Organic Carbon, and Organic Matter, pp. 539–579. *In* *Methods Soil Anal. Part 2. Chem. Microbiol. Prop.*
- Ngo, X. Q., N. Smol, and A. Vanreusel. 2013.** The meiofauna distribution in correlation with environmental characteristics in 5 Mekong estuaries, Vietnam. *Cah. Biol. Mar.* 54: 71–83.
- Nicholls, R. J., F. M. J. Hoozemans, and M. Marchand. 1999.** Increasing flood risk and wetland losses due to global sea-level rise: Regional and global analyses, pp. S69–S87. *In* *Glob. Environ. Chang.* Elsevier Ltd.
- Nordström, M. C., C. A. Currin, T. S. Talley, C. R. Whitcraft, and L. A. Levin. 2014.** Benthic food-web succession in a developing salt marsh. *Mar. Ecol. Prog. Ser.* 500: 43–55.
- Norén, M., and U. Jondelius. 1999.** Phylogeny of the Prolecithophora (Platyhelminthes) Inferred from 18S rDNA Sequences. *Cladistics.* 15: 103–112.
- Nyman, J. A. 2014.** Integrating Successional Ecology and the Delta Lobe Cycle in Wetland Research and Restoration. *Estuaries and Coasts.* 37: 1490–1505.
- Nyman, J. A., M. Carloss, R. D. Delaune, and W. H. Patrick. 1994.** Erosion rather than plant dieback as the mechanism of marsh loss in an estuarine marsh. *Earth Surf. Process.*

Landforms. 19: 69–84.

Nyman, J. A., R. D. Delaune, and W. H. Patrick. 1990. Wetland soil formation in the rapidly subsiding Mississippi River Deltaic Plain: Mineral and organic matter relationships. *Estuar. Coast. Shelf Sci.* 31: 57–69.

Odum, E. P. 1971. Estuarine Ecology, pp. 352–362. *In* Fundam. Ecol. W.B. Saunders Company, Philadelphia, PA.

Odum, W. E. 1988. Comparative ecology of tidal freshwater and salt marshes. *Annu. Rev. Ecol. Syst.* Vol. 19. 147–176.

Odum, W. E., T. J. Smith, J. K. Hoover, and C. Mcivor. 1984. The ecology of tidal freshwater marshes of the United States East Coast: a community profile. *Environ. Sci.*

Oksanen, J., F. G. Blanchet, M. Friendly, R. Kindt, P. Legendre, D. McGlinn, P. R. Minchin, R. B. O'Hara, G. L. Simpson, P. Solymos, M. H. H. Stevens, E. Szoecs, and H. Wagner. 2018. vegan: Community Ecology Package.

Olson, G. M., B. M. Meyer, and R. J. Portier. 2016. Assessment of the toxic potential of polycyclic aromatic hydrocarbons (PAHs) affecting Gulf menhaden (*Brevoortia patronus*) harvested from waters impacted by the BP Deepwater Horizon Spill. *Chemosphere.* 145: 322–328.

Orescanin, M. M., R. P. Hamilton, and B. Hoffnagle. 2018. Tidal choking in an anthropologically modified salt marsh estuary: Improving circulation through constriction removal. *Estuar. Coast. Shelf Sci.*

Paine, R. T., J. L. Ruesink, A. Sun, E. L. Soulanille, M. J. Wonham, C. D. G. Harley, D. R. Brumbaugh, and D. L. Secord. 1996. Trouble on oiled waters: Lessons from the Exxon valdez oil spill. *Annu. Rev. Ecol. Syst.* 27: 197–235.

Palaseanu-Lovejoy, M., C. Kranenburg, J. A. Barras, and J. C. Brock. 2013. Land Loss Due to Recent Hurricanes in Coastal Louisiana, U.S.A. *J. Coast. Res.* 63: 97–109.

Palmisano Jr., A. W. 1970. Plant community-soil relationships in Louisiana coastal marshes. LSU Hist. Diss. Theses.

Park, C., J. H. Wormuth, and G. A. Wolff. 1989. Sample variability of zooplankton in the nearshore off Louisiana with consideration of sampling design. *Cont. Shelf Res.* 9: 165–179.

Penfound, W. T., and E. S. Hathaway. 1938. Plant Communities in the Marshlands of Southeastern Louisiana. *Ecol. Monogr.* 8: 4–56.

Penland, S., and K. E. Ramsey. 1990. Relative Sea-Level Rise in Louisiana and the Gulf of Mexico : 1908-1988. *J. Coast. Res.* 6: 323–342.

Perret, W. S., and B. B. Barrett. 1971. Cooperative Gulf of Mexico Estuarine Inventory and Study, Louisiana: Phase II, hydrology, and Phase III, sedimentology. New Orleans.

Peterson, C. H., S. D. Rice, J. W. Short, D. Esler, J. L. Bodkin, B. E. Ballachey, and D. B. Irons.

- 2003.** Long-Term Ecosystem Response to the Exxon Valdez Oil Spill. *Science* (80-.).
- Peterson, G. W., and R. E. Turner. 1994.** The value of salt marsh edge vs interior as a habitat for fish and decapod crustaceans in a Louisiana tidal marsh. *Estuaries*. 17: 235–262.
- La Peyre, M. K., B. S. Eberline, T. M. Soniat, and J. F. La Peyre. 2013.** Differences in extreme low salinity timing and duration differentially affect eastern oyster (*Crassostrea virginica*) size class growth and mortality in Breton Sound, LA. *Estuar. Coast. Shelf Sci.* 135: 146–157.
- Peyronnin, N., M. Green, C. P. Richards, A. Owens, D. Reed, J. Chamberlain, D. G. Groves, W. K. Rhinehart, and K. Belhadjali. 2013.** Louisiana’s 2012 Coastal Master Plan: Overview of a Science-Based and Publicly Informed Decision-Making Process. *J. Coast. Res.* 67: 1–15.
- Phillips, J. D., D. J. Gillis, and R. H. Hanner. 2019.** Incomplete estimates of genetic diversity within species: Implications for DNA barcoding. *Ecol. Evol.* 9: 2996–3010.
- Poirrier, M. A., and M. M. Mulino. 1977.** The Impact of the 1975 Bonnet Carré Spillway Opening on Epifaunal Invertebrates in Southern Lake Pontchartrain. *J. Elisha Mitchell Sci. Soc.* 93: 11–18.
- Polak, R., A. Fillion, S. Fortier, J. Lanier, and K. Cooper. 1978.** Observations on Argo Merchant oil in zooplankton of Nantucket Shoals, pp. 109–115. *In* Wake Argo Merch. Center for Ocean Management Studies, University of Rhode Island, Kingston, RI.
- Porazinska, D. L., R. M. Giblin-Davis, L. Faller, W. Farmerie, N. Kanzaki, K. Morris, T. O. Powers, A. E. Tucker, W. Sung, and W. K. Thomas. 2009.** Evaluating high-throughput sequencing as a method for metagenomic analysis of nematode diversity. *Mol. Ecol. Resour.* 9: 1439–1450.
- Porazinska, D. L., W. Sung, R. M. Giblin-Davis, and W. K. Thomas. 2010.** Reproducibility of read numbers in high-throughput sequencing analysis of nematode community composition and structure. *Mol. Ecol. Resour.* 10: 666–676.
- Posey, M. H., T. D. Alphin, H. Harwell, and B. Allen. 2005.** Importance of low salinity areas for juvenile blue crabs, *Callinectes sapidus* Rathbun, in river-dominated estuaries of southeastern United States, pp. 81–100. *In* J. Exp. Mar. Bio. Ecol. Elsevier.
- Powell, R. T., and M. R. Alexander. 2003.** Trace metal contamination in sediments of Barataria Bay, Louisiana. *Bull. Environ. Contam. Toxicol.* 71: 308–314.
- Price, M. N., P. S. Dehal, and A. P. Arkin. 2010.** FastTree 2 - Approximately maximum-likelihood trees for large alignments. *PLoS One*. 5: e9490.
- Purcell, J. E., U. Båmstedt, and A. Båmstedt. 1999.** Prey, feeding rates, and asexual reproduction rates of the introduced oligohaline hydrozoan *Moerisia lyonsi*. *Mar. Biol.* 134: 317–325.
- Qiu, D., J. Yan, X. Ma, F. Gao, F. Wang, L. Wen, J. Bai, and B. Cui. 2019.** How vegetation influence the macrobenthos distribution in different saltmarsh zones along coastal topographic gradients. *Mar. Environ. Res.* 151: 104767.

- Quast, C., E. Pruesse, P. Yilmaz, J. Gerken, T. Schweer, P. Yarza, J. Peplies, and F. O. Glöckner. 2013.** The SILVA ribosomal RNA gene database project: improved data processing and web-based tools. *Nucleic Acids Res.* 41: D590–D596.
- Rabalais, N. N., and R. E. Turner. 2016.** Effects of the Deepwater Horizon Oil Spill on Coastal Marshes and Associated Organisms. *Oceanography.* 29: 150–159.
- Rangoonwala, A., C. E. Jones, and E. Ramsey III. 2016.** Wetland shoreline recession in the Mississippi River Delta from petroleum oiling and cyclonic storms. *Geophys. Res. Lett.* 43: 652–11,660.
- Reddy, K. R., W. H. Patrick, and C. W. Lindau. 1989.** Nitrification-denitrification at the plant root-sediment interface in wetlands. *Limnol. Oceanogr.* 34: 1004–1013.
- Rhoades, J. D. 1982.** Soluble Salts, pp. 167–179. *In* Methods Soil Anal. Part 2. Chem. Microbiol. Prop.
- Ricci, C., and M. Balsamo. 2000.** The biology and ecology of lotic rotifers and gastrotrichs. *Freshw. Biol.* 44: 15–28.
- Riera, P., P. Montagna, R. Kalke, and P. Richard. 2000.** Utilization of estuarine organic matter during growth and migration by juvenile brown shrimp *Penaeus aztecus* in a South Texas estuary. *Mar. Ecol. Prog. Ser.* 199: 205–216.
- Ritz, K., H. I. J. Black, C. D. Campbell, J. A. Harris, and C. Wood. 2009.** Selecting biological indicators for monitoring soils: A framework for balancing scientific and technical opinion to assist policy development. *Ecol. Indic.* 9: 1212–1221.
- Roberts, H. H., and J. M. Coleman. 1996.** Holocene evolution of the deltaic plain: A perspective - From Fisk to present. *Eng. Geol.* 45: 113–138.
- Rognes, T., T. Flouri, B. Nichols, C. Quince, and F. Mahé. 2016.** VSEARCH: a versatile open source tool for metagenomics. *PeerJ.* 4: e2584.
- Roman, C. T. 2017.** Salt Marsh Sustainability: Challenges During an Uncertain Future. *Estuaries and Coasts.* 40: 711–716.
- Rozas, L. P., and T. J. Minello. 2011.** Variation in penaeid shrimp growth rates along an estuarine salinity gradient: Implications for managing river diversions. *J. Exp. Mar. Bio. Ecol.* 397: 196–207.
- Rozas, L. P., T. J. Minello, and M. S. Miles. 2014.** Effect of Deepwater Horizon Oil on Growth Rates of Juvenile Penaeid Shrimps. *Estuaries and Coasts.* 37: 1403–1414.
- Rublee, P., and B. E. Dornseif. 1978.** Direct counts of bacteria in the sediments of a North Carolina salt marsh. *Estuaries.* 1: 188–191.
- Ruppert, K. M., R. J. Kline, and M. S. Rahman. 2019.** Past, present, and future perspectives of environmental DNA (eDNA) metabarcoding: A systematic review in methods, monitoring, and applications of global eDNA. *Glob. Ecol. Conserv.*

- Russell, R. J. 1940.** Quaternary history of Louisiana. *Bull. Geol. Soc. Am.* 51: 1199–1233.
- Rutledge, P. A., and J. W. Fleeger. 1993.** Abundance and seasonality of meiofauna, including harpacticoid copepod species, associated with stems of the salt-marsh cord grass, *Spartina alterniflora*. *Estuaries*. 16: 760–768.
- Saiki, R. K., D. H. Gelfand, S. Stoffel, S. J. Scharf, R. Higuchi, G. T. Horn, K. B. Mullis, and H. A. Erlich. 1988.** Primer-Directed Enzymatic Amplification of DNA with a Thermostable DNA Polymerase. *Science* (80-.). 239: 487–491.
- Sakata, M. K., S. Yamamoto, R. O. Gotoh, M. Miya, H. Yamanaka, and T. Minamoto. 2020.** Sedimentary eDNA provides different information on timescale and fish species composition compared with aqueous eDNA. *Environ. DNA*. 2: 505–518.
- Sanders, H. L., J. F. Grassle, and G. R. Hampson. 1980.** Anatomy of an oil spill: Long-term effects from the grounding of the barge Florida off West Falmouth, Massachusetts. *J. Mar. Res.* 38: 265–380.
- Santschi, P. H., B. J. Presley, T. L. Wade, B. Garcia-Romero, and M. Baskaran. 2001.** Historical contamination of PAHs, PCBs, DDTs, and heavy metals in Mississippi River Delta, Galveston Bay and Tampa Bay sediment cores. *Mar. Environ. Res.* 52: 51–79.
- Sapkota, Y., and J. R. White. 2019.** Marsh Edge Erosion and Associated Carbon Dynamics in Coastal Louisiana: A Proxy for Future Wetland-Dominated Coastlines World-Wide. *Estuar. Coast. Shelf Sci.* In Review: 106289.
- Sasser, C. E., M. D. Dozier, J. G. Gosselink, and J. M. Hill. 1986.** Spatial and temporal changes in Louisiana's Barataria Basin marshes, 1945-1980. *Environ. Manage.* 10: 671–680.
- Scaife, W. W., R. E. Turner, and R. Costanza. 1983.** Coastal Louisiana recent land loss and canal impacts. *Environ. Manage.* 7: 433–442.
- Schärer, L., J. N. Brand, P. Singh, K. S. Zadesenets, C. P. Stelzer, and G. Viktorin. 2020.** A phylogenetically informed search for an alternative *Macrostomum* model species, with notes on taxonomy, mating behavior, karyology, and genome size. *J. Zool. Syst. Evol. Res.* 58: 41–65.
- Schockaert, E. R., M. Hooge, R. Sluys, S. Schilling, S. Tyler, and T. Artois. 2008.** Global diversity of free living flatworms (Platyhelminthes, "Turbellaria") in freshwater. *Hydrobiologia*.
- Schroeder, A., A. Pallavicini, M. Pansera, D. Stankovic, E. Camatti, M. Biology, and S. Piran. 2019.** SUITABILITY OF METABARCODING FOR ZOOPLANKTON BIODIVERSITY ASSESSMENT-A COMPARISON BETWEEN CLASSICAL AND MOLECULAR APPROACHES. 23.
- Schuchert, P. 2017.** Systematic notes on some leptomedusa species with a description of *Neotima galeai* n. spec. (Hydrozoa, Cnidaria). *Rev. Suisse Zool.* 124: 351–375.
- Schutte, C. A., J. M. Marton, A. E. Bernhard, A. E. Giblin, and B. J. Roberts. 2020.** No Evidence for Long-term Impacts of Oil Spill Contamination on Salt Marsh Soil Nitrogen Cycling Processes. *Estuaries and Coasts*.

- Semprucci, F., C. Sbrocca, M. Rocchi, and M. Balsamo. 2015.** Temporal changes of the meiofaunal assemblage as a tool for the assessment of the ecological quality status. *J. Mar. Biol. Assoc. United Kingdom*. 95: 247–254.
- Sherman, K. M., and B. C. Coull. 1980.** The response of meiofauna to sediment disturbance. *J. Exp. Mar. Bio. Ecol.* 46: 59–71.
- Shigenaka, G. 2014.** Twenty-Five Years After the Exxon Valdez Oil Spill: NOAA's Scientific Support, Monitoring, and Research. Seattle.
- Sibbald, S. J., and J. M. Archibald. 2017.** More protist genomes needed. *Nat. Ecol. Evol.* 1: 145.
- Silliman, B. R., J. van de Koppel, M. W. McCoy, J. Diller, G. N. Kasozi, K. Earl, P. N. Adams, and A. R. Zimmerman. 2012.** Degradation and resilience in Louisiana salt marshes after the BP–Deepwater Horizon oil spill. *Proc. Natl. Acad. Sci.* 109: 11234–11239.
- Smith, C. J., R. D. Delaune, W. H. Patrick, and J. W. Fleeger. 1984.** Impact of dispersed and undispersed oil entering a Gulf Coast salt marsh. *Environ. Toxicol. Chem.* 3: 609–616.
- Smutná, M., K. Hilscherová, V. Pašková, and B. Maršálek. 2008.** Biochemical parameters in *Tubifex tubifex* as an integral part of complex sediment toxicity assessment. *J. Soils Sediments*. 8: 154–164.
- Snelgrove, P. V. R. 1997.** The Importance of Marine Sediment Biodiversity in Ecosystem Processes. *Ambio*. 26: 578–583.
- Soergel, D. A. W., N. Dey, R. Knight, and S. E. Brenner. 2012.** Selection of primers for optimal taxonomic classification of environmental 16S rRNA gene sequences. *ISME J.* 6: 1440–1444.
- Soetaert, K., M. Vincx, J. Wittoeck, and M. Tulkens. 1997.** Meiobenthic distribution and nematode community structure in five European estuaries. *Hydrobiologia*. 77: 211–227.
- Solomon, E. A., M. Kastner, I. R. MacDonald, and I. Leifer. 2009.** Considerable methane fluxes to the atmosphere from hydrocarbon seeps in the Gulf of Mexico. *Nat. Geosci.* 2: 561–565.
- Sørensen, T. 1948.** A method of establishing groups of equal amplitude in plant sociology based on similarity of species content. *Bull. Soc. Plant Ecol.* 1: 56.
- Soto, L. A., A. V. Botello, S. Licea-DurÃ¡n, M. L. LizÃ¡rraga-Partida, and A. YÃ¡Ã±ez-Arancibia. 2014.** The environmental legacy of the Ixtoc-I oil spill in Campeche Sound, southwestern Gulf of Mexico. *Front. Mar. Sci.* 1: 57.
- Souza, G. 1970.** Report of the Shellfish Warden. Pp. 161-165 in Annual report of the finances of the town of Falmouth for the year ending December 31, 1970.
- Stagg, C. L., and I. A. Mendelssohn. 2010.** Restoring Ecological Function to a Submerged Salt Marsh. *Restor. Ecol.* 18: 10–17.
- Stoeck, T., D. Bass, M. Nebel, R. Christen, M. D. M. Jones, H. W. Breiner, and T. A. Richards. 2010.** Multiple marker parallel tag environmental DNA sequencing reveals a highly

- complex eukaryotic community in marine anoxic water. *Mol. Ecol.* 19: 21–31.
- Suir, G. M., C. E. Sasser, R. D. Delaune, and E. O. Murray. 2019.** Comparing carbon accumulation in restored and natural wetland soils of coastal Louisiana, *Int. J. Sediment Res. International Research and Training Centre on Erosion and Sedimentation / the World Association for Sedimentation and Erosion Research.*
- Syvitski, J. P. M., A. J. Kettner, I. Overeem, E. W. H. Hutton, M. T. Hannon, G. R. Brakenridge, J. Day, C. Vörösmarty, Y. Saito, L. Giosan, and R. J. Nicholls. 2009.** Sinking deltas due to human activities. *Nat. Geosci.* 2: 681–686.
- Teal, J. M., J. W. Farrington, K. A. Burns, J. J. Stegeman, B. W. Tripp, B. Woodin, and C. Phinney. 1992.** The West Falmouth oil spill after 20 years: Fate of fuel oil compounds and effects on animals. *Mar. Pollut. Bull.* 24: 607–614.
- Teal, J. M., and R. W. Howarth. 1984.** Oil spill studies: A review of ecological effects. *Environ. Manage.* 8: 27–43.
- Teal, J. M., and L. Weishar. 2005.** Ecological engineering, adaptive management, and restoration management in Delaware Bay salt marsh restoration. *Ecol. Eng.* 25: 304–314.
- Temmerman, S., P. Meire, T. J. Bouma, P. M. J. Herman, T. Ysebaert, and H. J. De Vriend. 2013.** Ecosystem-based coastal defence in the face of global change. *Nature.*
- Thebeau, L. C., J. W. Tunnell, Q. R. Dokken, and M. E. Kindinger. 1981.** EFFECTS OF THE IXTOC I OIL SPILL ON THE INTERTIDAL AND SUBTIDAL INFAUNAL POPULATIONS ALONG LOWER TEXAS COAST BARRIER ISLAND BEACHES., pp. 467–475. *In* *Int. Oil Spill Conf. Proc. API (Publication 4334).*
- Thorne, K. M., C. M. Freeman, J. A. Rosencranz, N. K. Ganju, and G. R. Guntenspergen. 2019.** Thin-layer sediment addition to an existing salt marsh to combat sea-level rise and improve endangered species habitat in California, USA. *Ecol. Eng.* 0–1.
- Tidwell, M. A. 1970.** Tabanidae (Diptera): Some Systematic Aspects.
- Tito de Morais, L., and J. Y. Bodiou. 1984.** Predation on meiofauna by juvenile fish in a Western Mediterranean flatfish nursery ground. *Mar. Biol.* 82: 209–215.
- Tonelli, M., S. Fagherazzi, and M. Petti. 2010.** Modeling wave impact on salt marsh boundaries. *J. Geophys. Res. Ocean.* 115: C09028.
- Turner, R. E., and G. McClenachan. 2018.** Reversing wetland death from 35,000 cuts: Opportunities to restore Louisiana’s dredged canals. *PLoS One.* 13: 1–10.
- Turner, R. E., N. N. Rabalais, E. B. Overton, B. M. Meyer, G. McClenachan, E. M. Swenson, M. Besonen, M. L. Parsons, and J. Zingre. 2019.** Oiling of the continental shelf and coastal marshes over eight years after the 2010 Deepwater Horizon oil spill. *Environ. Pollut.* 252: 1367–1376.
- Turner, R. E., E. M. Swenson, and C. S. Milan. 2005.** Organic and Inorganic Contributions to

- Vertical Accretion in Salt Marsh Sediments, pp. 583–595. *In* Concepts Controv. Tidal Marsh Ecol. Kluwer Academic Publishers.
- Venter, P. C., F. Nitsche, and H. Arndt. 2018.** The Hidden Diversity of Flagellated Protists in Soil. *Protist.* 169: 432–449.
- Waeyenberge, L., N. de Sutter, N. Viaene, and A. Haegeman. 2019.** New Insights Into Nematode DNA-metabarcoding as Revealed by the Characterization of Artificial and Spiked Nematode Communities. *Diversity.* 11: 1–22.
- Wamsley, T. V., M. A. Cialone, J. M. Smith, J. H. Atkinson, and J. D. Rosati. 2010.** The potential of wetlands in reducing storm surge. *Ocean Eng.* 37: 59–68.
- Warren, R. S., P. E. Fell, R. Rozsa, A. H. Brawley, A. C. Orsted, E. T. Olson, V. Swamy, and W. A. Niering. 2002.** Salt marsh restoration in Connecticut: 20 years of science and management. *Restor. Ecol.* 10: 497–513.
- Warwick, R. M. 1981.** Survival Strategies of Meiofauna, pp. 39–52. *In* Feed. Surviv. Strategies Estuar. Org. Springer US, Boston, MA.
- Weiss, S., Z. Z. Xu, S. Peddada, A. Amir, K. Bittinger, A. Gonzalez, C. Lozupone, J. R. Zaneveld, Y. Vázquez-Baeza, A. Birmingham, E. R. Hyde, and R. Knight. 2017.** Normalization and microbial differential abundance strategies depend upon data characteristics. *Microbiome.* 5: 27.
- Whaley, S. D., and T. J. Minello. 2002.** The Distribution of Benthic Infauna of a Texas Salt Marsh In Relation to the Marsh Edge. *Wetlands.* 22: 753–766.
- Whitcraft, C. R., and L. A. Levin. 2007.** Regulation of benthic algal and animal communities by salt marsh plants: Impact of shading. *Ecology.* 88: 904–917.
- Whittaker, R. H. 1972.** Evolution and Measurement of Species Diversity. *Taxon.* 21: 213–251.
- Wilber, D. H., G. L. Ray, D. G. Clarke, and R. J. Diaz. 2008.** Responses of Benthic Infauna to Large-Scale Sediment Disturbance in Corpus Christi Bay, Texas. *J. Exp. Mar. Bio. Ecol.* 365: 13–22.
- Wilson, B. H. 1963.** Some Aspects of the Biology , Ecology , and Behavior of Horse Flies (Diptera , Tabanidae) in Louisiana .
- Wolfe, D. A., M. J. Hameedi, J. A. Galt, G. Watabayashi, J. Short, C. O’claire, S. Rice, J. Michel, J. R. Payne, J. Braddock, S. Hanna, and D. Sale. 1994.** The Fate of the Oil Spilled from the Exxon Valdez: The Mass Balance Is the Most Complete and Accurate of Any Major Oil Spill. *Environ. Sci. Technol.* 28.
- Wolters, M., A. Garbutt, and J. P. Bakker. 2005.** Salt-marsh restoration: Evaluating the success of de-embankments in north-west Europe. *Biol. Conserv.* 123: 249–268.
- Wong, W. H., N. N. Rabalais, and R. E. Turner. 2010.** Abundance and ecological significance of the clam *Rangia cuneata* (Sowerby, 1831) in the upper Barataria Estuary (Louisiana, USA).

Hydrobiologia. 651: 305–315.

Xia, K., G. Hagood, C. Childers, J. Atkins, B. Rogers, L. Ware, K. Armbrust, J. Jewell, D. Diaz, N. Gatian, and H. Folmer. 2012. Polycyclic aromatic hydrocarbons (PAHs) in Mississippi seafood from areas affected by the deepwater horizon oil spill. *Environ. Sci. Technol.* 46: 5310–5318.

Yandell, B. S. 1997. Practical data analysis for designed experiments. Chapman & Hall.

Yuill, B., D. Lavoie, and D. J. Reed. 2009. Understanding Subsidence Processes in Coastal Louisiana. *J. Coast. Res.* 10054: 23–36.

Zeppilli, D., J. Sarrazin, D. Leduc, P. M. Arbizu, D. Fontaneto, C. Fontanier, A. J. Gooday, R. M. Kristensen, V. N. Ivanenko, M. V. Sørensen, A. Vanreusel, J. Thébault, M. Mea, N. Allio, T. Andro, A. Arvigo, J. Castrec, M. Danielo, V. Foulon, R. Fumeron, L. Hermabessiere, V. Hulot, T. James, R. Langonne-Augen, T. Le Bot, M. Long, D. Mahabror, Q. Morel, M. Pantalos, E. Pouplard, L. Raimondeau, A. Rio-Cabello, S. Seite, G. Traisnel, K. Urvoy, T. Van Der Stegen, M. Weyand, and D. Fernandes. 2015. Is the meiofauna a good indicator for climate change and anthropogenic impacts? *Mar. Biodivers.* 45: 505–535.

Zhang, S., Z. Hu, and H. Wang. 2018. A retrospective review of microbiological methods applied in studies following the Deepwater Horizon oil spill. *Front. Microbiol.*

Zhang, Z., B. Cui, X. Fan, K. Zhang, H. Zhao, and H. Zhang. 2012. Wetland Network Design for Mitigation of Saltwater Intrusion by Replenishing Freshwater in an Estuary. *CLEAN - Soil, Air, Water.* 40: 1036–1046.

Zimmerman, R. J., T. J. Minello, and L. P. Rozas. 2002. Salt Marsh Linkages to Productivity of Penaeid Shrimps and Blue Crabs in the Northern Gulf of Mexico. *In* Weinstein, M.P., Kreeger, D.A. (eds.), *Concepts Controv. Tidal Marsh Ecol.* Springer, Dordrecht.

Zinger, L., A. Bonin, I. G. Alsos, M. Bálint, H. Bik, F. Boyer, A. A. Chariton, S. Creer, E. Coissac, B. E. Deagle, M. De Barba, I. A. Dickie, A. J. Dumbrell, G. F. Ficetola, N. Fierer, L. Fumagalli, M. T. P. Gilbert, S. Jarman, A. Jumpponen, H. Kauserud, L. Orlando, J. Pansu, J. Pawlowski, L. Tedersoo, P. F. Thomsen, E. Willerslev, and P. Taberlet. 2019. DNA metabarcoding—Need for robust experimental designs to draw sound ecological conclusions. *Mol. Ecol. mec.* 15060.

Vita

Patrick Michael Rayle attained his Bachelor of Science degree in biology from Louisiana State University in May of 2015. Following graduation, he sought out employment in a number of places before joining the lab of Dr. Lane Foil as a master's student in the fall of 2017. He anticipates graduating in May of 2021.